

**The chiral cyclobutane motif in the synthesis  
of dendrimers and multifunctional platforms.  
Applications as contrast agents, cell-penetrating  
peptides, and NPY analogues**

**Raquel Gutiérrez Abad**

Doctoral Thesis

Programa de doctorat en Química

Supervised by Prof. Rosa María Ortuño and Dr. Ona Illa

Departament de Química

Facultat de Ciències

2012



This thesis is presented for graduation as Doctor by **Raquel Gutiérrez Abad**

Read and approved,

**Prof. Rosa María Ortuño Mingarro**

**Dr. Ona Illa i Soler**

Bellaterra, 4<sup>th</sup> June 2012



## **Acknowledgements**

The present thesis has been carried out in the Department of Chemistry of Universitat Autònoma de Barcelona under the direction of Prof. Rosa María Ortuño and Dr. Ona Illa. I would like to thank them for the opportunity they gave me to work on this passionating research field.

I would also like to thank AGAUR and Ministerio de Educación for awarding me with the FI and FPU fellowships, which allowed the development of this thesis.

The COST action CM-083, Foldamers allowed me to establish contact with Prof. Oliver Reiser who kindly welcomed me in his laboratory at the Universität Regensburg during 4 months. Ministerio de Educación is also thanked for the fellowship which permitted this doctoral stay. I wish to thank Dr. Melanie Kaske and Ludwig Pils for their precious help during this period, Paula and all the “Italians” for the funny moments.

I am also very grateful to Dr. Miriam Royo and Dr. Daniel Carbajo for their collaboration in the development of the CPPs part of this thesis.

Fundamental results have been obtained with the help of Dr. Silvia Lope and Dr. Pau Nolis from the Servei de Ressonància Magnètica Nuclear, thank you for your efficiency and fruitful explanations.

Prof. Vicenç Branchadell and Dr. Carles Acosta are also deeply thanked for their help and their patience to explain me the basis of theoretical calculations.

This work wouldn't have been possible without the kind assistance received from the members of Servei d'Anàlisi Química, Servei de Ressonància Magnètica Nuclear and Proteomics facility from UAB.

This hard task has been facilitated by the friendly lab-atmosphere, thank you all for the laughs, support, chats and useful advices.

The last steps of the writing of this thesis took place while I was working in ATLB team, thank you to all my mates for your patience and support.

I can't finish without mentioning my friends and running mates for all the time that we have spend together. Thanks to them, during this period I have not only grown as a chemist but also in a personal way.

Finally, I would have never succeeded without the reconforting support of my Family.

Moltes gràcies a tots!



A mi Abuela Miguela





Part of the results reported in this thesis has been published in the following scientific articles:

- **Stereoselective synthesis of cyclobutyl  $\gamma$ -amino acids leading to branched peptides with a cyclobutane core.**

Aguilera, J.; Gutiérrez-Abad, R.; Mor, A.; Moglioni, A. G.; Moltrasio, G.; Ortuño, R. M.  
*Tetrahedron: Asymmetry* **2008**, *19*, 2864-2869.

- **Synthesis of chiral cyclobutane containing  $C_3$ -symmetric peptide dendrimers.**

Gutiérrez-Abad, R.; Illa, O.; Ortuño, R. M.  
*Org. Lett.* **2010**, *12*, 3148-3151.

- **Synthesis and structural study of highly constrained hybrid cyclobutane-proline  $\gamma,\gamma$ -peptides.**

Gutiérrez-Abad, R.; Carbajo, D.; Nolis, P.; Acosta-Silva, C.; Cobos, J. A.; Illa, O.; Royo, M.; Ortuño, R. M.  
*Amino Acids* **2011**, *41*, 673-686.

- **Searching for new cell-penetrating agents: hybrid cyclobutane-proline  $\gamma,\gamma$ -peptides**

Gorrea, E.; Carbajo, D.; Gutiérrez-Abad, R.; Illa, O.; Branchadell, V.; Royo, M.; Ortuño, R. M.  
*Org. Biomol. Chem.* **2012**, *10*, 4050-4057.



**Abbreviations**

|        |   |
|--------|---|
| B3LYP  | Becke 3-Parameter exchange functional, Lee, Yang and Parr                               |
| Bn     | Benzyl  |
| Boc    | <sup>t</sup> Butyloxycarbonyl   |
| CA     | Contrast Agent  |
| Cbz    | Benzyloxycarbonyl   |
| CF     | 5(6)-carboxyfluorescein   |
| CPP    | Cell Penetrating Peptide  |
| CNS    | Central Nervous System  |
| COSY   | Correlated Spectroscopy   |
| CT     | Computed Tomography   |
| DCC    | Dicyclohexyl Carbodiimide   |
| DEPT   | Distortionless Enhancement by Polarization Transfer                                     |
| DFT    | Density Functional Theory   |
| DIPEA  | <i>N,N</i> -Diisopropylethylamine   |
| DMAP   | 4-Dimethylaminopyridine   |
| DMF    | <i>N,N</i> -Dimethylformamide   |
| DMSO   | Dimethyl Sulfoxide  |
| DOTA   | 1,4,7,10-Tetraazacyclododecane-1,4,7,10-tetraacetic acid                                |
| EDAC   | 1-Ethyl-3-(3-dimethylaminopropyl)carbodiimide   |
| ee     | Enantiomeric Excess   |
| ESI-MS | Electrospray ionization mass spectrometry   |
| FDPP   | Pentafluorophenyl Diphenylphosphinate   |
| Fmoc   | 9-Fluorenylmethoxycarbonyl  |
| GABA   | $\gamma$ -Amino butiryc acid  |
| HATU   | O-(7-Azabenzotriazol-1-yl)- <i>N,N,N',N'</i> -tetramethyluronium<br>hexafluorophosphate |
| HOBt   | 1-hydroxy-1 <i>H</i> -benzotriazole   |
| HPP    | Human Pancreatic Polypeptide  |
| HRMS   | High Resolution Mass Spectroscopy   |

## Abbreviations

---

|       |   |
|-------|---|
| HSQC  | Heteronuclear Single Quantum Spectrum                               |
| IR    | Infrared Spectroscopy   |
| MM    | Molecular mechanics   |
| MRI   | Magnetic Resonance Imaging  |
| MTT   | 3-(4,5-dimethylthiazol-2-yl)-2,5-diphenyltetrazolium bromide        |
| NMR   | Nuclear Magnetic Resonance  |
| NOE   | Nuclear Overhauser Effect   |
| NOESY | Nuclear Overhauser Effect Spectroscopy                              |
| NPY   | Neuropeptide Y  |
| PDC   | Pyridinium dichromate   |
| PPTS  | Pyridinium <i>para</i> -toluenesulfonate                            |
| PyBOP | (Benzotriazol-1-yloxy)tripyrrolidinophosphonium hexafluorophosphate |
| PYY   | Peptide YY  |
| ROESY | Rotating frame Overhauser Effect Spectroscopy                       |
| SEM   | 2-(Trimethylsilyl)ethoxymethyl                                      |
| TAT   | Trans-Activating Transcriptional activator                          |
| TBAF  | Tetra-( <i>n</i> -butylammonium) fluoride                           |
| TFA   | Trifluoroacetic acid  |
| THF   | Tetrahydrofuran   |
| TLC   | Thin Layer Chromatography   |

**TABLE OF CONTENTS**

|  |    |
|--|----|
| <b>1. GENERAL INTRODUCTION</b> .....   | 23 |
| 1.1. USE OF PEPTIDES AS DRUGS .....  | 23 |
| 1.2. PEPTIDE STRUCTURE OF NON PROTEINOGENIC AMINO ACIDS AND PEPTIDES .....   | 25 |
| 1.3. AMINO ACIDS CONTAINING A CYCLOBUTANE MOIETY .....   | 27 |
| 1.3.1 Natural amino acids containing a cyclobutane moiety .....  | 27 |
| 1.3.2 Synthetic amino acids and peptides containing a cyclobutane moiety .....   | 28 |
| 1.4..... PRECEDENTS IN THE RESEARCH GROUP IN THE SYNTHESIS OF CYCLOBUTANE AMINO ACIDS AND PEPTIDES .....                                       | 31 |
| 1.4.1 Synthesis of 1,2-functionalised cyclobutane derivatives .....  | 32 |
| 1.4.2 Synthesis of 1,3-functionalised cyclobutane derivatives .....  | 35 |
| <b>2. CHAPTER I: CYCLOBUTANE CONTAINING C<sub>3</sub>-SYMMETRIC PEPTIDE DENDRIMERS</b> .....   | 41 |
| 2.1. INTRODUCTION .....  | 41 |
| 2.1.1 Biological relevance of $\gamma$ -amino acids .....  | 41 |
| 2.1.2 Secondary structure of $\gamma$ -peptides .....  | 42 |
| 2.1.3 Precedents in the synthesis of ring-containing $\gamma$ -amino acids .....   | 44 |
| 2.1.4 Precedents in the research group in the synthesis of ring-containing $\gamma$ -amino acids .....   | 45 |
| 2.1.5 Dendrimers .....   | 47 |
| 2.2. OBJECTIVES .....  | 55 |
| 2.3. RESULTS AND DISCUSSION .....  | 57 |
| 2.3.1 Synthesis of orthogonally protected cyclobutane $\gamma$ , $\epsilon$ -amino diacid, 15 .....  | 57 |
| 2.3.2 Synthesis of a differently protected family of GABA-residues .....   | 58 |
| 2.3.3 Synthesis and structural properties of cyclobutane-cored first generation dendrimers.....  | 61 |
| 2.3.4 Structural study in solution of the series of hybrid cyclobutane-GABA peptides .....   | 64 |
| 2.3.5 Synthesis of a cyclobutane-containing family of C <sub>3</sub> -symmetric benzene-cored dendritic molecules .....                        | 68 |
| 2.4. SUMMARY AND CONCLUSIONS: Cyclobutane Containing C <sub>3</sub> -Symmetric Peptide Dendrimers .....  | 82 |
| <b>3. CHAPTER II: HYBRID CYCLOBUTANE-PROLINE <math>\gamma</math>, <math>\gamma</math>-PEPTIDES: STRUCTURE AND CELL-UPTAKE PROPERTIES</b> ..... | 87 |
| 3.1. INTRODUCTION .....  | 87 |
| 3.1.1 Foldamers with heterogeneous backbones .....   | 87 |
| 3.1.2 Use of 4-amino-prolines in peptide chemistry .....   | 92 |
| 3.1.3 Cell penetrating peptides .....  | 94 |
| 3.2. OBJECTIVES .....  | 99 |

|   |            |
|---|------------|
| 3.3.RESULTS AND DISCUSSION.....   | 100        |
| 3.3.1 Synthesis of both enantiomers of orthogonally protected cyclobutane $\gamma$ -amino acid, (-)-47 and (+)-47 .....                         | 100        |
| 3.3.2.....  | 102        |
| Synthesis of partially protected 4-amino proline 54.....  | 102        |
| 3.3.3 Synthesis of (1 <i>S</i> ,3 <i>R</i> )-cyclobutane-proline $\gamma,\gamma$ -peptides series.....  | 102        |
| 3.3.4 Synthesis of (1 <i>R</i> ,3 <i>S</i> )-cyclobutane-proline $\gamma,\gamma$ -peptides series.....  | 104        |
| 3.3.5 Conformational study in solution.....   | 105        |
| 3.3.6 Theoretical calculations of orthogonally protected diastereomeric series of hybrid cyclobutane-proline $\gamma$ , $\gamma$ -peptides..... | 116        |
| 3.3.7 Self assembly studies for both diastereomeric series of hybrid cyclobutane-proline $\gamma$ , $\gamma$ -peptides.....                     | 118        |
| 3.3.8 Evaluation of the series of hybrid cyclobutane-proline $\gamma,\gamma$ -peptides as CPPs .....  | 119        |
| 3.4.SUMMARY AND CONCLUSIONS: Hybrid cyclobutane-proline $\gamma,\gamma$ -peptides: Structure and cell-uptake properties.....                    | 124        |
| <b>4. CHAPTER III: NPY ANALOGUES.....</b>   | <b>129</b> |
| 4.1.INTRODUCTION .....  | 129        |
| 4.1.1 Neuropeptide Y (NPY).....   | 129        |
| 4.1.2 NPY analogues containing constricted amino acids.....   | 131        |
| 4.2.OBJECTIVES.....   | 133        |
| 4.3.RESULTS AND DISCUSSION.....   | 135        |
| 4.3.1 Synthesis of $\beta$ -cyclobutane building block.....   | 135        |
| 4.3.2 Synthesis of $\gamma$ -cyclobutane building block .....   | 137        |
| 4.3.3 Solid-phase synthesis of truncated NPY analogues.....   | 138        |
| 4.3.5 Functional activity at the NPY $Y_4$ receptor determined in the steady state GTPase assay   | 146        |
| 4.4.SUMMARY AND CONCLUSIONS: NPY analogues .....  | 149        |
| <b>5. CHAPTER IV: CHIRAL CYCLOBUTANE PLATFORMS: Magnetic Resonance Imaging (MRI) CONTRAST AGENTS.....</b>                                       | <b>153</b> |
| 5.1.INTRODUCTION .....  | 153        |
| 5.1.1 Polyfunctional platforms .....  | 153        |
| 5.1.2 Magnetic Resonance Imaging (MRI).....   | 155        |
| 5.1.3 MRI Contrast Agents (CAs) .....   | 157        |
| 5.2.OBJECTIVES.....   | 161        |
| 5.3.RESULTS AND DISCUSSION.....   | 162        |
| 5.3.1 Synthesis of chiral polyfunctional cyclobutane platforms .....  | 162        |

|   |     |
|---|-----|
| 5.3.2 Synthesis of hybrid DOTA-cyclobutane CAs .....  | 170 |
| 5.3.3 <i>In vitro</i> evaluation of the new CAs .....   | 173 |
| 5.3.4 <i>In vivo</i> evaluation of the new CAs .....  | 177 |
| 5.4.SUMMARY AND CONCLUSIONS: Chiral polyfunctional cyclobutane platforms.....   | 181 |
| <b>6. GENERAL CONCLUSIONS</b> .....   | 185 |
| <b>7. EXPERIMENTAL PROCEDURES</b> .....   | 189 |
| 7.1.General methodology .....   | 189 |
| 7.2.Experimental Section .....  | 191 |
| (1 <i>S</i> ,3 <i>R</i> )-3-Acetyl-2,2-dimethylcyclobutanecarboxylic acid [( <i>-</i> )-( <i>cis</i> )-pinononic acid], <b>2</b> .....  | 191 |
| (1 <i>S</i> ,3 <i>R</i> )-Methyl-3-acetyl-2,2-dimethylcyclobutanecarboxylate, <b>3</b> .....  | 192 |
| Pyridinium <i>p</i> -toluenesulfonate (PPTS), <b>4</b> .....  | 193 |
| (1 <i>S</i> ,3 <i>R</i> )-Methyl-2,2-dimethyl-3-(2'-methyl-[1',3']-dioxolan-2'-yl)cyclobutane- carboxylate, <b>5</b> ..   | 193 |
| (1 <i>S</i> ,3 <i>R</i> )-3-(2'-Methyl-[1',3']-dioxolan-2'-yl)-2,2-dimethylcyclobutylmethanol, <b>6</b> .....   | 194 |
| (1 <i>S</i> ,3 <i>R</i> )-2,2-Dimethyl-3-(2'-methyl-[1',3']-dioxolan-2'-yl)cyclobutanecarbal-dehyde, <b>7</b> .....   | 195 |
| <i>tert</i> -Butyl 3-[(1' <i>R</i> ,3' <i>R</i> )-2',2'-dimethyl-3'-(2-methyl-1,3-dioxolan-2-yl)cyclobutyl]-acrylate, <b>8+9</b><br>( <i>Z+E</i> ).....   | 196 |
| ( <i>S</i> )- <i>tert</i> -Butyl 3-[(1' <i>R</i> ,3' <i>R</i> )-2',2'-dimethyl-3'-(2-methyl-1,3-dioxolan-2-yl)cyclobutyl]-4-<br>nitrobutanoate, <b>10</b> .....                                 | 197 |
| ( <i>S</i> )- <i>tert</i> -Butyl 4-amino-3-[(1' <i>R</i> ,3' <i>R</i> )-2',2'-dimethyl-3'-(2-methyl-1,3-dioxolan-2-<br>yl)cyclobutyl]butanoate, <b>11</b> .....                                 | 198 |
| ( <i>S</i> )- <i>tert</i> -Butyl 4-(benzyloxycarbonylamino)-3-[(1' <i>R</i> ,3' <i>R</i> )-2',2'-dimethyl-3'-(2-methyl-1,3-dioxolan-<br>2-yl)cyclobutyl]butanoate, <b>12</b> .....              | 199 |
| ( <i>S</i> )- <i>tert</i> -Butyl 3-[(1' <i>R</i> ,3' <i>R</i> )-3-acetyl-2',2'-dimethylcyclobutyl]-4-(benzyloxy-<br>carbonylamino)butanoate, <b>13</b> .....                                    | 200 |
| Benzyl (2 <i>S</i> ,1' <i>R</i> ,3' <i>R</i> )-3-( <i>tert</i> -butoxycarbonyl)-2-(2',2'-dimethyl-3'-carboxycyclobutyl)-<br>propylcarbamate, <b>14</b> .....                                    | 201 |
| (1' <i>R</i> ,3' <i>R</i> )-Methyl 3-[( <i>S</i> )-1-(benzyloxycarbonylamino)-4- <i>tert</i> -butoxy-4-oxobutan-2-yl)-2',2'-<br>dimethylcyclobutanecarboxylate, <b>15</b> .....                 | 202 |
| 4-(Benzyloxycarbonylamino)butanoic acid, <b>17</b> .....  | 203 |
| Methyl 4-(benzyloxycarbonylamino)butanoate, <b>18</b> .....   | 204 |
| <i>tert</i> -Butyl 4-(benzyloxycarbonylamino)butanoate, <b>19</b> .....   | 205 |
| Trifluoroacetate salt of methyl 4-ammoniobutanoate, <b>20</b> .....   | 206 |
| <i>tert</i> -Butyl 4-aminobutanoate, <b>21</b> .....  | 207 |
| <i>tert</i> -Butyl 4-(4-(benzyloxycarbonylamino)butanamido)-3-( <i>S</i> )-[(1' <i>R</i> ,3' <i>R</i> )-2',2'-dimethyl-3'-(2-<br>methyl-1,3-dioxolan-2-yl)cyclobutyl]butanoate, <b>22</b> ..... | 208 |

## Table of Contents

|   |     |
|---|-----|
| <i>tert</i> -Butyl 3-((1' <i>R</i> ,3' <i>R</i> )-3'-acetyl-2',2'-dimethylcyclobutyl)-4-(4-(benzyloxycarbonylamino)butanamido)butanoate, <b>23</b> .....                                  | 209 |
| (1' <i>R</i> ,3' <i>R</i> )-3-(( <i>S</i> )-15,15-Dimethyl-3,8,13-trioxo-1-phenyl-2,14-dioxa-4,9 diazahexadecan-11-yl)-2',2'-dimethylcyclobutanecarboxylic acid, <b>24</b> .....          | 211 |
| <i>tert</i> -butyl 4-(4-(benzyloxycarbonylamino)butanamido)-3-((1' <i>R</i> ,3' <i>R</i> )-3'-(4-methoxy-4-oxobutylcarbamoyl)-2',2'-dimethylcyclobutyl)butanoate, <b>25</b> .....         | 212 |
| 4-(4-(benzyloxycarbonylamino)butanamido)-3-((1' <i>R</i> ,3' <i>R</i> )-3'-(4-methoxy-4-oxobutylcarbamoyl)-2',2'-dimethylcyclobutyl)butanoic acid, <b>27</b> .....                        | 214 |
| 4- <i>tert</i> -Butoxycarbonylaminobutyric acid, <b>I</b> .....   | 215 |
| <i>tert</i> -Butyl (4-azido-4-oxobutyl)carbamate, <b>II</b> .....   | 216 |
| <i>tert</i> -Butyl (3-aminopropyl)carbamate, <b>III</b> .....   | 217 |
| Benzene-1,3,5-tricarbonyl azide, <b>30</b> .....  | 218 |
| Benzene-1,3,5-triamine, <b>33</b> .....   | 219 |
| C-Centered triamide <b>34</b> .....   | 220 |
| C-Centered triamide <b>35</b> .....   | 222 |
| Triurea <b>36</b> .....   | 223 |
| N-Centered triamide <b>37</b> .....   | 225 |
| (1 <i>R</i> ,3 <i>R</i> )-Methyl 3-(( <i>S</i> )-1-amino-4- <i>tert</i> -butoxy-4-oxobutan-2-yl)-2,2'-dimethylcyclobutanecarboxylate, <b>38</b> .....                                     | 226 |
| <i>tert</i> -Butyl 4-(( <i>S</i> )-4-(4-aminobutanamido)-3-((1' <i>R</i> ,3' <i>R</i> )-3'-(4-methoxy-4-oxobutylcarbamoyl)-2',2'-dimethylcyclobutyl)butanamido)butanoate, <b>39</b> ..... | 227 |
| Triurea <b>40</b> .....   | 228 |
| N-Centered triamide <b>41</b> .....   | 230 |
| C-Centered triamide <b>42</b> .....   | 232 |
| C-Centered triamide <b>43</b> .....   | 234 |
| (1 <i>S</i> ,3 <i>R</i> )-3-Acetyl-2,2-dimethylcyclobutanecarbonyl azide, <b>44</b> .....   | 235 |
| (1 <i>S</i> ,3 <i>R</i> )- Benzyl-3-acetyl-2,2-dimethylcyclobutylcarbamate, <b>45</b> .....   | 236 |
| (1 <i>R</i> ,3 <i>S</i> )-3-(Benzyloxycarbonylamino)-2,2-dimethylcyclobutanecarboxylic acid, <b>(-)-46</b> .....  | 237 |
| Diazomethane distillation from Diazald® .....   | 238 |
| (1 <i>R</i> ,3 <i>S</i> )-Methyl-3-(benzyloxycarbonylamino)-2,2-dimethylcyclobutanecarboxylate, <b>(-)-47</b> .....   | 239 |
| (1 <i>S</i> ,3 <i>R</i> )- <i>tert</i> -Butyl-3-acetyl-2,2-dimethylcyclobutane-1-carboxylate, <b>48</b> .....   | 241 |
| (1 <i>R</i> ,3 <i>S</i> )-3- <i>tert</i> -Butoxycarbonyl-2,2-dimethylcyclobutane-1-carboxylic acid, <b>49</b> .....   | 241 |
| (1 <i>S</i> ,3 <i>R</i> )- <i>tert</i> -Butyl 3-(azidocarbonyl)-2,2-dimethylcyclobutanecarboxylate, <b>50</b> .....   | 242 |
| (1 <i>R</i> ,3 <i>S</i> )- <i>tert</i> -Butyl-3-(benzyloxycarbonylamino)-2,2-dimethylcyclobutane carboxylate, <b>51</b> .....   | 243 |
| (1 <i>S</i> ,3 <i>R</i> )-3-benzyloxycarbonylamino-2,2-dimethylcyclobutanecarboxylic acid, <b>(+)-46</b> .....  | 244 |



|   |     |
|---|-----|
| (1 <i>S</i> ,3 <i>R</i> )-Methyl-3-(benzyloxycarbonylamino)-2,2-dimethylcyclobutane- carboxylate, <b>(+)-47</b> ...   | 245 |
| (2 <i>S</i> ,4 <i>S</i> )-4-(benzyloxycarbonylamino)-1-( <i>tert</i> -butoxycarbonyl)pyrrolidine-2-carboxylic acid, <b>54</b><br>.....  | 247 |
| (2 <i>S</i> ,4 <i>S</i> )-1- <i>tert</i> -Butyl 2-methyl 4-(benzyloxycarbonylamino)pyrrolidine-1,2-dicarboxylate, <b>55</b> ...   | 248 |
| (1 <i>S</i> ,3 <i>R</i> )-Methyl 3-amino-2,2-dimethylcyclobutanecarboxylate, <b>(+)-56</b> .....  | 249 |
| $\gamma$ -Dipeptide <b>57</b> .....   | 250 |
| $\gamma$ -Dipeptide <b>58</b> .....   | 252 |
| $\gamma$ -Dipeptide <b>59</b> .....   | 253 |
| $\gamma$ -Tetrapeptide <b>60</b> .....  | 254 |
| $\gamma$ -Tetrapeptide <b>61</b> .....  | 256 |
| $\gamma$ -Hexapeptide <b>62</b> .....   | 256 |
| (1 <i>R</i> ,3 <i>S</i> )-methyl 3-amino-2,2-dimethylcyclobutanecarboxylate, <b>(-)-56</b> .....  | 257 |
| $\gamma$ -Dipeptide <b>63</b> .....   | 258 |
| $\gamma$ -Dipeptide <b>64</b> .....   | 260 |
| $\gamma$ -Dipeptide <b>65</b> .....   | 261 |
| $\gamma$ -Tetrapeptide <b>66</b> .....  | 262 |
| $\gamma$ -Tetrapeptide <b>67</b> .....  | 264 |
| $\gamma$ -Hexapeptide <b>68</b> .....   | 265 |
| (1 <i>R</i> ,5 <i>S</i> )-3-Oxabicyclo[3.2.0]heptane-2,4-dione <b>IV</b> .....  | 266 |
| (1 <i>R</i> ,2 <i>S</i> )-Dimethyl-cyclobutane-1,2-dicarboxylate , <b>V</b> .....   | 267 |
| (1 <i>S</i> ,2 <i>R</i> )-2-(Methoxycarbonyl)cyclobutane carboxylic acid <b>VI</b> .....  | 268 |
| (1 <i>R</i> ,2 <i>S</i> )-Methyl 2-(azidocarbonyl)cyclobutane carboxylate, <b>VII</b> .....   | 269 |
| (1 <i>R</i> ,2 <i>S</i> )-Methyl 2-(benzyloxycarbonylamino)cyclobutane carboxylate, <b>VIII</b> .....   | 270 |
| (1 <i>R</i> ,2 <i>S</i> )-Methyl 2-( <i>tert</i> -butoxycarbonylamino)cyclobutane carboxylate, <b>69</b> .....  | 271 |
| (1 <i>R</i> ,2 <i>S</i> )-2-( <i>tert</i> -butoxycarbonylamino)cyclobutanecarboxylic acid, <b>70</b> .....  | 272 |
| (1 <i>R</i> ,2 <i>S</i> )-Benzyl 2-( <i>tert</i> -butoxycarbonylamino)cyclobutanecarboxylate, <b>71</b> .....   | 273 |
| (1 <i>R</i> ,2 <i>S</i> )-Benzyl 2-(2-((9 <i>H</i> -fluoren-9-yl)methoxycarbonylamino)-5-(3-((2,2,5,7,8-<br>pentamethylchroman-6-yl)sulfonyl)guanidino)pentanamido)cyclobutane carboxylate, <b>72</b> ..... | 274 |
| (1 <i>R</i> ,2 <i>S</i> )-2-(2-((9 <i>H</i> -Fluoren-9-yl)methoxycarbonylamino)-5-(3-((2,2,5,7,8-pentamethylchroman-6-<br>yl)sulfonyl)guanidino)pentanamido)cyclobutane carboxylic acid, <b>73</b> .....    | 276 |
| (1 <i>R</i> ,3 <i>S</i> )-3-Amino-2,2-dimethylcyclobutanecarboxylic acid, <b>74</b> .....   | 277 |
| (1 <i>R</i> ,3 <i>S</i> )-3-((9 <i>H</i> -Fluoren-9-yl)methoxycarbonylamino)-2,2-dimethylcyclobutane carboxylic acid, <b>75</b><br>.....  | 278 |
| NPY Analogue <b>76</b> .....  | 283 |

## Table of Contents

|   |     |
|---|-----|
| NPY Analogue <b>76a</b> .....   | 283 |
| NPY Analogue <b>77</b> .....  | 284 |
| NPY Analogue <b>77a</b> .....   | 284 |
| NPY Analogue <b>77b</b> .....   | 285 |
| NPY Analogue <b>78</b> .....  | 286 |
| NPY Analogue <b>78a</b> .....   | 286 |
| NPY Analogue <b>79</b> .....  | 287 |
| NPY Analogue <b>79a</b> .....   | 287 |
| Elongated NPY analogue <b>80</b> .....  | 288 |
| Elongated NPY analogue <b>81</b> .....  | 289 |
| Elongated NPY analogue <b>81a</b> .....   | 289 |
| HPP Analogue <b>82</b> .....  | 290 |
| HPP Analogue <b>82a</b> .....   | 290 |
| HPP Analogue <b>83a</b> .....   | 291 |
| HPP Analogue <b>83b</b> .....   | 292 |
| Modified HPP analogue <b>84</b> .....   | 292 |
| Elongated HPP analogue <b>85</b> .....  | 293 |
| Elongated HPP analogue <b>85a</b> .....   | 293 |
| ( <i>S</i> )-4-(Benzyloxycarbonylamino)-3-((1 <i>R</i> ,3 <i>R</i> )-3-methoxycarbonyl-2,2-dimethylcyclobutyl) butanoic acid, <b>86</b> .....                                   | 294 |
| (1 <i>R</i> ,3 <i>R</i> )-Methyl 3-(( <i>S</i> )-4-azido-1-(benzyloxycarbonylamino)-4-oxobutan-2-yl)-2,2-dimethylcyclobutane carboxylate, <b>87</b> .....                       | 295 |
| (1 <i>R</i> ,3 <i>R</i> )-Methyl 3-(3,9-dioxo-1,11-diphenyl-2,10-dioxa-4,8-diazaundecan-6-yl)-2,2-dimethylcyclobutane carboxylate, <b>88</b> .....                              | 296 |
| (1 <i>R</i> ,3 <i>R</i> )-3-(3,9-Dioxo-1,11-diphenyl-2,10-dioxa-4,8-diazaundecan-6-yl)-2,2-dimethylcyclobutane carboxylic acid, <b>90</b> .....                                 | 298 |
| Dibenzyl (2-((1 <i>R</i> ,3 <i>R</i> )-3-(azidocarbonyl)-2,2-dimethylcyclobutyl)propane-1,3-diyl)dicarbamate, <b>91</b> .....   | 299 |
| Cyclobutane triamine, <b>92</b> .....   | 300 |
| ( <i>S</i> )- <i>tert</i> -Butyl 4-((dibenzoyloxycarbonylamino)-3-((1 <i>R</i> ,3 <i>R</i> )-2,2-dimethyl-3-(2-methyl-1,3-dioxolan-2-yl)cyclobutyl)butanoate, <b>93</b> .....   | 301 |
| ( <i>S</i> )-benzyl 4-((1 <i>R</i> ,3 <i>R</i> )-3-acetyl-2,2-dimethylcyclobutyl)-2-oxopyrrolidine-1-carboxylate, <b>94</b> : ....  | 303 |
| ( <i>S</i> )- <i>tert</i> -Butyl 4-(benzyloxycarbonylmethylamino)-3-((1 <i>R</i> ,3 <i>R</i> )-2,2-dimethyl-3-(2-methyl-1,3-dioxolan-2-yl)cyclobutyl)butanoate, <b>95</b> ..... | 304 |
| 4-((1 <i>R</i> ,3 <i>R</i> )-2,2-Dimethyl-3-(2-methyl-1,3-dioxolan-2-yl)cyclobutyl)-1-methylpyrrolidin-2-one, <b>97</b> .....   | 306 |

|  |     |
|--|-----|
| ( <i>S</i> )- <i>tert</i> -Butyl 3-((1 <i>R</i> ,3 <i>R</i> )-2,2-dimethyl-3-(2-methyl-1,3-dioxolan-2-yl)cyclobutyl)-4-( <i>N</i> -methylsulfonyl)methylsulfonamido)butanoate, <b>98</b> .....   | 307 |
| ( <i>S</i> )- <i>tert</i> -Butyl 4-(di( <i>tert</i> -butoxycarbonyl)amino)-3-((1 <i>R</i> ,3 <i>R</i> )-2,2-dimethyl-3-(2-methyl-1,3-dioxolan-2-yl)cyclobutyl)butanoate, <b>99</b> .....   | 307 |
| (1 <i>R</i> ,3 <i>R</i> )-Methyl 3-(( <i>S</i> )-14,14-dimethyl-3,8-dioxo-1-phenyl-2,9,11-trioxa-4-aza-14-silapentadecan-6-yl)-2,2-dimethylcyclobutanecarboxylate, <b>100</b> .....  | 308 |
| (1 <i>R</i> ,3 <i>R</i> )-Methyl 2,2-dimethyl-3-(( <i>S</i> )-2,2,15,15-tetramethyl-8,13-dioxo-5,7,14-trioxa-12-aza-2-silahexadecan-10-yl)cyclobutane carboxylate, <b>101</b> .....  | 309 |
| ( <i>S</i> )- <i>tert</i> -Butyl 4-((1 <i>R</i> ,3 <i>R</i> )-3-(methoxycarbonyl)-2,2-dimethylcyclobutyl)-2-oxopyrrolidine-1-carboxylate, <b>102</b> .....   | 310 |
| (1 <i>R</i> ,3 <i>R</i> )-Methyl 3-(( <i>S</i> )-1-(benzyloxycarbonyl(methyl)amino)-4-( <i>tert</i> -butoxy)-4-oxobutan-2-yl)-2,2-dimethylcyclobutanecarboxylate, <b>103</b> .....   | 311 |
| ( <i>S</i> )-4-(Benzyloxycarbonyl(methyl)amino)-3-((1 <i>R</i> ,3 <i>R</i> )-3-(methoxycarbonyl)-2,2-dimethylcyclobutyl)butanoic acid, <b>104</b> .....  | 312 |
| (1 <i>R</i> ,3 <i>R</i> )-methyl 3-(( <i>S</i> )-4-azido-1-(benzyloxycarbonyl(methyl)amino)-4-oxobutan-2-yl)-2,2-dimethylcyclobutanecarboxylate, <b>105</b> .....  | 313 |
| (1 <i>R</i> ,3 <i>R</i> )-Methyl 2,2-dimethyl-3-(( <i>R</i> )-4-methyl-3,9-dioxo-1,11-diphenyl-2,10-dioxa-4,8-diazaundecan-6-yl)cyclobutanecarboxylate, <b>106</b> .....   | 314 |
| (1 <i>R</i> ,3 <i>R</i> )-2,2-Dimethyl-3-(( <i>R</i> )-4-methyl-3,9-dioxo-1,11-diphenyl-2,10-dioxa-4,8-diazaundecan-6-yl)cyclobutanecarboxylic acid, <b>107</b> .....  | 315 |
| Benzyl (( <i>R</i> )-2-((1 <i>R</i> ,3 <i>R</i> )-3-(azidocarbonyl)-2,2-dimethylcyclobutyl)-3-((benzyloxycarbonylamino)propyl)(methyl)carbamate, <b>108</b> .....  | 315 |
| <i>N</i> -methyl cyclobutane triamine, <b>109</b> .....  | 316 |
| (1 <i>S</i> ,3 <i>R</i> )-Methyl 3-( <i>tert</i> -butoxycarbonylamino)-2,2-dimethylcyclobutane carboxylate, <b>110</b> .....   | 317 |
| <i>tert</i> -Butyl ((1 <i>R</i> ,3 <i>S</i> )-3-(hydroxymethyl)-2,2-dimethylcyclobutyl)carbamate, <b>111</b> .....   | 318 |
| <i>tert</i> -Butyl ((1 <i>R</i> ,3 <i>S</i> )-3-formyl-2,2-dimethylcyclobutyl)carbamate, <b>112</b> .....  | 319 |
| ((1 <i>R</i> ,3 <i>S</i> )-3-(1-hydroxy-2-nitroethyl)-2,2-dimethylcyclobutyl)carbamate, <b>113+114</b> .....   | 320 |
| <i>tert</i> -Butyl ((1 <i>R</i> ,3 <i>R</i> )-2,2-dimethyl-3-(2-nitrovinyl)cyclobutyl)carbamate, <b>115+116</b> .....  | 320 |
| <i>tert</i> -Butyl ((1 <i>R</i> ,3 <i>R</i> )-3-(1,3-dinitropropan-2-yl)-2,2-dimethylcyclobutyl)carbamate, <b>117</b> .....  | 321 |
| <i>tert</i> -Butyl ((1 <i>R</i> ,3 <i>R</i> )-3-(1,3-diaminopropan-2-yl)-2,2-dimethylcyclobutyl)carbamate, <b>118</b> .....  | 322 |
| (1 <i>R</i> ,2 <i>S</i> )-Methyl 2-(((benzyloxycarbonylamino)cyclobutanecarboxylate, <b>92</b> .....   | 323 |
| Dibenzyl (2-((1 <i>R</i> ,3 <i>R</i> )-3-amino-2,2-dimethylcyclobutyl)propane-1,3-diyl)dicarbamate, <b>119</b> .....   | 324 |
| Benzyl (( <i>R</i> )-2-((1 <i>R</i> ,3 <i>R</i> )-3-amino-2,2-dimethylcyclobutyl)-3-((benzyloxycarbonylamino)propyl)(methyl)carbamate, <b>120</b> .....  | 325 |
| Tri- <i>tert</i> -butyl 2,2',2''-(10-(2-(((1 <i>R</i> ,3 <i>R</i> )-3-(3,9-dioxo-1,11-diphenyl-2,10-dioxa-4,8-diazaundecan-6-yl)-2,2-dimethylcyclobutyl)amino)-2-oxoethyl)-1,4,7,10-tetraazacyclododecane-1,4,7-triyl)triacetate, <b>121</b> ..... | 327 |

|  |     |
|--|-----|
| Tri- <i>tert</i> -butyl 2,2',2''-(10-(2-(((1 <i>R</i> ,3 <i>R</i> )-2,2-dimethyl-3-(( <i>R</i> )-4-methyl-3,9-dioxo-1,11-diphenyl-2,10-dioxa-4,8-diazaundecan-6-yl)cyclobutyl)amino)-2-oxoethyl)-1,4,7,10-tetraazacyclododecane-1,4,7-triyl)triacetate, <b>122</b> ..... | 328 |
| 2,2',2''-(10-(2-(((1 <i>R</i> ,3 <i>R</i> )-3-(3,9-dioxo-1,11-diphenyl-2,10-dioxa-4,8-diazaundecan-6-yl)-2,2-dimethylcyclobutyl)amino)-2-oxoethyl)-1,4,7,10-tetraazacyclododecane-1,4,7-triyl)triacetic acid, <b>123</b> .....   | 329 |
| 2,2',2''-(10-(2-(((1 <i>R</i> ,3 <i>R</i> )-2,2-Dimethyl-3-(( <i>R</i> )-4-methyl-3,9-dioxo-1,11-diphenyl-2,10-dioxa-4,8-diazaundecan-6-yl)cyclobutyl)amino)-2-oxoethyl)-1,4,7,10-tetraazacyclododecane-1,4,7-triyl)triacetic acid, <b>124</b> .....                     | 329 |
| <b>8. ANNEX I: COUPLING REAGENTS</b> .....   | 333 |
| <b>9. ANNEX II: NMR STUDIES OF CYCLOBUTANE-CORED DENDRIMERS</b> .....  | 341 |
| <b>10. ANNEX III: DETAILED NMR STUDIES ON HYBRID CYCLOBUTANE-PROLINE <math>\gamma,\gamma</math>-PEPTIDES</b> .....   | 349 |
| Compound 55 .....  | 349 |
| Dipeptide 63 .....   | 360 |
| Tetrapeptide 66 .....  | 369 |
| Hexapeptide 68 .....   | 376 |
| Dipeptide 57 .....   | 378 |
| Tetrapeptide 60 .....  | 385 |
| Hexapeptide 62 .....   | 390 |
| <b>11. ANNEX IV: COMPUTATIONAL METHODS FOR CYCLOBUTANE-PROLINE <math>\gamma,\gamma</math>-PEPTIDES MODELLING</b> .....   | 395 |
| Tetrapeptides 60 and 66 results .....  | 395 |
| Hexapeptides 62 and 68 results .....   | 398 |
| <b>12. ANNEX V: BIOLOGICAL ASSAYS OF CPPs</b> .....  | 403 |
| MTT cytotoxicity assay .....   | 403 |
| Flow cytometry .....   | 403 |
| <b>13. ANNEX VI: BIOLOGICAL ASSAYS OF NPY ANALOGUES</b> .....  | 407 |
| 13.1 Assay Protocols .....   | 407 |
| 13.1.1 Binding studies: Flow cytometric binding studies .....  | 407 |
| 13.1.2 Functional Studies: GTPase assay .....  | 408 |
| <b>14. BIBLIOGRAPHY</b> .....  | 415 |

## **Introduction**



## 1. GENERAL INTRODUCTION

The present doctoral thesis has been developed in the context of the Synthesis, Structure and Chemical Reactivity research group. Taking advantage of the broad experience of this group in the synthesis of highly constrained cyclobutane amino acids and their inclusion into peptides, a series of new compounds with potential very interesting applications have been prepared:

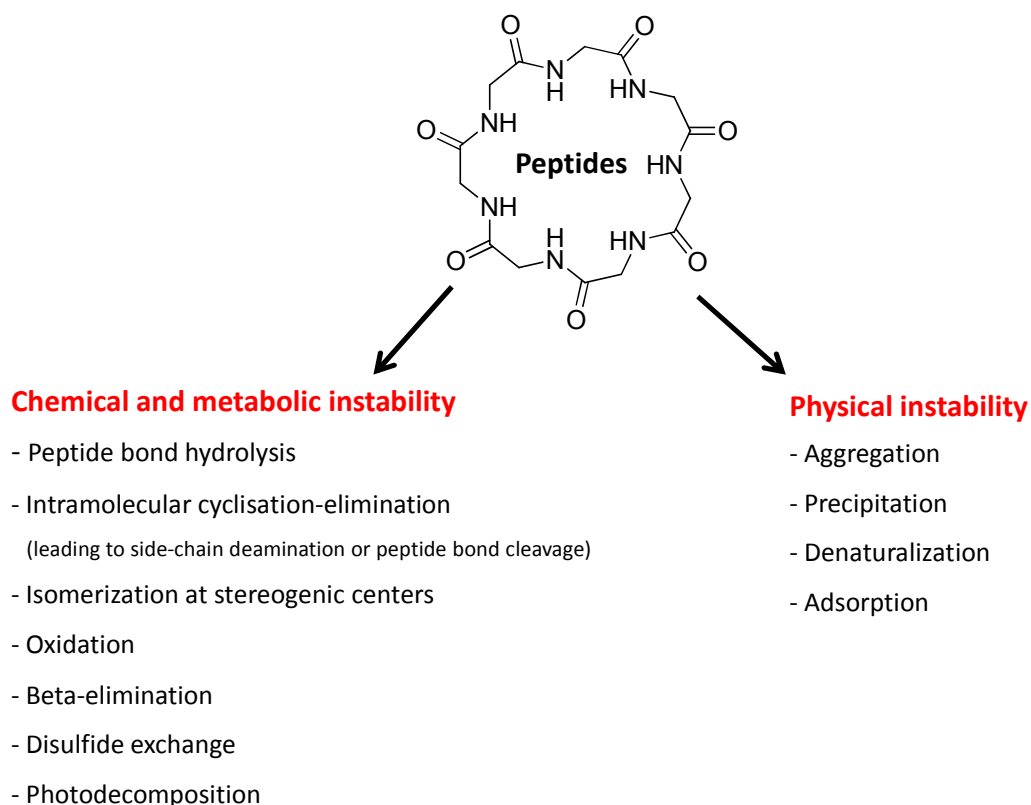
- Cyclobutane ring has been both used as core and dendron for the synthesis of a first generation family of chiral peptide dendrimers.
- The capability of the four-membered ring to induce defined secondary structures has been exploited in the preparation of hybrid cyclobutane-proline  $\gamma,\gamma$ -peptides which were suitable for their evaluation as Cell Penetrating Peptides (CPPs).
- In an analogous way, a series of cyclobutane-containing NPY analogues have been synthesised. It is expected that the intrinsic ability of the cyclobutane ring to induce defined folding will be useful to mimic NPY bioactive conformation.
- Furthermore, the possibility of preparing multivalent cyclobutane compounds encouraged us to design new chiral polyfunctional cyclobutane platforms which could lead to a new class of Magnetic Resonance Imaging (MRI) contrast agents (CAs).

### 1.1. USE OF PEPTIDES AS DRUGS

It is broadly known that amino acids, peptides and proteins are involved in nearly all physiological processes at some level. Up to the moment a great number of examples of how natural and unnatural amino acids and peptides contribute to regulate basic cell functions and metabolic processes involved in communication between neurons, among others, have been found. Due to that, peptide therapeutics has become once again the focus of innovative drug development reinforced by venture funds and biotechnology companies

that have re-energised this field. They are considered as viable alternatives to small molecule therapeutics, thanks to their high specificity and low toxicity profile. The historically used peptide vaccines against viral infections and antibacterial peptides led the way in clinical development, but recently many other diseases have been targeted, including the big sellers for AIDS, cancer, and Alzheimer's disease.<sup>1</sup>

Nevertheless, clinical applications of peptide-based drug are limited by several major considerations, which arise from peptide nature (**Scheme 1**).



**Scheme 1:** Chemical, metabolic and physical processes of instability in pharmaceutical peptides.

Apart from those physico-chemical instabilities, amino acids and peptides offer the ability to extensively explore conformational space. As a result from this richness they suffer from two important drawbacks for their use as drugs:



- **Conformational flexibility:** It allows the peptide to bind to more than one receptor or receptor subtype leading to undesirable side effects.
- **Poor absorption and transportation** because of their high molecular mass or the lack of specific delivery systems, especially for some peptides which require the passage through the blood-brain-barrier (BBB) to act in the central nervous system (CNS).<sup>2</sup>

With the aim of counteracting these problems, peptidomimetic drug design has emerged as an important tool for both *peptide chemists* and medicinal chemists. As a result, an interdisciplinary scientific endeavour has appeared, which combines organic chemistry, biochemistry and pharmacology.

From the one hand organic chemists have designed a variety of molecules which are capable of mimicking the secondary structures of peptides, such as  $\alpha$ -helices,  $\beta$ -turns, and  $\beta$ -sheets. Additionally, a number of strategies, which allow to explore structure-activity relationships of bioactive peptides, have been developed by incorporation of conformationally constrained amino acids, modification of the peptide backbone by amide bond isosteres, cyclizations, attachment of pharmacophores to a template or scaffold, and the synthesis of non-peptide analogues. With that, the advantage of peptidomimetics over the native peptides has been demonstrated by increasing the potency and selectivity, decreasing the side effects and by improving oral bioavailability and the half-life of the activity through minimizing enzymatic degradation.<sup>3</sup>

## **1.2. PEPTIDE STRUCTURE OF NON PROTEINOGENIC AMINO ACIDS AND PEPTIDES**

The imitation and improvement of structural features of peptides and proteins has always been a great challenge for chemists and biochemists. As it has been mentioned before, the application of native peptides for pharmacological and pharmaceutical purposes often suffers from their insufficient resistance to proteases and their unfavourable transport

properties. During many years scientists have tried to overcome this hindrance by substituting one or several natural amino acids in the sequence for non-proteinogenic amino acids. Nevertheless, in the last years, the consistent extension of this idea led to the search of oligomers that are composed only of non-proteinogenic amino acids.<sup>4, 5</sup> As previously mentioned, natural proteins function is essentially determined by characteristic secondary-structure elements such as helices, sheets and turns. Due to that, it is a requirement for the modified compounds to reflect the steric and electronic properties of their native counterparts in order to keep, or even to improve, their biological activity. Therefore, such oligomers should be able to adopt definite backbone conformations.<sup>6</sup>

All polypeptides can adopt a random coil structure, which is a flexible polymer conformation where the monomer subunits are oriented randomly while still being bonded to adjacent units (denatured state of the protein) at elevated temperature, in the presence of disruptive solvents or by pH changes. Due to the fact that the protein does not present an ordered arrangement, denatured protein is non-functional. This certainly highlights the enormous importance of the structural knowledge of amino acids, peptides and proteins. Through the study of secondary structure of proteins the components that make up a whole protein can be understood. Seizing the structure of the whole protein is often vital to understanding its function and the knowledge derived from these studies can be used to explore the mechanisms of enzymes, and to create inhibitory drugs to fight disease.

As designated by Gellman, those oligomers built from chemical monomer units with a strong tendency to adopt a specific conformation are known as foldamers. Owing to the wide variety of chemical monomer units, foldamers with specific properties could be expected, and these are interesting in other fields as, for instance, in material sciences.<sup>6</sup>

### 1.3. AMINO ACIDS CONTAINING A CYCLOBUTANE MOIETY

#### 1.3.1 Natural amino acids containing a cyclobutane moiety

Organic compounds containing four-membered rings in their structure belong to a unique group of compounds that includes both natural and synthetic products. Cyclobutane ring is found as an important structural moiety in a broad number of natural-occurring compounds produced by bacteria, fungi, plants and marine invertebrates, as well as in biosynthetic intermediates generated in primary and secondary metabolism in vertebrates.<sup>7</sup> It is worth pointing out that those compounds show many biological activities and may serve as potential drug leads or provide new ideas for the study of enzyme mechanisms and/or organic synthesis.<sup>8</sup>

Even though cyclobutane-containing compounds have been known for more than a century, their use in synthetic chemistry has only thrived on the last 30 years. The existence of cyclobutane ring in nature was not demonstrated until 1980, when Bell and co-workers<sup>9</sup> isolated 2,4-methanoglutamic acid and 2,4-methanoproline from *Ateleia's Herbert smithii* (Sophoreae, Leguminosae) seeds. Soon after, in 1987, Austin and co-workers<sup>10</sup> isolated a third non-proteinogenic amino acid: *cis*-1-amino-3-hydroxymethylcyclobutan-1-carboxylic acid (**Figure 1**). From that point on, many other cyclobutane amino acids and peptides have been isolated from natural sources. Some of those have displayed activities as antiviral or antimicrobial agents, neurotropics and analgesics.<sup>11, 12, 13</sup>

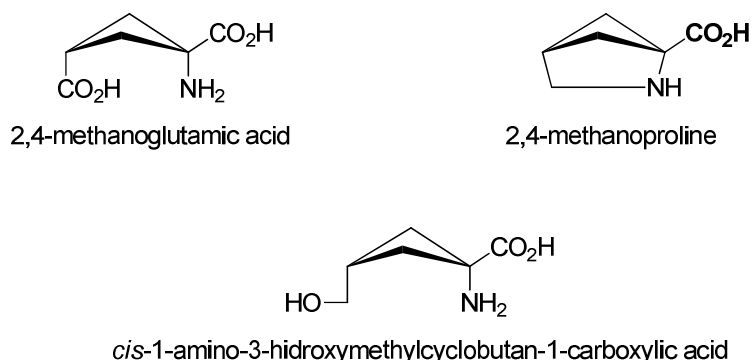


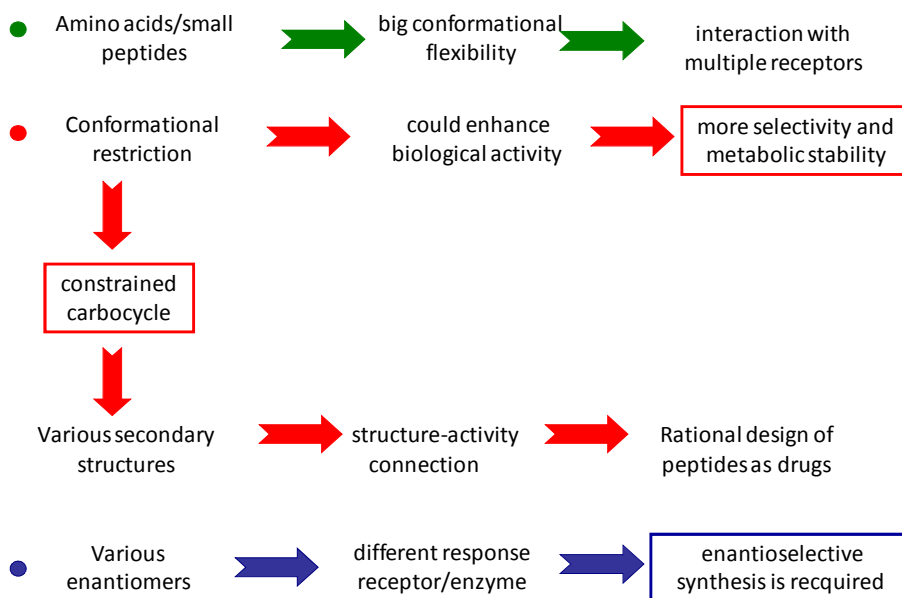
**Figure 1:** Natural amino acids isolated from seeds of *Ateleia herbert smithii*.

### 1.3.2 Synthetic amino acids and peptides containing a cyclobutane moiety

In the last years the syntheses of cyclobutanoid fatty acids, amino acids, monoterpenes, sesquiterpenes, diterpenes, triterpenes and steroids, among others, have been reported.<sup>14, 15</sup>

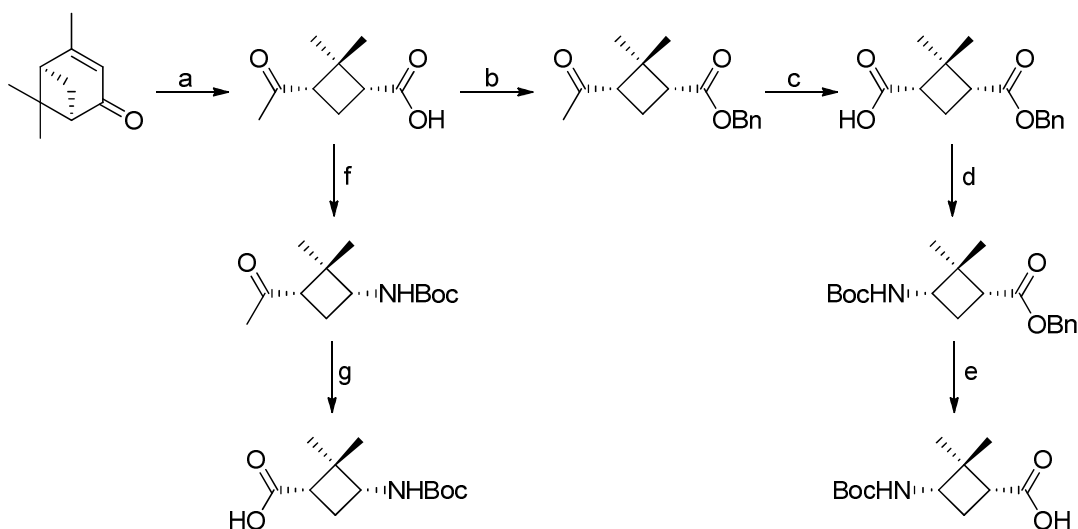
On the one hand, the biological properties showed as antiviral and antitumoral agents by cyclobutane-containing amino acids and peptides, and on the other hand, the constriction offered by the four-membered ring, have awakened the interest of chemists in this kind of compounds.

As cited before, the conformational restriction in small molecules with potential biological activity is crucial in many cases to guarantee unique interactions with the target receptor and to increase their metabolic stability and activity (**Scheme 2**). Owing to that, there are many examples in the literature on the synthesis of restricted amino acids by action of a tensioned ring. Nevertheless, there are few examples of amino acids and peptides containing a four-membered ring.



**Scheme 2**

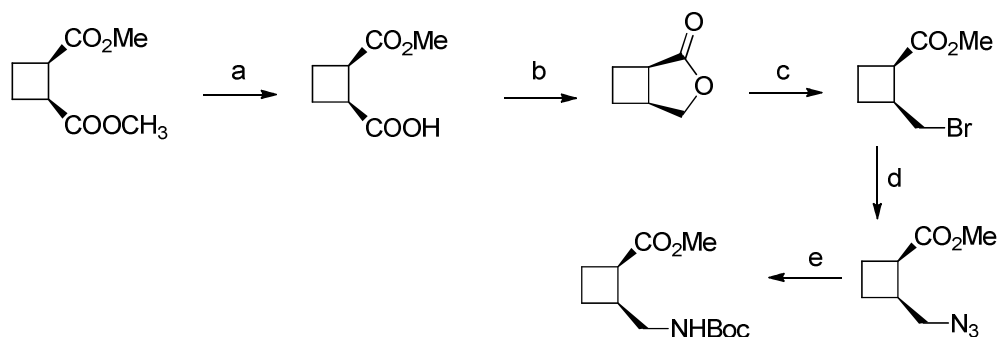
One of the first examples that are found is the synthesis of both enantiomers of optically active cyclobutane  $\gamma$ -amino acids carried out by Burgess et al.<sup>16</sup> using terpenoids from the natural chiral pool (**Scheme 3**). Starting from (+)-verbenone, oxidative cleavage of the carbon-carbon double bond, followed by concomitant loss of CO<sub>2</sub> was carried out using a catalytic amount of RuO<sub>4</sub>, to afford the corresponding cyclobutane keto-acid. This compound led to both enantiomers of optically active cyclobutane  $\gamma$ -amino acids just by modifying the order of the synthetic sequence. If the carboxylic acid is submitted to Curtius rearrangement in the presence of *tert*-butanol, followed by haloform degradation, (1*S*, 3*R*)-cyclobutane amino acid is isolated. For the synthesis of the other enantiomer steps were juxtaposed.



**Scheme 3:** a) NaIO<sub>4</sub>, RuCl<sub>3</sub>, H<sub>2</sub>O, CCl<sub>4</sub>, CH<sub>3</sub>CN, (94%); b) Benzyl chloride, (72%); c) NaOBr, dioxane, (83%); d) DPPA, <sup>t</sup>BuOH, (58%); e) H<sub>2</sub>, Pd/C, (79%); f) DPPA, <sup>t</sup>BuOH, (79 %); g) NaOBr, dioxane, (83%).

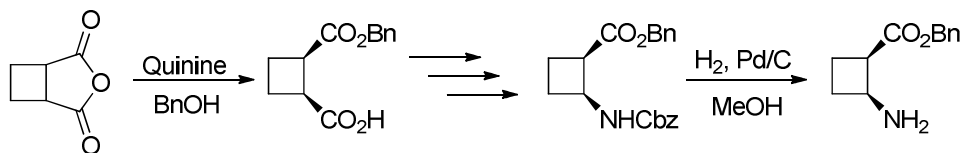
Another versatile example was developed by Ley and co-workers, who used pig liver esterase (PLE) in the desymmetrization of a *meso* diester (**Scheme 4**).<sup>17</sup> The key step of this synthetic route consists in the desymmetrisation of a *meso*-diester with polymer-supported PLE, to afford a half-ester in high yield and with very good enantiomeric excess. Afterwards, the selective reduction of the carboxylic acid using BH<sub>3</sub>.DMS was carried out, followed by treatment with polymer-supported RN<sup>+</sup>(Bn)<sub>3</sub>OH<sup>-</sup> to afford the corresponding  $\gamma$ -lactone. Next,

the  $\gamma$ -lactone was treated with thionyl bromide and subsequent addition of poly(4-vinylpyridine) was carried out to produce the analogous bromoester, which was converted into the corresponding azide using polymer-supported  $\text{RN}^+(\text{Me})_3\text{N}_3^-$ . Finally, catalytic hydrogenation in the presence of  $(\text{Boc})_2\text{O}$  gave *N*-Boc-amino ester.



**Scheme 4:** a) PLE, buffer, (98%); b) 1)  $\text{BH}_3 \cdot \text{DMS}$  2) Polymer-supported  $\text{RN}^+(\text{Bn})_3\text{OH}^-$ , (67%); c) 1)  $\text{SOBr}_2$  2) poly(4-vinylpyridine), (85%); d) Polymer-supported  $\text{RN}^+(\text{Me})_3\text{N}_3^-$ , (95%); e)  $\text{H}_2$ , Pd/C,  $(\text{Boc})_2\text{O}$ , (84%).

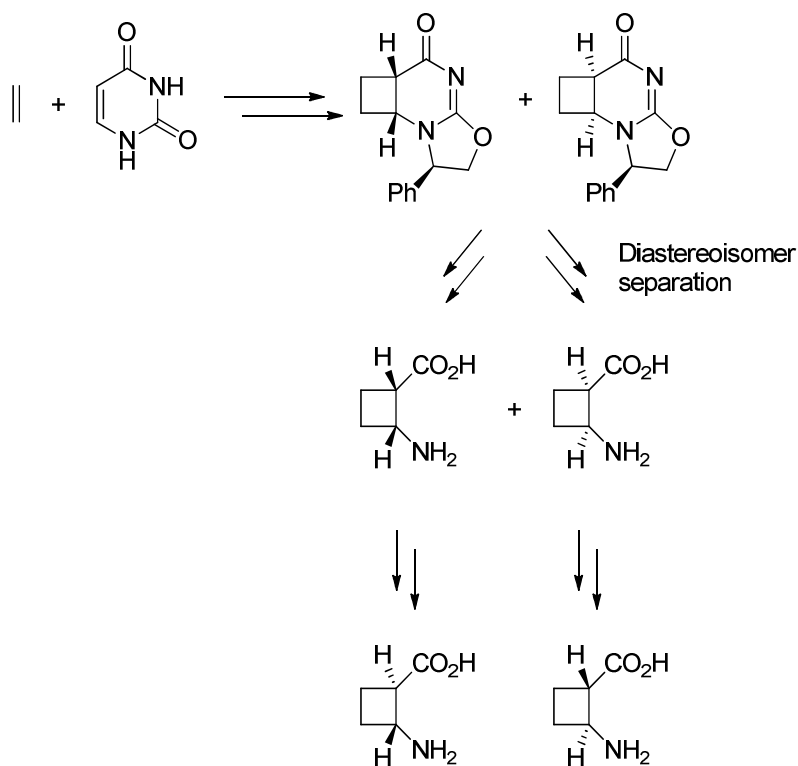
Another notable example corresponds to the synthesis of cyclobutane  $\beta$ -amino acids and other derivatives accomplished by Bolm and co-workers,<sup>18</sup> starting from the corresponding *meso* cyclic anhydride which is opened with benzyl alcohol using quinine as a chiral auxiliary (**Scheme 5**) to afford optically active *cis*-hemiester. Transformation of carboxylic acid group, in the previously mentioned compound, into an amine moiety, can be accomplished through Curtius rearrangement in the presence of benzyl alcohol.



**Scheme 5**

In turn, Aitken and co-workers<sup>19, 20</sup> synthesised the racemic form of cyclobutane  $\beta$ -amino acids through the [2+2] photochemical addition between ethylene and a chiral derivative from uracil, obtaining, after the degradation of the heterocyclic ring, the *cis*-amino acid function (**Scheme 6**). Next, the molecule was orthogonally protected and a

regioselective epimerization allowed to obtain (+) and (-)-*trans*-2-aminocyclobutan-1-carboxylic acids respectively.



Scheme 6

#### 1.4. PRECEDENTS IN THE RESEARCH GROUP IN THE SYNTHESIS OF CYCLOBUTANE AMINO ACIDS AND PEPTIDES

In the last decade, our research group has been focused in the synthesis of unnatural amino acids containing a cyclobutane ring, which have shown a high constriction capability. Some of those monomers could be used as biologically active drugs by themselves, but many others have been incorporated in peptides which could be used both in the medicinal<sup>21, 22</sup> and new materials field.<sup>23</sup> In the last case, our laboratory has accomplished the synthesis of new  $\beta$ - and  $\gamma$ -peptides containing a cyclobutane moiety in their skeleton. The presence of

the highly constricted four-membered ring in those peptides induces the formation of defined secondary structures that have been deeply studied.<sup>24-26</sup>

### 1.4.1 Synthesis of 1,2-functionalised cyclobutane derivatives

Highly effective synthetic routes leading to the four stereoisomers of cyclobutane  $\beta$ -amino acids have been set up (**Figure 2**).

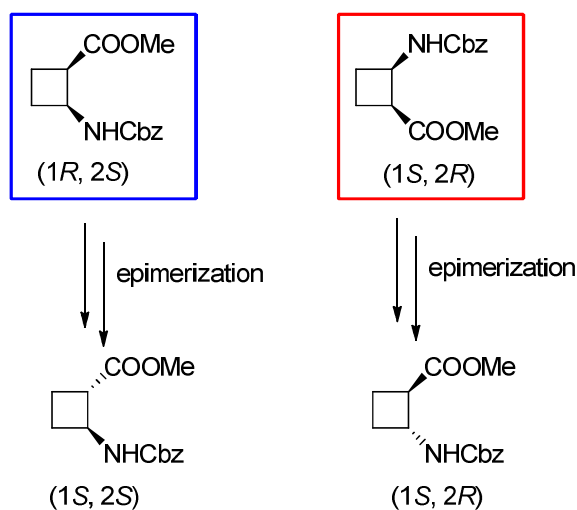
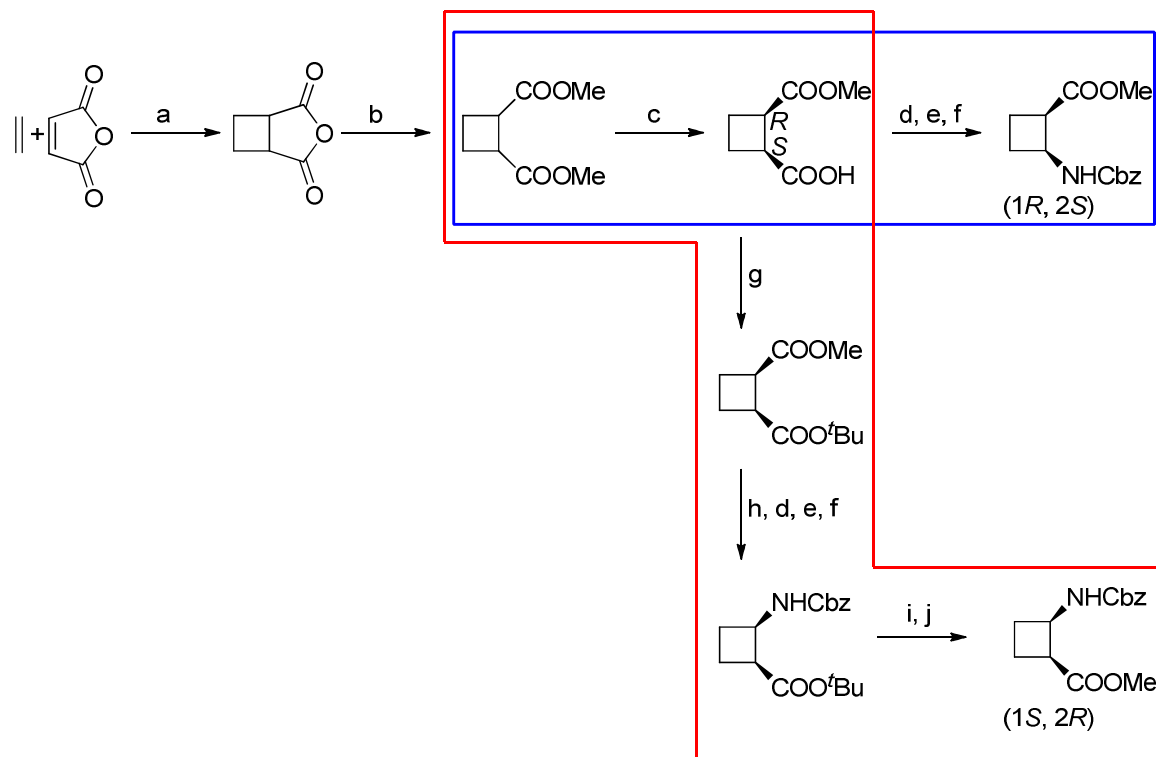


**Figure 2:** Four stereoisomers forms of  $\beta$ -cyclobutane amino acid.

In a first step, a [2+2] photochemical addition takes place between ethylene and maleic anhydride, generating in that way the four-membered ring (**Scheme 7**). Next, the anhydride is esterified under Fischer conditions to generate a *meso* cyclobutane diester. The key step of the synthetic route is the selective chemoenzymatic hydrolysis of pro-*S* ester (using PLE), thus affording the desymmetrisation of the *meso* cyclobutane diester. From the chiral cyclobutane hemiester both enantiomers of the corresponding protected amino acid can be generated only by changing the order of the synthetic sequence. Therefore, if the previously generated hemiester is activated through the formation of a mixed anhydride, the corresponding acyl azide can be obtained from reaction with sodium azide. Afterwards, the



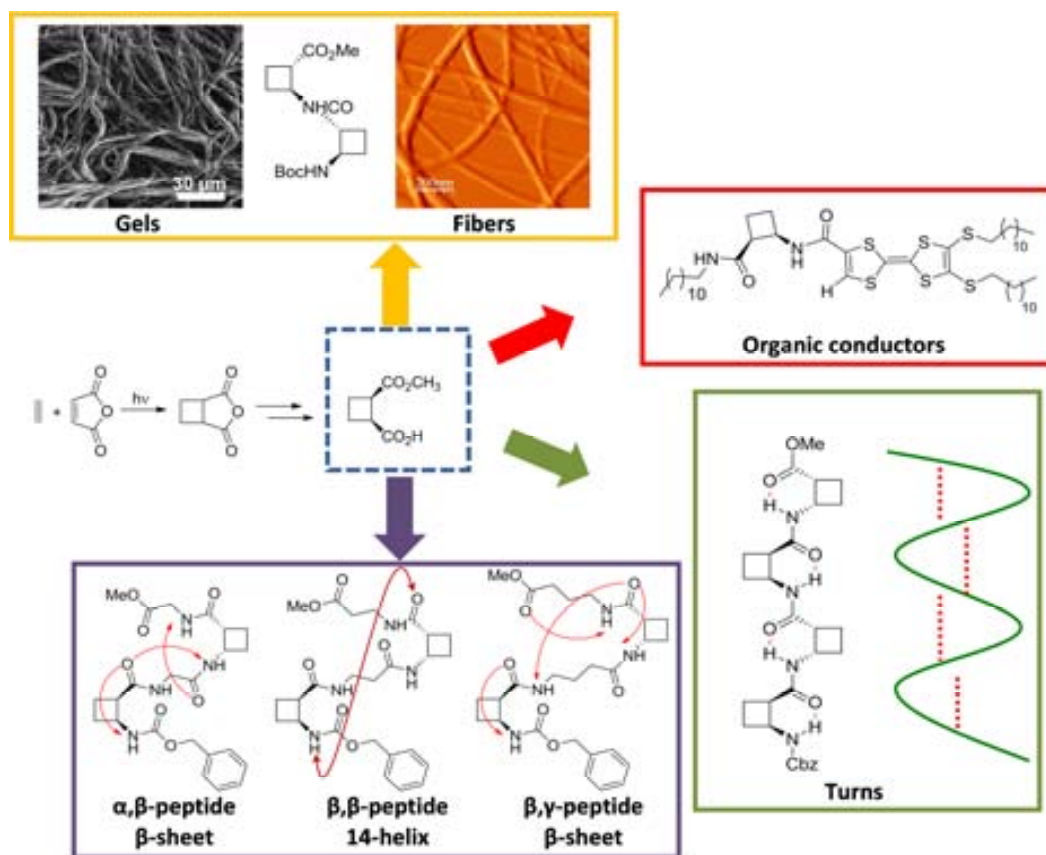
acyl azide can be submitted to Curtius rearrangement in the presence of benzyl alcohol, to isolate orthogonally protected (1*R*,2*S*)-cyclobutane  $\beta$ -amino acid.



**Scheme 7:** Synthetic route leading to both enantiomers of cyclobutane *cis*- $\beta$ -amino acids. Reagents, conditions, yields: (a) hv, acetone, quantitative; (b) H<sub>2</sub>SO<sub>4</sub>, methanol, (68%); (c) PLE, pH=7, quantitative; (d) ClCO<sub>2</sub>Et; (e) NaN<sub>3</sub>; (f) BnOH, toluene, reflux (68% for (1*R*, 2*S*), 55% for (1*S*, 2*R*), three steps); (g) Cl<sub>3</sub>CO<sup>t</sup>Bu, CH<sub>2</sub>Cl<sub>2</sub>, (74%); (h) NaOH, quantitative; (i) TFA, Et<sub>3</sub>SiH; (j) CH<sub>2</sub>N<sub>2</sub>, (98%, two steps).

On the other hand, the chiral hemiester can be esterified using *tert*-butyl trichloroacetimidate. Afterwards, the methyl ester can be saponified, and following the same procedure as for the other enantiomer the desired benzyl carbamate can be obtained. Next, there is only a need to change the protecting groups in order to obtain orthogonally protected (1*S*,2*R*)-cyclobutane  $\beta$ -amino acid.<sup>27, 28</sup>

All four stereoisomers of the cyclobutane  $\beta$ -amino acid have been incorporated in peptides, showing in most cases that the presence of the highly constricted four-membered ring induces the formation of defined secondary structures that have been deeply studied.<sup>24-28</sup> More concretely, cyclobutane  $\beta$ -peptides have shown a great ability to self-assemble into fibers and vesicles, turning to be often good organogelators (**Scheme 8**).<sup>26, 24, 29</sup> The aggregation properties of these molecules have been broadly studied with a wide range of experimental techniques and the obtained results have been nicely explained by computational studies. Moreover, recently a computational study to predict the secondary structure of peptides composed by *cis* and/or *trans*-cyclobutane amino acids has been carried out.<sup>30</sup>



**Scheme 8:** Previous studies of Ortuño's research group in the field of  $\beta$ -amino acids and  $\beta$ -peptides containing cyclobutane moieties.

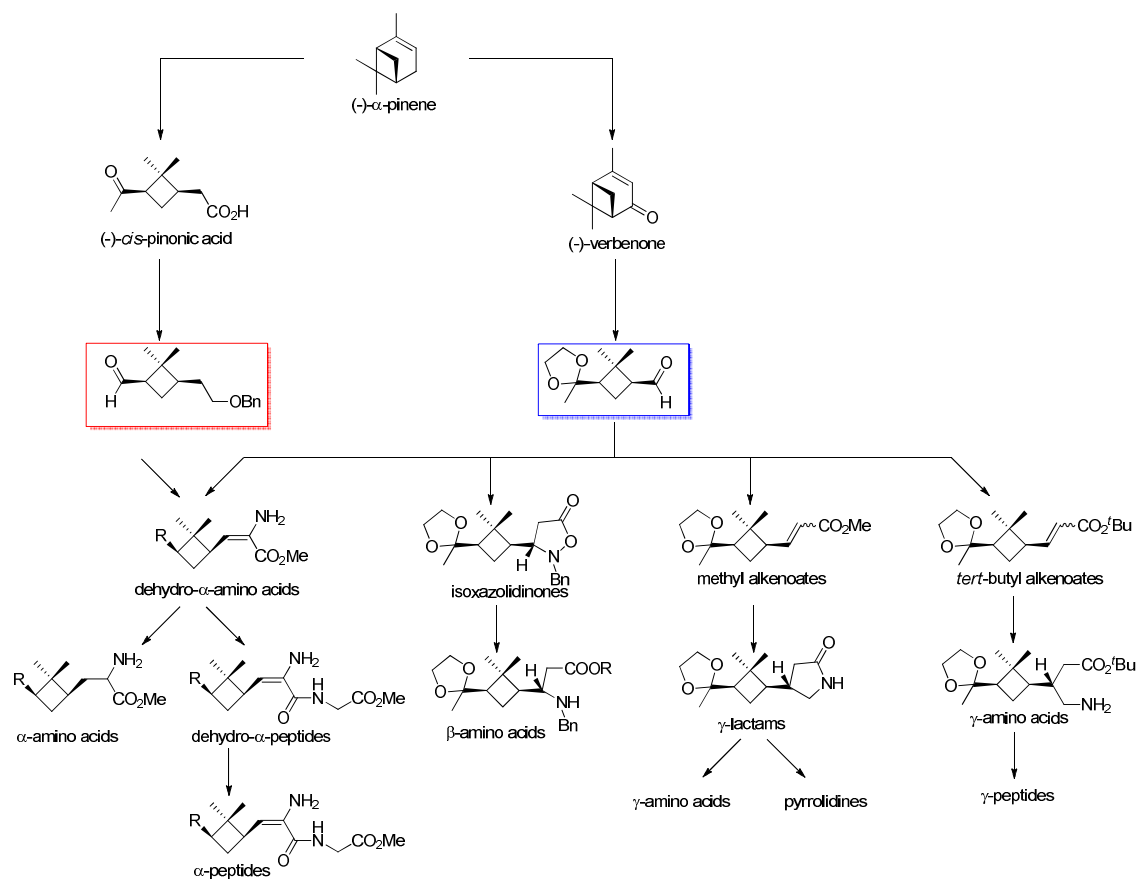
In all cases, structural studies performed for those compounds have demonstrated cyclobutane's inherent capability to promote defined secondary structures in  $\beta$ -peptides.

A series of hybrid oligomers constructed with (1*R*,2*S*)-2-aminocyclobutane-1-carboxylic acid and glycine,  $\beta$ -alanine, and  $\gamma$ -amino butyric acid (GABA), respectively, joined in alternation have been synthesised and studied by means of NMR and CD experiments as well as with computational calculations. Results account for the spacer length effect on folding and show that conformational preference for these hybrid peptides can be tuned from  $\beta$ -sheet-like folding for those containing a  $C_2$  or  $C_4$  linear segment to a helical folding for those with a  $C_3$  spacer between cyclobutane residues (**Scheme 8**).<sup>31, 32</sup>

Apart from the proved ability of these molecules to self-assemble, our research group has also pointed out some interesting physical and biological properties of these materials, such as being chiral organic conductors<sup>23</sup> and protease inhibitors.<sup>22</sup>

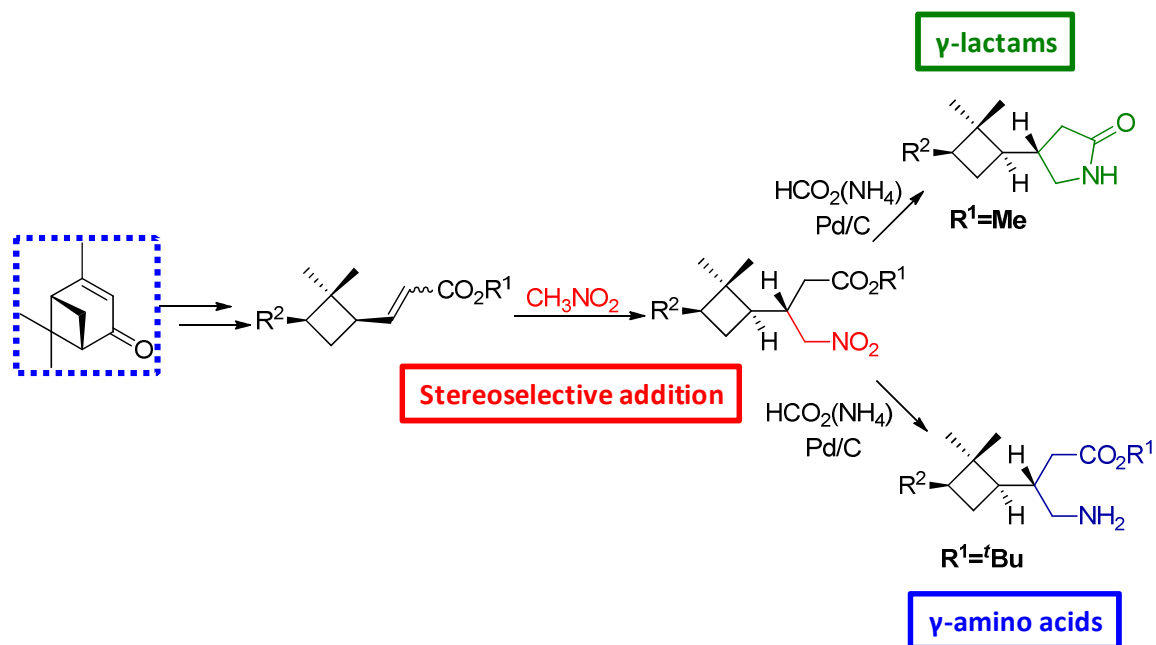
### **1.4.2 Synthesis of 1,3-functionalised cyclobutane derivatives**

Starting from natural-occurring terpenes such as (-)- $\alpha$ -pinene a series of enantiomerically pure cyclobutane-containing  $\alpha$ ,  $\beta$ ,  $\gamma$  and  $\delta$ -amino acids have been prepared. In all cases, cyclobutane aldehydes have been used as key intermediates. In **Scheme 9**, the families of synthesised products starting from (-)-verbenone and (-)-*cis*-pinonic acid are depicted. Among others,  $\alpha$ -deshydro-amino acids,  $\alpha$ -amino acids<sup>33</sup>,  $\alpha$ -peptides,<sup>34, 35, 36, 37, 38</sup> as well as  $\beta$ -amino acids,<sup>39</sup>  $\gamma$ -lactams,<sup>40</sup>  $\gamma$ -amino acids<sup>41, 42</sup> and  $\gamma$ -peptides<sup>43</sup> have been prepared.



Scheme 9

Most of these synthetic routes proceed through asymmetric 1,4-addition to  $\alpha,\beta$ -unsaturated carbonyl compounds (**Scheme 10**). The Michael type addition of nitromethane to the alkenoate derived from (-)-verbenone has shown to be totally diastereoselective.



**Scheme 10:** Synthesis of cyclobutyl  $\gamma$ -lactams from (-)-verbenone.

It is worth emphasizing the fact that one of the faces in the *cis*-substituted cyclobutane is sterically hindered due to the presence of the *gem*-dimethyl group, thus promoting the nucleophilic addition by the *re* face. The absolute configuration of the generated stereocenter could be unambiguously assigned by X-ray diffraction of the corresponding  $\gamma$ -lactam (**Figure 3**).<sup>42</sup>

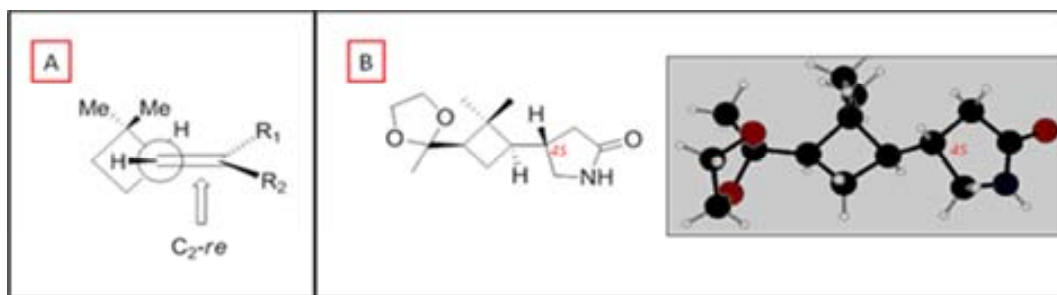
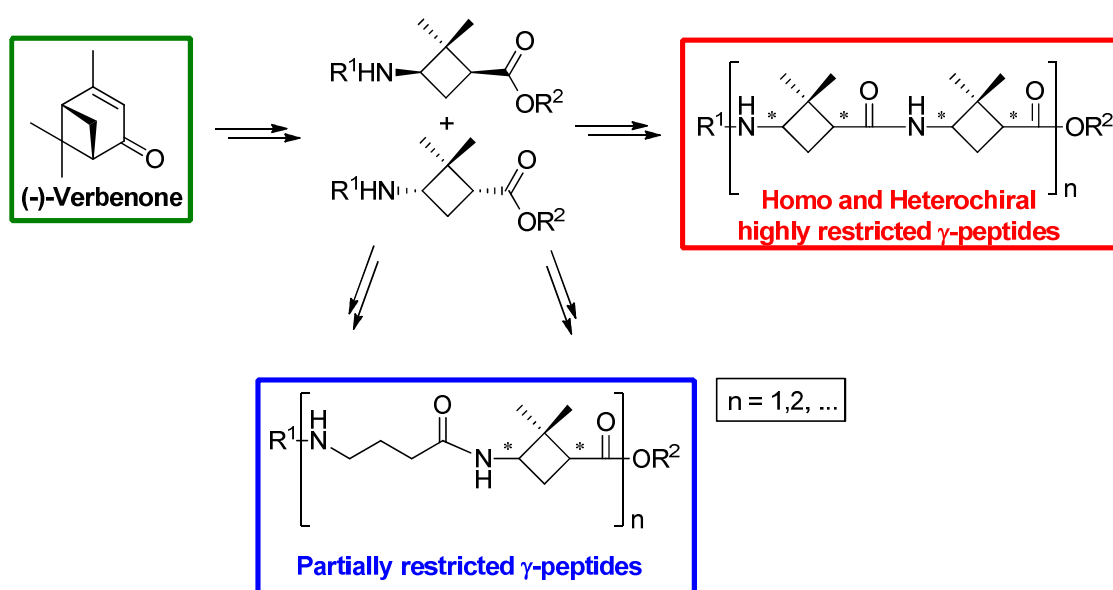


**Figure 3:** A, *re* face of the olefin is more accessible. B, X-ray diffractogram of the  $\gamma$ -lactam that allows the assignment of the absolute configuration in carbon 4 as *S*.

The synthesis of optically pure cyclobutane  $\gamma$ -amino acids and their inclusion into  $\gamma$ -peptides with modifiable conformational restriction has also been achieved in our group (**Scheme 11**).<sup>43</sup> It was thought that the presence of cyclobutane moiety could promote compact folding by the formation of long distance intramolecular hydrogen bonds. However, as a result of the preliminary structural studies, these cyclobutane  $\gamma$ -peptides present an extended conformation. This tendency contrasts with the natural trend of  $\gamma$ -peptides to fold by the action of hydrogen bonds between the nearest neighbour amides.<sup>44</sup>



**Scheme 11:** Synthesis of differently restricted hybrid  $\gamma$ -peptides.

**Chapter I**

**Cyclobutane Containing  $C_3$ -Symmetric Peptide Dendrimers**





## **2. CHAPTER I: CYCLOBUTANE CONTAINING C<sub>3</sub>-SYMMETRIC PEPTIDE DENDRIMERS**

### **2.1. INTRODUCTION**

#### **2.1.1 Biological relevance of $\gamma$ -amino acids**

Since 1950, when Roberts and Frankel discovered in mammalian's Central Nervous System (CNS) a common non proteinogenic amino acid, identified as  $\gamma$ -amino butyric acid (GABA, **16**),<sup>45</sup>  $\gamma$ -amino acids have awakened a great interest among scientific community.

GABA is known to be the major inhibitory neurotransmitter in mammalian CNS, which means that acts in neural synapse lowering or modulating electrochemical activities. It is mainly found in the brain, and is an agonist at three receptor subtypes (GABA<sub>A</sub>, GABA<sub>B</sub>, GABA<sub>C</sub>).<sup>46, 47</sup> Consequently, altered GABAergic function in the brain is believed to be responsible of some psychiatric and neurological disorders in humans such as schizophrenia (mental disorder involving a breakdown in the relation between thought, emotion, and behaviour, leading to faulty perception, inappropriate actions and feelings, and withdrawal from reality into fantasy and delusion).<sup>2</sup>

GABA not only serves as inhibitory neurotransmitter but also plays a part in the regulation of several physiological mechanisms (secretion of hormones such as prolactin and growth hormone), and is involved in the control of cardiovascular functions, pain processes, anxiety's synaptic mechanisms, feeding and aggressive behaviour.<sup>48</sup>

As a result of its multiple regulation functions, medicinal chemistry has been deeply interested in the synthesis of GABA agonists and antagonists for the treatment of related disorders (**Figure 4**).

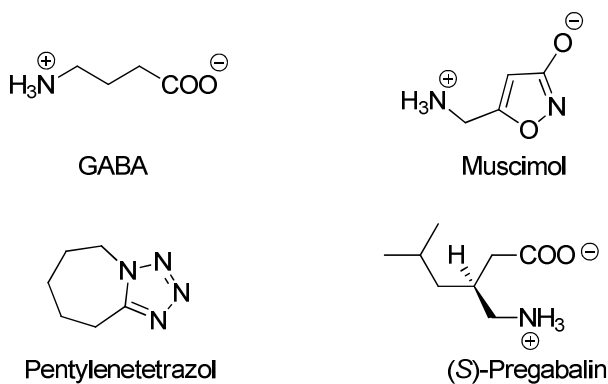


**Figure 4:** Some GABA Agonists and Antagonists

Even though  $\gamma$ -amino acids are interesting by their inherent biological properties, their capability to induce certain secondary structures in peptides has been object of many studies.<sup>49</sup> Moreover, it has been observed that those structures can lead to new materials, such as nanotubes or structures with inner cavities which could have interesting applications in biology and materials fields.<sup>50, 51</sup>

### **2.1.2 Secondary structure of $\gamma$ -peptides**

Special attention towards the secondary structure of homologated peptides has been paid by Seebach and co-workers who described the synthesis of various  $\gamma$ -peptides with only one side chain per amino acid ( $\gamma^2$ -,  $\gamma^3$ -,  $\gamma^4$ -hexapeptides).<sup>52, 53</sup> NMR analysis only led to a defined structure in solution in one instance ( $\gamma^4$ ) which was shown to be a 2.6<sub>14</sub>-helix (**Figure 5**).

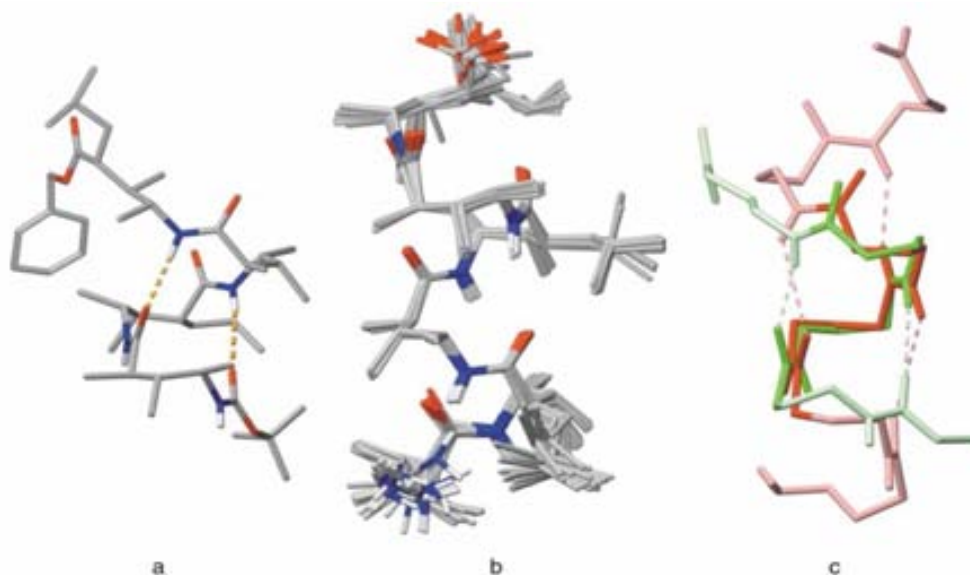


**Figure 5:** a) Structure of a  $\gamma^4$ -tetrapeptide in the crystal state determined by X-ray structure analysis. b) Bundle of 20 conformers of a  $\gamma^4$ -hexapeptide in MeOH obtained by simulated annealing calculations using restraints from NMR data. c) Superposition of the peptide backbones from the X-ray diffraction structure (green) and NMR structure (red)

From more highly substituted compounds, such as those with two side chains ( $\gamma^{2,4}$ ) studied by Hanessian et al.<sup>54, 55</sup> or trisubstituted  $\gamma^{2,3,4}$ -amino acid-based species described by Seebach and co-workers<sup>52, 56</sup> it has been possible to determine NMR structures in solution and X-ray crystal structures showing the same 2.6<sub>14</sub>-helix pattern as in the mono side-chain-substituted derivatives (**Figure 6**).<sup>57</sup> Depending upon the relative configuration of the  $\gamma$ -2,4-residues, turn motifs can also be constructed.

For both secondary structures to be observed in solution, the required chain length can be even shorter than in the case of  $\beta$ -peptides: four residues for the helix and two for the turn. The alkyl chain backbone takes control, while the number of hydrogen bonds per chain atom decreases. The structural diversity of  $\gamma$ -amino acids and  $\gamma$ -peptides has not been elucidated as well as that of  $\beta$ -peptides but it is expected to be richer.

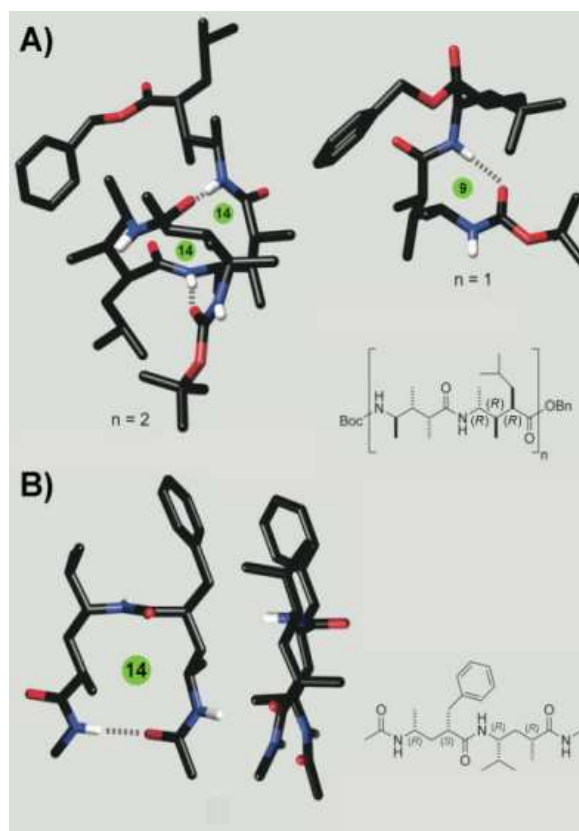


**Figure 6:**  $\gamma$ -Peptidic helix and turn. The  $\gamma$ -amino acids with three substituents in the tetrapeptide A, where  $n = 2$ , can be assigned D-configuration, and the helix is (M) or left-handed. L- $\gamma^4$ -Residues give rise to a (P)-helix (top left). The  $\gamma$ -dipeptide (top right) forms a nine-membered hydrogen-bonded ring. Turns as the one shown in B can be used as scaffolds for  $\alpha$ -peptidic turn mimics, given the proper side chains adjacent to the peptide bond.<sup>49</sup>

### 2.1.3 Precedents in the synthesis of ring-containing $\gamma$ -amino acids

As it has been pointed out before, it is a requirement to constrict conformational states in molecules with a potential biological activity. Two of the most successfully used elements for this purpose are the introduction of small cyclic structures and the use of  $\gamma$ -amino acids. Due to that, the synthesis of 3, 5 or 6 membered cyclic  $\gamma$ -amino acids has been extensively studied.<sup>17, 58, 59</sup> However, the syntheses of  $\gamma$ -amino acids and  $\gamma$ -peptides containing a four membered ring are few.

A remarkable example of those syntheses was carried out by Burgess *et al.*<sup>16</sup> using terpenoids from the chiral pool as it has been commented in the General Introduction.

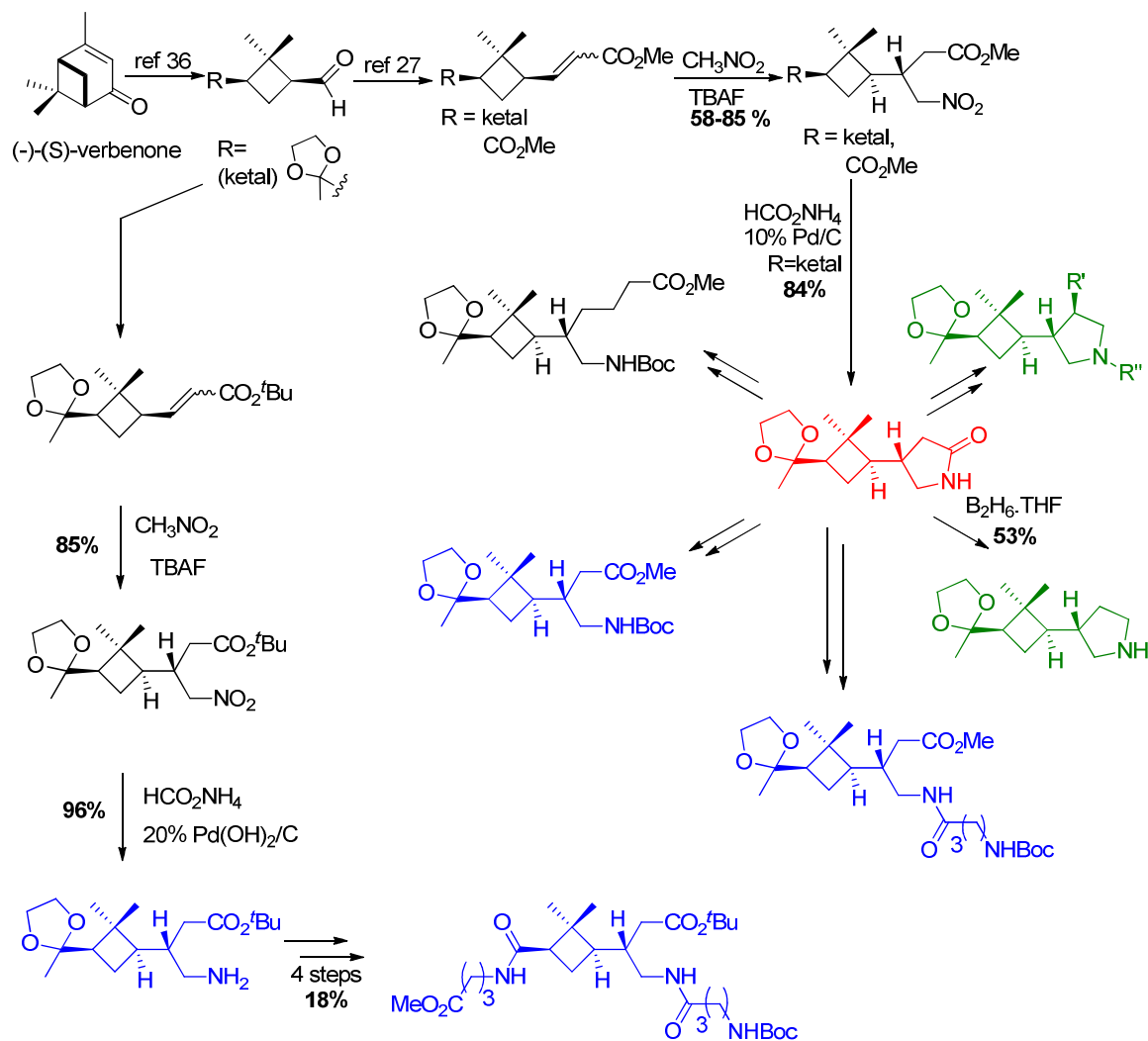
Another versatile example was developed by Ley and co-workers, who used PLE in the desymmetrization of a meso diester with polymer-supported PLE as it has been commented in the General Introduction.<sup>17</sup>

#### **2.1.4 Precedents in the research group in the synthesis of ring-containing $\gamma$ -amino acids**

As described in the General Introduction, most of the synthetic routes proceed through asymmetric 1,4-addition to  $\alpha$ ,  $\beta$ -unsaturated compounds. Moreover, the Michael type addition of nitromethane to the alkenoates derived from (-)-verbenone has showed to be totally diastereoselective.

Dr. Moglioni, Dr. Mor and Dr. Aguilera (unpublished results) took advantage of this stereospecific 1,4-addition in the synthesis of cyclobutane  $\gamma$ -lactams,  $\gamma$ -amino acids,  $\gamma$ -peptides and pyrrolidines that are not only interesting intermediates, but also compounds with high potential biological activity (**Scheme 9**). As previously commented, (-)-verbenone has been used as a chiral precursor in the synthesis of cyclobutyl aldehydes, bearing different substitutions on the ring.<sup>36</sup> Wittig olefination of these compounds by using suitable phosphoranes afforded differently protected alkenoates as mixtures of *Z/E* isomers, which could be chromatographically separated and isolated. On these substrates, the stereoselective addition of nitromethane in the presence of tetrabutylammonium fluoride was carried out in order to introduce a synthon providing the additional carbon atom of the  $\gamma$ -amino acid skeleton and a functional group that could be easily transformed into the amino function. Reduction of the nitro group was accomplished by treatment of the nitro esters with ammonium formate in the presence of Pd/C in boiling methanol. In the case of methyl esters the corresponding lactams were obtained without isolation of the intermediate amino esters, which underwent *in situ* cyclization. Lactams turned to be a highly versatile intermediate allowing the preparation of  $\gamma$ - and  $\epsilon$ -amino acids and pyrrolidines. On the contrary, in the case of the very low electrophilic *tert*-butyl ester, the compound resulting from nitromethane addition and subsequent reduction could be isolated. This product is already suitable for its incorporation into peptides as verified by its

coupling with two partially protected GABA residues under the usual conditions (HOBt, EDAC) to provide after 4 steps a tripeptide in 18% overall yield (**Scheme 13**).



**Scheme 13:** Previous syntheses of cyclobutane  $\gamma$ -amino acids and  $\gamma$ -peptides,  $\gamma$ -lactams and pyrrolidines, accomplished in our laboratory.

It should be noted that the above reported synthetic routes enable the access to multifunctional branched cyclobutane amino acids and peptides. The multifunctional nature of these molecules could be of great interest in the preparation of dendrimers, making them suitable both as cores and as dendrons as described below.

### 2.1.5 Dendrimers

Dendrimers are a new class of polymeric materials. They are highly branched, monodisperse macromolecules.<sup>60</sup> The structure of these materials has a great impact on their physical and chemical properties. As a result of their unique behaviour, dendrimers are suitable for a wide range of biomedical and industrial applications.

Polymer chemistry and technology have traditionally focused on linear polymers, which are widely used. Linear macromolecules only occasionally contain some smaller or longer branches. In the recent past it has been found that the properties of highly branched macromolecules can be very different from conventional polymers.<sup>60</sup> The structure of these materials has also a great influence on their applications.

It was not until the late 1970s when dendrimers appeared as a new kind of compounds that was in between of small organic molecules and polymers. Vögtle and co-workers were the pioneers in the synthesis of multi-branched compounds with the preparation in 1978 of the so called “cascade molecules”.<sup>61</sup> Short after, in the middle 1980s, Newkome<sup>62</sup> synthesised tree-kind of molecules known as “arborols”, and Tomalia<sup>63</sup> described the synthesis of poly(amino amides) at the same time that coined the term “dendrimer” [Greek, *dendra* (tree) and *meros* (part)] for these compounds.

Since their discovery, dendrimers have awakened a great interest among the scientific community as a result of the important applications that have been conferred to them: biomaterials, drugs or vaccines, hosts/transporters (catalysts, drugs, genes...) among others.<sup>64</sup> This fact has been reflected in the exponential increase in the number of publications related to this topic since dendrimers appeared (**Figure 7**).

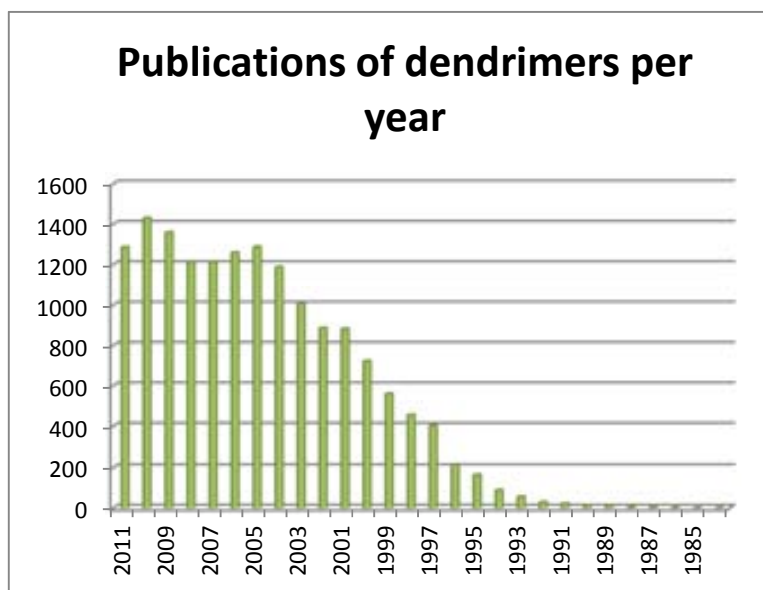


**Figure 7:** Data extracted from SciFinder Scholar under the research topic “Dendrimers”

On account of what has been said, dendrimers are polymeric molecules consisting of multiple branched monomers that emanate from a central core, reminiscent of a tree. When the core of a dendrimer is removed, a number of identical fragments called dendrons remain, their number depending on the multiplicity of the central core (2, 3, 4 or more). Consequently, dendrimers have three distinguishable regions: the nucleus or core, the internal cavity or branches, and the periphery or terminal groups (**Figure 8**).<sup>65</sup> The number of branch points encountered upon moving outward from the core of the dendron to its periphery defines its generation (G-1, G-2, G-3); dendrimers of higher generations are larger, more branched and have more end groups at their periphery than dendrimers of lower generations. What makes them extremely interesting is the possibility of modulating and controlling their size, shape, solubility and chemical properties through the modification of any of their regions.



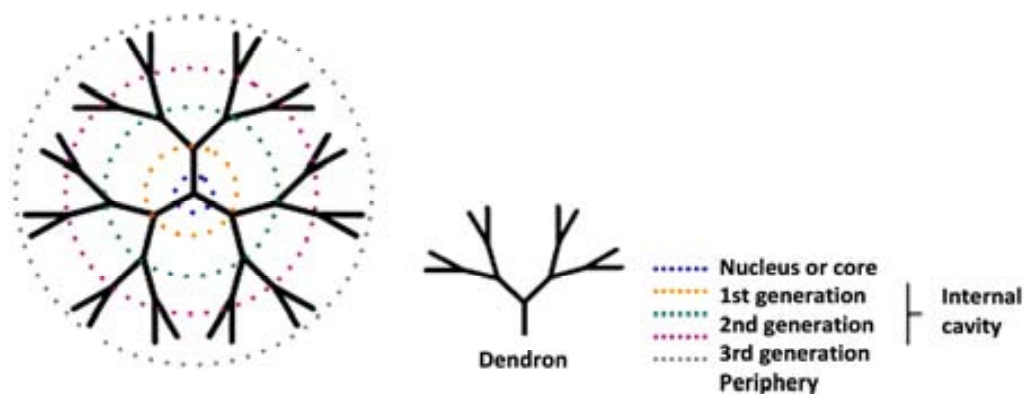
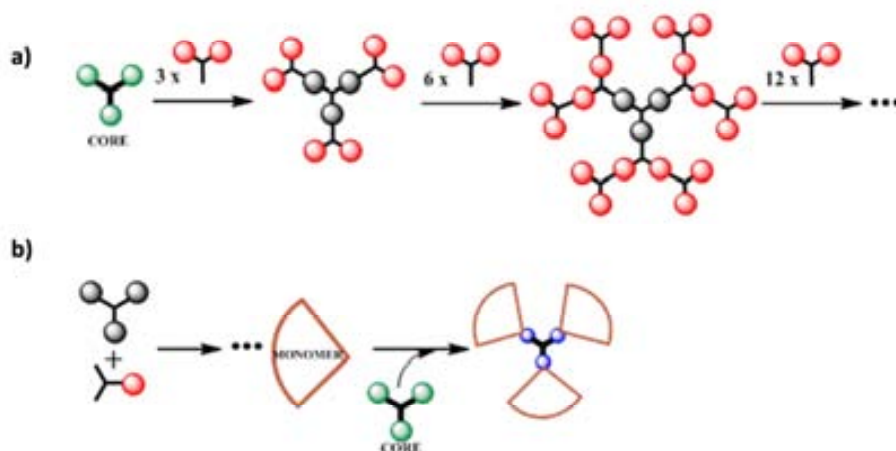


Figure 8: Anatomy of a dendrimer

Dendrimers are generally prepared using either a divergent method or a convergent one.<sup>66</sup> There is a fundamental difference between these two construction concepts. In the divergent methods, dendrimer grows outwards from a multifunctional core molecule. The core molecule reacts with monomer molecules containing one reactive and two dormant groups giving the first generation dendrimer. Then the new periphery of the molecule is activated for reactions with more monomers. The process is repeated for several generations and a dendrimer is built layer after layer (**Figure 9a**). The divergent approach is successful for the production of large quantities of dendrimers. Problems occur from side reactions and incomplete reactions of the end groups that lead to structure defects. To prevent side reactions and to force reactions to completion, large excess of reagents is required. This causes some difficulties in the purification of the final product.



**Figure 9:** a) The divergent growth method. b) The convergent growth method.

The convergent methods were developed as a response to the weaknesses of the divergent synthesis.<sup>67</sup> In the convergent approach, the dendrimer is constructed stepwise, starting from the end groups and progressing inwards. When the growing branched polymeric arms, called dendrons, are large enough, they are attached to a multifunctional core molecule (**Figure 9b**). The convergent growth method has several advantages. It is relatively easy to purify the desired product and the occurrence of defects in the final structure is minimised. It becomes possible to introduce subtle engineering into the dendritic structure by precise placement of functional groups at the periphery of the macromolecule. The convergent approach does not allow the formation of high generations because steric problems occur in the reactions of the dendrons and the core molecule.

### 2.1.5.1 $C_3$ -Symmetric benzene cored molecules

$C_3$ -Symmetric benzene-cored molecules are useful compounds with very different applications. Of special interest are those linked to the core through a urea, *C*-amide, or *N*-amide group (**Figure 10**). They have been described as good nucleation agents for polymers,<sup>68, 69, 70</sup> as new materials,<sup>71, 72, 73, 74, 75, 76, 77</sup> and especially as organogelators,<sup>78, 79,</sup>

<sup>80, 81, 82</sup> some of them with conducting<sup>83</sup> or photoresponsive properties,<sup>84</sup> and as ligands for metals.<sup>85, 86, 87</sup> Some also have interesting biological applications.<sup>85, 88, 89</sup> Nevertheless, there are very scarce examples of benzene-cored dendrimers containing a peptide nature in their dendron structure.<sup>74, 80, 89, 90, 91, 92, 93</sup>

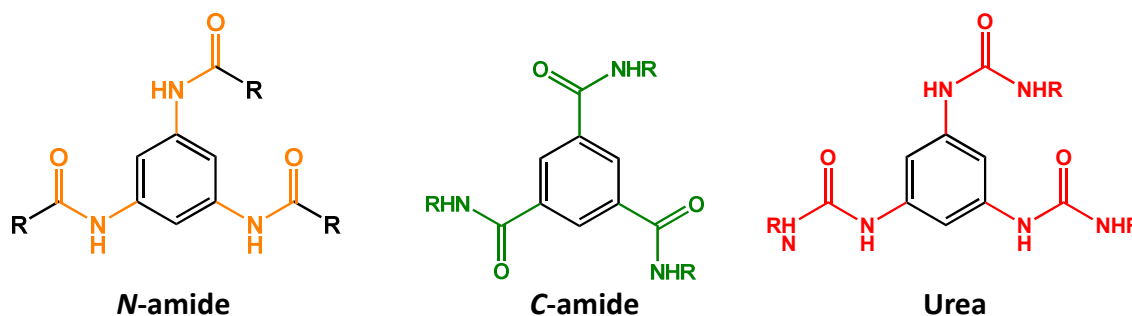
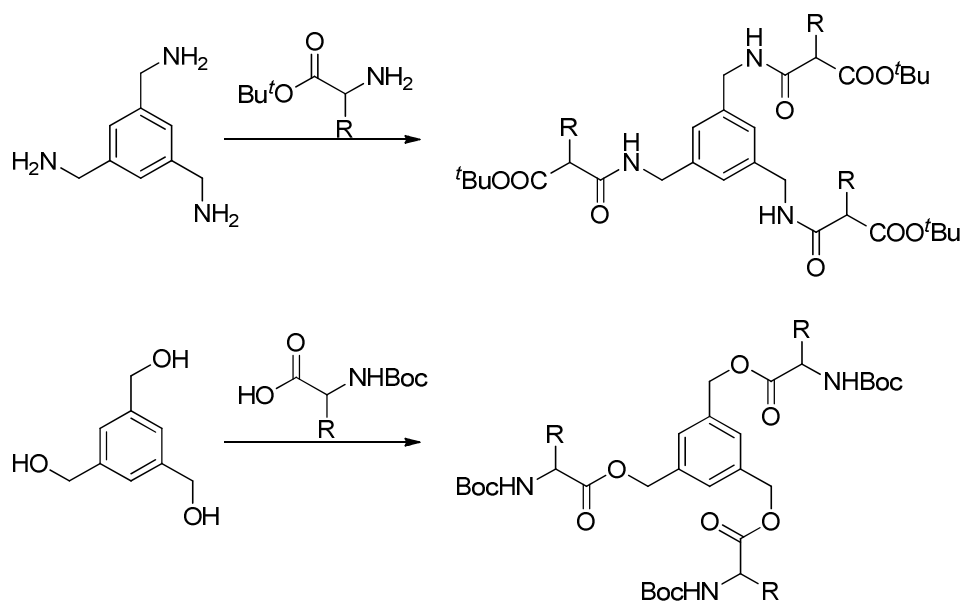


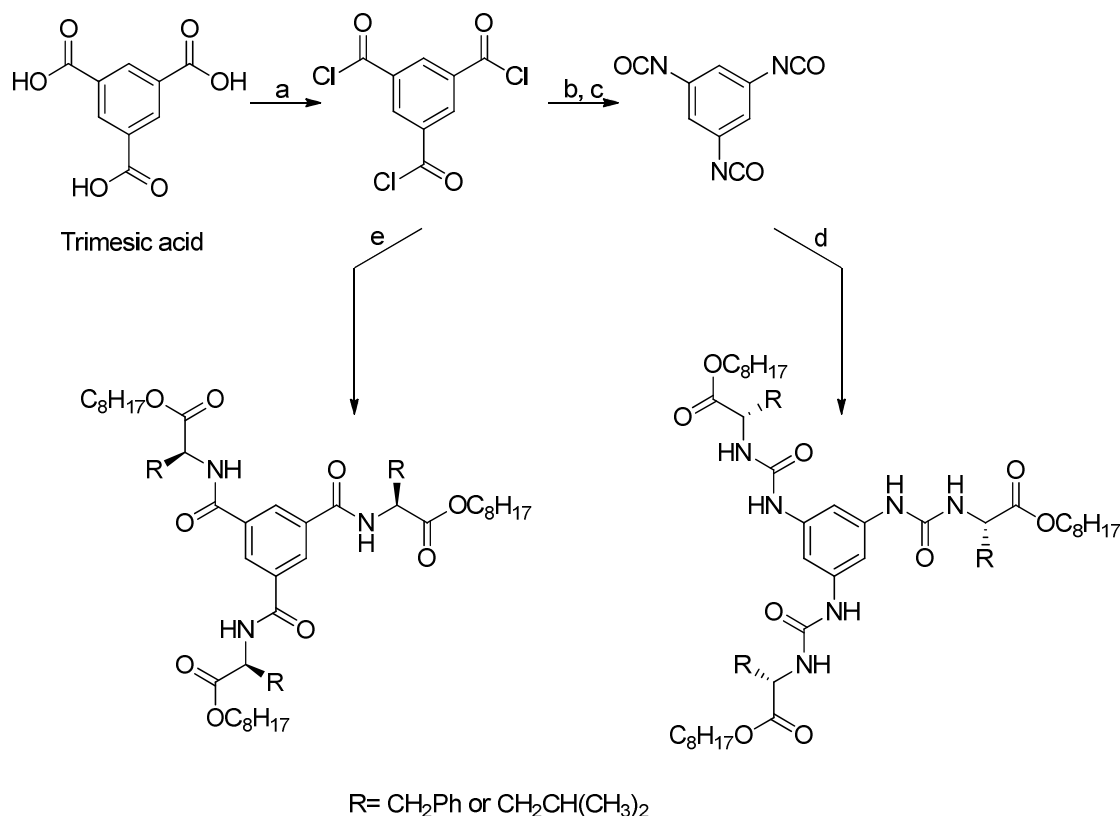
Figure 10

One of the first examples of  $C_3$ -symmetric benzene-cored molecules containing a peptide nature in their dendron structure was reported by Tor *et al.* (Scheme 14).<sup>93</sup> In their work they describe the synthesis of two different families: 1,3,5-tris(aminomethyl)benzene (TRAM) and 1,3,5-tris(hydroxymethyl)benzene. Only the first one contains peptidic bonds. The structural study of the TRAM family concluded that the peptides existed as an equilibrium mixture of mainly two classes of conformations, each with a unique pattern of interstrand H-bonds. Nevertheless, in none of those cases the peptide function is directly connected to the aromatic core as depicted in Figure 10.



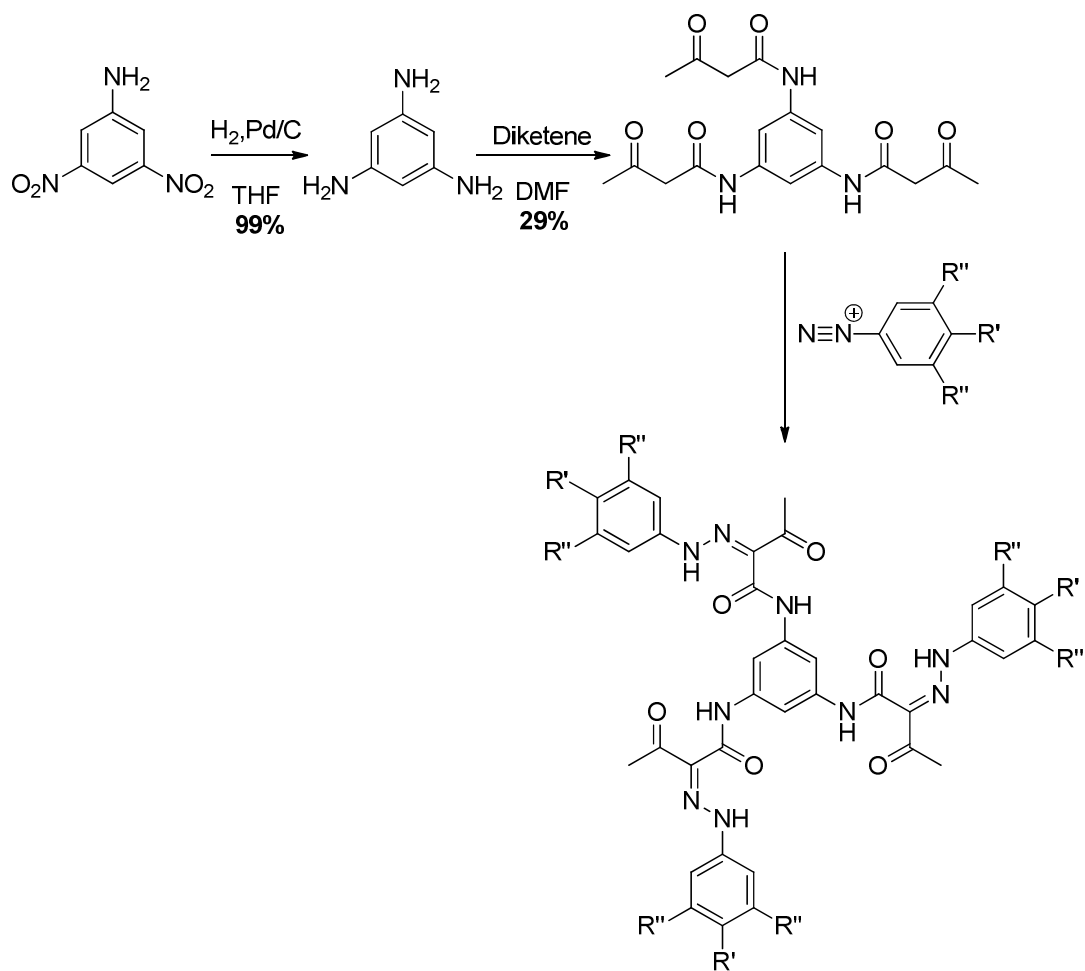
**Scheme 14:** Synthetic routes leading to  $C_3$ -symmetric molecules with peptide nature.

An interesting work concerning amide core-linked  $C_3$ -symmetric molecules is the one carried out by Feringa and co-workers who carried out a systematic study concerning the nature of the bond between the core and the branches and the side chain length.<sup>80</sup> With this aim they synthesised, starting from trimesic acid, both benzene-cored tris-amides and tris-ureas through reaction with  $\alpha$ -amino acids bearing different side chains (**Scheme 15**). It was found that the nature of the linking unit had a strong influence on the number of possible hydrogen bonds and therefore the strength of the intermolecular interactions. The side chain influenced the magnitude of the steric hindrance and the possible presence/absence of  $\pi$ - $\pi$  stacking. It seems that too strong intermolecular hydrogen bonding interactions (leading to insolubility, crystallisation or precipitation) can be compensated by the introduction of steric hindrance to yield effective gelators. Weaker hydrogen bonding interactions (amides) seem to be strengthened by the presence of  $\pi$ -stacking interactions and less steric hindrance.



**Scheme 15:** Synthesis of the 1,3,5-benzene tris-urea and tris-amide derivatives. Reagents and conditions: (a) SOCl<sub>2</sub>, DMF (cat.), 3 h, (100% conversion); (b) NaN<sub>3</sub>, water/THF, 0 °C, 2 h; (c) toluene; (d) 3.3 equiv RNH<sub>2</sub>, toluene, rt, 18 h, (20–40)%; (e) 3 equiv RNH<sub>2</sub>, Et<sub>3</sub>N, CH<sub>2</sub>Cl<sub>2</sub>, (50–60)%.

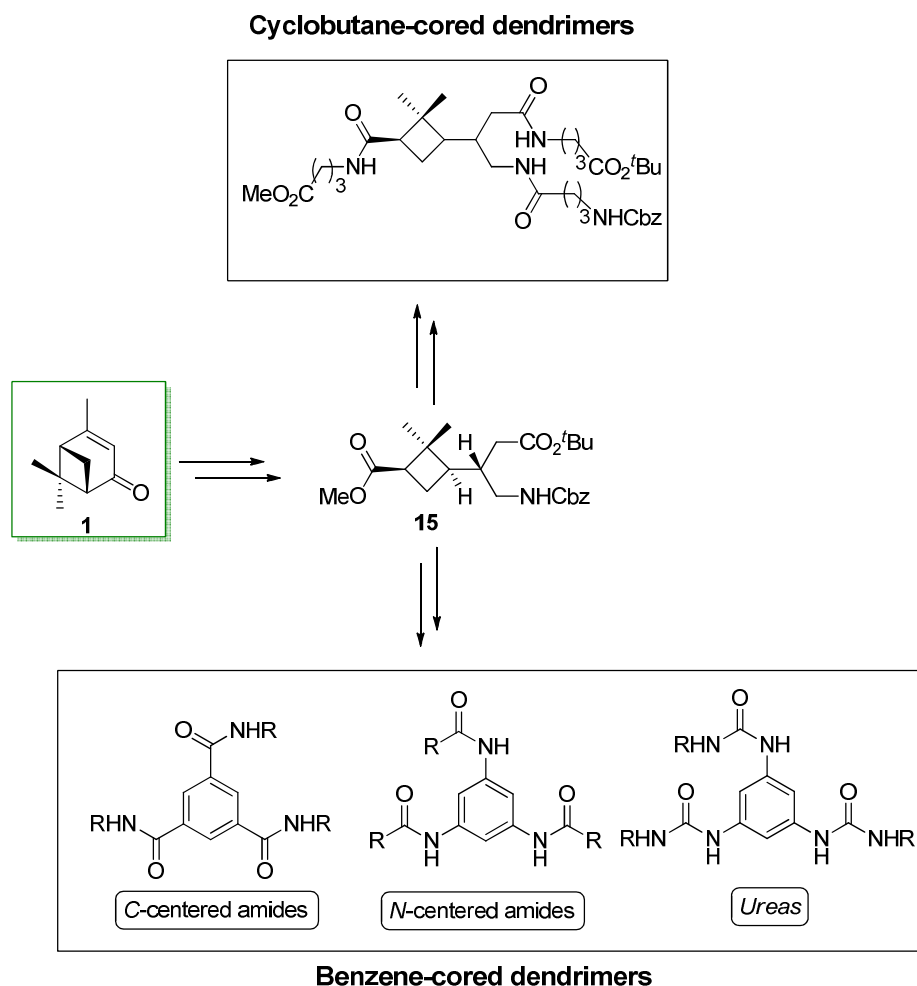
Apart from the reported example, many others concerning benzene-cored C<sub>3</sub>-symmetric C-amides and ureas can be found in the literature, however almost no examples of N-amides can be found. Jeong *et al.* described the synthesis of 1,3,5-tris(acetoacetamido)benzene starting from dinitroaniline, which led to discotic liquid crystalline hydrazones through diazo coupling reaction between 1,3,5-(trisacetoacetamido)benzene and diazonium salts of 4-alkyloxyphenylamines (**Scheme 16**).<sup>94</sup>



**Scheme 16:** Synthesis of discotic liquid crystalline compounds.

## 2.2. OBJECTIVES

The broad experience held by our research group in the preparation of enantiomerically pure cyclobutane  $\gamma$ -amino acids and peptides, the intrinsic potential biological activity of such molecules and the capability that they might have to induce defined secondary structures, prompted our group to start a research program in the field of applications of branched cyclobutane  $\gamma$ -amino acids. Therefore, the first objective of this chapter consists on the synthesis of an orthogonally protected cyclobutane  $\gamma$ ,  $\epsilon$ -amino diacid, like **15**, starting from the natural chiral pool (**Scheme 17**).



**Scheme 17:** Objective molecules from chapter 1.

Next, the capability of **15** to induce defined secondary structures will be tested through the coupling to 3 conveniently protected GABA residues (**Figure 11**), leading to the first example of cyclobutane-cored dendrimers.

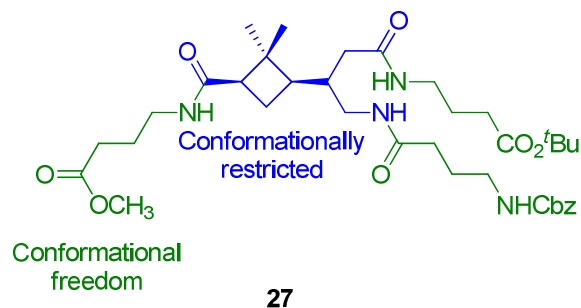


**Figure 11**

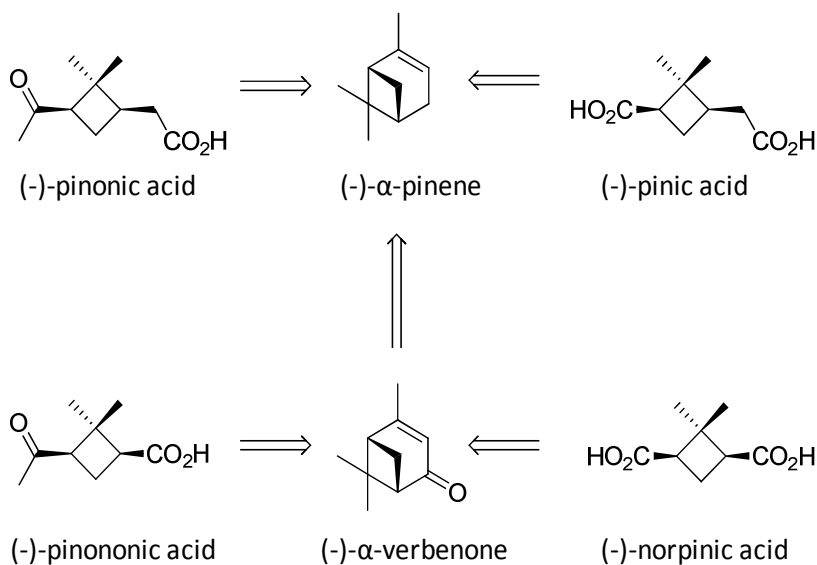
Finally, these newly synthesised multifunctional molecules could be used as dendrons in the preparation of benzene-cored  $C_3$ -symmetric dendritic molecules. In that way, the effect of the constricted nature of cyclobutane on the folding of the dendrimers would also be studied (**Scheme 17**).



## 2.3. RESULTS AND DISCUSSION

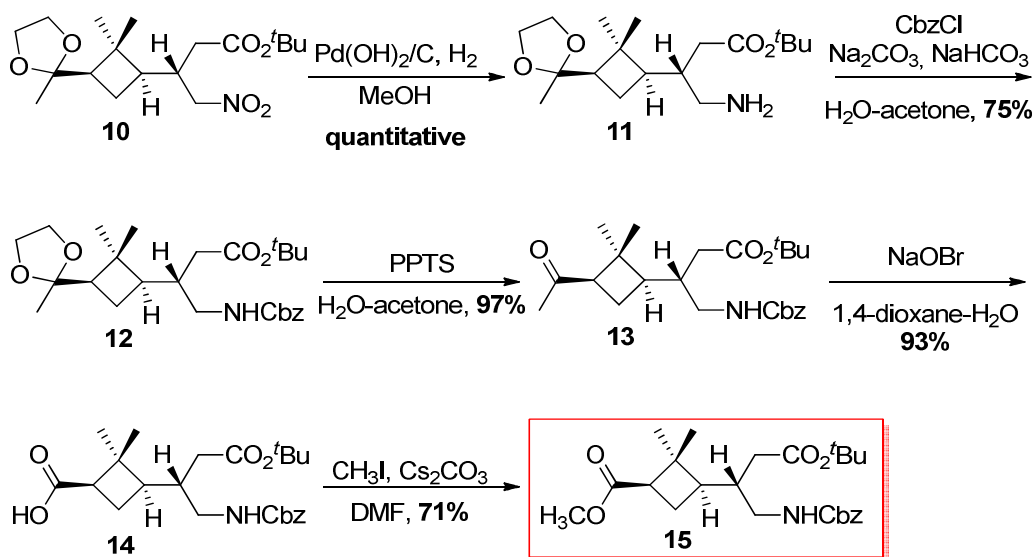
### 2.3.1 Synthesis of orthogonally protected cyclobutane $\gamma$ , $\epsilon$ -amino diacid, **15**

The use as precursor of chiral bicyclic terpenoids derivatives (**Scheme 18**) such as (-)-verbenone, has been traditionally the preferred choice in our laboratory. This is due to the fact that these molecules are available with high purity and enantiomeric excess at reasonable prices.



**Scheme 18:** Some products of the  $\alpha$ -pinene family which contain a four-membered ring.

Starting from previously synthesised nitro ester **10**, reduction of the nitro group (**Scheme 19**) was accomplished chemoselectively by treatment with ammonium formate (its thermal decomposition permits to generate hydrogen *in situ*) in the presence of 20% Pd(OH)<sub>2</sub>/C in boiling methanol. Due to the poor electrophilic nature of the carboxylic carbon in the *tert*-butyl nitro ester and to the hindrance around this center, amino ester **10** could be isolated, without lactam formation. Lactams had been obtained when the same sequence had been carried out on molecules containing methyl esters instead of in *tert*-butyl ones.<sup>42</sup> Compound **10** was already suitable for incorporation into peptides, although first it was protected as a benzyl carbamate using CbzCl and a 2:1 mixture of Na<sub>2</sub>CO<sub>3</sub>/NaHCO<sub>3</sub> as a base<sup>95</sup> to afford the orthogonally protected  $\gamma$ -amino acid **11** in 75% yield.

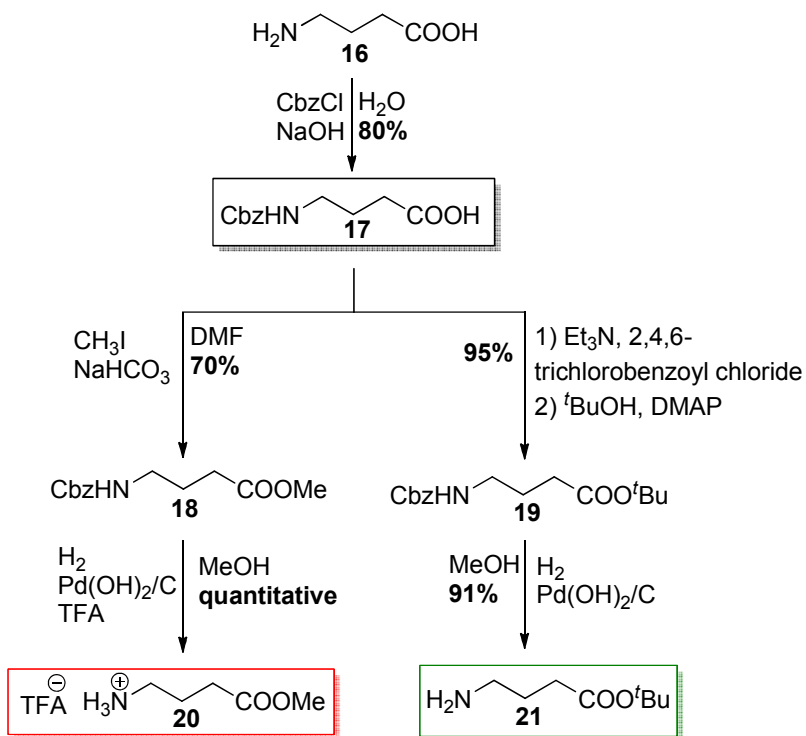
Scheme 19: Synthesis of  $\gamma,\epsilon$ -amino diacid **15**

Cyclobutyl  $\gamma$ -amino acid **11** presents an ethylene glycol ketal, which is a masked ketone that could be transformed into different functional groups to modulate the properties of these compounds. With this purpose, **12** was heated to reflux in wet acetone in the presence of catalytic amount of PPTS to afford quantitatively the free ketone **13** without observing epimerization. The so obtained methyl ketone was submitted to the haloform reaction conditions (NaOBr, 1,4-dioxane, water) at  $-5\text{ }^\circ\text{C}$  for 5 hours to provide the corresponding carboxylic acid **14** in a quantitative yield. Finally, **14** was methylated using  $\text{CH}_3\text{I}$  and  $\text{Cs}_2\text{CO}_3$  to afford enantiomerically pure orthogonally protected  $\gamma, \epsilon$ -amino diacid **15** in 71% yield.

### 2.3.2 Synthesis of a differently protected family of GABA-residues

As it has been previously mentioned, one of the objectives of this work consists on the evaluation of the capability of the cyclobutane ring to induce defined secondary structures through the coupling of 3 conveniently protected GABA residues with **15**. Taking this into account, it is of crucial importance to have at one's disposal a family of differently protected GABA-residues.

Starting from commercially available GABA (**16**), partially protected amino acid **17** was prepared through reaction with benzyl chloroformate using NaOH as a base (**Scheme 20**). This compound has been used as a key intermediate that enables the access to differently protected  $\gamma$ -amino acids through its esterification with different substrates.



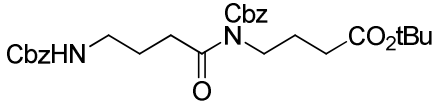
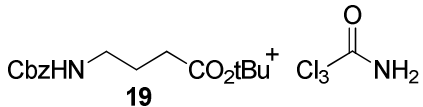
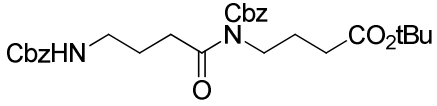
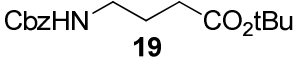
**Scheme 20:** Synthesis of a family of differently protected GABA-residues

As depicted in **Scheme 20**, compound **17** was methylated with CH<sub>3</sub>I and Cs<sub>2</sub>CO<sub>3</sub> in an analogous manner as that for **15**, to obtain an orthogonally protected lineal  $\gamma$ -amino acid (**18**). Note that it is not possible to synthesise the methyl ester of GABA when the amine group is not protected because the lactamization takes place instantaneously. Therefore, partially protected compound **20** was obtained through selective cleavage of benzyl carbamate group by hydrogenation over Pd(OH)<sub>2</sub>/C in the presence of trifluoroacetic acid (ammonium salts can be stored for longer times).

Concerning compound **19**, direct esterification of **17** using *tert*-butanol could not be performed due to the poor nucleophilicity of this alcohol. Consequently, different methods

were evaluated as summarised in **Table 1**. On a first attempt, the carboxylic acid was activated under peptide coupling conditions in the presence of *t*BuOH. However, due to the higher nucleophilicity of the nitrogen atom in the carbamate group in comparison to *t*BuOH, peptide coupling product between two GABA residues was obtained instead of the desired product (entry 1 from **Table 1**).

**Table 1:** Assayed methodologies for the preparation of **19**.

| Entry | Methodology   | Products   |
|-------|---|--|
| 1     | Peptide coupling conditions<br>( <i>t</i> BuOH/DMAP/EDAC/Et <sub>3</sub> N)       |    |
| 2     | <i>tert</i> -butyl trichloroacetimidate   |    |
| 3     | 1) Ethyl chloroformate/Et <sub>3</sub> N<br>2) <i>t</i> BuOH/DMAP                 |    |
| 4     | 1) 2,4,6-trichlorobenzene<br>chloride/Et <sub>3</sub> N<br>2) <i>t</i> BuOH, DMAP |  |

For that reason, we decided to prepare **19** through reaction with *tert*-butyl trichloroacetimidate. This methodology had been successfully used in our group, and once again it led to the expected esterification product. However, the separation of **19** from the obtained by-product (trichloroacetamide) turned out to be difficult, and resulted in an important yield lowering (entry 2, **Table 1**).

In view of the previous results, a new methodology, in which the carbonyl group was more activated, was performed. Therefore, the preparation of the corresponding mixed anhydride from **17** through reaction with ethyl chloroformate, followed by alcoholysis under basic catalysis seemed to be an appropriate method. Nevertheless, once again the peptide coupling product was obtained by following this procedure, as it is summarised in entry 3 of **Table 1**. Consequently, we decided to seek for alternative methods in the literature for the

preparation of *tert*-butyl esters, and Yamaguchi's esterification seemed to be a suitable option for the synthesis of **19**.<sup>96, 97</sup>

As stated in entry 4 of **Table 1**, the followed procedure is identical as the one in entry 3: mixed anhydride formation, followed by alcoholysis under basic conditions. However, this last case differs in the chloride used for the mixed anhydride formation, which is able to activate the carbonyl group towards the nucleophilic attack of *t*BuOH through a double mode of action: electronic effects (leaving group stabilisation) and steric effects (higher hindrance). Consequently, compound **19** was prepared quantitatively, following the Yamaguchi's esterification procedure, through reaction with 2,4,6-trichlorobenzene chloride and *t*BuOH in the presence of DMAP.

After that, partially protected compound **21** was obtained through selective cleavage of benzyl carbamate group through hydrogenation over Pd(OH)<sub>2</sub>/C with a very good yield.

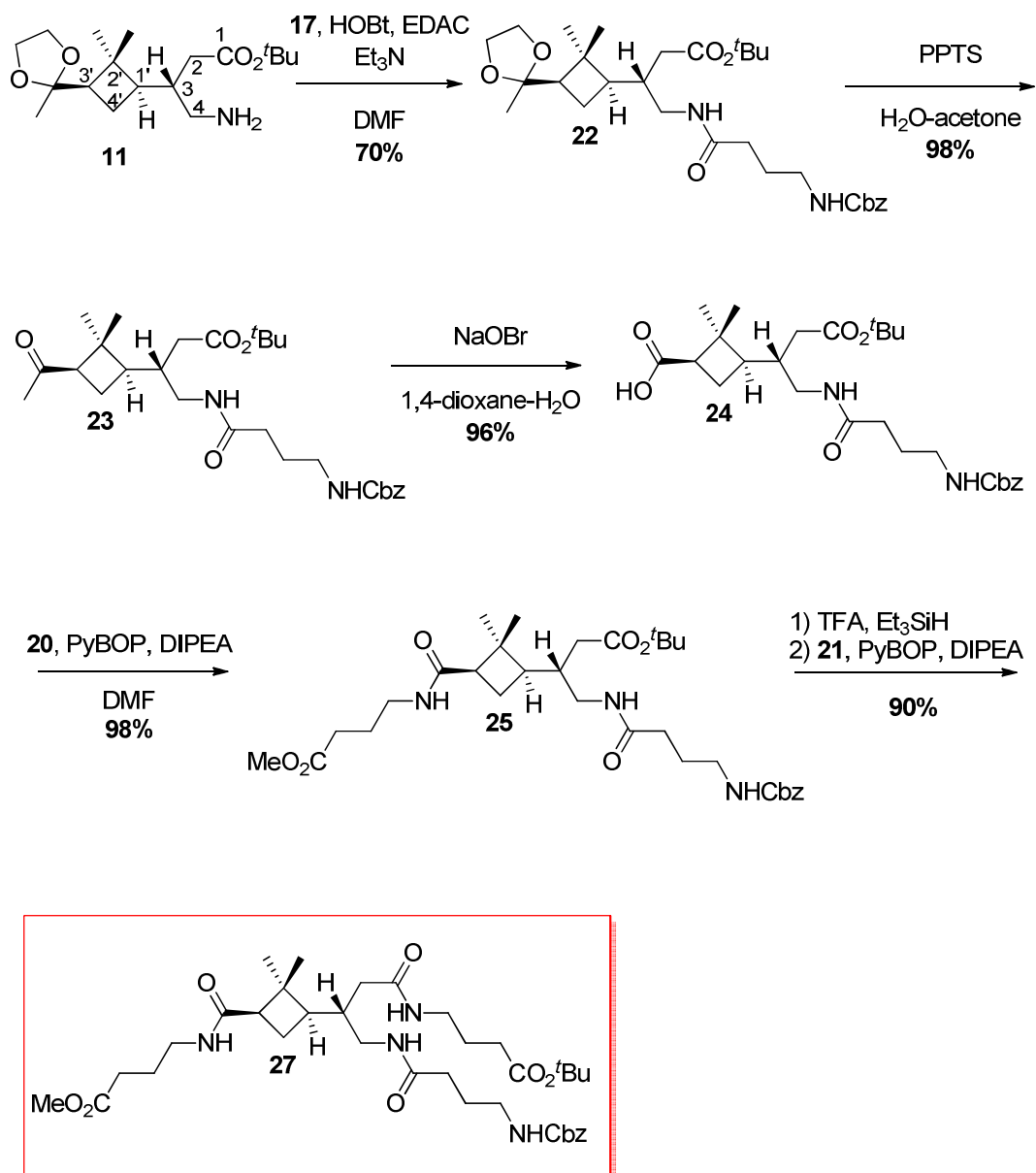
### **2.3.3 Synthesis and structural properties of cyclobutane-cored first generation dendrimers**

It has been previously commented that the cyclobutane ring is a rigid moiety which could be used as a constriction motive to induce defined secondary structures. With the aim to prove it, a series of hybrid cyclobutane-GABA peptides have been synthesised, which are the first example of cyclobutane-cored chiral dendrimers.

Using previously described **11** as key intermediate, conveniently modifying 3' position of cyclobutane ring, and the family of differently protected GABA residues, a series of orthogonally protected hybrid peptides has been obtained (**Scheme 21**). Both carbodiimide-based and phosphonium-based coupling agents have been tested, but here are shown only those conditions that have afforded best results.

In the first step, free carboxylic acid **11** and partially protected GABA **17** were coupled using EDAC as coupling agent and the acid catalyst HOBt to obtain fully protected dipeptide **22** with a good yield and with complete optical integrity. After that, position 3' of the cyclobutane ring was conveniently transformed. Therefore methyl ketone group was

deprotected, without epimerization, by heating dipeptide **22** to reflux in wet acetone and in the presence of catalytic amount of PPTS. The obtained product was submitted to the haloform reaction conditions (NaOBr, 1,4-dioxane, water) at -5° C for 5 hours to provide the corresponding carboxylic acid **24** in an almost quantitative yield as a white highly hygroscopic solid.



**Scheme 21:** Followed synthetic route for the preparation of a series of orthogonally protected hybrid  $\gamma$ -peptides and a cyclobutane-cored dendrimer.

Next, partially protected dipeptide **24** was coupled to conveniently protected GABA residue **20** using PyBOP as a coupling agent in the presence of DIPEA, to obtain, enantiomerically pure tripeptide **25** in an almost quantitative yield after purification. Finally, *tert*-butyl protecting group was removed through acidolysis with TFA using Et<sub>3</sub>SiH as a carbocation scavenger, to afford the free carboxylic acid, which was directly coupled to partially protected GABA **21** to obtain optically active branched tetrapeptide **27** in a 90% yield over the two steps. It is important to highlight that tetrapeptide **27** represents the first example of cyclobutane-cored dendrimers.

In order to understand the aggregation behaviour in solution of cyclobutane-cored dendrimer **27**, TEM images of aggregates from methanol solutions were recorded. It was found that concentration had a strong influence in the intermolecular interactions. As it can be seen in **Figure 12**, highly concentrated 250 mM solution showed the formation of almost crystalline aggregates with a rectangular shape, which were diffracted without success. When lowering the concentration to 50 mM (**Figure 12b**) molecules interacted forming a dense net. In highly diluted solutions (0.5 mM) the intermolecular interactions led to a very loose net (**Figure 12c**).

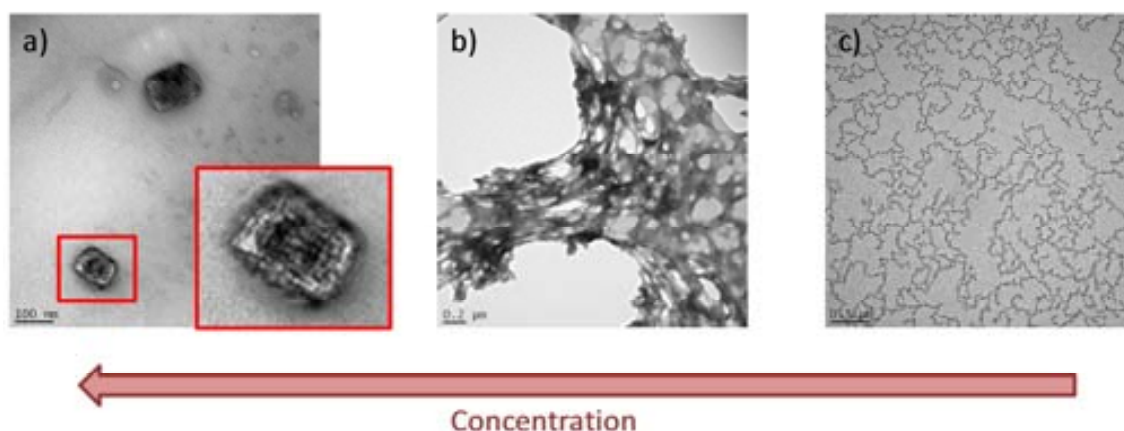
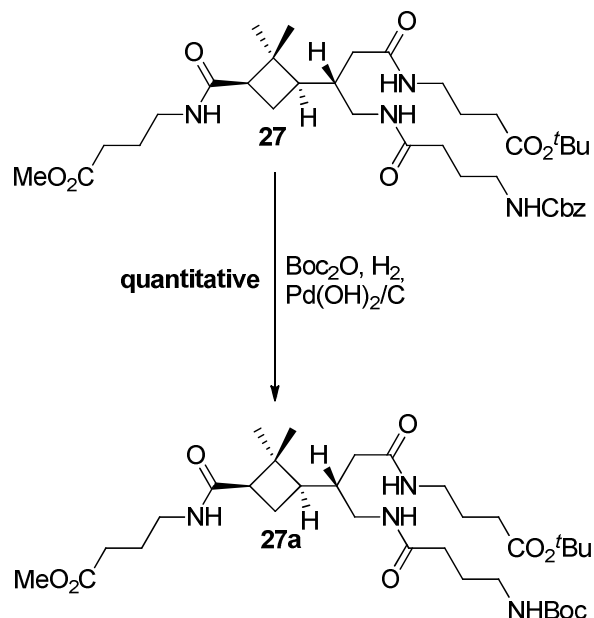


**Figure 12:** TEM micrographs of tetrapeptide **27** stained with uranyl acetate from a) 250 mM. b) 50 mM. c) 0.5 mM methanol solutions.

Additionally, the benzyl carbamate protecting group in **27** was exchanged by a *tert*-butyl carbamate by hydrogenation with Pd/C in MeOH in the presence of di-*tert*-butyl dicarbonate, in order to determine which was the influence of the protecting group nature (**Scheme 22**).



**Scheme 22:** Procedure for the synthesis of **27a**

The newly obtained tetrapeptide **27a** gellified readily (12 mM) in chloroform, whereas **27** did not, showing that the self-assembling properties of these types of compounds are highly influenced by the nature of the protecting groups.<sup>98</sup>

### **2.3.4 Structural study in solution of the series of hybrid cyclobutane-GABA peptides**

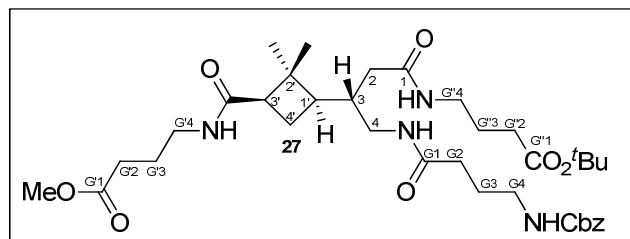
In order to test the capability of cyclobutane ring to induce defined secondary structures in solution, a structural study using different NMR techniques was carried out for the series of orthogonally protected hybrid cyclobutane-GABA peptides. The followed procedure can be summarised in the following steps:

1. NMR spectra of the peptide series assignment (<sup>1</sup>H and <sup>13</sup>C)
2. Recording of SELTOCSY spectra (bond coupling) for each NH
3. Recording of SELTOCSY spectra (space coupling) for each NH
4. Superposition and comparison of SELTOCSY and SELNOESY spectra



After complete assignment of the <sup>1</sup>H and <sup>13</sup>C NMR spectra for all the studied peptides, we realised that in all cases some of the NHs resonated at higher positions than expected. This downfield displacement could be a consequence of an intramolecular hydrogen bond formation (**Table 2**).

**Table 2:** Chemical shifts for the NHs in the series of hybrid cyclobutane-GABA peptides



| Proton                  | Dipeptide 22<br>( $\delta$ in ppm) | Tripeptide 25<br>( $\delta$ in ppm) | Tetrapeptide 27<br>( $\delta$ in ppm) |
|-------------------------|------------------------------------|-------------------------------------|---------------------------------------|
| NH <sub>amide</sub>     | 6.53                               | 6.39                                | 6.99                                  |
| NH <sub>carbamate</sub> | 5.60                               | 5.28                                | 5.38                                  |
| NH <sub>amide G'</sub>  |                                    | 5.69                                | 5.70                                  |
| NH <sub>amide G''</sub> |                                    |                                     | 7.14                                  |

As a consequence of this first evidence of the existence of a certain folding pattern, SELTOCSY spectra were recorded for all the NHs present in the different peptides. In that way, we were able to separate the different spin systems for each NH and assign them unequivocally. Afterwards, SELNOESY spectra were recorded to obtain information about the spatial disposition of the molecule, because a signal is generated only for close protons.

Finally, both SELTOCSY and SELNOESY spectras were overlaid in all cases. In that way, the appearance of new peaks in the SELNOESY spectra could be understood as a consequence of an intramolecular hydrogen bond formation. To illustrate this, the specific case of dipeptide **22** will be explained. As depicted in **Figure 13** SELNOESY spectrum from NH<sub>amide</sub> proton of **22** shows peaks for the three methylenes of the GABA residue, that do not appear in the corresponding SELTOCSY spectrum. Therefore, the mentioned amide proton is spatially close to the three methylenes of the GABA residue. This fact could be a

consequence of the formation of an intramolecular hydrogen bond that brought these protons close.

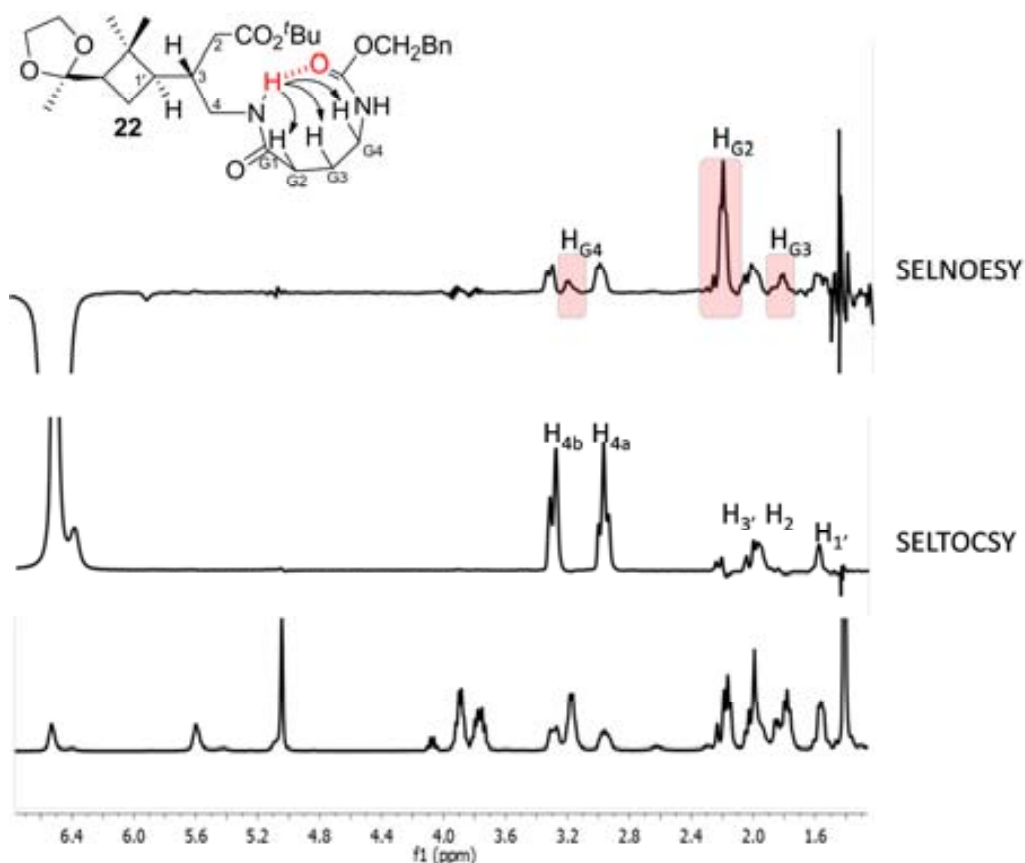


**Figure 13:** Overlay of the <sup>1</sup>H, SELTOCSY (6.53 ppm) and SELNOESY (6.53 ppm) spectra of dipeptide **22**.

To prove these results, a preliminary theoretical study was carried out in collaboration with Dr. Carles Acosta, of our research group. Firstly, a conformational search using molecular mechanics (MMFFs) was accomplished. Afterwards, the geometry of the most representative conformers was optimised both in gas phase [DFT (B3LYP/6-31G(d))] and in CHCl<sub>3</sub> [DFT (B3LYP/6-31G(d))]. The most stable conformer showed an intramolecular hydrogen bond between the NH<sub>amide</sub> proton and the carbonyl oxygen in the carbamate group, which led to a 9-membered ring (**Figure 14**). These results are in complete accordance with the experimental ones, providing a first evidence of the cyclobutane capability to induce defined secondary structures. Those calculations were not carried out for the larger peptides as a consequence of the high computational cost.

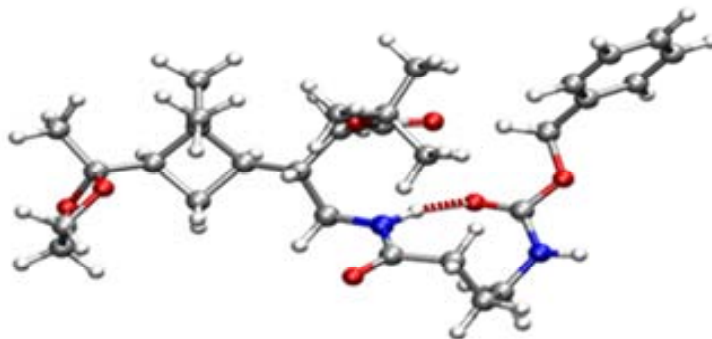


**Figure 14:** Most thermodynamically stable conformer of dipeptide **22**.

The followed procedure for the NMR structural study of dipeptide **22** in solution was also accomplished for tripeptide **25** and tetrapeptide **27** (further details can be found in Annex II). The obtained results are summarised in **Figure 15**, where we can see that the tendency to form intramolecular hydrogen bonds is preserved both in the tripeptide (**25**) and in the tetrapeptide (**27**). Therefore, it can be concluded that the synthesised  $\gamma$ ,  $\epsilon$ -amino diacid (**15**) is a good constriction motive and if we sum up its polyfunctional nature and its branched structure it could be a good candidate for the synthesis of dendrimers.

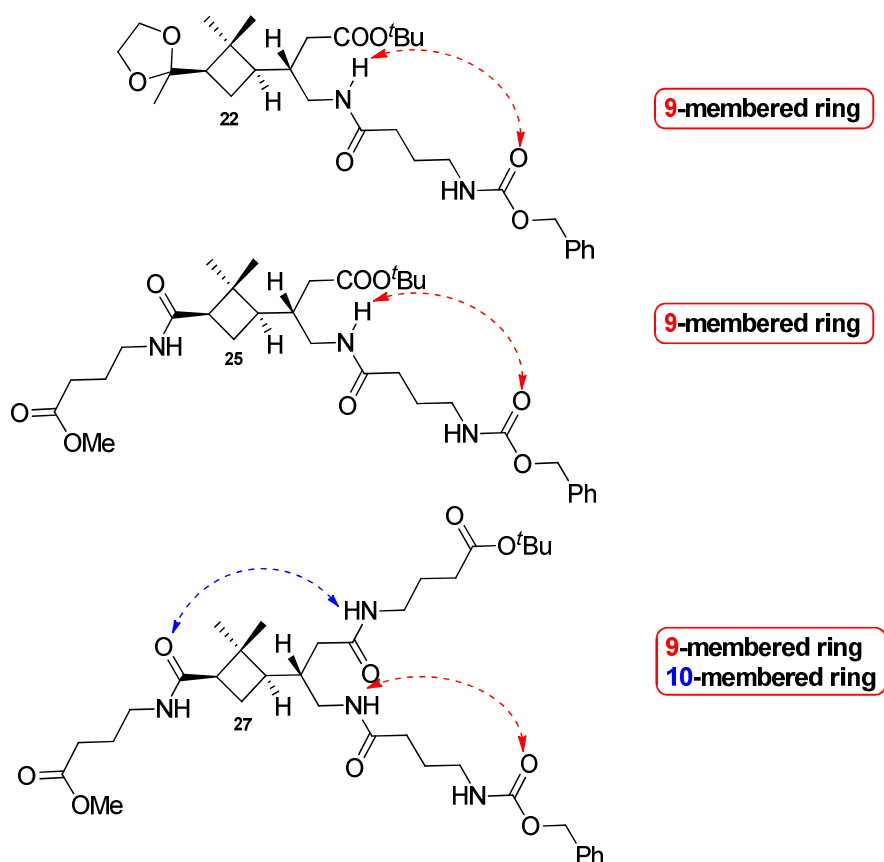
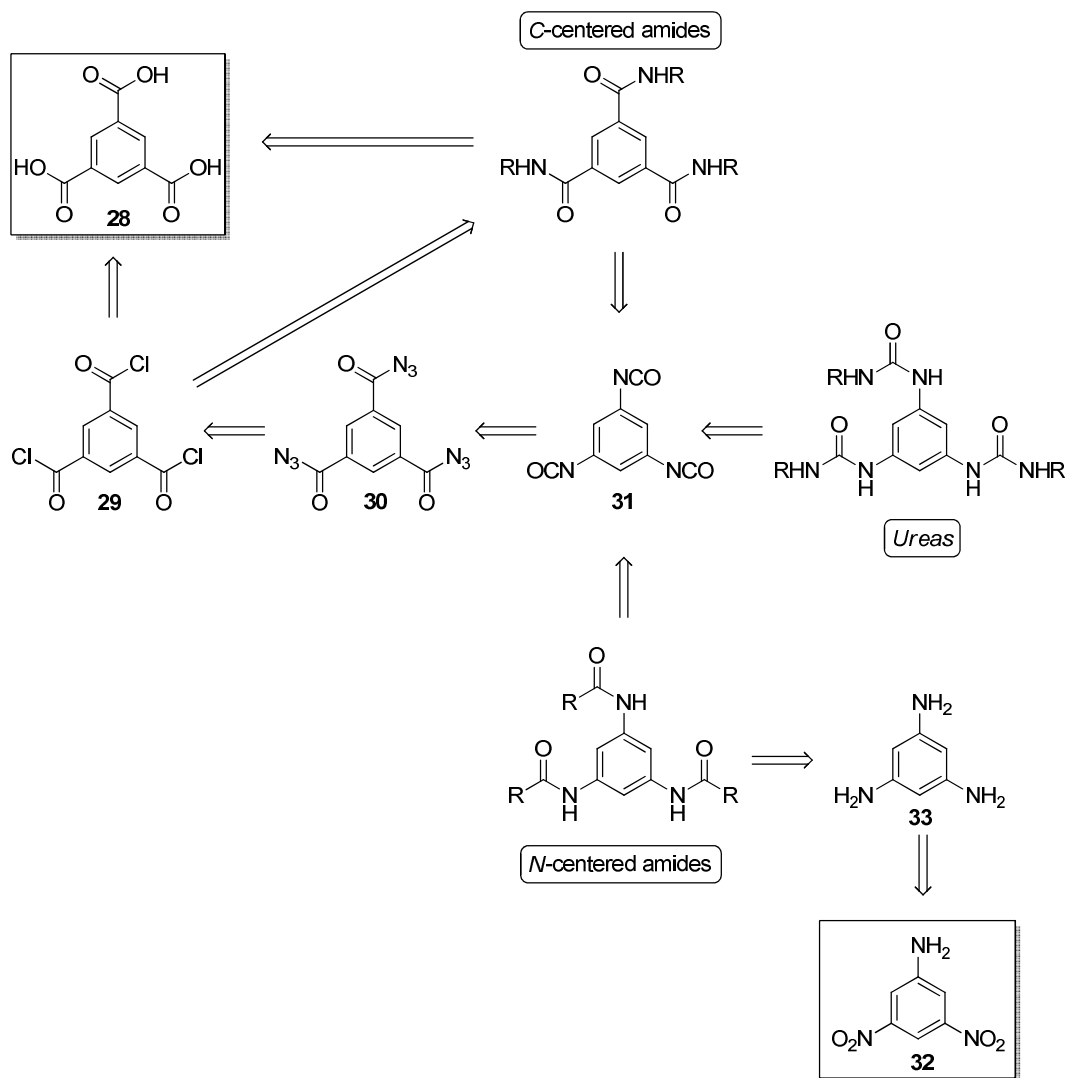


**Figure 15:** Intramolecular hydrogen bonds derived from the NMR structural study in solution for the series of peptides.

### **2.3.5 Synthesis of a cyclobutane-containing family of $C_3$ -symmetric benzene-cored dendritic molecules**

The high performance of  $C_3$ -symmetric benzene-cored molecules has been previously highlighted. Moreover, we wanted to verify if the role performed by the cyclobutane ring (nucleus or dendron) in the dendritic molecules, played any influence on their properties. According to that, a family of *C*-amide, *N*-amide and urea core-linked cyclobutane dendrimers was synthesised. These molecules were prepared following a convergent approach. This synthetic strategy, which consists of the attachment of presynthesised dendrons to the core, leads to dendrimers of monodisperse molecular weight which are easy to purify.

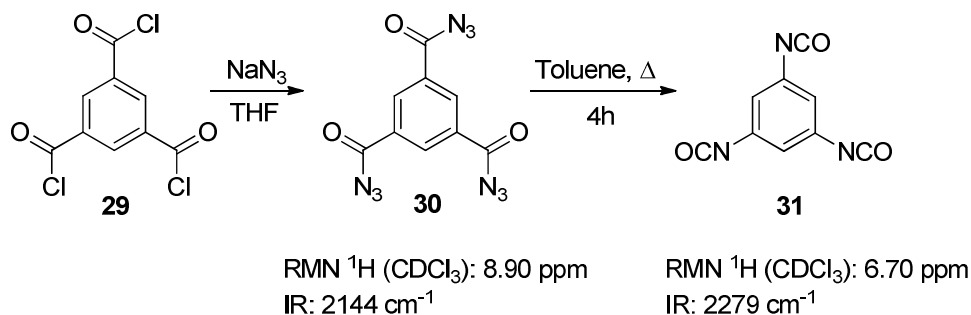
Accordingly, on a first stage the different compounds that could be used as nucleus were synthesised and characterised (**Scheme 23**).



**Scheme 23:** Target compounds and retrosynthetic analysis.

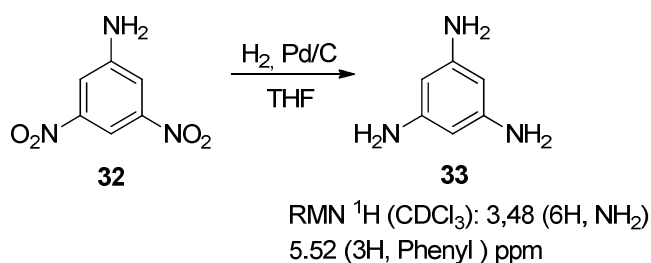
Starting from commercially available 1,3,5-benzenetricarbonyl trichloride, the corresponding triacyl azide (**30**) was prepared through reaction with sodium azide (**Scheme 24**). It is noteworthy to comment that **30** is an explosive compound which should be manipulated carefully, so it was never evaporated to dryness and metal spatula were avoided. This compound could be used for the preparation of C-centered triamides through reaction with primary amines, and when submitted to Curtius rearrangement could furnish N-centered amides and ureas. Therefore, a toluene solution of **30** was heated to reflux for 4

hours to obtain quantitatively triisocyanate **31**, which was readily reacted both with amines (leading to ureas) and carboxylic acids (leading to *N*-centered amides).



**Scheme 24:** Synthetic route leading to different C<sub>3</sub>-symmetric benzene nucleus.

Additionally, triaminobenzene **33** was obtained by reducing dinitroaniline with molecular hydrogen in the presence of palladium over carbon (**Scheme 25**). It is important to highlight that this compound was extremely unstable and it should be manipulated under inert atmosphere and used immediately in the following step. The so prepared nucleus, **33**, could be useful for the preparation of *N*-centered amides through reaction with activated carbonyls as well as for the synthesis of ureas through reaction with isocyanates.

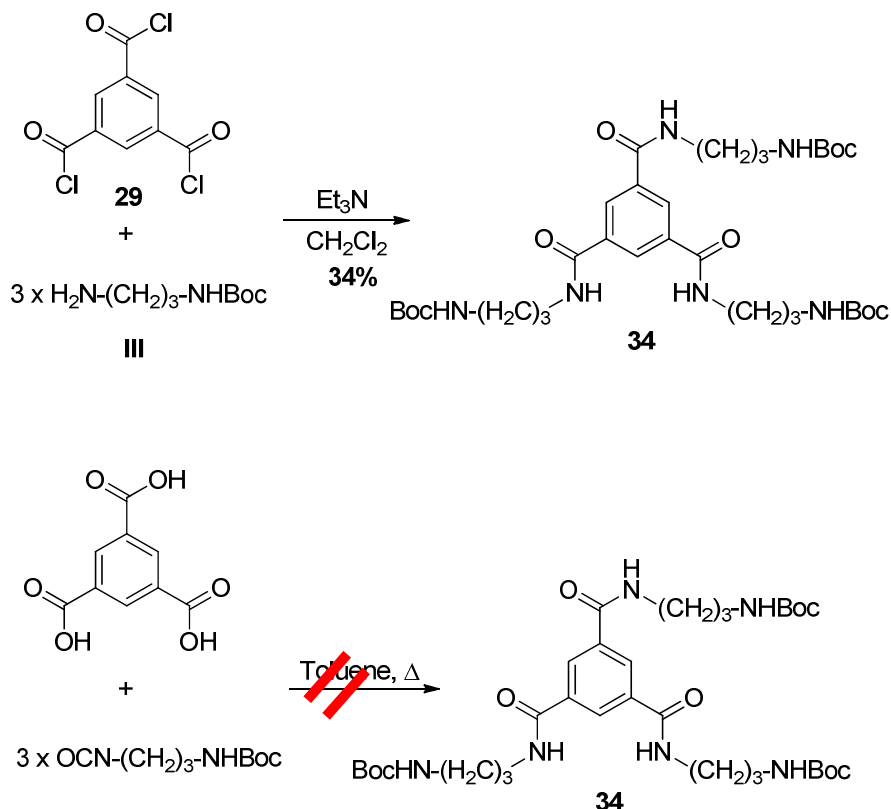


**Scheme 25:** Synthetic route leading to different C<sub>3</sub>-symmetric benzene nucleus.

Once we had a wide variety of cores we proceeded to explore their reactivity in order to design the best synthetic strategy for the preparation of a family of cyclobutane containing C<sub>3</sub>-symmetric benzene-cored dendrimers, as depicted in **Scheme 23**.

To explore the possible methodologies to use, model compounds were used. The tested methodologies for the preparation of *C*-centered benzene-cored triamides are

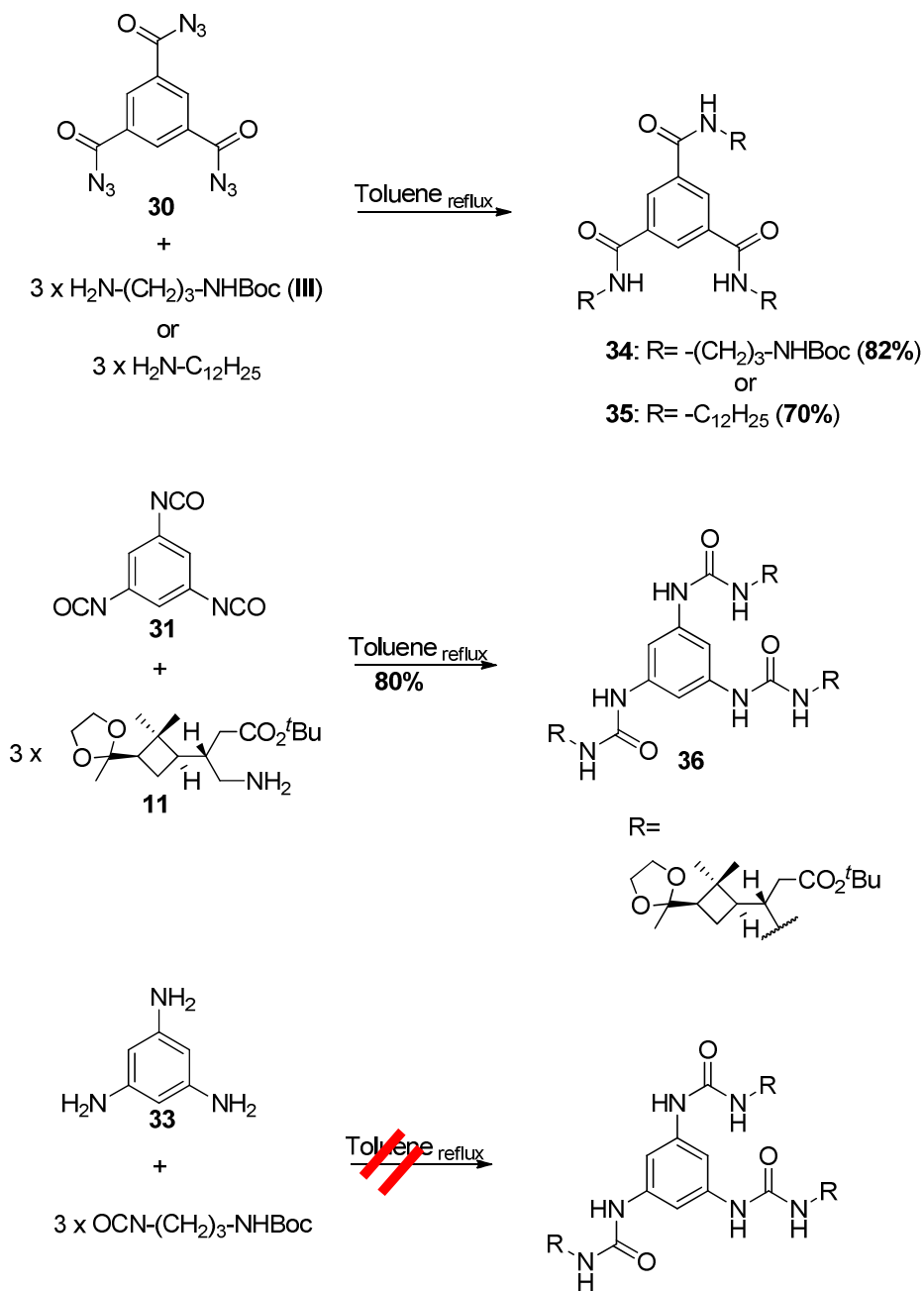
summarised in **Scheme 26**. Direct reaction of aliphatic amine **III** with 1,3,5-benzenetricarbonyl trichloride **29** afforded the corresponding triamide **34** with acceptable yields. The yield lowering of that reaction could be a consequence of the instability of trichloride **29**. Addition of trimesic acid to the isocyanate resulting from the Curtius rearrangement of acyl azide **I** was also performed, recovering unreacted trimesic acid.



**Scheme 26:** Tested reactions for the preparation of C-centered benzene triamides.

For the synthesis of benzene-cored triureas three different procedures were assayed (**Scheme 27**). Firstly, a 1 to 3 stoichiometric mixture of acyl azide **30** and amine (**III** or dodecylamine), in boiling anhydrous toluene gave the corresponding triamides. This is a consequence of the high electrophilicity of the carbonyl groups in **30**, therefore they undergo faster nucleophilic addition-elimination reaction than Curtius rearrangement. For that reason, the same reaction was carried out in two steps: Curtius rearrangement of **30** in

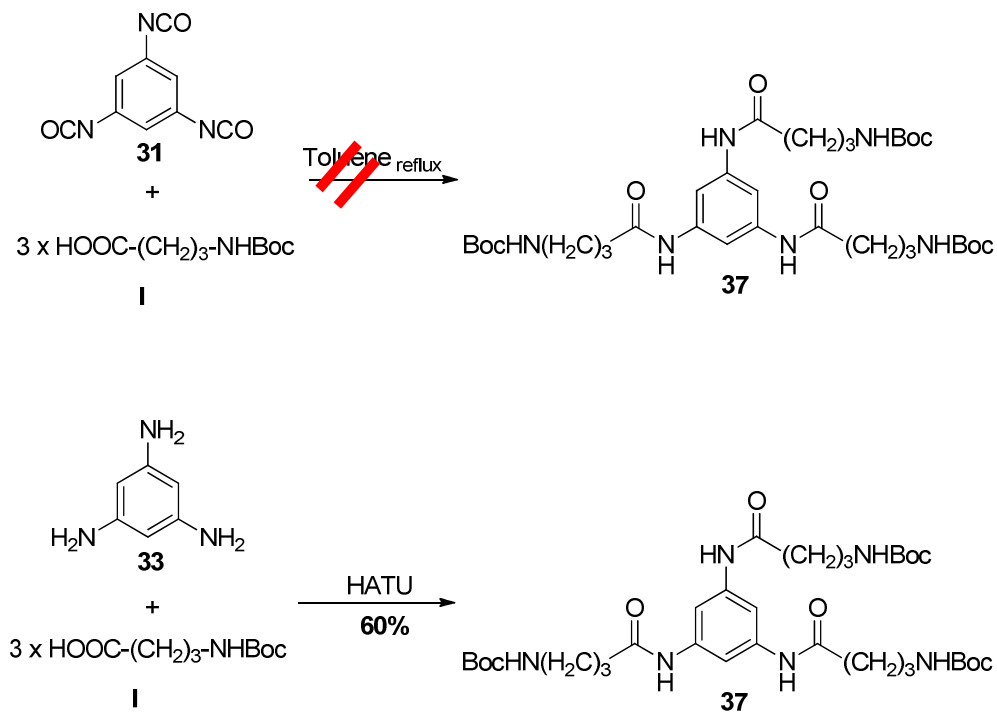
refluxing toluene to afford triisocyanate **31**, followed by addition of amine **11** to obtain desired triurea **36** with a very good yield and excellent purity. The inverse strategy was also tested, in that way triaminobenzene (**33**) was heated to reflux in the presence of three equivalents of previously prepared isocyanate from **I**. Due to the low nucleophilicity of triaminobenzene **33** unreacted product was recovered.



Scheme 27: Tested reactions for the preparation of benzene triureas.



Finally, methodologies for the synthesis of *N*-centered benzene-cored triamides were evaluated (**Scheme 28**). In a first attempt, triisocyanate **31** was heated to reflux in toluene in the presence of carboxylic acid **I**, recovering unreacted starting material. Therefore another methodology was tested: After testing several coupling reagent (EDAC, HBTU and HATU) triaminobenzene **33** was coupled to carboxylic acid **I** using HATU in the presence of DIPEA as a coupling agent, to obtain the desired *N*-centered benzene-cored triamide in 60% yield.



**Scheme 28:** Tested reactions for the preparation of *N*-centered benzene triamides.

In conclusion, when the dendron contains an amine group, both *C*-centered triamides and ureas can be synthesised. By contrast, when the dendron possesses a carboxylic group only *N*-centered triamides can be prepared.

Once we had adequate synthetic procedures leading to the differently core-linked dendrons available, it was feasible to synthesise a cyclobutane-containing family of C<sub>3</sub>-symmetric benzene-cored dendritic molecules, which are structurally interesting due to the fact that up to the moment no other example of this kind of molecules can be found in the literature.

A chart with the target dendrimers accompanied with their retrosynthetic analysis is found in **Figure 16**. As previously mentioned, we followed a convergent approach which consists of the attachment of presynthesised dendrons to the core. For the synthesis of dendrons, we used optically pure polyfunctional orthogonally protected cyclobutane  $\gamma$ -amino ester **15** and some convenient derivatives (**11** and **14**), as well as tetrapeptide **27** (**Scheme 29**).

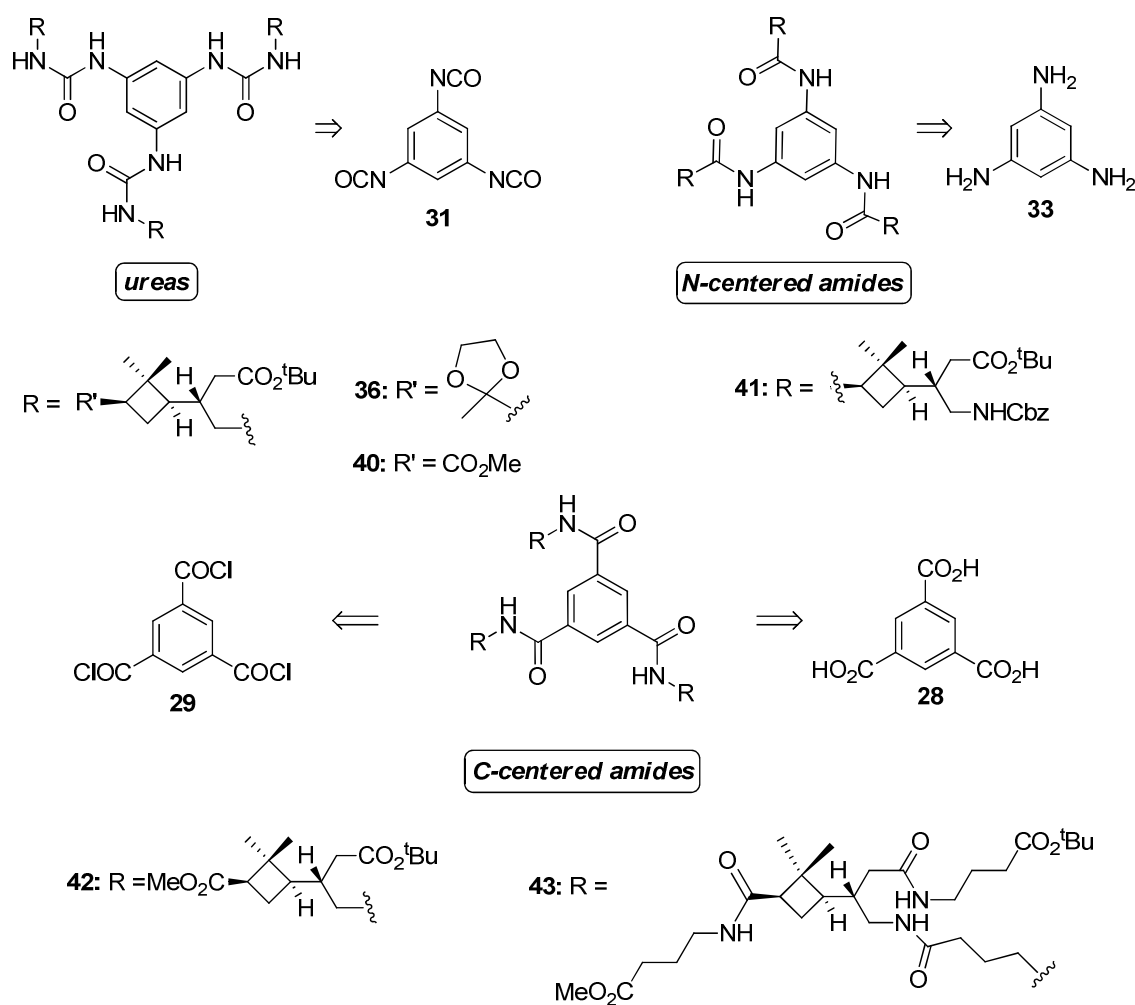
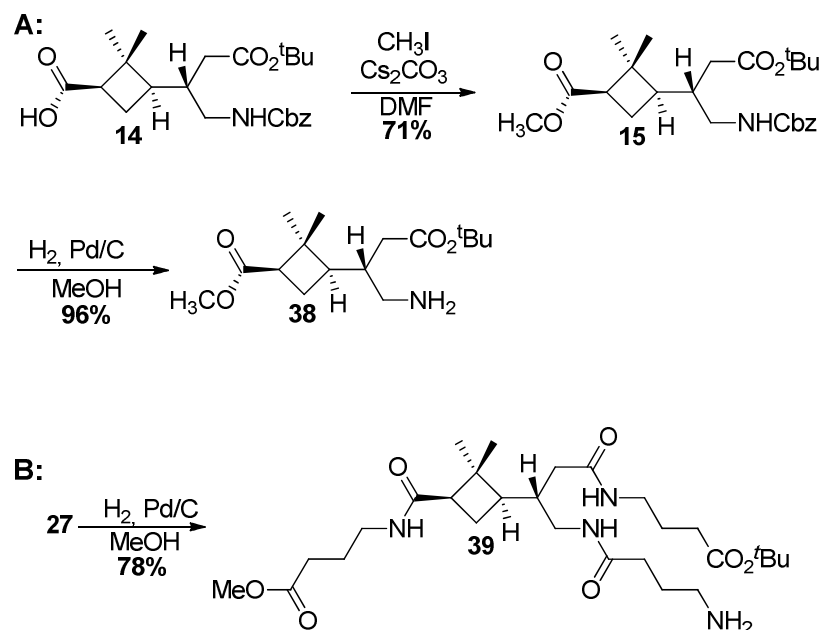


**Figure 16:** Target dendrimers and retrosynthetic analysis

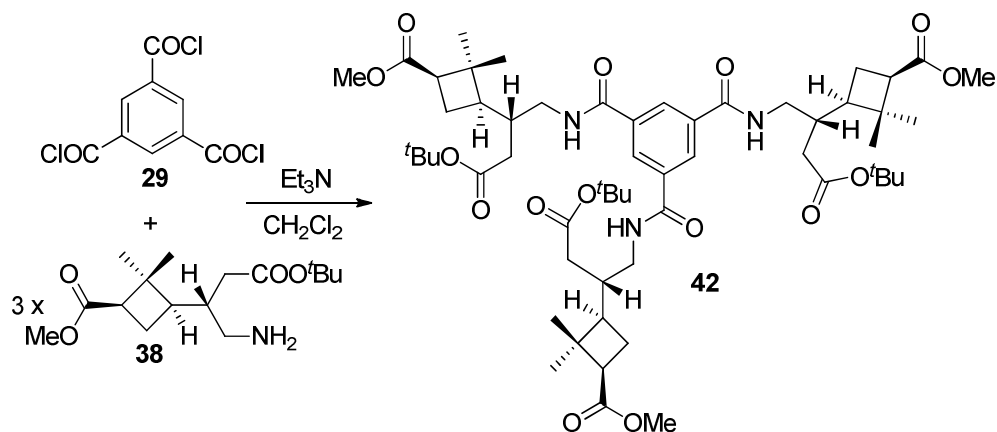
Totally protected amino diacid **15** and mixed tetrapeptide **27** were hydrogenated under 5 atm. of pressure in the presence of a catalytic amount of 10% Pd/C to provide amines **38** and **39** (96% and 78% yield respectively) (**Scheme 29**).



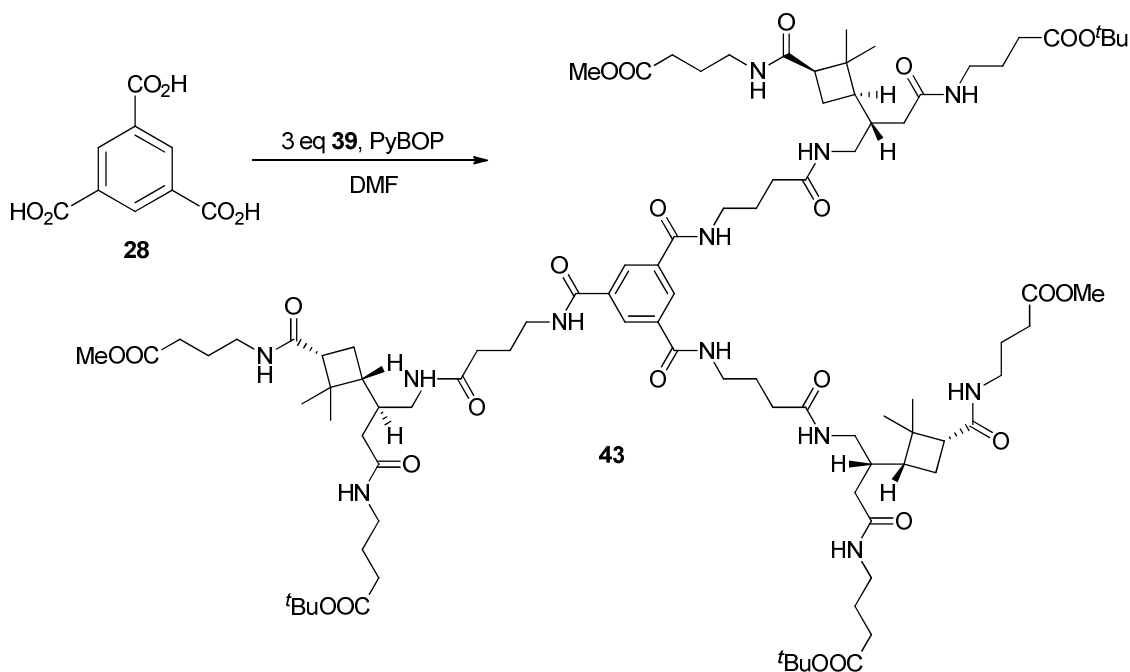
**Scheme 29:** Synthesis of cyclobutane based dendrons (**A**) and mixed cyclobutane-GABA dendrons (**B**).

All of the dendrons deriving from **15** contain a cyclobutane ring which confers rigidity and provides functional groups that can be selectively manipulated. The dendron deriving from cyclobutane-cored dendrimer **27** is based on a cyclobutane and three pending  $\gamma$ -aminobutyric acid (GABA) segments that tune up the flexibility of the molecule. This dendron is also interesting because it is known that oligomers derived from  $\gamma$ -amino acids tend to adopt defined structures.<sup>49, 52</sup>

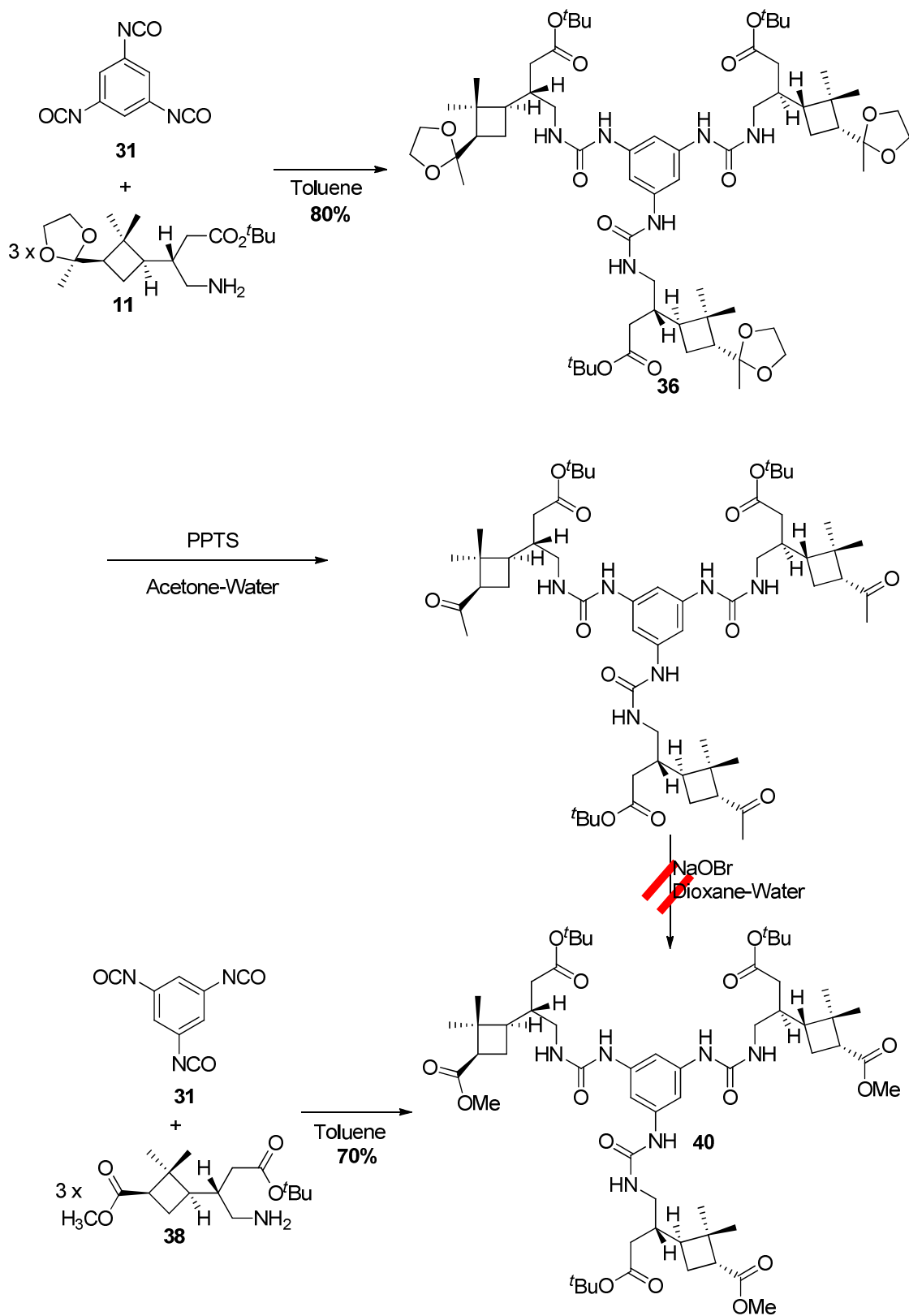
Following the previously optimised methodology for the preparation of C-centered amides, freshly prepared free amine **38** (3.1 eq) was reacted with benzyl trichloroformate **29** using triethylamine as a base in anhydrous dichloromethane. After stirring for 21 hours at room temperature the solvents were evaporated and the resulting C-centered triamide **42** was obtained in 58% yield (**Scheme 30**).

Scheme 30: Synthesis of C-centered triamide **42**.

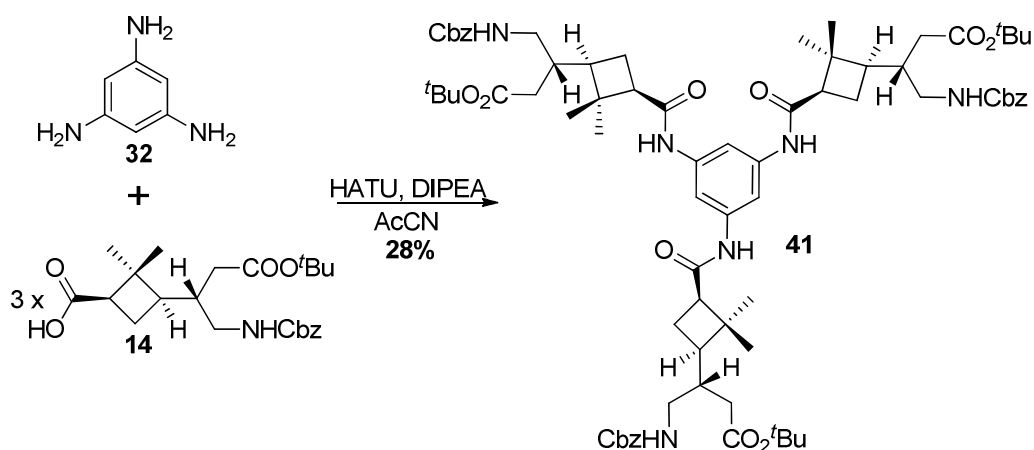
As it has been mentioned before, it is possible that the yield of the coupling reaction becomes lowered as a consequence of the intrinsic instability of benzyl trichloroformate (**29**). For that reason, C-centered triamide **43** was prepared through peptide coupling of trimesic acid and free amine **39** using PyBOP as a coupling agent to obtain the desired enantiomerically pure product **43** as a white solid in 75% yield after purification (Scheme 31).

Scheme 31: Synthesis of C-centered triamide **43**.

Triurea **36** was synthesised from freshly prepared 1,3,5-benzenetriisocyanate and aminoester **11** in anhydrous toluene at room temperature overnight (80% yield) (**Scheme 32**). Triurea **36** contains a ketal-protected methyl ketone and a *tert*-butyl ester as side groups that can be selectively deprotected for further functionalization. We were interested in testing whether it was possible to manipulate triurea **36** to synthesise triurea **40**. Deprotection of the methyl ketones worked satisfactorily, but attempts to convert it to the triacid through a Lieben degradation were unsuccessful. Transformations on the dendron amino ester **11** to prepare amine **38**, which could be then coupled to 1,3,5-benzenetriisocyanate, proved to be a much better strategy to obtain triurea **40** (70% yield). This molecule contains methyl ester and *tert*-butyl ester protecting groups, which can also be selectively removed if desired.

Scheme 32: Synthesis of triureas **36** and **40**.

As an example of a third type of dendrimer, *N*-centered triamide **41** was synthesised starting from acid **14** (Scheme 33). Previous model reactions had shown that 1,3,5-triaminobenzene **32** reacts better with a carboxylic acid in the presence of a coupling agent than with an isocyanate. This fact led us to use acid **14** in this reaction with 1,3,5-triaminobenzene, **35**, in the presence of HATU as coupling agent and DIPEA in anhydrous acetonitrile. After refluxing for 48 h, triamide **41** was obtained in a moderate yield (28%), probably due to the intrinsic instability of the 1,3,5-triaminobenzene (**32**). This convergent approach to triamide **41** is the first example in the synthesis of *N*-centered amides starting from a carboxylic acid and **32**. Product **41** contains three orthogonally protected  $\gamma$ -amino acids and is very attractive for further transformations.



Scheme 33: Synthesis of *N*-centered triamide **41**.

In summary, we have presented a very versatile synthesis of highly functionalised enantiopure peptide dendrimers with C<sub>3</sub>-symmetry. These dendrimers are also orthogonally protected, which could allow us to elongate selectively their structures and introduce further modifications.

Finally, in order to determine if the use of cyclobutane as dendron instead of as core had any influence in the structural behaviour of the resulting dendrimers, TEM images of methanol solutions of the family of the prepared benzene-cored dendrimers were recorded. Nevertheless, none of the molecules showed the formation of aggregates. For that reason, the IR spectra of all the synthesised compounds were recorded in solution. In order to

determine if any intermolecular interaction that allowed the formation of supramolecular structures was taking place, the IR spectra were recorded at different concentrations. As it can be seen in **Figure 17**, in none of the cases a significant variation of the spectra's profile through modification of the concentration can be observed. Therefore, we can conclude that in this kind of dendrimers no intermolecular interactions take place. It is important to note that all compounds show bands over  $3300\text{ cm}^{-1}$ , which indicate the formation of intramolecular hydrogen bonds that probably are more stable than the intermolecular ones.

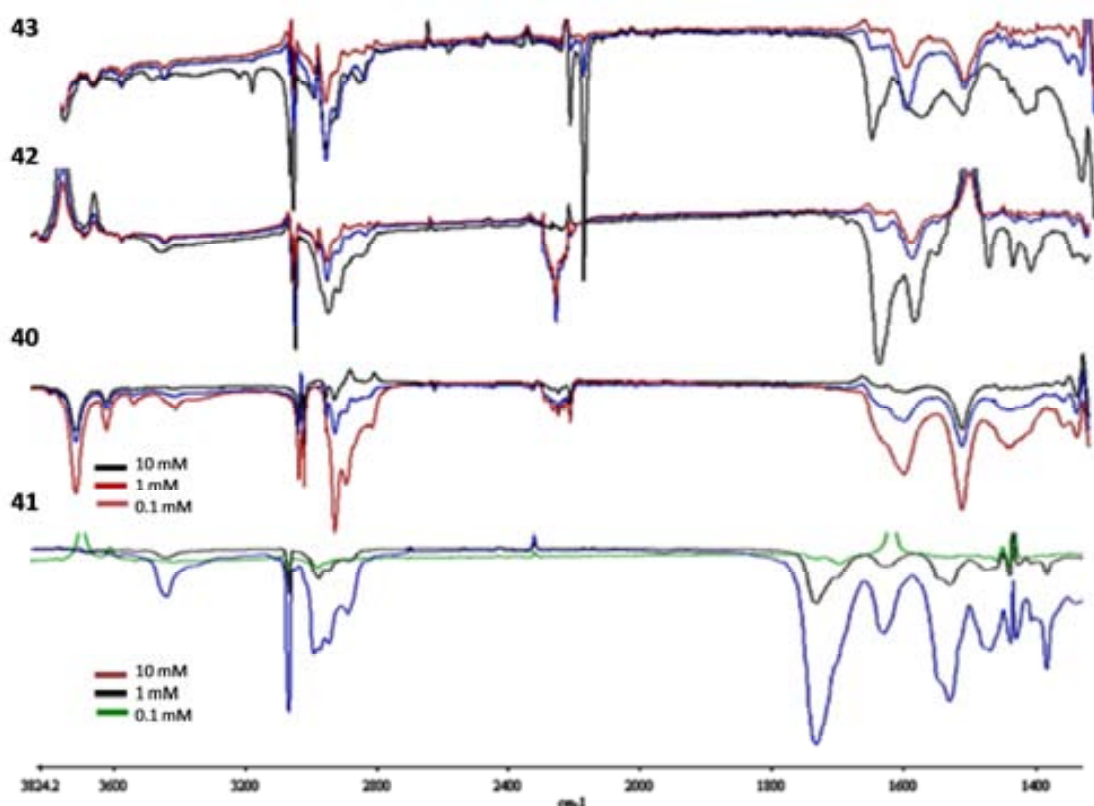


**Figure 17:** IR spectras at different concentrations of compounds **41-43**.

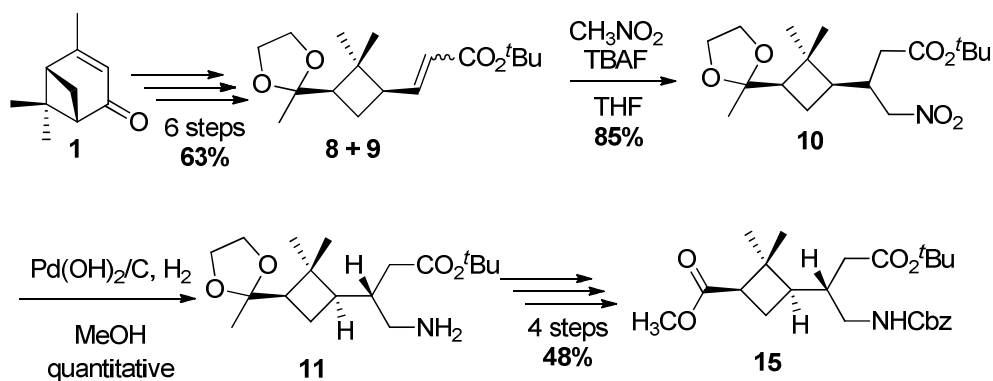
Having seen that some of the cyclobutane-core dendrimers were organogelators, the ability of the synthesised cyclobutane-containing benzene-cored dendrimers to gelate was also tested. Nevertheless, in contrast to what happened with cyclobutane-cored dendrimers, none of them showed to be suitable as organogelators.



Taking all these results into account, we can conclude that the role performed by the cyclobutane ring (nucleus or dendron) in the dendritic molecules, has a strong influence on the properties of the resulting dendrimers.

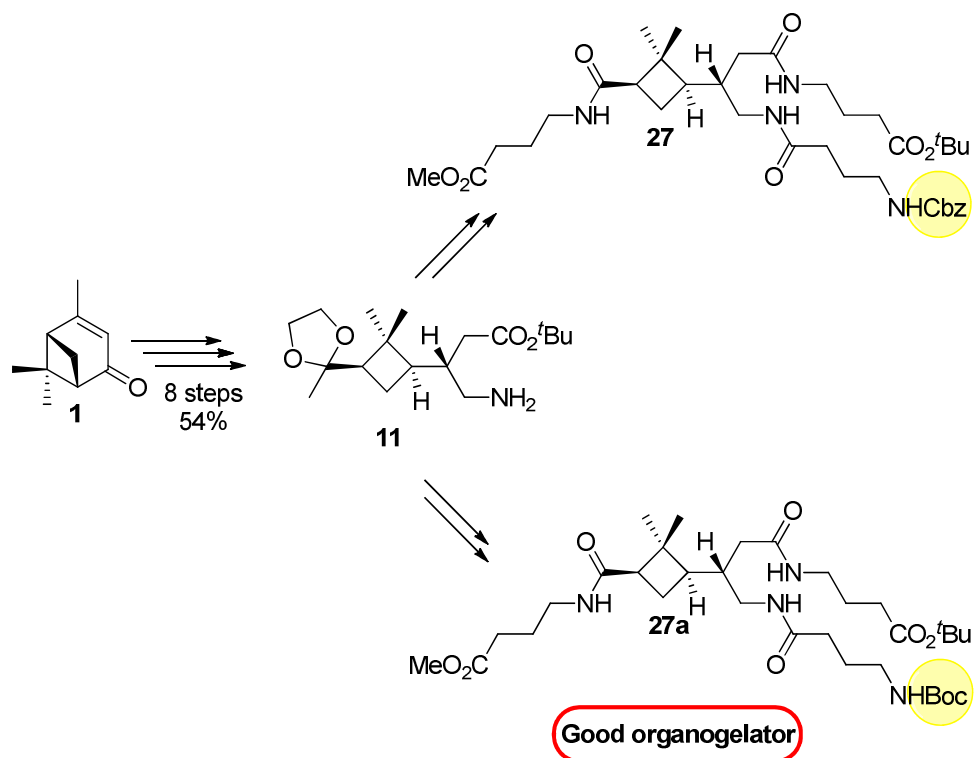
## 2.4. SUMMARY AND CONCLUSIONS: Cyclobutane Containing C<sub>3</sub>-Symmetric Peptide Dendrimers

- i) The synthesis of an orthogonally protected cyclobutane  $\gamma$ ,  $\epsilon$ -amino diacid, using (-)-verbenone as starting material has been achieved by stereoselective and high yielding transformations (**Scheme 34**) in 12 steps and with a 30% overall yield.



**Scheme 34:** Synthesis of cyclobutane  $\gamma$ ,  $\epsilon$ -amino diacid **15**.

- ii) The synthesis of a family of cyclobutane-cored first generation dendrimers has been accomplished using key intermediate **11** (**Scheme 35**).



**Scheme 35:** Synthesis of cyclobutane-cored dendrimers

- iii) The ability of the cyclobutane ring to induce secondary structures has been proved through a structural study in solution of the series of orthogonally protected peptides **22**, **25** and **27**. In all cases the rigid cyclobutane moiety induces the formation of intramolecular hydrogen bonds.
- iv) Some of the cyclobutane-cored dendrimers have shown to be good organogelators (**Scheme 35**), proving that the nature of the protecting groups allows modulating the properties of this kind of compounds.
- v) The first example of cyclobutane containing C<sub>3</sub>-symmetric peptide dendrimers has been prepared using a convergent approach (**Figure 18**). These dendrimers are highly functionalised and orthogonally protected, which could allow us to elongate selectively their structures and introduce further modifications in the future.

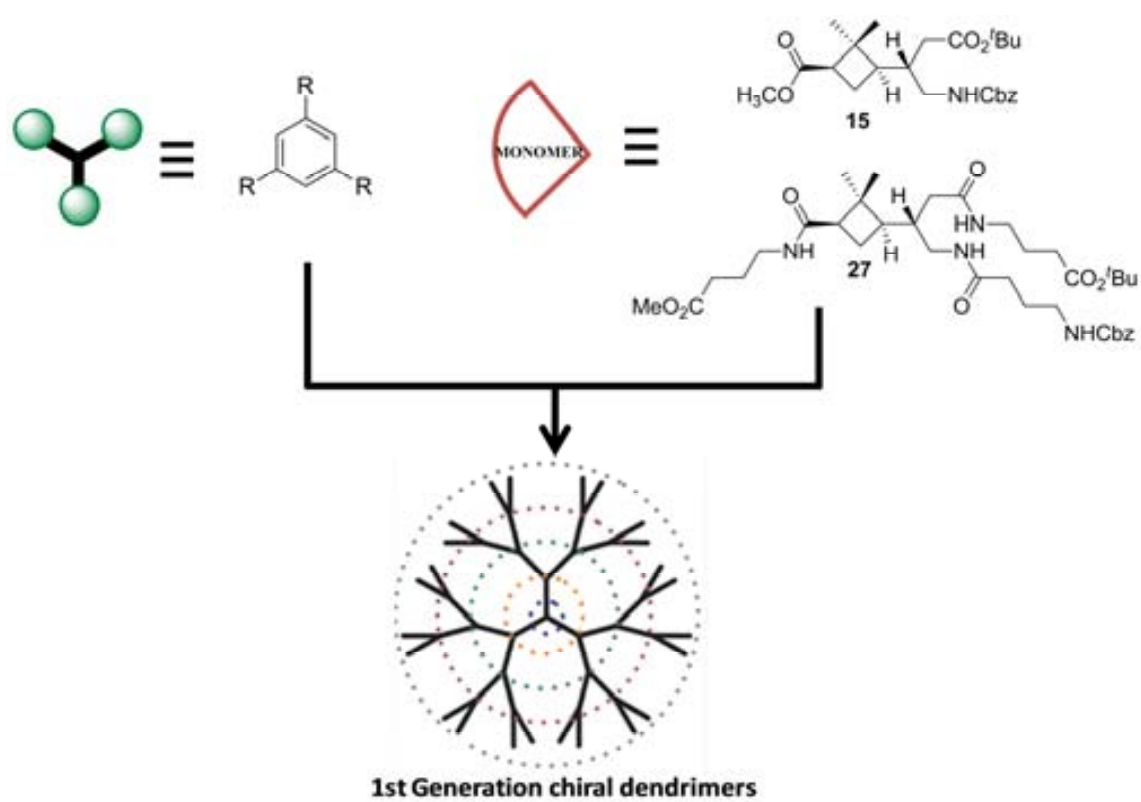


**Figure 18:** Core and dendrons used in the synthesis of cyclobutane containing  $C_3$ -symmetric peptide dendrimers.

## **Chapter II**

**Hybrid cyclobutane-proline  $\gamma$ ,  $\gamma$ -peptides:**

**Structure and cell-uptake properties**



### **3. CHAPTER II: HYBRID CYCLOBUTANE-PROLINE $\gamma$ , $\gamma$ -PEPTIDES: STRUCTURE AND CELL-UPTAKE PROPERTIES**

#### **3.1. INTRODUCTION**

##### **3.1.1 Foldamers with heterogeneous backbones**

Proteins and nucleic acids perform a wide range of complex functions in biological systems. Nearly all of these molecular operations require the biopolymer chain to adopt a compact and specific folding pattern. The conformational behaviour of biopolymers is usually analysed hierarchically: secondary structure reflects local features of the backbone (helix and sheet are the secondary structures with long-range order) which normally are a consequence of the intramolecular hydrogen bond formation, tertiary structure is formed when secondary structure elements pack against one another in intramolecular fashion, and quaternary structure arises when molecules with discrete secondary and/or tertiary structure assemble noncovalently into specific complexes. Over the past two decades many researchers have sought biopolymer-like folding behaviour in unnatural oligomers ("foldamers"), with the long-range goal of using compact and specific conformations to generate biopolymer-like functions.<sup>4</sup> Gellman and co-workers showed the ability of certain  $\alpha$  and  $\beta$ -homopolypeptides to adopt helical structures that clearly remind of those found in nature (**Figure 19**).

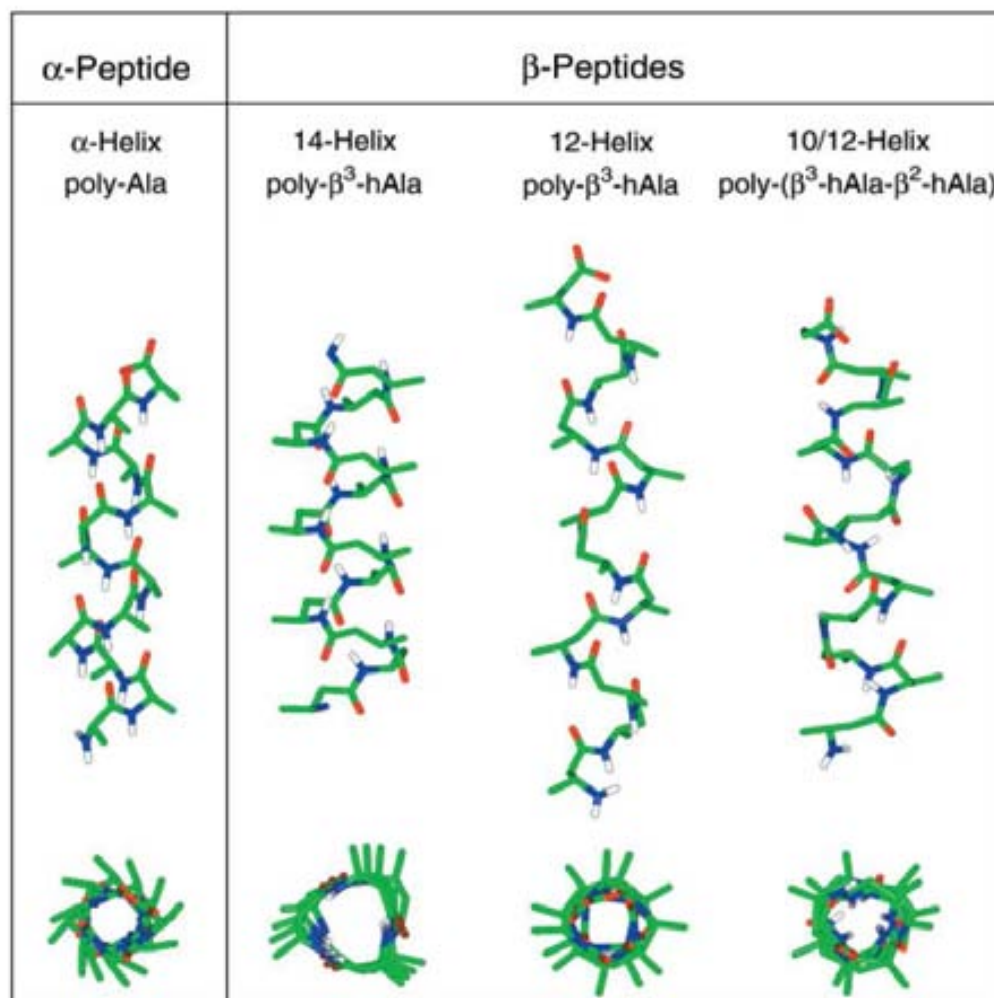


**Figure 19:** Structure of the  $\alpha$ -helix, 14-helix, 12-helix, and 10/12-helix. The hydrogens are omitted for clarity, except for the amide hydrogens (white). Carbon atoms are shown in green, nitrogen in blue, and oxygen in red.<sup>99</sup>

Most foldamers consist of homooligopeptides, but recently some examples of foldamers containing two or more different residues (hybrid peptides) have been reported. In most cases  $\alpha,\beta$ -,  $\beta,\gamma$ - or  $\alpha,\gamma$ - peptides have been prepared with the aim to enhance the ability of peptide oligomers to fold in defined manners.

The first systematic structural studies of linear oligomers with backbone alternation of  $\alpha$  and  $\beta$  residues were conducted independently by Zerbe, Reiser, and co-workers<sup>100</sup> on one hand, and by Gellman and co-workers<sup>101, 102</sup> on the other. In both cases, they were able



to demonstrate that hybrid peptides with 1:1  $\alpha,\beta$  alternation display conformational preferences unknown in shorter non-cyclic peptides containing only  $\alpha$ -amino acids.

For instance Reiser et al. reported the formation of surprisingly stable helical conformations in  $\alpha,\beta$  short peptides (from pentamer to nonamer) by incorporation of (*S*)-alanine and *cis*- $\beta$ -aminocyclopropane carboxylic acids. Those foldamers showed a tendency to form 13-helices (**Figure 20a**). Gellman and co-workers also reported the first example of  $\beta,\gamma$ - and  $\alpha,\gamma$ - mixed peptides, showing in both cases stable helical conformations (**Figures 20b and 20c**).

Recently, a collaboration between Prof. Fülöp and Prof. Reiser has revealed that  $\alpha,\beta$  and  $\alpha,\alpha,\beta,\beta$  alternation of (*S*)-alanine and *cys*- $\beta$ -amino-cyclopentanecarboxylic acid leads to stable helical structures with unprecedented 16/18 and 9/12/9/10 helices respectively.<sup>103</sup>

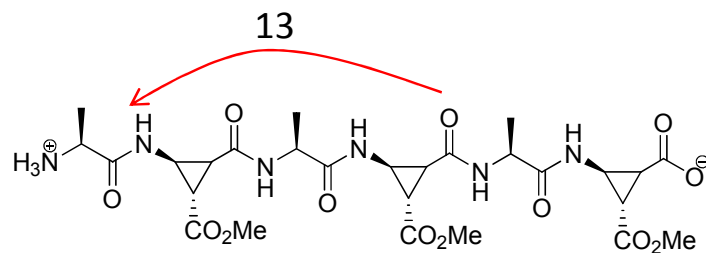
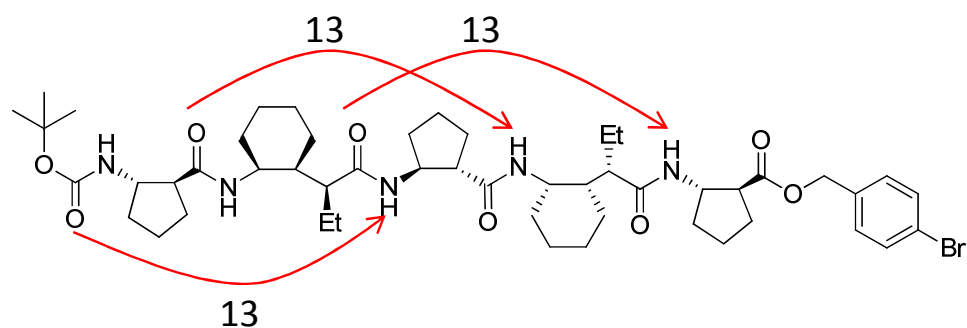
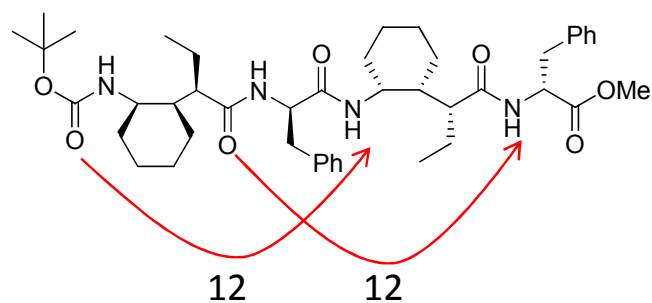
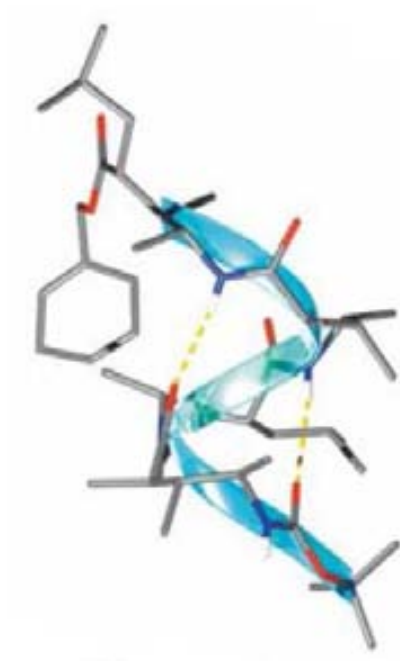
a)  $\alpha,\beta$  Foldamersb)  $\beta,\gamma$  Foldamersc)  $\alpha,\gamma$  Foldamers

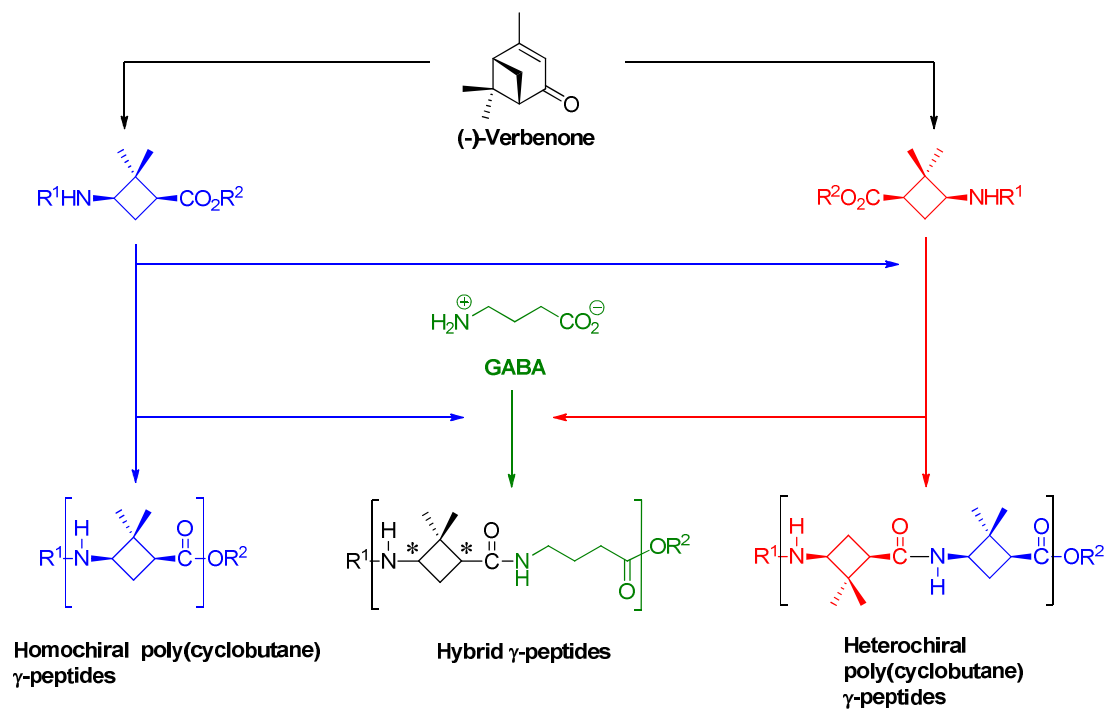
Figure 20: Hybrid foldamers helicity.

Also, combinations of different  $\beta,\beta$ <sup>32, 99</sup> and, in less extent,  $\gamma,\gamma$ -amino acids<sup>56, 43, 104</sup> have been used for these purposes. These last compounds, when using differently substituted linear monomers, led to 14-helices (**Figure 21**).



**Figure 21:** X-Ray analysis of a mixed  $\gamma,\gamma$ -tetrapeptide synthesised by Seebach and co-workers.<sup>104</sup>

In our laboratory, we have also prepared both enantiomeric forms of fully-protected cyclobutane  $\gamma$ -amino acids, which have been used for the preparation of short  $\gamma$ -peptides consisting of all-cyclobutane amino acids, with the same or different configuration, and of hybrid  $\gamma$ -peptides obtained by sequential alternation of a cyclobutane unit with GABA residues (**Scheme 36**).<sup>43</sup> Preliminary results show the tendency of these oligomers to adopt extended conformations due to the capability of cyclobutane ring to disrupt the natural tendency of  $\gamma$ -peptides to form the nearest neighbouring hydrogen bond.<sup>44</sup>



Scheme 36: Family of  $\gamma,\gamma$ -peptides synthesised in our laboratory.

Moreover, some authors have shown that replacement of linear residues by alicyclic ones has resulted, in some instances, in the formation of strong secondary structures and in changing their biological properties.<sup>105, 106</sup>

### 3.1.2 Use of 4-amino-prolines in peptide chemistry

4-Aminoprolines when included in oligomers, can behave both as an  $\alpha$ - and as a  $\gamma$ -amino acid with an additional amino function. The key lies on which amino group is involved in the peptide bond (Figure 22).

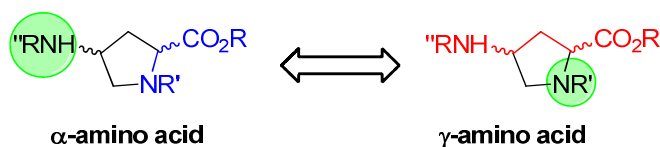
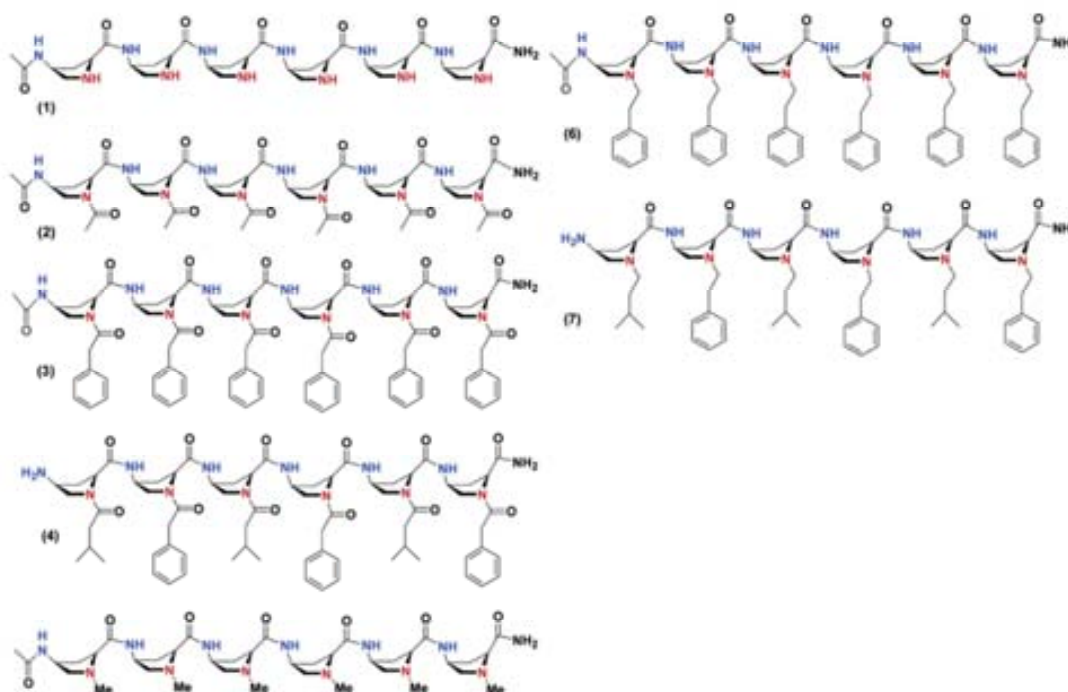


Figure 22: 4-Aminoprolines  $\alpha$ - or  $\gamma$ -amino acid behaviour.

They are useful scaffolds for the construction of  $\gamma$ -oligomers that can be modified by introduction of alkyl chains or other functional groups by manipulation of the free pyrrolidine N $^{\alpha}$ . The ability of homopeptides containing some of these moieties to fold into defined secondary structures, has been investigated by Giralt and co-workers,<sup>107</sup> who synthesised a family of *cis*- $\gamma$ -amino-L-proline  $\gamma$ -hexapeptides with different side-chains in the  $\alpha$ -amino group (**Figure 23**). From the NMR structural study in solution they concluded these compounds were found in equilibrium with several conformations.



**Figure 23:** Chemical structures of the *cis*- $\gamma$ -aminoproline oligomers synthesised by Giralt and co-workers.

To mention some applications, 4-aminoprolines and derivatives have been used for the synthesis of distamycin analogues with DNA binding affinity,<sup>108</sup> for the synthesis of helical dendronised polymers<sup>109, 110</sup> and for the preparation of cell-penetrating peptides.<sup>111</sup>

### 3.1.3 Cell penetrating peptides

The process of introducing drugs into cells has always proved to be a major challenge for research scientists and for the pharmaceutical industry. The cell membrane is selectively permeable and supports no generic mechanism for their uptake. A drug must be either highly lipophilic or very small to stand a chance of cellular internalization. These restrictions mean that the repertoire of possible drug molecules is limited. Similarly, novel therapeutic approaches such as gene and protein therapy also have limited potential due to the cell-impermeable nature of peptides and oligonucleotides. The existing methods for delivery of macromolecules, such as viral vectors<sup>112</sup> and membrane perturbation techniques,<sup>113</sup> can result in high toxicity, immunogenicity and low delivery yield. However, in 1988 the remarkable ability of a peptide to traverse a cell's plasma membrane independent of a membrane receptor was revealed. Known as TAT (Trans-Activating Transcriptional activator) peptide, the transcription activator of the human immunodeficiency virus type 1 (HIV-1) viral genome was shown to enter cells in a non-toxic and highly efficient manner.<sup>114</sup> In light of such properties TAT became known as the first 'cell-penetrating peptide' (CPP) and nowadays is used as reference peptide. From that moment up to nowadays, several CPPs have been described in the literature<sup>115, 116, 117, 118</sup> as a consequence of the remarkable advantages offered by them over other known cellular delivery systems, including low toxicity, high efficiency toward different cell lines, and even inherent therapeutic potential (Figure 24).

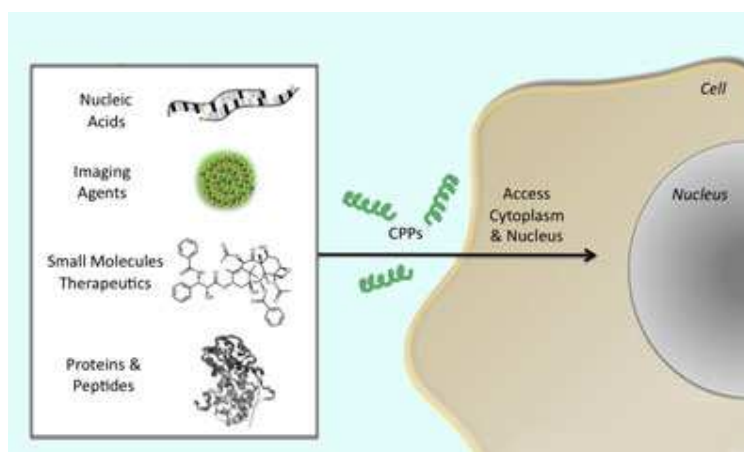


Figure 24: Molecules that can be carried by CPPs into cytoplasm and/or nucleus.

Nevertheless, these peptide-based compounds are limited by their low protease resistance and, sometimes, low membrane permeability.<sup>119, 120</sup> Hence, compounds with greater proteolytic resistance, such as oligomers,<sup>121, 122</sup> have been evaluated as drug delivery agents. However, amino acid homologation has become the most effective strategy, as a consequence of the high resistance towards proteases as well as the chance that they offer to generate biomolecular mimetics, such as  $\beta$ - or  $\gamma$ -foldamers<sup>111, 123, 124, 125</sup> which have been evaluated as drug delivery agents.

Peptides capable of translocating the cell membrane can be classified into two groups:

- (i) Cationic peptides with at least six charged amino acids (Lys or Arg) such as TAT peptide
- (ii) Hydrophobic peptides, such as those based on the H-region of signal-sequence proteins.<sup>126</sup>

Previous works reported that proline-rich peptides<sup>111, 127, 128</sup> and proline dendrimers<sup>64</sup> can be internalised by eukaryotic cells. The most important advantage of proline-rich peptides in biological systems is their solubility in water. In this context, the use of 4-aminoproline would be interesting, as a consequence of its free amine group which enables to modulate the hydrophobic/hydrophilic character of the peptides. A remarkable example has been reported by Giralt and co-workers who synthesised cis- $\gamma$ -amino-proline oligomers functionalised at the pyrrolidine nitrogen with several groups that mimicked the side chains of natural amino acids (**Figure 25**).<sup>111</sup>

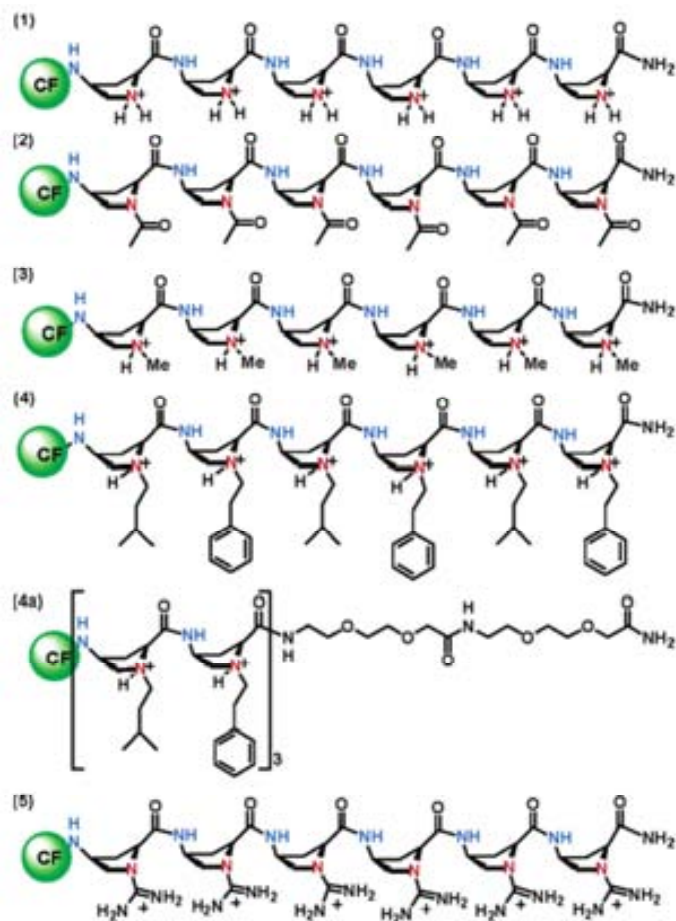


**Figure 25:**  $\gamma$ -Aminoproline monomer based  $\gamma$ -peptides labelled with 5(6)-carboxyfluorescein prepared by Giralt and co-workers.<sup>111</sup>

The capability of the mentioned peptides to enter into the eukaryotic cells was evaluated using a variety of techniques, such as plate fluorimetry (**Figure 26**), flow cytometry, and confocal microscopy to determine subcellular localization.



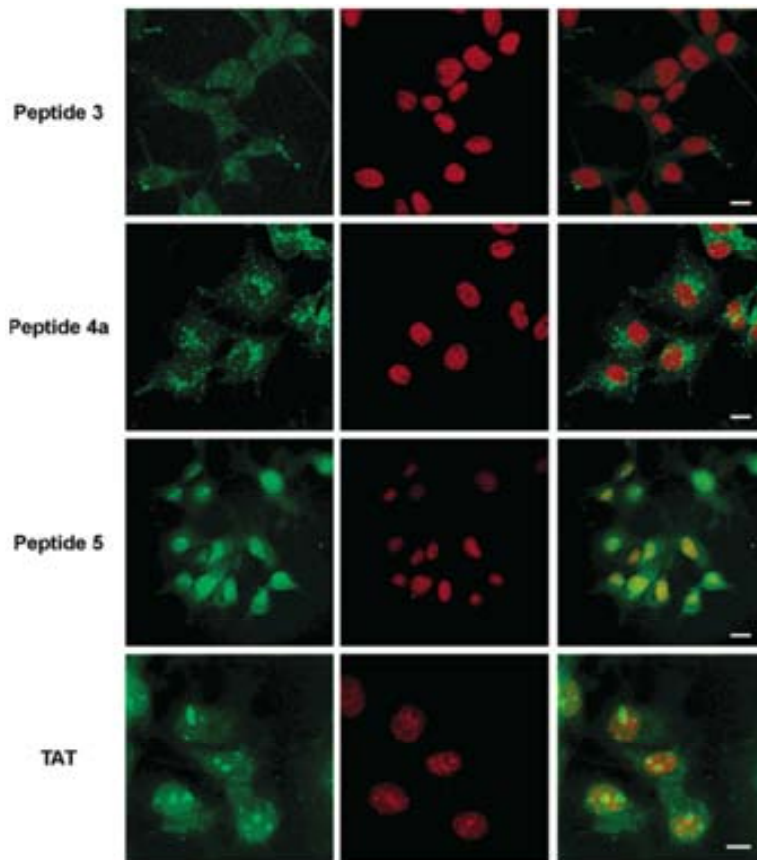


**Figure 26:** Confocal images of COS-1 cells illustrating the internalization of some of the peptides tested by Giralt and co-workers.<sup>111</sup>

In addition to their capability of entering into cells, these unnatural short length oligomers offered the important advantages over the reference TAT peptide of being less toxic and having higher protease resistance (**Figure 27**).

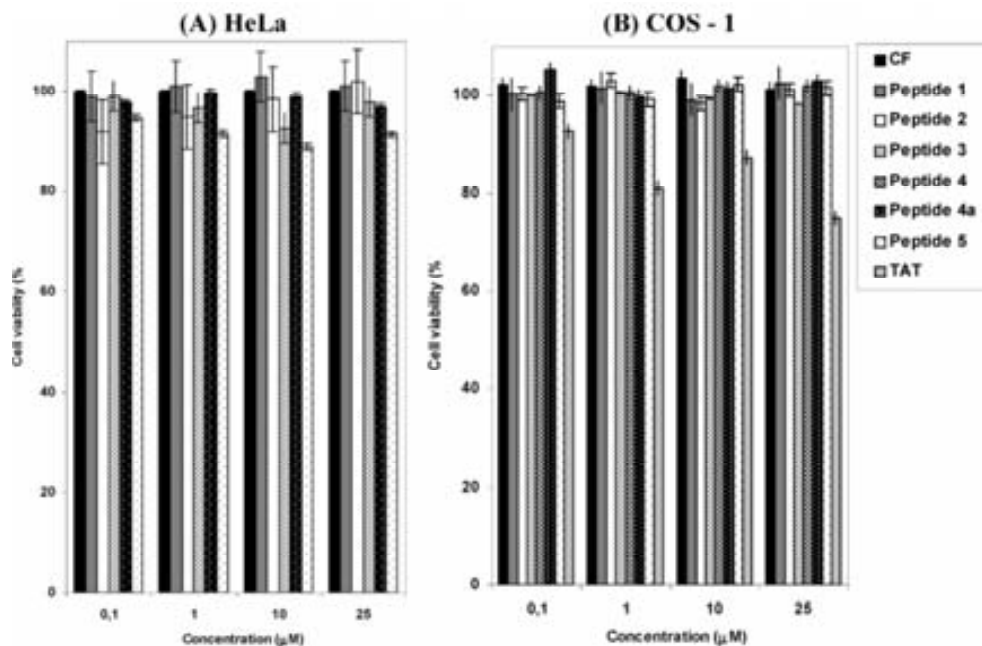
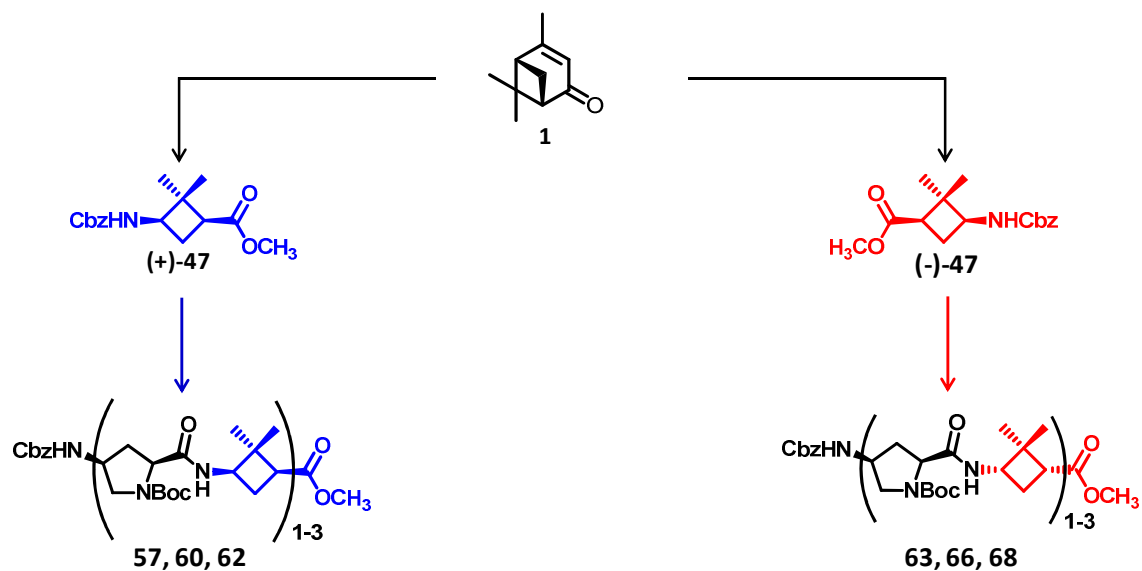


**Figure 27:** Cell viability of the different  $\gamma$ -peptides described by Giralt and co-workers as monitored in (A) HeLa and (B) COS-1 cell lines. Cell death was quantified using the MTT assay after 1 day of incubation using different peptide concentrations.<sup>111</sup>

### 3.2. OBJECTIVES

Foldamers with heterogeneous backbones (hybrid peptides) consisting of  $\alpha,\beta$ -,  $\beta,\gamma$ - or  $\alpha,\gamma$ -amino acids, and in less extent  $\gamma,\gamma$ -amino acids, have been prepared with the aim to enhance the ability of peptide oligomers to fold in defined manners. Moreover, proline-rich peptides have shown to be very useful monomers in the preparation of CPPs, being of special interest 4-aminoproline because through side chain modification enables the modulation of the hydrophobic/hydrophilic character of the resulting peptides.

In this context, we planned to use the experience in our laboratory in the synthesis and structural study of enantiomerically pure highly constricted cyclobutane  $\gamma$ -amino acids and peptides, to prepare a family of hybrid cyclobutane-proline  $\gamma$ ,  $\gamma$ -peptides (**Scheme 37**).



Scheme 37: Objective 1.

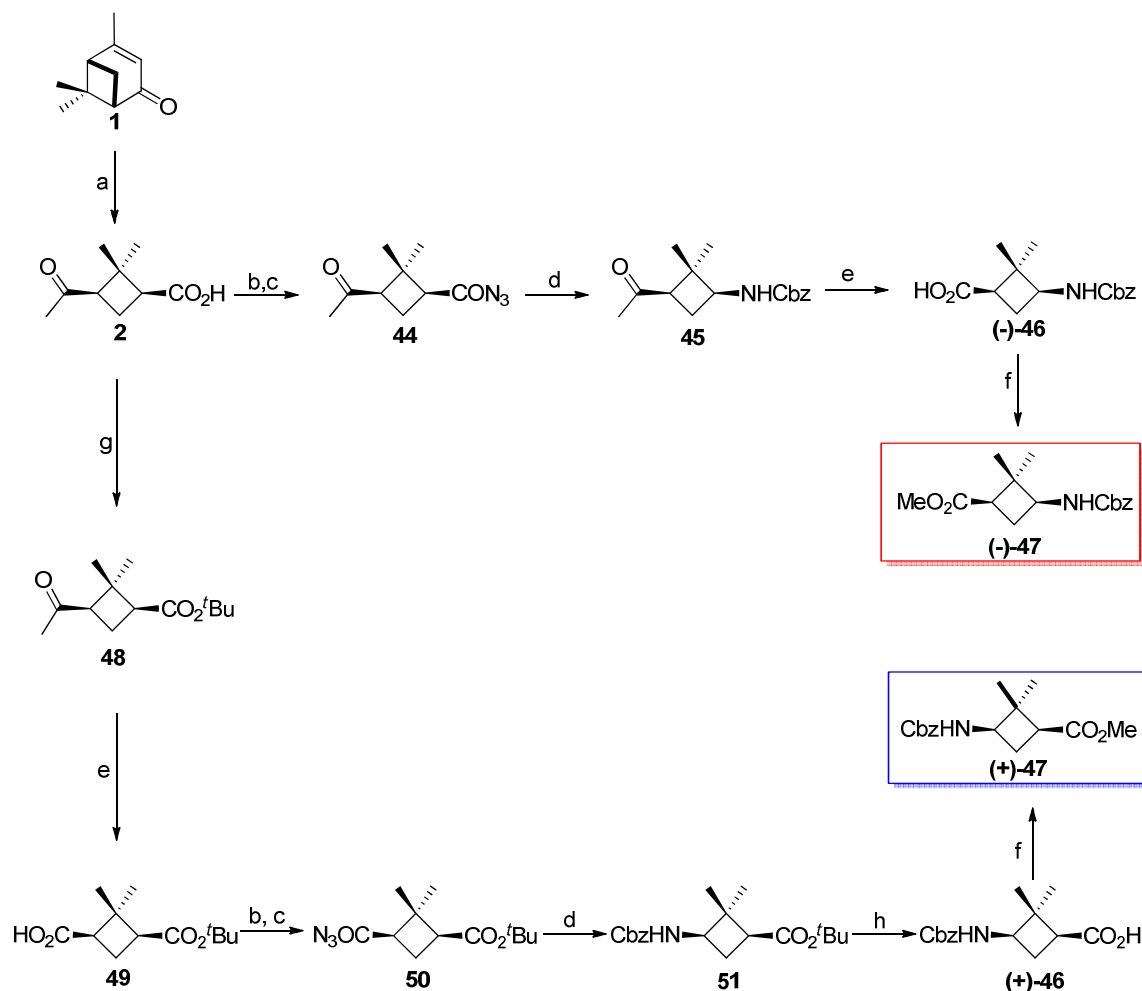
Next, a structural study in solution of the orthogonally protected peptides was carried out in order to determine their conformational bias.

Finally, the capability of these peptides to penetrate into cells was tested.

### 3.3. RESULTS AND DISCUSSION

#### 3.3.1 Synthesis of both enantiomers of orthogonally protected cyclobutane $\gamma$ -amino acid, (-)-47 and (+)-47

As previously described, catalytic oxidation of commercially available (-)-verbenone leads to (-)-*cis*-pinononic acid **2** (Scheme 38) without epimerization.<sup>36</sup>



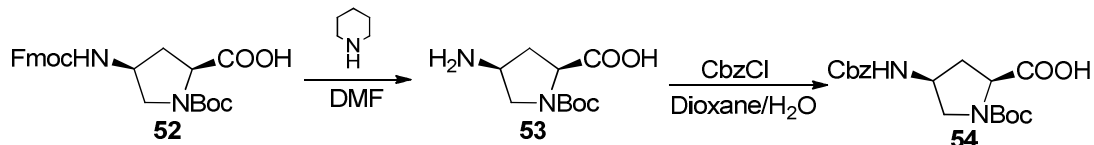
**Scheme 38:** Reagents, conditions, yields: (a) RuCl<sub>3</sub>, NaIO<sub>4</sub>, CH<sub>2</sub>Cl<sub>2</sub>/CH<sub>3</sub>CN/H<sub>2</sub>O, rt, quantitative; (b) ClCO<sub>2</sub>Et; (c) NaN<sub>3</sub>, (90% for **2**, 98% for **45**, two steps); (d) BnOH, toluene, reflux, (92%); (e) NaOBr, dioxane/H<sub>2</sub>O, (80% for **44**, 93% for (+)-**46**); (f) CH<sub>3</sub>I, Cs<sub>2</sub>CO<sub>3</sub>, DMF, (95%); (g) <sup>t</sup>BuOH, DMAP, EDAC, Et<sub>3</sub>N, anhydrous THF, 0 °C, (60%); (h) TFA, Et<sub>3</sub>SiH, CH<sub>2</sub>Cl<sub>2</sub>, (94%).

Carboxyl group from pinonic acid, **2**, was activated by formation of a mixed anhydride through reaction with ethyl chloroformate and subsequent reaction with sodium azide afforded acyl azide **44**, which was submitted to Curtius rearrangement by heating in toluene in the presence of benzyl alcohol to afford benzyl carbamate **45** with a 90% yield from pinonic acid **2**. Lieben degradation of the methyl ketone in **45** and esterification of the resulting carboxylic acid with methyl iodide produced orthogonally protected (1*R*,3*S*)-cyclobutane amino acid (-)-**47** with a 88% overall yield of the two steps. Two different methodologies were tested for this last step, on the one hand carboxylic acid was methylated through the action of diazomethane, which was generated *in situ* from diazald, which undergoes an internal rearrangement. Even though this methodology allows the access to the corresponding methyl esters with a quantitative yield, it is limited by the high instability and toxicity of diazomethane, thus allowing the performance of the reaction only in small amounts. Therefore, when working in a multi-gram scale the reaction was performed with methyl iodide using Cs<sub>2</sub>CO<sub>3</sub> as base to isolate the corresponding methyl ester in 86% yield

To obtain the enantiomeric form of (-)-**47**, the same procedure was followed but the order of the steps was exchanged. Alternatively, protection of the free carboxylic acid as a *tert*-butyl ester using <sup>t</sup>BuOH in the presence of EDAC and a catalytic amount of DMAP, led to **48** in 60% yield after purification. Next, methyl ketone **48** was submitted to Lieben degradation to afford carboxylic acid **49**. This was transformed into benzyl carbamate **51** following a 3-step procedure: activation of the carboxyl group by formation of a mixed anhydride through reaction with ethyl chloroformate and subsequent reaction with sodium azide afforded acyl azide **50**, which was submitted to Curtius rearrangement by heating it in toluene in the presence of benzyl alcohol. In this way, orthogonally protected amino acid **51** was obtained in 90% yield. Finally, *tert*-butyl ester in **51** was exchanged in order to make it suitable for the peptide synthesis (N <sup>$\alpha$</sup>  in 4-amino-proline **54** is protected with a *tert*-butyl carbamate). Acydolysis of the *tert*-butyl ester in **51** afforded free carboxylic acid (+)-**46** which was subsequently methylated to afford enantiomerically pure (1*S*,3*R*)-cyclobutane amino acid (+)-**47** in 89% overall yield, which is the enantiomeric form of orthogonally protected amino acid (-)-**47**.

### 3.3.2 Synthesis of partially protected 4-amino proline **54**

Commercially available *N*-Boc-*cis*-4-*N*-Fmoc-amino-L-proline does not bear adequate protecting groups for synthesis in solution of hybrid cyclobutane-proline peptides using (-)-**47** and (+)-**47** as monomers. In consequence, Fmoc (9-fluorenyl-methyloxycarbonyl) protecting group was cleaved by dissolving **52** in a 20% solution of piperidine in DMF and stirring for 15 minutes (**Scheme 39**). Afterwards, the previously obtained free amine **53** was suspended in a 1:1 mixture of dioxane/water, pH was adjusted to 9 through the addition of NaHCO<sub>3</sub> and CbzCl was added. The reaction was stirred for 3 hours to isolate, after column purification *N*-Boc-*cis*-4-*N*-Cbz-amino-L-proline **54** with a 60% overall yield.



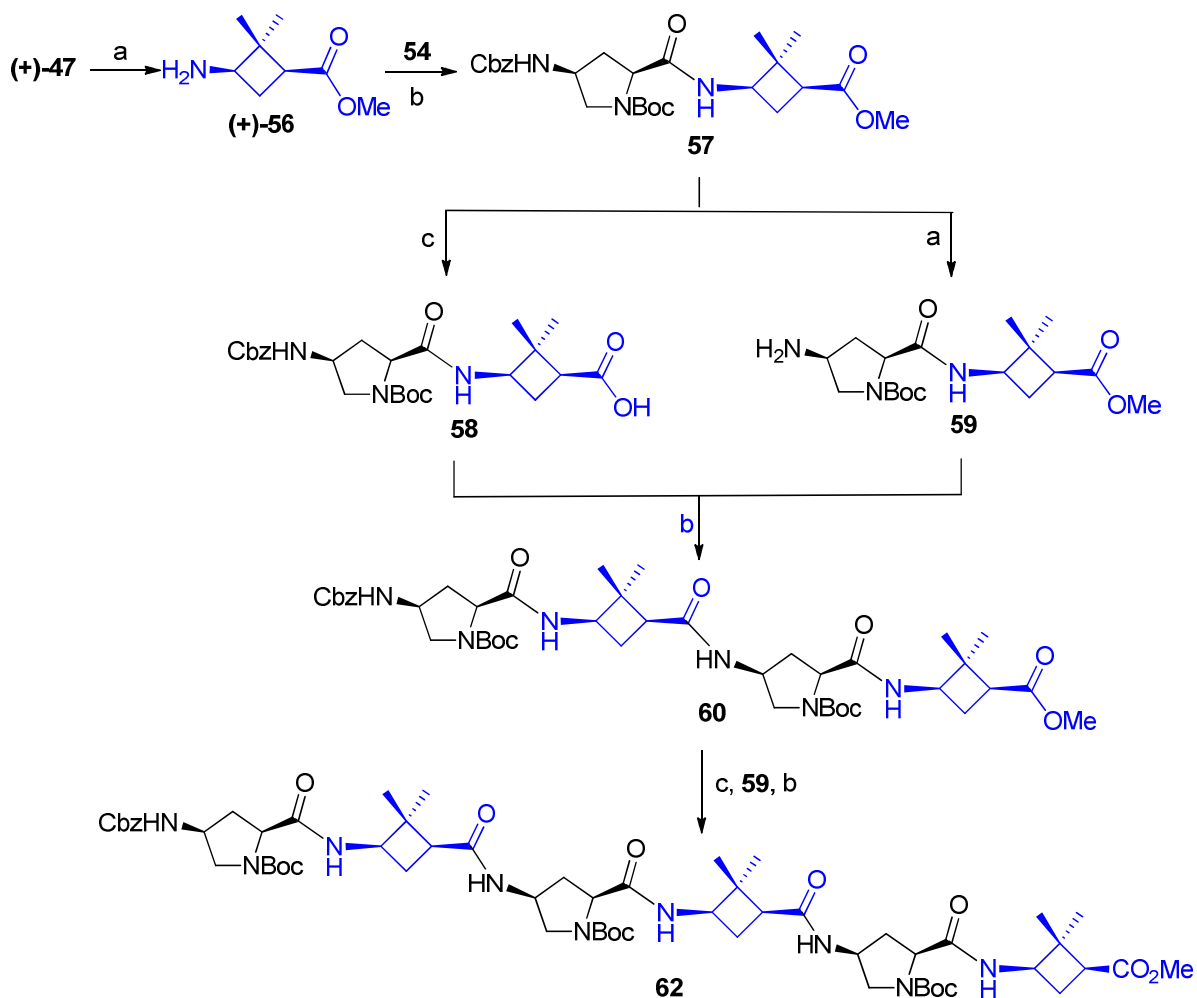
**Scheme 39:** Synthetic route leading to partially protected 4-amino proline **54**

### 3.3.3 Synthesis of (1*S*,3*R*)-cyclobutane-proline $\gamma,\gamma$ -peptides series

Once we had synthesised both orthogonally protected enantiomers of the desired cyclobutane  $\gamma$ -amino acid, and prepared partially protected 4-amino proline bearing adequate protecting groups, we were able to deprotect selectively the amine group of cyclobutane amino acid to perform the couplings to obtain both diastereomeric series of hybrid-peptides.

Starting with (1*S*,3*R*) series, benzyl carbamate in compound (+)-**47** was reductively cleaved by reaction with ammonium formate in the presence of 10% Pd/C in refluxing methanol affording free amine (+)-**56** within a quantitative yield (**Scheme 40**). This compound was reacted with partially protected 4-amino proline **54** under usual coupling conditions by using PyBOP and DIPEA in anhydrous dichloromethane to provide hybrid  $\gamma,\gamma$ -dipeptide **57** as a white solid and in quantitative yield after purification.

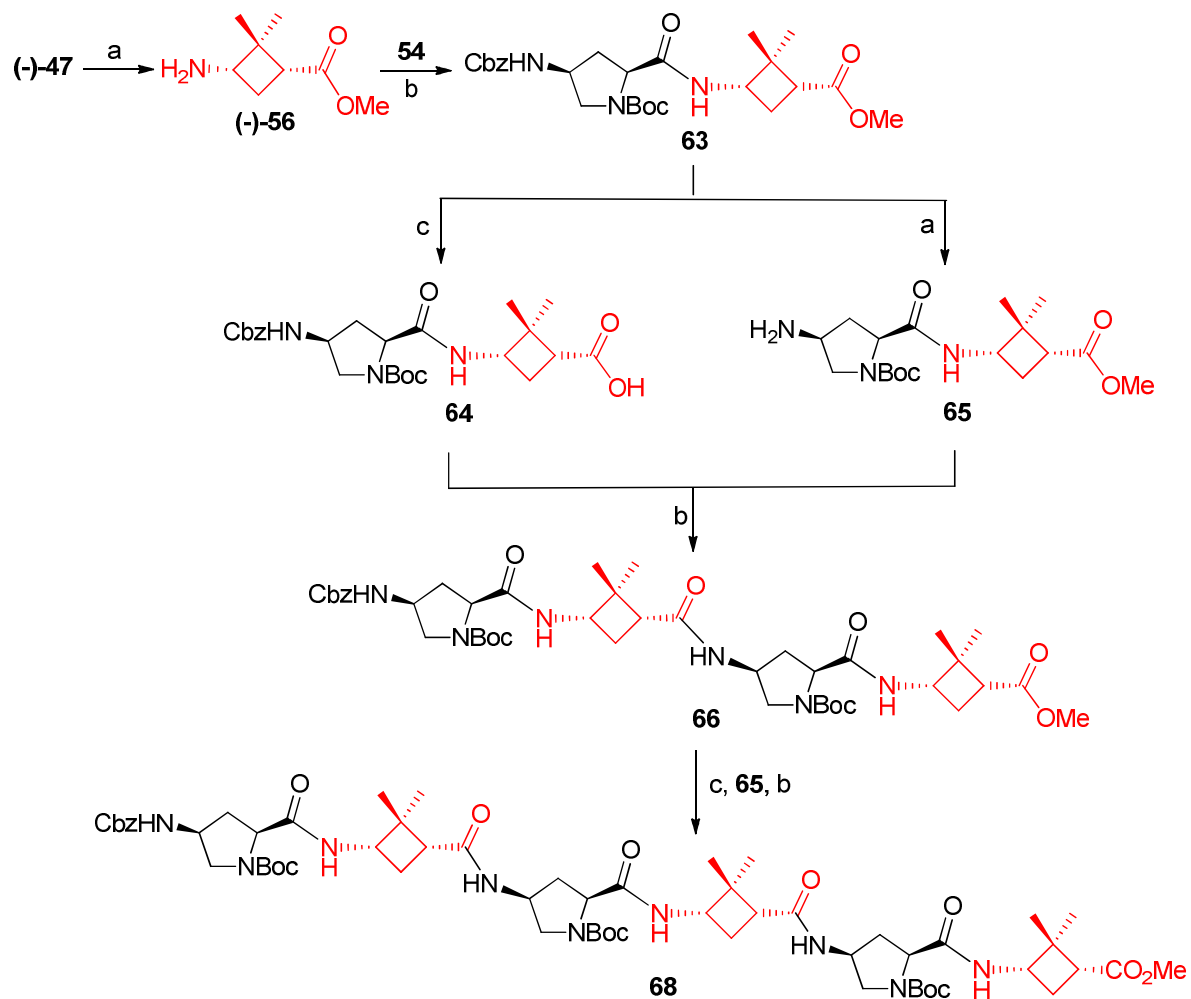
Tetrapeptide **60** was prepared through a convergent synthesis by coupling acid **58**, obtained from **57** by mild saponification with 1 M LiOH during 48 hours, and the amine resulting from removal of the benzyl carbamate in a second molecule of **57**, using the same procedure as for the cyclobutane amino acid. In this way, **60** was obtained in 96% yield as an enantiomerically pure white solid. Finally, quantitative deprotection of the carboxyl group in **60** followed by coupling with amine **59** afforded hexamer **62** in 81% yield as a white solid.



**Scheme 40:** Reagents, conditions, yields: (a)  $(\text{NH}_4)\text{HCO}_2$ , 10% Pd/C, MeOH, reflux, (quantitative); (b) PyBOP, DIPEA, anhydrous  $\text{CH}_2\text{Cl}_2$ , (quantitative for **57**, 96% for **60**, 81% for **62**); (c) 1 M LiOH, 2:10 THF/ $\text{H}_2\text{O}$ , (quantitative for **61**).

**3.3.4 Synthesis of (1*R*,3*S*)-cyclobutane-proline  $\gamma, \gamma$ -peptides series**

Similarly, the diastereomeric (1*R*,3*S*) series of hybrid  $\gamma, \gamma$ -peptides **63**, **66** and **68** (Scheme 41) was synthesised.



**Scheme 41:** Reagents, conditions, yields: (a)  $(\text{NH}_4)\text{HCO}_2$ , 10% Pd/C, MeOH, reflux, (96% for **(-)-56**, 86% for **65**); (b) PyBOP, DIPEA, anhydrous  $\text{CH}_2\text{Cl}_2$ , (95% for **63**, 92% for **66**, 84% for **67**); (c) 1 M LiOH, 2:10 THF/ $\text{H}_2\text{O}$ , (85% for **64**, 90% for **67**).

Once again, benzyl carbamate in orthogonally protected amino acid **(-)-47** was reductively cleaved by reaction with ammonium formate in the presence of 10% Pd/C in refluxing methanol affording free amine **(-)-56** in 68% yield (Scheme 41). This compound was readily reacted with partially protected 4-amino proline **54** under usual coupling conditions



by using PyBOP and DIPEA in anhydrous dichloromethane to provide a white solid identified as hybrid  $\gamma, \gamma$ -dipeptide **63** in 95% yield after purification.

In a similar way, tetrapeptide **66** was prepared through a convergent synthesis by coupling acid **64**, obtained from **63** by mild saponification with 1 M LiOH during 48 hours, and the amine resulting from removal of the benzyl carbamate in a second molecule of **63**, using the same procedure as for the cyclobutane amino acid. In this way, **66** was obtained in 92% yield in enantiomerically pure form as a white solid. Finally, deprotection of the carboxyl group in **66** (quantitative) followed by coupling with amine **65** afforded a white solid identified as enantiomerically pure hexamer **68** in 81% yield.

It is important to note that, both diastereomeric series of hybrid cyclobutane-proline  $\gamma, \gamma$ -peptides have been synthesised in solution. Even though this procedure is slower and more arduous than alternative solid-phase synthesis, it has been chosen due to the fact that it requires a smaller amount of starting material.

### **3.3.5 Conformational study in solution**

#### **Conformational study in solution of orthogonally protected 4-amino proline, 55**

Next, in collaboration with Dr. Pau Nolis, from Servei de Ressonància Magnètica at UAB, we decided to investigate the conformational bias of these products in solution. We started studying fully protected 4-aminoproline **55** itself because no detailed data were provided in the literature on this compound. 600 MHz  $^1\text{H-NMR}$  spectrum of **55** acquired at 273 K clearly showed split resonances in most of the protons. It is widely known that dynamic rotation of the conjugated N-C bond in Boc group is very slow within the NMR time scale giving rise to *cis/trans* conformers. The key point for the unambiguous assignment of both conformers was the NOE contacts observed for the *tert*-butyl group. While *trans* isomer correlates *tert*-butyl protons with  $\text{H}^5$  protons, *cis* isomers does it with  $\text{Me}^1$  and  $\text{H}^3$  protons. Both conformers are almost equally populated (**Figure 28**).

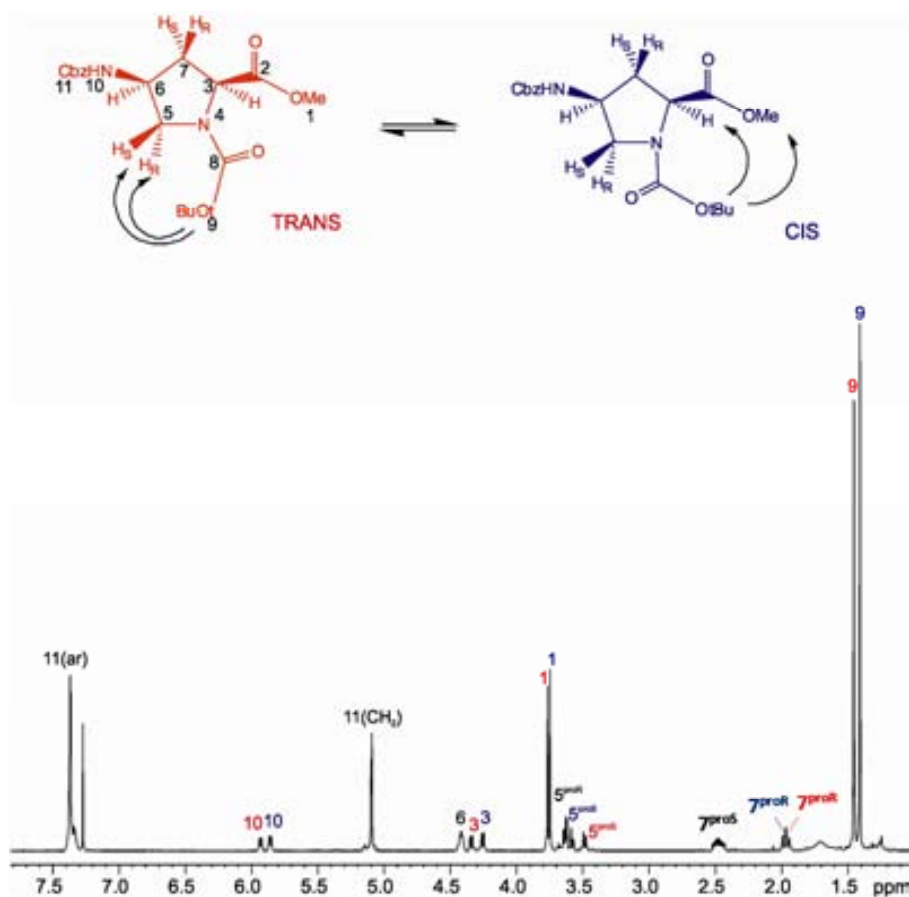


**Figure 28:**  $^1\text{H}$ -NMR spectrum of **55** acquired in a 600 MHz spectrometer at 273 K. *trans* isomer is marked red and *cis* isomer is marked blue. Overlapped *trans/cis* signals are not colored.

1D selective TOCSY experiments irradiating at  $\text{H}^{10}$  protons allowed us to obtain *cis/trans* proline protons in separate subspectra thus facilitating the *cis/trans* chemical shift assignment.  $^{13}\text{C}$ -NMR spectrum acquired at 273 K also exhibited split resonances for most of the signals due to *cis/trans* isomers. It is noticeable that  $\text{CO}^8$  signal difference between *cis* and *trans* isomer was about 113 Hz, while the difference found between *cis/trans* isomers in  $\text{CO}^2$  in the methyl ester and  $\text{CO}^{11}$  in the Cbz group was much lower (16 Hz and 9 Hz, respectively), therefore confirming that conformational rotational barrier is due to N-C bond in the Boc group. 2D-NOESY spectrum acquired at 273K was the key point to assign unequivocally *cis* and *trans* isomers. The expanded region showing *tert*-butyl cross peaks indicated that the slightly major component has cross peaks with  $\text{H}^3$  and  $\text{Me}^1$  protons and,

therefore, can be attributed to *cis* conformer. On the other hand, minor component correlates with H<sup>5</sup> protons, consequently assigned to *trans* conformer.

Interestingly, while inverting H<sup>10</sup> proton in 1D selective NOE experiment, independently of *cis* or *trans* isomer, NOE effects were observed at *pro-S* H<sup>5</sup> (H<sup>5S</sup>) and *pro-R* H<sup>7</sup> (H<sup>7R</sup>) protons, suggesting that NH<sup>10</sup> proton in both conformers is pointing to the carbonyl oxygen of the methyl ester group probably due to the presence of a hydrogen bond (**Figure 29**).

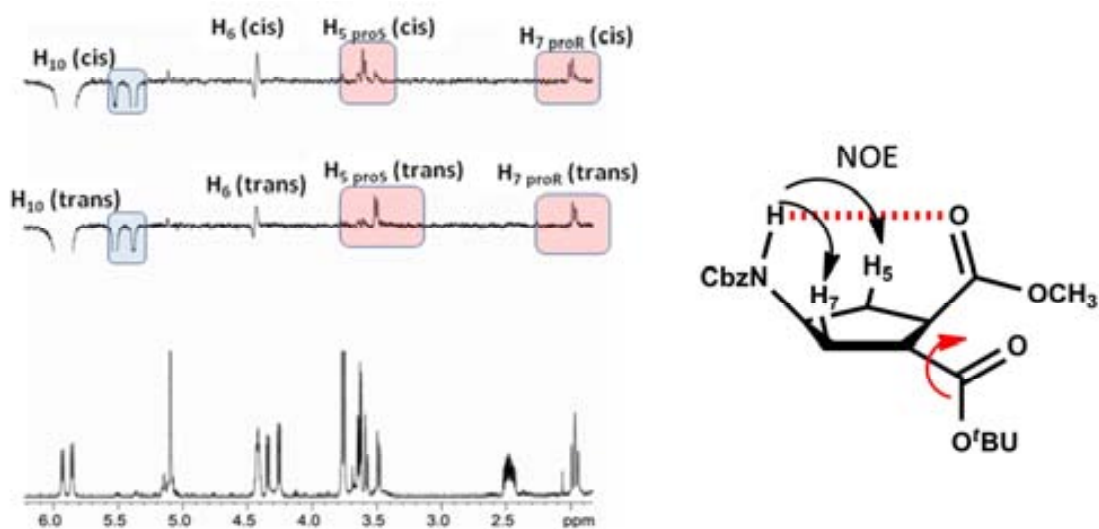


**Figure 29:** SELNOESY spectrum at 273K of each conformer of **55**.

Also, conformational exchange signals were detected in that experiment between *cis* and *trans* isomers. Furthermore, two small signals resonating at approximately 0.5 ppm downfield with respect to the major signals were observed and were assigned to minor conformations without such hydrogen bonding. According to all NMR experiments performed, the conformational equilibrium of modified proline **55** can be depicted as shown in **Figure 30**.

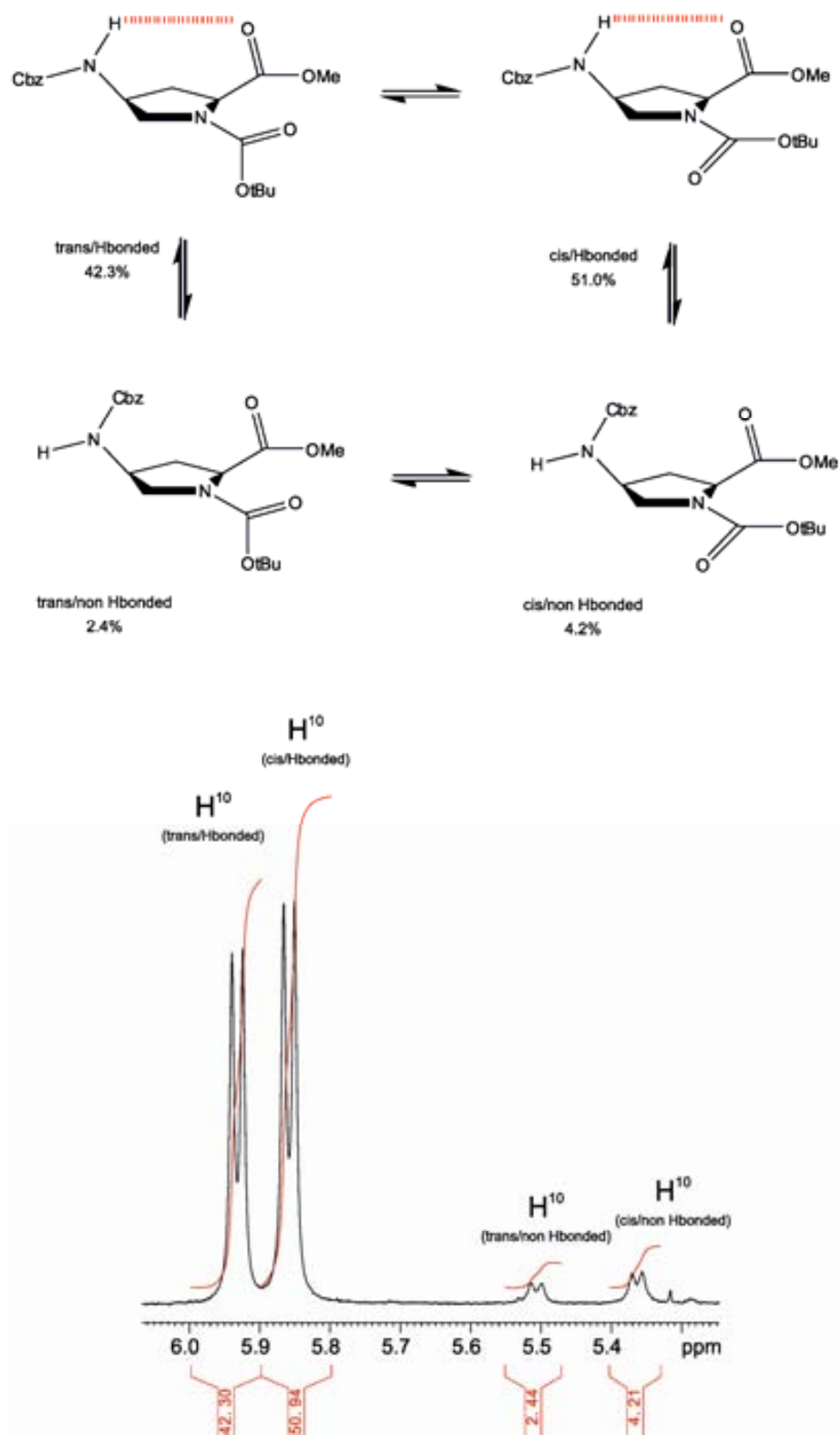


**Figure 30:** Expanded region of  $^1\text{H-NMR}$  spectrum at 273K with the detailed integration values for each conformer of 55.

Finally, variable  $^1\text{H-NMR}$  temperature experiments led to visualize the coalescence temperature between major *cis/trans* Boc isomers (**Figure 31**). The coalescence temperature is defined as the temperature at which the appearance of a peak corresponding to a certain proton changes from that of two separate peaks to that of a single, flattopped peak. For **55** it was determined to be at 323K. As conformer populations are almost equal, Eyring's equation was used to approximately determine a rotational barrier of 18.1 kcal/mol for the *cis/trans* equilibrium.<sup>129</sup>

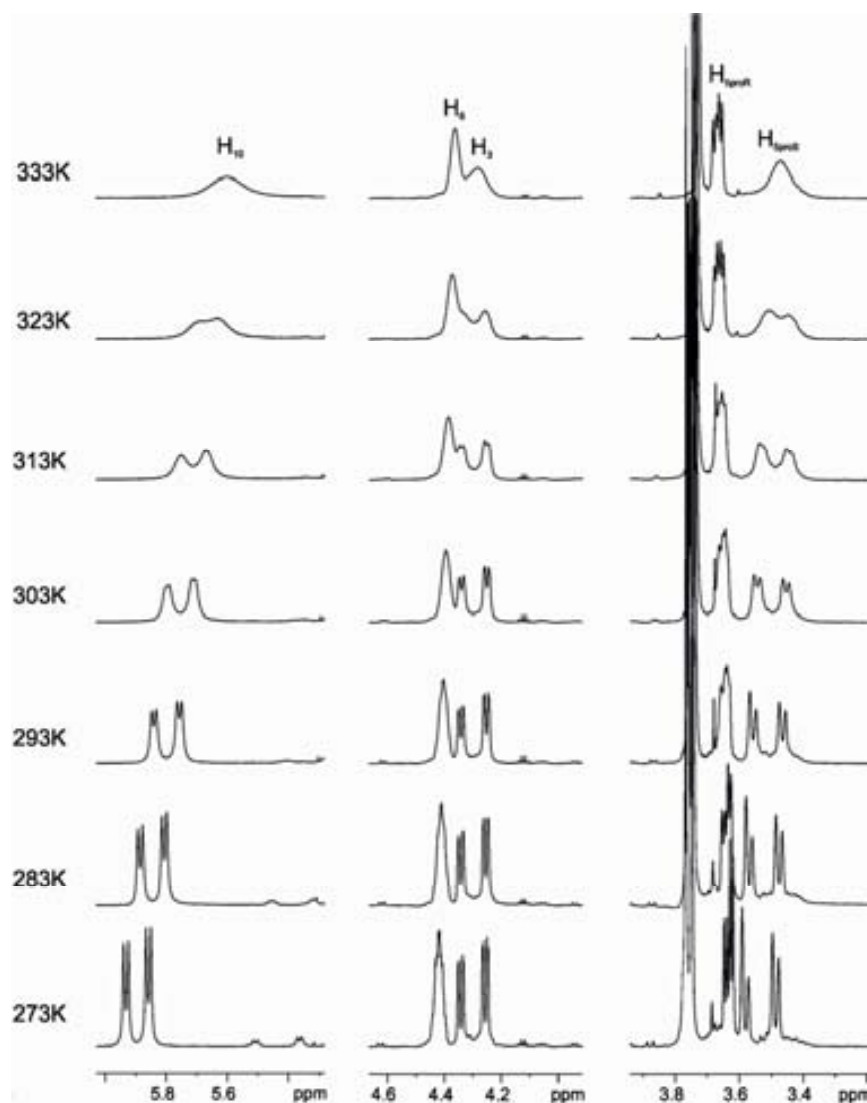


**Figure 31:** Variable temperature experiments, acquired at 600 MHz Bruker spectrometer. Temperature equilibration period was set to 10 minutes.

### Conformational study in solution of orthogonally protected diastereomeric series of hybrid cyclobutane-proline $\gamma$ , $\gamma$ -peptides

The next step was to investigate if the presence of the cyclobutane residues in the hybrid oligomers has any influence on this equilibrium and if preferred conformations change with respect to proline. Therefore, the two diastereomeric dipeptides **57** and **63** were studied. Differently to 4-aminoproline **55**, the respective  $^1\text{H-NMR}$  spectra of both **57** and **63** clearly showed a single major conformation. As an example, for **63** strongly deshielded position of  $\text{H}^9$  suggested a hydrogen bond between  $\text{NH}^9$  and  $\text{CO}^{16}$  building a 7-membered ring stacked to the 5-membered proline ring fixing, therefore, Boc rotamer to *trans* position (**Figure 32**). NOE experiments confirmed such hypothesis as described below. 1D selective TOCSY experiment irradiating at the  $\text{NH}$  protons allows the separation of proline and cyclobutane subspectra, which affords a clear visualization of the correct proton assignment of the molecule.

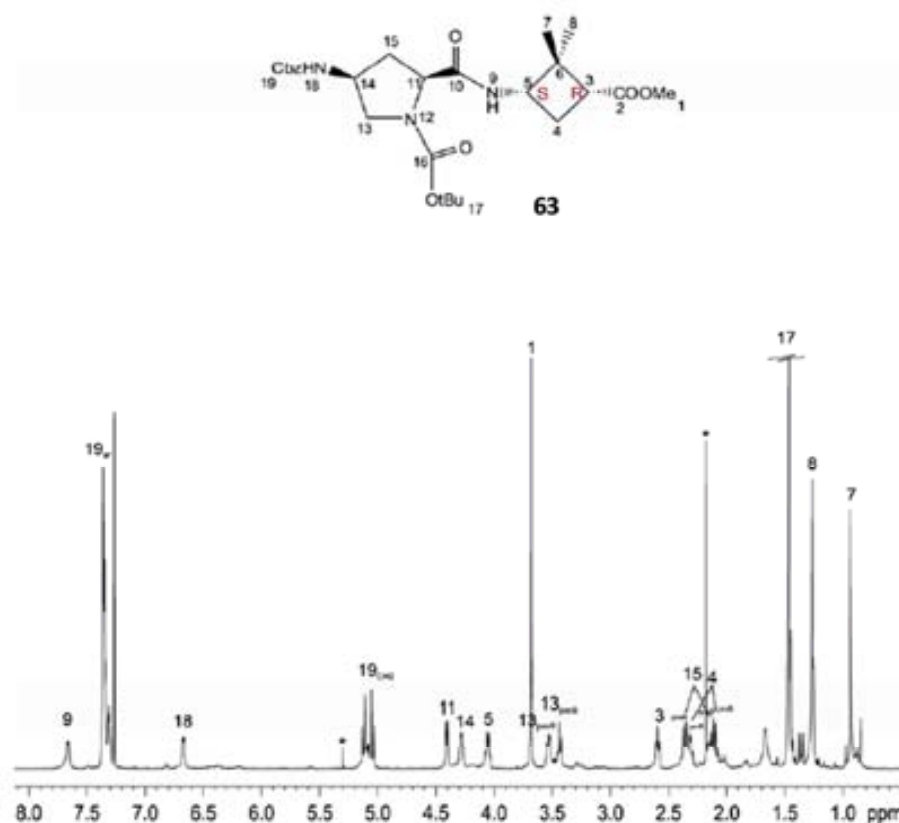


**Figure 32:**  $^1\text{H}$  NMR spectrum of dipeptide **63** acquired in a Bruker 600 MHz spectrometer at 298 K.

Considering dipeptide **63**,  $J$  coupling values together with 1D selective NOE experiments (**Figure 33**) over  $NH$  protons give an excellent visualization of the conformational structure of the molecule. Selective inversion of  $H^9$  gives a strong NOE effect with  $H^{11}$ . This fact, together with the highly deshielded position found for that proton, clearly indicates a strong hydrogen bond formation with Boc carbonyl group. Furthermore, coupling constant  $^3J_{H^9H^5} = 7.8$  Hz (dihedral angle  $\sim 150^\circ$ ) and NOE effects observed with  $H^5$ ,  $H^{4S}$  and  $Me^8$  indicate the spatial disposition of the cyclobutane ring.

Similarly to that observed in 4-aminoproline **55**,  $NH^{18}$  proton in Cbz group has an unusual deshielded position suggesting the formation of a hydrogen bond with  $CO^{10}$ . A similar hydrogen bond was previously reported for a  $\gamma$ -dipeptide consisting of two residues of 4-aminoproline protected in a different manner than compound **55**.<sup>107</sup> In our case, this is corroborated by NOE effects observed on  $H^{15R}$  and  $H^{13S}$  protons. However, there are slight differences in NOE intensities compared with **55**. In the dipeptide **63**, more NOE intensity is observed in  $H^{15R}$  with respect to  $H^{13S}$  proton indicating a shift toward this proton. This can be explained due to the conformational restriction of  $CO^{10}$  that belongs to the new 7-membered ring, which consequently shifts the hydrogen bond  $CO^{10}-NH^{18}$ . The slight change is also noticeable in  $^3J_{H^{14}H^{18}}$  coupling value, which changed from 8.8 Hz (dihedral angle  $\sim 160^\circ$ ) in triprotected proline **55** to 6.5 Hz in the dipeptide (dihedral angle  $\sim 140^\circ$ ).

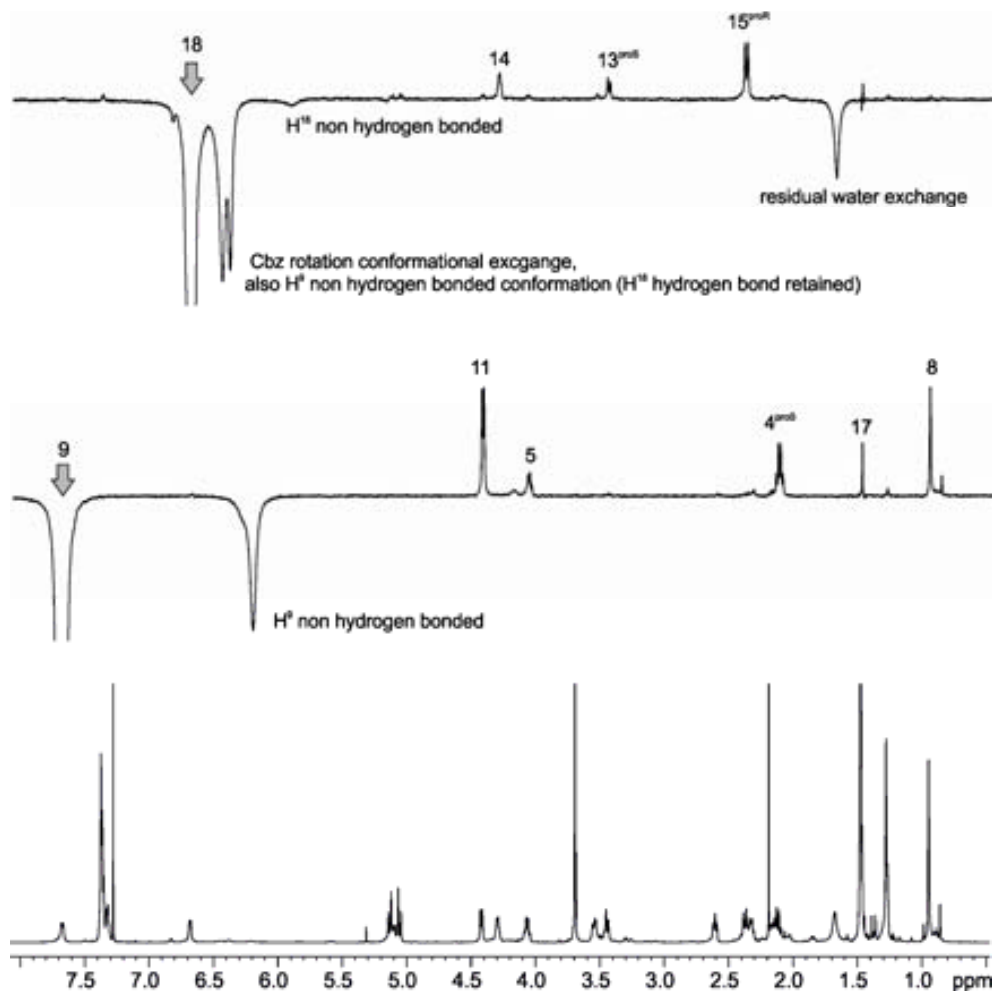


**Figure 33:** 1D selective NOESY experiments irradiating NH protons in **63**. Mixing time was set to 500 ms.  $^1\text{H}$ -NMR spectrum is added for comparison. Besides NOE peaks, exchange peaks are also observed.

A pictorial conformational structure of the major conformer of dipeptide **63** is presented in **Figure 34** (a).



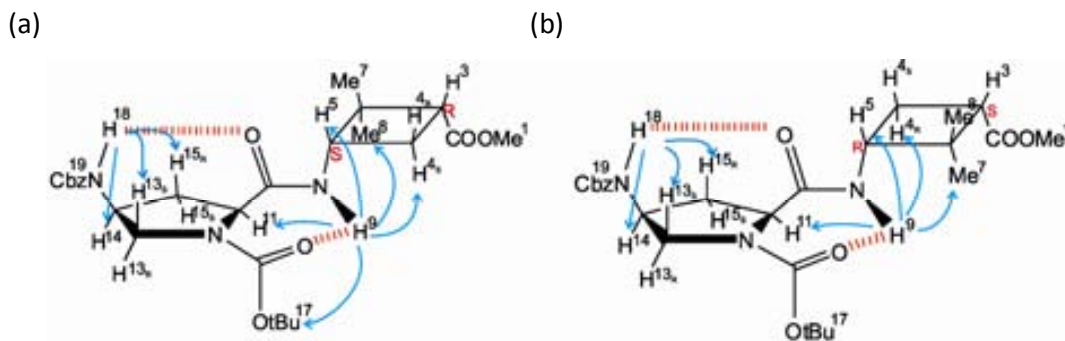


**Figure 34:** Conformation of (a) dipeptide **63** and (b) dipeptide **57** deduced from NOEs and  $J$  coupling values. NOE effects are indicated with blue arrows and hydrogen bond indicated with red lines.

A similar study was carried out on dipeptide **57** leading to the same conclusions. The conformation for **57** deduced from NOEs and  $J$  coupling values is depicted in **Figure 34** (b).

In order to qualitatively compare hydrogen bonding strength of  $NH^9$  and  $NH^{18}$  in these dipeptides, 50  $\mu$ L of deuterated methanol were added into the NMR tube. The tube was then hand-shaken and left to equilibrate for 10 minutes. The spectrum clearly shows that, while approximately half of the signal of  $NH^9$  prevails,  $NH^{18}$  has completely disappeared indicating a total deuterium exchange, therefore being experimentally demonstrated that  $NH^9$  hydrogen bond is less accessible than  $NH^{18}$  one, thus suggesting a stronger hydrogen bond (**Figure 35**). Variable  $^1H$ -NMR temperature experiments corroborate such hypothesis.

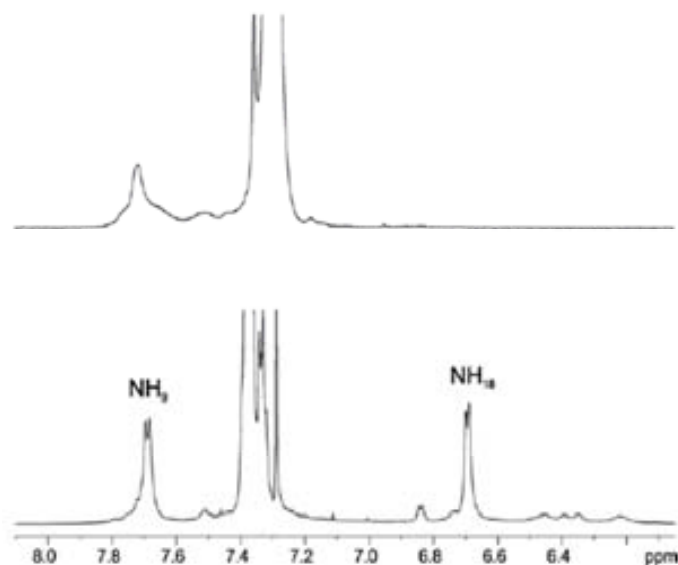


**Figure 35:** MeOD exchange experiment for dipeptide **63**

To ascertain if this conformation was preserved in tetramers,  $\gamma$ -tetrapeptides **60** and **66** were investigated. The respective  $^1\text{H}$ -NMR spectra clearly showed a single major conformation although several minor conformers are visible in the spectrum and as exchange peaks in 2D ROESY spectra. All  $^1\text{H}$  and  $^{13}\text{C}$  resonances have been assigned with the help of standard 2D NMR experiments which can be found in the annex (TOCSY, ROESY, HSQC and HMBC). The result of these studies was the confirmation of the same preferred conformation found for  $\gamma$ -dipeptides **57** and **63**. These conformers are depicted in **Figure 36** in which the inter residue strongest ROE contacts are indicated by bold arrows.

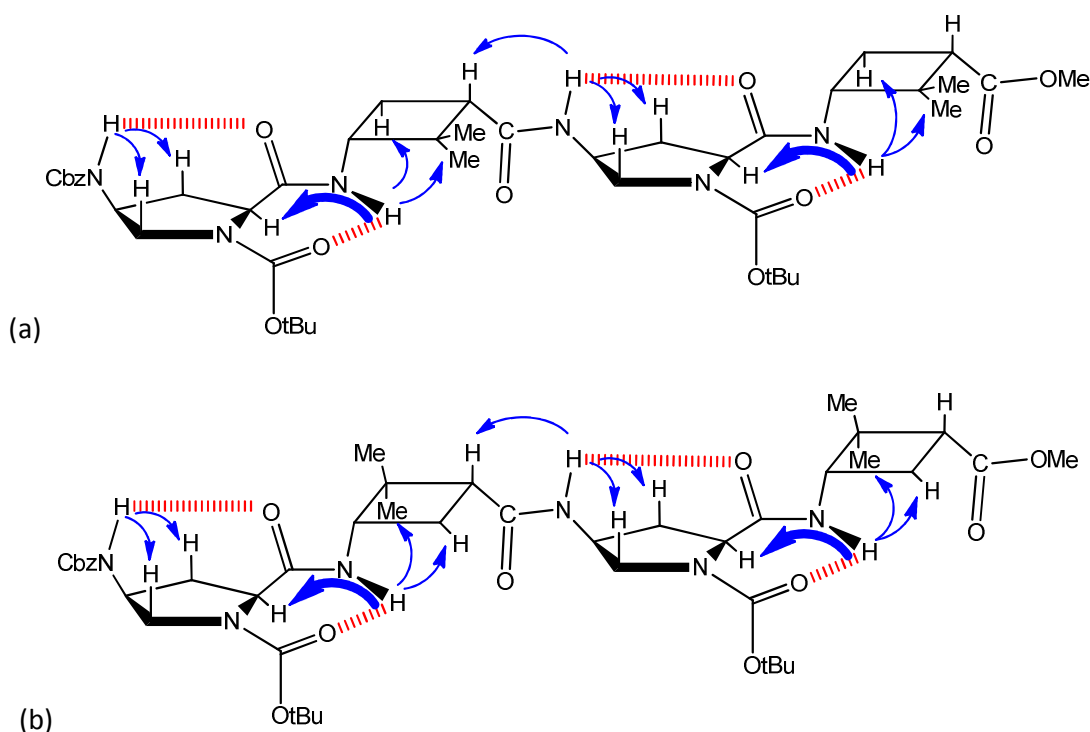


**Figure 36:** Main conformation for: (a) tetrapeptide **60** and (b) tetrapeptide **66** deduced from ROE connections and  $^3J_{\text{NHCH}}$  coupling values. Hydrogen bonds are indicated with red lines. ROE contacts are indicated with blue arrows. The bold ones correspond to the strongest contacts in each peptide.

$\gamma$ -Hexapeptides **62** and **68** were also examined by  $^1\text{H}$  NMR. A similar preferential conformation as that for dipeptides and tetrapeptides was concluded. Nevertheless, other minor conformers were also observed (See Annex III for detailed information about NMR studies).

Compared analysis of the amide *NH* region in the  $^1\text{H}$  NMR spectra of these  $\gamma$ -tetra- and  $\gamma$ -hexapeptides showed that **60** and **62** in one diastereomeric series, and **66** and **68** in the other one presented different peak splitting. Thus, while all *NH* signals presented differentiated chemical shifts for **60** and **62**, overlapped *NH* signals were observed for **66** and **68**. On the basis of these results, we could suggest different molecular arrangements for the two  $\gamma$ -peptide series in good agreement with the observed signatures in the CD spectra (Figure 37).

Figure 37 shows the CD spectra of all the synthesised  $\gamma$ -peptides as 0.01 M solutions in MeOH. This concentration is low enough to avoid self-aggregation. We can observe a different pattern and also a different sign of the maximum absorption peaks in each series thus reflecting the opposite chirality of the cyclobutane residues in **57**, **60** and **62** with respect to diastereomers **63**, **66** and **68**. Well defined Cotton effects were observed for tetra- and hexapeptides **60** and **62**, respectively.

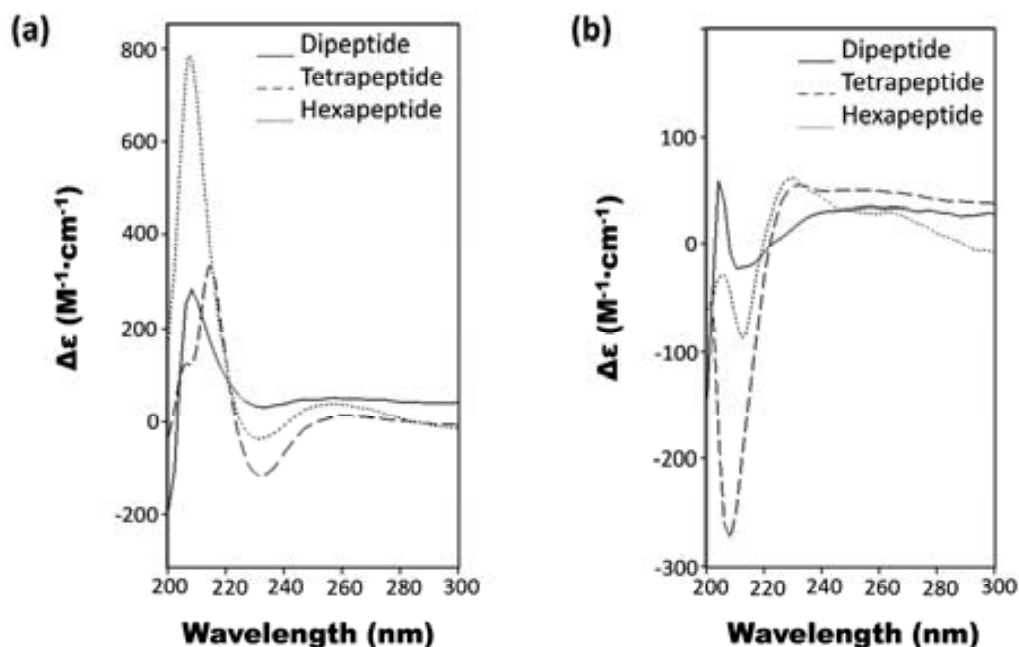
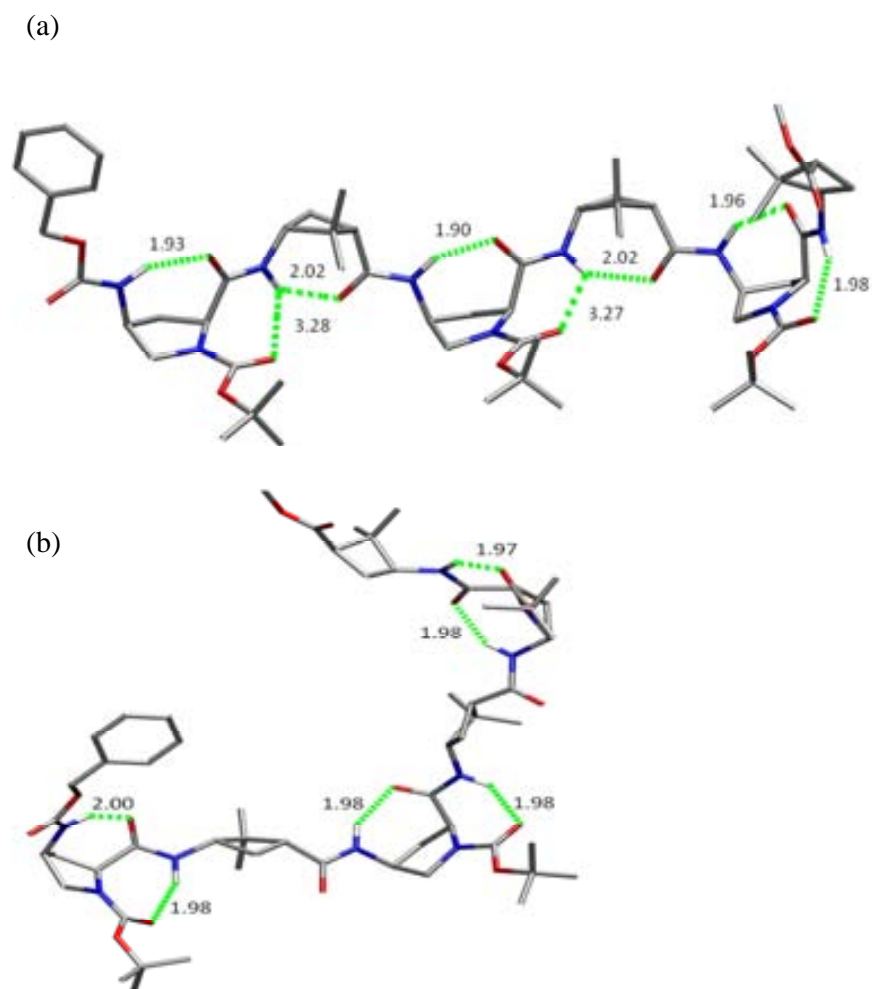


Figure 37: CD spectra of (a)  $\gamma$ -peptides **57**, **60** and **62**, and (b) **63**, **66** and **68** as 0.01 mM solutions in MeOH.

### **3.3.6 Theoretical calculations of orthogonally protected diastereomeric series of hybrid cyclobutane-proline $\gamma$ , $\gamma$ -peptides**

In collaboration with Dr. Carles Acosta, theoretical calculations on tetrapeptides and hexapeptides were performed to understand the differences observed for both diastereomeric series (see Computational Methods in Annex IV for detailed information).

Molecular Dynamics were performed on the significant structures obtained from the conformational search. It is remarkable that the inter residue hydrogen bond is always present during the dynamics while the proline intra residue one is not. This fact accounts for the higher strength of the former as deduced from  $^1\text{H}$  NMR experiments. The geometries of the resultant structures were optimised at B3LYP/6-31G(d) level of theory in chloroform solution for tetrapeptides **60** and **66** (see Computational Methods in Annex IV for detailed information) and in gas phase for hexapeptides **62** and **68** (**Figure 38**). Structural trends are similar for tetra- and hexapeptides in each series.



**Figure 38:** Preferred conformations for hexapeptides **62** (a) and **68** (b) as obtained at B3LYP/6-31G(d) level of theory in gas phase. Distances are in Å. All hydrogen atoms except *NH* have been omitted for clarity.

Comparing the calculated structures for **62** and **68** some features are remarkable. The first one is that, in **62**, each cyclobutane *NH* proton is involved, in average, in a bifurcated hydrogen bond, that means an inter residual  $\text{NH}^{(i)} \cdots \text{OC}^{(i-1)}$  hydrogen bond with the carbamate of the sequentially preceding proline moiety and a second one with the amide carbonyl of the same residue,  $\text{NH}^{(i)} \cdots \text{OC}^{(i)}$ . This last interaction is not observed in the terminal cyclobutane residue. In contrast, for hexapeptide **68**, only inter residual hydrogen bonding is predicted due to steric effects resulting from *gem*-dimethyl and the molecule is more twisted than **62** (**Figure 38**). The presence of the intra and inter residue hydrogen bonds in **62** originates a differentiated chemical environment for each *NH* proton, which in turn explains the split pattern in the *NH* region of the  $^1\text{H}$  NMR spectra. In contrast, the preferred

conformation for **68** presents a similar environment for all *NH* protons, thus resulting in an overlapping of the corresponding *NH* signals. Therefore, there is a tight relationship between cyclobutane stereochemistry and secondary structure of hybrid peptide.

### 3.3.7 Self assembly studies for both diastereomeric series of hybrid cyclobutane-proline $\gamma$ , $\gamma$ -peptides

Once the conformational bias in solution was verified, we explored the ability of some of these compounds to self-assemble. Thus, 2 mM solutions of the hybrid  $\gamma$ -peptides in MeOH were prepared and incubated for 24 h. TEM micrographs showed the formation of nicely defined sphere vesicles of nanometric size, as shown in **Figure 39** for compounds **57**, **60**, **63** and **66**. Incubation of samples for a week did not alter the shape of these assemblies. Hexapeptides **62** and **68** required longer incubation times to form defined aggregates.

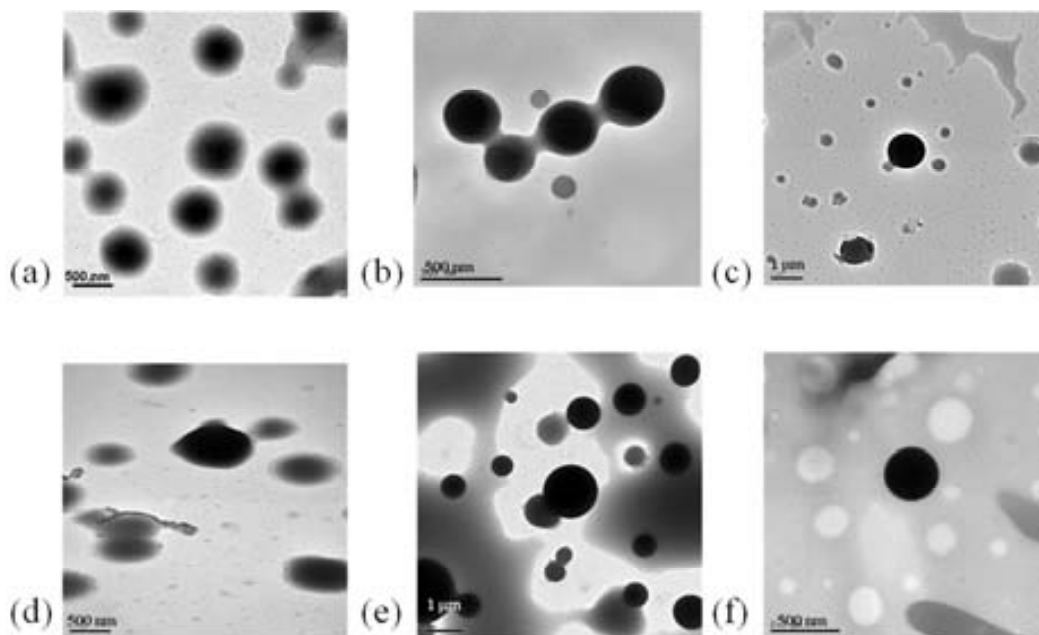


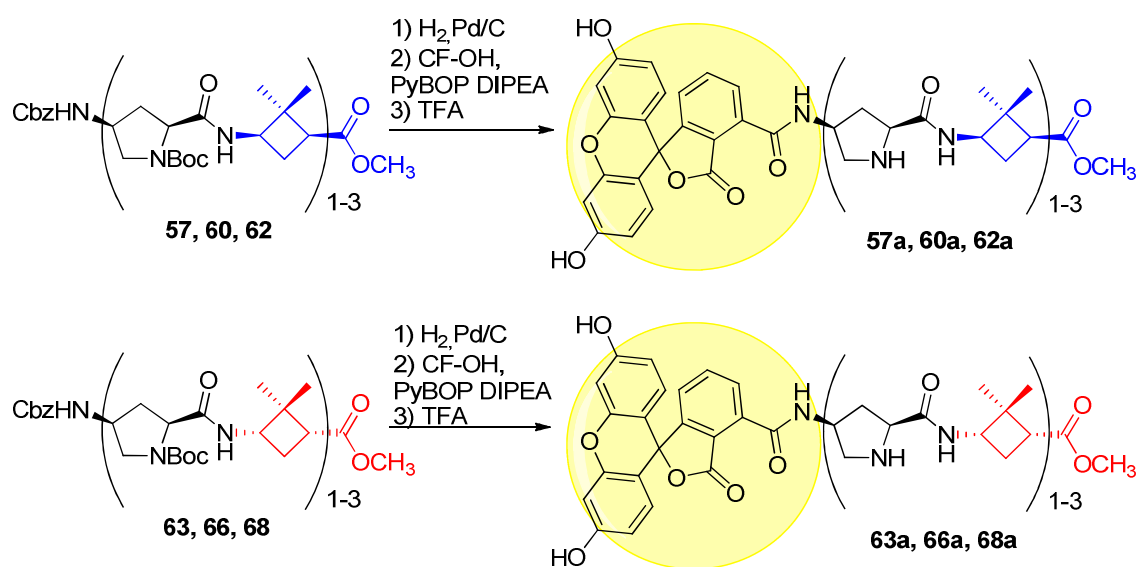
**Figure 39:** TEM images of the vesicles formed by (a) dipeptide **57**, (b) tetrapeptide **60**, (c) hexapeptide **62**, (d) dipeptide **63**, (e) tetrapeptide **66**, (f) hexapeptide **68** from 2 mM solutions in MeOH (1 day incubation for a, b, d, e and 4 days incubation for c,f) placed onto a carbon-film coated copper grid.

A similar behaviour has been observed for other peptides.<sup>130-135</sup> Self-assembled peptide-based vesicles have been used for biological purposes such as DNA delivery and release in cells.<sup>130-135</sup>

### 3.3.8 Evaluation of the series of hybrid cyclobutane-proline $\gamma$ , $\gamma$ -peptides as CPPs

Once the two diastereomeric series of hybrid cyclobutane-proline  $\gamma$ , $\gamma$ -peptides had been synthesised and their conformation in solution had been assigned unambiguously, their evaluation as CPPs was accomplished in collaboration with Dr. Miriam Royo and Dr. Daniel Carbajo of Scientific Park, UB.

The ability of the prepared compounds to penetrate into cells, was tested using HeLa cells<sup>136</sup> and quantified by means of flow cytometry techniques. Therefore, a fluorescent marker was incorporated. The chosen group for this purpose was 5(6)-carboxyfluorescein (CF) which was introduced using PyBOP after hydrogenolysis of *N*-terminal proline  $\gamma$ -amino group of previously synthesised peptides. Subsequently, *N*-Boc protecting group was removed by acidolysis with TFA (**Scheme 41**).



**Scheme 41:** Synthesis of CF-labelled hybrid cyclobutane-proline  $\gamma$ , $\gamma$ -peptides.

Firstly, the toxicity of CF-labelled  $\gamma,\gamma$ -peptides was tested using the 3-(4,5-dimethylthiazol-2-yl)-2,5-diphenyltetrazolium bromide (MTT) assay (see CPPs Biological Assays in Annex V for detailed information). Then, their cell-uptake properties were assayed by using HeLa cells by means of flow cytometry quantification techniques using TAT peptide as a reference (**Figure 40**).

The viability of HeLa cells after their treatment with 500  $\mu$ M solutions of the hybrid cyclobutane-proline  $\gamma,\gamma$ -peptides for 2 h was always higher than 80%, except for dipeptides **57a** and **66a** that showed a cell survival lower than 20%. In that way, we can conclude that there is a clear influence of peptide length on compound's cytotoxicity, being longer peptides less toxic than short ones. Nevertheless, cytotoxicity is almost not influenced by cyclobutane stereochemistry, showing similar results for both diastereomeric series. As it can be seen in **Figure 40**, tetrapeptides and hexapeptides showed much lower cytotoxicity than already known TAT peptide, which was used as reference. For this reason, this first generation of hybrid peptides seemed to be good candidates for biological applications, such as CPPs.

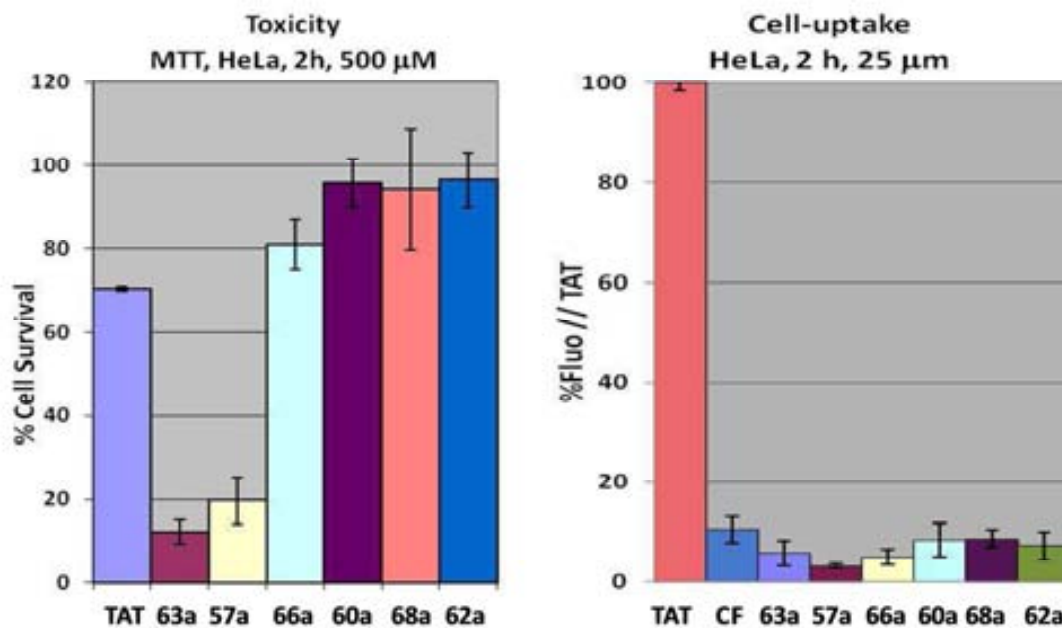


**Figure 40:** Representation of the cytotoxicity and cell-uptake properties of hybrid  $\gamma,\gamma$ -peptides in relation to the reference peptide TAT.



Once their toxicity was tested, their ability to penetrate HeLa cells was studied at 37 °C by flow cytometry (**Figure 40b**). When quantification by flow cytometry is carried out, the signals of the peptide that has been internalised and those of the peptide linked to the cell membrane have to be distinguished. To discriminate between the two situations, the cells are treated with an acid solution to reach a pH around 6, in which CF is not fluorescent and the cells remain intact, allowing the measure of the marking inside the cell and thus discriminating the ones at the cell surface. All of them showed to have some cell-uptake abilities albeit the results obtained were not as good as expected when compared with the current reference TAT peptide. Moreover, it was concluded that the length of the peptide was important to detect some advance in cell-uptake properties, being the  $\gamma,\gamma$ -hexapeptides (**67a** and **74a**) the ones giving the best results. Referring to the chirality of the cyclobutane moieties, it was shown to be not relevant for their penetration capability.

In conclusion, a new family of hybrid proline-cyclobutane  $\gamma,\gamma$ -peptides showing low cytotoxicity and certain cell uptake, has been synthesised. With these preliminary results, a second generation of hybrid peptides has been carried out by Dr. Esther Gorrea in our research group, by modification of 4-amino proline side chain in a series of hexapeptides. Using solid phase peptide synthesis a series of  $\gamma$ ,  $\gamma$ -hybrid peptides has been prepared, which have a common backbone and distinct side chains introduced with different linkage types through the  $N^\alpha$  atom of the proline monomer. Based on the linkage type, three different peptide families, namely  $N^\alpha$ -acyl- $\gamma,\gamma$ -hexapeptides,  $N^\alpha$ -alkyl- $\gamma,\gamma$ -hexapeptides, and  $N^\alpha$ -guanidylated- $\gamma,\gamma$ -hexapeptides have been obtained (**Figure 41**).

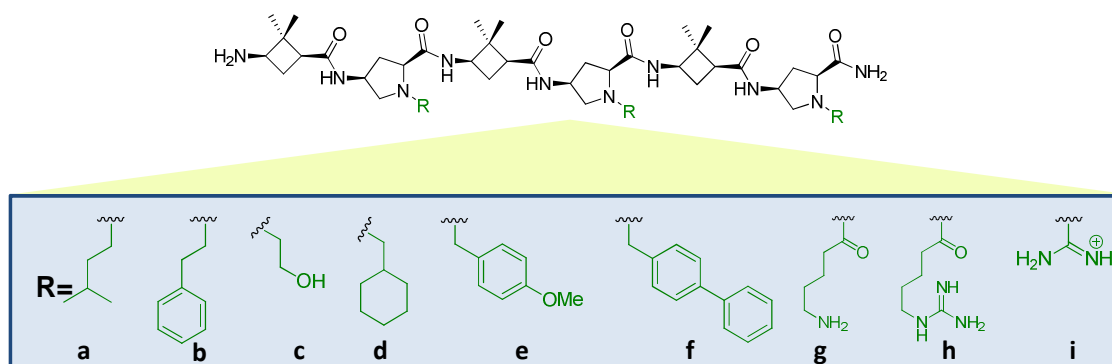


**Figure 41:** Chemical structure of the second generation of hybrid  $\gamma,\gamma$ -proline-cyclobutane hexapeptides synthesised.

The highest increase on the cell-uptake properties has been obtained for a hybrid  $\gamma,\gamma$ -hexapeptide in which  $N^\alpha$  atom of the proline residues is linked to a guanidinium group through a pentanoyl chain (**Figure 42**). The role of the spacer appears to be crucial for enhancing activity as deduced from comparison of results for  $N^\alpha$ -guanidylated peptide. Probably, in the most active peptide, guanidinium is more accessible to interaction with the cell membrane. On the contrary,  $N^\alpha$ -alkyl- $\gamma,\gamma$ -hexapeptides bearing hydrophobic carbon side-chains, evidenced much lower penetration activity.

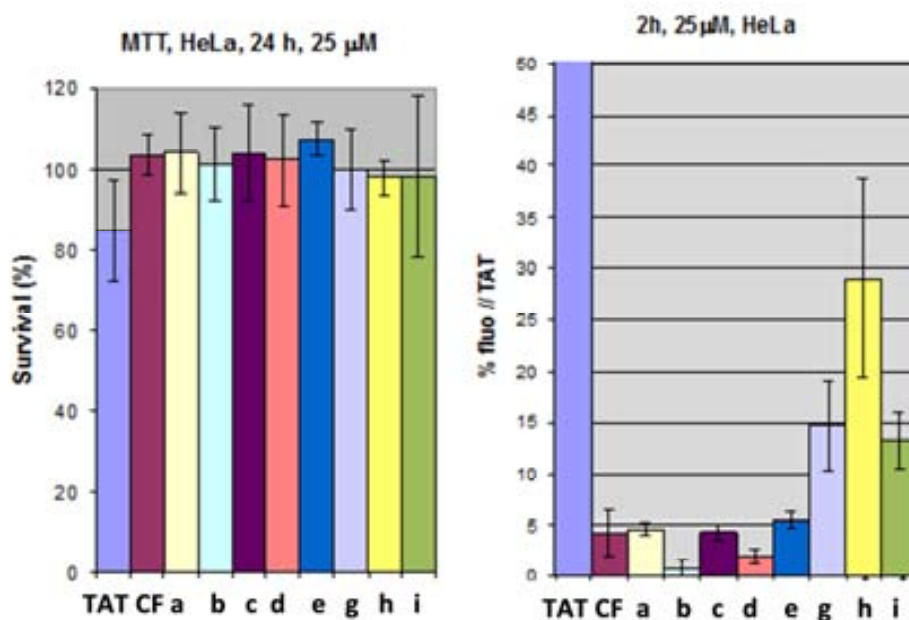


**Figure 42:** Representation of the cytotoxicity and cell-uptake properties of hybrid  $\gamma,\gamma$ -peptides in relation to the reference peptide TAT.

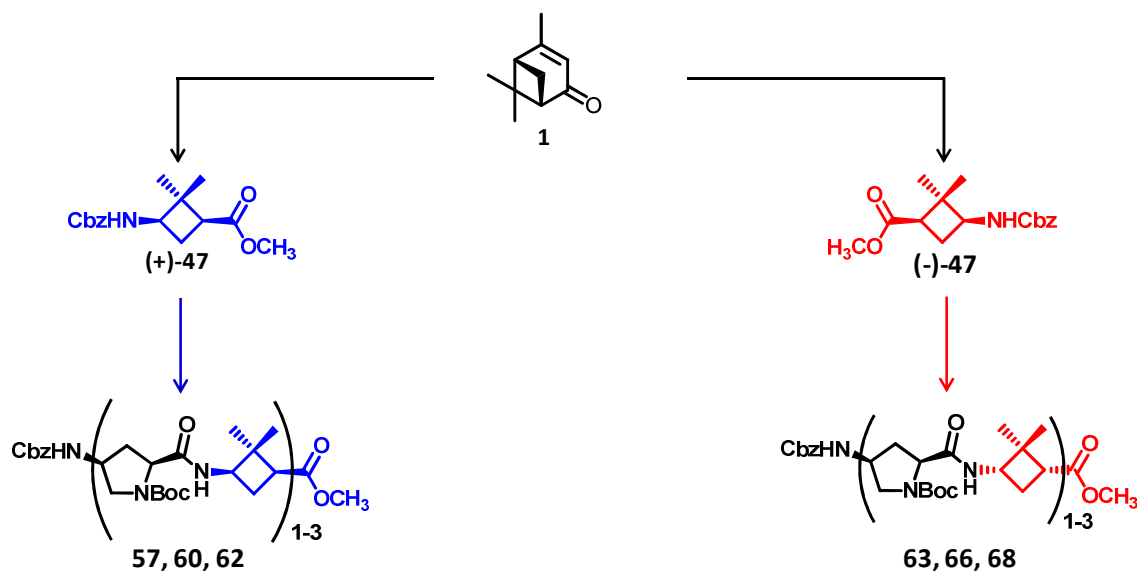
Differently to previously reported all-4-aminoproline  $\gamma$ -hexapeptides, in which six guanidinium groups are directly linked to the peptide backbone,<sup>111</sup> prepared hybrid  $\gamma,\gamma$ -hexapeptide presents only three guanidinium groups pending on an  $N^\alpha$ -alkyl chain. Therefore, charge balance is improved by the reduction of the total number of charges and the increase of hydrophobicity.<sup>137</sup> As a consequence, it presents similar up-take properties to those described for earlier peptides but lower toxicity.

Although the effectiveness of penetration revealed by the studied  $\gamma,\gamma$ -hexapeptides does not reach the level of some peptides described in the literature, their value as transporters could be guaranteed by establishing a favourable balance between their ability

to penetrate, the capacity to accumulate inside different cellular organelles, and their low toxicity. Subcellular localization studies as well as synthesis of longer hybrid  $\gamma,\gamma$ -peptides are currently on-going in our laboratories.

### 3.4. SUMMARY AND CONCLUSIONS: Hybrid cyclobutane-proline $\gamma$ , $\gamma$ -peptides: Structure and cell-uptake properties

- (i) The synthesis of optically pure cyclobutane  $\gamma$ -amino acids and their inclusion into two diastereomeric series of hybrid cyclobutane-proline  $\gamma$ ,  $\gamma$ -peptides has been accomplished (**Scheme 42**).



- (ii) The presence of the cyclobutane moiety in these compounds leads to well defined conformations in solution affording compact structures as the result of two kinds of hydrogen-bonded ring formation, as proved by NMR structural studies in solution and theoretical calculations (**Figure 43**).

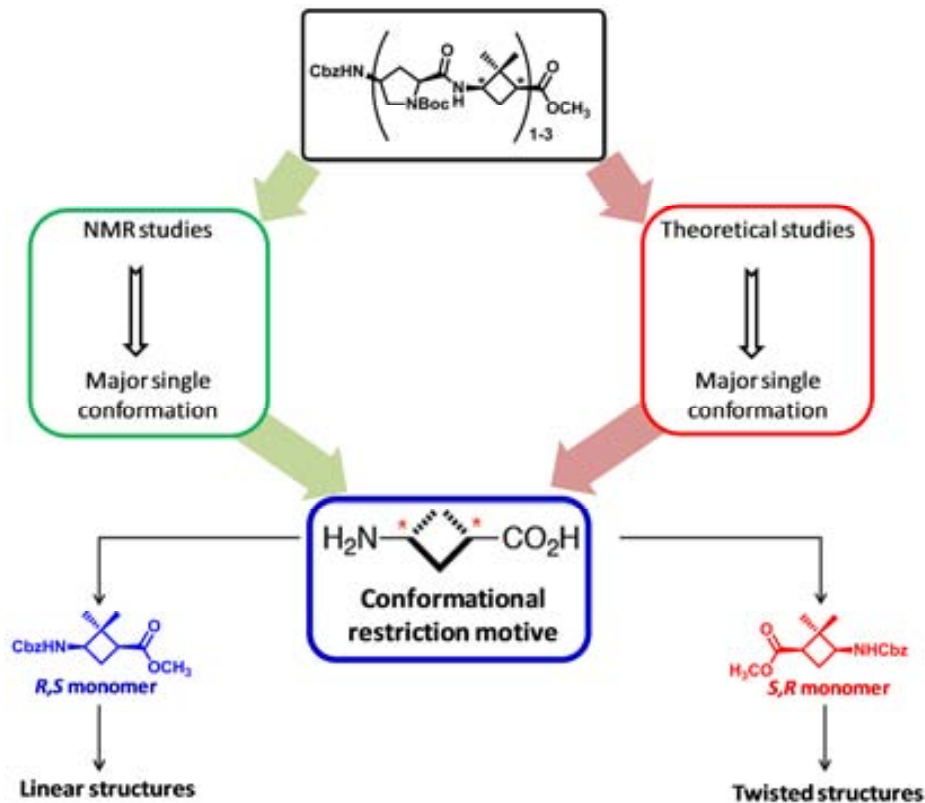


Figure 43

- (iii) The cytotoxicity and the ability of these molecules to cross the cell membrane have been evaluated. Tetrapeptides and hexapeptides, independently of their stereochemistry, showed to be non-toxic. The best cell uptake was performed by hexapeptides. In view of this preliminary results obtained on the first generation of CPPs, a second generation has been synthesised by Dr. Esther Gorrea and screened by Dr. Daniel Carbajo.



**Chapter III**

**NPY Analogues**





## 4. CHAPTER III: NPY ANALOGUES

### 4.1. INTRODUCTION

#### 4.1.1 Neuropeptide Y (NPY)

In order to enable life to occur, a high level of regulation takes place controlling every event in every living cell at any time. This control is achieved through the ability of biomolecules to recognise and identify each other. Normally, cells present certain molecules in their surface, called receptors. These are exposed to the environment, making possible the communication with it through the interaction with specific compounds called ligands. This interaction allows the transmission of information about events taking place inside and outside the cell and the promotion of appropriate responses (**Figure 44**).

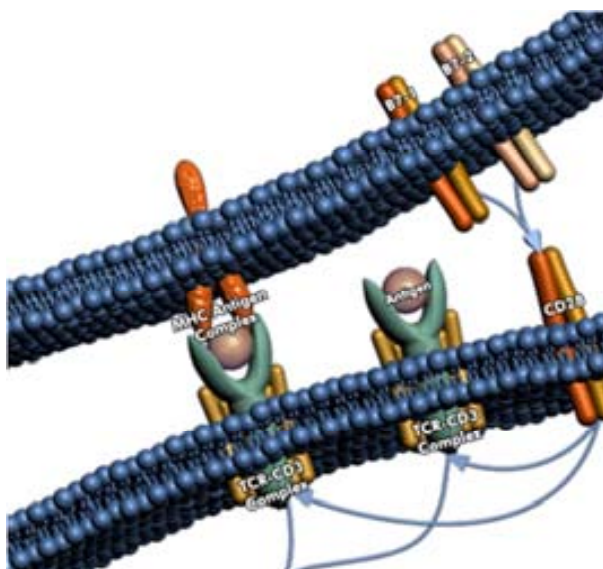


**Figure 44:** Molecular recognition at cell surface.

Neuropeptide Y (NPY) is one of the most abundant neuropeptides in central nervous system in mammals, and belongs, together with peptide YY (PYY) and pancreatic polypeptide (HPP), to the NPY hormone family. It is composed by 36 natural  $\alpha$ -amino acids and presents an amide group at the C-terminus extreme. NPY is the strongest known stimulator of food intake, and is also involved in peripheral vascular resistance, sexual functioning, anxiety and stress response.<sup>138</sup> In mammals, the functions of NPY are regulated

by five different G protein coupled receptors ( $Y_1$ ,  $Y_2$ ,  $Y_4$ ,  $Y_5$  and  $Y_6$ ).<sup>139</sup> However, the exact role of each of them is still unknown. NPY shows sub-nanomolar affinity towards all receptors, and consequently it is still difficult to distinguish the physiological roles of each one *in vivo*. To address this problem, the knowledge of the particular bioactive conformation at each receptor is indispensable for the further development of subtype-selective ligands.

NPY exhibits a three-dimensional structure called PP-fold, which is characterised by an extended type II polyproline helix (residues 1-8) that is followed by a turn (residues 9-13) and an amphiphatic  $\alpha$ -helix (residues 14-31). But the C-terminus (residues 32-36), which mainly interacts with the receptor binding site, has no regular structure (**Figure 45**).<sup>140</sup>

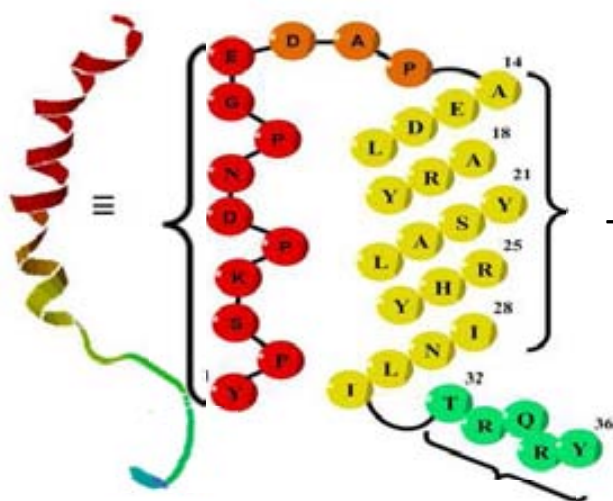


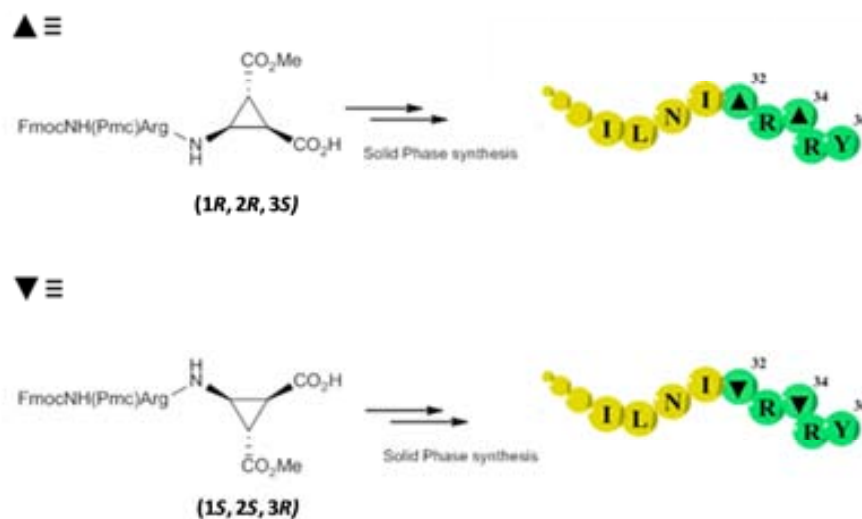
**Figure 45:** Three-dimensional model of NPY.

A. G. Beck-Sickinger and co-workers investigated the contribution of the side chain of each amino acid in NPY to the receptor by systematic single exchange of each residue of NPY by L-Ala<sup>141</sup> revealing that especially the highly conserved C-terminal part of NPY, with its arginine residues in positions 33 and 35 and the tyrosine amide in position 36, plays a crucial role during the recognition process by the respective receptor. However, this segment is highly flexible and no defined structure could be assigned to this important part of the molecule to date. It is assumed that different secondary structure motifs of the C-terminus are responsible for receptor subtype selectivity.

For that reason, the synthesis of NPY analogues with a stabilised secondary structure at the C-terminus can clarify the role of the NPY receptors and the bioactive conformation of NPY. If the analogue fits into only one receptor, only the bioprocesses correlated to this receptor will be activated. On the other hand, if the affinity of an analogue is higher than that of the natural sequence, its conformation should be very close to the bioactive one.

#### 4.1.2 NPY analogues containing constricted amino acids

In order to rigidify the peptide's backbone, and with the aim to induce or stabilise different secondary structures, a series of truncated (25-36) NPY analogues containing  $\beta$ -aminocyclopropane carboxylic acids ( $\beta$ -ACC) were synthesised by Reiser and co-workers (**Scheme 43**).<sup>105</sup>



**Scheme 43:** Synthesis of NPY truncated analogues starting from  $\beta$ -ACC containing dipeptides.

As can be seen in **Scheme 43**, a family of NPY truncated analogues was synthesised, incorporating both enantiomers of a  $\beta$ -ACC in positions 32 and 34 which are in direct proximity to the most important amino acids Arg<sup>33</sup> and Arg<sup>35</sup>. Differently to what happened with native sequence, some of these peptides, which are composed of only 11 residues, showed nanomolar affinity towards Y<sub>1</sub> receptor, being the shortest linear peptides that are selective for Y<sub>1</sub> receptor (**Table 3**). It was also demonstrated that chirality of  $\beta$ -ACC had a

high influence on the activity of the resulting peptide, being active only the ones bearing ( $\blacktriangle$ )-configuration (1*R*,2*R*,3*S*).

**Table 3:** Sequences and affinities of shortened  $\beta$ -ACC-containing NPY analogues at the Y receptors, synthesised by Reiser and co-workers . The affinities are expressed as  $K_i$  values [nm].

| Sequences <sup>[a]</sup>   | Y <sub>1</sub> | Y <sub>2</sub>    | Y <sub>3</sub> | $\Delta[\theta]_R$ <sup>[d]</sup> |
|--|----------------|-------------------|----------------|-----------------------------------|
| RHYINLITRQRY-NH <sub>2</sub>   | > 1000         | 21 <sup>[d]</sup> | > 1000         | 17.5                              |
| RHYINLITR $\blacktriangle$ RY-NH <sub>2</sub>                        | 37( $\pm$ 20)  | > 1000            | 724            | 5.6                               |
| RHYINLITR $\blacktriangledown$ RY-NH <sub>2</sub>                    | > 1000         | > 1000            | > 1000         | 3.7                               |
| RHYINLI $\blacktriangle$ RQRY-NH <sub>2</sub>                        | > 1000         | > 1000            | > 1000         | 1.5                               |
| RHYINLI $\blacktriangledown$ RQRY-NH <sub>2</sub>                    | > 1000         | > 1000            | > 1000         | 1.6                               |
| RHYINLI $\blacktriangle$ $\blacktriangle$ RY-NH <sub>2</sub>         | 50( $\pm$ 10)  | > 1000            | 617            | 2.9                               |
| RHYINLI $\blacktriangledown$ $\blacktriangle$ RY-NH <sub>2</sub>     | > 150          | > 1000            | > 1000         | 3.5                               |
| RHYINLR $\blacktriangle$ $\blacktriangle$ RY-NH <sub>2</sub>         | 29( $\pm$ 13)  | > 1000            | 118            | 3.3                               |
| RHYINLR $\blacktriangledown$ $\blacktriangledown$ RY-NH <sub>2</sub> | 1000           | > 1000            | > 1000         | 2.2                               |
| NLR $\blacktriangle$ $\blacktriangle$ RY-NH <sub>2</sub>             | 235            | > 1000            | > 1000         | 2.0                               |
| RHYINLITR $\beta$ RY-NH <sub>2</sub>                                 | > 1000         | > 1000            | > 1000         | 5.1                               |
| RHYINLI $\beta$ R $\beta$ RY-NH <sub>2</sub>                         | > 1000         | > 1000            | > 1000         | 1.4                               |
| RHYINLITR $\beta$ RY-NH <sub>2</sub>                                 | > 1000         | > 1000            | > 1000         | 9.9                               |

## 4.2. OBJECTIVES

Taking into account the important role developed by NPY in mammals and the need of possessing sub-selective ligands towards a single receptor which could bring a better understanding of the bioactive conformations of NPY, we set ourselves the target of synthesising highly constricted truncated NPY analogues.

Within the framework of an existing COST Action (CM-083, Foldamers) we started a collaboration with the group of Prof. Oliver Reiser, who has broad experience in this topic. With this aim I carried out a doctoral stay in the Universität Regensburg during 4 months.

Therefore, the first objective of this chapter was the synthesis of cyclobutane monomers which are convenient for their incorporation into peptides using solid-phase synthesis (**Figure 46**).

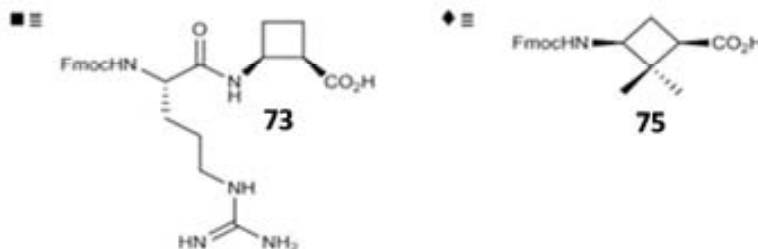
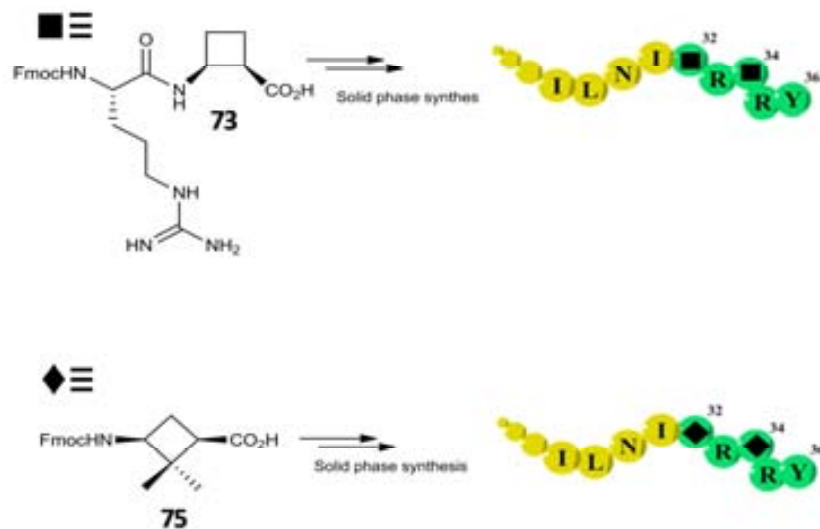


Figure 46

Next, the previously prepared compounds will be used in the synthesis of truncated NPY analogues, introducing them in positions 32 and 34 which are in direct proximity to the most important amino acids Arg<sup>33</sup> and Arg<sup>35</sup> (**Scheme 44**).



Scheme 44: Target compounds.

The affinity of the prepared analogues towards the different receptors was evaluated. In that way information concerning the following items was obtained:

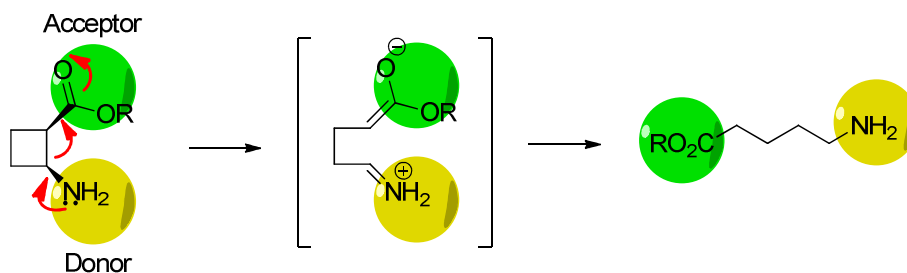
- Effect of ring size
- Effect of homologation ( $\beta$  and  $\gamma$ )
- Effect of truncated peptide length

### 4.3. RESULTS AND DISCUSSION

#### 4.3.1 Synthesis of $\beta$ -cyclobutane building block

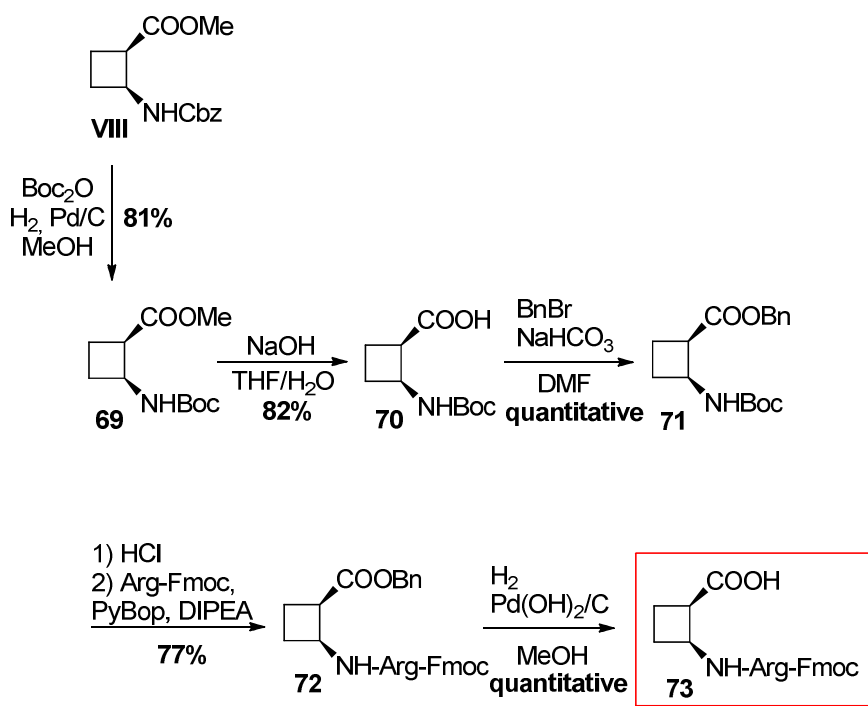
In previous works carried out by Koglin et al. it was proved that monomer chirality had a strong influence on the final peptide activity.<sup>105</sup> In that way, they reported that only cyclopropane  $\beta$ -amino acids bearing a (*R,S*) configuration led to active compounds. With this precedent and with the wide experience held by our research group on the synthesis of cyclobutane  $\beta$ -amino acids, we decided to synthesise the (*1R,2S*) cyclobutane amino acid enantiomer with an adequate functionalisation which could enable its incorporation into peptides using solid phase peptide synthesis.

Starting from previously described orthogonally protected amino acid **VIII**, a convenient monomer for solid-phase peptide synthesis was prepared. As already mentioned, this monomer will be incorporated into the final NPY analogue through solid-phase peptide synthesis. Therefore it is required that it bears convenient protecting groups. As done in previous works,<sup>105</sup> Wang-resin was used and therefore an Fmoc/*tert*-butyl strategy was followed, requiring the monomer to be added as a free acid. Therefore, methyl ester in **VIII** has to be hydrolysed and benzyl carbamate protecting group exchanged by an Fmoc moiety. This last step required the use of the *N*-unprotected form of the  $\beta$ -cyclobutane amino acid, which afterwards could be protected using Fmoc-O-succinimide. However, it is important to take into account the fact that the 1,2-donor-acceptor cyclobutane substitution makes its *N*-unprotected form unstable (**Scheme 45**).



**Scheme 45:** Push-Pull effect.

For that reason, there was a need to seek an alternative strategy that avoided the *N*-unprotected form of the  $\beta$ -cyclobutane amino acid. It seemed that the best way consisted in incorporating the  $\beta$ -cyclobutane amino acid into the NPY analogue as a pre-formed dipeptide with the consecutive residue (Arg). With this aim, benzyl carbamate in orthogonally protected amino acid **VIII** was hydrogenated in the presence of Pd/C and *tert*-butyl dicarbonate to afford *tert*-butyl carbamate **69** in 82% yield (**Scheme 46**) without observing ring opening. Afterwards, the protecting group from the carboxylic acid was exchanged by a more convenient one. For that reason, the methyl ester in compound **69** was hydrolysed and the resulting carboxylic acid was esterified using benzyl bromide and sodium bicarbonate affording the corresponding benzyl ester **71** in a quantitative yield.



**Scheme 46:** Synthetic route leading to conveniently functionalised  $\beta$ -cyclobutane building block.

As it has been commented, the coupling of the *N*-terminus requires a particular protocol to avoid cyclobutane ring-opening. The protocol of choice to accomplish the coupling of  $\beta$ -cyclobutane amino acids such as **71** is based on a previously set-up methodology in Prof. Reiser research group, which consists in the *tert*-butyl carbamate cleavage by treatment with a saturated solution of HCl in ethyl acetate. The resulting

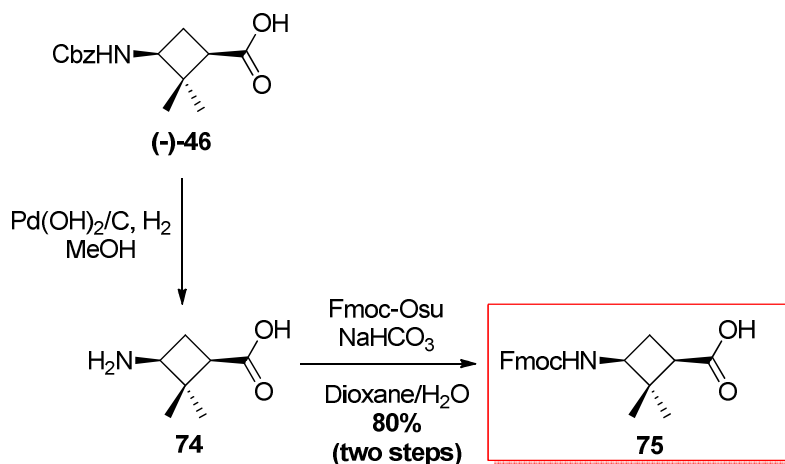


ammonium salt is stable enough, and can be liberated by the addition of a mild base (DIPEA) in the presence of preactivated Arg-Fmoc (with PyBOP) to obtain the corresponding dipeptide **72** without observing ring opening products and in 77% yield after purification. Finally, benzyl ester in dipeptide **72** was cleaved by hydrogenolysis in the presence of Pd(OH)<sub>2</sub>/C to afford quantitatively carboxylic acid **73** which is an adequate building block for solid-phase peptide synthesis.

### **4.3.2 Synthesis of $\gamma$ -cyclobutane building block**

In order to determine the effect of homologation of the unnatural amino acid in the resulting NPY analogues, a conveniently protected cyclobutane  $\gamma$ -amino acid was synthesised. As it has been previously mentioned monomer chirality has a strong influence on the final peptide activity<sup>105</sup> and only amino acids bearing a (*R,S*) configuration lead to active compounds. With this precedent in mind and the experience held by our research group on the synthesis of cyclobutane  $\gamma$ -amino acids, we decided to synthesise the (*1R,2S*) cyclobutane amino acid enantiomer with adequate protecting groups for solid phase peptide synthesis.

As described in Chapter 2, our research group possesses effective synthetic routes leading to both enantiomeric forms of orthogonally protected cyclobutane  $\gamma$ -amino acids. As previously commented, partially protected cyclobutane  $\gamma$ -amino acid (**-**)-**46** is synthesised, starting from (**-**)-verbenone (**1**) with a 73% overall yield. Nevertheless, the protecting groups present in (**-**)-**46** are not convenient for solid-phase peptide synthesis. As explained before, Wang-resin was used and therefore an Fmoc/*tert*-butyl strategy was followed, requiring that the monomer is incorporated as a free acid. Due to that, hydrogenolysis of benzyl carbamate in (**-**)-**46** was carried out in the presence of Pd(OH)<sub>2</sub>/C (**Scheme 47**). Right after, the obtained free amine was protected as Fmoc using Fmoc-O-succinimide and sodium bicarbonate as a base, to isolate partially protected cyclobutane  $\gamma$ -amino acid as a single enantiomer in 80% yield after the two steps.



**Scheme 47:** Synthetic route leading to conveniently functionalised  $\gamma$ -cyclobutane building-block.

### 4.3.3 Solid-phase synthesis of truncated NPY analogues

Solid-phase peptide synthesis is a good alternative when preparing peptides of a certain length. The solid phase synthesis can be mainly performed by two alternative protecting group strategies: Boc (temporary PG)/Bn (permanent PG) and Fmoc (temporary PG)/*t*Bu (permanent PG). The first one implies the use of Merrifield linker (**Figure 47**) which requires liquid HF for the cleavage of the peptide from the resin. For that reason this procedure has to be carried out in specialised apparatus and moreover, due to the highly acidic conditions several rearrangements can take place. Oppositely, when following the Fmoc/*t*Bu strategy the cleavage of the peptide from the resin occurs under milder acidic conditions (50% TFA in  $\text{CH}_2\text{Cl}_2$  for the Wang linker), for that reason the Fmoc protection is widely used. In order to introduce extremely mild cleaving conditions, Rink amide has been developed. It is very labile to acids (10% TFA in  $\text{CH}_2\text{Cl}_2$ ) and allows the cleavage of side chain protected peptides, thus being suitable for combinatorial chemistry and peptide synthesis. However, when using this resin, the isolated peptides are amidated in the C-terminus extreme.

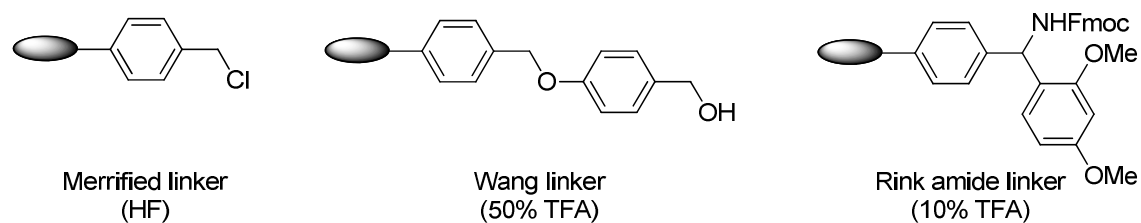


**Figure 47:** Mainly used linkers in solid-phase peptide synthesis (cleavage conditions).

Taking into account the inconveniences showed by Merrifield linker and the fact that the NPY analogues are amidated in the C-terminus, we decided to use Rink amide linker to prepare a family of cyclobutane-containing truncated NPY analogues.

To begin with the solid-phase peptide synthesis, the resin has to be swollen by stirring it during 30 min with an adequate amount of DMF/NMP 80:20 (v/v). Since Rink amide resin is already sold in the NHFmoc protected form, the next step consists in the removal of the Fmoc protecting group using piperidine.

Afterwards, the first monomer is coupled to the linker using a high excess of reagent, HBT/HOBt as coupling agent and DIPEA as a mild base. After shaking for 60-70 minutes the excess of reagent is eliminated by filtration (**Figure 48**) and the resin is washed with DMF.

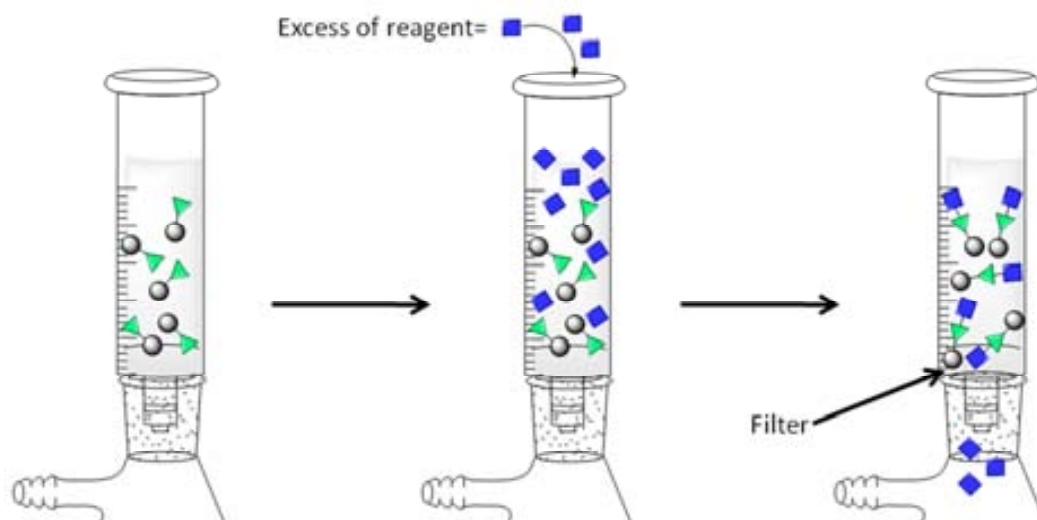


**Figure 48:** Purification of compounds bound to the solid support from those in solution by simple filtration.

In order to prove the completion of the peptide coupling (absence of primary amines) both the Ninhydrin test (Kaiser test) and the TNBS test can be carried out, which are based on colorimetric reaction with primary amines. When the coupling reaction has been completed the Fmoc protecting group of the terminal amine is cleaved through reaction with 20% piperidine. In that way a new reactive site is exposed and synthesis continues in a repetitive way (**Figure 49**).

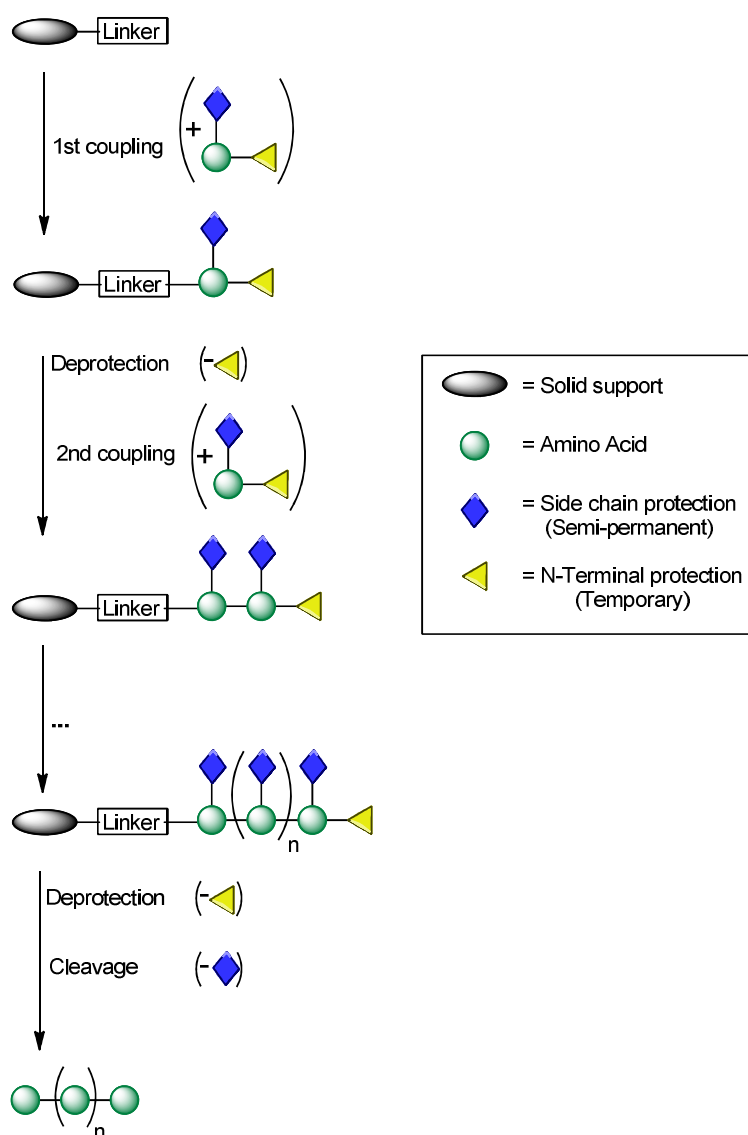


**Figure 49:** General scheme for solid-phase peptide synthesis.

Based on orthogonal protection concept, only takes place the deprotection of the portion of the molecule where further reaction is desired to occur in subsequent couplings, while preventing reaction at side-chain functional groups (**Figure 49**).

Finally, the peptide is cleaved from the resin using an acidic cleavage cocktail. Their selection depends on the nature of the cleavable linker attaching the peptide to the support, the nature of the protecting groups and the reactive properties of the unprotected side-chain. Due to the fact that we wanted to obtain the fully-deprotected peptides, a highly acidic cocktail was used (90:5:5; TFA/Et<sub>3</sub>SiH/H<sub>2</sub>O;). After precipitation and purification of the compounds by preparative HPLC (see Experimental procedures), peptides **76-85** were obtained (**Table 4**). More details concerning the followed procedure for solid-phase peptide synthesis can be found in “Experimental Procedures” section of the present Thesis.

**Table 4:** Isolated truncated cyclobutane-containing NPY analogues. Where ■ = **84** and ◆ = **86**.

| Code       | Sequence  |
|------------|---|
| <b>76</b>  | Ac-RHYINLITR■RY-NH <sub>2</sub>                         |
| <b>76a</b> | Ac-RHYINLITR■RY-NH <sub>2</sub> (SO <sub>3</sub> )      |
| <b>77</b>  | Ac-RHYINLITR◆RY-NH <sub>2</sub>                         |
| <b>77a</b> | Ac-RHYINLITR◆RY-NH <sub>2</sub> (SO <sub>3</sub> )      |
| <b>77b</b> | Ac-RHYINLITR◆RY-NH <sub>2</sub> (2SO <sub>3</sub> )     |
| <b>78</b>  | Ac-RHYINLR■R■RY-NH <sub>2</sub>                         |
| <b>78a</b> | Ac-RHYINLR■R■RY-NH <sub>2</sub> (SO <sub>3</sub> )      |
| <b>79</b>  | Ac-RHYINLI◆R◆RY-NH <sub>2</sub>                         |
| <b>79a</b> | Ac-RHYINLI◆R◆RY-NH <sub>2</sub> (SO <sub>3</sub> )      |
| <b>80</b>  | Ac-YYSALRHYINLITR■RY-NH <sub>2</sub>                    |
| <b>80a</b> | Ac-YYSALRHYINLITR■RY-NH <sub>2</sub> (SO <sub>3</sub> ) |
| <b>81</b>  | Ac-YYSALRHYINLR■R■RY-NH <sub>2</sub>                    |
| <b>81a</b> | Ac-YYSALRHYINLR■R■RY-NH <sub>2</sub> (SO <sub>3</sub> ) |
| <b>82</b>  | Ac-RRYIN-NLe-LTR■RY-NH <sub>2</sub>                     |

|            |   |
|------------|---|
| <b>82a</b> | Ac-RRYIN-NLe-LTR■RY-NH <sub>2</sub> (SO <sub>3</sub> )      |
| <b>83a</b> | Ac-RRYIN-NLe-LTR◆RY-NH <sub>2</sub> (SO <sub>3</sub> )      |
| <b>83b</b> | Ac-RRYIN-NLe-LTR◆RY-NH <sub>2</sub> (2SO <sub>3</sub> )     |
| <b>84</b>  | Ac-RRYINNLTR■RY-NH <sub>2</sub>                             |
| <b>85</b>  | Ac-YAADLRRYIN-NLe-LTR■RY-NH <sub>2</sub>                    |
| <b>85a</b> | Ac-YAADLRRYIN-NLe-LTR■RY-NH <sub>2</sub> (SO <sub>3</sub> ) |

Compounds **76-79** correspond to 12 amino acid cyclobutane-containing NPY analogues. In order to determine the influence in the bioactivity of the analogue's length, 17 amino acid long peptides **80-81** were synthesised. Moreover, 12 amino acid cyclobutane-containing HPP analogues, **82-84**, were synthesised as well as the corresponding elongated HPP analogue **85**. Note that, entries **76a**, **77a**, **77b**, **78a**, **79a**, **80a**, **81a**, **82a**, **83a** and **83b** correspond to mono- or di-*O*-sulphated peptides. The sulphonation probably takes place in the tyrosine residues. Those by-products are formed during the cleavage of the Pmc group (2,2,5,7,8-pentamethylchroman-6-sulfonyl) which is used to protect arginine's side-chain (**Figure 52**), in the future this fact could be avoided by using Pbf (pentamethyl-2,3-dihydrobenzofuran-5-sulfonyl) (**Figure 50**) instead of Pmc. Fortunately, those products could be isolated (except **80a**), therefore we possess a wider range of NPY analogues. Moreover, it is worth to consider that *O*-sulfation is one of the most common *in vivo* post-translational modifications. Hence, the effect of peptide's *O*-sulfation will be evaluated.

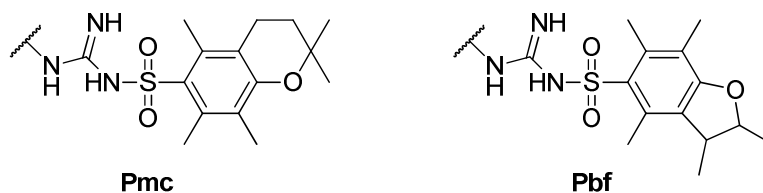


**Figure 50:** Molecular structures of Pmc and Pbf protecting groups.

#### 4.3.4 Determination of NPY analogues $Y_4$ Receptor affinity and subtype selectivity by flow cytometric binding studies

As it has been mentioned before, it is crucial to possess subtype selective NPY ligands which could aid to understand their different *in vivo* functions. With this aim, the affinity towards  $Y_4$ ,  $Y_1$ ,  $Y_2$  and  $Y_5$  receptors was evaluated. The investigated NPY analogues containing building-blocks **73** and **75** whose activity towards  $Y_1$ ,  $Y_2$ ,  $Y_4$  and  $Y_5$  receptors was compared with the natural truncated sequence (HPP and pNPY) are shown in **Table 7**.

Compounds **76-85** were investigated in the laboratories of the Prof. Buschauer from Universität Regensburg with respect to binding affinity to the  $Y_4R$ ,  $Y_1R$ ,  $Y_2R$  and  $Y_5R$  through the performance of saturation binding assays (see NPY analogues Biological assays in Annex VI for detailed information). As can be seen in **Figure 51**, this kind of assays are based on the addition of increasing concentrations of the evaluated ligand (**76-85**) to a suspension of cells whose receptors are completely binded by fluorescent ligands (cy5-[ $K^4$ ]-hP or cy5-pNPY). It is important to note that these assays were carried out with genetically engineered cells that expressed a single subtype receptor. After incubation of the samples for 90-120 min the amount of remaining fluorescent labelled ligand was determined by flow cytometry. The procedure and the instrument settings have been previously described in detail.<sup>142-144</sup>

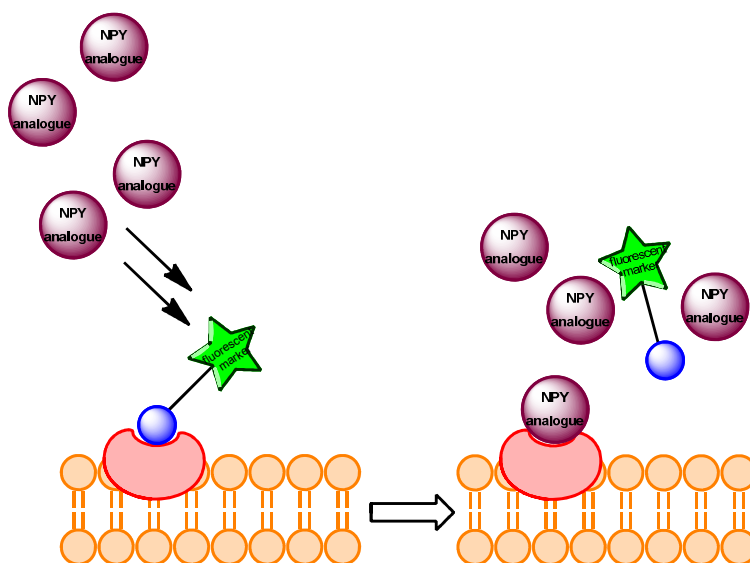


**Figure 51:** Saturation binding assay.

Saturation binding assays allow the determination of the  $K_i$  of each ligand towards each receptor (**Table 5**). The  $K_i$  is the concentration of the competing ligand that will bind to half the binding sites at equilibrium, in the absence of other competitors. If the  $K_i$  is low, the affinity of the receptor for the inhibitor is high.

**Table 5:** Summary of results of the binding studies at  $Y_4$  receptor.

|                          | CHO-hY <sub>4</sub> |      |
|--------------------------|---------------------|------|
|                          | K <sub>i</sub> [nM] |      |
|                          | mean                | sem  |
| 76                       | 71.6                | 7.2  |
| 77                       | > 1000              | /    |
| 77a                      | > 1000              | /    |
| 77b                      | > 1000              | /    |
| 78                       | 35.3                | 1.9  |
| 78a                      | 41.2                | 8.2  |
| 79                       | > 1000              | /    |
| 79a                      | > 1000              | /    |
| 80 + 80a                 | > 1000              | /    |
| 81                       | > 1000              | /    |
| 82                       | 92.8                | 4.3  |
| 82a                      | 563.4               | 59.8 |
| 83a                      | > 1000              | /    |
| 83b                      | > 1000              | /    |
| 84                       | 70.0                | 9.0  |
| 85                       | 119.9               | 29.5 |
| 85a                      | > 1000              | /    |
| HPP <sup>143</sup>       | 6.55                | 0.06 |
| pNPY <sup>142, 143</sup> | 9.62                | 0.07 |

$K_i$  was calculated according to the Cheng-Prusoff equation, mean and sem (standard error of mean) were calculated from three independent experiments performed in duplicate



As it has been previously mentioned, affinity towards  $Y_4$ ,  $Y_1$ ,  $Y_2$  and  $Y_5$  receptors was evaluated, nevertheless here are only shown results  $Y_4$  receptor (see NPY analogues Biological assays in Annex VI for detailed information). Affinity studies (**Table 5**) showed that none of the NPY analogues containing  $\gamma$ -amino acids (**77**, **77a**, **77b**, **79**, **79a**, **83a** and **83b**) exhibited any affinity towards any NPY receptor subtypes. Therefore unnatural amino acid homologation plays an important role in NPY analogues receptor affinity. In contrast, NPY analogues containing a  $\beta$ -cyclobutane moiety were sub-selective towards  $Y_4R$  receptor, differently to  $\beta$ -cyclopropane containing analogues which were sub-selective towards  $Y_1$  receptor.<sup>105</sup> Consequently, we can assume that ring size highly determines the structure of the resulting analogues, thus showing clearly different affinities. In the future, theoretical calculations will be carried out in order to establish the conformation of each of the analogues which leads to a different behaviour. Preliminary modelling carried out by Dr. Lukasz Berlicki (Wroclaw University of Technology) clearly showed that the presence of the cyclobutane ring in analogue **76** highly modifies the position of the side chains of the <sup>33</sup>Arg and <sup>35</sup>Arg residues compared to native sequence (**Figure 52**).

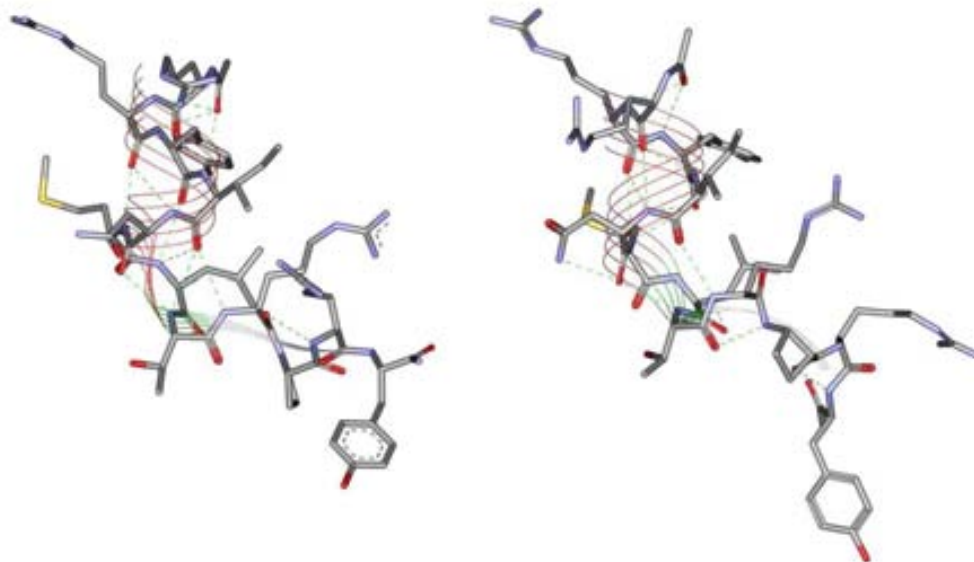


**Figure 52:** Comparison of structures of natural truncated peptide (left, PDB code 1LJV) and peptide containing cyclobutane unit **76** (right, modeled).

Best performance was shown by analogue **78** ( $K_i = 35.3$  nM), which contains two cyclobutane moieties preceding  $^{33}\text{Arg}$  and  $^{35}\text{Arg}$  that seem to be crucial in the receptor binding (**Figure 53**).

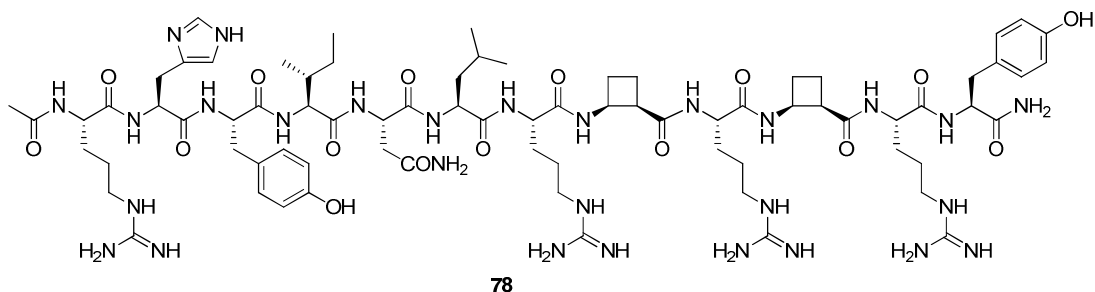


**Figure 53:** Structure of analogue **78**.

In most cases, sulphated peptides (**77a**, **77b**, **83a**, **83b**, **85a**) showed no  $Y_4R$  affinity or in the case of **82a** compared to **82**, reduced  $Y_4R$  affinity. The only exception was **78a** which showed  $Y_4R$  affinity comparable to that of the non-sulphated analogue **78**. We assume that  $^{36}\text{Tyr}$  is sulphated, hence this residue might not be involved in receptor binding. However, further structural studies should be carried out to confirm this hypothesis.

The NPY analogue **80 + 80a** which is extended by five amino acids with respect to **76**, did not show any affinity for the  $Y_4R$ , whereas the corresponding elongated HPP analogue **85** ( $K_i = 119$  nM) exhibited only a minimal decrease in affinity compared to the shorter analogue **82** ( $K_i = 92.8$  nM). Hence, peptide length has an important influence in NPY analogue's affinity.

#### **4.3.5 Functional activity at the NPY $Y_4$ receptor determined in the steady state GTPase assay**

As previously mentioned, NPY receptors belong to G protein-coupled receptors family, which are transmembrane receptors that sense molecules outside the cell and activate inside signal transduction pathways and, ultimately, cellular responses. Signal

molecules bind to a domain located outside the cell. An intracellular domain activates a G protein. This activates a cascade of further compounds, and finally causes a change downstream in the cell (**Figure 54**).

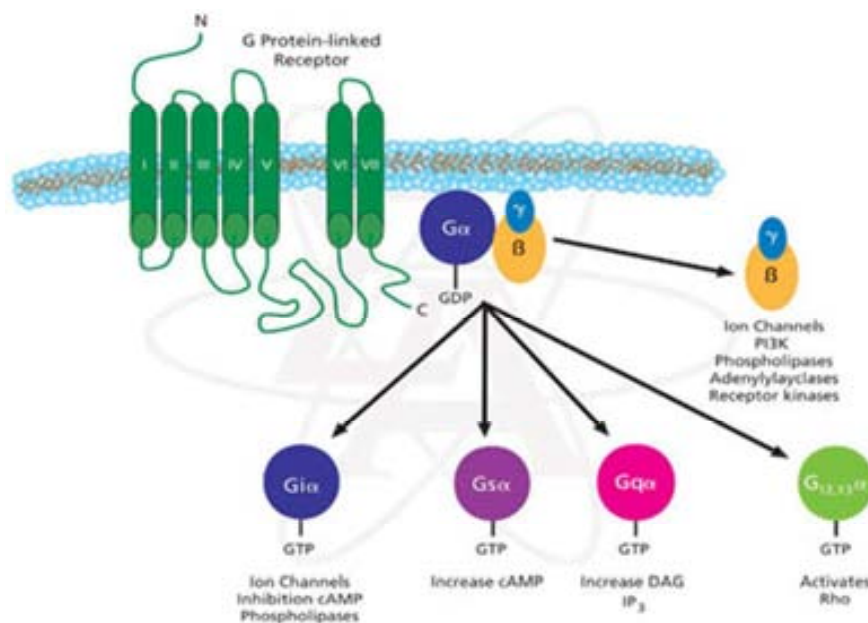


**Figure 54:** Cascade reactions induced by G protein-coupled receptors.

In view to determine the functional activity at the NPY  $Y_4$  receptor of those compounds that showed nanomolar affinities (**76**, **78**, **78a**, **82**, **82a**, **84** and **85**), a GTPase steady state assay was performed following previously described procedures.<sup>145-147</sup>

This kind of assays are based on the addition of increasing concentrations of the evaluated ligand (**76**, **78**, **78a**, **82**, **82a**, **84** and **85**) to a suspension of  $Y_4$ -containing cell membranes in the presence of radio-labelled [ $\gamma$ - $^{32}$ P]-GTP. The  $EC_{50}$  is the concentration of the evaluated ligand that will present a 50% of the maximum GTPase activity, in the absence of other competitors. If the  $EC_{50}$  is low, the activity of the ligand is high. The  $EC_{50}$  of each ligand can be determined through the measure of the final radioemission.

As summarised in **Table 6**, all analogues show partial agonism at the NPY  $Y_4$ R receptor in the steady state GTPase assay, and their  $EC_{50}$  values are much lower than those shown by native NPY, thus having a higher affinity towards  $Y_4$ R. Compound **78** ( $EC_{50}$  = 66.16 nM), which contains two cyclobutane moieties, was the analogue that exhibited the best performance. It is important to note that compound **78** was the one that showed higher

affinity towards Y<sub>4</sub>R. Therefore, it might be a good candidate to model bioactive Y<sub>4</sub>-selective conformation of NPY.

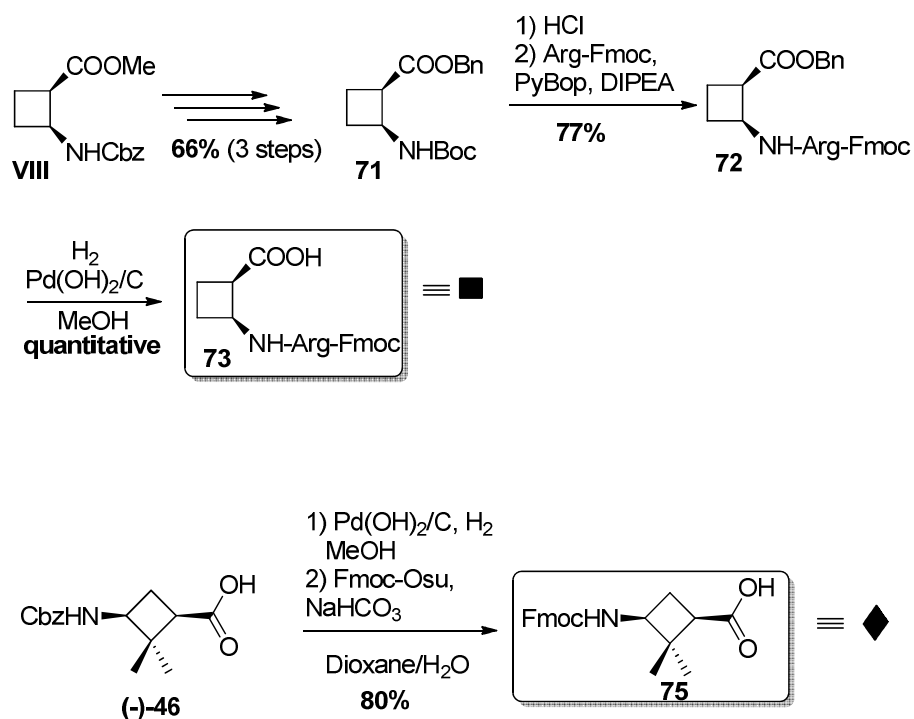
**Table 6:** Results of the GTPase assay (agonist mode) of all Y<sub>4</sub>R affinity ligands.

|                           | Y <sub>4</sub> R      |       |          |
|---------------------------|-----------------------|-------|----------|
|                           | EC <sub>50</sub> [nM] |       | Efficacy |
|                           | mean                  | sem   |          |
| <b>76</b>                 | 122.01                | 28.29 | 0.67     |
| <b>78</b>                 | 66.16                 | 25.48 | 0.76     |
| <b>78a</b>                | 69.95                 | 19.10 | 0.65     |
| <b>82</b>                 | 284.17                | 46.36 | 0.74     |
| <b>82a</b>                | 214.19                | 67.46 | 0.58     |
| <b>84</b>                 | 75.82                 | 21.06 | 0.70     |
| <b>85</b>                 | 223.70                | 34.08 | 0.51     |
| <b>HPP<sup>145</sup></b>  | 11.0                  | 3.6   | /        |
| <b>pNPY<sup>145</sup></b> | 416.9                 | 42    | /        |

Means ± sem were obtained in at least three independent experiments performed in duplicate.

#### 4.4. SUMMARY AND CONCLUSIONS: NPY analogues

- i) The synthesis of enantiomerically pure  $\beta$ - and  $\gamma$ -cyclobutane building blocks suitable for solid-phase peptide synthesis has been accomplished using stereoselective and high yielding transformations (**Scheme 48**).



**Scheme 48:** Synthesis of cyclobutane building-blocks suitable for solid-phase peptide synthesis.

- ii) A family of cyclobutane-containing NPY truncated analogues (**76-85**) has been prepared using solid-phase peptide synthesis. The products differ in:
- Homologation of unnatural amino acid ( $\beta$  and  $\gamma$ )
  - Number of unnatural amino acids
  - Peptide length (12 and 17 residues)
  - Sulphation of certain residues
- iii) Affinity and activity studies have been carried out revealing that:

- a.  $\beta$ -cyclobutane containing analogues (**76**, **78**, **78a**, **82**, **82a**, **84** and **85**) show high affinity towards  $Y_4$  receptor, in contrast to  $\beta$ -cyclopropane-containing ones that were subselective towards  $Y_1$  receptor.
- b. Best performance was shown by analogue **78** ( $K_i = 35.3$  nM), which contains two cyclobutane moieties preceding  $^{33}\text{Arg}$  and  $^{35}\text{Arg}$  that seem to be crucial in the receptor binding.
- c. Homologation of unnatural amino acid led to non-active compounds, none of all the NPY analogues containing  $\gamma$ -amino acids exhibited any affinity towards any of the sub-type receptors.
- d. Length of truncated NPY analogues has an important influence on their activity. In the case of NPY analogues, a better performance was showed by short ones, whereas elongated HPP analogues (**85**) were more active and exhibited similar affinity values.
- e. Sulphation is not a convenient modification, thus only **78a** showed  $Y_4R$  affinity comparable to that of the non-sulphated analogue **78**.

In that way, we can conclude that we possess a series of NPY analogues proximate to bioactive  $Y_4R$  sub-selective conformation. Therefore, theoretical calculations could help to clarify the secondary structure of  $Y_4R$  sub-selective conformation. Moreover, these analogues could be useful to understand which bioprocesses are correlated to  $Y_4R$ .

## **Chapter IV**

Chiral polyfunctional cyclobutane platforms:

Magnetic Resonance Imaging Contrast Agents





## 5. CHAPTER IV: CHIRAL CYCLOBUTANE PLATFORMS: Magnetic Resonance Imaging (MRI) CONTRAST AGENTS

### 5.1. INTRODUCTION

#### 5.1.1 Polyfunctional platforms

Polyfunctional platforms are molecules which have recently awakened the interest of chemists because they present promising applications as building-blocks. As a consequence of their multi-valent nature they can be used as organogelators themselves, or as cores which after convenient modification can lead to organogelators,<sup>76,81</sup> nucleation additives for polymers,<sup>68, 69, 70</sup> nano-wires,<sup>83, 148, 149</sup> liquid crystals,<sup>150</sup> among others. Nevertheless, the most appealing feature of polyfunctional platforms is the feasibility of preparing hybrid multifunctional materials as a consequence of their high versatility.<sup>151</sup>

In that way, hybrid multifunctional materials combine in a single material properties of organic and biological molecules with those of inorganic compounds (**Figure 55**). The inorganic material can play several roles: enhancing the mechanical and thermal stability, modulating the refractive index, providing an accessible and interconnected porous network for sensing or catalysts, or conferring specific magnetic, electronic, redox, electrochemical or chemical properties. Organic components offer opportunities to modify mechanical properties enabling the production of films and fibers, to obtain by simple casting various geometric structures for integrated optics, to control the porosity and connectivity of networks, and to adjust the balance hydrophilic/hydrophobic character. Organic components can also contribute to a specific physical or chemical property including electrical or optical characteristics, electrochemical behaviour, chemical or biochemical reactivity, etc.

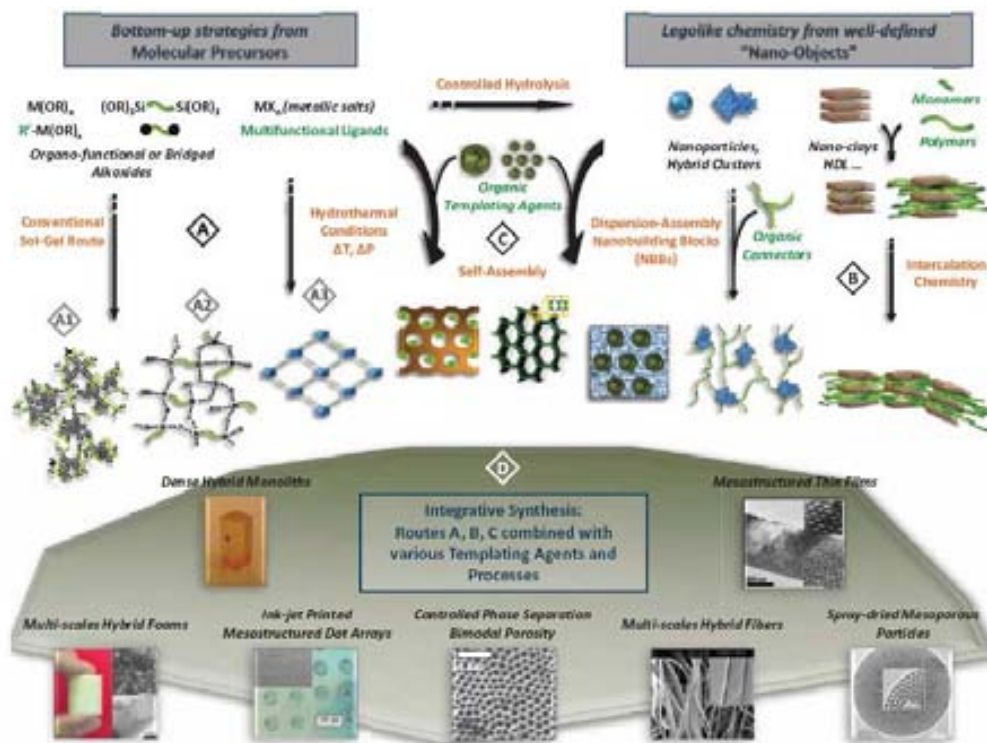


**Figure 55:** Scheme of the main chemical routes leading to nanostructured inorganic and hybrid organic/inorganic materials.<sup>151</sup>

Due to their importance, different hybrid materials can be classified into two main families depending on the nature of the interface combining the organic (or biological) components and inorganic.<sup>152</sup>

Class I corresponds to hybrid systems where the organic and mineral components interact by weak bonds including Van der Waals, electrostatic or hydrogen bonds.

Class II corresponds to hybrid materials in which these components are linked by covalent or ionic-covalent chemical bonds. Of course many hybrid materials have both types of interfaces, strong and weak, but due to the significance of the presence of strong chemical bonds on the final hybrid material properties, these types of hybrid are grouped into class II.

### 5.1.2 Magnetic Resonance Imaging (MRI)

In clinical diagnosis, non-invasive monitoring of internal organs and states of diseases has always been a challenge. With this purpose, a series of techniques named Medical Imaging have been used. There are two main medical imaging techniques: Magnetic Resonance Imaging (MRI) and Computed Tomography (CT). MRI uses radio frequencies and a magnetic field to generate images, whereas CT uses X-ray. The main advantage offered by MRI in comparison to CT is that it doesn't involve exposure to radiation. In addition, it offers excellent spatial resolution and is particularly useful for showing soft tissue. Nevertheless, its low sensitivity makes necessary the use of Contrast Agents (CAs) in order to increase the signal. Hydrogen ( $^1\text{H}$ ) is the most commonly measured nuclei, as it is the most sensitive and abundant element in the human body. It is present inside the body in the form of water and various other organic compounds, such as lipids and cholesterol.

The hydrogen atoms in the body normally point randomly in different directions, but they will line up parallel to each other in a magnetic field (**Figure 56**). When a pulse of radiofrequency (RF) is applied directly to the protons, they will be excited to a higher energy state. Once the RF is turned off, these higher energy protons will gradually relax and generate a detectable radio signal. These signals are detected by the magnetic coils in the machine, and the computer converts the signals into an image, based on the strength of the signal produced by different types of tissue. Generally, protons have to go through magnetization, excitation and relaxation before an MRI image is generated.<sup>153</sup>

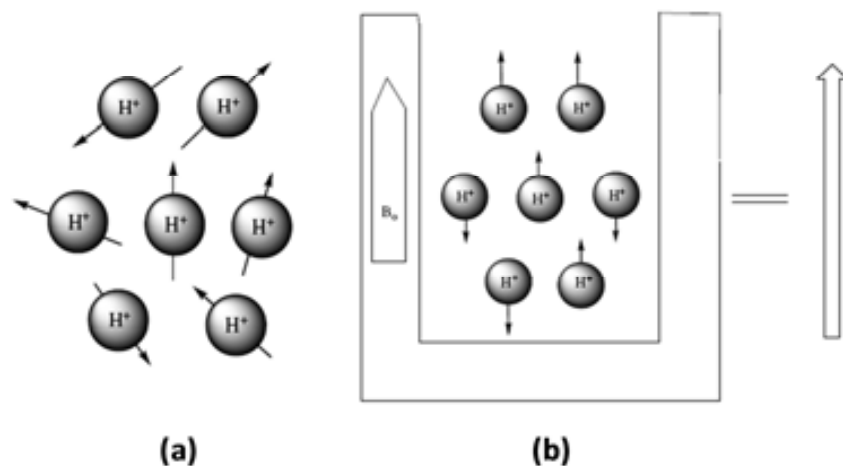


**Figure 56:** (a) dipoles are oriented in a random manner in the absence of magnetic field. (b) nuclei align in the presence of magnetic field.

Relaxation is the result of two different mechanisms: longitudinal relaxation and transverse relaxation.

**Longitudinal relaxation:** Longitudinal relaxation corresponds to the longitudinal magnetization recovery, and its rate is characterised by the time constant ( $T_1$ ), which is determined by thermal interactions between the resonating protons and other protons and other magnetic nuclei in the magnetic environment or "lattice". These interactions allow the energy absorbed by the protons during resonance to be dispersed to other nuclei in the lattice. The recovery of longitudinal magnetization follows an exponential curve (**Figure 57**).  $T_1$  values increase with the field strength.

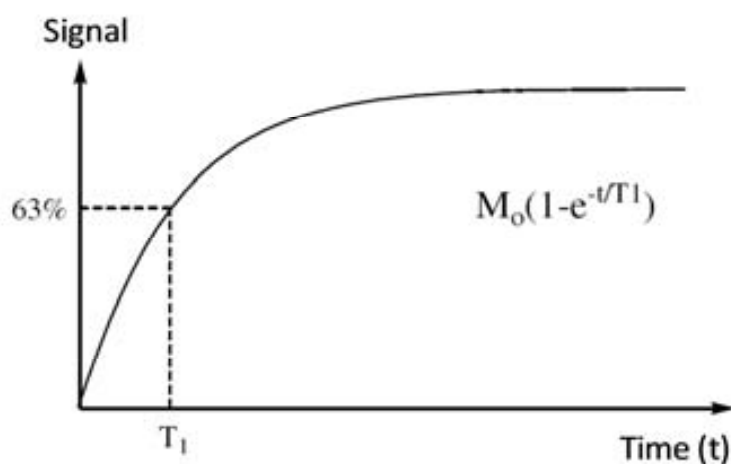


**Figure 57:** Plot of longitudinal magnetization *versus* time.

**Transverse relaxation:** It is a measure of how long transverse magnetization would last in a perfectly uniform external magnetic field as a result of the spins getting out of the phase. When spins move together, the temporary and random interactions between their magnetic field cause their precession rate to change, and result in a cumulative loss in phase. Transverse magnetization is decayed exponentially (**Figure 58**) and it is characterised by the time constant  $T_2$ . Unlike  $T_1$ ,  $T_2$  value is independent of the field strength.

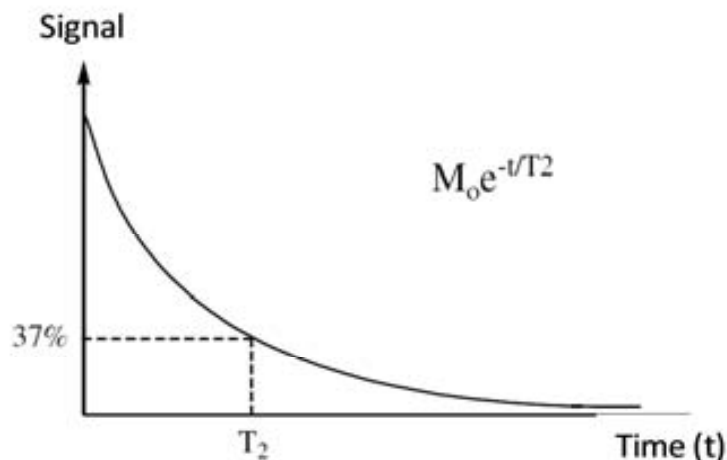


Figure 58: Plot of transverse magnetization *versus* time.

### 5.1.3 MRI Contrast Agents (CAs)

Contrast agents (CAs) shorten the relaxation time  $T_1$  and  $T_2$  of the water protons where they are distributed in a particular tissue. This enhances the contrast between the area of interest and the background. MRI contrast agents are classified into two types,  $T_1$  and  $T_2$  agents.  $T_1$  agents are also known as positive contrast agents, which alter  $T_1$  of tissue more effectively than  $T_2$ , and increase signal intensity on  $T_1$  weighted images.  $T_2$  agents are known as negative contrast agents, which largely reduce the  $T_2$  of tissue and cause a reduction in signal intensity.  $T_1$  contrast agents are more favourable than  $T_2$  contrast agents as the  $T_1$  relaxation time of diamagnetic water solution is typically five-times longer than  $T_2$  and, consequently easier to shorten. Therefore, much attention has been focused on the development of  $T_1$  contrast agents.

Best candidates for  $T_1$  contrast agents are paramagnetic substances (i.e. molecular oxygen), paramagnetic stable radicals (i.e. nitroxide) or paramagnetic metal ions (transition metals and lanthanides). However, only metal ions are suitable candidates for MRI contrast agents with clinical use. Gadolinium(III) ion, which contains seven unpaired electrons that make it highly paramagnetic, is the most favourable candidate. Moreover, the totally symmetric electronic state ( $^8S_{7/2}$  ground state) of  $Gd^{3+}$  results in a long electronic relaxation time ( $10^{-8} - 10^{-9}$  s), thus being a powerful contrast agent. Nevertheless,  $Gd^{3+}$  cannot be

directly administered to patients due to its toxicity, and for that reason ligands capable of forming stable complexes with  $Gd^{3+}$  have to be used.

$Gd^{3+}$  based MRI CAs catalytically shorten the relaxation time of the water protons through dipolar coupling between the electron magnetic moment of the  $Gd^{3+}$  ion and the nuclear magnetic moment of the water proton. The efficiency of a certain CA to catalyse the water proton relaxation is measured in terms of relaxivity ( $r$ ) and is expressed in units of  $mM^{-1}\cdot s^{-1}$ . Relaxivity can be obtained by plotting relaxation rate ( $R_i = 1/T_i$ ) against the concentration of the CA. The water molecules directly linked to the metal exchange with bulk water, and this exchange transmits the paramagnetic effect of  $Gd^{3+}$  to the surrounding environment. The efficacy of the agent is mainly related to the number of water molecules bound to  $Gd^{3+}$  (the hydration number),  $q$  (the exchange rate of the coordinated water molecule[s] with the surrounding water),  $k_{ex}$ , and the rotational correlation time  $\tau_R$  (**Figure 59**).

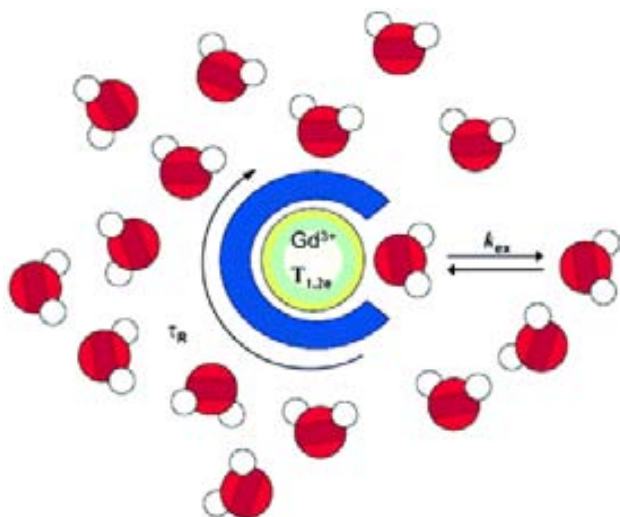


**Figure 59:** Diagram showing the parameters that govern longitudinal relaxivity.<sup>154</sup>

However, the efficacy of a certain MRI contrast agent is also governed by other factors. In addition to a high relaxivity, it must be also biocompatible. Therefore, an ideal MRI contrast agent should be effective at low concentration, present tissue specificity, and have basic pharmaceutical features, such as non-toxicity and low osmolality.

**Clinical contrast agents**

In the European Union (EU) there are nine clinically approved Gd<sup>3+</sup> based contrast agents as listed in **Figure 60**.<sup>155</sup>

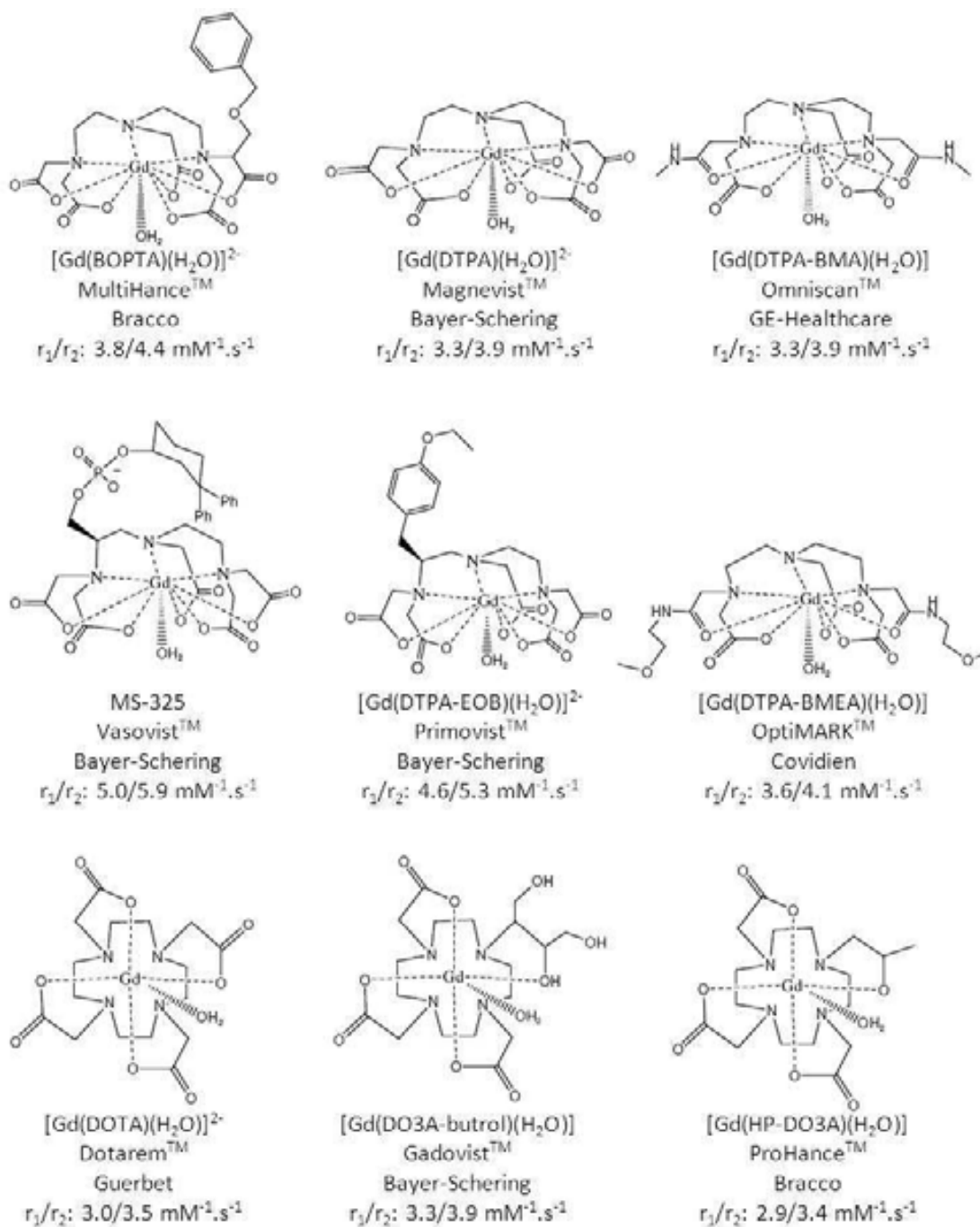


**Figure 60:** Clinically approved MRI contrast agents. Relaxivities were measured at 37 °C in water, using 1.5 T magnets.

All the clinically approved  $T_1$  agents have a molecular weight around 600 Da and relaxivities between 4 and 5  $\text{mM}^{-1}\cdot\text{s}^{-1}$  at 1.5 T and 310 K. They are regarded as non-specific agents or extracellular fluid space (EFS) agents, except MultiHance<sup>TM</sup> and Primovist<sup>TM</sup>, which are hepatobiliary agents. All of them are octa-coordinated gadolinium chelates, and the coordination sphere is completed with a water molecule in the inner sphere, achieving a total coordination number of nine.

As previously mentioned, apart from relaxivity values, biocompatibility is a critical factor. For that reason, the integrity of the gadolinium chelate must be maintained *in vivo* in order to ensure good tolerability. Dissociation of  $\text{Gd}^{3+}$  from an MRI contrast agent is undesirable, as both the free metal and unchelated ligands are generally more toxic than the chelate itself. Two sometimes confusing concepts have been proposed to describe the stability of gadolinium chelates: thermodynamic and kinetic stability, nevertheless what is clear is that chelate stability is much higher for macrocyclic than for linear ones. It appears that high kinetic stability (i.e. macrocyclic chelates in the order of kinetic stability: Gd-DOTA > Gd-DO3A-butrol > Gd-HP-DO3A) combined with high thermodynamic stability (i.e. macrocyclic chelates in the order of thermodynamic conditional stability: Gd-DOTA > Gd-HP-DO3A > Gd-DO3A-butrol) will minimize the amount of free gadolinium released *in vivo*.<sup>155</sup> Therefore, it seems that Dotarem<sup>TM</sup> is the best candidate for *in vivo* applications.

When designing new CAs, in order to achieve sufficient  $T_1$  change, relaxivity and/or the number of Gd per molecule should be increased. Perhaps the most important parameter influencing relaxivity is rotational motion. There are several approaches that control the rotational dynamics in order to increase relaxivity, the most effective ones consist in limiting rotation of  $\text{Gd}^{3+}$  through the use of rigid scaffolds, and the templated self-assembly approach of several monomers. Novel strategies for linking multiple gadolinium complexes are also beginning to appear.<sup>156</sup>



## 5.2. OBJECTIVES

As it has been previously mentioned, polyfunctional platforms are very versatile molecules which potentially possess a wide number of applications. For that reason the first objective of this chapter consists on the stereoselective synthesis of chiral cyclobutane platforms such as triamines **92** or **118** (Figure 61).

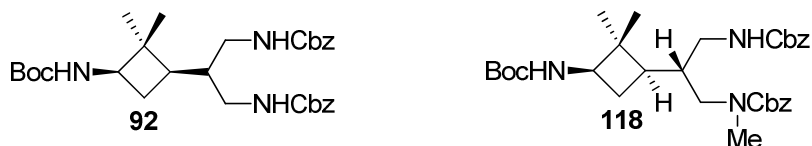


Figure 61

Chiral platforms **92** and **118** were used for the preparation of hybrid materials consisting of a new class of Gd-based multivalent MRI contrast agents using DOTA as complexing agent (Figure 62).

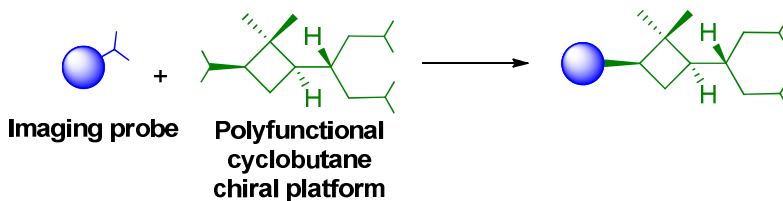


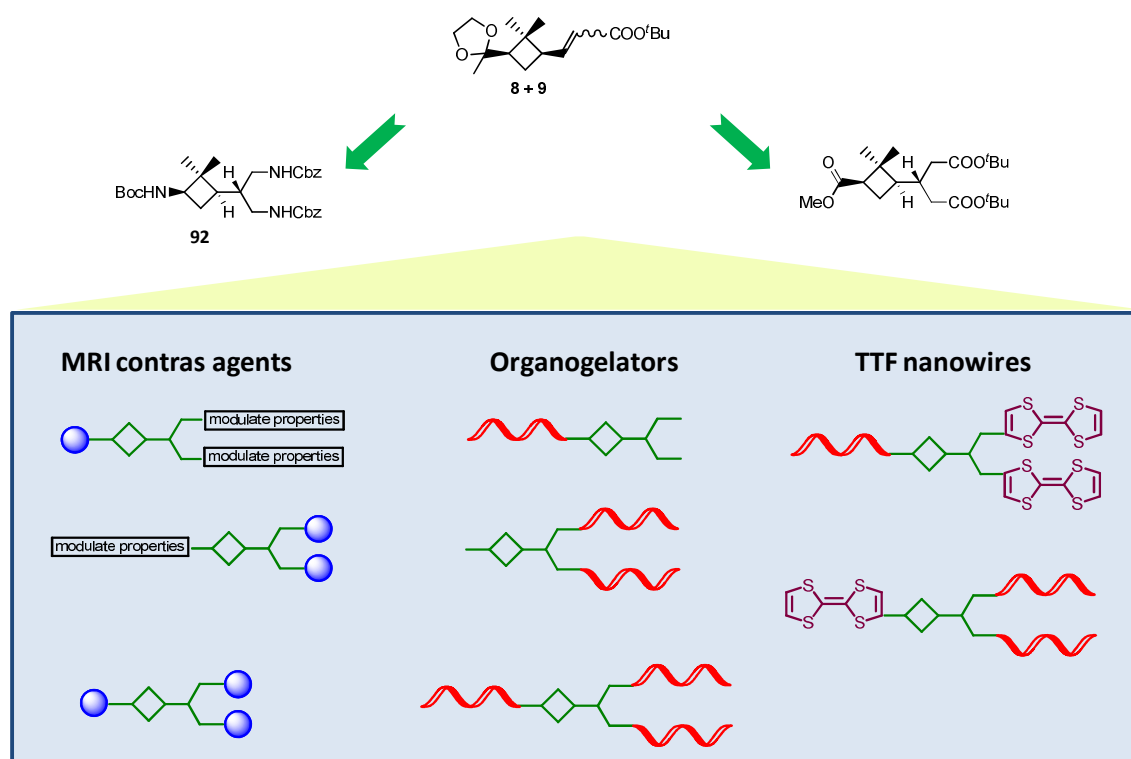
Figure 62

Finally, newly prepared CAs were evaluated both *in vitro* and *in vivo* using adequate MRI techniques.

### 5.3. RESULTS AND DISCUSSION

#### 5.3.1 Synthesis of chiral polyfunctional cyclobutane platforms

The recent interest that polyfunctional platforms have awakened among both materials and synthetic chemists, as a result of their high versatility leading to hybrid materials, made us think of the use of previously synthesised  $\gamma$ ,  $\epsilon$ -aminodiacid **15** as a precursor for the preparation of chiral polyfunctional cyclobutane platforms. One of the requirements of this kind of molecules is to lead easily to the final products, therefore we proposed ourselves the synthesis of both chiral cyclobutane triacid and triamine (**Scheme 49**) which could be functionalised in a single step.

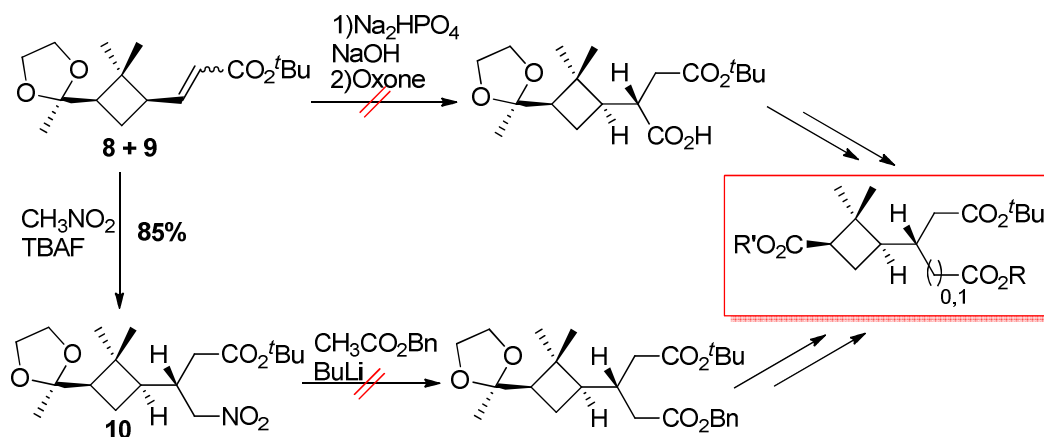


**Scheme 49:** Chiral polyfunctional cyclobutane platforms potentially leading to a wide range of hybrid materials.

#### Attempted synthesis of cyclobutane-cored tricarboxylic acid

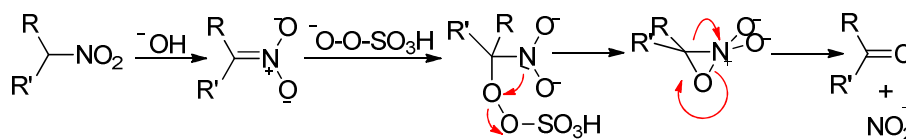
As it has been mentioned in Chapter 1, when designing new synthetic routes leading to chiral cyclobutane containing compounds it is essential to respect the optical purity of the

substances. For that reason, in most cases only mild conditions can be used. Accordingly, the first assayed procedure for the preparation of cyclobutane tricarboxylic acid consisted in submitting nitro ester **10** to Nef reaction which allows the transformation of nitro compounds into carbonyl derivatives (**Scheme 50**). In that way, the third chiral center had been already generated through the Michael addition of nitromethane to previously prepared *E/Z* mixture of alkenes **8** and **9** (see Chapter 1) and it was only required to find mild conditions which enabled the accomplishment of Nef reaction. P. Ceccherilli and co-workers had previously described the use of Oxone<sup>®</sup> as oxidizing agent to undergo Nef reaction under mild conditions.<sup>157</sup>



**Scheme 50:** Explored synthetic routes leading to cyclobutane carboxylic acid.

As depicted in **Scheme 51** the mechanism of Oxone-promoted Nef reaction is compatible with functional groups present in nitro-ester **10**. Hence, compound **10** was submitted to the conditions described by Ceccherilli *et al.*, only recovering the starting material. Probably, this result is the consequence of the electronic factors that deactivate nitro-ester **10** towards oxidative Nef reaction.



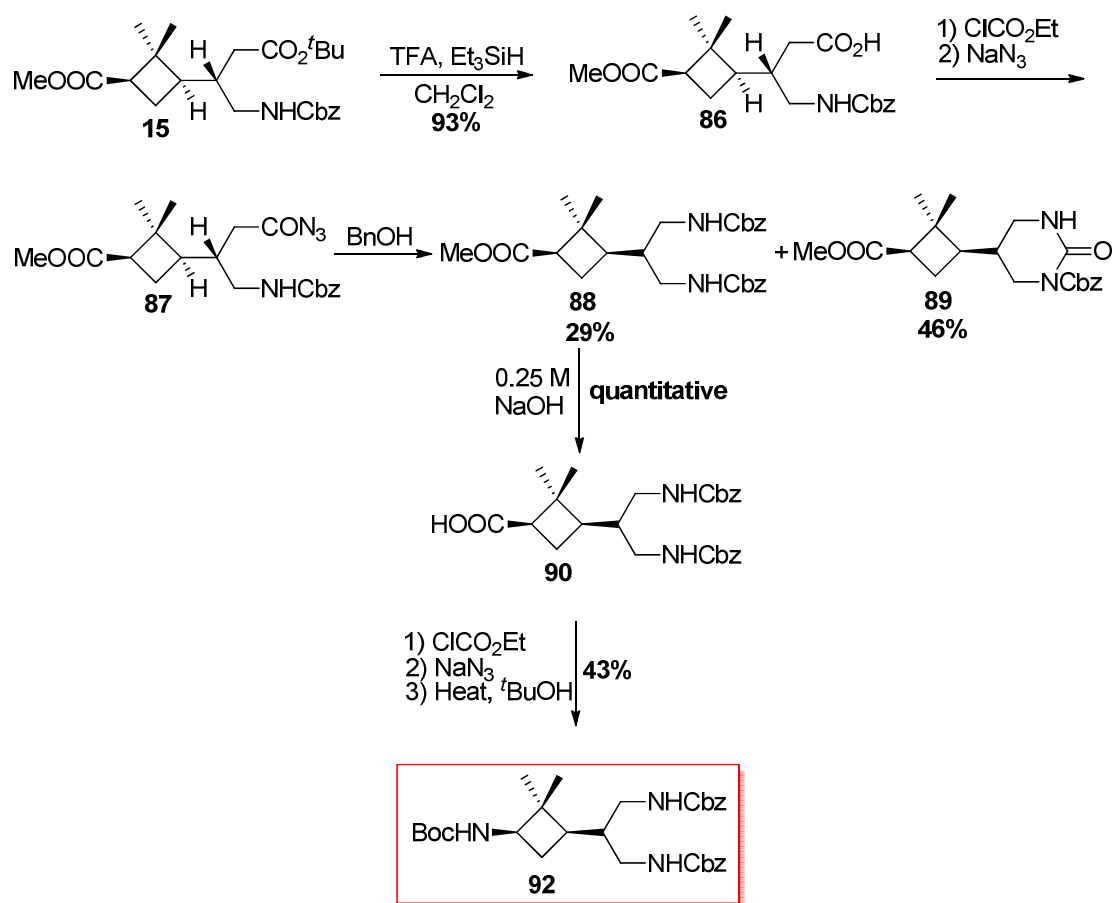
**Scheme 51:** Reaction mechanism of Oxone-promoted Nef Reaction

After not having succeeded in the transformation of nitro group into a oxo group, a new synthetic strategy was considered. It consisted in the addition to the double bond in **8** and **9**, of a synthon which already contained the carbonyl group. However, the requirement of generating a strong enough nucleophile almost limited it to dicarbonyl synthons which were not suitable due to the extreme conditions required for subsequent decarboxylation. Nevertheless, Iwasawa *et al.* had already described the addition of benzyl acetate to the double bond of alkenoates using BuLi as a base.<sup>158</sup> For that reason the same methodology was essayed with *E/Z* mixture of alkenes **8** and **9** without success, recovering starting material (**Scheme 50**).

In view of the obtained results, the synthesis of cyclobutane tricarboxylic acid was abandoned and all our efforts were focused in the synthesis of cyclobutane triamines.

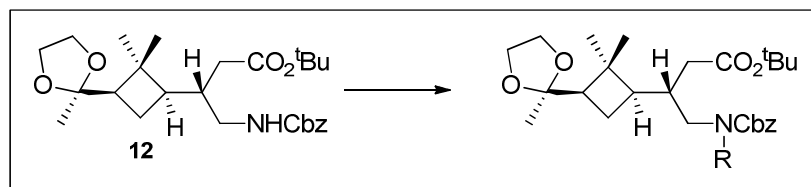
### Synthesis of cyclobutane-cored triamines

Taking into account the facile transformation of carboxylic acids into amines through Curtius rearrangement, we decided to use previously synthesised  $\gamma$ ,  $\epsilon$ -aminodiacid **15** (see Chapter 1) as starting material for the synthesis of cyclobutane-cored triamines. This compound is an excellent intermediate and only requires of two sequential deprotection/Curtius rearrangement sequences. With this aim, *tert*-butyl ester in compound **15** was cleaved under acid conditions using triethylsilane as a cation scavenger to afford free carboxylic acid **86** with an almost quantitative yield (**Scheme 52**). Next, carbonyl group in **86** was activated through the formation of a mixed anhydride, which was reacted with sodium azide to afford the corresponding acyl azide **87**. The so-obtained product was directly submitted to Curtius rearrangement in the presence of benzyl alcohol to afford the corresponding diamine **88** in 29% yield. This low yield was a consequence of the formation of the cyclic urea **89** which is more favourable due to the fact that the nucleophilic attack towards the isocyanate takes place intramolecularly. The desired diamine **88** could be easily isolated from the reaction crude and its methyl ester was hydrolysed using 0.25 M NaOH to afford quantitatively free carboxylic acid **90**. Without further purification, it was submitted to the activation/nucleophilic attack sequence yielding acyl azide **91** which directly underwent Curtius rearrangement in the presence of *tert*-butanol to afford cyclobutane-cored triamine **92** in 43% yield after the 3 steps.



**Scheme 52:** Synthetic scheme leading to cyclobutane-cored triamine **92**.

In order to avoid the side-reaction of formation of urea **89**, amine group in **15** should be diprotected. Moreover, this would lead to a new kind of platform which would enable us to investigate the influence of an additional chiral center on its final properties. With this aim, a series of methodologies were assayed using as model compound **12**, as summarised in **Table 7**. As it can be seen, only one of all the evaluated procedures afforded the desired diprotected amine with an acceptable yield which corresponds to amine methylation using methyl iodide and silver oxide after 7 days of reaction. However, due to the long time required for the reaction to complete, summed to the non-reverse nature of this protection, other alternatives were investigated.

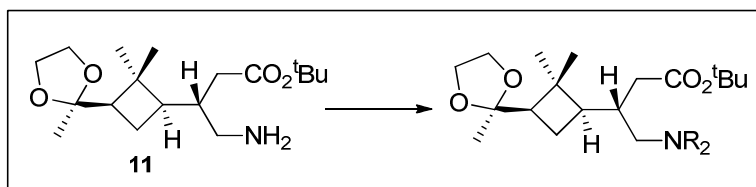
**Table 7:** Essayed methodologies for the diprotection of amine group in **12**.

| Reactants                                       | $t_{\text{REAC}}$ | Products  |
|---|-------------------|---|
| CbzCl, NaHCO <sub>3</sub>                       | 18h               | Starting material   |
| CbzCl, LHMDS                                    | 1h                | Starting material   |
| CbzCl, LHMDS                                    | 18h               | 58% conversion ( <b>93</b> , R= Cbz)<br>Low reproducibility |
| Cbz <sub>2</sub> O, DMAP                        | 18h               | Starting material   |
| TsCl, Pyr                                       | 18h               | Starting material   |
| MsCl, Pyr                                       | 18h               | Starting material   |
| MsCl, BuLi                                      | 18h               | <br><b>94</b>   |
| CH <sub>3</sub> I, Ag <sub>2</sub> O            | 7 days            | 25 % conversion ( <b>95</b> , R= CH <sub>3</sub> )          |
| CH <sub>3</sub> I, BuLi                         | 18h               | <br><b>97</b><br>2 epimers                                  |
| CH <sub>3</sub> I, NaH                          | 18h               | <br><b>97</b>   |
| F <sub>3</sub> CSO <sub>3</sub> CH <sub>3</sub> | 18h               | <br><b>96</b> + Product ( <b>95</b> )                       |

In this case, direct diprotection of free amine in compound **11** was tested as summarised in **Table 8**. As stated in the second entry, diprotection of free amine using *tert*-

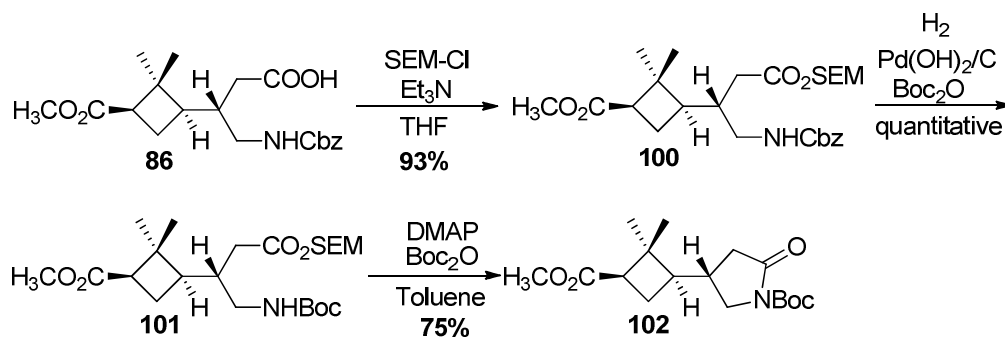
butyl dicarbonate and a catalytic amount of DMAP afforded the desired product with a 75% conversion after 60 hours and allowed the recovery of unreacted material. Nevertheless, this protecting group did not allow selective cleavage of *tert*-butyl ester, therefore a different protecting group for the carboxyl group was required.

**Table 8:** Essayed methodologies for the diprotection of free amine group in **11**.



| Reactants                | $t_{\text{REAC}}$ | Products  |
|--------------------------|-------------------|---|
| MsCl, Pyr                | 18h               | Product ( <b>98</b> , R= Ms)<br>+ Side products |
| Boc <sub>2</sub> O, DMAP | 60h               | Product ( <b>99</b> , R= Boc)<br>75% conversion |

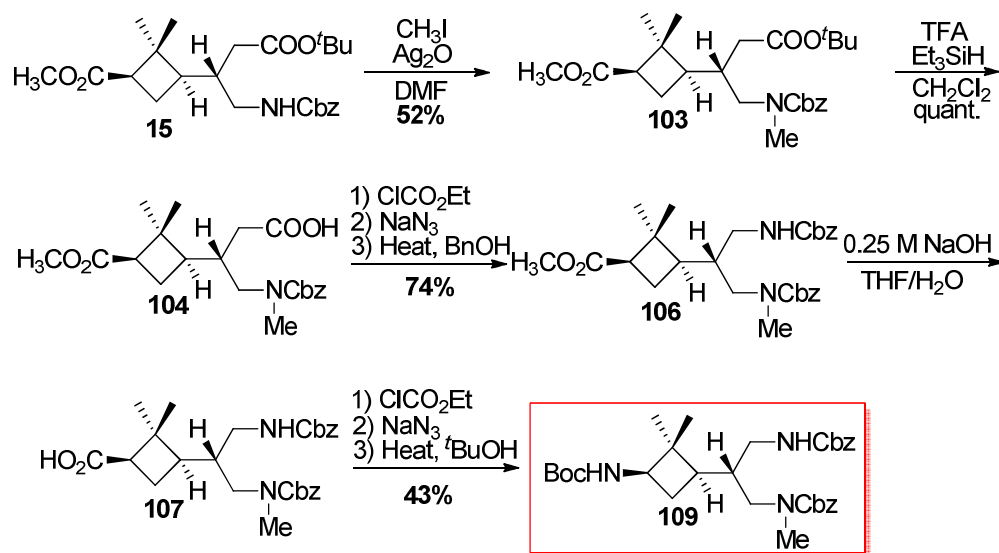
2-Trimethylsilyloxyethyl ester (SEM) which is stable under a wide range of pHs and is easily removed using fluoride ion, seemed to be a good option for the protection of the carboxylic acid. With this purpose, free carboxylic acid in **86** was protected as a SEM-ester using SEM chloride and triethylamine as a base, to obtain the desired SEM-protected product **100** in 93% yield (**Scheme 53**). Afterwards, benzyl carbamate was cleaved through hydrogenolysis in the presence of *tert*-butyl dicarbonate to afford orthogonally protected  $\gamma$ ,  $\epsilon$ -aminodiacid **101** which was used without further purification in the next step. Then, Boc mono-protected amine **101** was heated to reflux in toluene in order to obtain the corresponding diprotected product. However, SEM protecting group turned to be labile under high temperatures and cyclic lactam **102** was obtained instead of the desired product.



Scheme 53: SEM-based synthetic route.

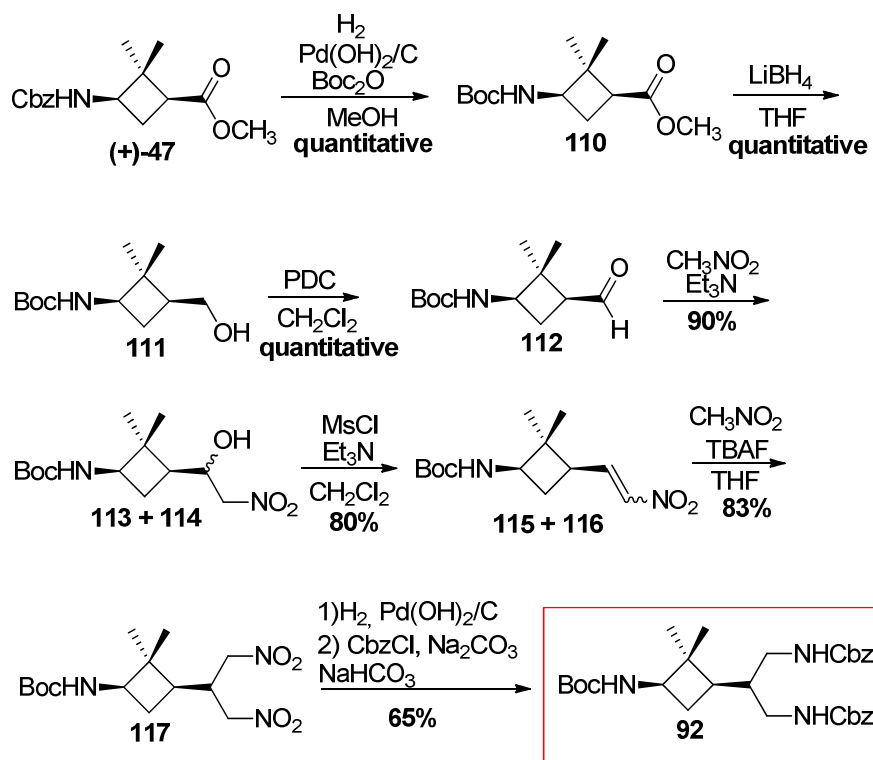
As a consequence of the described results, finally the methodology involving methyl iodide and silver oxide was chosen as the best one. In that way, mono-protected amine in **15** was methylated following the previously described methodology, to obtain the desired product in 52% yield after 7 days (Scheme 54). Next, *tert*-butyl ester in **103** was cleaved using TFA and triethylsilyl ether as a cation scavenger, yielding quantitatively free carboxylic acid **104**. Next, acyl azide **105** was prepared through a two-step methodology consisting of carbonyl activation and subsequent nucleophilic attack by sodium azide. Right after, acyl azide **105** was submitted to Curtius rearrangement in the presence of benzyl alcohol to afford diamine **106** in 74% yield. Afterwards, methyl ester was hydrolysed using 0.25 M NaOH and yielded free carboxylic acid **107**, from which acyl azide **108** was prepared. Curtius rearrangement in the presence of *tert*-butanol afforded pure cyclobutane-cored triamine **109** in 43% yield after 4 steps.





**Scheme 54:** Synthetic route leading to diprotected cyclobutane-cored triamine **109**.

Even though two different cyclobutane-cored triamines had been prepared, we persisted in the seek for an efficient synthetic route leading to triamine **92** (**Scheme 55**). Starting from previously prepared, orthogonally protected  $\gamma$ -amino acid **(+)-47**, benzyl carbamate was exchanged by a Boc protecting group through catalytic hydrogenation in the presence of Boc anhydride, isolating pure compound **110** with a quantitative yield. Orthogonally protected amino acid **110** was reduced to alcohol **111** with  $\text{LiBH}_4$  followed by controlled oxidation with PDC to the corresponding aldehyde **112** which was immediately submitted to Henry reaction in order to afford a mixture of nitro alcohols **114** and **115** in 90% yield. The diastereomeric mixture of alcohols underwent mesylate elimination followed by *in situ* nitromethane addition isolating enantiopure dinitro derivative **117** in 66% overall yield. Finally, reduction of both nitro groups by catalytic hydrogenation led to partially deprotected triamine **118** and subsequent amine protection as benzyl carbamate led to enantiopure cyclobutane-cored triamine **92** in 65% yield.

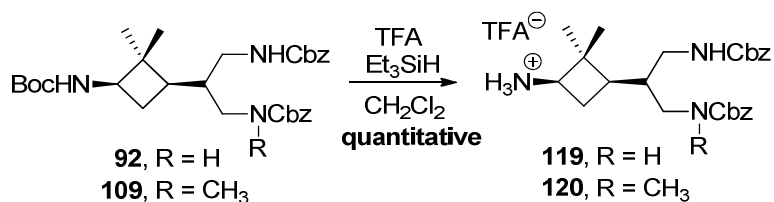


**Scheme 55:** More efficient alternative synthetic route leading to cyclobutane-cored triamine **92**.

It is important to note, that this last synthetic strategy is much more effective than the described in **Scheme 52**. The Henry reaction-based synthetic route presents a 15% overall yield after 16 steps, starting from (-)-verbenone (**1**). In contrast, the other one consists of 20 steps which have a 3% overall yield.

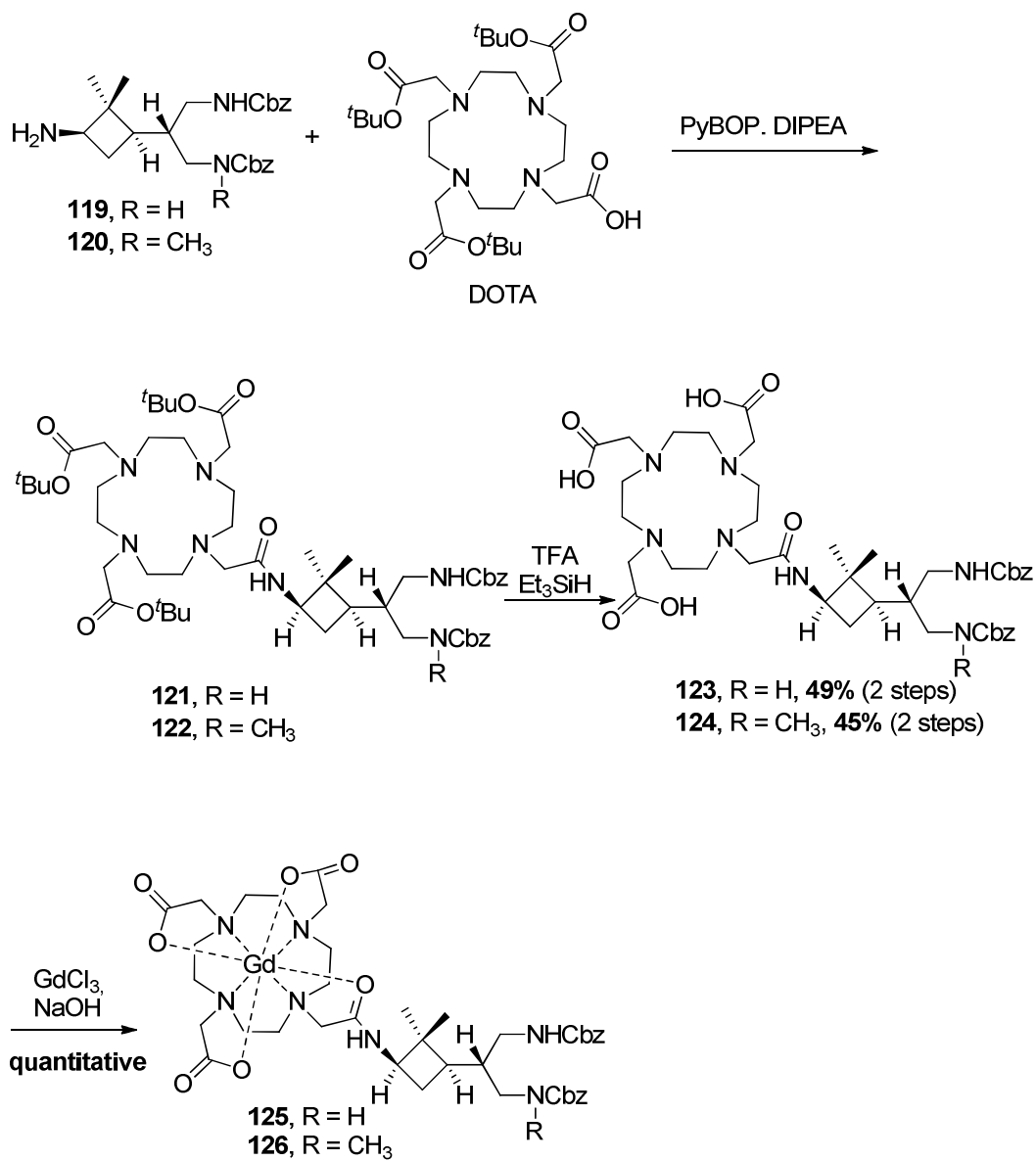
### 5.3.2 Synthesis of hybrid DOTA-cyclobutane CAs

Once we possessed a series of chiral polyfunctional cyclobutane platforms we proceeded to link them to DOTA in order to obtain a new generation of highly versatile contrast agents. With this purpose, first of all, acidolytic mono-deprotection of both orthogonally protected triamines **92** and **109** was carried out obtaining respectively **119** and **120** in quantitative yield (**Scheme 56**).



**Scheme 56:** Selective deprotection of triamines **92** and **109**.

After selective mono-deprotection it was possible to carry out the peptide coupling of one equivalent of DOTA. Taking into account earlier results described in previous chapters, as well as the precedents found in the literature, PyBOP was used as coupling agent together with DIPEA affording hybrid DOTA-cyclobutane compounds **121** and **122** (**Scheme 57**), which were not purified and used straightforward in the next step. Afterwards, *tert*-butyl esters were cleaved using TFA and, after precipitation in MeOH/Et<sub>2</sub>O, pure free acids **123** and **124** were obtained in 49% and 45% overall yield, respectively. Finally, Gd<sup>3+</sup> was complexed obtaining compounds **125** and **126** through reaction of deprotected triacids **123** and **124** with GdCl<sub>3</sub> at room temperature and at pH=6. The completion of the process was checked using the single-drop xylenol orange test (**Figure 63**), which consists on a colourimetric reaction between xylenol orange and free Gd<sup>3+</sup>.<sup>159</sup> At a buffered pH, xylenol orange has a orange/yellow coloration. In the presence of free Gd<sup>3+</sup> cations, xylenol orange complexes them and its color turns to purple. As it can be seen in **Figure 63**, none of the tested reactions presented free Gd<sup>3+</sup> cations.



Scheme 57: Synthesis of hybrid DOTA-cyclobutane contrast agents.

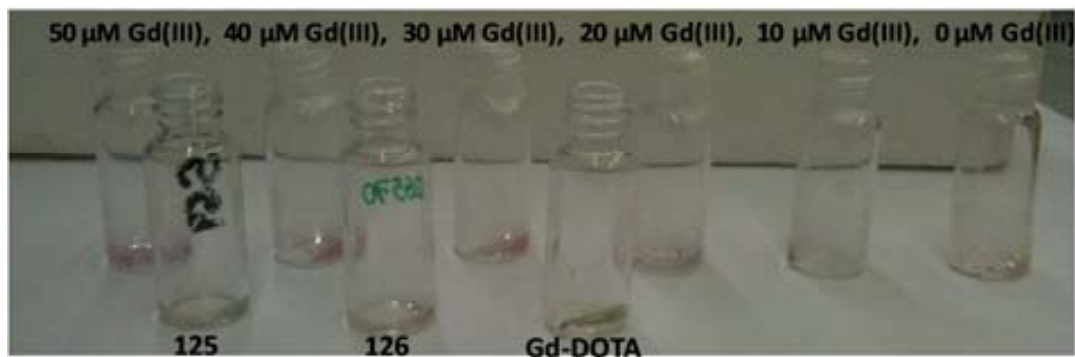


**Figure 63:** Xylenol orange test used to detect free  $Gd^{3+}$  ions. As can be clearly seen in the picture none of the samples contained free  $Gd^{3+}$ .

All these deprotection and complexation synthetic steps, were also carried out for DOTA itself, leading to compound Gd-DOTA. In that way, the resulting molecule complex could be used as control in the MRI experiments.

### **5.3.3 In vitro evaluation of the new CAs**

In collaboration with Dr. Lope-Piedrafita from Servei de Resonància Magnètica, UAB, a series of MRI measurements were carried out in order to determine *in vitro*  $T_1$  and  $T_2$  values of the previously synthesised compounds. All the  $^1H$ -magnetic resonance studies were performed in a 7 Tesla horizontal magnet (*BioSpec 70/30*, Bruker Biospin, Ettlingen, Germany). To perform relaxivity measurements, phantoms of Milli-Q water solutions containing compounds **125**, **126** and Gd-DOTA at various concentrations (1.250, 0.625, 0.312, 0.156, 0.078, 0.039, 0.019 and 0.00 mM) were prepared (**Figure 64**).

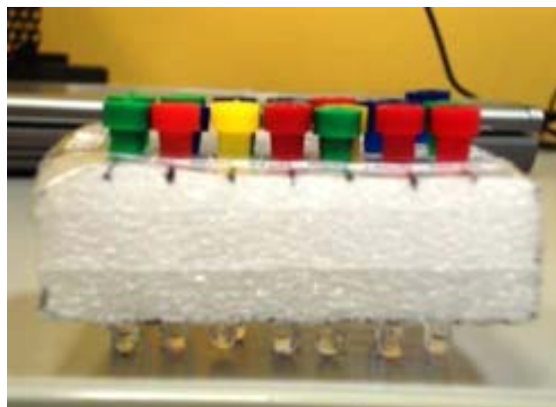


**Figure 64:** Phantom solutions of the different evaluated compounds.

Longitudinal and transverse relaxivity values,  $r_1$  and  $r_2$ , were obtained from the linear regression of the relaxation rates  $R_1$  and  $R_2$  (as the inverse of the relaxation times  $T_1$  and  $T_2$ ) versus Gd concentration:

$$R_i = (R_i)_0 + r_i [\text{Gd}]; \quad i = 1, 2$$

where  $(R_i)_0$  refers to the relaxation rate in the absence of paramagnetic species.

Longitudinal  $r_1$  and transverse  $r_2$  relaxivities for compounds **125**, **126** and reference Gd-DOTA were derived and are compared in **Table 9**. Those values were obtained by fitting of the experimental relaxation rates ( $R_1$  and  $R_2$ ) into a line using the linear least squares regression method. The slope of the resulting line corresponds to the relaxivity ( $r_1$  or  $r_2$ ) value (Figures **65** and **66**).

**Table 19:** Longitudinal  $r_1$  and transverse  $r_2$  relaxivities of CAs **136**, **137** and Gd-DOTA measured at 7 T magnetic field and 295 K.

|                      | $r_1 [s^{-1} \cdot mM^{-1}]$ |         |         | $r_2 [s^{-1} \cdot mM^{-1}]$ |         |         |
|----------------------|------------------------------|---------|---------|------------------------------|---------|---------|
|                      | Prepared Gd-DOTA             | 125     | 126     | Prepared Gd-DOTA             | 125     | 126     |
| <b>1st replicate</b> | 2.3±0.1                      | 3.3±0.1 | 1.7±0.1 | 2.6±0.1                      | 4.6±0.8 | 2.4±0.2 |
| <b>2nd replicate</b> | 2.3±0.1                      | 3.2±0.2 | 1.7±0.1 | 2.6±0.1                      | 4.3±0.7 | 2.3±0.1 |
| <b>Mean</b>          | 2.3±0.1                      | 3.2±0.2 | 1.7±0.1 | 2.6±0.1                      | 4.5±0.7 | 2.3±0.2 |

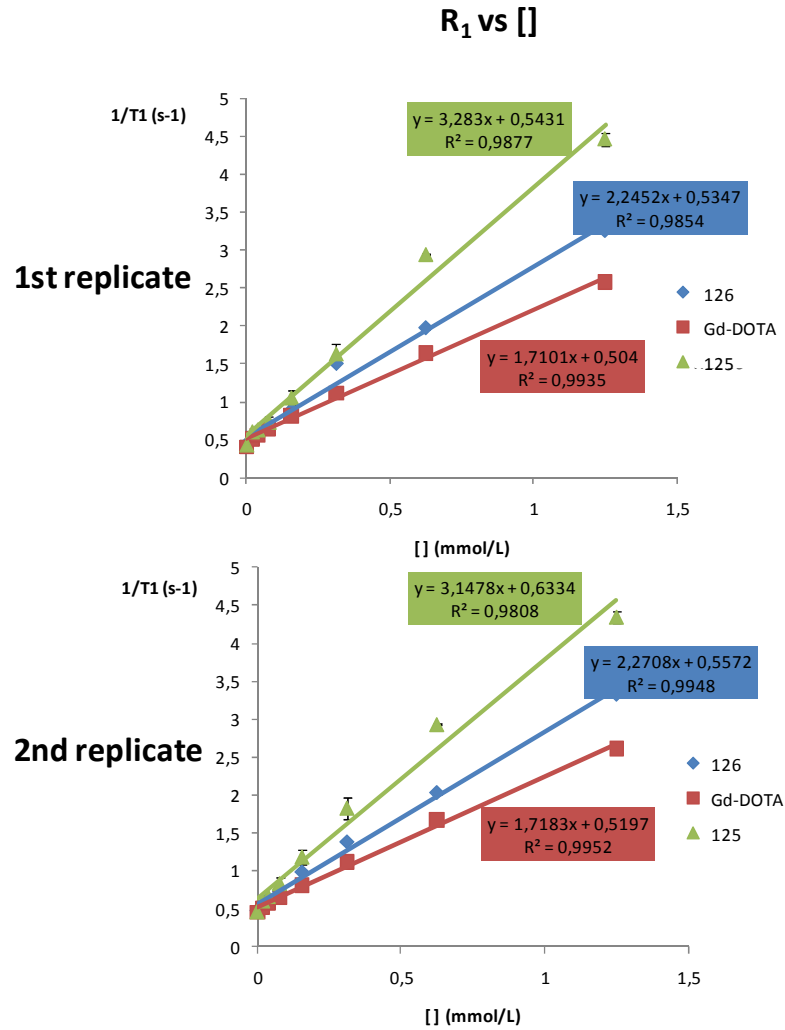
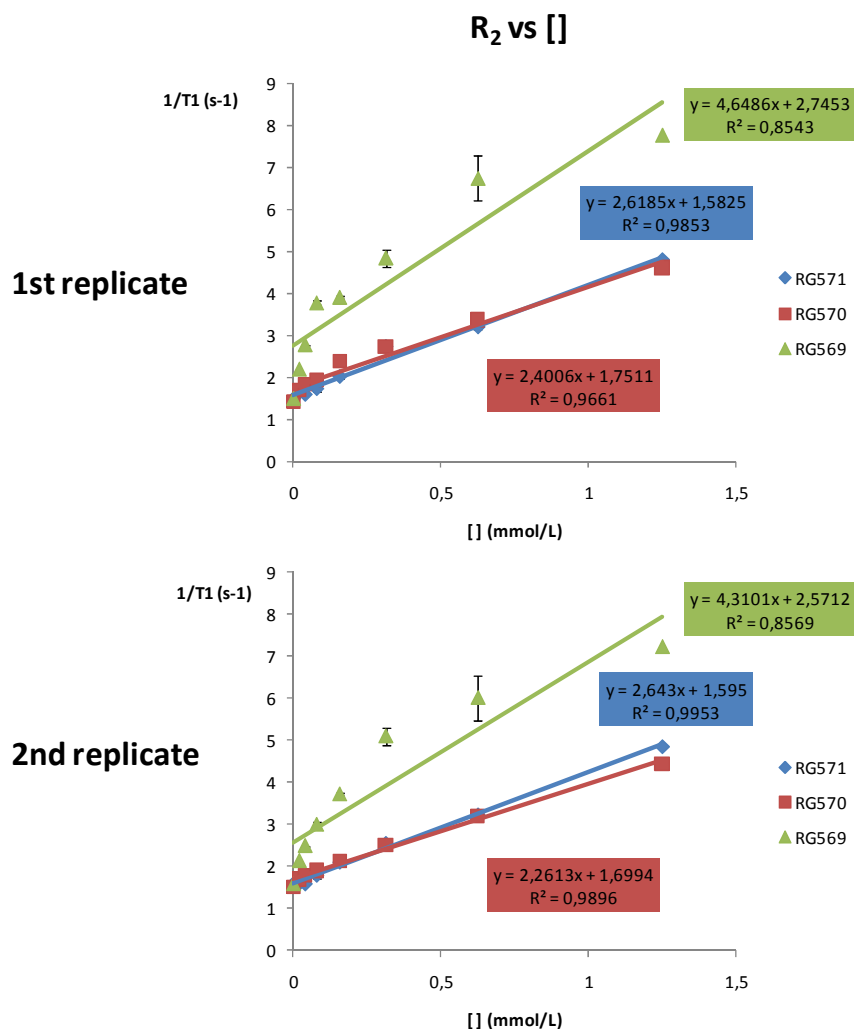


Figure 65: R<sub>1</sub> vs concentration.



**Figure 66:** R<sub>2</sub> vs concentration.

As it can be seen in **Table 19**, compound **125** exhibited an  $r_1$  value ( $3.2 \text{ mM}^{-1} \cdot \text{s}^{-1}$ ) higher than Gd-DOTA used as reference, showing stronger contrast enhancement in T<sub>1</sub>-weighted images (**Figure 67**). As it can be seen in **Figure 67**, T<sub>1</sub>-weighted images are brighter for **125** than for Gd-DOTA and R<sub>1</sub> map also shows higher values for the first one. The  $r_2$  value for **125** ( $4.5 \text{ mM}^{-1} \cdot \text{s}^{-1}$ ) was even much higher compared with  $r_2$  relaxivity of Gd-DOTA ( $2.6 \text{ mM}^{-1} \cdot \text{s}^{-1}$ ), resulting in negative contrast in T<sub>2</sub>-weighted images. As it can be seen in **Figure 67**, T<sub>2</sub>-weighted images are darker for **125** than for Gd-DOTA and R<sub>2</sub> map shows higher values for the first one.

In contrast,  $r_1$  and  $r_2$  relaxivities for **126** were comparable to Gd-DOTA although lower than those of **125** ( $1.7$  and  $2.3 \text{ mM}^{-1} \cdot \text{s}^{-1}$ , respectively). This different behaviour of **125** and



**126** as a result of the functionalisation of one of the amines is currently under study through theoretical modelling of the compounds in order to establish which structural features lead to such significant differences.

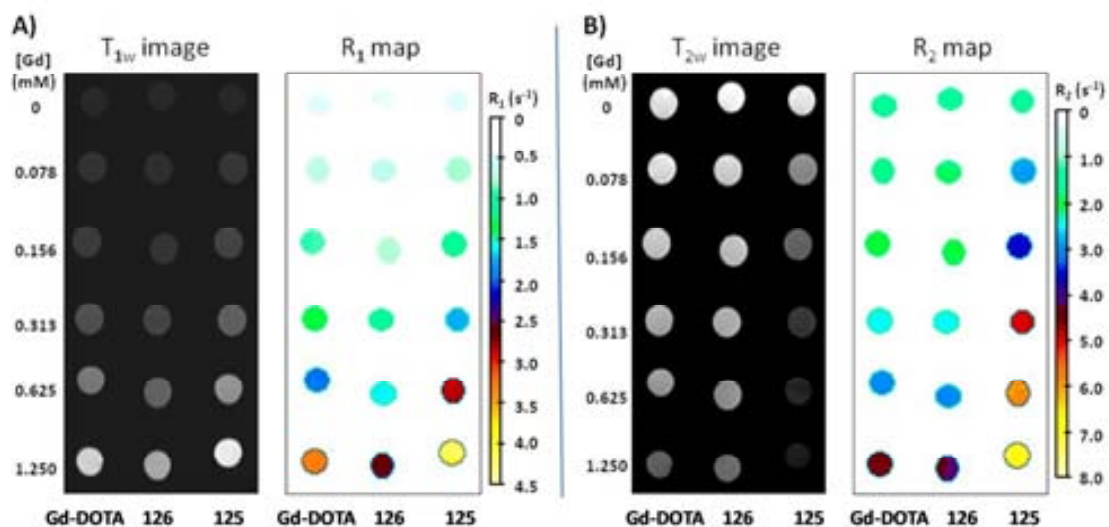


**Figure 67:** *In vitro* MRI. A)  $T_{1w}$ -weighted image and  $R_1$  map and B)  $T_{2w}$ -weighted image and  $R_2$  map of phantoms of water solutions containing compounds **125**, **126**, and Gd-DOTA at various Gd concentrations.

### 5.3.4 *In vivo* evaluation of the new CAs

The good performance showed by **125** in the *in vitro* studies encouraged ourselves to carry out preliminary *in vivo* animal experiments which could provide certain information about their possible clinical application.

White mice were the chosen animals for the study. First, they were exposed to UV-light to dilate the blood vessels (**Figure 68**). Afterwards they were anaesthetised using inhaled isoflurane. Next, the mice were cannulated in the tail, placed in the bed and introduced in the MRI machine. Their vital constants were monitored during the whole imaging experiments.

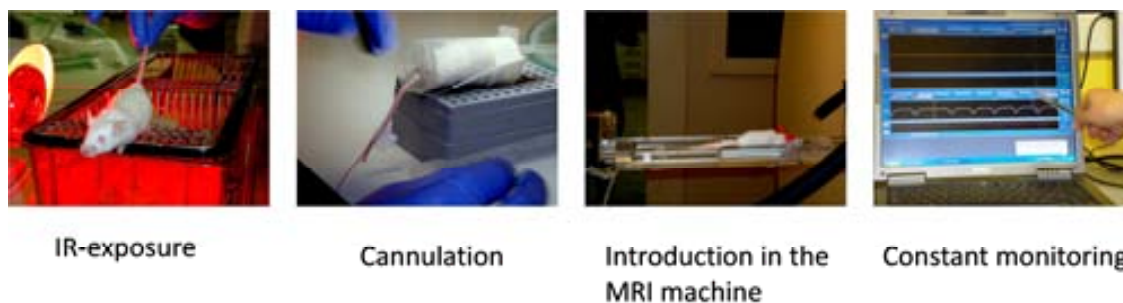


**Figure 68:** Followed procedure for the preparation of the studied mice for *in vivo* MRI. Coded

In order to determine if the prepared CAs behaved in a similar way *in vivo*, a solution containing the Gd-compounds **125** and **126** (0.2 mmol/Kg) was intravenously injected into mice and no apparent acute toxicity or side-effects health problems were observed. MR images were acquired before and after gadolinium injection to address biodistribution of these compounds (**Figure 69**).

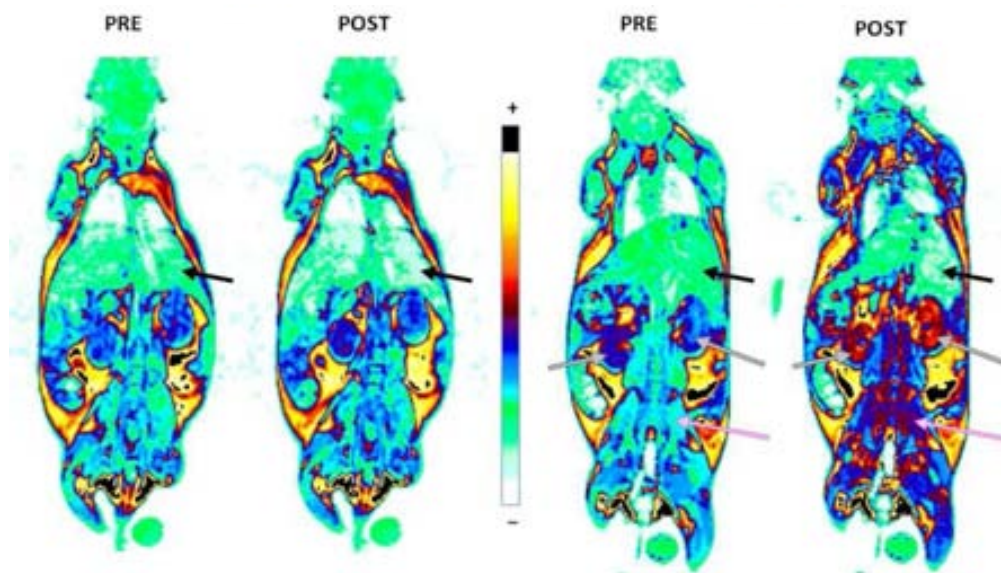


**Figure 69:** *In vivo* MRI colour coded  $T_1$ -weighted images of the mouse body acquired prior to (PRE) and 8 minutes post (POST) intravenous injection of contrast agent **125** (left) and **126** (right). Arrows indicating the liver (black), kidneys (grey), and muscular tissue (pink).

As it can be seen in **Diagram 1**,  $T_1$ -weighted MR images showed positive enhancement of the kidney and muscle tissue post agent **126** injections and negative

contrast in the liver was also observed for both compounds **125** and **126** due to strong  $T_2$  effect. This influence on  $T_2$  is noteworthy because only very few data on this effect are reported with gadolinium-based agents.<sup>156, 160, 161</sup> This property could be used for negative contrast images as complementary to positive contrast MRI.

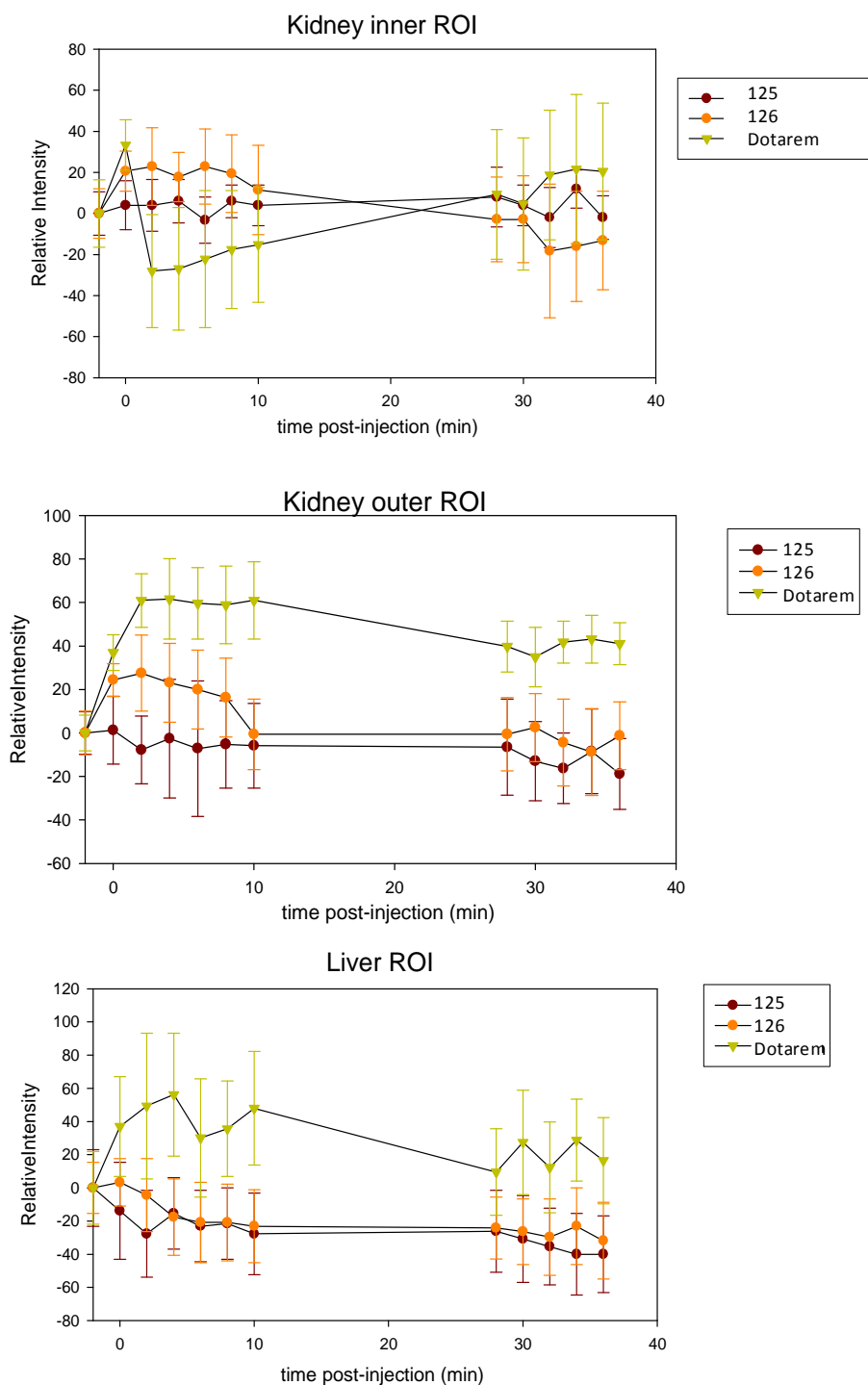
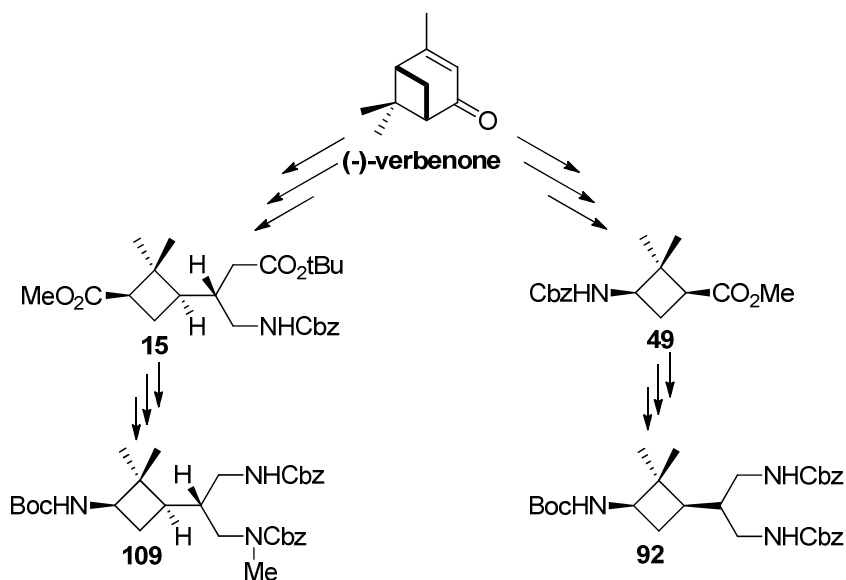


**Diagram 1:** Biodistribution of the different CAs at different after-injection times.

Preliminary MRI *in vivo* studies turned to be very encouraging and taking advantage of multivalent nature of the prepared compounds, much effort is being focused in the introduction of modifications on both tested CAs which could lead to new compounds showing a better *in vivo* performance.

#### 5.4. SUMMARY AND CONCLUSIONS: Chiral polyfunctional cyclobutane platforms

- i) The synthesis of two new triamine-based chiral polyfunctional cyclobutane platforms has been accomplished (**Scheme 58**).



Scheme 58

- ii) Hybrid DOTA-cyclobutane materials **125** and **126** have been synthesised through peptide coupling between DOTA and cyclobutane-cored triamines **92** and **109** (**Scheme 57**).
- iii) Preliminary results from both *in vitro* and *in vivo* MRI experiments are very encouraging, showing that **125** (**Figure 70**) is a most powerful *in vitro* CA than reference Gd-DOTA. Active investigation is currently ongoing to model their action mode with the aim to develop multiplexed and/or modular magnetic resonance probes by chirality modification and/or functional group manipulation, taking advantage of the synthetic versatility of these cyclobutane containing compounds.

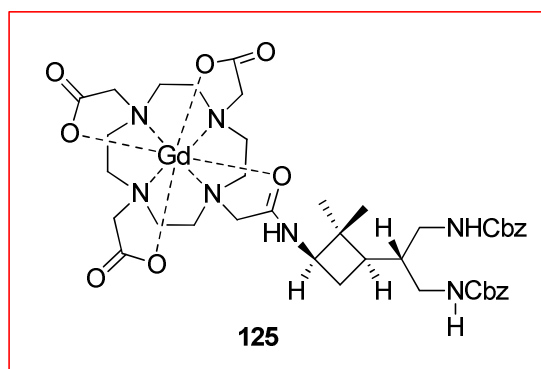


Figure 70

## **General Conclusions**





## 6. GENERAL CONCLUSIONS

The highly constrained cyclobutane ring has been used in the synthesis of chiral  $\beta$ - and  $\gamma$ -amino acids and derivatives which have been used in the preparation of a series of new compounds with very interesting applications. Therefore, the synthesised cyclobutane-containing compounds have been used in the preparation of the following compounds:

- **First generation of cyclobutane-containing peptide dendrimers.** Cyclobutane ring has been both used as core and dendron. Those molecules are the first example of its class. Some of them showed properties as organogelators.
- **Hybrid cyclobutane-proline  $\gamma,\gamma$ -peptides** which have shown certain ability to penetrate into cells. The presence of the cyclobutane ring in such compounds induced defined secondary structures.
- **Cyclobutane-containing NPY truncated analogues.**  $\beta$ -cyclobutane containing analogues showed high affinity towards  $Y_4$  receptor, in contrast to natural truncated NPY which exhibits no affinity towards any receptor subtype. Therefore, we can conclude that we possess a series of NPY analogues proximate to bioactive  $Y_4R$  sub-selective conformation.
- **Hybrid DOTA-cyclobutane CAs for MRI.** Preliminary results from both *in vitro* and *in vivo* MRI experiments are very encouraging, showing that compound **125** is a most powerful *in vitro* CA than reference Gd-DOTA.



## **Experimental Procedures**



## 7. EXPERIMENTAL PROCEDURES

### 7.1. General methodology

- Solvents were distilled under nitrogen atmosphere using standard procedures:
  - THF, toluene, Et<sub>2</sub>O: sodium/benzophenone
  - CH<sub>2</sub>Cl<sub>2</sub>, DMF, CH<sub>3</sub>CN: CaH<sub>2</sub>
  - MeOH, acetone: CaCl<sub>2</sub>
- Column chromatography was performed on silica gel (mean pore: 60 Å; particle size: 0.04-0.06 mm, 230-400 mesh).
- Reverse phase column chromatography was performed on C18 modified silica gel (mean pore: 60 Å; particle size: 0.04-0.06 mm).
- Commercially available reagents were used as received.
- All reactions were monitored by analytical thin-layer chromatography (TLC) using silica gel (60 Å) precoated aluminium plates (0.20 mm thickness).
- Solutions were concentrated using a rotary evaporator at 68 Torr.
- Infrared spectra were recorded on a Sapphire-ATR Spectrophotometer and peaks are reported in cm<sup>-1</sup>.
- High resolution mass spectra (HRMS) were recorded at *Servei d'Anàlisi Química de la Universitat Autònoma de Barcelona* in a Bruker micrOTOFQ spectrometer using ESI-MS (QTOF).
- Microanalyses were performed at *Servei d'Anàlisi Química de la Universitat Autònoma de Barcelona*.
- Melting points were determined on a hot stage and are uncorrected.
- Optical rotations were measured at 22±2 °C in a polarimeter Propol Automatishes (Dr. Kermchen model).

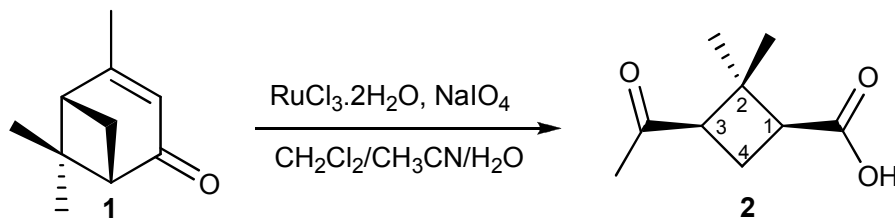
- In the case of products that derive from verbenone, the enantiomeric excess (ee) of all compounds was assumed to be 95%, the same as for (-)-verbenone starting material, as determined by  $^1\text{H}$  NMR after derivatization (unless otherwise mentioned).

- $^1\text{H}$ -NMR (at 250, 360, 400 or 600 MHz),  $^{13}\text{C}$ -NMR (at 62.5, 90, 100 or 150 MHz) were recorded at *Servei de Ressonància Magnètica Nuclear de la Universitat Autònoma de Barcelona*. The chemical shift of every signal is given in reference to:

| Deuterated solvent       | $^1\text{H}$ -NMR (ppm) | $^1\text{H}$ -NMR of residual $\text{H}_2\text{O}$<br>(ppm) | $^{13}\text{C}$ -NMR<br>(ppm) |
|--------------------------|-------------------------|---|-------------------------------|
| Acetone- $d_6$           | 2.05                    | 2.8   | 206.0, 29.8                   |
| $\text{CDCl}_3$          | 7.26                    | 1.55  | 77.0                          |
| DMSO- $d_6$              | 2.50                    | 3.31  | 39.5                          |
| $\text{H}_2\text{O}-d_2$ | 4.80                    | 4.80  | ---                           |
| MeOH- $d_4$              | 3.31                    | 4.84  | 49.0                          |

- NMR signals were assigned with help of DEPT, COSY, HMBC and HMQC experiments.

## 7.2. Experimental Section

**(1*S*,3*R*)-3-Acetyl-2,2-dimethylcyclobutanecarboxylic acid [(-)-(*cis*)-pinonic acid], 2:**

To a stirred solution of (-)-verbenone (4.4 mL, 28.6 mmol) in a 2:2:3 mixture of dichloromethane-acetonitrile-water (232 mL) were added catalytic  $\text{RuCl}_3$  hydrate (162 mg, 0.6 mmol, 0.02 eq) and  $\text{NaIO}_4$  (25.4 g, 120.3 mmol, 4.2 eq). The mixture was stirred at room temperature for 18 h. Then, the inorganic salts were filtered and the organic layer was extracted with dichloromethane (3x40 mL). The combined organic extracts were dried over  $\text{MgSO}_4$  and concentrated under reduced pressure to afford quantitatively crude (-)-*cis*-pinonic acid (4.76 g), which can be crystallised but which is used without further purification for practical purposes.

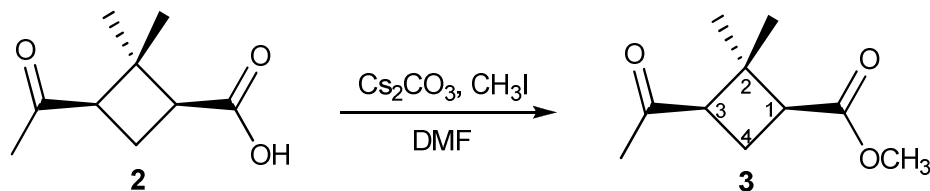
**Spectroscopic data for compound 2:**

$^1\text{H NMR}$  (250 MHz,  $\text{CDCl}_3$ )  $\delta$  0.97 (s, 3H, *trans*- $\text{CH}_3$ ), 1.45 (s, 3H, *cis*- $\text{CH}_3$ ), 1.91 (ddd,  $^2J_{\text{H-H}} = 11.5$  Hz,  $^3J_{\text{H-H}} = 7.8$  Hz,  $^3J_{\text{H-H}} = 7.7$  Hz, 1H,  $\text{H}_{4a}$ ), 2.07 (s, 3H,  $\text{CH}_3\text{CO-}$ ), 2.64 (ddd,  $^2J_{\text{H-H}} = 11.5$  Hz,  $^3J_{\text{H-H}} = 10.7$  Hz,  $^3J_{\text{H-H}} = 10.5$  Hz, 1H,  $\text{H}_{4b}$ ), 2.83 (dd,  $^3J_{\text{H-H}} = 10.7$  Hz,  $^3J_{\text{H-H}} = 7.8$  Hz, 1H,  $\text{H}_3$ ), 2.91 (dd,  $^3J_{\text{H-H}} = 10.5$  Hz,  $^3J_{\text{H-H}} = 7.7$  Hz, 1H,  $\text{H}_1$ ).

$^{13}\text{C NMR}$  (62.5 MHz, acetone- $d_6$ )  $\delta$  18.3 (*cis*- $\text{CH}_3$ ), 19.3 ( $\text{C}_4$ ), 30.2 (*trans*- $\text{CH}_3$ ), 31.0 ( $\text{CH}_3\text{CO}$ ), 44.8 ( $\text{C}_2$ ), 45.4 ( $\text{C}_1$ ), 53.1 ( $\text{C}_3$ ), 178.8 ( $\text{CO}_{\text{acid}}$ ), 206.1 ( $\text{CO}_{\text{ketone}}$ ).

Spectroscopic data are consistent with those reported in reference:

Burgess, K; Li, S.; Rebenspies, J. *Tetrahedron Lett.* **1997**, *38*, 1681-1684.

**(1S,3R)-Methyl-3-acetyl-2,2-dimethylcyclobutanecarboxylate, 3:**

A mixture containing (-)-*cis*-pinonic acid (4.8 g, 28.2 mmol), cesium carbonate (11.0 g, 33.8 mmol, 1.2 eq) and 2.1 mL of methyl iodide (33.7 mmol, 1.2 eq) in anhydrous DMF (65 mL) was stirred at room temperature for 18 h. Then, ethyl acetate (50 mL) was added and the resultant solution was washed with saturated aqueous sodium bicarbonate (4 x 25 mL). The organic liquors were dried over magnesium sulfate and solvent was evaporated under vacuum to provide (-)-*cis*-pinonic methyl ester **3** (4.5 g, 85% yield).

**Spectroscopic data for compound 3:**

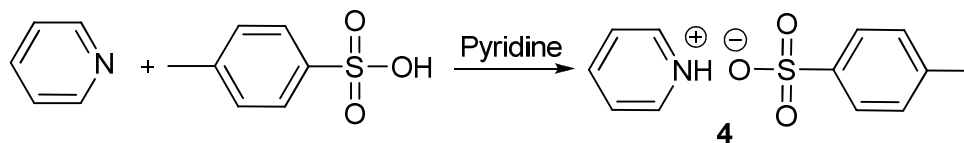
$^1\text{H NMR}$  (250 MHz,  $\text{CDCl}_3$ )  $\delta$  0.90 (s, 3H, *trans*- $\text{CH}_3$ ), 1.43 (s, 3H, *cis*- $\text{CH}_3$ ), 1.90 (ddd,  $^2J_{\text{H-H}} = 11.3$  Hz,  $^3J_{\text{H-H}} = ^3J'_{\text{H-H}} = 7.8$  Hz, 1H,  $\text{H}_{4a}$ ), 2.66 (ddd,  $^2J_{\text{H-H}} = 11.3$  Hz,  $^3J_{\text{H-H}} = 10.8$  Hz,  $^3J_{\text{H-H}} = 10.3$  Hz, 1H,  $\text{H}_{4b}$ ), 2.78 (dd,  $^3J_{\text{H-H}} = 10.7$  Hz,  $^3J_{\text{H-H}} = 7.7$  Hz, 1H,  $\text{H}_1$ ), 2.88 (dd,  $^3J_{\text{H-H}} = 10.3$  Hz,  $^3J_{\text{H-H}} = 7.7$  Hz, 1H,  $\text{H}_3$ ), 3.61 (s, 3H,  $\text{CO}_2\text{CH}_3$ ).

$^{13}\text{C NMR}$  (62,5 MHz, acetone- $d_6$ )  $\delta$  18.3 (*trans*- $\text{CH}_3$ ), 19.3 ( $\text{C}_4$ ), 30.2 (*cis*- $\text{CH}_3$ ), 31.0 ( $\text{CH}_3\text{CO}$ ), 44.8 ( $\text{C}_2$ ), 45.4 ( $\text{C}_1$ ), 51.3 ( $\text{CH}_3$  ester), 53.1 ( $\text{C}_3$ ), 172.8 ( $\text{CO}_{\text{ester}}$ ), 206.1 ( $\text{CO}_{\text{ketone}}$ ).

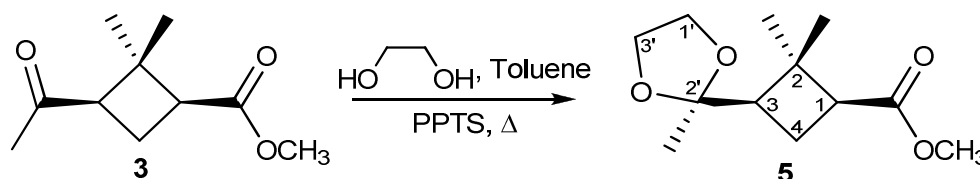
Spectroscopic data are consistent with those reported in reference:

Aguado, G. P.; Moglioni, A. G.; Brousse, B. N.; Ortuño, R. M. *Tetrahedron: Asymmetry* **2003**, *14*, 2445.



**Pyridinium *p*-toluenesulfonate (PPTS), 4.**

A mixture containing *p*-toluenesulfonic acid (7.23 g, 38 mmol) and pyridine (15 mL) was stirred for 10 minutes; afterwards the pyridine excess was evaporated to dryness under vacuum. The white solid formed was recrystallised in acetone to afford pure PPTS in a quantitative yield.

**(1*S*,3*R*)-Methyl-2,2-dimethyl-3-(2'-methyl-[1',3']-dioxolan-2'-yl)cyclobutane-carboxylate, 5.**

A mixture of ketone **3** (4.5 g, 24.4 mmol), ethylene glycol (12 mL, 215.0 mmol, 8.8 eq), and PPTS (1.28 g, 5.0 mmol, 0.2 eq) in toluene (50 mL) was heated to reflux for 4 h, using a Dean-Stark apparatus to remove water from the reaction mixture. Solvent was evaporated under reduced pressure, and the residue was poured into EtOAc (100 mL). The resultant solution was subsequently washed with a saturated aqueous solution of  $\text{NaHCO}_3$  (3 x 30 mL) and brine (30 mL) and dried over  $\text{MgSO}_4$ . Solvent was removed to dryness, and the residue was chromatographed (1:5 ethyl acetate/hexane) to afford pure ketal **5** as a colourless oil (4.95 g, 89% yield).

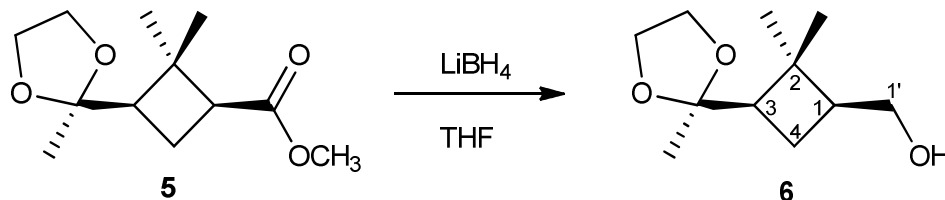
**Spectroscopic data for compound 5:**

$^1\text{H NMR}$  (250 MHz,  $\text{CDCl}_3$ )  $\delta$  1.04 (s, 3H, *trans*- $\text{CH}_3$ ), 1.23 (s, 3H, *cis*- $\text{CH}_3$ ), 1.25 (s, 3H,  $\text{CH}_3$  ketal), 1.85-1.91 (m, 1H,  $\text{H}_{4a}$ ), 2.21-2.24 (m, 2H,  $\text{H}_3$ ,  $\text{H}_{4b}$ ), 2.58-2.65 (m, 1H,  $\text{H}_1$ ), 3.65 (s, 3H,  $\text{CO}_2\text{CH}_3$ ), 3.80-3.86 (m, 2H,  $-\text{OCH}_2\text{CH}_2\text{O}-$ ), 3.94-4.00 (m, 2H,  $-\text{OCH}_2\text{CH}_2\text{O}-$ ).

$^{13}\text{C NMR}$  (62.5 MHz,  $\text{acetone-}d_6$ )  $\delta$  20.5 (*trans*- $\text{CH}_3$ ), 22.9 ( $\text{C}_4$ ), 26 (*cis*- $\text{CH}_3$ ), 33.6 ( $\text{CH}_3$  ketal), 45.9 ( $\text{C}_2$ ), 48.4 ( $\text{C}_1$ ), 52.1 ( $\text{CH}_3$  ester), 53.3 ( $\text{C}_3$ ), 66.4 and 68.1 (2C,  $-\text{OCH}_2\text{CH}_2\text{O}-$ ), 112.1 ( $\text{C}_{\text{ketalic}}$ ), 175.3 ( $\text{CO}_2\text{CH}_3$ ).

Spectroscopic data are consistent with those reported in reference:

Mogliani, A.G; Muray, E; Castillo, J. A; Álvarez-Larena, Á; Moltrasio, G. Y; Branchadell, V; Ortuño, R. M. *J. Org. Chem.* **2002**, *67*, 2402-2410.

**(1*S*,3*R*)-3-(2'-Methyl-[1',3']-dioxolan-2'-yl)-2,2-dimethylcyclobutylmethanol, 6.**

To a solution of ester **5** (3.9 g, 17.1 mmol) in anhydrous THF (50 mL) was added a 2 M solution of  $\text{LiBH}_4$  in THF (24 mL, 48.0 mmol, 2.8 eq). The mixture was heated to reflux under nitrogen atmosphere for 18 h. Excess hydride was eliminated by slow addition of methanol (5 mL) and water (30 mL). The resultant solution was extracted with dichloromethane, and the combined extracts were dried over  $\text{MgSO}_4$ . Solvents were removed at reduced pressure, and the residue was chromatographed (EtOAc-hexane 1:2) to provide alcohol **6** as a colourless oil (2.95 g, 87 % yield).

**Spectroscopic data for compound 6:**

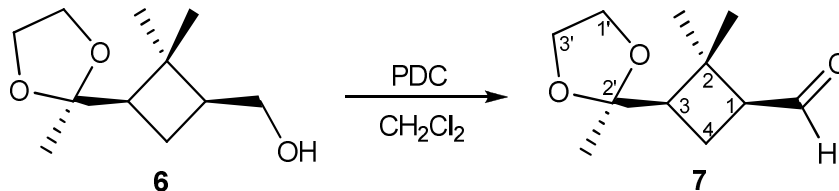
$^1\text{H NMR}$  (250 MHz,  $\text{CDCl}_3$ )  $\delta$  1.09 (s, 3H, *trans*- $\text{CH}_3$ ), 1.17 (s, 3H, *cis*- $\text{CH}_3$ ), 1.22 (s, 3H,  $\text{CH}_3$  ketal), 1.55 (m, 1H,  $\text{H}_{4a}$ ), 1.81-1.92 (m, 1H,  $\text{H}_{4b}$ ), 1.93-2.05 (m, 1H,  $\text{H}_3$ ), 2.14 (dd,  $^3J_{\text{H-H}} = 7.5$  Hz,  $^3J_{\text{H-H}} = 3.23$  Hz, 1H,  $\text{H}_1$ ), 3.54 (dd,  $^2J_{\text{H-H}} = 10.7$  Hz,  $^3J_{\text{H-H}} = 6.3$  Hz, 1H,  $\text{H}_{1'a}$ ), 3.65 (dd,  $^2J_{\text{H-H}} = 10.7$  Hz,  $^3J_{\text{H-H}} = 7.9$  Hz, 1H,  $\text{H}_{1'b}$ ), 3.79-4.02 (c.a., 4H,  $-\text{OCH}_2\text{CH}_2\text{O}-$ ).

$^{13}\text{C NMR}$  (62.5 MHz, acetone- $d_6$ )  $\delta$  17.1 (*trans*- $\text{CH}_3$ ), 22.2 ( $\text{C}_4$ ), 23.9 (*cis*- $\text{CH}_3$ ), 32.3 ( $\text{CH}_3$  ketal), 40.8 ( $\text{C}_2$ ), 44.9 ( $\text{C}_1$ ), 50.2 ( $\text{C}_3$ ), 63.2, 64.1 (2C,  $-\text{OCH}_2\text{CH}_2\text{O}-$ ), 65.8 ( $\text{CH}_2\text{OH}$ ), 110.2 ( $\text{C}_{\text{ketalic}}$ ).

Spectroscopic data are consistent with those reported in reference:

Mogliani, A.G; Muray, E; Castillo, J. A; Álvarez-Larena, Á; Moltrasio, G. Y; Branchadell, V; Ortuño, R. M. *J. Org. Chem.* **2002**, *67*, 2402-2410.

**(1*S*,3*R*)-2,2-Dimethyl-3-(2'-methyl-[1',3']-dioxolan-2'-yl)cyclobutanecarbal-dehyde, 7:**



A mixture of alcohol **6** (2.1 g, 10.5 mmol) and PDC (4.3 g, 11.3 mmol, 1.1 eq) in anhydrous dichloromethane was stirred at room temperature overnight under nitrogen atmosphere (the reaction progress was monitored by TLC. If needed, more PDC was added). Then a small portion of Florisil was added and stirring was continued for 30 minutes. The reaction mixture was filtered on Celite® and solvent was removed at reduced pressure to afford crude aldehyde **7** (1.5-1.9 g, 79-90% yield) as a rather unstable oil that was identified by its IR and  $^1\text{H NMR}$  spectroscopic data and immediately used in the condensation step without purification.

**Spectroscopic data for compound 7:**

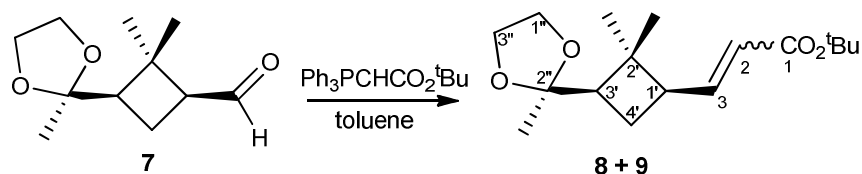
IR (ATR): 2982 (CH<sub>st</sub>), 2957(CH<sub>st</sub>), 2713 (CH<sub>aldehyde</sub>), 1715 (CO<sub>aldehyde</sub>), 1371, 1089, 1048.

<sup>1</sup>H NMR (250 MHz, CDCl<sub>3</sub>) δ 1.11 (s, 3H, *trans*-CH<sub>3</sub>), 1.16 (s, 3H, *cis*-CH<sub>3</sub>), 1.32 (s, 3H, CH<sub>3</sub> ketal), 1.85-1.95 (m, 1H, H<sub>4a</sub>), 2.02-2.14 (m, 1H, H<sub>4b</sub>), 2.21-2.44 (m, 1H, H<sub>3</sub>), 2.65-2.75 (m, 1H, H<sub>1</sub>), 3.81-4.07 (c.a., 4H, -OCH<sub>2</sub>CH<sub>2</sub>O-), 9.70 (d, <sup>3</sup>J<sub>H-H</sub> = 1.4 Hz, H<sub>aldehyde</sub>).

Spectroscopic data are consistent with those reported in reference:

Mogliani, A.G; Muray, E; Castillo, J. A; Álvarez-Larena, Á; Moltrasio, G. Y; Branchadell, V; Ortuño, R. M. *J. Org. Chem.* **2002**, *67*, 2402-2410.

***tert*-Butyl 3-[(1'*R*,3'*R*)-2',2'-dimethyl-3'-(2-methyl-1,3-dioxolan-2-yl)cyclobutyl]-acrylate, 8+9 (*Z+E*):**



To a solution of *tert*-butyl (triphenylphosphoranylidene)acetate (8.3 g, 14.9 mmol, 1.2 eq) in 20 mL of anhydrous toluene under nitrogen atmosphere was added a solution of aldehyde **7** (12.4 mmol) in 80 mL of anhydrous toluene and the resulting mixture was stirred during 18 hours. Afterwards, the solvent was evaporated under vacuo, the resulting crude was solved in hot diethyl ether and the solution was filtered through sintered glass funnel. Again, the solvent was evaporated under vacuo and the resulting crude was purified by flash chromatography (1:1 hexane-ethyl acetate) to afford a mixture of olefins **8** and **9** as a colourless oil (ratio *E/Z* 47:53, 3.4 g, 96% yield).

**Spectroscopic data for compound 8 (E) and 9 (Z):**

**IR (ATR):** 2979 (CH<sub>st</sub>), 2935(CH<sub>st</sub>), 2879(CH<sub>st</sub>), 1717 (CO<sub>ester</sub>), 1713 (CO<sub>ester</sub>), 1647, 1420, 1368.

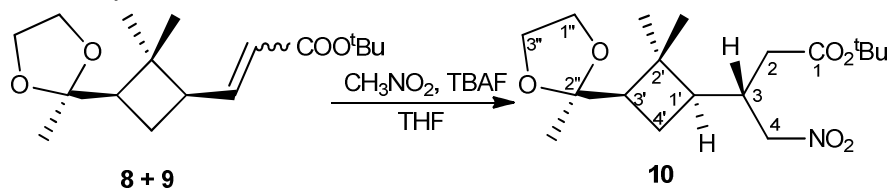
**<sup>1</sup>H NMR** (250 MHz, CDCl<sub>3</sub>) for isomer *E* δ 1.04 (s, 3H, *trans*-CH<sub>3</sub>), 1.17 (s, 3H, *cis*-CH<sub>3</sub>), 1.26 (s, 3H, CH<sub>3</sub><sub>ketal</sub>), 1.50 (s, 9H, <sup>t</sup>Bu), 1.72-1.83 (m, 1H, H<sub>4'a</sub>), 2.05-2.10 (m, 1H, H<sub>1'</sub>), 2.20-2.30 (m, 1H, H<sub>3'</sub>), 2.46-2.55 (m, 1H, H<sub>4'b</sub>), 3.82-4.05 (c.a., 4H, -OCH<sub>2</sub>CH<sub>2</sub>O-), 5.64-5.75 (m, 1H, H<sub>2</sub>), 6.84 (dd, <sup>3</sup>J<sub>H-H</sub>=15.6 Hz, <sup>4</sup>J<sub>H-H</sub>= 7.4 Hz).

**<sup>1</sup>H NMR** (250 MHz, CDCl<sub>3</sub>) for isomer *Z* δ 1.08 (s, 3H, *trans*-CH<sub>3</sub>), 1.17 (s, 3H, *cis*-CH<sub>3</sub>), 1.26 (s, 3H, CH<sub>3</sub><sub>ketal</sub>), 1.50 (s, 9H, <sup>t</sup>Bu), 1.93-1.98 (m, 1H, H<sub>4'a</sub>), 2.05-2.10 (m, 1H, H<sub>1'</sub>), 2.20-2.30 (m, 1H, H<sub>3'</sub>), 2.46-2.55 (m, 1H, H<sub>4'b</sub>), 3.82-4.05 (c.a., 4H, -OCH<sub>2</sub>CH<sub>2</sub>O-), 5.64-5.75 (m, 1H, H<sub>2</sub>), 6.06 (dd, <sup>3</sup>J<sub>H-H</sub>= 11.6 Hz, <sup>4</sup>J<sub>H-H</sub>=10.2 Hz, 1H).

**<sup>13</sup>C NMR** (62.5 MHz, CDCl<sub>3</sub>) δ 18.11 (*trans*-CH<sub>3</sub>), 23.18 (C<sub>4'</sub>), 23.68 (C<sub>4'</sub>), 25.17 (CH<sub>3</sub><sub>ketal</sub>), 28.08 (C(CH<sub>3</sub>)<sub>3</sub>), 28.14 (C(CH<sub>3</sub>)<sub>3</sub>), 30.91 (*cis*-CH<sub>3</sub>), 31.41 (*cis*-CH<sub>3</sub>), 39.83 (C<sub>2'</sub>), 43.66 (C<sub>2'</sub>), 44.16 (C<sub>1'</sub>), 44.69 (C<sub>1'</sub>), 49.73 (C<sub>3'</sub>), 49.87 (C<sub>3'</sub>), 63.62 (-OCH<sub>2</sub>CH<sub>2</sub>O-), 65.45 (-OCH<sub>2</sub>CH<sub>2</sub>O-), 65.51 (-OCH<sub>2</sub>CH<sub>2</sub>O-), 79.98 (C(CH<sub>3</sub>)<sub>3</sub>), 109.55 (C<sub>ketalic</sub>), 109.76 (C<sub>ketalic</sub>), 121.94 (C<sub>2</sub>), 123.08 (C<sub>2</sub>), 147.68 (C<sub>3</sub>), 148.62 (C<sub>3</sub>), 165.77 (CO<sub>2</sub><sup>t</sup>Bu), 165.97 (CO<sub>2</sub><sup>t</sup>Bu).

**Elemental analysis:** Calculated for C<sub>17</sub>H<sub>28</sub>O<sub>4</sub>: C, 68.89; H, 9.52. Found C, 69.08; H 9.55.

**(S)-tert-Butyl 3-[(1'*R*,3'*R*)-2',2'-dimethyl-3'-(2-methyl-1,3-dioxolan-2-yl)cyclobutyl]-4-nitrobutanoate, 10:**



To a solution of alkenes **8** and **9** (4.1 g, 13.9 mmol) in 150 mL of anhydrous THF under nitrogen atmosphere were subsequently added nitromethane (0.9 mL, 15.8 mmol, 1.1 eq) and 1.0 M TBAF in THF (16.1 mL, 16.8 mmol, 1.2 eq). The resulting mixture was let to stir for 18 h. Next, the solvent was evaporated at reduced pressure, and the resulting crude was

chromatographed on silica gel (hexane–ethyl acetate, 4:1) to afford compound **10** as a colourless oil (4.2 g, 85%).

**Spectroscopic data and physical constants for compound 10:**

$[\alpha]_D = -22.0$  (c 1.00, CH<sub>2</sub>Cl<sub>2</sub>).

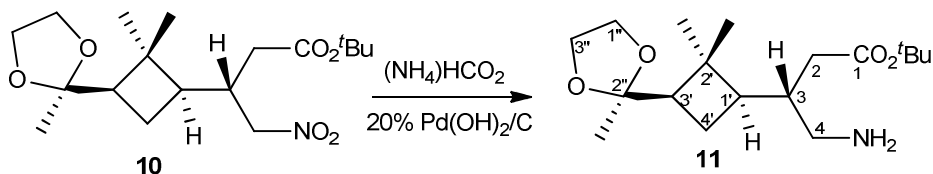
IR (ATR): 2980 (CH<sub>st</sub>), 2950 (CH<sub>st</sub>), 2876 (CH<sub>st</sub>), 1724 (CO<sub>ester</sub>), 1549 (NO<sub>st</sub>), 1463, 1428, 1369 (NO<sub>st</sub>).

<sup>1</sup>H NMR (250 MHz, CDCl<sub>3</sub>) δ 1.11 (s, 3H, *trans*-CH<sub>3</sub>), 1.17 (s, 3H, *cis*-CH<sub>3</sub>), 1.22 (s, 3H, CH<sub>3</sub><sub>ketal</sub>), 1.45 (s, 9H, <sup>t</sup>Bu), 1.52–1.64 (m, 1H, H<sub>3</sub>), 1.70–1.82 (m, 1H, H<sub>4'a</sub>), 1.86–1.95 (m, 1H, H<sub>4'b</sub>), 2.01–2.12 (m, 1H, H<sub>2a</sub>), 2.19–2.38 (c.a., 2H, H<sub>1'</sub> and H<sub>2b</sub>), 2.38–2.53 (m, 1H, H<sub>3'</sub>), 3.78–3.96 (c.a., 4H, -OCH<sub>2</sub>CH<sub>2</sub>O-), 4.36–4.51 (c.a., 2H, -CH<sub>2</sub>NO<sub>2</sub>)

<sup>13</sup>C NMR (62.5 MHz, CDCl<sub>3</sub>) δ 16.4 (*trans*-CH<sub>3</sub>), 23.2 (C<sub>4'</sub>), 23.7 (CH<sub>3</sub><sub>ketal</sub>), 28.0 (C(CH<sub>3</sub>)<sub>3</sub>), 31.8 (*cis*-CH<sub>3</sub>), 35.5 (C<sub>3</sub>), 35.9 (C<sub>2'</sub>), 41.2 (C<sub>2</sub>), 42.9 (C<sub>1'</sub>), 49.0 (C<sub>3'</sub>), 63.6 (-OCH<sub>2</sub>CH<sub>2</sub>O-), 65.4 (-OCH<sub>2</sub>CH<sub>2</sub>O-), 76.4 (C<sub>4</sub>, CH<sub>2</sub>NO<sub>2</sub>), 81.11 (C(CH<sub>3</sub>)<sub>3</sub>), 109.4 (C<sub>ketalic</sub>), 170.5 (CO<sub>2</sub><sup>t</sup>Bu).

**High resolution mass spectrum:** Calculated for C<sub>18</sub>H<sub>31</sub>NNaO<sub>6</sub> (M+Na)<sup>+</sup>: 380.2044. Found: 380.2040.

**(S)-tert-Butyl 4-amino-3-[(1'R,3'R)-2',2'-dimethyl-3'-(2-methyl-1,3-dioxolan-2-yl)cyclobutyl]butanoate, 11:**



To a solution of **10** (5.0 g, 14.0 mmol) in 125 mL of anhydrous methanol were subsequently added ammonium formate (3.2 g, 49.4 mmol, 3.5 eq) and 20% Pd(OH)<sub>2</sub>/C (1.1 g, 4% in weight). The resulting mixture was heated at reflux for 2 h. Afterwards, the reaction

mixture was filtered through Celite<sup>®</sup>, and the solvent was eliminated under vacuo to obtain a yellow oil identified as amine **11** (4.6 g, 96% yield).

**Spectroscopic data and physical constants for compound 11:**

$[\alpha]_D = -8.3$  (c 0.48, CH<sub>2</sub>Cl<sub>2</sub>).

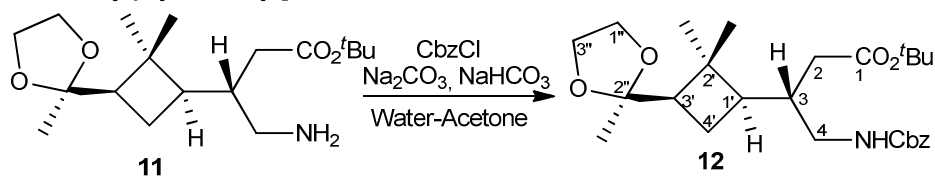
IR (ATR): 3384 (NH<sub>st</sub>), 2978 (CH<sub>st</sub>), 1725 (CO<sub>ester</sub>), 1461, 1428, 1392, 1368, 1256 (CN<sub>st</sub>), 1224 (CN<sub>st</sub>).

<sup>1</sup>H NMR (250 MHz, CDCl<sub>3</sub>) δ 1.10 (s, 3H, *trans*-CH<sub>3</sub>), 1.18 (s, 3H, *cis*-CH<sub>3</sub>), 1.23 (s, 3H, CH<sub>3</sub><sub>ketal</sub>), 1.45 (s, 9H, <sup>t</sup>Bu), 1.55–1.72 (c.a., 2H, H<sub>4'a</sub>, H<sub>1'</sub>), 1.81–1.97 (c.a., 2H, H<sub>4'b</sub>, H<sub>3</sub>), 2.02–2.16 (c.a., 4H, H<sub>3'</sub>, H<sub>2a</sub>, NH<sub>2</sub>), 2.26 (dd, *J*<sub>H-H</sub> = 14.5 Hz, *J*<sub>H-H</sub> = 3.6 Hz, 1H, H<sub>2b</sub>), 2.57 (dd, *J*<sub>H-H</sub> = 12.9 Hz, *J*<sub>H-H</sub> = 6.7 Hz, 1H, H<sub>4a</sub>), 2.75 (dd, *J*<sub>H-H</sub> = 12.9 Hz, *J*<sub>H-H</sub> = 3.9 Hz, 1H, H<sub>4b</sub>), 3.78–3.97 (c.a., 4H, -OCH<sub>2</sub>CH<sub>2</sub>O-)

<sup>13</sup>C NMR (62.5 MHz, CDCl<sub>3</sub>) δ 16.5 (*trans*-CH<sub>3</sub>), 23.4 (C<sub>4'</sub>), 23.8 (CH<sub>3</sub><sub>ketal</sub>), 28.0 (C(CH<sub>3</sub>)<sub>3</sub>), 32.0 (*cis*-CH<sub>3</sub>), 36.7 (C<sub>3</sub>), 41.0 (C<sub>1'</sub>), 42.0 (C<sub>2</sub>), 43.7 (C<sub>4</sub>), 49.2 (C<sub>2'</sub>) 50.9 (C<sub>3'</sub>), 63.6 (-OCH<sub>2</sub>CH<sub>2</sub>O-), 65.4 (-OCH<sub>2</sub>CH<sub>2</sub>O-), 80.7 (C(CH<sub>3</sub>)<sub>3</sub>), 109.6 (C<sub>ketalic</sub>), 172.5 (CO<sub>2</sub><sup>t</sup>Bu).

**High resolution mass spectrum:** Calculated for C<sub>18</sub>H<sub>33</sub>NNaO<sub>4</sub> (M+Na)<sup>+</sup>: 328.2482. Found: 328.2484.

**(S)-tert-Butyl 4-(benzyloxycarbonylamino)-3-[(1'R,3'R)-2',2'-dimethyl-3'-(2-methyl-1,3-dioxolan-2-yl)cyclobutyl]butanoate, 12:**



To a solution of **11** (1.12 g, 3.5 mmol) in water-acetone (10:1, 110 mL) were subsequently added Na<sub>2</sub>CO<sub>3</sub> (0.72 g, 7.0 mmol, 2.0 eq), NaHCO<sub>3</sub> (0.29 g, 3.5 mmol, 1.0 eq) and CbzCl (0.6 mL, 4.4 mmol, 1.25 eq). The resulting mixture was stirred at room temperature for 3 h. afterwards, the reaction mixture was extracted with dichloromethane,

and the combined extracts were dried over  $\text{MgSO}_4$ . Solvents were removed at reduced pressure, and the residue was chromatographed (hexane-ethyl acetate, 1:4) to provide carbamate **12** as a colourless oil (1.20 g, 75 % yield).

#### Spectroscopic data and physical constants for compound **12**:

$[\alpha]_D^{25} = +14.6$  (c 0.55,  $\text{CH}_2\text{Cl}_2$ ).

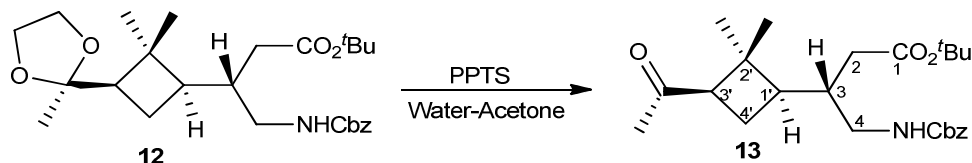
**IR** (ATR): 3339 ( $\text{NH}_{\text{st}}$ ), 2977 ( $\text{CH}_{\text{st}}$ ), 2952 ( $\text{CH}_{\text{st}}$ ), 2880 ( $\text{CH}_{\text{st}}$ ), 1724 (bs,  $\text{CO}_{\text{ester}} + \text{CO}_{\text{carbamate}}$ ), 1518, 1455, 1368, 1247 ( $\text{CN}_{\text{st}}$ ).

**$^1\text{H}$  NMR** (250 MHz,  $\text{CDCl}_3$ )  $\delta$ : 1.07 (s, 3H, *trans*- $\text{CH}_3$ ), 1.14 (s, 3H, *cis*- $\text{CH}_3$ ), 1.20 (s, 3H,  $\text{CH}_3_{\text{ketal}}$ ), 1.41 (s, 9H,  $^t\text{Bu}$ ), 1.54–1.66 (c.a., 2H,  $\text{H}_{4'a}$ ,  $\text{H}_{1'}$ ), 1.87–2.05 (c.a., 4H,  $\text{H}_{4'b}$ ,  $\text{H}_3$ ,  $\text{H}_{3'}$ ,  $\text{H}_{2a}$ ), 2.23 (dd,  $J_{\text{H-H}} = 18.5$  Hz,  $J_{\text{H-H}} = 7.2$  Hz, 1H,  $\text{H}_{2b}$ ), 2.92–3.02 (m, 1H,  $\text{H}_{4a}$ ), 3.32 (ddd,  $J_{\text{H-H}} = 12.7$  Hz,  $J_{\text{H-H}}' = 5.7$  Hz,  $J_{\text{H-H}} = 3.2$  Hz, 1H,  $\text{H}_{4b}$ ), 3.72–3.98 (c.a., 4H,  $-\text{OCH}_2\text{CH}_2\text{O}-$ ), 5.07 (s, 2H,  $\text{CH}_2\text{Bn}$ ), 5.20 (dd,  $J_{\text{H-H}} = 5.7$  Hz,  $J_{\text{H-H}} = 6.0$  Hz, 1H, NH), 7.24–7.38 (c.a., 5H,  $\text{H}_{\text{Ar}}$ ).

**$^{13}\text{C}$  NMR** (62.5 MHz,  $\text{CDCl}_3$ )  $\delta$ : 16.5 (*trans*- $\text{CH}_3$ ), 23.6 ( $\text{C}_{4'}$ ), 23.7 ( $\text{CH}_3_{\text{ketal}}$ ), 27.9 ( $\text{C}(\text{CH}_3)_3$ ), 32.0 (*cis*- $\text{CH}_3$ ), 36.8 ( $\text{C}_3$ ), 37.3 ( $\text{C}_2$ ), 41.0 ( $\text{C}_{2'}$ ), 42.5 ( $\text{C}_4$ ), 44.0 ( $\text{C}_{1'}$ ), 49.3 ( $\text{C}_{3'}$ ), 63.5 ( $-\text{OCH}_2\text{CH}_2\text{O}-$ ), 65.3 ( $-\text{OCH}_2\text{CH}_2\text{O}-$ ), 66.4 ( $\text{CH}_2\text{Bn}$ ), 80.6 ( $\text{C}(\text{CH}_3)_3$ ), 109.6 ( $\text{C}_{\text{ketalic}}$ ), 127.8, 127.9, 128.3, 136.6 ( $6\text{C}$ ,  $\text{C}_{\text{Ar}}$ ), 156.3 ( $\text{CO}_{\text{carbamate}}$ ) 172.2 ( $\text{CO}_2^t\text{Bu}$ ).

**High resolution mass spectrum:** Calculated for  $\text{C}_{26}\text{H}_{39}\text{NNaO}_6$  ( $\text{M}+\text{Na}$ ) $^+$ : 484.2670. Found: 484.2671.

#### (*S*)-*tert*-Butyl 3-[(1'*R*,3'*R*)-3-acetyl-2',2'-dimethylcyclobutyl]-4-(benzyloxy-carbonylamino]butanoate, **13**:



A mixture containing compound **12** (250 mg, 0.5 mmol) and PPTS (41 mg, 0.2 mmol, 0.4 eq) in a mixture of water-acetone (1:20, 42 mL) was heated at reflux for 2 h. Afterwards, acetone was evaporated under vacuo. The resulting crude was poured into 40 mL of ethyl



acetate, and the solution was washed with saturated aqueous sodium bicarbonate (3 × 20 mL). The organic phase was dried over magnesium sulfate. The solvent was removed at reduced pressure, and the residue was chromatographed on silica gel (ethyl acetate) to afford pure methyl-ketone **13** (220 mg, 97%) as an oil.

#### Spectroscopic data and physical constants for compound **13**:

$[\alpha]_D^{25} = +243.5$  (*c* 0.61, CH<sub>2</sub>Cl<sub>2</sub>).

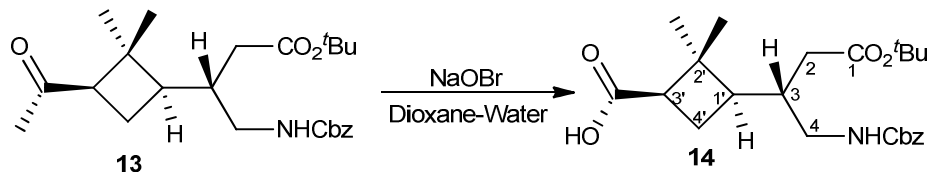
IR (ATR): 3365 (NH<sub>st</sub>), 2954 (CH<sub>st</sub>), 1724 and 1705 (bs, CO<sub>carbamate</sub> + CO<sub>ester</sub> + CO<sub>ketone</sub>), 1523, 1455.

<sup>1</sup>H NMR (250 MHz, CDCl<sub>3</sub>) δ 0.92 (s, 3H, *trans*-CH<sub>3</sub>), 1.35 (s, 3H, *cis*-CH<sub>3</sub>), 1.44 (s, 9H, <sup>t</sup>Bu), 1.73–2.26 (c.a., 9H, H<sub>4'a</sub>, H<sub>1'</sub>, COCH<sub>3</sub>, H<sub>3'</sub>, H<sub>3</sub>, H<sub>4'b</sub>, H<sub>2a</sub>), 2.65–2.82 (m, 1H, H<sub>2b</sub>), 2.98–3.14 (m, 1H, H<sub>4a</sub>), 3.19–3.34 (m, 1H, H<sub>4b</sub>), 5.00–5.28 (c.a., 3H, CH<sub>2</sub>Bn, NH), 7.29–7.41 (c.a., 5H, H<sub>Ar</sub>).

<sup>13</sup>C NMR (62.5 MHz, CDCl<sub>3</sub>) δ 17.2 (*trans*-CH<sub>3</sub>), 22.9 (C<sub>4'</sub>), 28.5 (C(CH<sub>3</sub>)<sub>3</sub>), 30.7 (COCH<sub>3</sub>), 31.6 (*cis*-CH<sub>3</sub>), 37.3 (C<sub>3</sub>), 37.6 (C<sub>2</sub>), 42.8 (C<sub>2'</sub>), 43.7 (C<sub>4</sub>), 44.3 (C<sub>1'</sub>), 54.1 (C<sub>3'</sub>), 67.7 (CH<sub>2</sub>Bn), 81.5 (C(CH<sub>3</sub>)<sub>3</sub>), 124.4, 128.9, 137.1 (6C, C<sub>Ar</sub>), 156.3 (CO<sub>carbamate</sub>), 172.1 (CO<sub>2</sub><sup>t</sup>Bu), 207.9 (COCH<sub>3</sub>).

High resolution mass spectrum: Calculated for C<sub>24</sub>H<sub>35</sub>NNaO<sub>5</sub> (M+Na)<sup>+</sup>: 440.2407. Found: 440.2398.

#### Benzyl (2*S*,1'*R*,3'*R*)-3-(*tert*-butoxycarbonyl)-2-(2',2'-dimethyl-3'-carboxycyclobutyl)-propylcarbamate, **14**:



To an ice cooled solution of ketone **13** (1.15 g, 2.8 mmol) in a mixture of dioxane–water (90 mL, 7:2), was added 160 mL of a sodium hypobromite solution, prepared from bromine (0.6 mL, 12.6 mmol, 4.5 eq) and sodium hydroxide (1.67 g, 40.6 mmol, 14.5 eq) in a mixture of water–dioxane (160 mL, 3:1). The resulting mixture was stirred for 4.5 h at -5 °C.

Next, 10 mL of sodium bisulfite were added, and the mixture was brought to acidic pH by adding 5% hydrochloric acid. The acid solution was extracted with dichloromethane (4 × 30 mL), the organic extracts were dried over anhydrous magnesium sulfate, and the solvent was removed to afford carboxylic acid **14** (1.16 g, quantitative yield).

#### Spectroscopic data and physical constants for compound **14**:

$[\alpha]_D = +93.3$  (*c* 0.15, CH<sub>2</sub>Cl<sub>2</sub>).

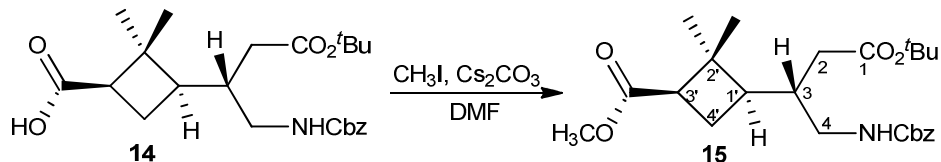
IR (ATR): 3341 (OH<sub>st</sub>, NH<sub>st</sub>), 2957 (CH<sub>st</sub>), 1709 and 1707 (bs, CO<sub>carbamate</sub> + CO<sub>ester</sub> + CO<sub>acid</sub>), 1524, 1455.

<sup>1</sup>H NMR (250 MHz, CDCl<sub>3</sub>) δ 1.12 (s, 3H, *trans*-CH<sub>3</sub>), 1.29 (s, 3H, *cis*-CH<sub>3</sub>), 1.45 (s, 9H, <sup>t</sup>Bu), 1.75–1.89 (m, 1H, H<sub>4'a</sub>), 1.90–2.14 (c.a., 4H, H<sub>4'b</sub>, H<sub>1'</sub>, H<sub>3</sub>, H<sub>2a</sub>), 2.17–2.32 (m, 1H, H<sub>2b</sub>), 2.59–2.75 (m, 1H, H<sub>3'</sub>), 3.00–3.15 (m, 1H, H<sub>4a</sub>), 3.20–3.38 (m, 1H, H<sub>4b</sub>), 5.03–5.23 (c.a., 3H, CH<sub>2</sub>Bn, NH), 7.30–7.43 (c.a., 5H, H<sub>Ar</sub>).

<sup>13</sup>C NMR (62.5 MHz, CDCl<sub>3</sub>) δ 17.4 (*trans*-CH<sub>3</sub>), 24.0 (C<sub>4'</sub>), 28.5 (C(CH<sub>3</sub>)<sub>3</sub>), 30.1 (*cis*-CH<sub>3</sub>), 31.3 (C<sub>3</sub>), 37.6 (C<sub>2</sub>), 42.8 (C<sub>2'</sub>), 43.4 (C<sub>4</sub>), 44.4 (C<sub>1'</sub>), 45.9 (C<sub>3'</sub>), 67.1 (CH<sub>2</sub>Bn), 81.5 (C(CH<sub>3</sub>)<sub>3</sub>), 128.5, 128.9, 136.9 (6C, C<sub>Ar</sub>), 157.0 (CO<sub>carbamate</sub>), 172.5 (CO<sub>2</sub><sup>t</sup>Bu), 178.21 (COOH).

High resolution mass spectrum: Calculated for C<sub>23</sub>H<sub>33</sub>NNaO<sub>6</sub> (M+Na)<sup>+</sup>: 442.2200. Found: 442.2197.

#### (1'*R*,3'*R*)-Methyl 3-[(*S*)-1-(benzyloxycarbonylamino)-4-*tert*-butoxy-4-oxobutan-2-yl]-2',2'-dimethylcyclobutanecarboxylate, **15**:



To a solution of carboxylic acid **14** (150 mg, 0.4 mmol) in 40 mL of dimethylformamide, cesium carbonate (140 mg, 0.4 mmol, 1.0 eq) and iodomethane (0.1 mL, 1.60 mmol, 4.0 eq) were subsequently added. The resulting mixture was left to stir for 16 h at room temperature. Afterwards, ethyl acetate (40 mL) was added, and the solution

was washed with saturated aqueous sodium bicarbonate (4 × 20 mL). The organic phase was dried over magnesium sulfate, and the solvent was removed at reduced pressure. The residue was chromatographed on silica gel (hexane–diethyl ether, 1:1) to afford pure ester **15** (110 mg, 71% yield) as a colourless oil.

#### Spectroscopic data and physical constants for compound **15**:

$[\alpha]_D^{25} = +64.4$  (*c* 0.29, CH<sub>2</sub>Cl<sub>2</sub>).

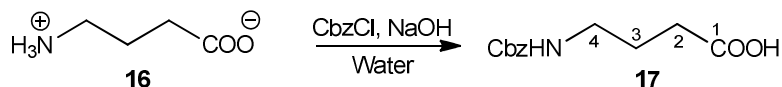
IR (ATR): 3366 (NH<sub>st</sub>), 2951 (CH<sub>st</sub>), 1721 and 1720 (bs, CO<sub>carbamate</sub> + CO<sub>esters</sub>), 1518, 1455.

<sup>1</sup>H NMR (250 MHz, CDCl<sub>3</sub>) δ 0.98 (s, 3H, *trans*-CH<sub>3</sub>), 1.26 (s, 3H, *cis*-CH<sub>3</sub>), 1.45 (s, 9H, <sup>t</sup>Bu), 1.71–1.85 (m, 1H, H<sub>4'a</sub>), 1.90–2.11 (c.a., 4H, H<sub>4'b</sub>, H<sub>1'</sub>, H<sub>3</sub>, H<sub>2a</sub>), 2.16–2.34 (m, 1H, H<sub>2b</sub>), 2.54–2.71 (m, 1H, H<sub>3'</sub>), 2.98–3.12 (m, 1H, H<sub>4a</sub>), 3.20–3.35 (m, 1H, H<sub>4b</sub>), 3.67 (s, 3H, CO<sub>2</sub>CH<sub>3</sub>), 5.00–5.21 (c.a., 3H, CH<sub>2</sub>Bn, NH), 7.29–7.44 (c.a., 5H, H<sub>Ar</sub>)

<sup>13</sup>C NMR (62.5 MHz, CDCl<sub>3</sub>) δ 17.0 (*trans*-CH<sub>3</sub>), 23.7 (C<sub>4'</sub>), 28.0 (C(CH<sub>3</sub>)<sub>3</sub>), 30.9 (*cis*-CH<sub>3</sub>), 37.1 (C<sub>2</sub>), 42.3 (C<sub>2'</sub>), 42.7 (C<sub>4</sub>), 43.9 (C<sub>1'</sub>), 45.6 (C<sub>3'</sub>), 51.1 (CO<sub>2</sub>CH<sub>3</sub>), 66.5 (CH<sub>2</sub>Bn), 80.9 (C(CH<sub>3</sub>)<sub>3</sub>), 128.0, 128.4, 136.3 (6C, C<sub>Ar</sub>), 156.4 (CO<sub>carbamate</sub>), 171.8 and 172.8 (CO<sub>2</sub><sup>t</sup>Bu + CO<sub>2</sub>CH<sub>3</sub>).

High resolution mass spectrum: Calculated for C<sub>24</sub>H<sub>35</sub>NNaO<sub>6</sub> (M+Na)<sup>+</sup>: 456.2357. Found: 456.2349.

#### 4-(Benzyloxycarbonylamino)butanoic acid, **17**:



Benzyl chloroformate (31.5 mL, 3 M solution in THF, 94.5 mmol, 1.3 eq) was added to an aqueous solution (40 mL) of  $\gamma$ -aminobutyrate, **16** (GABA, 7.5 g, 75.0 mmol) and NaOH (6.04 g, 150 mmol, 2 eq) cooled at -5 °C. The reaction mixture was stirred at this temperature for 1 h and at room temperature for 3 h, then CH<sub>2</sub>Cl<sub>2</sub> (3 × 30 mL) was added and the organic phase was separated to remove the excess benzyl chloroformate and THF. The aqueous phase was then cooled down at 0 °C and acidified with concentrated HCl to pH

3 and the white precipitate formed was filtered and washed with 5% HCl to give pure compound **17** (14.29 g, 60.2 mmol, 80% yield).

**Spectroscopic data for compound 17:**

**Melting point:** 60-62 °C (H<sub>2</sub>O)

**IR (ATR):** 3329 (NH<sub>st</sub>), 1685 (bs, CO<sub>carbamate</sub> + CO<sub>ester</sub>), 1545.

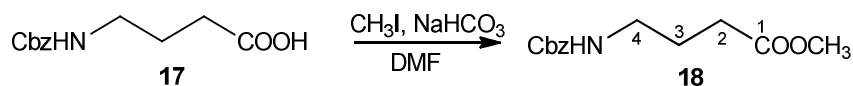
**<sup>1</sup>H NMR** (250 MHz, CDCl<sub>3</sub>) δ 1.98 – 1.72 (m, 2H, H<sub>3</sub>), 2.41 (t, *J*<sub>H,H</sub> = 7.00 Hz, 2H, H<sub>2</sub>), 3.17-3.35 (m, 2H, H<sub>4</sub>), 4.95 (bs, 1H, N-H), 5.11 (s, 2H, CH<sub>2</sub>Bn), 7.29-7.42 (m, 5H, H<sub>Ar</sub>). 0.

**<sup>13</sup>C NMR** (62.5 MHz, CDCl<sub>3</sub>) δ 25.0 (C<sub>3</sub>), 31.1 (C<sub>2</sub>), 40.2 (C<sub>4</sub>), 66.8 (CH<sub>2</sub>Bn), 128.2, 128.5, 136.3 (6C, C<sub>Ar</sub>), 156.7 (CO<sub>carbamate</sub>), 178.4 (CO<sub>acid</sub>).

Spectroscopic data are consistent with those reported in reference:

García-Álvarez, I.; Garrido, L.; Fernández-Mayoralas, A. *ChemMedChem* **2007**, *2*, 496-504.

**Methyl 4-(benzyloxycarbonylamino)butanoate, 18:**



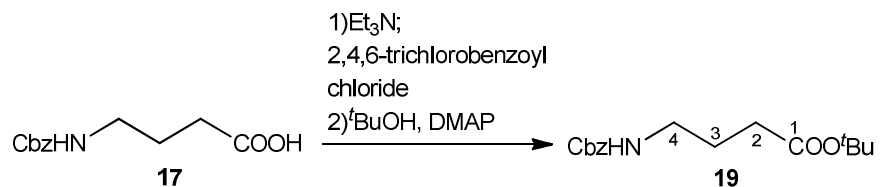
Compound **17** (4.00 g, 17.9 mmol) and NaHCO<sub>3</sub> (3.02 g, 35.9 mmol, 2 eq) were dissolved in DMF (60 mL). Afterwards, CH<sub>3</sub>I (5.6 mL, 89.7 mmol, 5 eq) was added and the resulting mixture was stirred at room temperature for 18 hours. Then the mixture was diluted with water (15 mL) and extracted with ethyl acetate (3 x 30 mL). The combined organic extracts were dried over magnesium sulfate and concentrated under reduced pressure. The crude residue was purified by flash column chromatography (hexane-ethyl acetate, 2:1) to afford pure methyl ester **18** (3.10 g, 70% yield) as a colourless oil.

**Spectroscopic data for compound 18:**

$^1\text{H NMR}$  (250 MHz,  $\text{CDCl}_3$ )  $\delta$  1.78-1.91 (m, 2H,  $\text{H}_3$ ), 2.39 (t,  $J_{\text{H,H}} = 7.2$  Hz, 2H,  $\text{H}_2$ ), 3.19-3.32 (m, 2H,  $\text{H}_4$ ), 3.68 (s, 3H,  $\text{CO}_2\text{CH}_3$ ), 4.92 (bs, 1H, NH), 5.11 (s, 2H,  $\text{CH}_2\text{Bn}$ ), 7.32-7.44 (m, 5H,  $\text{H}_{\text{Ar}}$ ).

Spectroscopic data are consistent with those reported in reference:

García-Álvarez, I.; Garrido, L.; Fernández-Mayoralas, A. *ChemMedChem* **2007**, *2*, 496-504.

***tert*-Butyl 4-(benzyloxycarbonylamino)butanoate, 19:**

Carboxylic acid **17** (834 mg, 3.5 mmol) was dissolved in anhydrous toluene under nitrogen atmosphere and previously distilled triethylamine (480  $\mu\text{L}$ , 3.5 mmol, 1 eq) was added. After 40 minutes, a solution of *t*-BuOH (673  $\mu\text{L}$ , 7.0 mmol, 2 eq) and DMAP (860 mg, 7.0 mmol, 2 eq) in anhydrous toluene (5 mL) was cannulated over the mixed anhydride and the resulting crude was stirred for 1.5 hours. Then the mixture was diluted with diethyl ether (30 mL) and washed with saturated aqueous sodium bicarbonate (3 x 20 mL). The organic liquors were dried over magnesium sulfate and the solvent was evaporated under vacuum. The resulting crude was purified by flash column chromatography (hexane-ethyl acetate, 3:1) to afford pure *tert*-butylester **19** (980 mg, 95% yield) as a colourless oil.

**Spectroscopic data for compound 19:**

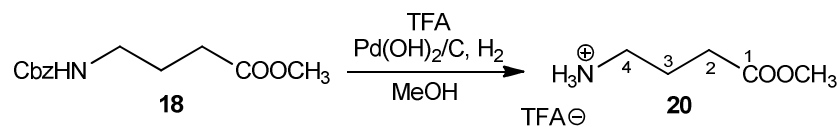
$^1\text{H NMR}$  (250 MHz,  $\text{CDCl}_3$ )  $\delta$  1.41 (s, 9H,  $^t\text{Bu}$ ), 1.64-1.84 (m, 2H,  $\text{H}_3$ ), 2.22 (t,  $J_{\text{H, H}} = 7.2$  Hz, 2H,  $\text{H}_2$ ), 3.08-3.23 (m, 2H,  $\text{H}_4$ ), 5.06 (s, 2H,  $\text{CH}_2\text{Bn}$ ), 5.28 (bs, 1H, NH), 7.32-7.44 (m, 5H,  $\text{H}_{\text{Ar}}$ ).

$^{13}\text{C NMR}$  (62.5 MHz,  $\text{CDCl}_3$ )  $\delta$  25.6 ( $\text{C}_3$ ), 28.4 ( $\text{C}(\text{CH}_3)_3$ ), 33.2 ( $\text{C}_2$ ), 40.8 ( $\text{C}_4$ ), 66.9 ( $\text{CH}_2\text{Bn}$ ), 80.7 ( $\text{C}(\text{CH}_3)_3$ ), 128.4, 128.8, 137.1 (6C,  $\text{C}_{\text{Ar}}$ ), 156.9 ( $\text{CO}_{\text{carbamate}}$ ), 173.0 ( $\text{CO}_{\text{ester}}$ ).

Spectroscopic data are consistent with those reported in reference:

Lee, K.; Kim, D.-K. *Journal of the Korean Chemical Society* **2003**, *48*, 161-170.

García-Álvarez, I.; Garrido, L.; Fernández-Mayoralas, A. *ChemMedChem* **2007**, *2*, 496-504.

**Trifluoroacetate salt of methyl 4-ammoniobutanoate, 20:**

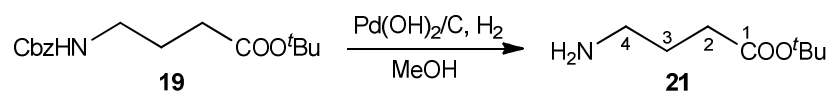
Compound **18** (3.00 g, 12.0 mmol) in methanol (30 mL) was hydrogenated under 5 atmospheres of pressure in the presence of 20%  $\text{Pd}(\text{OH})_2/\text{C}$  (0.35 g, 2% Pd in weight) and TFA (14.4 mL, 18.7 mmol, 1.6 eq) overnight. The reaction mixture was filtered through Celite® and solvent was removed under reduced pressure to provide ammonium salt **20** (2.58 g, quantitative yield) as a yellowish oil.

**Spectroscopic data for compound 20:**

$^1\text{H NMR}$  (250 MHz,  $\text{D}_2\text{O}$ )  $\delta$  1.73-1.93 (m, 2H,  $\text{H}_3$ ), 2.48 (t,  $J_{\text{H,H}} = 7.2$  Hz, 2H,  $\text{H}_2$ ), 3.00 (t,  $J_{\text{H,H}} = 7.2$  Hz, 2H,  $\text{H}_4$ ), 3.59 (s, 3H,  $\text{CO}_2\text{CH}_3$ ).

Spectroscopic data are consistent with those reported in reference:

García-Álvarez, I.; Garrido, L.; Fernández-Mayoralas, A. *ChemMedChem* **2007**, *2*, 496-504.

**tert-Butyl 4-aminobutanoate, 21**

Compound **19** (170 mg, 0.6 mmol) in methanol (15 mL) was hydrogenated under 5 atmospheres of pressure in the presence of 20%  $\text{Pd}(\text{OH})_2/\text{C}$  (20 mg, 2% Pd in weight) overnight. The reaction mixture was filtered through Celite<sup>®</sup> and solvent was removed under reduced pressure to provide amine **21** (83.4 mg, 91% yield) as a colourless oil.

**Spectroscopic data for compound 21:**

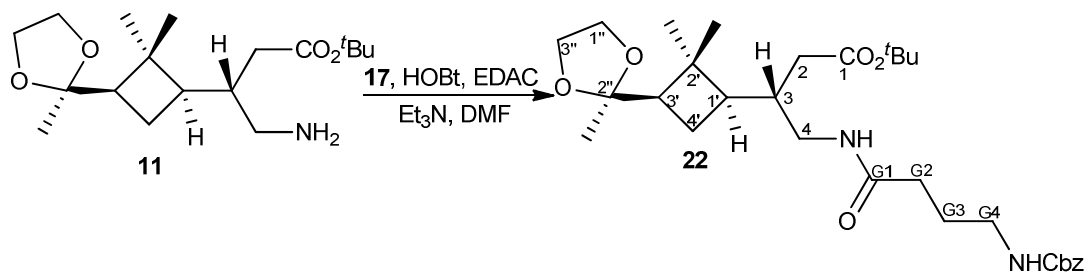
$^1\text{H NMR}$  (250MHz,  $\text{D}_2\text{O}$ )  $\delta$  1.44 (s, 9H,  $^t\text{Bu}$ ), 1.95-2.14 (m, 2H,  $\text{H}_3$ ), 2.40 (t,  $J_{\text{H,H}} = 7.2$  Hz, 2H,  $\text{H}_2$ ), 3.08 (t,  $J_{\text{H,H}} = 7.2$  Hz, 2H,  $\text{H}_4$ ), 6.00 (bs, 2H,  $\text{NH}_2$ ).

$^{13}\text{C NMR}$  (62.5 MHz,  $\text{CDCl}_3$ )  $\delta$  28.0 ( $\text{C}_3$ ), 28.8 ( $\text{C}(\text{CH}_3)_3$ ), 32.9 ( $\text{C}_2$ ), 41.4 ( $\text{C}_4$ ), 80.2 ( $\text{C}(\text{CH}_3)_3$ ), 172.8 ( $\text{CO}_{\text{ester}}$ ).

Spectroscopic data are consistent with those reported in reference:

Lee, K.; Kim, D.-K. *J. Korean Chem. Soc.* **2003**, *48*, 161-170.

***tert*-Butyl 4-(4-(benzyloxycarbonylamino)butanamido)-3-(*S*)-((1'*R*,3'*R*)-2',2'-dimethyl-3'-(2-methyl-1,3-dioxolan-2-yl)cyclobutyl)butanoate, **22**:**



A mixture containing carboxylic acid **17** (448 mg, 1.9 mmol, 1.1 eq), HOBt (375 mg, 2.8 mmol, 1.5 eq), EDAC (773 mg, 4.0 mmol, 2.2 eq) and triethylamine (0.6 mL, 4.4 mmol, 2.4 eq) in anhydrous DMF was stirred for 20 minutes under nitrogen atmosphere, and then amine **11** (600 mg, 1.8 mmol) in anhydrous DMF (10 mL) was added. After stirring at room temperature for 21 hours, the reaction crude was diluted with ethyl acetate (50 mL) and washed with a saturated aqueous sodium bicarbonate solution. The organic phase was dried over magnesium sulfate and the solvents were removed under vacuum. The reaction crude was purified by column chromatography on neutral silica gel (hexane-ethyl acetate, 1:4) to afford pure dipeptide **22** (700 mg, 70% yield) as a yellow oil.



**Spectroscopic data and physical constants for compound 22:**

$[\alpha]_D = -7.0$  (c 1.42, CH<sub>2</sub>Cl<sub>2</sub>).

**Melting point:** 92-93 °C (EtOAc).

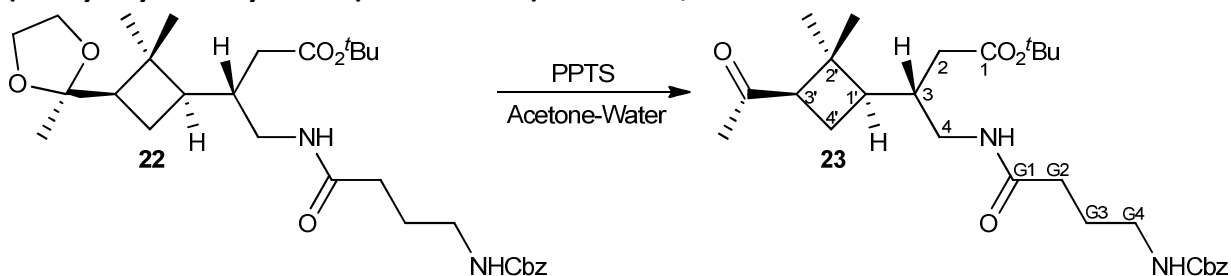
**IR (ATR):** 3315 (NH<sub>st</sub>), 2936 (CH<sub>st</sub>), 2876 (CH<sub>st</sub>), 1718 (CO<sub>amide</sub>), 1649 (CO<sub>ester</sub>), 1531, 1454.

**<sup>1</sup>H NMR** (360 MHz, CDCl<sub>3</sub>) δ 1.01 (s, 3H, *trans*-CH<sub>3</sub>), 1.10 (s, 3H, *cis*-CH<sub>3</sub>), 1.15 (s, 3H, CH<sub>3</sub><sub>ketal</sub>), 1.40 (s, 9H, <sup>t</sup>Bu), 1.47-1.61 (c.a., 2H, H<sub>4'a</sub>, H<sub>3</sub>), 1.74-1.82 (m, 2H, H<sub>G3</sub>), 1.82-1.88 (m, 1H, H<sub>4'b</sub>), 1.97-2.01 (m, 2H, H<sub>2</sub>), 2.02-2.06 (m, 2H, H<sub>1'</sub>, H<sub>3'</sub>), 2.17 (t, *J*<sub>H,H</sub> = 7.2 Hz, 2H, H<sub>G2</sub>), 2.90-3.02 (m, 1H, H<sub>4a</sub>), 3.13-3.23 (m, 2H, H<sub>G4</sub>), 3.25-3.34 (m, 1H, H<sub>4</sub>), 3.70-3.83 (m, 2H, -OCH<sub>2</sub>CH<sub>2</sub>O-), 3.84-3.95 (m, 2H, -OCH<sub>2</sub>CH<sub>2</sub>O-), 5.04 (s, 2H, CH<sub>2</sub>Bn), 5.60 (bs, 1H, NH<sub>carbamate</sub>), 6.53 (bs, 1H, NH<sub>amide</sub>), 7.28-7.33 (m, 5H, H<sub>Ar</sub>).

**<sup>13</sup>C NMR** (90 MHz, CDCl<sub>3</sub>) δ 16.6 (*trans*-CH<sub>3</sub>), 21.0 (C<sub>4'</sub>), 23.8 (CH<sub>3</sub><sub>ketal</sub>), 25.9 (C<sub>G3</sub>), 28.0 (C(CH<sub>3</sub>)<sub>3</sub>), 32.1 (*cis*-CH<sub>3</sub>), 33.7 (C<sub>G2</sub>), 36.3 (C<sub>2</sub>), 37.5 (C<sub>1'</sub>), 40.4 (C<sub>G4</sub>), 41.0 (C<sub>4</sub>), 41.4 (C<sub>2'</sub>), 44.3 (C<sub>3</sub>), 49.3 (C<sub>3'</sub>), 63.6 (-OCH<sub>2</sub>CH<sub>2</sub>O-), 65.4 (-OCH<sub>2</sub>CH<sub>2</sub>O-), 66.4 (CH<sub>2</sub>Bn), 80.8 (C(CH<sub>3</sub>)<sub>3</sub>), 109.6 (C<sub>ketalic</sub>), 127.9, 128.0, 128.4, 136.7 (6C, C<sub>Ar</sub>), 156.7 (CO<sub>carbamate</sub>), 172.6, 172.7 (CO<sub>amide</sub>, CO<sub>ester</sub>).

**Elemental analysis:** calculated for C<sub>30</sub>H<sub>46</sub>N<sub>2</sub>O<sub>7</sub>: 65.91% C, 8.48% H, 5.12% N. Found: C: 65.48% C, 8.70% H, 5.12% N.

***tert*-Butyl 3-(S)-((1'*R*,3'*R*)-3'-acetyl-2',2'-dimethylcyclobutyl)-4-(4-(benzyloxycarbonylamino)butanamido)butanoate, 23:**



A mixture of ketal **22** (2.66 g, 4.9 mmol) and PPTS (0.40 g, 1.6 mmol, 0.3 eq) in wet acetone (45 mL) was heated to reflux for 2 hours. The reaction mixture was cooled and solvent was removed at reduced pressure. The residue was poured into ethyl acetate (50 mL) and the resulting solution was washed with saturated aqueous sodium bicarbonate and then dried over magnesium sulfate. The solvent was evaporated under vacuum to afford a yellow oil identified as ketone **23** (2.40 g, 98% yield).

**Spectroscopic data and physical constants for 23:**

$[\alpha]_D^{25} = -14.23$  (c 1.26, CH<sub>2</sub>Cl<sub>2</sub>).

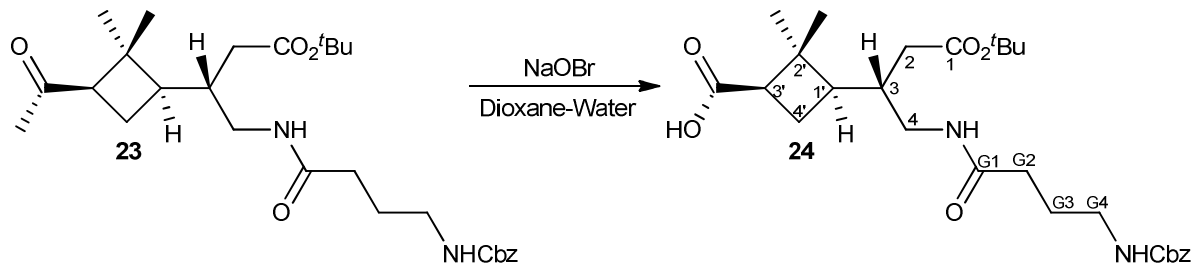
**IR** (ATR): 3336 (NH<sub>st</sub>), 2957 (CH<sub>st</sub>), 2880 (CH<sub>st</sub>), 1705 and 1657 (bs, CO<sub>carbamate</sub> + CO<sub>ester</sub> + CO<sub>ketone</sub> + CO<sub>amide</sub>), 1533, 1456.

**<sup>1</sup>H NMR** (360 MHz, CDCl<sub>3</sub>)  $\delta$  0.90 (s, 3H, *trans*-CH<sub>3</sub>), 1.34 (s, 3H, *cis*-CH<sub>3</sub>), 1.45 (s, 9H, <sup>t</sup>Bu), 1.75-2.10 (c.a., 10H, CH<sub>3</sub>CO, H<sub>4'</sub>, H<sub>1'</sub>, H<sub>3</sub>, H<sub>2a</sub> and H<sub>G3</sub>), 2.18-2.26 (c.a., 3H, H<sub>2b</sub> and H<sub>G2</sub>), 2.74 (dd,  $J_{H,H} = 10.3$  Hz,  $J_{H,H} = 7.4$  Hz, 1H, H<sub>3'</sub>), 3.03-3.12 (m, 1H, H<sub>4a</sub>), 3.20-3.30 (m, 3H, H<sub>G4</sub> i H<sub>4b</sub>), 5.10 (s, 2H, CH<sub>2</sub>Bn), 5.20 (bs, 1H, NH<sub>carbamate</sub>), 6.31 (bs, 1H, NH<sub>amide</sub>), 7.29-7.38 (m, 5H, H<sub>Ar</sub>).

**<sup>13</sup>C NMR** (90 MHz, CDCl<sub>3</sub>)  $\delta$  16.8 (*trans*-CH<sub>3</sub>), 22.4 (C<sub>4'</sub>), 25.8 (C<sub>G3</sub>), 28.0 (C(CH<sub>3</sub>)<sub>3</sub>), 30.2 (CH<sub>3</sub>CO), 31.2 (*cis*-CH<sub>3</sub>), 33.6 (C<sub>G2</sub>), 36.3 (C<sub>1'</sub>), 37.2 (C<sub>2</sub>), 40.4 (C<sub>G4</sub>), 40.9 (C<sub>4</sub>), 43.8 (C<sub>2'</sub>), 44.3 (C<sub>3</sub>), 53.4 (C<sub>3'</sub>), 66.4 (CH<sub>2</sub>Bn), 81.0 (C(CH<sub>3</sub>)<sub>3</sub>), 127.9, 128.4, 128.5, 136.7 (6C, C<sub>Ar</sub>), 156.8 (CO<sub>carbamate</sub>), 172.3, 172.7 (CO<sub>amide</sub>, CO<sub>ester</sub>), 207.6 (CO<sub>ketone</sub>).

**High resolution mass spectrum:** Calculated for C<sub>28</sub>H<sub>42</sub>N<sub>2</sub>NaO<sub>6</sub> (M+Na)<sup>+</sup>: 525.2935. Found: 525.2939.

**(1'*R*,3'*R*)-3-((*S*)-15,15-Dimethyl-3,8,13-trioxo-1-phenyl-2,14-dioxo-4,9 diazahexadecan-11-yl)-2',2'-dimethylcyclobutanecarboxylic acid, **24**:**



To an ice cooled solution of compound **23** (1.60 g, 3.2 mmol) in a mixture of dioxane-water (7:2, 46 mL) was added a sodium hypobromite solution, prepared from bromine (0.58 mL, 11.5 mmol, 3.5 eq) and sodium hydroxide (0.97 g, 23.0 mmol, 7.2 eq) in a 3:1 mixture of water-dioxane (87 mL). The resulting mixture was stirred for 5 hours at -5 °C. Then, sodium bisulfite was added (10 mL) and the mixture was brought to acidic pH by adding 5% hydrochloric acid. The acid solution was extracted with dichloromethane (4 x 30 mL), the organic extracts were dried over anhydrous magnesium sulfate and solvent was removed to afford carboxylic acid **24** as a white powder (1.55 g, 96% yield).

**Spectroscopic data and physical constants for 24:**

$[\alpha]_D = +26.7$  ( $c$  1.65,  $\text{CH}_2\text{Cl}_2$ ).

**Melting point:** below 25 °C ( $\text{CH}_2\text{Cl}_2$ ).

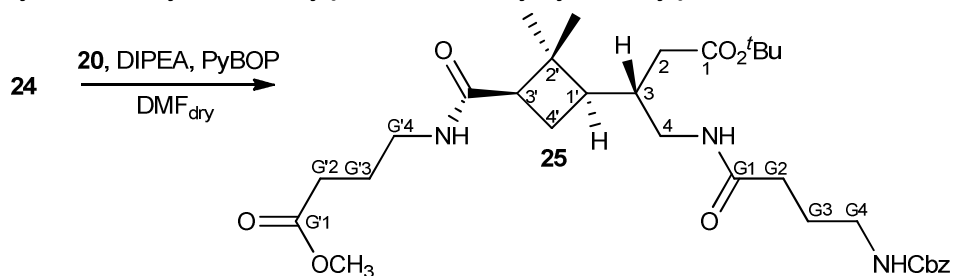
**IR (ATR):** 3700 ( $\text{OH}_{\text{st}}$ ), 3336 ( $\text{NH}_{\text{st}}$ ), 2937 ( $\text{CH}_{\text{st}}$ ), 1701 and 1640 (bs,  $\text{CO}_{\text{carbamate}} + \text{CO}_{\text{ester}} + \text{CO}_{\text{acid}} + \text{CO}_{\text{amide}}$ ), 1558, 1414.

**$^1\text{H}$  NMR** (250 MHz,  $\text{CDCl}_3$ )  $\delta$  1.03 (s, 3H, *trans*- $\text{CH}_3$ ), 1.26 (s, 3H, *cis*- $\text{CH}_3$ ), 1.44 (s, 9H,  $^t\text{Bu}$ ), 1.70-1.90 (c.a., 3H,  $\text{H}_{4'a}$  i  $\text{H}_{G3}$ ), 1.91-2.12 (c.a., 4H,  $\text{H}_{G2}$ ,  $\text{H}_3$ ,  $\text{H}_{4'b}$ ), 2.13-2.30 (c.a., 3H,  $\text{H}_2$ ,  $\text{H}_{1'}$ ), 2.54-2.72 (m, 1H,  $\text{H}_{3'}$ ), 2.92-3.11 (m, 1H,  $\text{H}_4$ ), 3.12-3.37 (m, 3H,  $\text{H}_{G4}$ ,  $\text{H}_4$ ), 5.08 (s, 2H,  $\text{CH}_2\text{Bn}$ ), 5.44 (bs, 1H,  $\text{NH}_{\text{carbamate}}$ ), 6.64 (bs, 1H,  $\text{NH}_{\text{amide}}$ ), 7.29-7.38 (m, 5H,  $\text{H}_{\text{Ar}}$ ), 9.41 (s, 1H,  $\text{H}_{\text{acid}}$ ).

**$^{13}\text{C}$  NMR** (62.5 MHz,  $\text{CDCl}_3$ )  $\delta$  17.4 (*trans*- $\text{CH}_3$ ), 24.1 ( $\text{C}_{4'}$ ), 26.3 ( $\text{C}_{G3}$ ), 28.5 ( $\text{C}(\text{CH}_3)_3$ ), 31.3 (*cis*- $\text{CH}_3$ ), 34.0 ( $\text{C}_{G2}$ ), 36.9 ( $\text{C}_{1'}$ ), 37.7 ( $\text{C}_2$ ), 40.8 ( $\text{C}_{G4}$ ), 41.6 ( $\text{C}_4$ ), 43.2 ( $\text{C}_3$ ), 44.6 ( $\text{C}_{3'}$ ), 45.9 ( $\text{C}_{2'}$ ), 67.0 ( $\text{CH}_2\text{Bn}$ ), 81.7 ( $\text{C}(\text{CH}_3)_3$ ), 128.4, 129.0, 137.0 (6C,  $\text{C}_{\text{Ar}}$ ), 157.3 ( $\text{CO}_{\text{carbamate}}$ ), 173.1, 173.7, 177.2 ( $\text{CO}_{\text{amide}}$ ,  $\text{CO}_{\text{ester}}$ ,  $\text{CO}_{\text{acid}}$ ).

**High resolution mass spectrum:** Calculated for  $\text{C}_{27}\text{H}_{40}\text{N}_2\text{NaO}_7$  ( $\text{M}+\text{Na}$ ) $^+$ : 527.2728. Found: 527.2724.

***tert*-butyl 4-(4-(benzyloxycarbonylamino)butanamido)-3-(*S*)-((1'*R*,3'*R*)-3'-(4-methoxy-4-oxobutylcarbamoyl)-2',2'-dimethylcyclobutyl)butanoate, 25:**



Compound **24** (1.18 g, 2.3 mmol), DIPEA (2.00 mL, 11.5 mmol, 5.0 eq) and PyBOP (1.80 g, 3.5 mmol, 1.5 eq) were dissolved in anhydrous dimethylformamide (40 mL), the mixture was stirred for 5 minutes under nitrogen atmosphere. Then, a solution of amine **20** (0.64 g, 2.8 mmol, 1.2 eq) in anhydrous dimethylformamide (10 mL) was added via cannula.

After stirring at room temperature for 2 hours, the reaction crude was diluted with ethyl acetate (40 mL) and washed with a saturated aqueous sodium bicarbonate solution. The organic phase was dried over magnesium sulfate and the solvents were removed under vacuum. The reaction crude was purified by column chromatography on neutral silica gel (ethyl acetate to methanol) to afford pure tripeptide **25** (1.36 g, 98% yield) as a yellow oil.

**Spectroscopic data and physical constants for 25:**

$[\alpha]_D^{25} = +22.5$  (*c* 1.81, CH<sub>2</sub>Cl<sub>2</sub>).

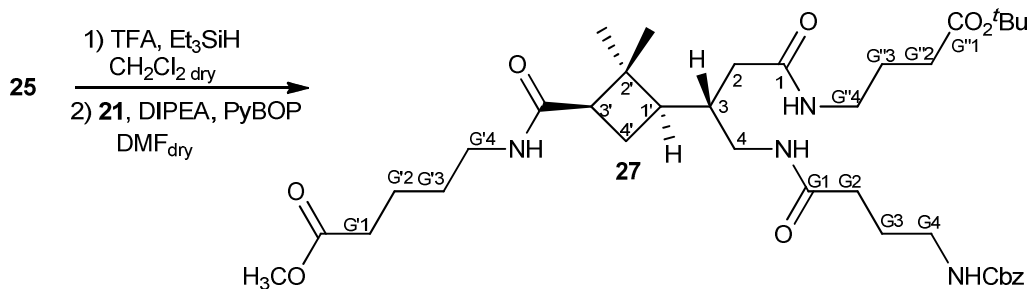
**IR** (ATR): 3443 (NH<sub>st</sub>), 2956 (CH<sub>st</sub>), 1721 and 1665 (bs, CO<sub>carbamate</sub> + CO<sub>esters</sub> + CO<sub>amides</sub>), 1518, 1455, 1440.

**<sup>1</sup>H NMR** 360 MHz, CDCl<sub>3</sub> δ 0.97 (s, 3H, *trans*-CH<sub>3</sub>), 1.25 (s, 3H, *cis*-CH<sub>3</sub>), 1.45 (s, 9H, <sup>t</sup>Bu), 1.71-1.83 (m, 1H, H<sub>3</sub>), 1.78-1.91 (m, 2H, H<sub>4'</sub>), 1.84 (tt, *J*<sub>H,H</sub> = 6.3 Hz, *J*<sub>H,H</sub> = 7.1 Hz, 2H, H<sub>G'3</sub>), 1.86 (tt, *J*<sub>H,H</sub> = 7.0 Hz, *J*<sub>H,H</sub> = 6.1 Hz, 2H, H<sub>G3</sub>), 2.22 (t, *J*<sub>H,H</sub> = 6.7 Hz, 2H, H<sub>G2</sub>), 2.17-2.26 (c.a., 3H, H<sub>2</sub> and H<sub>1'</sub>), 2.37 (t, *J*<sub>H,H</sub> = 7.1 Hz, 2H, H<sub>G'2</sub>), 2.45 (dd, *J*<sub>H,H</sub> = 10.3 Hz, *J*<sub>H,H</sub> = 7.6 Hz, 1H, H<sub>3'</sub>), 3.00-3.11 (m, 1H, H<sub>4</sub>), 3.24-3.34 (m, 1H, H<sub>4</sub>), 3.25 (td, *J*<sub>H,H</sub> = 6.8 Hz, *J*<sub>H,H</sub> = 6.1 Hz, 2H, H<sub>G'4</sub>), 3.29 (td, *J*<sub>H,H</sub> = 6.8 Hz, *J* = 6.2 Hz, 2H, H<sub>G4</sub>), 3.67 (s, 3H, CO<sub>2</sub>CH<sub>3</sub>), 5.09 (s, 2H, CH<sub>2</sub>Bn), 5.28 (bs, 1H, NH<sub>carbamate</sub>), 5.69 (bs, 1H, NH<sub>amide G'</sub>), 6.39 (bs, 1H, NH<sub>amide</sub>), 7.29-7.38 (m, 5H, H<sub>Ar</sub>).

**<sup>13</sup>C NMR** (90 MHz, CDCl<sub>3</sub>) δ 16.7 (*trans*-CH<sub>3</sub>), 24.0 (C<sub>4'</sub>), 24.8, 25.8 (C<sub>G3</sub>, C<sub>G'3</sub>), 28.1 (C(CH<sub>3</sub>)<sub>3</sub>), 31.3 (*cis*-CH<sub>3</sub>), 31.5, 33.7 (C<sub>G2</sub>, C<sub>G'2</sub>), 36.7 (C<sub>1'</sub>), 37.5 (C<sub>2</sub>), 38.8 (C<sub>G4</sub>), 40.5 (C<sub>4</sub>), 41.6 (C<sub>G'4</sub>), 43.4 (C<sub>3</sub>), 44.1 (C<sub>3'</sub>), 47.1 (C<sub>2'</sub>), 51.7 (CO<sub>2</sub>CH<sub>3</sub>), 66.6 (CH<sub>2</sub>Bn), 81.2 (C(CH<sub>3</sub>)<sub>3</sub>), 128.1, 128.5, 136.5 (6C, C<sub>Ar</sub>), 156.8 (CO<sub>carbamate</sub>), 171.5, 172.3, 173.8, 174.1 (CO<sub>amides</sub>, CO<sub>esters</sub>)

**High resolution mass spectrum:** Calculated for C<sub>32</sub>H<sub>49</sub>N<sub>3</sub>NaO<sub>8</sub> (M+Na)<sup>+</sup>: 626.3412. Found: 626.3410.

**4-(4-(benzyloxycarbonylamino)butanamido)-3-(S)-((1'R,3'R)-3'-(4-methoxy-4-oxobutylcarbamoyl)-2',2'-dimethylcyclobutyl)butanoic acid, **27**:**



A mixture containing compound **25** (1.44 g, 2.4 mmol), trifluoroacetic acid (1.5 mL, 20.7 mmol, 8.6 eq) and triethyl silane (0.6 mL, 3.6 mmol, 1.5 eq) in anhydrous dichloromethane (30 mL) was stirred at room temperature for 2 h. Then, solvent was evaporated and the excess of trifluoroacetic acid was removed by lyophilization affording quantitatively compound **26** (1.30 g) as a white solid. Compound **26** (1.3 g, 2.4 mmol), DIPEA (2.09 mL, 12.0 mmol, 5 eq) and PyBOP (1.90 g, 3.7 mmol, 1.5 eq) were then dissolved in anhydrous dimethylformamide (40 mL), the mixture was stirred for 5 minutes under nitrogen atmosphere, and then a solution of **21** (0.46 g, 2.9 mmol, 1.2 eq) in anhydrous dimethylformamide (10 mL) was added via cannula. After stirring at room temperature for 2 hours the reaction crude was diluted with ethyl acetate (40 mL) and washed with a saturated aqueous sodium bicarbonate solution. The organic phase was dried over magnesium sulfate and the solvents were removed under vacuum. The reaction crude was purified by column chromatography on neutral silica gel (ethyl acetate to methanol) to afford pure tetrapeptide **27** (1.40 g, 90% yield from **25**) as a yellow oil.

**Spectroscopic data and physical constants for 27:**

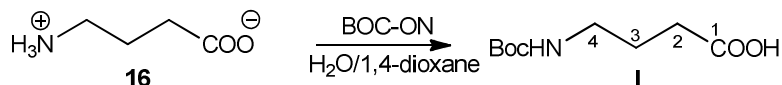
$[\alpha]_D = +15.3$  ( $c$  1.11,  $\text{CH}_2\text{Cl}_2$ ).

**IR (ATR):** 3301 ( $\text{NH}_{\text{st}}$ ), 2933 ( $\text{CH}_{\text{st}}$ ), 1716 and 1650 (bs,  $\text{CO}_{\text{carbamate}}$  +  $\text{CO}_{\text{esters}}$  +  $\text{CO}_{\text{amides}}$ ), 1539, 1455.

**$^1\text{H}$  NMR** (400 MHz,  $\text{CDCl}_3$ )  $\delta$  1.00 (s, 3H, *trans*- $\text{CH}_3$ ), 1.25 (s, 3H, *cis*- $\text{CH}_3$ ), 1.42 (s, 9H,  $^t\text{Bu}$ ), 1.73-1.78 (m, 1H,  $\text{H}_3$ ), 1.78 (tt,  $J_{\text{H,H}} = 7.2$  Hz,  $J_{\text{H,H}} = 7.5$ , 2H,  $\text{H}_{\text{G}''3}$ ), 1.82 (tt,  $J_{\text{H,H}} = 7.0$  Hz,  $J_{\text{H,H}} = 7.2$  Hz, 2H,  $\text{H}_{\text{G}''3}$ ), 1.83 (tt,  $J_{\text{H,H}} = 6.3$  Hz,  $J'' = 7.0$  Hz, 2H,  $\text{H}_{\text{G}3}$ ), 1.85-1.93 (m, 2H,  $\text{H}_{4'}$ ), 1.92-1.99 (m, 2H,  $\text{H}_2$ ), 2.09-2.12 (m, 1H,  $\text{H}_{1'}$ ), 2.24 (t,  $J_{\text{H,H}} = 6.7$  Hz, 2H,  $\text{H}_{\text{G}2}$ ), 2.26 (t,  $J_{\text{H,H}} = 7.2$  Hz, 2H,  $\text{H}_{\text{G}''2}$ ), 2.36 (t,  $J_{\text{H,H}} = 7.1$  Hz, 2H,  $\text{H}_{\text{G}''2}$ ), 2.39-2.48 (m, 1H,  $\text{H}_{3'}$ ), 2.98-3.07 (m, 1H,  $\text{H}_{4a}$ ), 3.24 (td,  $J_{\text{H,H}} = 7.2$  Hz,  $J_{\text{H,H}} = 5.7$  Hz, 2H,  $\text{H}_{\text{G}4}$ ), 3.24 (td,  $J_{\text{H,H}} = 6.1$  Hz,  $J_{\text{H,H}} = 6.1$  Hz, 2H,  $\text{H}_{\text{G}''4}$ ), 3.28 (td,  $J_{\text{H,H}} = 6.6$  Hz,  $J_{\text{H,H}} = 6.4$  Hz, 2H,  $\text{H}_{\text{G}''4}$ ), 3.26-3.36 (m, 1H,  $\text{H}_{4b}$ ), 3.67 (s, 3H,  $\text{CO}_2\text{CH}_3$ ), 5.08 (s, 2H,  $\text{CH}_2\text{Bn}$ ), 5.38 (bs, 1H,  $\text{NH}_{\text{carbamate}}$ ), 5.70 (bs, 1H,  $\text{NH}_{\text{amide G}'}$ ), 6.99 (bs, 1H,  $\text{NH}_{\text{amide}}$ ), 7.14 (bs, 1H,  $\text{NH}_{\text{amide G}''}$ ), 7.30-7.38 (m, 5H,  $\text{H}_{\text{Ar}}$ ).

**$^{13}\text{C}$  NMR** (100 MHz,  $\text{CDCl}_3$ )  $\delta$  17.0 (*trans*- $\text{CH}_3$ ), 23.8 ( $\text{C}_{4'}$ ), 24.6, 24.9, 26.4 ( $\text{C}_{\text{G}3}$ ,  $\text{C}_{\text{G}''3}$ ,  $\text{C}_{\text{G}''3}$ ), 28.2 ( $\text{C}(\text{CH}_3)_3$ ), 31.6 (*cis*- $\text{CH}_3$ ), 31.7, 33.3, 33.8 ( $\text{C}_{\text{G}2}$ ,  $\text{C}_{\text{G}''2}$ ,  $\text{C}_{\text{G}''2}$ ), 37.7 ( $\text{C}_{1'}$ ), 37.9 ( $\text{C}_2$ ), 38.5, 39.0, 39.3 ( $\text{C}_{\text{G}4}$ ,  $\text{C}_{\text{G}''4}$ ,  $\text{C}_{\text{G}''4}$ ), 40.4 ( $\text{C}_4$ ), 41.6 ( $\text{C}_3$ ), 44.2 ( $\text{C}_{3'}$ ), 47.2 ( $\text{C}_2'$ ), 51.9 ( $\text{CO}_2\text{CH}_3$ ), 66.9 ( $\text{CH}_2\text{Bn}$ ), 80.7 ( $\text{C}(\text{CH}_3)_3$ ), 128.2, 128.3, 128.7, 136.7 (6C,  $\text{C}_{\text{Ar}}$ ), 157.2 ( $\text{CO}_{\text{carbamate}}$ ), 171.7, 172.3, 173.0, 173.6, 174.1 ( $\text{CO}_{\text{amides}}$ ,  $\text{CO}_{\text{esters}}$ ).

**High resolution mass spectrum:** Calculated for  $\text{C}_{36}\text{H}_{56}\text{N}_4\text{NaO}_9$  ( $\text{M}+\text{Na}$ ) $^+$ : 711.3940. Found: 711.3935.

**4-tert-Butoxycarbonylamino butyric acid, I:**

To a solution of GABA, **16** ( $\gamma$ -aminobutyric acid, 1 g, 9.69 mmol) and triethylamine (2.02 mL, 14.54 mmol, 1.5 eq) in water (20 mL) was added 1,4-dioxane (20 mL) and BOC-ON

(2-(*tert*-butoxycarbonyloxyimino)-2-phenylacetonitrile), 2.62 g, 10.7 mmol, 1.1 eq) at room temperature with continuous stirring. The mixture became homogeneous within 15 minutes and stirring was continued for 3 h at room temperature. After addition of water (60 mL) and EtOAc (30 mL) to the mixture, the aqueous layer was separated, washed with EtOAc (5 x 30 mL), to remove the oxime by-product, and then acidified with 5% aqueous citric acid to pH = 3 and extracted with dichloromethane (2 x 50 mL). The organic layer was evaporated under reduced pressure and the acid **I** was obtained as a white crystalline solid in 83% yield without need of further purification.

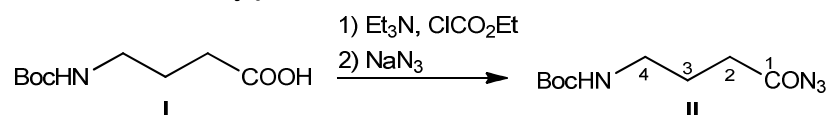
#### Spectroscopic data for compound **I**:

$^1\text{H NMR}$  (250MHz,  $\text{CDCl}_3$ )  $\delta$  1.44 (s, 9H,  $^t\text{Bu}$ ), 1.81 (m, 2H,  $\text{H}_3$ ), 2.39 (t,  $J_{\text{H,H}} = 7.3$  Hz, 2H,  $\text{H}_2$ ), 3.18 (m, 2H,  $\text{H}_4$ ).

Spectroscopic data are consistent with those reported in reference:

Zhao, L-X.; Park, J. G.; Moon, Y-S.; Basnet, A.; Choi, J.; Kim, E-K.; Jeong, T. C.; Jahng, Y.; Lee, E-S. *Il Farmaco* **2004**, *59*, 381-387.

#### *tert*-Butyl (4-azido-4-oxobutyl)carbamate, **II**:



To an ice-cooled solution of carboxylic acid **I** (300 mg, 1.5 mmol) in anhydrous acetone, triethylamine (0.33 mL, 2.3 mmol, 1.5 eq) and ethyl chloroformate (0.23 mL, 2.3 mmol, 1.5 eq) were subsequently added. The mixture was stirred at 0 °C for 30 minutes. Then, sodium azide (167 mg, 2.5 mmol, 1.7 eq) in 5 mL of water was added and the resultant solution was stirred at room temperature for 1.5 h. The reaction mixture was extracted with dichloromethane (4 x 15 mL), and the organic extracts were dried over magnesium sulfate. Solvents were removed under reduced pressure to give acyl azide **II** as a white powder (335



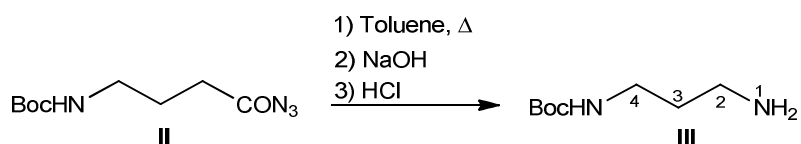
mg, 98% yield), which was characterised by its spectroscopic data and used in the next step without further purification. WARNING: This product should be carefully manipulated because of its explosive nature.

**Spectroscopic data for compound II:**

**IR** (ATR): 3344 (NH<sub>st</sub>), 2977 (CH<sub>st</sub>), 2932 (CH<sub>st</sub>), 2136 (N<sub>3</sub>), 1691 (bs, CO<sub>ester</sub> + CO<sub>acylazide</sub>), 1517.

**<sup>1</sup>H NMR** (250 MHz, CDCl<sub>3</sub>) δ 1.33 (s, 9H, <sup>t</sup>Bu), 1.64-1.82 (m, 2H, H<sub>3</sub>), 2.21-2.39 (m, 2H, H<sub>2</sub>), 2.97-3.18 (m, 2H, H<sub>4</sub>), 4.99 (bs, 1H, NH).

**<sup>13</sup>C NMR** (62.5 MHz, CDCl<sub>3</sub>) δ 25.6 (C<sub>3</sub>), 28.7 (C(CH<sub>3</sub>)<sub>3</sub>), 34.6 (C<sub>2</sub>), 40.0 (C<sub>4</sub>), 79.7 (C(CH<sub>3</sub>)<sub>3</sub>), 156.5 (CO<sub>carbamate</sub>), 181.0 (CON<sub>3</sub>).

***tert*-Butyl (3-aminopropyl)carbamate, III:**

Acyl azide **II** (335 mg, 1.47 mmol) was dissolved in toluene (15 mL) and the mixture was heated to reflux overnight. Afterwards the solution was cooled to room temperature and added to NaOH (0.11 g, 2.72 mmol, 1.7 eq) in H<sub>2</sub>O (5 mL). After vigorously stirring for 15 h at room temperature, no isocyanate was detected by IR in the toluene phase. The mixture was acidified to pH<1 by careful addition (CO<sub>2</sub> evolution) of concentrated HCl, the layers were separated and the aqueous phase was washed with Et<sub>2</sub>O (2 x 10 mL). The aqueous phase was then made basic by slow addition of NaOH pellets (pH = 14) and extracted with CH<sub>2</sub>Cl<sub>2</sub> (2 x 15 mL). The combined organic extracts were dried over magnesium sulfate and concentrated under reduced pressure to yield amine **III** (128 mg, 50% yield) as a colourless oil.

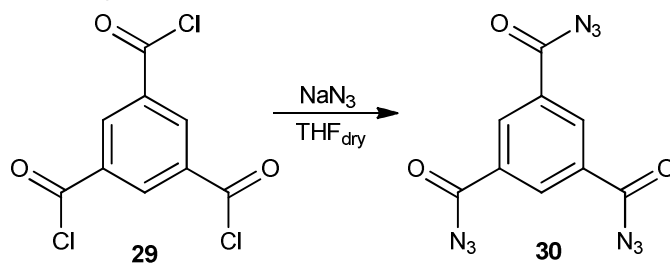
**Spectroscopic data for compound III:**

$^1\text{H NMR}$  (250 MHz,  $\text{CDCl}_3$ )  $\delta$  1.42 (s, 9H,  $^t\text{Bu}$ ), 1.51-1.66 (m, 2H,  $\text{H}_3$ ), 2.69-2.80 (m, 2H,  $\text{H}_2$ ), 3.11-3.26 (m, 2H,  $\text{H}_4$ ).

$^{13}\text{C NMR}$  (62.5 MHz,  $\text{CDCl}_3$ )  $\delta$  27.8 ( $\text{C}(\text{CH}_3)_3$ ), 33.3 ( $\text{C}_3$ ), 38.1 ( $\text{C}_4$ ), 39.7 ( $\text{C}_2$ ), 78.6 ( $\text{C}(\text{CH}_3)_3$ ), 156.3 ( $\text{CO}_{\text{carbamate}}$ ).

Spectroscopic data are consistent with those reported in reference:

Plouvier, B.; Bailly, C.; Houssin, R.; Henichart, J.-P. *Heterocycles*, **32** (1991), 693-701.

**Benzene-1,3,5-tricarbonyl azide, 30:**

A solution of trimesoyl chloride, **29** (100 mg, 0.38 mmol) in anhydrous THF (1 mL) was added dropwise to a solution of  $\text{NaN}_3$  (250 mg, 3.8 mmol, 10 eq) in water (2 mL) while cooling with an ice bath. After stirring for 30 minutes the reaction mixture was extracted with dichloromethane (4 x 15 mL), and the organic extracts were dried over magnesium sulfate. Solvents were removed under reduced pressure to give acyl azide **30** as a white powder (97 mg, 90% yield), which was characterised by its spectroscopic data and used in the next step without further purification. **WARNING:** This product should be carefully manipulated because of its explosive nature.

**Spectroscopic data for compound 30:**

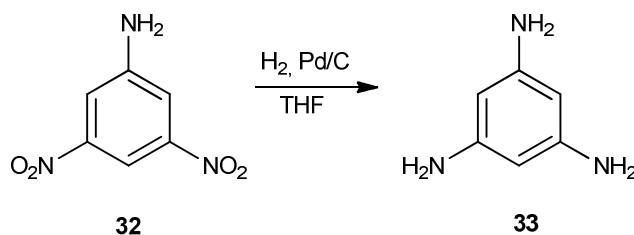
IR (ATR): 3053 (=C-H<sub>st</sub>), 2144 (N<sub>3</sub>), 1697 (CO<sub>acylazide</sub>), 1193.

<sup>1</sup>H NMR (250 MHz, CDCl<sub>3</sub>) δ 8.90 (s, 3H, H<sub>orto</sub>)

<sup>13</sup>C NMR (62.5 MHz, CDCl<sub>3</sub>) δ 132.9 (C<sub>orto</sub>), 135.7 (CCO), 181.0 (CON<sub>3</sub>).

Spectroscopic data are consistent with those reported in reference:

van Gorp, J. J.; Vekemans, J. A. J. M.; Meijer, E. W. J. *Am. Chem. Soc.* **2002**, *124*, 14759-14769.

**Benzene-1,3,5-triamine, 33:**

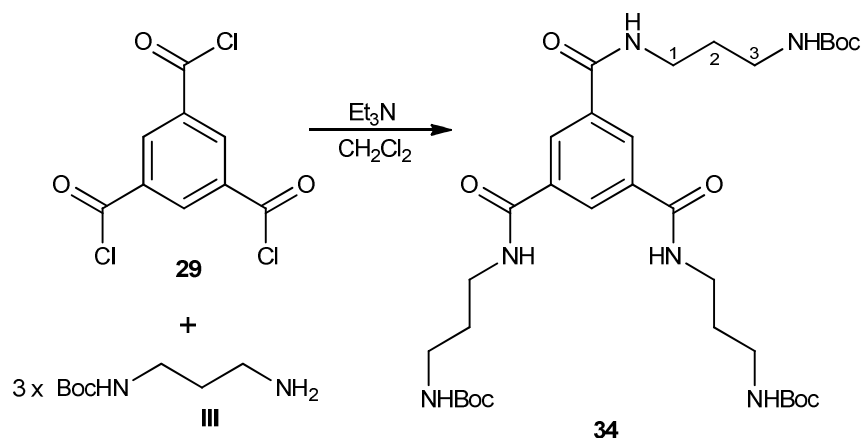
3,5-Dinitroaniline, **32** (0.50 g, 2.7 mmol) was hydrogenated in anhydrous tetrahydrofuran (15 mL) in the presence of 10% Pd/C (0.05 g, 1% Pd in weight) under hydrogen atmosphere (5 atm). After filtration under inert atmosphere, the filtrate was concentrated to dryness by evaporation under reduced pressure to give 1,3,5-triaminobenzene **33** (0.33 g, 99% yield).

**Spectroscopic data for compound 33:**

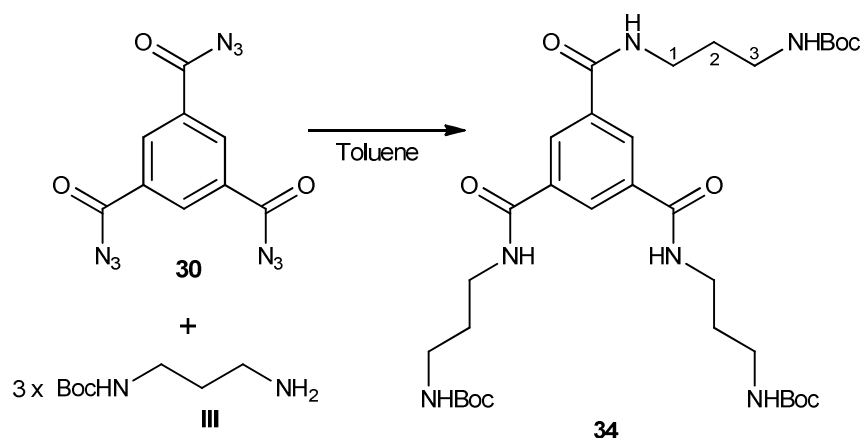
<sup>1</sup>H NMR (250 MHz, CDCl<sub>3</sub>) δ 3.48 (bs, 6H, NH<sub>2</sub>), 5.52 (s, 3H, H<sub>orto</sub>).

Spectroscopic data are consistent with those reported in reference:

Jeong, M. J.; Park, J. H.; Lee, C.; Chang, J. Y. *Org. Lett.* **2006**, *8*, 2221-2224.

**C-Centered triamide 34:**Method 1:

To a cooled solution of compound **III** (170 mg, 1.0 mmol, 3.3 eq) and triethylamine (0.13 mL, 1.0 mmol, 3 eq) in anhydrous dichloromethane (15 mL) was added a solution of 1,3,5-benzenetricarbonyl trichloride (80 mg, 0.3 mmol) in anhydrous dichloromethane (5 mL). The solution was slowly brought to room temperature and stirred for 21 hours. The reaction mixture was diluted with ethyl acetate (20 mL) and the solution was washed with 5% aqueous citric acid (3 x 20 mL), saturated aqueous sodium bicarbonate solution (3 x 20 mL) and brine (3 x 20 mL). The organic layer was dried over magnesium sulfate and the solvent was evaporated in vacuo. The resulting crude was dissolved in diethyl ether, filtered through a sintered funnel and the filtrate was evaporated to afford pure C-centered triamide **34** (70 mg, 34% yield) as a yellow solid.

Method 2:

A mixture containing acyl azide **30** (160 mg, 0.6 mmol) and amine **III** (0.32 g, 1.8 mmol, 3.3 eq) in anhydrous toluene (15 mL) was heated to reflux for 18 hours (reaction progress was monitored by IR following the signals for the acyl azide at  $2136\text{ cm}^{-1}$  and the isocyanate, at  $2260\text{ cm}^{-1}$ ). After elimination of toluene under reduced pressure, the residue was chromatographed on silica gel (dichloromethane) to afford C-centered triamide **34** as a yellow solid (310 mg, 82% yield).

**Spectroscopic data for compound 34:**

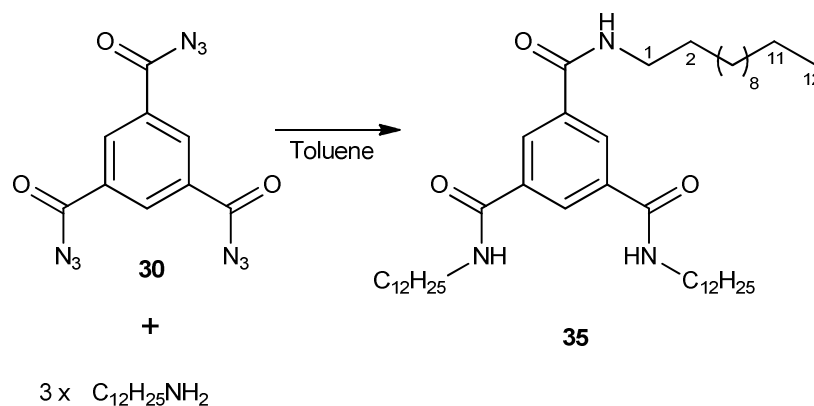
**Melting point:** 172-174 °C (dichloromethane)

**IR (ATR):** 3318 ( $\text{NH}_{\text{st}}$ ), 3077 ( $=\text{C}-\text{H}_{\text{st}}$ ), 2976 ( $\text{CH}_{\text{st}}$ ), 2932 ( $\text{CH}_{\text{st}}$ ), 2360, 2341 and 2247 (overtones), 1688 ( $\text{CO}_{\text{carbamate}}$ ), 1650 ( $\text{CO}_{\text{amide}}$ ), 1529 ( $\text{C}-\text{C}_{\text{Ar}}$ ).

**$^1\text{H}$  NMR** (250 MHz,  $\text{CDCl}_3$ )  $\delta$  1.44 (s, 27H,  $^t\text{Bu}$ ), 1.67-1.83(m, 6H,  $\text{H}_2$ ), 3.13-3.27 (m, 6H,  $\text{H}_3$ ), 3.4-3.57 (m, 6H,  $\text{H}_1$ ), 5.27 (bs, 3H,  $\text{NH}_{\text{carbamate}}$ ) 7.77 (bs, 3H,  $\text{NH}_{\text{amide}}$ ), 8.14 (bs, 3H,  $\text{H}_{\text{Ar}}$ ).

**$^{13}\text{C}$  NMR** (62.5 MHz,  $\text{CDCl}_3$ )  $\delta$  28.9 ( $\text{C}(\text{CH}_3)_3$ ), 30.2 ( $\text{C}_2$ ), 37.2 ( $\text{C}_3$ ), 37.9 ( $\text{C}_1$ ), 80.0 ( $\text{C}(\text{CH}_3)_3$ ), 128.6 ( $\text{C}_{\text{orto}}$ ), 135.8 ( $\text{C}_{\text{ipso}}$ ), 157.2 ( $\text{CO}_{\text{carbamate}}$ ), 167.3 ( $\text{CO}_{\text{amide}}$ ).

**High resolution mass spectrum:** Calculated for  $\text{C}_{33}\text{H}_{54}\text{N}_6\text{NaO}_9$  ( $\text{M}+\text{Na}$ ) $^+$ : 701.3844. Found: 701.3817.

C-Centered triamide **35**:

A mixture containing acyl azide **30** (257 mg, 0.9 mmol) and dodecylamine (580 mg, 3.1 mmol, 3.3 eq) in anhydrous toluene (25 mL) was heated to reflux for 18 hours (reaction progress was monitored by IR following the signals for the acyl azide at  $2136\text{ cm}^{-1}$  and the isocyanate, at  $2260\text{ cm}^{-1}$ ). After elimination of toluene under reduced pressure, the residue was chromatographed on silica gel (hexane-ethyl acetate, 1:2) to afford C-centered triamide **35** (448 mg, 70 % yield) as a white solid.

**Spectroscopic data for compound 35:**

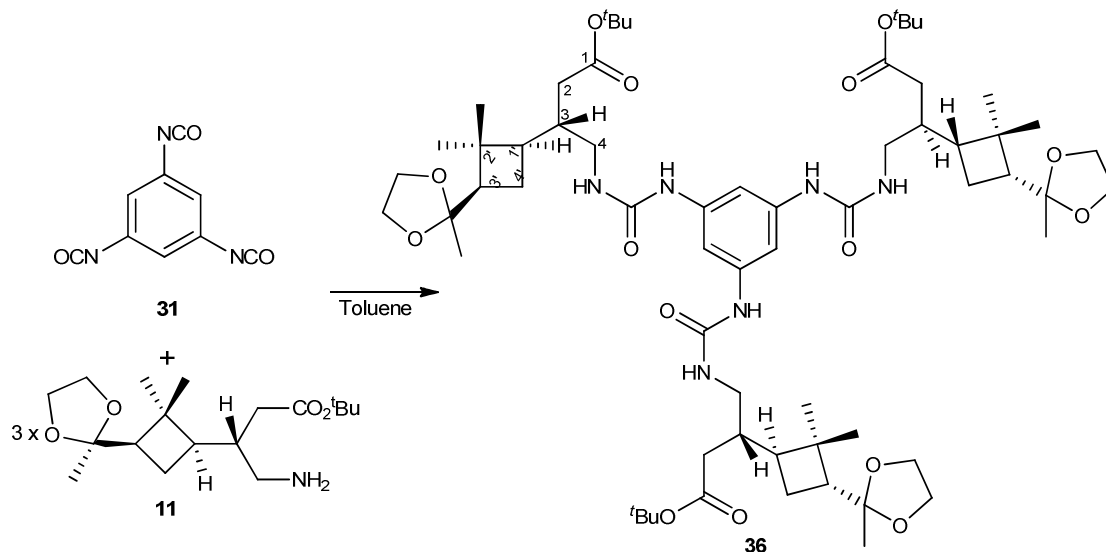
**Melting point:** 158-161 °C (hexane-ethyl acetate)

**IR (ATR):** 3236 (NH<sub>st</sub>), 3071 (=C-H<sub>st</sub>), 2921.2 (CH<sub>st</sub>), 2852 (CH<sub>st</sub>), 1641 (CO<sub>amide</sub>), 1561 (C-C<sub>Ar</sub>), 1465.

**<sup>1</sup>H NMR** (250 MHz, CDCl<sub>3</sub>) δ 1.44 (s, 27H, <sup>t</sup>Bu), 1.67-1.83 (m, 6H, H<sub>2</sub>), 3.13-3.27 (m, 6H, H<sub>3</sub>), 3.4-3.57 (m, 6H, H<sub>1</sub>), 5.27 (bs, 3H, NH<sub>carbamate</sub>) 7.77 (bs, 3H, NH<sub>amide</sub>), 8.14 (s, 3H, H<sub>Ar</sub>).

**<sup>13</sup>C NMR** (62.5 MHz, CDCl<sub>3</sub>) δ 28.9 (C(CH<sub>3</sub>)<sub>3</sub>), 30.2 (C<sub>2</sub>), 37.2 (C<sub>3</sub>), 37.9 (C<sub>1</sub>), 80.0 (C(CH<sub>3</sub>)<sub>3</sub>), 128.6 (C<sub>orto</sub>), 135.8 (C<sub>ipso</sub>), 157.2 (CO<sub>carbamate</sub>), 167.3 (CO<sub>amide</sub>).

**High resolution mass spectrum:** Calculated for C<sub>33</sub>H<sub>54</sub>N<sub>6</sub>NaO<sub>9</sub> (M+Na)<sup>+</sup>: 701.3844. Found: 701.3817.

Triurea **36**:

To an ice cooled solution of **1**, 3,5-trimesic acid (64 mg, 0.3 mmol) in anhydrous acetone (15 mL) were added triethylamine (0.15 mL, 1.2 mmol, 4.0 eq) and ethyl chloroformate (0.11 mL, 1.2 mmol, 4.0 eq). After that was added a solution of  $\text{NaN}_3$  (95 mg, 1.5 mmol, 5.0 eq) in  $\text{H}_2\text{O}$  (10 mL) and the mixture was stirred for 1.5 h at room temperature resulting in the formation of 1,3,5-benzenetricarbonyl triazide **30** as a white precipitate. The reaction crude was diluted with ethyl acetate (40 mL) and washed with a saturated aqueous sodium bicarbonate solution. The organic phase was dried over magnesium sulfate and the solvents were removed under vacuum to afford an acyl azide. (250-MHz,  $^1\text{H-NMR}$  ( $\text{CDCl}_3$ )  $\delta$  8.86 (s, 3H), characteristic signal) WARNING: This product should be carefully manipulated because of its explosive nature.

The resulting acyl azide was dissolved in anhydrous toluene (30 mL) and was gradually heated to reflux and stirred until gas evolution stopped, yielding in situ the corresponding triisocyanate **31**. (250-MHz,  $^1\text{H-NMR}$  ( $\text{CDCl}_3$ )  $\delta$  6.70 (s, 3H), characteristic signal). The solution was allowed to cool to room temperature and amine **11** (320 mg, 1.0 mmol, 3.3 eq) in anhydrous toluene (10 mL) was added. The mixture was stirred for one night at room temperature, after which the solvents were evaporated in vacuo. The resulting crude was purified by column chromatography on neutral silica gel (hexane to ethyl acetate to methanol). The fraction containing the product was redissolved in diethyl ether, filtrated

and the corresponding filtrate was evaporated to afford pure compound **36** (280 mg, 80% yield) as a yellow solid.

**Spectroscopic data for compound 36:**

$[\alpha]_D = -12.7$  (c 0.79, CH<sub>2</sub>Cl<sub>2</sub>).

**Melting point:** Over 350 °C (diethyl ether)

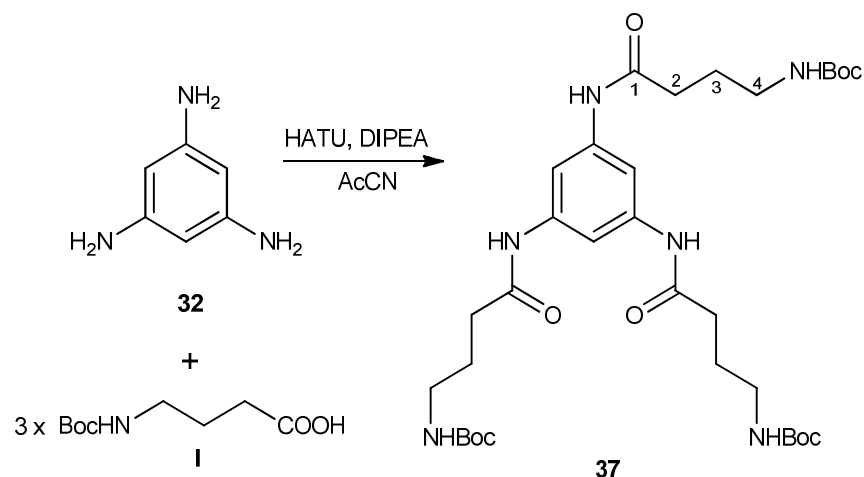
**IR (ATR):** 3347 (NH<sub>st</sub>), 2961 (CH<sub>st</sub>), 2924 (CH<sub>st</sub>), 2853 (CH<sub>st</sub>), 1727 (CO<sub>carbamate</sub>), 1664 (CO<sub>urea</sub>), 1552 (C-C<sub>Ar</sub>), 1457.

**<sup>1</sup>H NMR** (360 MHz, DMSO-*d*<sub>6</sub>) δ 1.00 (s, 9H, *trans*-CH<sub>3</sub>), 1.11 (s, 9H, *cis*-CH<sub>3</sub>), 1.13 (s, 9H, CH<sub>3</sub> ketal), 1.39 (s, 27H, <sup>t</sup>Bu), 1.49-1.60 (c.a., 6H, H<sub>4'a</sub>, H<sub>1'</sub>), 1.76-1.89 (c.a., 6H, H<sub>4'b</sub>, H<sub>3</sub>), 1.91-2.05 (c.a., 6H, H<sub>3'</sub>, H<sub>2a</sub>), 2.06-2.20 (m, 3H, H<sub>2b</sub>), 2.85-2.99 (m, 3H, H<sub>4a</sub>), 3.05-3.19 (m, 3H, H<sub>4b</sub>), 3.68-3.79 (m, 6H, -OCH<sub>2</sub>CH<sub>2</sub>O-), 3.82-3.93 (m, 6H, -OCH<sub>2</sub>CH<sub>2</sub>O-), 5.85 (bs, 3H, NH<sub>monomer</sub>), 7.12 (s, 3H, H<sub>orto</sub>), 8.37 (bs, 3H, NH<sub>Ar</sub>)

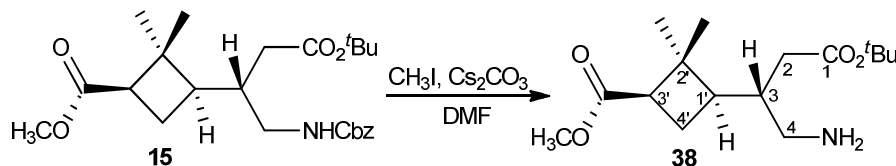
**<sup>13</sup>C NMR** (90 MHz, CDCl<sub>3</sub>) δ 16.8 (*trans*-CH<sub>3</sub>), 23.8 (C<sub>4'</sub>), 28.3 (CH<sub>3</sub> ketal), 29.8 (C(CH<sub>3</sub>)<sub>3</sub>), 31.9 (*cis*-CH<sub>3</sub>), 36.0 (C<sub>3</sub>), 37.2 (C<sub>2'</sub>), 41.0 (C<sub>2</sub>), 44.1 (C<sub>1'</sub>), 49.6 (C<sub>3'</sub>), 52.1 (C<sub>4</sub>), 63.7 (-OCH<sub>2</sub>CH<sub>2</sub>O-), 65.6 (-OCH<sub>2</sub>CH<sub>2</sub>O-), 80.7 (C(CH<sub>3</sub>)<sub>3</sub>), 110.0 (C<sub>ketalic</sub>), 128.7 (C<sub>orto</sub>), 140.4 (C<sub>ipso</sub>), 156.3 (CO<sub>urea</sub>), 173.0 (CO<sub>2</sub><sup>t</sup>Bu).

**High resolution mass spectrum:** Calculated for C<sub>63</sub>H<sub>102</sub>N<sub>15</sub>NaO<sub>6</sub> (M+Na)<sup>+</sup>: 1205.7295.  
Found: 1205.7248.



***N*-Centered triamide **37**:**

Acid **I** (284 mg, 1.4 mmol, 3.5 eq), DIPEA (0.7 mL, 3.9 mmol, 9.5 eq) and HATU (510 mg, 1.4 mmol, 3.5 eq) were dissolved in anhydrous acetonitrile (20 mL), the mixture was stirred for 5 minutes under nitrogen atmosphere, and then a solution of triamine **32** (74 mg, 0.4 mmol) in anhydrous acetonitrile (10 mL) was added via cannula. The mixture was heated to reflux and let to stir for 48 hours. After that, solvent was evaporated and the reaction crude was dissolved into ethyl acetate (40 mL) and washed with a saturated aqueous sodium bicarbonate solution. The organic phase was dried over magnesium sulfate and the solvents were removed under vacuum. The reaction crude was purified by column chromatography on neutral silica gel (hexane to ethyl acetate to methanol) to afford pure *N*-centered triamide **37** (163 mg, 60% yield) as a yellow solid.

**Spectroscopic data for compound 37:****Melting point:** over 290 °C (methanol)**IR (ATR):** 3295 (NH<sub>st</sub>), 3112 (=C-H<sub>st</sub>), 2927 (CH<sub>st</sub>), 2853 (CH<sub>st</sub>), 1621 (CO<sub>amide</sub>), 1539 (C-C<sub>Ar</sub>), 1458.**<sup>1</sup>H NMR** (250 MHz, CDCl<sub>3</sub>) δ 1.43 (s, 27H, <sup>t</sup>Bu), 1.76-1.94 (m, 6H, H<sub>3</sub>), 2.27-2.45 (m, 6H, H<sub>2</sub>), 3.10-3.30 (m, 6H, H<sub>4</sub>), 5.31 (bs, 3H, NH<sub>carbamate</sub>), 7.32 (s, 3H, H<sub>orto</sub>), 8.73 (bs, 3H, NH<sub>amide</sub>).**<sup>13</sup>C NMR** (62.5 MHz, CDCl<sub>3</sub>) δ 25.9 (C<sub>3</sub>), 29.7 (C(CH<sub>3</sub>)<sub>3</sub>), 33.9 (C<sub>2</sub>), 39.8 (C<sub>3</sub>), 79.3 (C(CH<sub>3</sub>)<sub>3</sub>), 108.2 (C<sub>orto</sub>), 138.5 (C<sub>ipso</sub>), 156.6 (CO<sub>carbamate</sub>), 171.9 (CO<sub>amide</sub>).**High resolution mass spectrum:** Calculated for C<sub>33</sub>H<sub>54</sub>N<sub>6</sub>NaO<sub>9</sub> (M+Na): 701.3844. Found: 701.3832.**(1*R*,3*R*)-Methyl 3-((*S*)-1-amino-4-*tert*-butoxy-4-oxobutan-2-yl)-2,2-dimethylcyclobutanecarboxylate, 38:**

Compound **15** (450 mg, 1.0 mmol) in methanol (15 mL) was hydrogenated under 5 atmospheres of pressure in the presence of 10% Pd/C (400 mg, 10% Pd in weight) overnight. The reaction mixture was filtered through Celite<sup>®</sup> and solvent was removed under reduced pressure. The resulting crude was purified by column chromatography on silica gel (hexane to methanol) to provide amine **38** (300 mg, 96% yield) as a colourless oil.

**Spectroscopic data and physical constants for compound 38:**

$[\alpha]_D = -26.0$  ( $c$  0.77,  $\text{CH}_2\text{Cl}_2$ ).

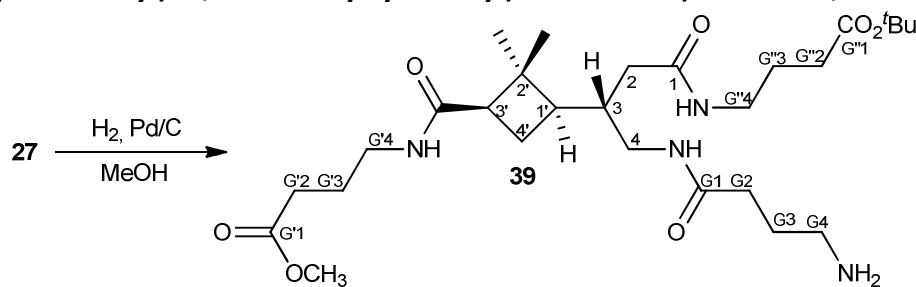
IR (ATR): 3371 ( $\text{NH}_{\text{st}}$ ), 2953 ( $\text{CH}_{\text{st}}$ ), 2926 ( $\text{CH}_{\text{st}}$ ), 1726 and 1677 ( $\text{CO}_{\text{esters}}$ ), 1557, 1445, 1436

$^1\text{H NMR}$  (360 MHz,  $\text{CDCl}_3$ )  $\delta$  0.99 (s, 3H, *trans*- $\text{CH}_3$ ), 1.27 (s, 3H, *cis*- $\text{CH}_3$ ), 1.46 (s, 9H,  $^t\text{Bu}$ ), 1.83-2.05 (c.a., 4H,  $\text{H}_{4'a}$ ,  $\text{H}_{4'b}$ ,  $\text{H}_{1'}$ ,  $\text{H}_3$ ), 2.12-2.21 (m, 1H,  $\text{H}_{2a}$ ), 2.27-2.35 (m, 1H,  $\text{H}_{2b}$ ), 2.60-2.71 (c.a., 2H,  $\text{H}_{3'}$ ,  $\text{H}_{4a}$ ), 2.79-2.90 (m, 1H,  $\text{H}_{4b}$ ), 3.67 (s, 3H,  $\text{CO}_2\text{CH}_3$ ), 5.13 (bs, 2H,  $\text{CH}_2\text{Bn}$ ).

$^{13}\text{C NMR}$  (90 MHz,  $\text{CDCl}_3$ )  $\delta$  17.0 (*trans*- $\text{CH}_3$ ), 23.5 ( $\text{C}_{4'}$ ), 28.1 ( $\text{C}(\text{CH}_3)_3$ ), 30.9 (*cis*- $\text{CH}_3$ ), 36.5 ( $\text{C}_3$ ), 36.9 ( $\text{C}_{2'}$ ), 42.1 ( $\text{C}_2$ ), 42.7 ( $\text{C}_{1'}$ ), 43.6 ( $\text{C}_{3'}$ ), 45.6 ( $\text{C}_4$ ), 51.3 ( $\text{CO}_2\text{CH}_3$ ), 81.0 ( $\text{C}(\text{CH}_3)_3$ ), 172.3 and 172.9 ( $\text{CO}_2^t\text{Bu} + \text{CO}_2\text{CH}_3$ ).

**High resolution mass spectrum:** Calculated for  $\text{C}_{16}\text{H}_{29}\text{NNaO}_4$  ( $\text{M}+\text{Na}$ ) $^+$ : 322.1989. Found: 322.1985.

***tert*-Butyl 4-((*S*)-4-(4-aminobutanamido)-3-((*1'R,3'R*)-3'-(4-methoxy-4-oxobutylcarbamoyl)-2',2'-dimethylcyclobutyl)butanamido)butanoate, 39:**



Compound **27** (800 mg, 1.2 mmol) in methanol (15 mL) was hydrogenated under 5 atmospheres of pressure in the presence of 10% Pd/C (400 mg, 5% in weight of Pd) overnight. The reaction mixture was filtered through Celite<sup>®</sup> and solvent was removed under reduced pressure. The resulting crude was purified by column chromatography on silica gel  $\text{C}_{18}$ -reversed phase (ethyl acetate to methanol) to provide tetrapeptide **39** (500 mg, 78% yield) as a colourless oil.

**Spectroscopic data and physical constants for 39:**

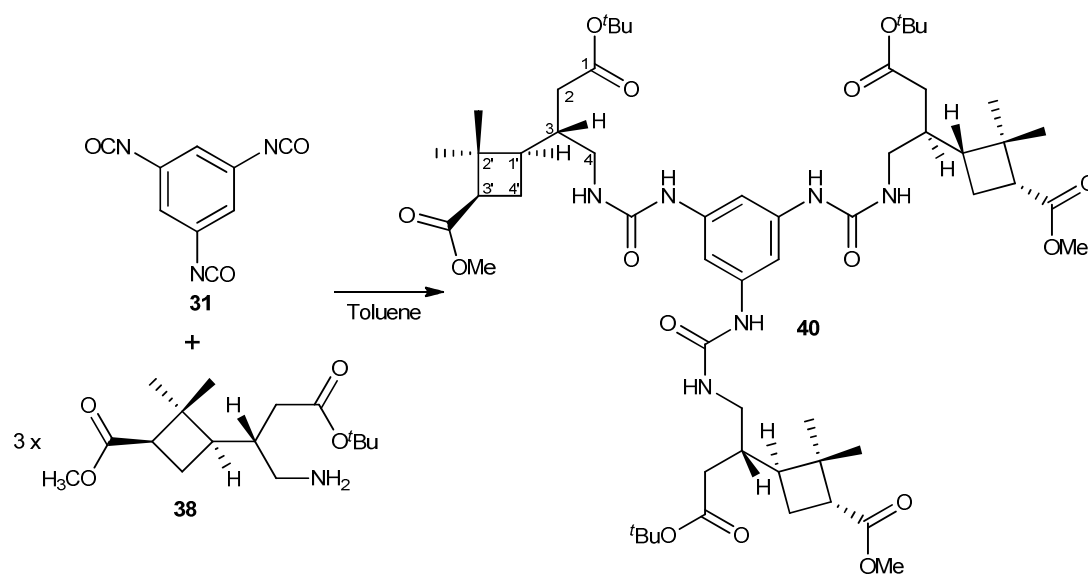
$[\alpha]_D = +17.6$  (c 1.03, CH<sub>2</sub>Cl<sub>2</sub>).

**IR (ATR):** 3303 (NH<sub>st</sub>), 3076 (NH<sub>st</sub>), 2960 (CH<sub>st</sub>), 2925 (CH<sub>st</sub>), 2854 (CH<sub>st</sub>), 1729 and 1648, (bs, CO<sub>esters</sub> + CO<sub>amides</sub>), 1542, 1452

**<sup>1</sup>H NMR** (360 MHz, CDCl<sub>3</sub>) δ 0.97 (s, 3H, *trans*-CH<sub>3</sub>), 1.29 (s, 3H, *cis*-CH<sub>3</sub>), 1.48 (s, 9H, <sup>t</sup>Bu), 1.74-1.94 (c.a., 5H, H<sub>3</sub>, H<sub>G'3</sub>, H<sub>G'3</sub>), 1.96-2.12 (c.a., 3H, H<sub>G3</sub>, H<sub>4'a</sub>), 2.20-2.44 (c.a., 6H, H<sub>4'b</sub>, H<sub>2</sub>, H<sub>1'</sub>, H<sub>G2</sub>), 2.44-2.59 (c.a., 2H, H<sub>G'2</sub>), 2.69-2.87 (m, 2H, H<sub>G4</sub>), 3.04-3.50 (c.a., 9H, H<sub>G'2</sub>, H<sub>3'</sub>, H<sub>4</sub>, H<sub>G'4</sub>, H<sub>G'4</sub>), 3.71 (s, 3H, CO<sub>2</sub>CH<sub>3</sub>).

**<sup>13</sup>C NMR** (100 MHz, CDCl<sub>3</sub>) δ 16.8 (*trans*-CH<sub>3</sub>), 22.0 (C<sub>4'</sub>), 24.8, 26.4, 28.0 (C<sub>G3</sub>, C<sub>G'3</sub>, C<sub>G'3</sub>), 29.6 (C(CH<sub>3</sub>)<sub>3</sub>), 31.3 (*cis*-CH<sub>3</sub>), 31.4, 33.0, 34.3 (C<sub>G2</sub>, C<sub>G'2</sub>, C<sub>G'2</sub>), 37.5 (C<sub>1'</sub>), 38.1 (C<sub>2</sub>), 38.7, 38.9, 42.3 (C<sub>G4</sub>, C<sub>G'4</sub>, C<sub>G'4</sub>), 44.0 (C<sub>4</sub>), 46.3 (C<sub>3</sub>), 46.8 (C<sub>3'</sub>), 49.0 (C<sub>2'</sub>), 51.6 (CO<sub>2</sub>CH<sub>3</sub>), 80.2 (C(CH<sub>3</sub>)<sub>3</sub>), 171.7, 171.8, 172.2, 172.7, 174.0 (CO<sub>amides</sub>, CO<sub>esters</sub>).

**High resolution mass spectrum:** Calculated for C<sub>28</sub>H<sub>51</sub>N<sub>4</sub>NaO<sub>7</sub> (M+Na)<sup>+</sup>: 555.3752. Found: 555.3760.

**Triurea 40:**

To an ice cooled solution of 1,3,5-trimesic acid (70 mg, 0.3 mmol) in anhydrous acetone (15 mL) were added triethylamine (0.16 mL, 1.3 mmol, 4 eq) and ethylchloroformate (0.12 mL, 1.3 mmol, 4 eq). After that was added a solution of sodium azide (105 mg, 1.6 mmol, 5 eq) in water (10 mL) and the mixture was stirred for 1.5 h at room temperature resulting in the formation of 1,3,5-benzenetricarbonyl triazide **30** as a white precipitate. The reaction crude was diluted with ethyl acetate (40 mL) and washed with a saturated aqueous sodium bicarbonate solution. The organic phase was dried over magnesium sulfate and the solvents were removed under vacuum to afford an acyl azide. (250-MHz,  $^1\text{H-NMR}$  ( $\text{CDCl}_3$ )  $\delta$  8.86 (s, 3H), characteristic signal) WARNING: This product should be carefully manipulated because of its explosive nature. The resulting acyl azide was dissolved in anhydrous toluene (30 mL) and was gradually heated to reflux and stirred until gas evolution stopped, yielding *in situ* the corresponding triisocyanate **31**.  $^1\text{H RMN}$   $\delta_{\text{H}}$  (250 MHz,  $\text{CDCl}_3$ ): 6.70 (s, 3H), characteristic signal. The solution was allowed to cool to room temperature and amine **38** (300 mg, 1.00 mmol) in anhydrous toluene (10 mL) was added. The mixture was stirred for one night at room temperature, after which the solvents were evaporated *in vacuo*. The resulting crude was purified by column chromatography on neutral silica gel (hexane to ethyl acetate to methanol). The fraction containing the product was redissolved in diethyl ether, filtrated and the corresponding filtrate was evaporated to afford pure compound **40** (253 mg, 70% yield) as a white solid.

**Spectroscopic data and physical constants for compound 40:**

$[\alpha]_D = -26.7$  ( $c$  0.15,  $\text{CH}_2\text{Cl}_2$ ).

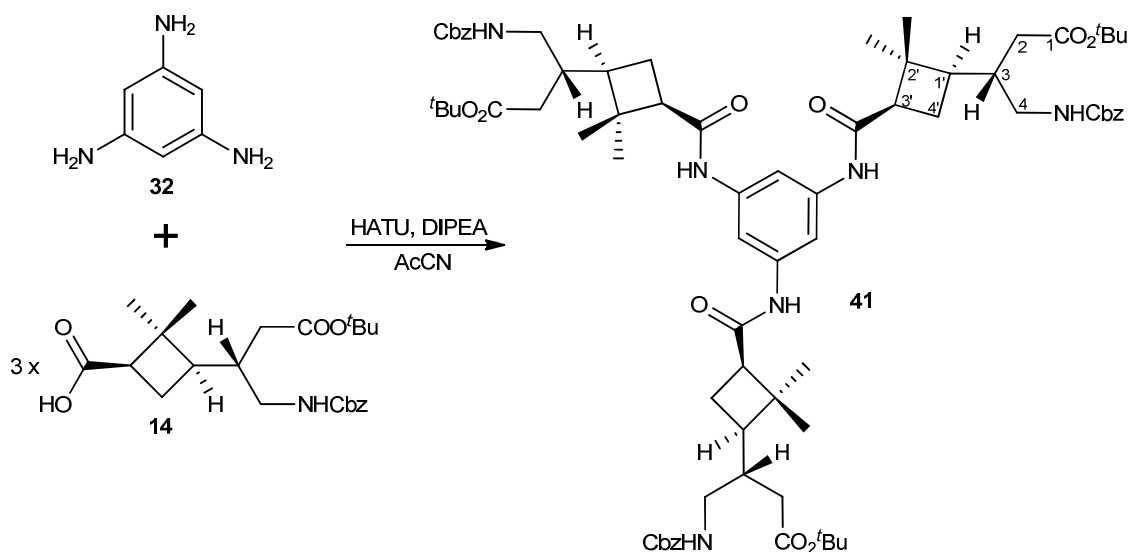
**Melting point:** 61-64 °C (diethyl ether)

**IR (ATR):** 3359 ( $\text{NH}_{\text{st}}$ ), 3194 ( $\text{NH}_{\text{st}}$ ), 2954 ( $\text{CH}_{\text{st}}$ ), 2923 ( $\text{CH}_{\text{st}}$ ), 2853 ( $\text{CH}_{\text{st}}$ ), 1726 and 1660 ( $\text{CO}_{\text{esters}}$ ), 1632 ( $\text{CO}_{\text{urea}}$ ), 1558 ( $\text{C-C}_{\text{Ar}}$ ), 1457.

**$^1\text{H}$  NMR** (400 MHz,  $\text{CDCl}_3$ )  $\delta$  0.90 (s, 9H, *trans*- $\text{CH}_3$ ), 1.25 (s, 9H, *cis*- $\text{CH}_3$ ), 1.45 (s, 27H,  $^t\text{Bu}$ ), 1.89-2.07 (c.a., 6H,  $\text{H}_{4'a}$ ,  $\text{H}_{4'b}$ ), 2.09-2.40 (c.a., 9H,  $\text{H}_{1'}$ ,  $\text{H}_3$ ,  $\text{H}_{2a}$ ), 2.41-2.56 (m, 3H,  $\text{H}_{2b}$ ), 2.58-2.73 (m, 3H,  $\text{H}_{3'}$ ), 2.91-3.21 (c.a., 6H,  $\text{H}_{4a}$ ,  $\text{H}_{4b}$ ), 3.65 (s, 9H,  $\text{CO}_2\text{CH}_3$ ), 7.35 (bs, 3H,  $\text{H}_{\text{orto}}$ ), 8.28-8.50 (c.a., 6H,  $\text{NH}_{\text{urea}}$ ).

**$^{13}\text{C}$  NMR** (100 MHz,  $\text{CDCl}_3$ )  $\delta$  17.0 (*trans*- $\text{CH}_3$ ), 23.4 ( $\text{C}_{4'}$ ), 28.0 ( $\text{C}(\text{CH}_3)_3$ ), 30.7 (*cis*- $\text{CH}_3$ ), 34.8 ( $\text{C}_3$ ), 36.2 ( $\text{C}_{2'}$ ), 41.0 ( $\text{C}_2$ ), 42.6 ( $\text{C}_{1'}$ ), 42.9 ( $\text{C}_{3'}$ ), 45.2 ( $\text{C}_4$ ), 51.2 ( $\text{CO}_2\text{CH}_3$ ), 81.9 ( $\text{C}(\text{CH}_3)_3$ ), 126.8, 128.0, 128.4, 129.0, 129.4, and 130.3 (6C,  $\text{C}_{\text{Ar}}$ ), 172.1, 172.2 and 172.7 ( $\text{CO}_2^t\text{Bu}$  +  $\text{CO}_2\text{CH}_3$  +  $\text{CO}_{\text{urea}}$ ).

**High resolution mass spectrum:** Calculated for  $\text{C}_{57}\text{H}_{90}\text{N}_6\text{NaO}_{15}$  ( $\text{M}+\text{Na}$ ) $^+$ : 1121.6356. Found: 1121.6384.

**N-Centered triamide 41:**

Acid **14** (570 mg, 1.4 mmol, 3.5 eq), DIPEA (0.7 mL, 3.9 mmol, 9.8 eq) and HATU (510 mg, 1.4 mmol, 3.5 eq) were dissolved in anhydrous acetonitrile (40 mL), the mixture was stirred for 5 minutes under nitrogen atmosphere, and then a solution of 1,3,5-triaminobenzene **32** (74 mg, 0.4 mmol) in anhydrous acetonitrile (10 mL) was added via cannula. The mixture was heated to reflux and let to stir for 48 hours. After that, solvent was evaporated and the reaction crude was dissolved into ethyl acetate (40 mL) and washed with a saturated aqueous sodium bicarbonate solution. The organic phase was dried over magnesium sulfate and the solvents were removed under vacuum. The reaction crude was purified by column chromatography on neutral silica gel (hexane to ethyl acetate to methanol) to afford pure *N*-centered triamide **41** (150 mg, 28% yield) as a yellow solid.

**Spectroscopic data and physical constants for compound 41:**

$[\alpha]_D = -66.7$  (c 0.18, CH<sub>2</sub>Cl<sub>2</sub>).

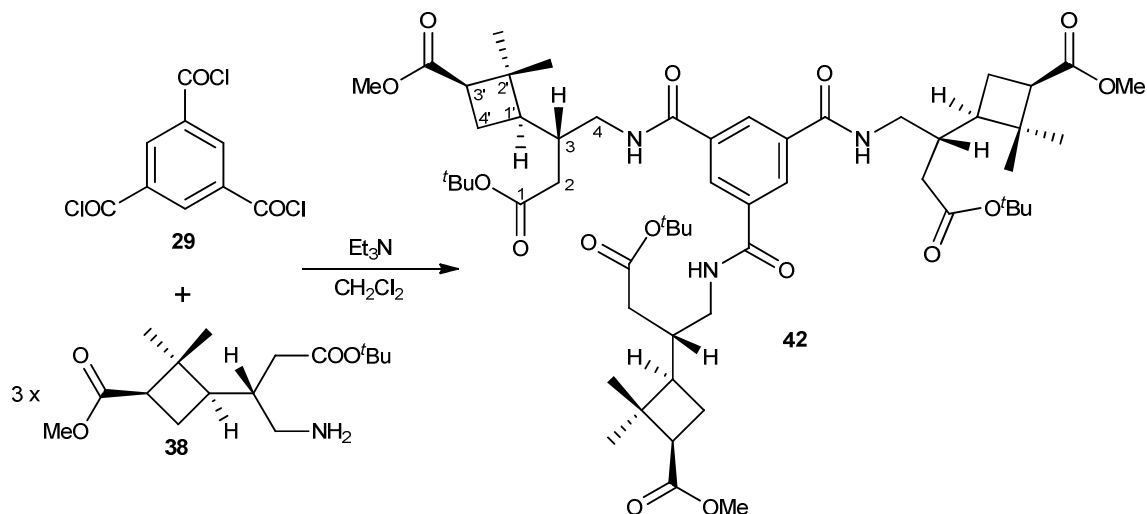
**Melting point:** over 290 °C (methanol)

**IR** (ATR): 3733 (NH<sub>st</sub>), 3628 (NH<sub>st</sub>), 3326 (NH<sub>st</sub>), 2925 (CH<sub>st</sub>), 2855 (CH<sub>st</sub>), 1707 (bs, CO<sub>carbamate</sub> + CO<sub>ester</sub>), 1617 (CO<sub>amide</sub>), 1541 (C-C<sub>Ar</sub>), 1456.

**<sup>1</sup>H NMR** (360 MHz, CDCl<sub>3</sub>) δ 1.00 (s, 9H, *trans*-CH<sub>3</sub>), 1.28 (s, 9H, *cis*-CH<sub>3</sub>), 1.44 (s, 27H, <sup>t</sup>Bu), 1.67-1.87 (m, 3H, H<sub>4'a</sub>), 1.90-2.15 (c.a., 12H, H<sub>4'b</sub>, H<sub>1'</sub>, H<sub>3</sub>, H<sub>2a</sub>), 2.14-2.41 (m, 3H, H<sub>2b</sub>), 2.46-2.67 (m, 3H, H<sub>3'</sub>), 2.94-3.17 (m, 3H, H<sub>4a</sub>), 3.19-3.40 (m, 3H, H<sub>4b</sub>), 5.00-5.44 (c.a., 9H, CH<sub>2</sub>Bn, NH<sub>carbamate</sub>), 6.79 (bs, 3H, NH<sub>amide</sub>), 7.17-7.50 (c.a., 18H, H<sub>Ar</sub>).

**<sup>13</sup>C NMR** (90 MHz, CDCl<sub>3</sub>) δ 16.9 (*trans*-CH<sub>3</sub>), 23.7 (C<sub>4'</sub>), 28.2 (C(CH<sub>3</sub>)<sub>3</sub>), 29.7 (*cis*-CH<sub>3</sub>), 31.1 (C<sub>3</sub>), 37.1 (C<sub>2'</sub>), 42.3 (C<sub>2</sub>), 43.2 (C<sub>1'</sub>), 43.9 (C<sub>3'</sub>), 48.1 (C<sub>4</sub>), 66.6 (CH<sub>2</sub>Bn), 81.1 (C(CH<sub>3</sub>)<sub>3</sub>), 102.7, 128.0, 128.5, 136.7 and 139.1 (18C, C<sub>Ar</sub>), 156.6 (CO<sub>carbamate</sub>), 170.3 and 172.3 (CO<sub>2</sub><sup>t</sup>Bu + CO<sub>amide</sub>).

**High resolution mass spectrum:** Calculated for C<sub>75</sub>H<sub>102</sub>N<sub>6</sub>NaO<sub>15</sub> (M+Na)<sup>+</sup>: 1349.7295. Found: 1349.7310.

C-Centered triamide **42**:

To an ice cooled solution of compound **38** (240 mg, 0.8 mmol, 3.1 eq) and triethylamine (0.1 mL, 0.8 mmol, 3.1 eq) in anhydrous dichloromethane (20 mL) was added a solution of 1,3,5-benzenetricarbonyl trichloride (0.04 mL, 0.3 mmol) in anhydrous dichloromethane (5 mL). The solution was slowly brought to room temperature and stirred for 21 hours. The reaction mixture was diluted with ethyl acetate (20 mL) and the solution was washed with 5% aqueous citric acid (3 x 20 mL), saturated aqueous sodium bicarbonate solution (3 x 20 mL) and brine (3 x 20 mL). The organic layer was dried over magnesium sulfate and the solvent was evaporated *in vacuo*. The resulting crude was dissolved in diethyl ether, filtered through a sintered funnel and the filtrate was evaporated to afford pure C-centered triamide **42** (159 mg, 58% yield) as a yellow oil.



**Spectroscopic data and physical constants for compound 42:**

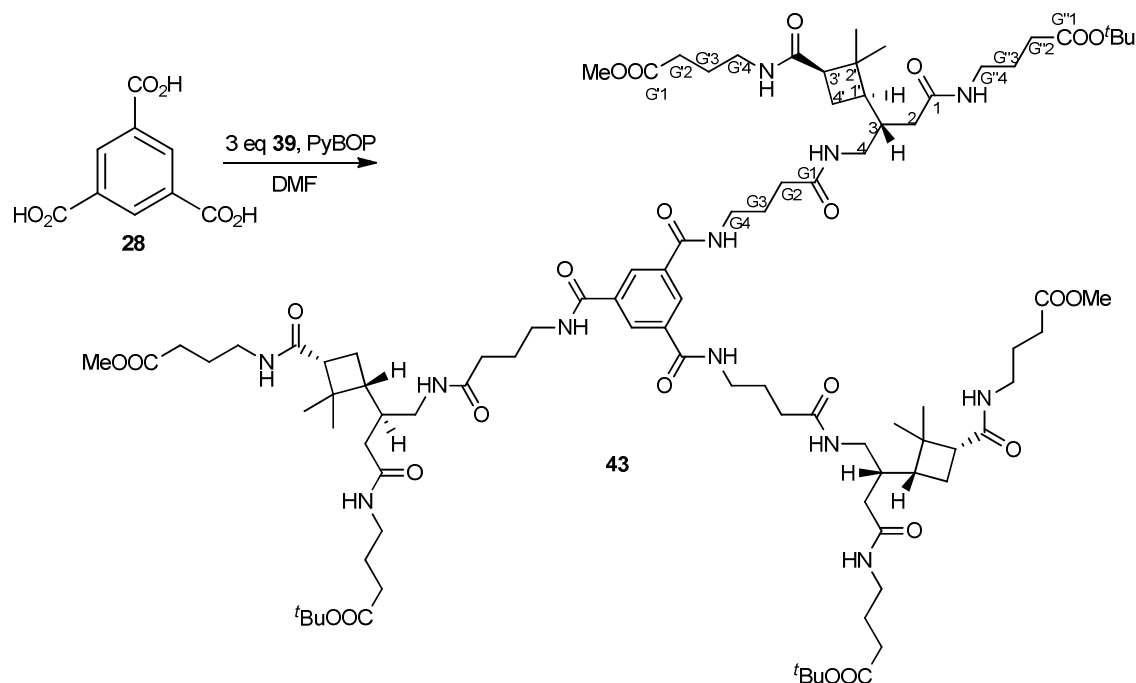
$[\alpha]_D = +40.0$  ( $c$  0.35,  $\text{CH}_2\text{Cl}_2$ ).

**IR** (ATR): 3734 ( $\text{NH}_{\text{st}}$ ), 3627 ( $\text{NH}_{\text{st}}$ ), 3299 ( $\text{NH}_{\text{st}}$ ), 2953 ( $\text{CH}_{\text{st}}$ ), 2925 ( $\text{CH}_{\text{st}}$ ), 2854 ( $\text{CH}_{\text{st}}$ ), 1731 (bs,  $\text{CO}_{\text{carbamate}}$  +  $\text{CO}_{\text{ester}}$ ), 1656 ( $\text{CO}_{\text{amide}}$ ), 1581, 1547, 1457, 1436.

**$^1\text{H}$  NMR** (250 MHz,  $\text{DMSO-}d_6$ )  $\delta$  0.98 (s, 9H, *trans-CH*<sub>3</sub>), 1.26 (s, 9H, *cis-CH*<sub>3</sub>), 1.43 (s, 27H, <sup>t</sup>Bu), 1.84-2.38 (c.a., 18H,  $\text{H}_{4'a}$ ,  $\text{H}_{4'b}$ ,  $\text{H}_{1'}$ ,  $\text{H}_3$ ,  $\text{H}_{2a}$ ,  $\text{H}_{2b}$ ), 2.55-2.72 (m, 3H,  $\text{H}_{3'}$ ), 3.25-3.42 (m, 3H,  $\text{H}_{4a}$ ), 3.43-3.58 (m, 3H,  $\text{H}_{4b}$ ), 3.66 (s, 9H,  $\text{CO}_2\text{CH}_3$ ), 6.63 (bs, 3H,  $\text{NH}_{\text{amide}}$ ), 7.33 (s, 3H, *Horto*).

**$^{13}\text{C}$  NMR** (90 MHz,  $\text{CDCl}_3$ )  $\delta$  17.6 (*trans-CH*<sub>3</sub>), 24.2 ( $\text{C}_{4'}$ ), 28.4 ( $\text{C}(\text{CH}_3)_3$ ), 31.3 (*cis-CH*<sub>3</sub>), 37.1 ( $\text{C}_3$ ), 37.3 ( $\text{C}_{2'}$ ), 41.4 ( $\text{C}_2$ ), 43.1 ( $\text{C}_{1'}$ ), 44.4 ( $\text{C}_{3'}$ ), 45.9 ( $\text{C}_4$ ), 51.6 ( $\text{CO}_2\text{CH}_3$ ), 81.7 ( $\text{C}(\text{CH}_3)_3$ ), 128.6, 135.4 ( $\text{C}_6$ ,  $\text{C}_{\text{Ar}}$ ), 164.2, 172.8 and 173.2 ( $\text{CO}_2^{\text{t}}\text{Bu}$  +  $\text{CO}_2\text{CH}_3$  +  $\text{CO}_{\text{amide}}$ ).

**High resolution mass spectrum:** Calculated for  $\text{C}_{53}\text{H}_{80}\text{N}_3\text{O}_{15}$  ( $\text{M}^{\text{t}}\text{Bu}+2\text{H}$ )<sup>+</sup>: 998.5589. Found: 998.5466; Calculated for  $\text{C}_{53}\text{H}_{79}\text{N}_3\text{NaO}_{15}$  ( $\text{M}^{\text{t}}\text{Bu}+\text{H}+\text{Na}$ )<sup>+</sup>: 1020.5409. Found: 1020.5286; Calculated for  $\text{C}_{49}\text{H}_{72}\text{N}_3\text{O}_{15}$  ( $\text{M}-2^{\text{t}}\text{Bu}+3\text{H}$ )<sup>+</sup>: 942.4963. Found: 942.4875; Calculated for  $\text{C}_{49}\text{H}_{71}\text{N}_3\text{NaO}_{15}$  ( $\text{M}-2^{\text{t}}\text{Bu}+2\text{H}+\text{Na}$ )<sup>+</sup>: 964.4783. Found: 964.4725; Calculated for  $\text{C}_{45}\text{H}_{64}\text{N}_3\text{O}_{15}$  ( $\text{M}-3^{\text{t}}\text{Bu}+4\text{H}$ )<sup>+</sup>: 886.4337. Found: 886.4209; Calculated for  $\text{C}_{45}\text{H}_{63}\text{N}_3\text{NaO}_{15}$  ( $\text{M}-3^{\text{t}}\text{Bu}+3\text{H}+\text{Na}$ )<sup>+</sup>: 908.4157. Found: 908.3955.

C-Centered triamide **43**:

1,3,5-Trimesic acid **28** (25 mg, 0.1 mmol), DIPEA (0.18 mL, 1.1 mmol, 10 eq) and PyBOP (280 mg, 0.5 mmol, 5 eq) were dissolved in anhydrous dimethylformamide (30 mL), the mixture was stirred for 2 hours under nitrogen atmosphere, and then a solution of amine **39** (200 mg, 0.4 mmol, 4 eq) in anhydrous dimethylformamide (5 mL) was added via cannula. After stirring at room temperature for 2 hours the reaction crude was diluted with ethyl acetate (20 mL) and washed with a saturated aqueous sodium bicarbonate solution. The organic phase was dried over magnesium sulfate and the solvents were removed under vacuum. The reaction crude was purified by subsequent liquid-solid extractions (diethyl ether and methanol) to afford pure triamide **43** (160 mg, 75% yield) as a white solid.

Spectroscopic data and physical constants for compound **43**:

$[\alpha]_D^{25} = +48.3$  (*c* 0.29, CH<sub>2</sub>Cl<sub>2</sub>).

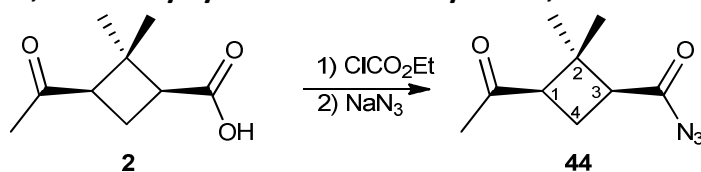
**IR** (ATR): 3736 (NH<sub>st</sub>), 3630 (NH<sub>st</sub>), 3361 (NH<sub>st</sub>), 2926 (CH<sub>st</sub>), 2855 (CH<sub>st</sub>), 1723, 1719, 1655 and 1651 (bs, CO<sub>carbamate</sub> + CO<sub>esters</sub> + CO<sub>amides</sub>), 1548, 1543, 1459.

**<sup>1</sup>H NMR** (400 MHz, DMSO-*d*<sub>6</sub>)  $\delta$  0.82 (s, 9H, *trans*-CH<sub>3</sub>), 1.14 (s, 9H, *cis*-CH<sub>3</sub>), 1.38 (s, 27H, <sup>*t*</sup>Bu), 1.54-2.03 (c.a., 33H, H<sub>3</sub>, H<sub>G'3</sub>, H<sub>G'3</sub>, H<sub>G3</sub>, H<sub>4'</sub>, H<sub>2</sub>), 2.14-2.21 (c.a., 9H, H<sub>1'</sub>, H<sub>G2</sub>) 2.24-2.32 (c.a., 15H, H<sub>G'2</sub>, H<sub>G'2</sub>, H<sub>3'</sub>), 2.90-3.12 (c.a., 24H, H<sub>4a</sub>, H<sub>G4</sub>, H<sub>G'4</sub>, H<sub>G'4</sub>, H<sub>4b</sub>), 3.58 (s, 9H, CO<sub>2</sub>CH<sub>3</sub>), 7.47 (s, 3H, H<sub>orto</sub>), 7.62-7.76 (c.a., 6H, NH<sub>amide</sub>), 7.80-7.90 (c.a., 6H, NH<sub>amide</sub>).

**<sup>13</sup>C NMR** (100 MHz, CDCl<sub>3</sub>)  $\delta$  16.8 (*trans*-CH<sub>3</sub>), 23.5 (C<sub>4'</sub>), 24.9, 26.3, 26.4 (C<sub>G3</sub>, C<sub>G'3</sub>, C<sub>G'3</sub>), 28.0 (C(CH<sub>3</sub>)<sub>3</sub>), 31.6 (*cis*-CH<sub>3</sub>), 31.5, 33.0, 33.7 (C<sub>G2</sub>, C<sub>G'2</sub>, C<sub>G'2</sub>), 37.5 (C<sub>1'</sub>), 38.0 (C<sub>2</sub>), 38.6, 39.0, 40.2 (C<sub>G4</sub>, C<sub>G'4</sub>, C<sub>G'4</sub>), 42.3 (C<sub>4</sub>), 44.1 (C<sub>3</sub>), 46.2 (C<sub>3'</sub>), 47.0 (C<sub>2'</sub>), 51.8 (CO<sub>2</sub>CH<sub>3</sub>), 80.6 (C(CH<sub>3</sub>)<sub>3</sub>), 128.5, 135.3 (6C, C<sub>Ar</sub>), 169.9, 171.7, 172.3, 172.8, 173.9, 174.1 (CO<sub>amides</sub>, CO<sub>esters</sub>).

**High resolution mass spectrum:** Calculated for C<sub>93</sub>H<sub>150</sub>N<sub>12</sub>O<sub>24</sub> (M+Na)<sup>+</sup>: 1843.0810. Found: 1843.0853.

**(1*S*,3*R*)-3-Acetyl-2,2-dimethylcyclobutanecarbonyl azide, **44**:**



To an ice-cooled solution of (-)-*cis*-pinonic acid **2**, (300 mg, 1.8 mmol) in anhydrous acetone (10 mL), triethylamine (0.75 mL, 5.3 mmol, 3 eq) and ethyl chloroformate (0.26 mL, 2.5 mmol, 1.5 eq) were subsequently added and the mixture was stirred at 0 °C for 30 minutes under nitrogen atmosphere. Then, sodium azide (191 mg, 3.0 mmol, 1.7 eq) in 7 mL of water was added and the resultant solution was stirred at room temperature for 1.5 h. The reaction mixture was extracted with dichloromethane (4 x 15 mL), and the organic

extracts were dried over magnesium sulfate. Solvents were removed under reduced pressure to give acyl azide **44** as a colourless oil (310 mg, 90% yield), which was characterised by its spectroscopic data and used in the next step without further purification.

**Spectroscopic data for compound 44:**

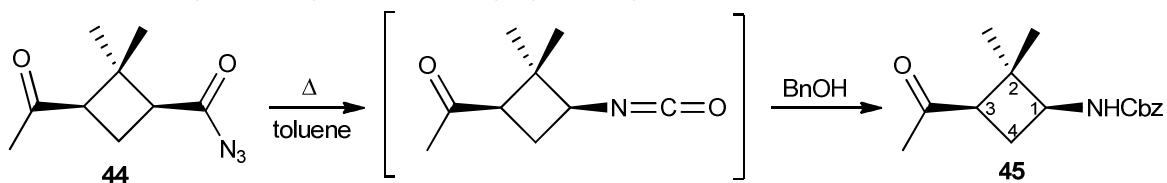
$^1\text{H NMR}$  (250 MHz, acetone- $d_6$ )  $\delta$  0.92 (s, 3H, *trans*- $\text{CH}_3$ ), 1.47 (s, 3H, *cis*- $\text{CH}_3$ ), 2.05 (s, 3H,  $\text{CH}_3\text{CO}$ ), 2.57 (dd,  $J_{\text{H,H}} = 20.5$  Hz,  $J_{\text{H,H}} = 8.75$  Hz, 1H,  $\text{H}_{4a}$ ), 2.79-2.98 (c.a., 2H,  $\text{H}_3$ ,  $\text{H}_{4b}$ ), 3.10 (dd,  $J_{\text{H,H}} = 11.25$  Hz,  $J_{\text{H,H}} = 8$  Hz, 1H,  $\text{H}_1$ ).

$^{13}\text{C NMR}$  (62.5 MHz, acetone- $d_6$ )  $\delta$  16.2 (*trans*- $\text{CH}_3$ ), 27.4 ( $\text{C}_4$ ), 27.9 ( $\text{CH}_3\text{CO}$ ), 30.3 (*cis*- $\text{CH}_3$ ), 45.5 ( $\text{C}_2$ ), 46.7 ( $\text{C}_3$ ), 53.8 ( $\text{C}_1$ ), 179.1 ( $\text{CON}_3$ ).

Spectroscopic data are consistent with those reported in reference:

Aguilera, J.; Moglioni, A. G.; Moltrasio, G. Y.; Ortuño, R. M. *Tetrahedron: Asymmetry* **2008**, *19*, 302-308.

**(1*S*,3*R*)- Benzyl-3-acetyl-2,2-dimethylcyclobutylcarbamate, 45:**



A solution of **44** (310 mg, 1.6 mmol) and benzyl alcohol (0.4 mL, 3.3 mmol) in toluene (9 mL) was heated to reflux for 3.5 hours (the reaction progress was monitored by IR following the signals for the acyl azide at  $2136\text{ cm}^{-1}$  and the isocyanate at  $2260\text{ cm}^{-1}$ ). Toluene was removed under reduced pressure and then the excess of benzyl alcohol was eliminated by vacuum distillation. The residue was chromatographed on silica gel (ethyl acetate-hexane, 1:1 to 2:1) to afford carbamate **45** as a white solid (402 mg, 92% yield).

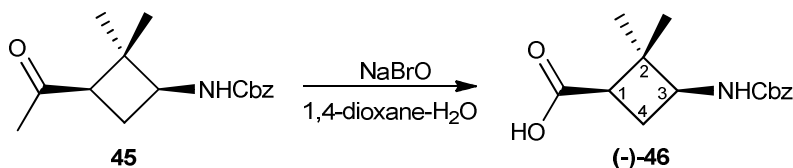
**Spectroscopic data and physical constants for compound 45:**

$^1\text{H NMR}$  (250 MHz,  $\text{CDCl}_3$ ): 0.84 (s, 3H, *trans*- $\text{CH}_3$ ), 1.41 (s, 3H, *cis*- $\text{CH}_3$ ), 2.08 (s, 3H,  $\text{CH}_3\text{CO}$ ), 2.10 (m, 2H,  $2\text{H}_4$ ), 2.75 (dd,  $J_{\text{H,H}} = 4.25$  Hz,  $J_{\text{H,H}} = 6.5$  Hz, 1H,  $\text{H}_3$ ), 3.93 (dd, 1H,  $\text{H}_1$ ), 4.82 (broad singlet, 1H, NH), 5.10 (dd,  $J_{\text{H,H}} = 6.5$  Hz,  $J_{\text{H,H}} = 11$  Hz, 2H,  $\text{CH}_2\text{Bn}$ ), 7.38 (c.a., 5H,  $\text{H}_{\text{Ar}}$ ).

$^{13}\text{C NMR}$  (62.5 MHz,  $\text{CDCl}_3$ )  $\delta$  16.4 (*trans*- $\text{CH}_3$ ), 24.8 ( $\text{C}_4$ ), 28.9 (*cis*- $\text{CH}_3$ ), 30.3 ( $\text{CH}_3\text{CO}$ ), 46.49 ( $\text{C}_2$ ), 50.7 ( $\text{C}_3$ ), 51.3 ( $\text{C}_1$ ), 66.8 ( $\text{CH}_2\text{Bn}$ ), 128.1, 128.2, 128.5 and 136.3 ( $\text{C}_{\text{Ar}}$ ), 155.9 ( $\text{CO}_{\text{carbamate}}$ ), 206.8 ( $\text{CH}_3\text{CO}$ ).

Spectroscopic data are consistent with those reported in reference:

Aguilera, J.; Moglioni, A. G.; Moltrasio, G. Y.; Ortuño, R. M. *Tetrahedron: Asymmetry* **2008**, *19*, 302-308.

**(1*R*,3*S*)-3-(Benzyloxycarbonylamino)-2,2-dimethylcyclobutanecarboxylic acid, (-)-  
46:**

To an ice cooled solution of ketone **45** (1.20 g, 4.5 mmol) in dioxane-water (7:2, 36 mL) was added a sodium hypobromite solution, prepared from bromine (0.82 mL, 16.2 mmol, 3.6 eq) and sodium hydroxide (1.25 g, 31.5 mmol, 7.0 eq) in a 3:1 mixture of water-dioxane (60 mL). The resulting mixture was stirred for 5 hours at -5 °C. Then, the reaction mixture was washed with dichloromethane (2x50 mL), treated with sodium sulfite and, finally, 5% HCl was added to reach pH 2-3. The acid solution was extracted with dichloromethane (4 x 50 mL) and the organic extracts were dried over magnesium sulfate. Solvent was removed to afford acid **(-)-46** as a white solid (1.1 g, 88% yield) which was identified by its  $^1\text{H NMR}$  spectrum and used in the next step without further purification.

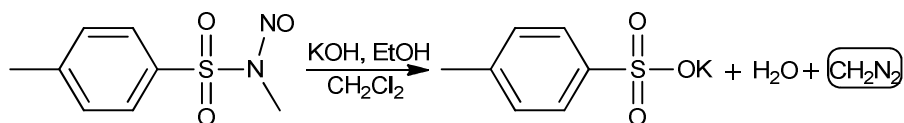
**Spectroscopic data for compound (-)-46:**

$^1\text{H NMR}$  (250 MHz,  $\text{CDCl}_3$ )  $\delta$  0.99 (s, 3H, *trans*- $\text{CH}_3$ ), 1.35 (s, 3H, *cis*- $\text{CH}_3$ ), 2.06 (s, 1H,  $\text{H}_{4a}$ ), 2.33 (m, 1H,  $\text{H}_{4b}$ ), 2.58 (m, 1H,  $\text{H}_1$ ), 3.94 (m, 1H,  $\text{H}_3$ ), 5.11 (c.a., 3H, NH,  $\text{CH}_2\text{Bn}$ ), 7.37 (c.a., 5H,  $\text{H}_{Ar}$ ), 10.15 (broad singlet, 1H, COOH).

$^{13}\text{C NMR}$  (62.5 MHz,  $\text{CDCl}_3$ )  $\delta$  17.2 (*trans*- $\text{CH}_3$ ), 26.8 ( $\text{C}_4$ ), 29.2 (*cis*- $\text{CH}_3$ ), 43.2 ( $\text{C}_2$ ), 46.8 ( $\text{C}_3$ ), 51.8 ( $\text{C}_1$ ), 67.3 ( $\text{CH}_2\text{Bn}$ ), 128.5, 128.2, 128.6 and 128.9 ( $\text{C}_{Ar}$ ), 156.5 ( $\text{CO}_{\text{carbamate}}$ ), 178.1 ( $\text{CO}_2\text{H}$ ).

Spectroscopic data are consistent with those reported in reference:

Aguilera, J.; Moglioni, A. G.; Moltrasio, G. Y.; Ortuño, R. M. *Tetrahedron: Asymmetry* **2008**, *19*, 302-308.

**Diazomethane distillation from Diazald®.**

Diazomethane reacts instantaneously with carboxylic acids to yield methyl esters quantitatively. However, it must be prepared from a precursor and care must be taken when handling this very reactive reagent:

- Diazomethane is a yellow gas at room temperature, liquifies at  $-23\text{ }^\circ\text{C}$ , and freezes at  $-145\text{ }^\circ\text{C}$ . It is extremely toxic.

- All edges of glassware used for diazomethane should be carefully firepolished and ground-glass joints cannot be employed. Care should be taken in cleaning the glassware used for diazomethane to avoid scratching the surfaces. Contact of diazomethane with alkali metals or anhydrous agents such as calcium sulfate can result in an explosion. The recommended desiccating agent for diazomethane is potassium hydroxide pellets.

· All diazomethane reactions should be performed in an efficient fume hood and behind a sturdy safety shield. Reactions of diazomethane are best performed at room temperature or below.

· Solutions of diazomethane should not be frozen because the rough edges of crystals could cause it to explode.

Procedure:

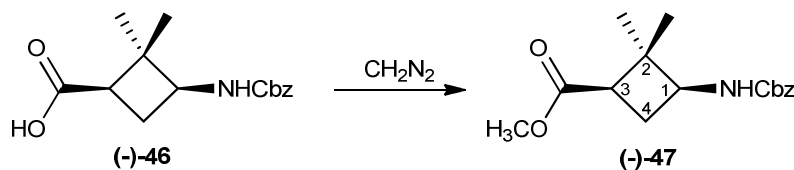
To a mixture containing Diazald® (5 g, 23 mmol) in dichloromethane (60 mL), a mixture of KOH in EtOH 96% (0.8 g in 70 mL) is added. The system is stirred for 10 minutes at room temperature before it is heated to 50 °C to promote the  $\text{CH}_2\text{N}_2$  distillation (as a yellow gas) over the reactant to be methylated. When the distillation is finished, the heating is turned off and the system is allowed to reach room temperature. Then the distillation apparatus is removed.

Silica gel is added slowly and carefully to the solution that initially contained the diazald to eliminate the diazomethane excess.

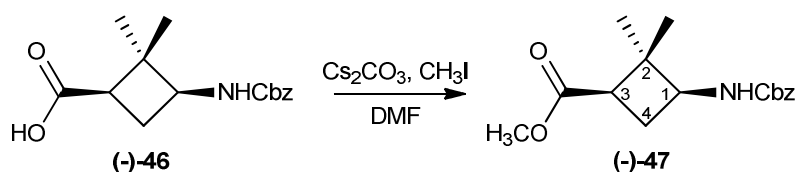
The excess of diazomethane in the flask that contains the methylated product is carefully removed using a gentle nitrogen flow.

**(1R,3S)-Methyl-3-(benzyloxycarbonylamino)-2,2-dimethylcyclobutanecarboxylate, (-)-47:**

Method 1:



Acid **(-)-46** (400 mg, 1.4 mmol) was methylated by the action of an excess of diazomethane (0.91 g of Diazald®, 4.2 mmol, 3 eq) in a dichloromethane solution to provide quantitatively the orthogonally protected amino acid **(-)-47** (420 mg).

Method 2:

A mixture containing acid **(-)-46** (2.00 g, 7.2 mmol), cesium carbonate (2.80 g, 8.6 mmol, 1.2 eq) and 0.5 mL of methyl iodide (8.6 mmol, 1.2 eq) in anhydrous DMF (40 mL) was stirred at room temperature for 18 h. Then, ethyl acetate (30 mL) was added and the resultant solution was washed with a saturated aqueous solution of sodium bicarbonate (4x25 mL). The organic liquors were dried over magnesium sulfate and solvent was evaporated under vacuum to provide methyl ester **(-)-47** (1.81 g, 86% yield).

**Spectroscopic data for compound (-)-47:**

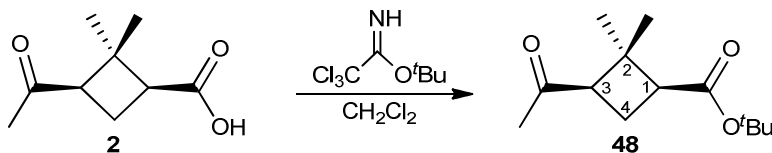
**<sup>1</sup>H NMR** (250 MHz, CDCl<sub>3</sub>) δ 0.90 (s, 3H, *trans*-CH<sub>3</sub>), 1.29 (s, 3H, *cis*-CH<sub>3</sub>), 2.05 (dd, *J*<sub>H,H</sub> = 21 Hz, *J*<sub>H,H</sub> = 9.75 Hz, 1H, H<sub>4a</sub>), 2.36 (m, 1H, H<sub>4b</sub>), 2.57 (dd, *J*<sub>H,H</sub> = 9.75 Hz, *J*<sub>H,H</sub> = 7 Hz, 1H, H<sub>3</sub>), 3.67 (s, 3H, COOCH<sub>3</sub>), 3.92 (dd, *J*<sub>H,H</sub> = 17.25 Hz, *J*<sub>H,H</sub> = 8 Hz, 1H, H<sub>1</sub>), 4.91 (d, *J*<sub>H,H</sub> = 11.75 Hz, 1H, NH), 5.05 (d, *J*<sub>H,H</sub> = 19 Hz, 1H, CH<sub>2</sub>Bn), 5.12 (d, *J*<sub>H,H</sub> = 20.25 Hz, 1H, CH<sub>2</sub>Bn), 7.36 (c.a., 5H, H<sub>Ar</sub>).

**<sup>13</sup>C NMR** (62.5 MHz, CDCl<sub>3</sub>) δ 16.7 (*trans*-CH<sub>3</sub>), 26.4 (C<sub>4</sub>), 28.5 (*cis*-CH<sub>3</sub>), 42.6 (C<sub>3</sub>), 45.8 (C<sub>2</sub>), 51.3 (COOCH<sub>3</sub>) 76.9 (C<sub>1</sub>), 66.6 (CH<sub>2</sub>Bn), 127.9, 128.5 and 136.0 (C<sub>Ar</sub>), 155.7 (CO<sub>carbamate</sub>), 172.6 (CO<sub>2</sub>CH<sub>3</sub>).

Spectroscopic data are consistent with those reported in reference:

Aguilera, J.; Moglioni, A. G.; Moltrasio, G. Y.; Ortuño, R. M. *Tetrahedron: Asymmetry* **2008**, *19*, 302-308.



**(1S,3R)-tert-Butyl-3-acetyl-2,2-dimethylcyclobutane-1-carboxylate, 48:**

*tert*-Butyl 2,2,2-trichloroacetimidate (8.5 mL, 48.0 mmol, 2 eq) was added to a solution of acid **2** (4 g, 23.5 mmol) in dichloromethane (120 mL) under nitrogen atmosphere and the mixture was stirred overnight. The mixture was evaporated to dryness under reduced pressure. The reaction crude was purified by column chromatography on neutral silica gel (1:3 ethyl acetate-hexane) to afford pure **48** (3.1 g, 86% yield).

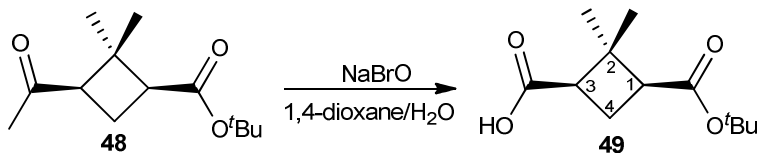
**Spectroscopic data for compound 48:**

$^1\text{H NMR}$  (250 MHz,  $\text{CDCl}_3$ )  $\delta$  0.90 (s, 3H, *trans*- $\text{CH}_3$ ), 1.39 (s, 3H, *cis*- $\text{CH}_3$ ), 1.42 (s, 9H,  $\text{C}(\text{CH}_3)_3$ ), 1.65-2.01 (m, 1H,  $\text{H}_{4a}$ ), 2.03 (s, 3H,  $\text{CH}_3\text{CO}$ ), 2.48-2.69 (c.a., 2H,  $\text{H}_{4b}$ ,  $\text{H}_1$ ), 2.81 (dd,  $^2J_{\text{H-H}} = 10.6 \text{ Hz}$ ,  $^3J_{\text{H-H}} = 7.9 \text{ Hz}$ , 1H,  $\text{H}_3$ ).

$^{13}\text{C NMR}$  (62.5 MHz,  $\text{CDCl}_3$ )  $\delta$  17.8 (*trans*- $\text{CH}_3$ ), 19.1 ( $\text{C}_4$ ), 28.2 ( $\text{C}(\text{CH}_3)_3$ ), 29.9 ( $\text{CH}_3\text{CO}$ ), 30.2 (*cis*- $\text{CH}_3$ ), 44.8 ( $\text{C}_2$ ), 45.8 ( $\text{C}_1$ ), 53 ( $\text{C}_3$ ), 80.4 ( $\text{C}(\text{CH}_3)_3$ ), 171.4 ( $\text{CO}_2^t\text{Bu}$ ), 207.2 ( $\text{CO}_{\text{ketone}}$ ).

Spectroscopic data are consistent with those reported in reference:

Rouge, P.; Moglioni, A.; Moltrasio, G.; Ortuño, R., M., *Tetrahedron: Asymmetry* **2003**, *142*, 193-195.

**(1R,3S)-3-tert-Butoxycarbonyl-2,2-dimethylcyclobutane-1-carboxylic acid, 49:**

To an ice cooled solution of ketone **48** (410 mg, 1.8 mmol) in dioxane-water (7:2, 13 mL) was added a sodium hypobromite solution, prepared from bromine (0.33 mL, 6.5 mmol, 3.6 eq) and sodium hydroxide (0.50 g, 12.6 mmol, 7.0 eq) in a 3:1 mixture of water and dioxane (24 mL). The resulting mixture was stirred for 5 hours at -5 °C. Then, sodium bisulfite was added (5 mL) and the mixture was brought to acidic pH by adding 5% hydrochloric acid. The acid solution was extracted with dichloromethane (4 x 30 mL), the organic extracts were dried over anhydrous magnesium sulfate and solvent was removed to dryness to afford carboxylic acid **49** as a white powder (383 mg, 93% yield).

**Spectroscopic data for compound 49:**

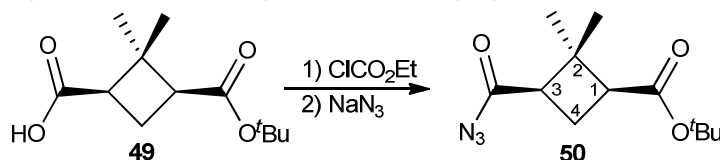
<sup>1</sup>H NMR (250 MHz, CDCl<sub>3</sub>) δ 1.01 (s, 3H, *trans*-CH<sub>3</sub>), 1.30 (s, 3H, *cis*-CH<sub>3</sub>), 1.41 (s, 9H, C(CH<sub>3</sub>)<sub>3</sub>), 1.90-2.05 (m, 1H, H<sub>4a</sub>), 2.39-2.55 (m, 1H, H<sub>4b</sub>), 2.59-2.86 (c.a., 2H, H<sub>3</sub>, H<sub>1</sub>), 5.42 (broad singlet, 1H, COOH).

<sup>13</sup>C NMR (62.5 MHz, CDCl<sub>3</sub>) δ 18.2 (*trans*-CH<sub>3</sub>), 20.1 (C<sub>4</sub>), 28.2 (C(CH<sub>3</sub>)<sub>3</sub>), 30 (*cis*-CH<sub>3</sub>), 44.4 (C<sub>2</sub>), 45.2 (C<sub>3</sub>), 46.1 (C<sub>1</sub>), 80.5 (C(CH<sub>3</sub>)<sub>3</sub>), 171.5 (CO<sub>2</sub><sup>t</sup>Bu), 177.9 (COOH).

Spectroscopic data are consistent with those reported in reference:

Aguado, G. P.; Moglioni, A. G.; Brousse, B. N.; Ortuño, R. M. *Tetrahedron: Asymmetry* **2003**, *14*, 2445-2451.

**(1*S*,3*R*)- tert-Butyl 3-(azidocarbonyl)-2,2-dimethylcyclobutanecarboxylate, 50:**



To an ice-cooled solution of half-ester **49** (300 mg, 1.3 mmol) in anhydrous acetone, triethylamine (0.29 mL, 2.0 mmol, 1.5 eq) and ethyl chloroformate (0.2 mL, 2.0 mmol, 1.5 eq) were subsequently added. The mixture was stirred at 0 °C for 30 minutes. Then, sodium azide (145 mg, 2.2 mmol, 1.7 eq) in 5 mL of water was added and the resultant solution was stirred at room temperature for 1.5 h. The reaction mixture was extracted with dichloromethane (4x15 mL), and the organic extracts were dried over magnesium sulfate. Solvents were removed under reduced pressure to give acyl azide **50** as a colourless oil (323 mg, 98% yield), which was characterised by its spectroscopic data and used in the next step without further purification.

#### Spectroscopic data for compound **50**:

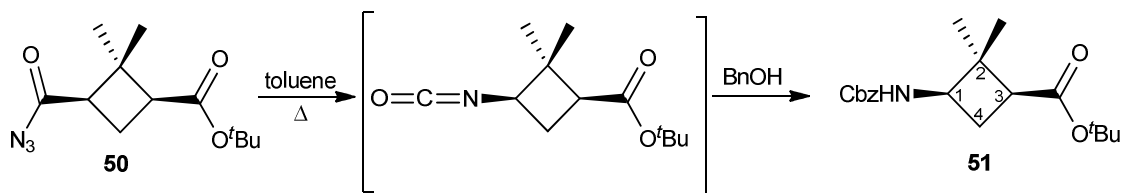
$^1\text{H NMR}$  (250 MHz, acetone- $d_6$ )  $\delta$  1.29 (s, 3H, *trans*- $\text{CH}_3$ ), 1.35 (s, 3H, *cis*- $\text{CH}_3$ ), 1.45 (s, 9H,  $\text{C}(\text{CH}_3)_3$ ), 1.87-1.99 (m, 1H,  $\text{H}_{4a}$ ), 2.43-2.56 (m, 1H,  $\text{H}_{4b}$ ), 2.78-2.96 (c.a., 2H,  $\text{H}_3$ ,  $\text{H}_1$ ).

$^{13}\text{C NMR}$  (62.5 MHz, acetone- $d_6$ )  $\delta$  18.1 (*trans*- $\text{CH}_3$ ), 20.1 ( $\text{C}_4$ ), 27.3 ( $\text{C}(\text{CH}_3)_3$ ), 30 (*cis*- $\text{CH}_3$ ), 45.1 ( $\text{C}_2$ ), 46.2 ( $\text{C}_3$ ), 47.6 ( $\text{C}_1$ ), 80.2 ( $\text{C}(\text{CH}_3)_3$ ), 171.2 ( $\text{CO}_2^t\text{Bu}$ ), 179.5 ( $\text{CON}_3$ ).

Spectroscopic data are consistent with those reported in reference:

Aguilera, J.; Moglioni, A. G.; Moltrasio, G. Y.; Ortuño, R. M. *Tetrahedron: Asymmetry* **2008**, *19*, 302-308.

#### (1*R*,3*S*)-*tert*-Butyl-3-(benzyloxycarbonylamino)-2,2-dimethylcyclobutane carboxylate, **51**:



A solution of acyl azide **50** (460 mg, 1.8 mmol) and benzyl alcohol (0.42 mL, 3.8 mmol, 2.1 eq) in toluene (9 mL) was heated to reflux for 3.5 hours under nitrogen atmosphere (the reaction progress was monitored by IR following the signals for the acyl azide at  $2136\text{ cm}^{-1}$  and the corresponding isocyanate at  $2260\text{ cm}^{-1}$ ). Toluene was removed at reduced pressure

and then excess of benzyl alcohol was eliminated by vacuum distillation. The residue was chromatographed on silica gel (ethyl acetate-hexane, 1:1 to 2:1) to afford carbamate as a white solid which was crystallised (ether/pentane) to afford pure orthogonally protected amino acid **51** (545 mg, 90% yield).

#### Spectroscopic data and physical constants for compound **51**:

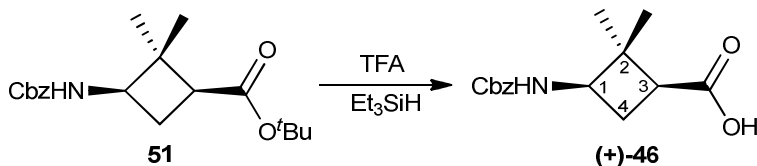
$^1\text{H NMR}$  (250 MHz,  $\text{CDCl}_3$ )  $\delta$  0.95 (s, 3H, *trans*- $\text{CH}_3$ ), 1.30 (s, 3H, *cis*- $\text{CH}_3$ ), 1.46 (s, 9H,  $\text{C}(\text{CH}_3)_3$ ), 2.02 (dd,  $J_{\text{H,H}} = 18.7$  Hz,  $J_{\text{H,H}} = 9.5$ , 1H,  $\text{H}_{4a}$ ), 2.25-2.36 (c.a, 1H,  $\text{H}_{4b}$ ), 2.51 (dd,  $J_{\text{H,H}} = 9.5$  Hz,  $J_{\text{H,H}} = 6.75$ ,  $\text{H}_3$ ), 3.90 (dd,  $J_{\text{H,H}} = 17.2$  Hz,  $J_{\text{H,H}} = 9.5$ , 1H,  $\text{H}_1$ ), 4.9 (d,  $J_{\text{H,H}} = 9$  Hz, 1H, NH), 5.10 (d,  $J_{\text{H,H}} = 20.75$  Hz, 1H,  $\text{CH}_2\text{Bn}$ ), 5.13 (d,  $J_{\text{H,H}} = 21.5$  Hz, 1H,  $\text{CH}_2\text{Bn}$ ), 7.37 (c.a., 5H,  $\text{H}_{\text{Ar}}$ ).

$^{13}\text{C NMR}$  (62.5 MHz,  $\text{CDCl}_3$ )  $\delta$  16.9 (*trans*- $\text{CH}_3$ ), 26.7 ( $\text{C}_4$ ), 28.3 ( $\text{C}(\text{CH}_3)_3$ ), 29.9 (*cis*- $\text{CH}_3$ ), 43.9 ( $\text{C}_2$ ), 45.9 ( $\text{C}_3$ ), 51.5 ( $\text{C}_1$ ), 66.8 ( $\text{CH}_2\text{Bn}$ ), 80.5 ( $\text{C}(\text{CH}_3)_3$ ), 128.2 and 128.6 ( $\text{C}_{\text{Ar}}$ ), 155.8 ( $\text{CO}_{\text{carbamate}}$ ), 171.5 ( $\text{CO}_2^t\text{Bu}$ ).

Spectroscopic data are consistent with those reported in reference:

Aguilera, J.; Moglioni, A. G.; Moltrasio, G. Y.; Ortuño, R. M. *Tetrahedron: Asymmetry* **2008**, *19*, 302-308.

#### (1*S*,3*R*)-3-benzoyloxycarbonylamino-2,2-dimethylcyclobutanecarboxylic acid, (+)-**46**:



A mixture containing compound **51** (700 mg, 2.1 mmol), trifluoroacetic acid (2.1 mL, 27.3 mmol, 13 eq) and triethyl silane (0.84 mL, 5.2 mmol, 2.5 eq) in anhydrous dichloromethane (6 mL) was stirred at room temperature for 2 h. Solvent was evaporated

and the excess of trifluoroacetic acid was removed by liophilization affording acid **(+)-46** as a white solid which was identified by its  $^1\text{H}$  NMR spectrum and used in the next step without purification (543 mg, 94% yield).

**Spectroscopic data for compound (+)-46:**

$^1\text{H}$  NMR (250 MHz,  $\text{CDCl}_3$ )  $\delta$  0.99 (s, 3H, *trans*- $\text{CH}_3$ ), 1.35 (s, 3H, *cis*- $\text{CH}_3$ ), 2.06 (m, 1H,  $\text{H}_{4a}$ ), 2.33 (m, 1H,  $\text{H}_3$ ), 2.58 (m, 1H,  $\text{H}_{4b}$ ), 3.94 (m, 1H,  $\text{H}_1$ ), 5.11 (c.a., 3H, NH,  $\text{CH}_2\text{Bn}$ ), 7.37 (c.a., 5H,  $\text{H}_{Ar}$ ), 10.15 (broad singlet, 1H, COOH).

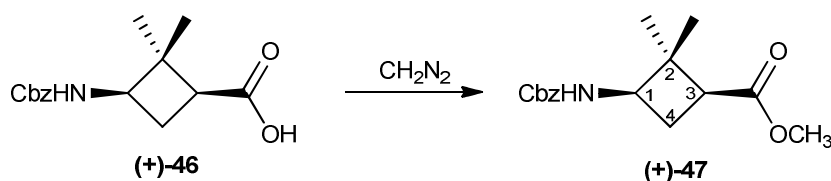
$^{13}\text{C}$  NMR (62.5 MHz,  $\text{CDCl}_3$ )  $\delta$  16.4 (*trans*- $\text{CH}_3$ ), 24.8 ( $\text{C}_4$ ), 28.9 (*cis*- $\text{CH}_3$ ), 30.3 ( $\text{CH}_3\text{CO}$ ), 46.49 ( $\text{C}_2$ ), 50.7 ( $\text{C}_3$ ), 51.3 ( $\text{C}_1$ ), 66.8 ( $\text{CH}_2\text{Bn}$ ), 128.1, 128.2, 128.5 and 136.3 ( $\text{C}_{Ar}$ ), 155.9 ( $\text{CO}_{\text{carbamate}}$ ), 206.8 ( $\text{CH}_3\text{CO}$ ).

Spectroscopic data are consistent with those reported in reference:

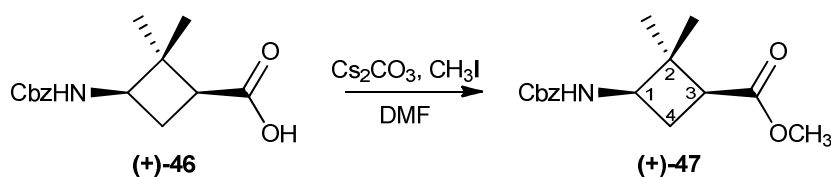
Aguilera, J.; Moglioni, A. G.; Moltrasio, G. Y.; Ortuño, R. M. *Tetrahedron: Asymmetry* **2008**, *19*, 302-308.

**(1S,3R)-Methyl-3-(benzyloxycarbonylamino)-2,2-dimethylcyclobutane- carboxylate, (+)-47:**

Method 1:



Acid **(+)-46** (500 mg, 1.8 mmol) was methylated by the action of an excess of diazomethane (1.17 g of Diazald<sup>®</sup>, 5.4 mmol, 3 eq) in a dichloromethane solution (30 mL) to provide quantitatively the orthogonally protected amino acid **(+)-47** (524 mg).

Method 2:

A mixture containing acid **(+)-46** (2.20 g, 7.9 mmol), cesium carbonate (3.07 g, 9.4 mmol, 1.2 eq) and 0.6 mL of methyl iodide (9.4 mmol, 1.2 eq) in anhydrous DMF (40 mL) was stirred at room temperature for 18 h. Then, ethyl acetate (30 mL) was added and the resultant solution was washed with saturated aqueous sodium bicarbonate (4 x 25 mL). The organic liquors were dried over magnesium sulfate and solvent was evaporated under vacuum to provide methyl ester **(+)-47** (2.01 g, 87% yield).

**Spectroscopic data and physical constants for compound (+)-47:**

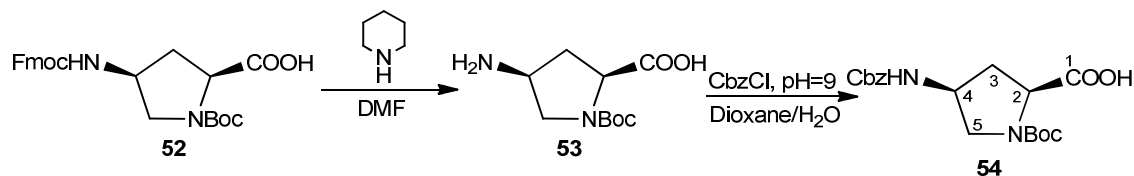
**<sup>1</sup>H NMR** (250 MHz, CDCl<sub>3</sub>) δ 0.90 (s, 3H, *trans*-CH<sub>3</sub>), 1.29 (s, 3H, *cis*-CH<sub>3</sub>), 2.05 (dd, <sup>2</sup>J<sub>H,H</sub> = 21 Hz, <sup>3</sup>J<sub>H,H</sub> = 9.75 Hz, 1H, H<sub>4a</sub>), 2.36 (m, 1H, H<sub>4b</sub>), 2.57 (dd, J<sub>H,H</sub> = 9.75 Hz, J<sub>H,H</sub> = 7 Hz, 1H, H<sub>3</sub>), 3.67 (s, 3H, COOCH<sub>3</sub>), 3.92 (dd, J<sub>H,H</sub> = 17.25 Hz, J<sub>H,H</sub> = 8 Hz, 1H, H<sub>1</sub>), 4.91 (d, J<sub>H,H</sub> = 11.75 Hz, 1H, NH), 5.05 (d, J<sub>H,H</sub> = 19 Hz, 1H, CH<sub>2</sub>Bn), 5.12 (d, J<sub>H,H</sub> = 20.25 Hz, 1H, CH<sub>2</sub>Bn), 7.36 (c.a., 5H, H<sub>Ar</sub>).

**<sup>13</sup>C NMR** (62.5 MHz, CDCl<sub>3</sub>) δ 16.7 (*trans*-CH<sub>3</sub>), 26.4 (C<sub>4</sub>), 28.5 (*cis*-CH<sub>3</sub>), 42.6 (C<sub>3</sub>), 45.8 (C<sub>2</sub>), 51.3 (COOCH<sub>3</sub>) 76.9 (C<sub>1</sub>), 66.6 (CH<sub>2</sub>Bn), 127.9, 128.6 and 136.1 (C<sub>Ar</sub>), 155.7 (CO<sub>carbamate</sub>), 172.6 (CO<sub>2</sub>CH<sub>3</sub>).

Spectroscopic data are consistent with those reported in reference:

Aguilera, J.; Moglioni, A. G.; Moltrasio, G. Y.; Ortuño, R. M. *Tetrahedron: Asymmetry* **2008**, *19*, 302-308.

**(2*S*,4*S*)-4-(benzyloxycarbonylamino)-1-(*tert*-butoxycarbonyl)pyrrolidine-2-carboxylic acid, **54**:**



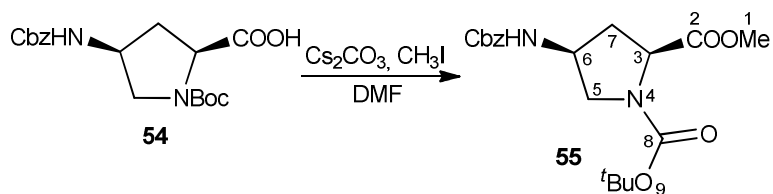
Fmoc-Proline **52** (1.00 g, 2.2 mmol) was dissolved in 20% piperidine solution in DMF (10 mL, 20.2 mmol, 9.2 eq) and was let to stir for 15 minutes. Afterwards, DMF was evaporated and the resulting crude was redissolved in a 1:1 mixture of dioxane and H<sub>2</sub>O (20 mL) and the pH was adjusted to 9 by the addition of NaHCO<sub>3</sub>. Benzyl chloroformate (0.35 mL, 2.7 mmol, 1.2 eq) was added and the solution was stirred for 3h at room temperature. The dioxane was evaporated under reduced pressure, water was added and the solution extracted with diethyl ether (2 x 25 mL). The aqueous phase was then acidified with 5% citric acid and the product extracted with CH<sub>2</sub>Cl<sub>2</sub> (3 x 20 mL). The organic layer was dried with magnesium sulfate and evaporated under reduced pressure. The residue was purified by silica gel chromatography (hexane-ethyl acetate, 1:4) to give pure **54** as a white solid (0.48 g, 60% yield).

**Spectroscopic data and physical constants for compound **54**:**

<sup>1</sup>H NMR (250 MHz, CDCl<sub>3</sub>) δ 1.52 (s, 9H, <sup>t</sup>Bu), 2.18-2.37 (m, 1H, H<sub>3a</sub>), 2.41-2.59 (m, 1H, H<sub>3b</sub>), 3.46-3.65 (m, 2H, H<sub>5</sub>), 4.21-4.37 (m, 1H, H<sub>4</sub>), 4.41-4.54 (m, 1H, H<sub>2</sub>), 5.01-5.24 (m, 2H, CH<sub>2</sub>Bn), 5.66 (bs, 1H, NH), 7.37 (c.a., 5H, H<sub>Ar</sub>)

Spectroscopic data are consistent with those reported in reference:

Torino, D.; Mollica, A.; Pinnen, F.; Feliciani, F.; Spisani, S.; Lucente, G. *Bioorg. Med. Chem.* **2009**, *17*, 251-259.

**(2*S*,4*S*)-1-*tert*-Butyl 2-methyl 4-(benzyloxycarbonylamino)pyrrolidine-1,2-dicarboxylate, 55:**

A mixture containing acid **54** (60 mg, 0.2 mmol), cesium carbonate (100 mg, 0.3 mmol, 2 eq) and 0.01 mL of methyl iodide (0.3 mmol, 2 eq) in anhydrous DMF (5 mL) was stirred at room temperature for 18 h. Then, ethyl acetate (30 mL) was added and the resultant solution was washed with saturated aqueous sodium bicarbonate (4 x 25 mL). The organic liquors were dried over magnesium sulfate and solvent was evaporated under vacuum to provide pure methyl ester **55** (57 mg, 95% yield) as a colourless oil.



**Spectroscopic data for compound 55:****cis conformer**

**<sup>1</sup>H NMR** (600 MHz, CDCl<sub>3</sub>) δ 1.41 (s, 9H, H<sub>9</sub>), 1.98 (d,  $J_{H,H} = 14.9$  Hz, 1H, H<sub>7 proR</sub>), 2.43-2.53 (m, 1H, H<sub>7 proS</sub>), 3.58 (d,  $J_{H,H} = 11.4$  Hz, 1H, H<sub>5 proS</sub>), 3.57-3.65 (m, 1H, H<sub>5 proR</sub>), 3.75 (s, 3H, H<sub>1</sub>), 4.26 (dd,  $J_{H,H} = 9.8$  Hz,  $J_{H,H} = 2.5$  Hz, 1H, H<sub>3</sub>), 4.41-4.43 (m, 1H, H<sub>6</sub>), 5.09-5.10 (m, 2H, H<sub>11 CH2</sub>), 5.86 (d,  $J_{H,H} = 9.2$  Hz, 1H, H<sub>10</sub>), 7.33-7.37 (m, 5H, H<sub>11 Ar</sub>).

**<sup>13</sup>C NMR** (150 MHz, CDCl<sub>3</sub>) δ 28.3 (C<sub>9</sub>), 35.8 or 36.8 (C<sub>7</sub>), 49.7 (C<sub>6</sub>), 52.6 (C<sub>1</sub>), 53.1 (C<sub>5</sub>), 57.7 (C<sub>3</sub>), 66.8 (C<sub>11 CH2</sub>), 80.7 (C<sub>9q</sub>), 128.2, 128.3 and 128.6 (C<sub>11 Ar</sub>), 136.3 (C<sub>11q</sub>), 153.5 (C<sub>8</sub>), 155.7 (C<sub>11 CO</sub>), 174.7 (C<sub>2</sub>).

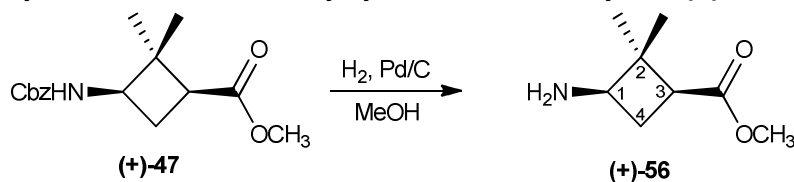
**trans conformer**

**<sup>1</sup>H NMR** (600 MHz, CDCl<sub>3</sub>) δ 1.46 (s, 9H, H<sub>9</sub>), 1.96 (d,  $J = 14.9$  Hz, 1H, H<sub>7 proR</sub>), 2.43-2.53 (m, 1H, H<sub>7 proS</sub>), 3.49 (d,  $J = 11.4$  Hz, 1H, H<sub>5 proS</sub>), 3.57-3.65 (m, 1H, H<sub>5 proR</sub>), 3.77 (s, 3H, H<sub>1</sub>), 4.34 (dd,  $J = 9.8$  Hz,  $J' = 2.3$  Hz, 1H, H<sub>3</sub>), 4.41-4.43 (m, 1H, H<sub>6</sub>), 5.09-5.10 (m, 2H, H<sub>11 CH2</sub>), 5.93 (d,  $J = 9.2$  Hz, 1H, H<sub>10</sub>), 7.33-7.37 (m, 5H, H<sub>11 Ar</sub>).

**<sup>13</sup>C NMR** (150 MHz, CDCl<sub>3</sub>) δ 28.3 (C<sub>9</sub>), 35.8 or 36.8 (C<sub>7</sub>), 50.7 (C<sub>6</sub>), 52.9 (C<sub>1</sub>), 53.7 (C<sub>5</sub>), 57.6 (C<sub>3</sub>), 66.8 (C<sub>11 CH2</sub>), 80.7 (C<sub>9q</sub>), 128.2, 128.3 and 128.6 (C<sub>11 Ar</sub>), 136.3 (C<sub>11q</sub>), 154.2 (C<sub>8</sub>), 155.8 (C<sub>11 CO</sub>), 174.8 (C<sub>2</sub>).

Spectroscopic data are consistent with those reported in reference:

Torino, D.; Mollica, A.; Pinnen, F.; Feliciani, F.; Spisani, S.; Lucente, G. *Bioorg. Med. Chem.* **2009**, *17*, 251-259.

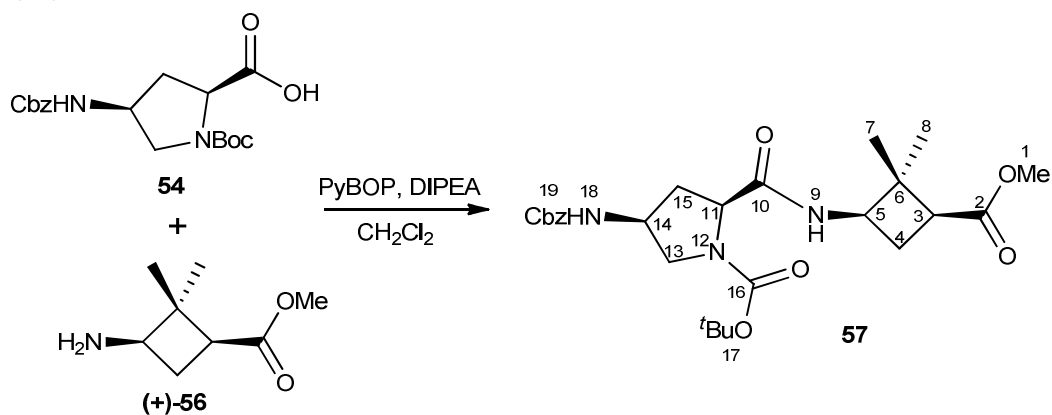
**(1S,3R)-Methyl 3-amino-2,2-dimethylcyclobutanecarboxylate, (+)-56:**

Compound **(+)-47** (200 mg, 0.7 mmol) in methanol (10 mL) was hydrogenated under 5 atmospheres of pressure in the presence of 10% Pd/C (50 mg, 2.5% Pd in weight) overnight. The reaction mixture was filtered through Celite<sup>®</sup> and solvent was removed under reduced pressure. The resulting crude was purified by column chromatography on silica gel (hexane to methanol) to provide amine **(+)-56** (103 mg, 94% yield) as a colourless oil which was identified by its <sup>1</sup>H and <sup>13</sup>C NMR spectra and used in the next step without further purification.

**Spectroscopic data for compound (+)-56:**

<sup>1</sup>H NMR (250 MHz, CDCl<sub>3</sub>) δ 0.93 (s, 3H, *trans*-CH<sub>3</sub>), 1.17 (s, 3H, *cis*-CH<sub>3</sub>), 2.00-2.15 (m, 1H, H<sub>4a</sub>), 2.16-2.31 (m, 1H, H<sub>4b</sub>), 2.45-2.58 (m, 1H, H<sub>3</sub>), 3.14 (t, J = 9 Hz, 1H, H<sub>1</sub>), 3.61 (s, 3H, CO<sub>2</sub>CH<sub>3</sub>).

<sup>13</sup>C NMR (62.5 MHz, CDCl<sub>3</sub>) δ 16.4 (*trans*-CH<sub>3</sub>), 23.2 (C<sub>4</sub>), 28.8 (*cis*-CH<sub>3</sub>), 29.9 (C<sub>3</sub>), 43.4 (C<sub>2</sub>), 51.9 (CO<sub>2</sub>CH<sub>3</sub>), 56.6 (C<sub>1</sub>), 173.4 (CO<sub>2</sub>CH<sub>3</sub>).

**γ-Dipeptide 57:**

Acid **54** (292 mg, 0.6 mmol), DIPEA (0.30 mL, 1.6 mmol, 2.7 eq) and PyBOP (420 mg, 0.8 mmol, 1.4 eq) were dissolved in anhydrous dichloromethane (15 mL). The mixture was

stirred for 5 minutes under nitrogen atmosphere, and then a solution of amine **(+)-56** (92 mg, 0.6 mmol) in anhydrous dichloromethane (10 mL) was added via cannula. After stirring at room temperature for 2 hours the reaction crude was washed with a saturated aqueous sodium bicarbonate solution. The organic phase was dried over magnesium sulfate and the solvents were removed under vacuum. The reaction crude was purified by column chromatography on neutral silica gel (ethyl acetate-hexane, 1:1) to afford pure dipeptide **57** (302 mg, quantitative yield) as a white solid.

**Spectroscopic data and physical constants for compound 57:**

$[\alpha]_D = -13.8$  (*c* 0.99, CH<sub>2</sub>Cl<sub>2</sub>).

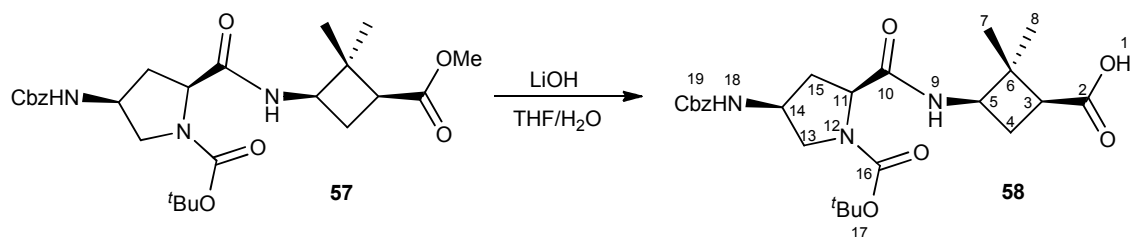
**Melting point:** 52-54 °C (diethyl ether).

**IR (ATR):** 3312 (NH<sub>st</sub>), 2956 (CH<sub>st</sub>), 2876 (CH<sub>st</sub>), 1677 (bs, CO<sub>carbamate</sub> + CO<sub>ester</sub> + CO<sub>amide</sub>), 1521, 1393.

**<sup>1</sup>H NMR** (600 MHz, CDCl<sub>3</sub>) δ 0.87 (s, 3H, H<sub>7</sub>), 1.27 (s, 3H, H<sub>8</sub>), 1.40 (s, 9H, H<sub>17</sub>), 2.17 (m, 2H, H<sub>4 proR</sub>, H<sub>15 proS</sub>), 2.25 (m, 1H, H<sub>4 proS</sub>), 2.40 (d, *J*<sub>H,H</sub> = 13.7 Hz, 1H, H<sub>15 proR</sub>), 2.62 (dd, *J*<sub>H,H</sub> = 10.0 Hz, *J*<sub>H,H</sub> = 8.0 Hz, 1H, H<sub>3</sub>), 3.47 (d, *J*<sub>H,H</sub> = 11.6 Hz, 1H, H<sub>13 proS</sub>), 3.55 (m, 1H, H<sub>13 proR</sub>), 3.70 (s, 3H, H<sub>1</sub>), 4.08 (dd, *J*<sub>H,H</sub> = 17.8 Hz, *J*<sub>H,H</sub> = 8.6 Hz, 1H, H<sub>5</sub>), 4.30 (m, 1H, H<sub>14</sub>), 4.43 (d, *J*<sub>H,H</sub> = 8.7 Hz, 1H, H<sub>11</sub>), 5.10 (m, 2H, H<sub>19 CH2</sub>), 6.85 (d, *J*<sub>H,H</sub> = 6.2 Hz, 1H, H<sub>18</sub>), 7.35 (m, 5H, H<sub>19 Ar</sub>), 7.72 (d, *J*<sub>H,H</sub> = 8.0 Hz, 1H, H<sub>9</sub>).

**<sup>13</sup>C NMR** (150 MHz, CDCl<sub>3</sub>) δ 17.0 (C<sub>7</sub>), 26.2 (C<sub>4</sub>), 28.3 (C<sub>17</sub>), 29.0 (C<sub>8</sub>), 31.5 (C<sub>15</sub>), 43.1 (C<sub>3</sub>), 46.3 (C<sub>6</sub>), 50.1 (C<sub>5</sub>), 50.7 (C<sub>14</sub>), 51.4 (C<sub>1</sub>), 55.1 (C<sub>13</sub>), 59.21 (C<sub>11</sub>), 66.4 (C<sub>19 CH2</sub>), 81.2 (C<sub>17q</sub>), 128.0 and 128.4 (C<sub>19 Ar</sub>), 136.7 (C<sub>19q</sub>), 156.0 (C<sub>19 CO</sub>), 156.2 (C<sub>16</sub>), 172.3 (C<sub>10</sub>), 172.8 (C<sub>2</sub>).

**High resolution mass spectrum:** calculated for C<sub>26</sub>H<sub>37</sub>N<sub>3</sub>NaO<sub>7</sub>, (M+Na)<sup>+</sup>: 526.2524, Found: 526.2506.

**$\gamma$ -Dipeptide 58:**

To an ice-cooled solution of ester **57** (95 mg, 0.2 mmol) in THF (6.5 mL) was added a 5% solution of LiOH in water (1.90 mL, 4.0 mmol, 20 eq). The reaction was let to stir for 48 hours (reaction progress was monitored by HPLC/Ms). Afterwards the crude was brought to pH 2-3 through the addition of a 5% solution of HCl in water. The acid solution was extracted with dichloromethane (4x30 mL), the organic extracts were dried over anhydrous magnesium sulfate and solvent was removed to afford carboxylic acid **58** as a white powder (90 mg, 98% yield) which was identified by its spectroscopic data and immediately used in the condensation step without purification.

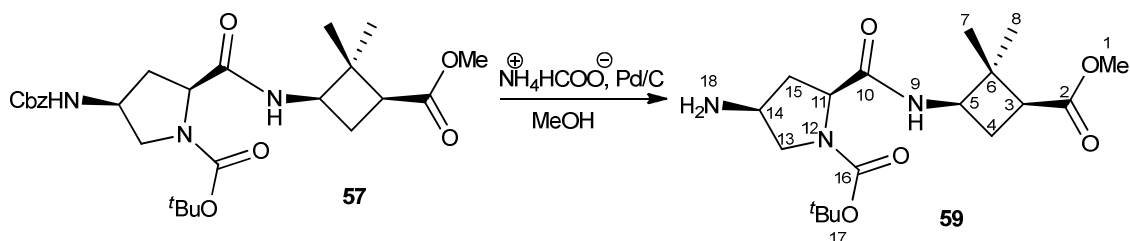
**Spectroscopic data and physical constants for compound 58:**

$[\alpha]_D = +6.9$  ( $c$  0.88, CH<sub>2</sub>Cl<sub>2</sub>).

**Melting point:** 79-81 °C (diethyl ether).

**IR (ATR):** 3323 (NH<sub>st</sub> + OH<sub>st</sub>), 2964 (CH<sub>st</sub>), 1675 (bs, CO<sub>carbamate</sub> + CO<sub>acid</sub> + CO<sub>amide</sub>), 1527, 1397.

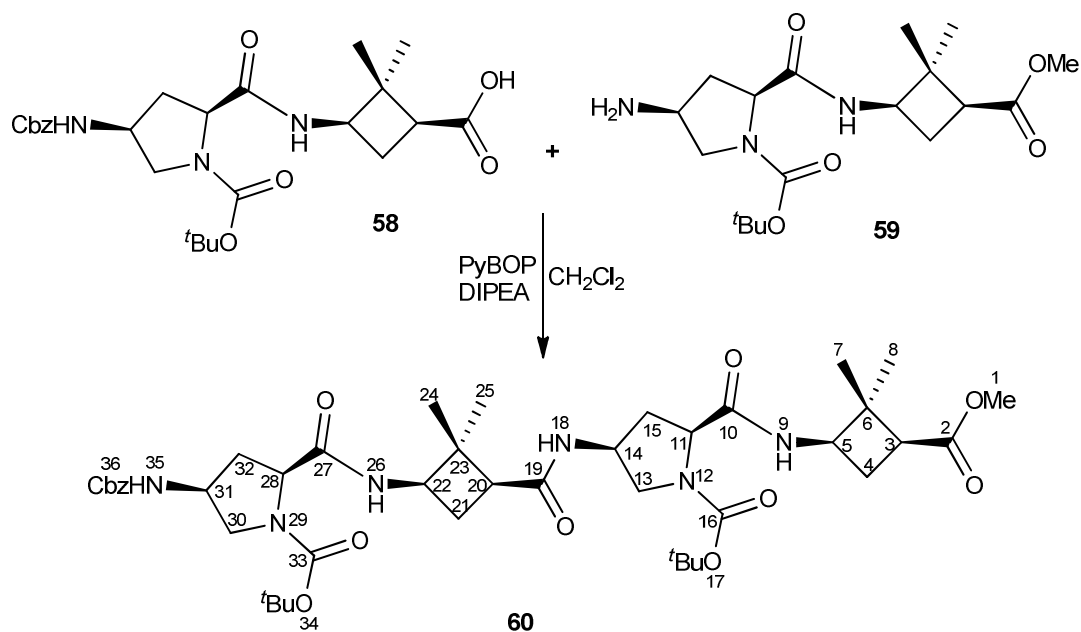
**High resolution mass spectrum:** calculated for C<sub>26</sub>H<sub>35</sub>N<sub>3</sub>NaO<sub>7</sub>, (M+Na)<sup>+</sup>: 512.2367, Found: 512.2360.

**$\gamma$ -Dipeptide 59:**

To a solution of **57** (95 mg, 0.2 mmol) in 15 mL of anhydrous methanol were subsequently added ammonium formate (120 mg, 1.5 mmol, 7.5 eq) and 10% Pd/C (50 mg, 5% Pd in weight). The resulting mixture was heated at reflux for 2 h (reaction progress was monitored by HPLC/MS). Afterwards, the reaction mixture was filtered through Celite<sup>®</sup>, and the solvent was eliminated under vacuo to obtain a white solid identified as amine **59** (65 mg, 93% yield) by its spectroscopic data and immediately used in the condensation step without purification.

**Spectroscopic data and physical constants for compound 59:**

IR (ATR): 3284 (NH<sub>st</sub>), 2954 (CH<sub>st</sub>), 1727 (CO<sub>ester</sub>), 1664 (CO<sub>amide</sub>), 1544, 1392, 1366.

**$\gamma$ -Tetrapeptide 60:**

Acid **58** (90 mg, 0.2 mmol), DIPEA (0.12 mL, 0.6 mmol, 3 eq) and PyBop (161 mg, 0.3 mmol, 1.5 eq) were dissolved in anhydrous dichloromethane (10 mL). The mixture was stirred for 5 minutes under nitrogen atmosphere, and then a solution of amine **59** (65mg, 0.2 mmol) in anhydrous dichloromethane (5 mL) was added via cannula. After stirring at room temperature for 2 hours, the reaction crude was washed with a saturated aqueous sodium bicarbonate solution. The organic phase was dried over magnesium sulfate and the solvents were removed under vacuum. The reaction crude was purified by column chromatography on neutral silica gel (ethyl acetate) to afford pure tetrapeptide **60** (145 mg, 96% yield) as a white solid.

**Spectroscopic data and physical constants for compound 60:**

$[\alpha]_D = -310.8$  ( $c$  0.06,  $\text{CH}_2\text{Cl}_2$ ).

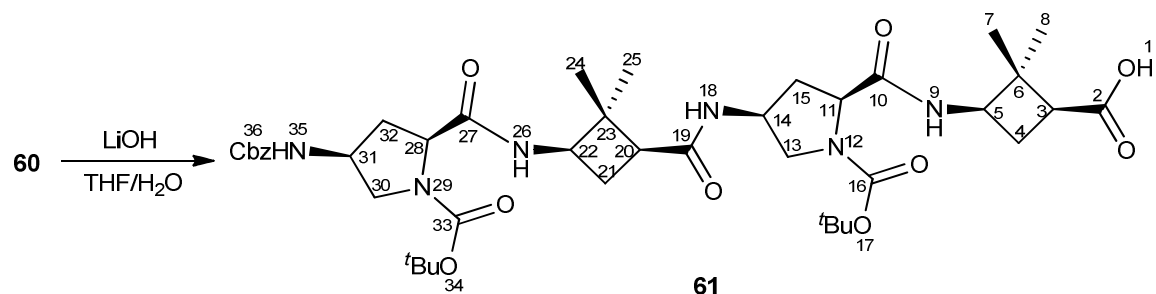
**Melting point:** 79-81 °C ( $\text{H}_2\text{O}$ ).

**IR (ATR):** 3355 ( $\text{NH}_{\text{st}}$ ), 2926 ( $\text{CH}_{\text{st}}$ ), 2854 ( $\text{CH}_{\text{st}}$ ), 1700 and 1671 (bs,  $\text{CO}_{\text{carbamates}}$  +  $\text{CO}_{\text{esters}}$  +  $\text{CO}_{\text{amides}}$ ), 1542, 1459, 1398.

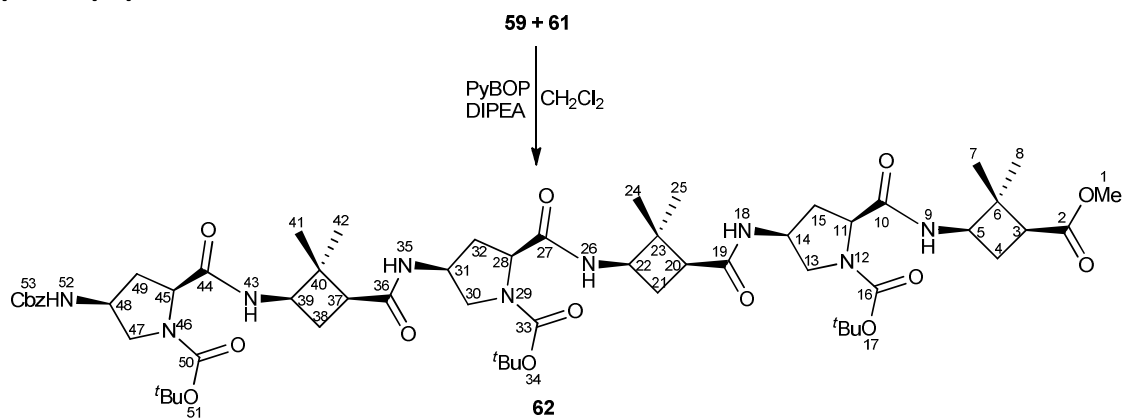
**$^1\text{H}$  NMR** (600 MHz,  $\text{CDCl}_3$ )  $\delta$  0.85 and 0.86 (s, 6H,  $\text{H}_7$  and  $\text{H}_{24}$ ), 1.22 (s, 3H,  $\text{H}_8$ ), 1.26 (s, 3H,  $\text{H}_{25}$ ), 1.45 (s, 18H,  $\text{H}_{17}$  and  $\text{H}_{34}$ ), 2.10-2.35 (m, 8H,  $\text{H}_{4 \text{ proS}}$ ,  $\text{H}_{4 \text{ proR}}$ ,  $\text{H}_{15 \text{ proS}}$ ,  $\text{H}_{15 \text{ proR}}$ ,  $\text{H}_{21 \text{ proS}}$ ,  $\text{H}_{21 \text{ proR}}$ ,  $\text{H}_{32 \text{ proS}}$ ,  $\text{H}_{32 \text{ proR}}$ ), 2.46-2.49 (m, 1H,  $\text{H}_{20}$ ), 2.58-2.61 (m, 1H,  $\text{H}_3$ ), 3.33-3.35 (m, 1H,  $\text{H}_{30 \text{ proS}}$ ), 3.43-3.44 (m, 1H,  $\text{H}_{13 \text{ proR}}$ ), 3.49-3.55 (m, 1H,  $\text{H}_{30 \text{ proR}}$ ), 3.68 (s, 3H,  $\text{H}_1$ ), 4.00-4.08 (m, 2H,  $\text{H}_5$  and  $\text{H}_{22}$ ), 4.29-4.31 (m, 1H,  $\text{H}_{31}$ ), 4.38-4.47 (m, 3H,  $\text{H}_{11}$ ,  $\text{H}_{14}$  and  $\text{H}_{28}$ ), 5.04-5.14 (m, 2H,  $\text{H}_{36 \text{ CH}_2}$ ), 6.93 (d,  $J_{\text{H,H}} = 6.1$  Hz, 1H,  $\text{H}_{35}$ ), 7.30-7.36 (m, 5H,  $\text{H}_{36 \text{ Ar}}$ ), 7.56 (d,  $J_{\text{H,H}} = 7.9$  Hz, 1H,  $\text{H}_{26}$ ), 7.70 (d,  $J_{\text{H,H}} = 8.4$  Hz, 1H,  $\text{H}_9$ ), 7.81 (d,  $J_{\text{H,H}} = 6.4$  Hz, 1H,  $\text{H}_{18}$ ).

**$^{13}\text{C}$  NMR** (150 MHz,  $\text{CDCl}_3$ )  $\delta$  16.5 ( $\text{C}_{24}$ ), 17.0 ( $\text{C}_7$ ), 26.0 ( $\text{C}_{21}$ ), 26.2 ( $\text{C}_4$ ), 28.3 (6C,  $\text{C}_{17}$  and  $\text{C}_{34}$ ), 29.0 ( $\text{C}_8$ ), 29.3 ( $\text{C}_{25}$ ), 31.1 ( $\text{C}_{15}$ ), 31.9 ( $\text{C}_{32}$ ), 43.0 ( $\text{C}_3$ ), 44.3 ( $\text{C}_{20}$ ), 45.8 ( $\text{C}_{23}$ ), 46.2 ( $\text{C}_6$ ), 49.1 ( $\text{C}_{14}$ ), 50.0 and 50.1 (2C,  $\text{C}_5$ ,  $\text{C}_{22}$ ), 50.7 ( $\text{C}_{31}$ ), 51.4 ( $\text{C}_1$ ), 55.2 ( $\text{C}_{30}$ ), 55.5 ( $\text{C}_{13}$ ), 59.2 ( $\text{C}_{11}$ ), 59.3 ( $\text{C}_{28}$ ), 66.4 ( $\text{C}_{36 \text{ CH}_2}$ ), 80.9 and 81.1 (2C,  $\text{C}_{17\text{q}}$ ,  $\text{C}_{34\text{q}}$ ), 127.9, 128.0 and 128.4 ( $\text{C}_{36 \text{ Ar}}$ ), 136.7 ( $\text{C}_{36\text{q}}$ ), 156.1 and 156.3 (3C,  $\text{C}_{16}$ ,  $\text{C}_{33}$ ,  $\text{C}_{36}$ ), 171.2 ( $\text{C}_{19,\text{CO}}$ ), 172.2 ( $\text{C}_{27}$ ), 172.4 ( $\text{C}_{10}$ ), 172.7 ( $\text{C}_2$ ).

**High resolution mass spectrum:** calculated for  $\text{C}_{43}\text{H}_{64}\text{N}_6\text{NaO}_{11}$  ( $\text{M}+\text{Na}$ ) $^+$ : 863.4525, Found: 863.4534.

**$\gamma$ -Tetrapeptide 61:**

To an ice-cooled solution of ester **60** (145 mg, 0.2 mmol) in THF (5 mL) was added a 5% solution of LiOH in water (2.2 mL, 1.7 mmol, 8.5 eq). The reaction was let to stir for 48 hours (reaction progress was monitored by HPLC/MS). Afterwards the crude was brought to pH 2-3 through the addition of a 5% solution of HCl in water. The acid solution was extracted with dichloromethane (4 x 30 mL), the organic extracts were dried over anhydrous magnesium sulfate and solvent was removed to afford carboxylic acid **61** as a white powder (140 mg, 98% yield) which was identified by its spectroscopic data and immediately used in the condensation step without purification.

 **$\gamma$ -Hexapeptide 62:**

Acid **61** (140 mg, 0.2 mmol), DIPEA (0.12 mL, 0.6 mmol, 3 eq) and PyBOP (161 mg, 0.3 mmol, 1.5 eq) were dissolved in anhydrous dichloromethane (10 mL), the mixture was stirred for 5 minutes under nitrogen atmosphere, and then a solution of amine **59** (70 mg, 0.2 mmol) in anhydrous dichloromethane (5 mL) was added via cannula. After stirring at room temperature for 2 hours the reaction crude was washed with a saturated aqueous



sodium bicarbonate solution. The organic phase was dried over magnesium sulfate and the solvents were removed under vacuum. The reaction crude was purified by column chromatography on neutral silica gel (ethyl acetate to ethyl acetate-methanol, 19:1) to afford pure hexapeptide **62** (180 mg, 81% yield) as a white solid.

**Spectroscopic data and physical constants for compound 62:**

$[\alpha]_D = +18.5$  ( $c$  0.10,  $\text{CH}_2\text{Cl}_2$ ).

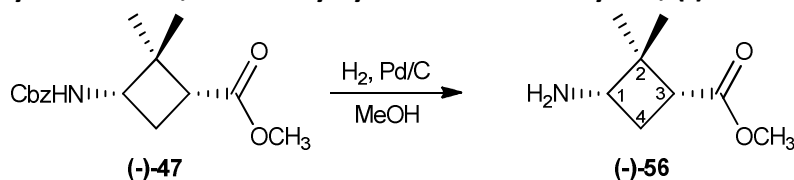
**Melting point:** 128-131 °C ( $\text{AcCN}/\text{H}_2\text{O}$ ).

**IR (ATR):** 3298 ( $\text{NH}_{\text{st}}$ ), 2957 ( $\text{CH}_{\text{st}}$ ), 1673 (bs,  $\text{CO}_{\text{carbamates}} + \text{CO}_{\text{esters}} + \text{CO}_{\text{amides}}$ ), 1520, 1392, 1367.

**$^1\text{H NMR}$**  (600 MHz,  $\text{CDCl}_3$ )  $\delta$  0.76-0.81 (m, 9H,  $\text{H}_7$ ,  $\text{H}_{24}$  and  $\text{H}_{41}$ ), 1.12-1.17 (m, 9H,  $\text{H}_8$ ,  $\text{H}_{25}$  and  $\text{H}_{42}$ ), 1.35-1.38 (m, 27H,  $\text{H}_{17}$ ,  $\text{H}_{34}$  and  $\text{H}_{51}$ ), 2.03-2.26 (m, 12H,  $\text{H}_4$ ,  $\text{H}_{15}$ ,  $\text{H}_{21}$ ,  $\text{H}_{32}$ ,  $\text{H}_{38}$  and  $\text{H}_{49}$ ), 2.41-2.44 (m, 2H,  $\text{H}_{20}$  and  $\text{H}_{37}$ ), 2.52-2.55 (m, 1H,  $\text{H}_3$ ), 3.26-3.44 (m, 6H,  $\text{H}_{13}$ ,  $\text{H}_{30}$  and  $\text{H}_{47}$ ), 3.61(s, 3H,  $\text{H}_1$ ), 3.96-3.97 (m, 3H,  $\text{H}_5$ ,  $\text{H}_{22}$  and  $\text{H}_{39}$ ), 4.20-4.21 (m, 1H,  $\text{H}_{48}$ ), 4.30-4.31 (m, 1H,  $\text{H}_{45}$ ), 4.33-4.35 (m, 1H,  $\text{H}_{28}$ ), 4.36-4.38 (m, 3H,  $\text{H}_{11}$ ,  $\text{H}_{14}$  and  $\text{H}_{31}$ ), 4.96-5.05 (m, 2H,  $\text{H}_{53 \text{ CH}_2}$ ), 6.93 (d,  $J_{\text{H,H}} = 6.8$  Hz, 1H,  $\text{H}_{52}$ ), 7.23-7.28 (m, 5H,  $\text{H}_{53 \text{ Ar}}$ ), 7.56 (d,  $J_{\text{H,H}} = 8.1$  Hz, 1H,  $\text{H}_{43}$ ), 7.60 (d,  $J_{\text{H,H}} = 8.9$  Hz, 1H,  $\text{H}_{26}$ ), 7.66 (d,  $J_{\text{H,H}} = 9.0$  Hz, 1H,  $\text{H}_9$ ), 7.94 (d,  $J_{\text{H,H}} = 7.1$  Hz, 1H,  $\text{H}_{18}$ ), 8.03 (d,  $J_{\text{H,H}} = 7.2$  Hz, 1H,  $\text{H}_{35}$ ).

**High resolution mass spectrum:** calculated for  $\text{C}_{60}\text{H}_{91}\text{N}_9\text{NaO}_{15}$ ,  $(\text{M}+\text{Na})^+$ : 1200.6527, Found: 1200.6521.

**(1R,3S)-methyl 3-amino-2,2-dimethylcyclobutanecarboxylate, (-)-56:**



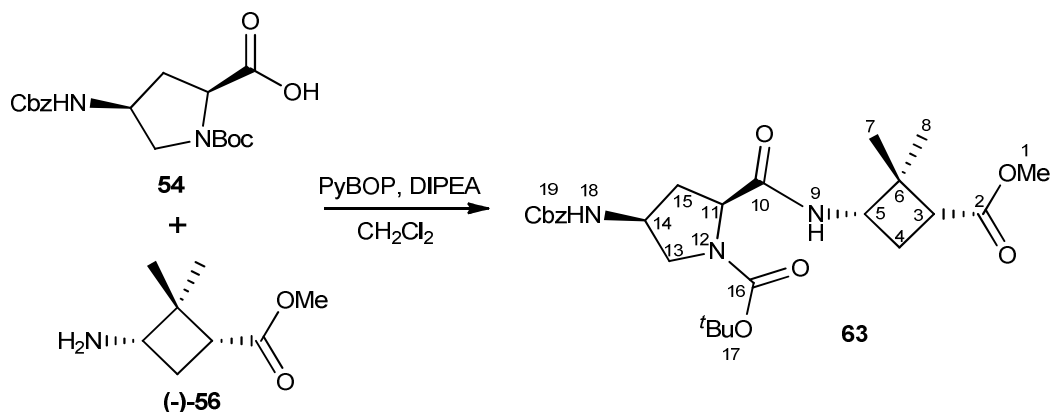
Compound **(-)-47** (400 mg, 1.4 mmol) in methanol (15 mL) was hydrogenated under 5 atmospheres of pressure in the presence of 10% Pd/C (100 mg, 2.5% Pd in weight) overnight. The reaction mixture was filtered through Celite<sup>®</sup> and solvent was removed under reduced pressure. The resulting crude was purified by column chromatography on silica gel (hexane to methanol) to provide amine **(-)-56** (210 mg, 96% yield) as a colourless oil which was identified by its <sup>1</sup>H and <sup>13</sup>C NMR spectra and used in the next step without further purification.

#### Spectroscopic data compound **(-)-56**:

<sup>1</sup>H NMR (250 MHz, CDCl<sub>3</sub>) δ 0.93 (s, 3H, *trans*-CH<sub>3</sub>), 1.17 (s, 3H, *cis*-CH<sub>3</sub>), 2.00-2.15 (m, 1H, H<sub>4a</sub>), 2.16-2.30 (m, 1H, H<sub>4b</sub>), 2.45-2.59 (m, 1H, H<sub>3</sub>), 3.14 (t, *J*<sub>H,H</sub> = 9 Hz, 1H, H<sub>1</sub>), 3.61 (s, 3H, CO<sub>2</sub>CH<sub>3</sub>).

<sup>13</sup>C NMR (62.5 MHz, CDCl<sub>3</sub>) δ 16.4 (*trans*-CH<sub>3</sub>), 23.2 (C<sub>4</sub>), 28.8 (*cis*-CH<sub>3</sub>), 29.9 (C<sub>3</sub>), 43.4 (C<sub>2</sub>), 51.9 (CO<sub>2</sub>CH<sub>3</sub>), 56.6 (C<sub>1</sub>), 173.4 (CO<sub>2</sub>CH<sub>3</sub>).

#### γ-Dipeptide **63**:



Acid **54** (210 mg, 0.6 mmol), DIPEA (0.34 mL, 1.7 mmol, 3.0 eq) and PyBOP (480 mg, 0.9 mmol, 1.5 eq) were dissolved in anhydrous dichloromethane (15 mL). The mixture was

stirred for 5 minutes under nitrogen atmosphere, and then a solution of amine (-)-**56** (90 mg, 0.6 mmol) in anhydrous dichloromethane (10 mL) was added via cannula. After stirring at room temperature for 2 hours the reaction crude was washed with a saturated aqueous sodium bicarbonate solution. The organic phase was dried over magnesium sulfate and the solvents were removed under vacuum. The reaction crude was purified by column chromatography on neutral silica gel (ethyl acetate-hexane, 1:1) to afford pure dipeptide **63** (276 mg, 95%) as a white solid.

**Spectroscopic data and physical constants for compound 63:**

$[\alpha]_D = -109.4$  (*c* 0.39, CH<sub>2</sub>Cl<sub>2</sub>).

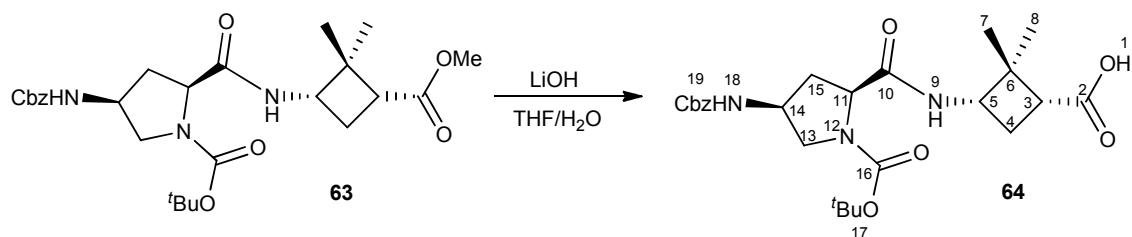
**Melting point:** 59-62 °C (diethyl ether).

**IR (ATR):** 3305 (NH<sub>st</sub>), 2958 (CH<sub>st</sub>), 1679 and 1671 (bs, CO<sub>carbamate</sub> + CO<sub>ester</sub> + CO<sub>amide</sub>), 1541, 1406.

**<sup>1</sup>H NMR** (600 MHz, CDCl<sub>3</sub>) δ 0.95 (s, 3H, H<sub>7</sub>), 1.28 (s, 3H, H<sub>8</sub>), 1.47 (s, 9H, H<sub>17</sub>), 2.09-2.13 (m, 1H, H<sub>4 proS</sub>), 2.14-2.17 (m, 1H, H<sub>15 proS</sub>), 2.30-2.34 (m, 1H, H<sub>4 proR</sub>), 2.36-2.39 (m, 1H, H<sub>15 proS</sub>), 2.61 (dd, *J*<sub>H,H</sub> = 8.9 Hz, 1H, H<sub>3</sub>), 3.45 (dd, *J*<sub>H,H</sub> = 10.8 Hz, 1H, H<sub>13 proS</sub>), 3.54 (dd, *J*<sub>H,H</sub> = 10.8 Hz, *J*<sub>H,H</sub> = 4.8 Hz, 1H, H<sub>13 proR</sub>), 3.69 (s, 3H, H<sub>1</sub>), 4.06 (dd, *J*<sub>H,H</sub> = 17.2 Hz, *J*<sub>H,H</sub> = 8.5 Hz, 1H, H<sub>5</sub>), 4.29-4.30 (m, 1H, H<sub>14</sub>), 4.42 (d, *J*<sub>H,H</sub> = 8.8 Hz, 1H, H<sub>11</sub>), 5.06 (d, *J*<sub>H,H</sub> = 12.3 Hz, 1H, H<sub>19 CH2</sub>), 5.13 (d, *J*<sub>H,H</sub> = 12.3 Hz, 1H, H<sub>19 CH2</sub>), 6.68 (d, *J*<sub>H,H</sub> = 6.4 Hz, 1H, H<sub>18</sub>), 7.32-7.37 (m, 5H, H<sub>19 Ar</sub>), 7.67 (d, *J*<sub>H,H</sub> = 7.6 Hz, 1H, H<sub>9</sub>).

**<sup>13</sup>C NMR** (150 MHz, CDCl<sub>3</sub>) δ 17.2 (C<sub>8</sub>), 26.3 (C<sub>4</sub>), 28.3 (3C, C<sub>17</sub>), 28.8 (C<sub>7</sub>), 31.8 (C<sub>15</sub>), 43.1 (C<sub>3</sub>), 46.0 (C<sub>6</sub>), 50.0 (C<sub>5</sub>), 50.7 (C<sub>14</sub>), 51.5 (C<sub>1</sub>), 55.1 (C<sub>13</sub>), 59.2 (C<sub>11</sub>), 66.5 (C<sub>19,CH2</sub>), 81.2 (C<sub>17q</sub>), 128.0, 128.2 and 128.5 (C<sub>19 Ar</sub>), 136.7 (C<sub>19q</sub>), 156.0 (C<sub>19,CO</sub>), 156.3 (C<sub>16</sub>), 172.1 (C<sub>2</sub>), 172.9 (C<sub>10</sub>).

**High resolution mass spectrum:** calculated for C<sub>26</sub>H<sub>37</sub>N<sub>3</sub>NaO<sub>7</sub>, (M+Na)<sup>+</sup>: 526.2524, Found: 526.2506.

**$\gamma$ -Dipeptide 64:**

To an ice-cooled solution of ester **63** (200 mg, 0.4 mmol) in THF (6.5 mL) was added a 5% solution of LiOH in water (2.46 mL, 5.2 mmol, 13 eq). The reaction was let to stir for 48 hours (reaction progress was monitored by HPLC/MS). Afterwards the crude was brought to pH 2-3 through the addition of a 5% solution of HCl in water. The acid solution was extracted with dichloromethane (4 x 30 mL), the organic extracts were dried over anhydrous magnesium sulfate and solvent was removed to afford carboxylic acid **64** as a white powder (170 mg, 85% yield) which was identified by its spectroscopic data and immediately used in the condensation step without purification.

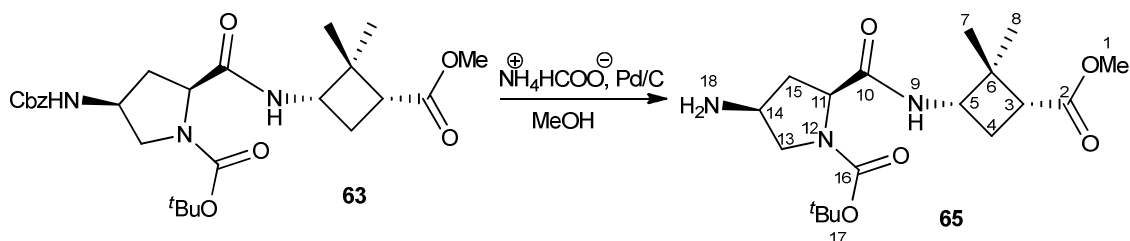
**Spectroscopic data and physical constants for compound 64:**

$[\alpha]_D = -54.2$  (*c* 0.48, CH<sub>2</sub>Cl<sub>2</sub>).

**Melting point:** 106-109 °C (diethyl ether).

**IR (ATR):** 3337 (NH<sub>st</sub> + OH<sub>st</sub>), 2960 (CH<sub>st</sub>), 2928 (CH<sub>st</sub>), 1701 and 1692 (bs, CO<sub>carbamate</sub> + CO<sub>acid</sub> + CO<sub>amide</sub>), 1531, 1410.

**High resolution mass spectrum:** calculated for C<sub>26</sub>H<sub>35</sub>N<sub>3</sub>NaO<sub>7</sub>, (M+Na)<sup>+</sup>: 512.2367, Found: 512.2360.

**$\gamma$ -Dipeptide 65:**

To a solution of **63** (206 mg, 0.4 mmol) in 15 mL of anhydrous methanol were subsequently added ammonium formate (240 mg, 3.0 mmol, 7.5 eq) and 10% Pd/C (100 mg, 5% Pd in weight). The resulting mixture was heated at reflux for 2 h (reaction progress was monitored by HPLC/MS). Afterwards, the reaction mixture was filtered through Celite<sup>®</sup>, and the solvent was eliminated under vacuo to obtain a white solid identified as amine **65** (130 mg, 86% yield) by its spectroscopic data and immediately used in the condensation step without purification.

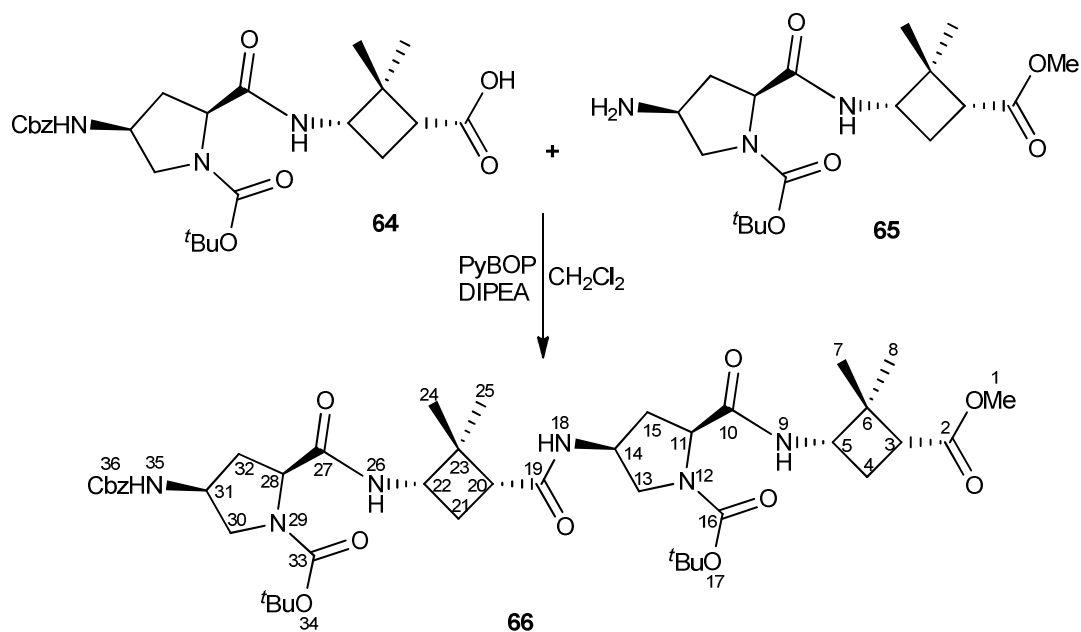
**Spectroscopic data and physical constants for compound 65:**

$[\alpha]_D = -64.9$  ( $c$  0.37,  $\text{CH}_2\text{Cl}_2$ ).

**Melting point:** 29-31 °C (diethyl ether).

**IR (ATR):** 3300 ( $\text{NH}_{\text{st}}$ ), 2957 ( $\text{CH}_{\text{st}}$ ), 1730 ( $\text{CO}_{\text{ester}}$ ), 1682 ( $\text{CO}_{\text{amide}}$ ), 1551, 1394.

**High resolution mass spectrum:** calculated for  $\text{C}_{18}\text{H}_{32}\text{N}_3\text{NaO}_5$ , ( $\text{M}+\text{Na}$ )<sup>+</sup>: 370.2336, Found: 370.2323.

**$\gamma$ -Tetrapeptide 66:**

Acid **64** (160 mg, 0.3 mmol), DIPEA (0.20 mL, 1.0 mmol, 3 eq) and PyBOP (280 mg, 0.5 mmol, 1.5 eq) were dissolved in anhydrous dichloromethane (15 mL). The mixture was stirred for 5 minutes under nitrogen atmosphere, and then a solution of amine **65** (120mg, 0.3 mmol) in anhydrous dichloromethane (5 mL) was added via cannula. After stirring at room temperature for 2 hours the reaction crude was washed with a saturated aqueous sodium bicarbonate solution. The organic phase was dried over magnesium sulfate and the solvents were removed under vacuum. The reaction crude was purified by column chromatography on neutral silica gel (ethyl acetate) to afford pure tetrapeptide **66** (255 mg, 92% yield) as a white solid.

**Spectroscopic data and physical constants for compound 66:**

$[\alpha]_D = -16.4$  ( $c$  0.57,  $\text{CH}_2\text{Cl}_2$ ).

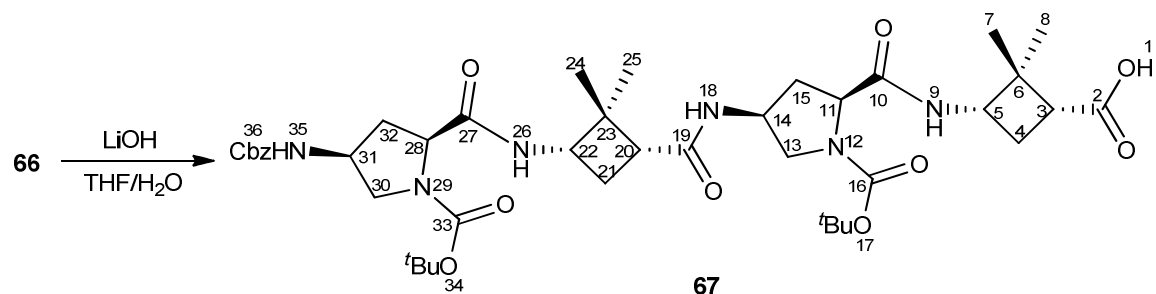
**Melting point:** 129-131 °C ( $\text{Et}_2\text{O}$ ).

**IR (ATR):** 3640 ( $\text{NH}_{\text{st}}$ ), 3571 ( $\text{NH}_{\text{st}}$ ), 3292 ( $\text{NH}_{\text{st}}$ ), 2956 ( $\text{CH}_{\text{st}}$ ), 1665 (bs,  $\text{CO}_{\text{carbamates}}$  +  $\text{CO}_{\text{esters}}$  +  $\text{CO}_{\text{amides}}$ ), 1524, 1391, 1368.

**$^1\text{H}$  NMR** (600 MHz,  $\text{CDCl}_3$ )  $\delta$  0.93 (s, 3H,  $\text{H}_{25}$ ), 0.95 (s, 3H,  $\text{H}_8$ ), 1.27 (s, 3H,  $\text{H}_7$ ), 1.31 (s, 3H,  $\text{H}_{24}$ ), 1.46 (s, 18H,  $\text{H}_{17}$  and  $\text{H}_{34}$ ), 2.10-2.20 (c.a., 4H,  $\text{H}_4$  proS,  $\text{H}_{15}$  proS,  $\text{H}_{21}$  proS and  $\text{H}_{32}$  proS), 2.24-2.27 (m, 1H,  $\text{H}_{15}$  proR), 2.30-2.46 (c.a., 4H,  $\text{H}_4$  proR,  $\text{H}_{20}$  proR,  $\text{H}_{21}$  proR and  $\text{H}_{32}$  proR), 2.63 (dd,  $J_{\text{H,H}} = 10.1$  Hz,  $J_{\text{H,H}} = 7.8$  Hz, 1H,  $\text{H}_3$ ), 3.38 (d,  $J_{\text{H,H}} = 11.6$  Hz, 1H,  $\text{H}_{13}$  proS), 3.45 (d,  $J_{\text{H,H}} = 11.5$  Hz, 1H,  $\text{H}_{30}$  proS), 3.49-3.55 (c.a., 2H,  $\text{H}_{13}$  proR and  $\text{H}_{30}$  proR), 3.70 (s, 3H,  $\text{H}_1$ ), 4.00-4.08 (c.a., 2H,  $\text{H}_5$  and  $\text{H}_{22}$ ), 4.26-4.32 (m, 1H,  $\text{H}_{31}$ ), 4.39-4.43 (c.a., 2H,  $\text{H}_{11}$  and  $\text{H}_{28}$ ), 4.45-4.50 (m, 1H,  $\text{H}_{14}$ ), 5.04 (d,  $J_{\text{H,H}} = 12.3$  Hz, 1H,  $\text{H}_{36}$  CH<sub>2</sub>), 5.12 (d,  $J_{\text{H,H}} = 12.3$  Hz, 1H,  $\text{H}_{36}$  CH<sub>2</sub>), 6.80 (d,  $J_{\text{H,H}} = 7.1$  Hz, 1H,  $\text{H}_{35}$ ), 7.29-7.41 (c.a., 5H,  $\text{H}_{36}$  Ar), 7.64-7.75 (m, 3H,  $\text{H}_9$ ,  $\text{H}_{18}$  and  $\text{H}_{26}$ ).

**$^{13}\text{C}$  NMR** (150 MHz,  $\text{CDCl}_3$ )  $\delta$  17.0 ( $\text{C}_{25}$ ), 17.3 ( $\text{C}_8$ ), 25.8 ( $\text{C}_4$ ), 26.3 ( $\text{C}_{21}$ ), 28.4 (6C,  $\text{C}_{17}$ ,  $\text{C}_{34}$ ), 28.8 ( $\text{C}_{24}$ ), 29.0 ( $\text{C}_7$ ), 31.9 ( $\text{C}_{15}$ ), 32.1 ( $\text{C}_{32}$ ), 43.0 ( $\text{C}_3$ ), 44.7 ( $\text{C}_{20}$ ), 45.6 and 45.9 (2C,  $\text{C}_{25}$ ,  $\text{C}_6$ ), 49.0 ( $\text{C}_1$ ), 49.9 (2C,  $\text{C}_5$ ,  $\text{C}_{22}$ ), 50.7 ( $\text{C}_{31}$ ), 51.7 ( $\text{C}_{14}$ ), 55.2 (2C,  $\text{C}_{13}$ ,  $\text{C}_{30}$ ), 59.2 (2C,  $\text{C}_{11}$ ,  $\text{C}_{28}$ ), 66.6 ( $\text{C}_{36}$  CH<sub>2</sub>), 81.2 and 81.3 (2C,  $\text{C}_{17\text{q}}$ ,  $\text{C}_{34\text{q}}$ ), 128.1, 128.3 and 128.5 ( $\text{C}_{36}$  Ar), 136.6 ( $\text{C}_{36\text{q}}$ ), 156.1 and 156.2 (3C,  $\text{C}_{16}$ ,  $\text{C}_{33}$ ,  $\text{C}_{36}$  CO), 171.1 ( $\text{C}_{19}$ ), 172.1 ( $\text{C}_{27}$ ), 172.5 ( $\text{C}_{10}$ ), 173.0 ( $\text{C}_2$ ).

**High resolution mass spectrum:** calculated for  $\text{C}_{43}\text{H}_{64}\text{N}_6\text{O}_{11}$ , ( $\text{M}+\text{Na}$ )<sup>+</sup>: 863.4525, Found: 841.4698.

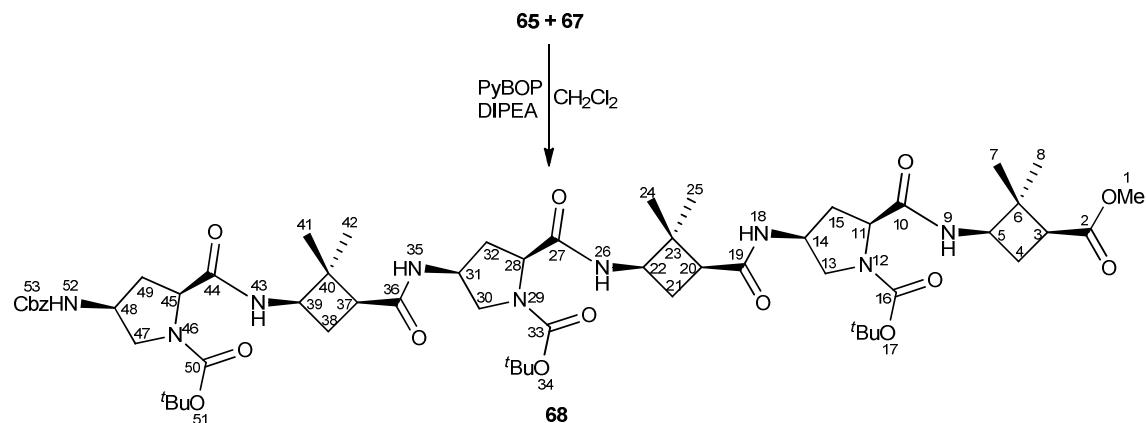
**$\gamma$ -Tetrapeptide 67:**

To an ice-cooled solution of ester **66** (101 mg, 0.1 mmol) in THF (5 mL) was added a 5% solution of LiOH in water (1.90 mL, 0.6 mmol, 6 eq). The reaction was let to stir for 48 hours (reaction progress was monitored by HPLC/MS). Afterwards the crude was brought to pH 2-3 through the addition of a 5% solution of HCl in water. The acid solution was extracted with dichloromethane (4 x 30 mL), the organic extracts were dried over anhydrous magnesium sulfate and solvent was removed to afford carboxylic acid **67** as a white powder (90 mg, 90% yield) which was identified by its spectroscopic data and immediately used in the condensation step without purification.

**Physical constants for compound 67:**

**Melting point:** 106-109 °C (Et<sub>2</sub>O).



**$\gamma$ -Hexapeptide 68:**

Acid **67** (90 mg, 0.1 mmol), DIPEA (0.06 mL, 0.3 mmol, 3 eq) and PyBop (80 mg, 0.2 mmol, 1.5 eq) were dissolved in anhydrous dichloromethane (10 mL), the mixture was stirred for 5 minutes under nitrogen atmosphere, and then a solution of amine **65** (60 mg, 0.1 mmol) in anhydrous dichloromethane (5 mL) was added via cannula. After stirring at room temperature for 2 hours the reaction crude was washed with a saturated aqueous sodium bicarbonate solution. The organic phase was dried over magnesium sulfate and the solvents were removed under vacuum. The reaction crude was purified by column chromatography on neutral silica gel (ethyl acetate to ethyl acetate-methanol, 19:1) to afford pure hexapeptide **68** (100 mg, 84% yield) as a white solid.

**Spectroscopic data and physical constants for compound 68:**

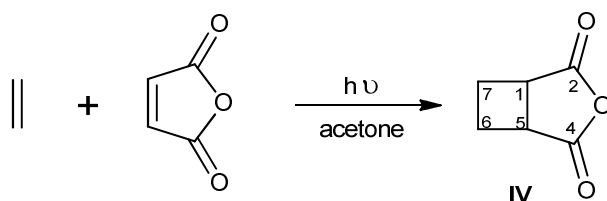
$[\alpha]_D = -131.0$  ( $c$  0.13,  $\text{CH}_2\text{Cl}_2$ ).

**Melting point:** 144-146 °C ( $\text{AcCN}/\text{H}_2\text{O}$ ).

**IR (ATR):** 3292 ( $\text{NH}_{\text{st}}$ ), 2957 ( $\text{CH}_{\text{st}}$ ), 1666 (bs,  $\text{CO}_{\text{carbamates}} + \text{CO}_{\text{esters}} + \text{CO}_{\text{amides}}$ ), 1534, 1392, 1368.

**$^1\text{H}$  NMR (600 MHz,  $\text{CDCl}_3$ )**  $\delta$  0.93-0.97 (m, 9H,  $\text{H}_8$ ,  $\text{H}_{25}$  and  $\text{H}_{42}$ ), 1.21-1.31 (m, 9H,  $\text{H}_7$ ,  $\text{H}_{24}$  and  $\text{H}_{41}$ ), 1.44-1.46 (m, 27H,  $\text{H}_{17}$ ,  $\text{H}_{34}$  and  $\text{H}_{51}$ ), 2.10-2.44 (m, 14H,  $\text{H}_4$ ,  $\text{H}_{15}$ ,  $\text{H}_{21}$ ,  $\text{H}_{32}$ ,  $\text{H}_{38}$ ,  $\text{H}_{49}$ ,  $\text{H}_{20}$  and  $\text{H}_{37}$ ), 2.62-2.65 (m, 1H,  $\text{H}_3$ ), 3.37-3.53 (m, 6H,  $\text{H}_{13}$ ,  $\text{H}_{30}$  and  $\text{H}_{47}$ ), 3.69 (s, 3H,  $\text{H}_1$ ), 4.02-4.07 (m, 3H,  $\text{H}_5$ ,  $\text{H}_{22}$  and  $\text{H}_{39}$ ), 4.28-4.29 (m, 1H,  $\text{H}_{48}$ ), 4.37-4.43 (m, 3H,  $\text{H}_{11}$ ,  $\text{H}_{28}$  and  $\text{H}_{45}$ ), 4.47-4.51 (m, 2H,  $\text{H}_{14}$  and  $\text{H}_{31}$ ), 5.04 (d,  $J_{\text{H,H}} = 12.3$  Hz, 1H,  $\text{H}_{53 \text{ CH}_2}$ ), 5.12 (d,  $J_{\text{H,H}} = 12.3$  Hz, 1H,  $\text{H}_{53 \text{ CH}_2}$ ), 6.81 (d,  $J_{\text{H,H}} = 7.2$  Hz, 1H,  $\text{H}_{52}$ ), 7.33-7.37 (m, 5H,  $\text{H}_{53 \text{ Ar}}$ ), 7.62 (d,  $J_{\text{H,H}} = 7.9$  Hz, 1H,  $\text{H}_{26}$ ), 7.67-7.75 (m, 4 H,  $\text{H}_9$ ,  $\text{H}_{18}$ ,  $\text{H}_{35}$  and  $\text{H}_{43}$ ).

**High resolution mass spectrum:** calculated for  $\text{C}_{60}\text{H}_{91}\text{N}_9\text{O}_{15}$ ,  $(\text{M}+\text{Na})^+$ : 1200.6527, Found: 1200.6509.

**(1R,5S)-3-Oxabicyclo[3.2.0]heptane-2,4-dione IV:**

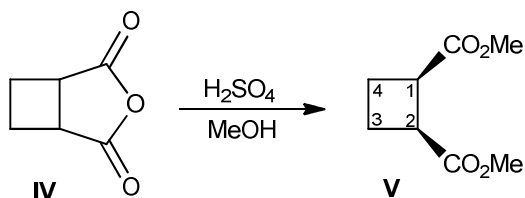
A solution containing 2.00 g (20.4 mmol) of maleic anhydride in 500 mL of acetone was placed in a photochemical reactor. The mixture was cooled at -40 °C and an ethylene flow connected until the solution was saturated. The system was stirred for 4-5 hours and recharged with ethylene the as many times as it was required (reaction progress was monitored by GC). Then, solvent was evaporated under vacuum to provide 2.57 g of **IV** as a pale yellow crystalline solid in a quantitative yield.

**Spectroscopic data of compound IV:**

$^1\text{H NMR}$  (250 MHz,  $\text{CDCl}_3$ )  $\delta$  2.33-2.48 (c.a., 2H,  $\text{H}_{7a}$ ,  $\text{H}_{6a}$ ), 2.67-2.87 (c.a., 2H,  $\text{H}_{6b}$ ,  $\text{H}_{7b}$ ), 3.45-3.58 (c.a., 2H,  $\text{H}_1$ ,  $\text{H}_5$ ).

Spectroscopic data are consistent with those reported in reference:

Zhao, L-X.; Park, J.G.; Moon, Y-S.; Basnet, A.; Choi, J.; Kim, E-K.; Jeong, T.C.; Jahng, Y.; Lee, E-S. *Il Farmaco* **2004**, *59*, 381-387.

**(1R,2S)-Dimethyl-cyclobutane-1,2-dicarboxylate, V:**

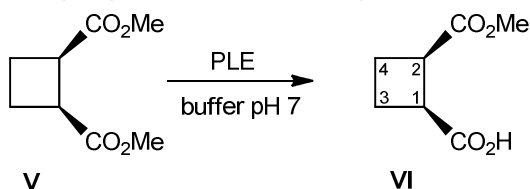
To a solution containing of cyclobutane anhydride **IV** (2.57 g, 20.4 mmol) in 50 mL of  $\text{MeOH}$ , 1 mL of concentrated  $\text{H}_2\text{SO}_4$  was added. The mixture was stirred at room temperature overnight. Then, solvent was evaporated under vacuum, 30 mL of  $\text{EtOAc}$  were added and the resulting solution was washed with  $\text{H}_2\text{O}$  (2 x 20 mL). The organic layer was dried over anhydrous  $\text{MgSO}_4$  and solvents removed under reduced pressure to afford 2.93 g of a pale brown dense oil. This one was later purified by reduced pressure distillation to provide **V** (2.39 g, 68% yield) as a colourless oil.

**Spectroscopic data of compound V:**

$^1\text{H NMR}$  (250 MHz,  $\text{CDCl}_3$ )  $\delta$  2.13-2.26 (c.a., 2H,  $\text{H}_{3a}$ ,  $\text{H}_{4a}$ ), 2.28-2.45 (c.a., 2H,  $\text{H}_{3b}$ ,  $\text{H}_{4b}$ ), 3.35-3.45 (c.a., 2H,  $\text{H}_1$ ,  $\text{H}_2$ ), 3.68 (s, 3H,  $\text{CH}_3$ ).

Spectroscopic data are consistent with those reported in reference:

Torres, E.; Gorrea, E.; Burusco, K.K.; Da Silva, E.; Nolis, P.; Rúa, F.; Bousset, S.; Díez-Pérez, I.; Dannenberg, S.; Izquierdo, S.; Giralt, E.; Jaime, C.; Branchadell, V.; Ortuño, R.M. *Org. Biomol. Chem.* **2010**, *8*, 564-575.

**(1S,2R)-2-(Methoxycarbonyl)cyclobutane carboxylic acid VI:**

Porcine Liver esterase (PLE) (115 mg, 1955 units) was added to a solution of diester **V** (2.13 g, 1.2 mmol) in 200 mL of  $\text{KH}_2\text{PO}_4/\text{K}_2\text{HPO}_4$  buffer at pH 7. The mixture was stirred for 24 hours at room temperature. After stirring at room temperature for 24 hours, the mixture was brought to pH 2 through the addition of 5%  $\text{HCl}_{(\text{aq})}$ . The crude was extracted with  $\text{Et}_2\text{O}$  (3x200 mL), the organic layers were combined, dried over anhydrous  $\text{MgSO}_4$  and the solvents removed under reduced pressure to afford **VI** (2.02 g) as a colourless oil in quantitative yield.

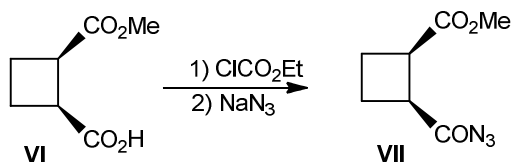
**Spectroscopic data of compound VI:**

$^1\text{H NMR}$  (250 MHz,  $\text{CDCl}_3$ )  $\delta$  2.16-2.32 (c.a. 2H,  $\text{H}_{3a}$ ,  $\text{H}_{4b}$ ), 2.32-2.47 (c.a., 2H,  $\text{H}_{3b}$ ,  $\text{H}_{4a}$ ), 3.38-3.49 (c.a., 2H,  $\text{H}_1$ ,  $\text{H}_2$ ), 3.70 (s, 3H,  $-\text{OCH}_3$ ).

$^{13}\text{C NMR}$  (62.5 MHz,  $\text{CDCl}_3$ )  $\delta$  21.9 and 22.1 ( $\text{C}_3$ ,  $\text{C}_4$ ), 40.5 (2C,  $\text{C}_1$ ,  $\text{C}_2$ ), 51.9 ( $\text{CO}_2\text{CH}_3$ ), 173.9 ( $\text{CO}_{\text{ester}}$ ), 179.4 ( $\text{CO}_{\text{acid}}$ ).

Spectroscopic data are consistent with those reported in reference:

Sabbioni, G.; Jones, J.B. *J. Org. Chem.* **1987**, *52*, 4565-4570.

**(1R,2S)-Methyl 2-(azidocarbonyl)cyclobutane carboxylate, VII:**

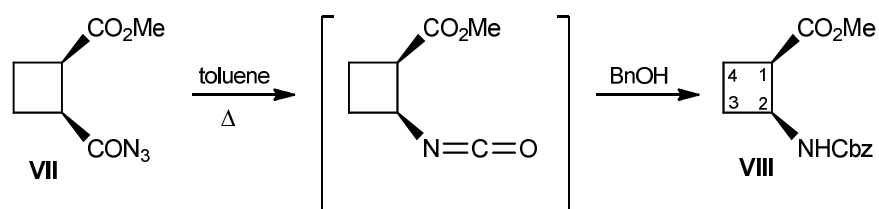
To an ice-cooled solution of half-ester **VI** (1.96 g, 12.4 mmol) in 40 mL of anhydrous acetone, triethylamine (2.8 mL, 20.2 mmol, 1.6 eq) and ethyl chloroformate (2.3 mL, 24.1 mmol, 1.9 eq) were subsequently added. The mixture was stirred at 0 °C for 30 minutes. Then, sodium azide (3.00 g, 46.1 mmol, 3.7 eq) in 5 mL of water was added and the resultant solution was stirred at room temperature for 1.5 h. The reaction mixture was extracted with dichloromethane (4 x 15 mL), and the organic extracts were dried over magnesium sulfate. Solvents were removed under reduced pressure to give acyl azide **VII** as a colourless oil (2.22 g, 98% yield), which was characterised by its spectroscopic data and used in the next step without further purification.

**Spectroscopic data of compound VII:**

IR (ATR): 3024 (NH<sub>st</sub>), 2952 (CH<sub>st</sub>), 2134 (N<sub>3</sub>), 1708 (CO).

Spectroscopic data are consistent with those reported in reference:

Martin-Vilà, M.; Muray, E.; Aguado, G. P.; Álvarez-Larena, A.; Branchadell, V.; Minguillón, C.; Giralt, E.; Ortuño, R.M. *Tetrahedron: Asymmetry* **2000**, *11*, 3569-3584.

**(1R,2S)-Methyl 2-(benzyloxycarbonylamino)cyclobutane carboxylate, VIII:**

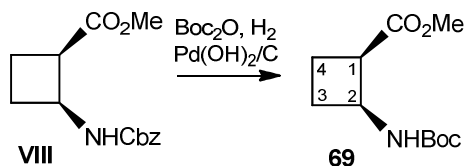
A solution of azyl azide **VII** (2.22 g, 12.2 mmol) and benzyl alcohol (1.7 mL, 16.4 mmol, 1.3 eq) in toluene (40 mL) was heated to reflux for 18 hours under nitrogen atmosphere (the reaction progress was monitored by IR following the signals for the acyl azide at 2134 cm<sup>-1</sup> and the corresponding isocyanate at 2260 cm<sup>-1</sup>). Toluene was removed at reduced pressure and then excess of benzyl alcohol was eliminated by vacuum distillation. The residue was chromatographed on silica gel (ethyl acetate-hexane, 1:2) to afford carbamate as a white solid which was crystallised (ether-pentane) to afford pure orthogonally protected amino acid **VIII** (2.19 g, 68% yield).

**Spectroscopic data of compound VIII:**

$^1\text{H NMR}$  (250 MHz,  $\text{CDCl}_3$ )  $\delta$  1.90-2.05 (c.a., 2H,  $\text{H}_{3a}$ ,  $\text{H}_{4a}$ ), 2.15-2.46 (c.a., 2H,  $\text{H}_{3b}$ ,  $\text{H}_{4b}$ ), 3.36-3.45 (m, 1H,  $\text{H}_1$ ), 3.66 (s, 3H,  $-\text{OCH}_3$ ), 4.54 (quint.,  $J_{\text{H,H}} = 8.5$  Hz, 1H,  $\text{H}_2$ ), 5.08 (s, 2H,  $\text{CH}_2_{\text{benzyl}}$ ), 5.65 (broad s, 1H,  $\text{NHCbz}$ ), 7.28-7.42 (c.a., 5H,  $\text{H}_{\text{Ar}}$ ).

Spectroscopic data are consistent with those reported in reference:

Martin-Vilà, M.; Muray, E.; Aguado, G. P.; Álvarez-Larena, A.; Branchadell, V.; Minguillón, C.; Giralt, E.; Ortuño, R.M. *Tetrahedron: Asymmetry* **2000**, *11*, 3569-3584.

**(1R,2S)-Methyl 2-(tert-butoxycarbonylamino)cyclobutane carboxylate, 69:**

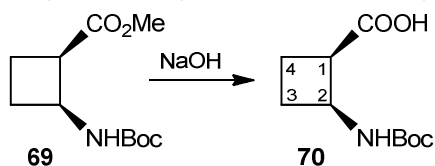
Compound **VIII** (484 mg, 1.8 mmol) in methanol (15 mL) was hydrogenated under 5 atmospheres of pressure in the presence of  $\text{Boc}_2\text{O}$  (0.6 mL, 2.7 mmol, 1.5 eq) and 20%  $\text{Pd}(\text{OH})_2/\text{C}$  (146 mg, 6% in weight of Pd) overnight. The reaction mixture was filtered through Celite<sup>®</sup> and solvent was removed under reduced pressure. The resulting crude was purified by column chromatography on silica gel (ethyl acetate-hexane, 1:4) to provide monomer **69** (340 mg, 81% yield) as a colourless oil.

**Spectroscopic data for compound 69:**

$^1\text{H NMR}$  (250 MHz,  $\text{CDCl}_3$ )  $\delta$  1.45 (s, 9H,  $^t\text{Bu}$ ), 1.90-2.07 (c.a., 2H,  $\text{H}_{3a}$ ,  $\text{H}_{4a}$ ), 2.14-2.46 (c.a., 2H,  $\text{H}_{3b}$ ,  $\text{H}_{4b}$ ), 3.34-3.48 (m, 1H,  $\text{H}_1$ ), 3.73 (s, 3H,  $-\text{OCH}_3$ ), 4.38-4.59 (m, 1H,  $\text{H}_2$ ), 5.36 (bs, 1H, NH).

Spectroscopic data are consistent with those reported in reference:

Izquierdo, S.; Rúa, F.; Sbai, A.; Parella, T.; Álvarez-Larena, A.; Branchadell, V.; Ortuño, R.M. *J. Org. Chem.* **2005**, *70*, 7963–7971.

**(1R,2S)-2-(tert-butoxycarbonylamino)cyclobutanecarboxylic acid, 70:**

A mixture of **69** (168 mg, 0.7 mmol) in  $\text{H}_2\text{O}$ -THF (7 mL, 10:1) and 0.25 M NaOH (6 mL, 1.5 mmol, 2.1 eq) was stirred at 0 °C for 3 h. Then the reaction mixture was washed with  $\text{CH}_2\text{Cl}_2$ , and 4 M HCl was added to the aqueous layer to reach pH 2. Then the acid aqueous phase was extracted with dichloromethane, and the solvent was removed at reduced pressure to afford acid **70** as a white solid (129 mg, 82% yield).

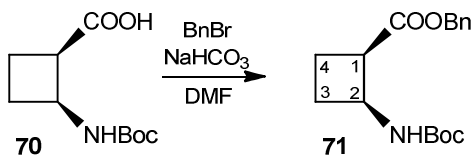
**Spectroscopic data for compound 70:**

$^1\text{H NMR}$  (250 MHz,  $\text{CDCl}_3$ )  $\delta$  1.45 (s, 9H,  $^t\text{Bu}$ ), 1.68-1.76 (m, 1H,  $\text{H}_{4a}$ ), 2.00-2.08 (m, 1H,  $\text{H}_{3a}$ ), 2.16-2.45 (c.a., 2H,  $\text{H}_{3b}$ ,  $\text{H}_{4b}$ ), 3.34-3.48 (m, 1H,  $\text{H}_1$ ), 4.36-4.57 (m, 1H,  $\text{H}_2$ ).

Spectroscopic data are consistent with those reported in reference:

Izquierdo, S.; Rúa, F.; Sbai, A.; Parella, T.; Álvarez-Larena, A.; Branchadell, V.; Ortuño, R.M. *J. Org. Chem.* **2005**, *70*, 7963–7971.



**(1*R*,2*S*)-Benzyl 2-(*tert*-butoxycarbonylamino)cyclobutanecarboxylate, 71:**

To a solution of acid **70** (140 mg, 0.7 mmol) in 10 mL of DMF were subsequently added NaHCO<sub>3</sub> (0.11 g, 1.3 mmol, 2.0 eq) and benzyl bromide (80 μL, 0.7 mmol, 1.1 eq). After being stirred for 48 h at room temperature, the solution was diluted with 30 mL of ethyl acetate and 30 mL of water. The organic layer was separated, and the aqueous layer was extracted with ethyl acetate (2 x 30 mL). The combined organic layers were washed with water and dried over MgSO<sub>4</sub>. The solvent was evaporated to afford pure **71** (200 mg, 0.65 mmol) in a quantitative yield as a white solid.

**Spectroscopic data and physical constants for compound 71:**

$[\alpha]_D = -72.5$  (*c* 1.00, CH<sub>2</sub>Cl<sub>2</sub>).

**Melting point:** 39-41 °C (Ethyl acetate).

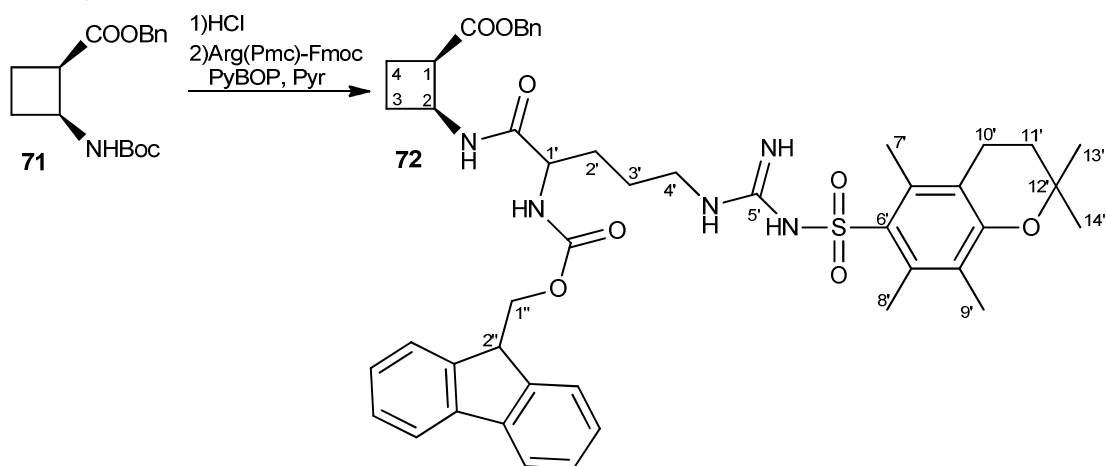
**IR (ATR):** 3364 (NH<sub>st</sub>), 2976 (CH<sub>st</sub>), 1711 (bs, CO<sub>carbamate</sub> + CO<sub>ester</sub>), 1501, 1338.

**<sup>1</sup>H NMR** (300 MHz, CDCl<sub>3</sub>) δ 1.38 (s, 9H, <sup>t</sup>Bu), 2.01-1.82 (c.a., 2H, H<sub>3a</sub>, H<sub>4a</sub>), 2.37-2.12 (c.a., 2H, H<sub>3b</sub>, H<sub>4b</sub>), 3.46-3.32 (m, 1H, H<sub>1</sub>), 4.53-4.39 (m, 1H, H<sub>2</sub>), 5.20-5.04 (m, 2H, CH<sub>2</sub>Bn), 5.40 (bs, 1H, NH), 7.35-7.28 (c.a., 5H, H<sub>Ar</sub>).

**<sup>13</sup>C NMR** (75 MHz, CDCl<sub>3</sub>) δ 18.5 (C<sub>4</sub>), 28.3 (C(CH<sub>3</sub>)<sub>3</sub>), 29.7 (C<sub>3</sub>), 45.5 (C<sub>1</sub>), 45.8 (C<sub>2</sub>), 66.4 (CH<sub>2</sub>Bn), 79.3 (C(CH<sub>3</sub>)<sub>3</sub>), 128.2, 128.6, 135.9 (6C, C<sub>Ar</sub>), 154.7 (CO<sub>carbamate</sub>), 174.0 (CO<sub>2</sub>Bn).

**High resolution mass spectrum:** calculated for C<sub>17</sub>H<sub>23</sub>NO<sub>4</sub>, (M<sup>+</sup>)<sup>+</sup>: 305.1627, Found: 305.1631.

**(1*R*,2*S*)-Benzyl 2-(2-((9*H*-fluoren-9-yl)methoxycarbonylamino)-5-(3-((2,2,5,7,8-pentamethylchroman-6-yl)sulfonyl)guanidino)pentanamido)cyclobutane carboxylate, **72**:**



A solution of **71** (200 mg, 0.7 mmol) in 3 M HCl in ethyl acetate (4.5 mL, 21 eq) was stirred at 0 °C for 3h. The solution was then evaporated, the resulting salt was resuspended in CH<sub>2</sub>Cl<sub>2</sub> (10 mL) and Fmoc-Arg(Pmc)-OH (562 mg, 0.8 mmol, 1.1 eq), PyBOP (417 mg, 0.8 mmol, 1.1 eq) and pyridine (119 μL, 1.5 mmol, 2.1 eq) were added. The mixture was stirred overnight at room temperature. The solution was washed with saturated NaHCO<sub>3</sub> (3 x 20 mL), the organic phase was dried over MgSO<sub>4</sub> and concentrated under vacuum. The resulting crude was purified by column chromatography on silica gel (ethyl acetate-petrol ether, 1:1 to ethyl acetate) to afford pure **72** as a white solid (429 mg, 77% yield).

**Spectroscopic data and physical constants for compound 72:**

$[\alpha]_D = -41.3$  (c 0.63, CH<sub>2</sub>Cl<sub>2</sub>).

**Melting point:** 101-102 °C (Ethyl acetate).

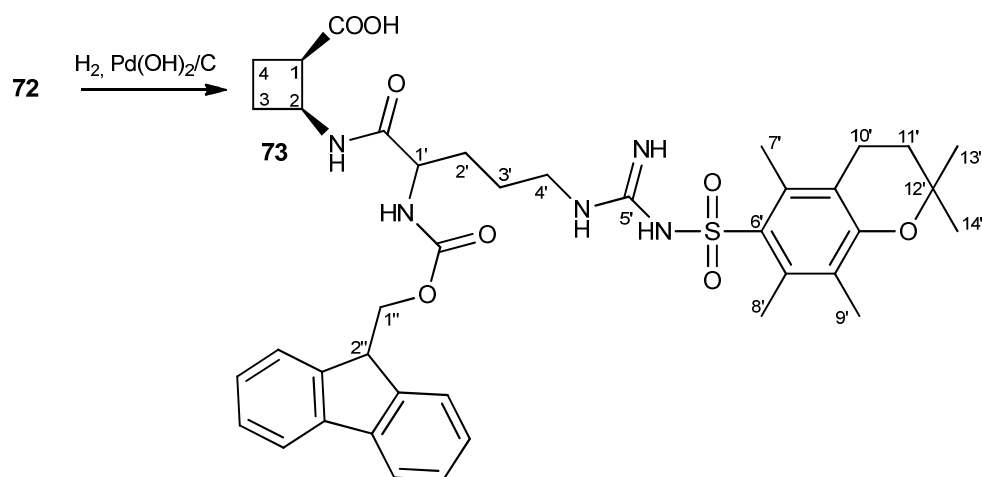
**IR (ATR):** 3464(NH<sub>st</sub>), 3332 (NH<sub>st</sub>), 2939 (CH<sub>st</sub>), 1724 (CO<sub>ester</sub>), 1677 (CO<sub>carbamate</sub>), 1621 (CO<sub>amide</sub>), 1548, 1451, 1391.

**<sup>1</sup>H NMR (300 MHz, CDCl<sub>3</sub>)**  $\delta$  1.24-1.37 (s, 6H, H<sub>13'</sub>, H<sub>14'</sub>), 1.45-1.55 (c.a., 3H, H<sub>3'</sub>, H<sub>4a</sub>), 1.74-1.82 (c.a., 3H, H<sub>2'</sub>, H<sub>4b</sub>), 2.00-2.17 (c.a., 5H, H<sub>9'</sub>, H<sub>3a</sub>, H<sub>3b</sub>), 2.23-2.42 (m, 2H, H<sub>11'</sub>), 2.52-2.67 (c.a., 8H, H<sub>7'</sub>, H<sub>8'</sub>, H<sub>10'</sub>), 3.08-3.32 (c.a., 2H, H<sub>4'</sub>), 3.36-3.49 (m, 1H, H<sub>1</sub>), 4.04-4.15 (m, 1H, H<sub>2</sub>), 4.15-4.23 (t,  $J_{H,H} = 6.8$  Hz, 1H, H<sub>1'</sub>), 4.38 (d,  $J_{H,H} = 7.0$  Hz, 2H, H<sub>1''</sub>), 4.62-4.79 (m, 1H, H<sub>2''</sub>), 5.10 (dd,  $J_{H,H} = 26.7$  Hz,  $J_{H,H} = 12.2$  Hz, 2H, CH<sub>2</sub>Bn), 5.70 (d,  $J_{H,H} = 7.2$  Hz, 1H, NH<sub>carbamate</sub>), 6.16 (bs, 2H, NH<sub>guanidino</sub>), 7.20 (d,  $J_{H,H} = 8.3$  Hz, 1H, NH<sub>amide</sub>), 7.29-7.35 (c.a., 7H, H<sub>Fmoc</sub>, H<sub>Bn</sub>), 7.40 (t,  $J_{H,H} = 7.2$  Hz, 2H, H<sub>Fmoc</sub>), 7.51-7.64 (m, 2H, H<sub>Fmoc</sub>), 7.76 (d,  $J_{H,H} = 7.6$  Hz, 2H, H<sub>Fmoc</sub>).

**<sup>13</sup>C NMR (75 MHz, CDCl<sub>3</sub>)**  $\delta$  12.1 (C<sub>7'</sub>), 18.5 (C<sub>9'</sub>), 19.3 (C<sub>8'</sub>), 21.4 (C<sub>4</sub>), 25.1 (C<sub>3'</sub>), 26.7 (2C, C<sub>13'</sub> and C<sub>14'</sub>), 28.6 (C<sub>11'</sub>), 30.0 (C<sub>3</sub>), 30.1 (C<sub>2'</sub>), 32.7 (C<sub>10'</sub>), 40.5 (C<sub>4'</sub>), 44.5 (C<sub>2''</sub>), 44.8 (C<sub>1</sub>), 47.0 (C<sub>2</sub>), 54.1 (C<sub>1'</sub>), 66.4 (CH<sub>2</sub>Bn), 67.2 (C<sub>1''</sub>), 73.6 (C<sub>12'</sub>), 117.9, 119.9, 124.1, 125.2, 127.1, 127.7, 128.0, 128.1, 128.3, 128.6, 133.1, 134.9, 135.5, 135.7, 141.2, 143.6, 143.8 (24C, C<sub>Ar</sub>), 153.6 (CO<sub>carbamate</sub>), 156.3 (CO<sub>guanidino</sub>), 171.2 (CO<sub>amide</sub>), 173.7 (CO<sub>ester</sub>).

**High resolution mass spectrum:** calculated for C<sub>47</sub>H<sub>56</sub>N<sub>5</sub>O<sub>8</sub>S, (MH<sup>+</sup>)<sup>+</sup>: 850.3850, Found: 850.3868.

**(1*R*,2*S*)-2-(2-((9*H*-Fluoren-9-yl)methoxycarbonylamino)-5-(3-((2,2,5,7,8-pentamethylchroman-6-yl)sulfonyl)guanidino)pentanamido)cyclobutane carboxylic acid, **73**:**



A solution of **72** (665 mg, 0.8 mmol) in 15 mL of methanol was hydrogenated under 5 atmospheres of pressure in the presence of 20%  $\text{Pd}(\text{OH})_2/\text{C}$  (50 mg, 1% Pd in weight) overnight. Afterwards, the reaction mixture was filtered through Celite<sup>®</sup>, and the solvent was eliminated under vacuo to obtain a white solid identified as carboxylic acid **73** (591 mg, quantitative yield) by its spectroscopic data and immediately used in the condensation step without purification.

**Spectroscopic data and physical constants for compound 73:**

$[\alpha]_D = -23.7$  ( $c$  0.66,  $\text{CH}_2\text{Cl}_2$ ).

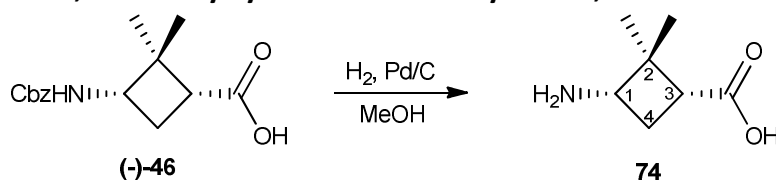
**Melting point:** 114-115 °C (EtOAc).

**IR (ATR):** 3450 ( $\text{NH}_{\text{st}} + \text{CO}_{\text{st}}$ ), 2975 ( $\text{CH}_{\text{st}}$ ), 2943 ( $\text{CH}_{\text{st}}$ ), 1709 ( $\text{CO}_{\text{acid}}$ ), 1653 ( $\text{CO}_{\text{carbamate}}$ ), 1630 ( $\text{CO}_{\text{amide}}$ ), 1547, 1450, 1385.

**$^1\text{H}$  NMR** (300 MHz,  $\text{CDCl}_3$ )  $\delta$  1.28 (s, 6H,  $\text{H}_{13'}$ ,  $\text{H}_{14'}$ ), 1.59-2.41 (c.a., 13H,  $\text{H}_{3'}$ ,  $\text{H}_{4a}$ ,  $\text{H}_{2'}$ ,  $\text{H}_{4b}$ ,  $\text{H}_{9'}$ ,  $\text{H}_{3a}$ ,  $\text{H}_{3b}$ ,  $\text{H}_{11'}$ ), 2.43-2.69 (c.a., 8H,  $\text{H}_{7'}$ ,  $\text{H}_{8'}$ ,  $\text{H}_{10'}$ ), 3.08-3.54 (c.a., 3H,  $\text{H}_{4'}$ ,  $\text{H}_1$ ), 3.99-4.44 (c.a., 4H,  $\text{H}_2$ ,  $\text{H}_{1'}$ ,  $\text{H}_{1''}$ ), 4.60-4.76 (m, 1H,  $\text{H}_{2''}$ ), 6.05-6.38 (c.a., 3H,  $\text{NH}_{\text{guanidino}}$ ), 7.25-7.30 (m, 3H,  $\text{H}_{\text{Fmoc}}$ ,  $\text{NH}_{\text{carbamate}}$ ), 7.31-7.43 (m, 3H,  $\text{H}_{\text{Fmoc}}$ ,  $\text{NH}_{\text{amide}}$ ), 7.50-7.62 (m, 2H,  $\text{H}_{\text{Fmoc}}$ ), 7.70-7.81 (m, 2H,  $\text{H}_{\text{Fmoc}}$ ).

**$^{13}\text{C}$  NMR** (75 MHz,  $\text{CDCl}_3$ )  $\delta$  12.2 ( $\text{C}_{7'}$ ), 17.5 ( $\text{C}_{9'}$ ), 18.6 ( $\text{C}_{8'}$ ), 21.4 ( $\text{C}_4$ ), 25.1 ( $\text{C}_{3'}$ ), 26.7 ( $\text{C}_{13'}$  and  $\text{C}_{14'}$ ), 27.5 ( $\text{C}_{11'}$ ), 29.5 ( $\text{C}_3$ ), 30.1 ( $\text{C}_{2'}$ ), 32.7 ( $\text{C}_{10'}$ ), 40.5 ( $\text{C}_{4'}$ ), 44.7 ( $\text{C}_{2''}$ ), 45.3 ( $\text{C}_1$ ), 47.0 ( $\text{C}_2$ ), 53.5 ( $\text{C}_{1'}$ ), 67.3 ( $\text{C}_{1''}$ ), 73.8 ( $\text{C}_{12'}$ ), 118.1, 119.9, 124.3, 125.2, 127.1, 127.7, 128.0, 128.2, 128.3, 128.5, 132.6, 132.7, 135.1, 135.6, 140.9, 141.2, 143.7, 143.9 ( $18\text{C}$ ,  $\text{C}_{\text{Ar}}$ ), 153.9 ( $\text{CO}_{\text{carbamate}}$ ), 156.5 ( $\text{CO}_{\text{guanidino}}$ ), 173.6 ( $\text{CO}_{\text{ester}}$ ), 176.5 ( $\text{CO}_{\text{acid}}$ ).

**High resolution mass spectrum:** calculated for  $\text{C}_{40}\text{H}_{49}\text{N}_5\text{NaO}_8\text{S}$ ,  $(\text{M}+\text{Na})^+$ : 782.3194, Found: 782.3196.

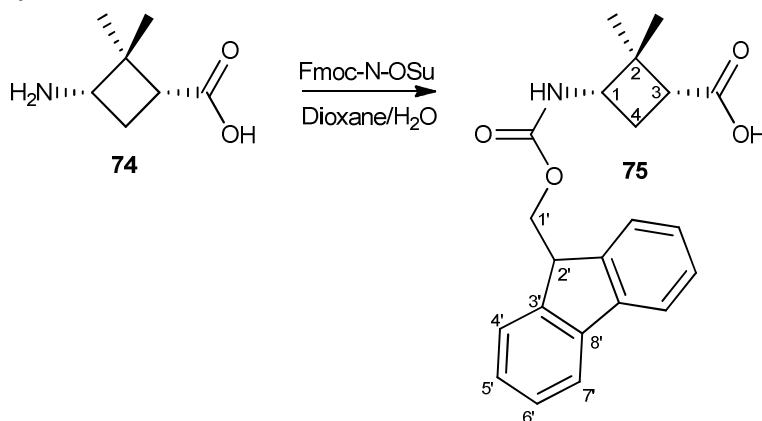
**(1R,3S)-3-Amino-2,2-dimethylcyclobutanecarboxylic acid, 74:**

Compound **(-)-47** (1.05 g, 3.8 mmol) in methanol (15 mL) was hydrogenated under 5 atmospheres of pressure in the presence of 20%  $\text{Pd}(\text{OH})_2/\text{C}$  (100 mg, 1.9% Pd in weight) overnight. The reaction mixture was filtered through Celite<sup>®</sup> and solvent was

removed under reduced pressure to provide amino acid **74** (543 mg, quantitative yield) as a white solid which was identified by its  $^1\text{H}$  spectrum and used in the next step without further purification.

**Spectroscopic data and physical constants for compound 74:**

$^1\text{H}$  NMR (250 MHz,  $\text{CDCl}_3$ )  $\delta$  0.95 (s, 3H, *trans*- $\text{CH}_3$ ), 1.15 (s, 3H, *cis*- $\text{CH}_3$ ), 1.95-2.10 (m, 1H,  $\text{H}_{4a}$ ), 2.11-2.25 (m, 1H,  $\text{H}_{4b}$ ), 2.55-2.69 (m, 1H,  $\text{H}_3$ ), 3.12 (t,  $J_{\text{H,H}} = 8.55$  Hz, 1H,  $\text{H}_1$ ).

**(1R,3S)-3-((9H-Fluoren-9-yl)methoxycarbonylamino)-2,2-dimethylcyclobutane carboxylic acid, 75:**

To a solution of amino acid **74** (585 mg, 4.09 mmol) in dioxane-water (50 mL, 1:1 mixture) at 0 °C were added Fmoc O-Su (1.37 g, 4.09 mmol) and  $\text{NaHCO}_3$  (0.71 g, 8.38 mmol). The mixture was stirred overnight at room temperature. Afterwards the dioxane was eliminated in the rotary evaporator and the resulting solution was diluted with saturated  $\text{NH}_4\text{Cl}$  and extracted with  $\text{CH}_2\text{Cl}_2$  (3 x 30mL). The organic extracts were dried over  $\text{MgSO}_4$  and concentrated under vacuo. The resulting crude was purified by flash chromatography ( $\text{CH}_2\text{Cl}_2$  + 2% Methanol) to afford **75** as a white solid which was crystallised (dichloromethane-petrol ether) to afford pure **75** (1.20 g, 80% yield).

**Spectroscopic data and physical constants for compound 75:**

$[\alpha]_D = +8.1$  (c 0.15, CH<sub>2</sub>Cl<sub>2</sub>).

**Melting point:** 155-157 °C (dichloromethane/petrol ether).

**IR (ATR):** 3307 (NH<sub>st</sub> + CO<sub>st</sub>), 2977 (CH<sub>st</sub>), 1700 (bs, CO<sub>acid</sub> + CO<sub>carbamate</sub>), 1533, 1449, 1371.

**<sup>1</sup>H NMR** (300 MHz, CDCl<sub>3</sub>)  $\delta$  0.97 (s, 3H, *trans*-CH<sub>3</sub>), 1.32 (s, 9H, *cis*-CH<sub>3</sub>), 2.06 (dd,  $J_{H,H} = 21.16$  Hz,  $J_{H,H} = 10.09$  Hz, 1H, H<sub>4a</sub>), 2.38 (dd,  $J_{H,H} = 19.50$  Hz,  $J_{H,H} = 8.02$  Hz, 1H, H<sub>4b</sub>), 2.56-2.73 (m, 1H, H<sub>3</sub>), 3.83-4.02 (m, 1H, H<sub>1</sub>), 4.21 (t,  $J_{H,H} = 6.79$  Hz, 1H, H<sub>2'</sub>), 4.34-4.50 (m, 2H, H<sub>1'</sub>), 4.83 (d,  $J_{H,H} = 8.59$  Hz, 1H, NH), 7.32 (t,  $J_{H,H} = 7.43$  Hz, 2H, H<sub>5'</sub>), 7.41 (t,  $J_{H,H} = 7.33$  Hz, 2H, H<sub>6'</sub>), 7.59 (d,  $J_{H,H} = 7.41$  Hz, 2H, H<sub>4'</sub>), 7.77 (t,  $J_{H,H} = 7.48$  Hz, 2H, H<sub>7'</sub>).

**<sup>13</sup>C NMR** (75 MHz, CDCl<sub>3</sub>)  $\delta$  16.9 (*trans*-CH<sub>3</sub>), 26.5 (*cis*-CH<sub>3</sub>), 28.8 (C<sub>4</sub>), 42.9 (C<sub>2</sub>), 46.1 (C<sub>2'</sub>), 47.3 (C<sub>3</sub>), 51.5 (C<sub>1</sub>), 66.6 (C<sub>1'</sub>), 120.0, 120.1 (C<sub>4'</sub>), 124.7 (2C, C<sub>5'</sub>), 125.0, 125.1 (C<sub>7'</sub>), 127.1, 127.7 (C<sub>6'</sub>), 141.4 (2C, C<sub>8'</sub>), 143.9 (2C, C<sub>3'</sub>), 155.7 (CO<sub>carbamate</sub>), 172.8 (CO<sub>acid</sub>).

**High resolution mass spectrum:** calculated for C<sub>22</sub>H<sub>23</sub>NNaO<sub>4</sub>, (M+Na)<sup>+</sup>: 388.15.25, Found: 388.1528.

## General procedure for solid-phase synthesis

### 1. Preparation of the resin

The desired mass of the resin is weighed in a syringe equipped with a frit. Rink-Amide resin (0.64 mmol/g loading) is already loaded with Fmoc so the synthesis can be started without prior preparation. In the case of the Wang Type resin, it has to be preloaded with the First Fmoc-amino acid.

The Fmoc-Rink-amide resin (150 mg) is swollen in 1 mL DMF/NMP 80:20 (v/v) for 30 min, then the solvent is sucked off.

### 2. Fmoc deprotection

Before coupling the amino acid, the Fmoc-protecting group has to be cleaved. This is done using piperidine:

- a) Add 1000 mL of 20% piperidine (DMF/NMP 80:20 v/v), shake for 15 min
- b) The solution is sucked off
- c) Repeat step a)
- d) The solution is sucked off, and the resin is washed with DMF (5 times with ca. 0.5 mL each time)

### 3. Single coupling of Fmoc-amino acid (Fmoc-AA)

- a) Add 4 eq of Fmoc-AA dissolved in 4 eq HOBt (0.38 M in DMF/NMP 80:20 v/v), 3.8 eq HBTU (0.37 M in DMF/NMP 80:20 v/v). Add 8 eq DIPEA (1.02 M in NMP) and shake for 60-70 min.
- b) The reaction mixture is sucked off, and the resin is washed with DMF (5 times with ca. 0.5 mL each time)

### 4. Fmoc deprotection

See point 2 above



**Repeat steps 2-4 for peptide chain elongation until the peptide chain is completed**

Before storing the resin it should be completely dried. Therefore it is washed with DMF, DCM and Et<sub>2</sub>O 5 times each.

**5. Ninhydrin test (optional)**

To test for the completeness of the coupling reaction it is possible to conduct a ninhydrin test (Kaiser test):

To a small amount (~10 beads) of the dried resin in an Eppendorf vial, one drop of each of the following reagents is added:

- 20 mM KCN in pyridine
- 0.28 M ninhydrine in ethanol
- 80% phenol in ethanol

Warm up at 95 °C for 5 min. If the Kaiser test is negative (no color change), go on with the elongation, otherwise (blue color) repeat step 3 another time.

**6. TNBS test (optional)**

To test for the completeness of the coupling reaction it is possible to conduct a TNBS test:

A few non-dried resin beads are placed in an Eppendorf vial, and the following amounts of reagents are added:

- 200 µL DMF
- 200 µL 10% DIPEA in DMF
- 100 µL 1% TNBS in DMF (2,4,6-trinitrobenzene-sulphonic acid)

After a short mixing, the mixture is left at room temperature for 10 min and the beads inspected. If the TNBS test is negative (colorless-yellow beads), go on with the elongation, otherwise (orange-red beads) repeat step 3 another time.

## 7. *N*-Acetylation (optional)

The *N*-acetylation is recommended for protein fragments as the acetylated *N*-terminus resembles the continuous amide bonds as present in the full-length protein. After the final Fmoc-deprotection the free amino group is acetylated using acetic anhydride.

- a) Add 10 eq of acetic anhydride, 10 eq of DIPEA (1.02 M in NMP) and shake for 30 min.
- b) The reaction mixture is sucked off, and the resin is washed with DMF, DCM and Et<sub>2</sub>O (5 times with ca. 0.5 mL each time)

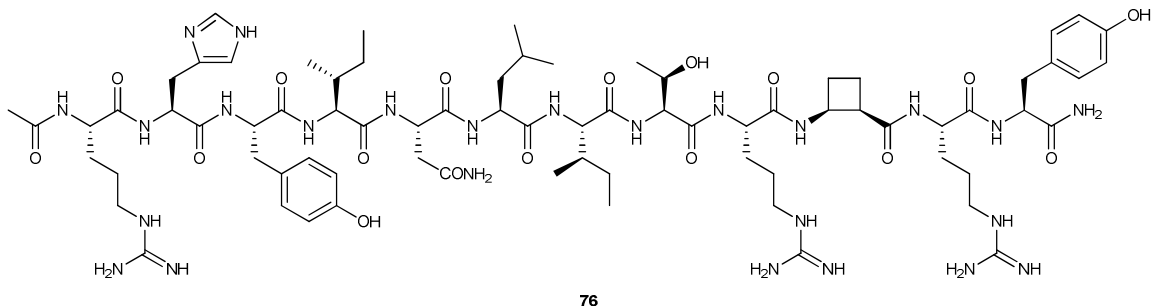
## 8. Cleavage of the resin

### 8.1 Small-scale cleavage

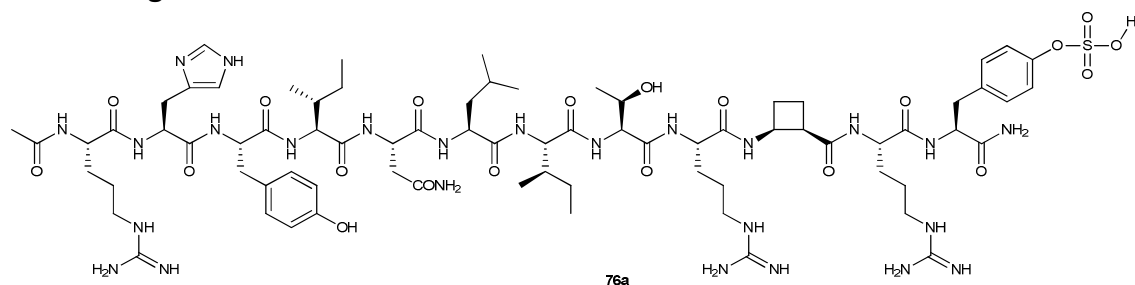
To monitor the progress of the synthesis it is possible to make a small-scale cleavage. Therefore, a small amount of resin (just few beads) is put in an Eppendorf vial and 100  $\mu$ L of the cleavage solution (TFA/Et<sub>3</sub>SiH/water 90:5:5) is added and the resulting mixture is stirred for 3 h. Then, filter the solution into a falcon, add ice-cold diethylether to the filtrate, keep 5 min at -20 °C, centrifuge 2 min, remove the ether, add new ether, shake, keep 5 min at -20 °C, centrifuge 2 min, remove the ether. Repeat the ether washings twice. Let the precipitate anhydrous under a nitrogen flow, and then dissolve the precipitate in 0.1% TFA in water/AcCN 1:1. Perform HPLC/MS.

### 8.2 Total cleavage

For the final TFA cleavage use 1.5-2.0 mL of a cleavage solution (TFA/Et<sub>3</sub>SiH/water 90:5:5). In the presence of cysteine, tryptophan and methionine, add also ethylenediaminetetraacetic acid (EDT) and/or thioanisole as scavenger.

**NPY Analogue 76:****Ac-Arg-His-Tyr-Ile-Asn-Leu-Ile-Thr-Arg-■-Arg-Tyr-NH<sub>2</sub> (76)**

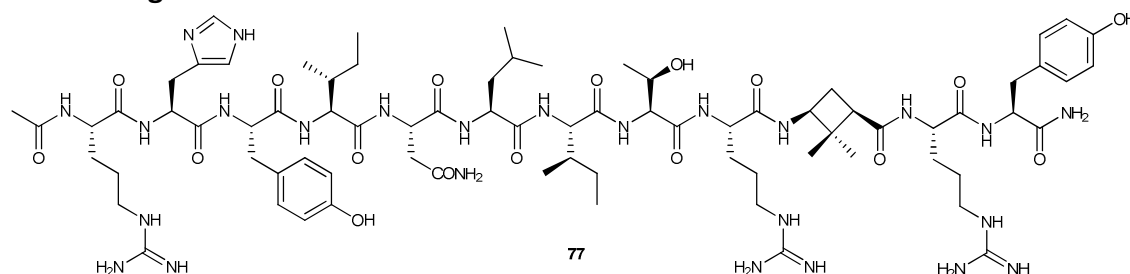
The crude peptide was purified by preparative HPLC using a non-linear gradient (5 % MeCN for 5 min, increased to 40% in 25 min, from 40 to 90% in 5 min, increased to 100% MeCN in 0.5 min, and finally the original conditions were re-established) of MeCN (containing 0.01% of TFA) and H<sub>2</sub>O (containing 0.01% of TFA). The purity of each fraction was verified by analytical HPLC and showed that the peptide had a purity higher than 95%. MS calcd for C<sub>75</sub>H<sub>122</sub>N<sub>25</sub>O<sub>17</sub> [M + 3H]<sup>3+</sup>: 548.4. found: 548.4.

**NPY Analogue 76a:****Ac-Arg-His-Tyr-Ile-Asn-Leu-Ile-Thr-Arg-■-Arg-Tyr(SO<sub>3</sub>)-NH<sub>2</sub> (76a)**

The crude peptide was purified by preparative HPLC using a non-linear gradient (5% MeCN for 5 min, increased to 40% in 25 min, from 40 to 90% in 5 min, increased to 100% MeCN in 0.5 min, and finally the original conditions were re-established) of MeCN (containing 0.01% of TFA) and H<sub>2</sub>O (containing 0.01% of TFA). The purity of each fraction was verified by analytical HPLC and showed that the peptide had a purity higher than

95%. MS calcd for  $C_{75}H_{121}N_{25}O_{20}S$   $[M + 2H]^{2+}$ : 862.4. found: 862.4.  $C_{75}H_{122}N_{25}O_{20}S$   $[M + 3H]^{3+}$ : 575.2. found: 575.2.

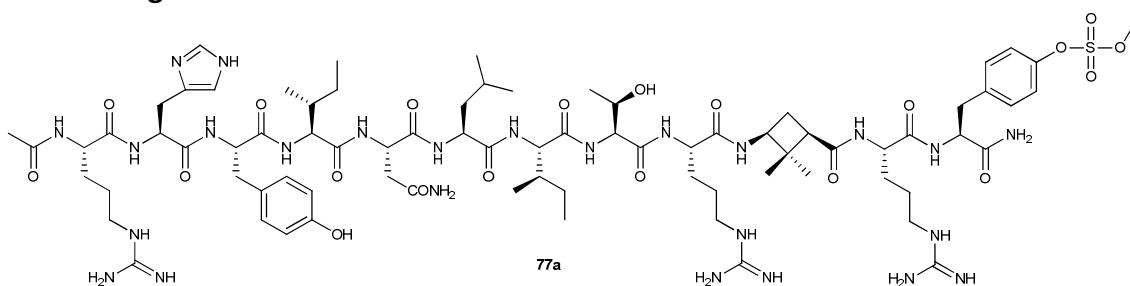
### NPY Analogue 77:



Ac-Arg-His-Tyr-Ile-Asn-Leu-Ile-Thr-Arg- $\blacklozenge$ -Arg-Tyr-NH<sub>2</sub> (**77**)

The crude peptide was purified by preparative HPLC using a non-linear gradient (5% MeCN for 5 min, increased to 40% in 25 min, from 40 to 90% in 5 min, increased to 100% MeCN in 0.5 min, and finally the original conditions were re-established) of MeCN (containing 0.01% of TFA) and H<sub>2</sub>O (containing 0.01% of TFA). The purity of each fraction was verified by analytical HPLC and showed that the peptide had a purity higher than 95%. MS calcd for  $C_{77}H_{126}N_{25}O_{17}$   $[M + 3H]^{3+}$ : 557.8. found: 557.8.

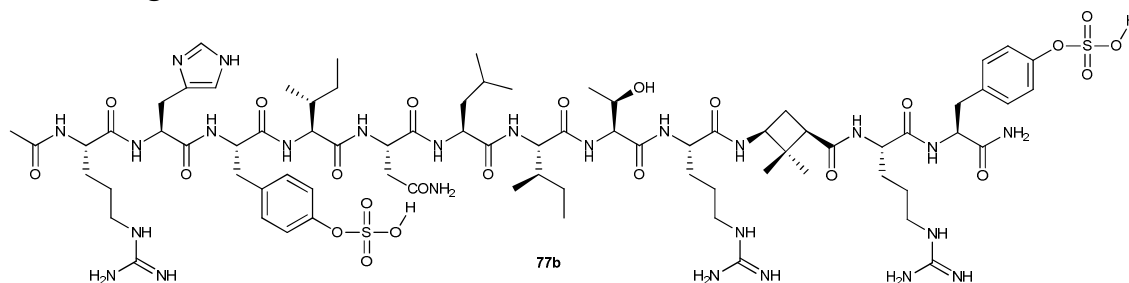
### NPY Analogue 77a:



Ac-Arg-His-Tyr-Ile-Asn-Leu-Ile-Thr-Arg- $\blacklozenge$ -Arg-Tyr(SO<sub>3</sub>)-NH<sub>2</sub> (**77a**)

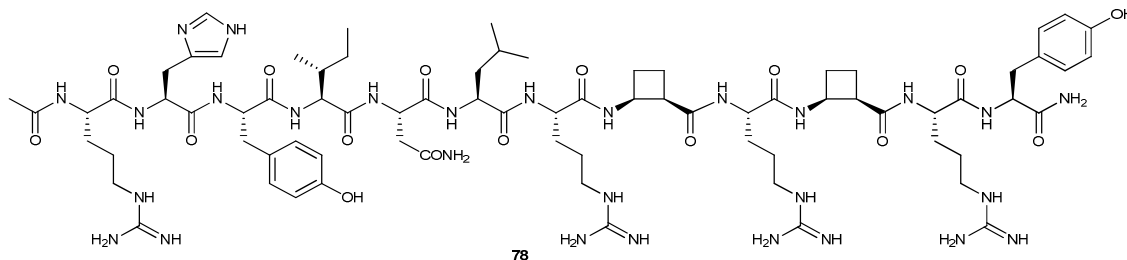
The crude peptide was purified by preparative HPLC using a non-linear gradient (5% MeCN for 5 min, increased to 40% in 25 min, from 40 to 90% in 5 min, increased to 100% MeCN in 0.5 min, and finally the original conditions were re-established) of MeCN (containing 0.01% of TFA) and H<sub>2</sub>O (containing 0.01% of TFA). The purity of each fraction was verified by analytical HPLC and showed that the peptide had a purity higher than 95%. MS calcd for C<sub>77</sub>H<sub>125</sub>N<sub>25</sub>O<sub>20</sub>S [M + 2H]<sup>2+</sup>: 876.4. found: 876.4. MS calcd for C<sub>77</sub>H<sub>126</sub>N<sub>25</sub>O<sub>20</sub>S [M + 3H]<sup>3+</sup>: 584.6. found: 584.6.

### NPY Analogue 77b:

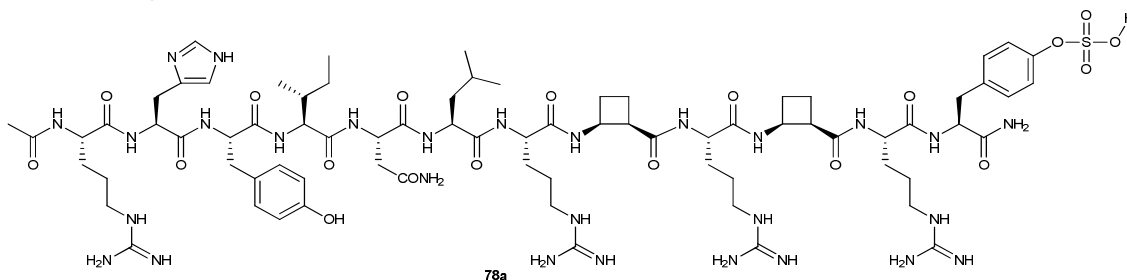


Ac-Arg-His-Tyr(SO<sub>3</sub>)-Ile-Asn-Leu-Ile-Thr-Arg-◆-Arg-Tyr(SO<sub>3</sub>)-NH<sub>2</sub> (**77b**)

The crude peptide was purified by preparative HPLC using a non-linear gradient (5% MeCN for 5 min, increased to 40% in 25 min, from 40 to 90% in 5 min, increased to 100% MeCN in 0.5 min, and finally the original conditions were re-established) of MeCN (containing 0.01% of TFA) and H<sub>2</sub>O (containing 0.01% of TFA). The purity of each fraction was verified by analytical HPLC and showed that the peptide had a purity higher than 95%. MS calcd for C<sub>77</sub>H<sub>125</sub>N<sub>25</sub>O<sub>23</sub>S<sub>2</sub> [M + 2H]<sup>2+</sup>: 916.4. found: 916.4. MS calcd for C<sub>77</sub>H<sub>126</sub>N<sub>25</sub>O<sub>23</sub>S<sub>2</sub> [M + 3H]<sup>3+</sup>: 611.3. found: 611.3.

**NPY Analogue 78:**Ac-Arg-His-Tyr-Ile-Asn-Leu-Arg-Arg-Arg-Tyr-NH<sub>2</sub> (**78**)

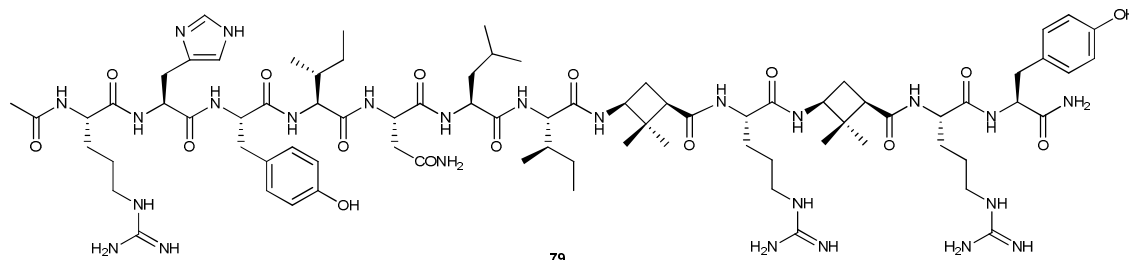
The crude peptide was purified by preparative HPLC using a non-linear gradient (5% MeCN for 5 min, increased to 40% in 25 min, from 40 to 90% in 5 min, increased to 100% MeCN in 0.5 min, and finally the original conditions were re-established) of MeCN (containing 0.01% of TFA) and H<sub>2</sub>O (containing 0.01% of TFA). The purity of each fraction was verified by analytical HPLC and showed that the peptide had a purity higher than 95%. MS calcd for C<sub>76</sub>H<sub>122</sub>N<sub>28</sub>O<sub>16</sub> [M + 2H]<sup>2+</sup>: 842.1. found: 842.1. MS calcd for C<sub>76</sub>H<sub>123</sub>N<sub>28</sub>O<sub>16</sub> [M + 3H]<sup>3+</sup>: 561.6. found: 561.6.

**NPY Analogue 78a:**Ac-Arg-His-Tyr-Ile-Asn-Leu-Arg-Arg-Arg-Tyr(SO<sub>3</sub>)-NH<sub>2</sub> (**78a**)

The crude peptide was purified by preparative HPLC using a non-linear gradient (5% MeCN for 5 min, increased to 40% in 25 min, from 40 to 90% in 5 min, increased to 100% MeCN in 0.5 min, and finally the original conditions were re-established) of MeCN (containing 0.01% of TFA) and H<sub>2</sub>O (containing 0.01% of TFA). The purity of each fraction was verified by analytical HPLC and showed that the peptide had a purity higher than

95%. MS calcd for  $C_{76}H_{122}N_{28}O_{19}S$   $[M + 2H]^{2+}$ : 881.8. found: 881.8. MS calcd for  $C_{76}H_{123}N_{28}O_{19}S$   $[M + 3H]^{3+}$ : 588.2. found: 588.2.

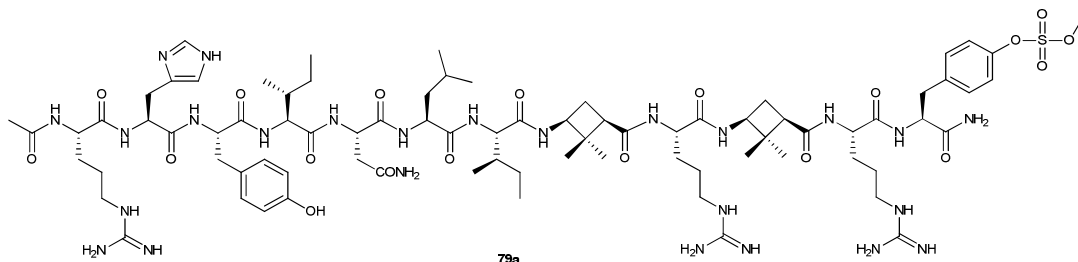
### NPY Analogue 79:



Ac-Arg-His-Tyr-Ile-Asn-Leu-Ile- $\blacklozenge$ -Arg- $\blacklozenge$ -Arg-Tyr-NH<sub>2</sub> (79)

The crude peptide was purified by preparative HPLC using a non-linear gradient 5% MeCN for 5 min, increased to 40% in 25 min, from 40 to 90% in 5 min, increased to 100% MeCN in 0.5 min, and finally the original conditions were re-established) of MeCN (containing 0.01% of TFA) and H<sub>2</sub>O (containing 0.01% of TFA). The purity of each fraction was verified by analytical HPLC and showed that the peptide had a purity higher than 95%. MS calcd for  $C_{80}H_{129}N_{25}O_{16}$   $[M + 2H]^{2+}$ : 848.4. found: 848.4. MS calcd for  $C_{80}H_{130}N_{25}O_{16}$   $[M + 3H]^{3+}$ : 565.9. found: 565.9.

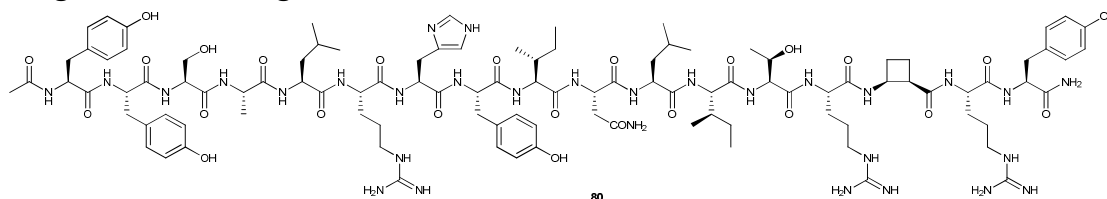
### NPY Analogue 79a:



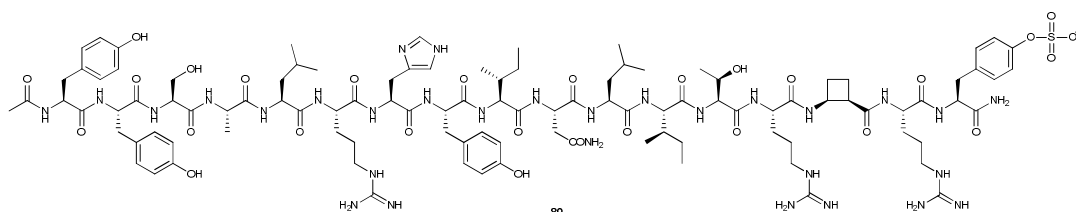
Ac-Arg-His-Tyr-Ile-Asn-Leu-Ile- $\blacklozenge$ -Arg- $\blacklozenge$ -Arg-Tyr(SO<sub>3</sub>)-NH<sub>2</sub> (79a)

The crude peptide was purified by preparative HPLC using a non-linear gradient (5% MeCN for 5 min, increased to 40% in 25 min, from 40 to 90% in 5 min, increased to 100% MeCN in 0.5 min, and finally the original conditions were re-established) of MeCN (containing 0.01% of TFA) and H<sub>2</sub>O (containing 0.01% of TFA). The purity of each fraction was verified by analytical HPLC and showed that the peptide had a purity higher than 95%. MS calcd for C<sub>80</sub>H<sub>129</sub>N<sub>25</sub>O<sub>19</sub>S [M + 2H]<sup>2+</sup>: 888.4. found: 888.4. MS calcd for C<sub>80</sub>H<sub>130</sub>N<sub>25</sub>O<sub>19</sub>S [M + 3H]<sup>3+</sup>: 592.6. found: 592.6.

### Elongated NPY analogue **80**:



Ac-Tyr-Tyr-Ser-Ala-Leu-Arg-His-Tyr-Ile-Asn-Leu-Ile-Thr-Arg-■-Arg-Tyr-NH<sub>2</sub> (**80**)



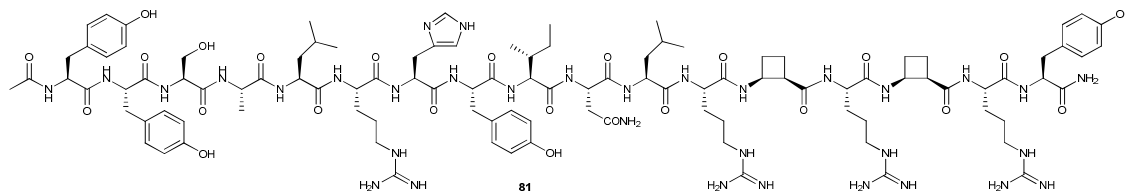
Ac-Tyr-Tyr-Ser-Ala-Leu-Arg-His-Tyr-Ile-Asn-Leu-Ile-Thr-Arg-■-Arg-Tyr(SO<sub>3</sub>)-NH<sub>2</sub> (**80a**)

The crude peptide was purified by preparative HPLC using a non-linear gradient (5% MeCN for 5 min, increased to 40% in 25 min, from 40 to 90% in 5 min, increased to 100% MeCN in 0.5 min, and finally the original conditions were re-established) of MeCN (containing 0.01% of TFA) and H<sub>2</sub>O (containing 0.01% of TFA). The purity of each fraction was verified by analytical HPLC and showed that the peptide was a mixture of **80** and **80a** with a purity higher than 95%. MS calcd for C<sub>105</sub>H<sub>160</sub>N<sub>30</sub>O<sub>25</sub> [M + 2H]<sup>2+</sup>: 1121.1. found: 1121.1.



MS calcd for  $C_{105}H_{161}N_{30}O_{25}$   $[M + 3H]^{3+}$ : 747.8. found: 747.8.  $C_{105}H_{160}N_{30}O_{28}S$   $[M + 2H]^{2+}$ : 1161.2. found: 1161.2. MS calcd for  $C_{105}H_{161}N_{30}O_{28}S$   $[M + 3H]^{3+}$ : 774.5. found: 774.5.

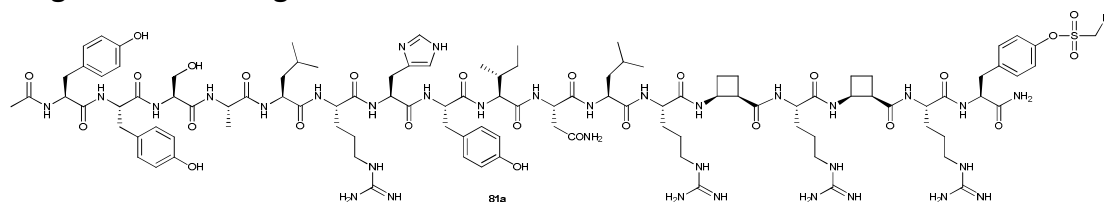
### Elongated NPY analogue 81:



Ac-Tyr-Tyr-Ser-Ala-Leu-Arg-His-Tyr-Ile-Asn-Leu-Arg-Arg-Arg-Tyr-NH<sub>2</sub> (**81**)

The crude peptide was purified by preparative HPLC using a non-linear gradient (5% MeCN for 5 min, increased to 40% in 25 min, from 40 to 90% in 5 min, increased to 100% MeCN in 0.5 min, and finally the original conditions were re-established) of MeCN (containing 0.01% of TFA) and H<sub>2</sub>O (containing 0.01% of TFA). The purity of each fraction was verified by analytical HPLC and showed that the peptide had a purity higher than 95%. MS calcd for  $C_{106}H_{161}N_{33}O_{24}$   $[M + 2H]^{2+}$ : 1181.0. found: 1181.0. MS calcd for  $C_{106}H_{162}N_{33}O_{24}$   $[M + 3H]^{3+}$ : 787.5. found: 787.5. MS calcd for  $C_{106}H_{163}N_{33}O_{24}$   $[M + 4H]^{4+}$ : 590.8. found: 590.8.

### Elongated NPY analogue 81a:

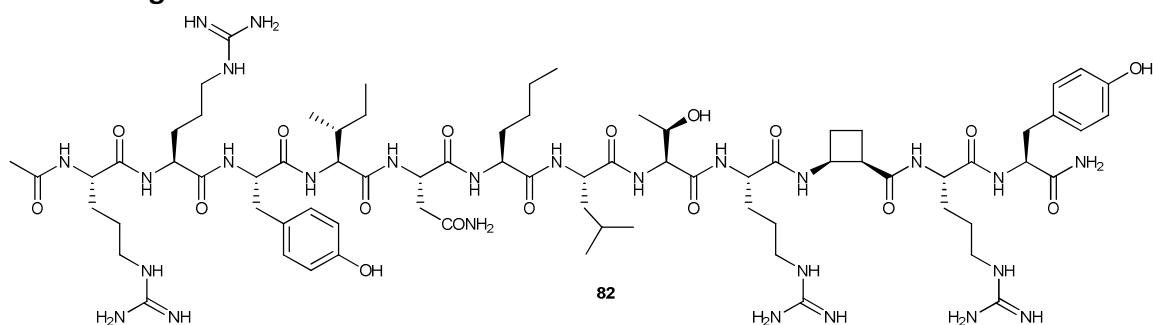


Ac-Tyr-Tyr-Ser-Ala-Leu-Arg-His-Tyr-Ile-Asn-Leu-Arg-Arg-Arg-Tyr(SO<sub>3</sub>)-NH<sub>2</sub> (**81a**)

The crude peptide was purified by preparative HPLC using a non-linear gradient (5% MeCN for 5 min, increased to 40% in 25 min, from 40 to 90% in 5 min, increased to 100% MeCN in 0.5 min, and finally the original conditions were re-established) of MeCN (containing 0.01% of TFA) and H<sub>2</sub>O (containing 0.01% of TFA). The purity of each fraction

was verified by analytical HPLC and showed that the peptide had a purity higher than 95%. MS calcd for  $C_{106}H_{161}N_{33}O_{27}S$   $[M + 2H]^{2+}$ : 1220.8. found: 1220.8. MS calcd for  $C_{106}H_{162}N_{33}O_{27}S$   $[M + 3H]^{3+}$ : 814.1. found: 814.1.

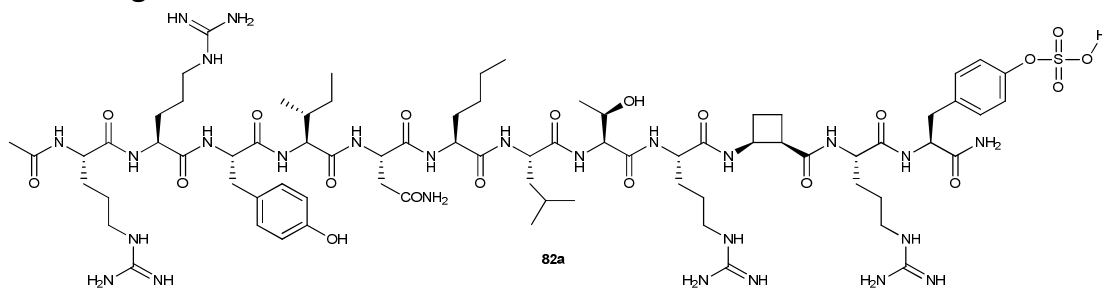
### HPP Analogue 82:



Ac-Arg-Arg-Tyr-Ile-Asn-NLe-Leu-Thr-Arg-Arg-Tyr-NH<sub>2</sub> (**82**)

The crude peptide was purified by preparative HPLC using a non-linear gradient (5% MeCN for 5 min, increased to 40% in 25 min, from 40 to 90% in 5 min, increased to 100% MeCN in 0.5 min, and finally the original conditions were re-established) of MeCN (containing 0.01% of TFA) and H<sub>2</sub>O (containing 0.01% of TFA). The purity of each fraction was verified by analytical HPLC and showed that the peptide had a purity higher than 95%. MS calcd for  $C_{75}H_{127}N_{26}O_{17}$   $[M + 3H]^{3+}$ : 554.7. found: 554.7.

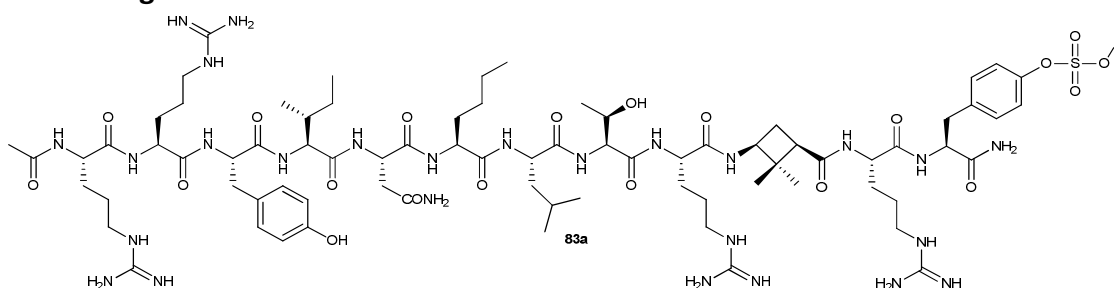
### HPP Analogue 82a:



Ac-Arg-Arg-Tyr-Ile-Asn-NLe-Leu-Thr-Arg-Arg-Tyr(SO<sub>3</sub>)-NH<sub>2</sub> (**82a**)

The crude peptide was purified by preparative HPLC using a non-linear gradient (5% MeCN for 5 min, increased to 40% in 25 min, from 40 to 90% in 5 min, increased to 100% MeCN in 0.5 min, and finally the original conditions were re-established) of MeCN (containing 0.01% of TFA) and H<sub>2</sub>O (containing 0.01% of TFA). The purity of each fraction was verified by analytical HPLC and showed that the peptide had a purity higher than 95%. MS calcd for C<sub>75</sub>H<sub>126</sub>N<sub>26</sub>O<sub>20</sub>S [M + 2H]<sup>2+</sup>: 871.8. found: 871.8. MS calcd for C<sub>75</sub>H<sub>127</sub>N<sub>26</sub>O<sub>20</sub>S [M + 3H]<sup>3+</sup>: 581.5. found: 581.5.

### HPP Analogue 83a:



Ac-Arg-Arg-Tyr-Ile-Asn-NLe-Leu-Thr-Arg- $\blacklozenge$ -Arg-Tyr(SO<sub>3</sub>)-NH<sub>2</sub> (**83a**)

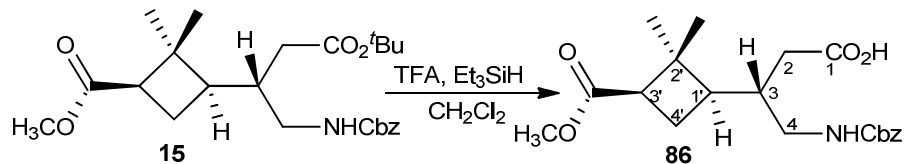
The crude peptide was purified by preparative HPLC using a non-linear gradient (5% MeCN for 5 min, increased to 40% in 25 min, from 40 to 90% in 5 min, increased to 100% MeCN in 0.5 min, and finally the original conditions were re-established) of MeCN (containing 0.01% of TFA) and H<sub>2</sub>O (containing 0.01% of TFA). The purity of each fraction was verified by analytical HPLC and showed that the peptide had a purity higher than 95%. MS calcd for C<sub>77</sub>H<sub>130</sub>N<sub>26</sub>O<sub>20</sub>S [M + 2H]<sup>2+</sup>: 885.9. found: 885.9. MS calcd for C<sub>77</sub>H<sub>131</sub>N<sub>26</sub>O<sub>20</sub>S [M + 3H]<sup>3+</sup>: 590.9. found: 590.9.





The crude peptide was purified by preparative HPLC using a non-linear gradient (5 % MeCN for 5 min, increased to 40 % in 25 min, from 40 to 90 % in 5 min, increased to 100 % MeCN in 0.5 min, and finally the original conditions were re-established) of MeCN (containing 0.01% of TFA) and H<sub>2</sub>O (containing 0.01% of TFA). The purity of each fraction was verified by analytical HPLC and showed that the peptide had a purity higher than 95%. MS calcd for C<sub>100</sub>H<sub>161</sub>N<sub>31</sub>O<sub>28</sub>S [M + 2H]<sup>2+</sup>: 1138.6. found: 1138.6. MS calcd for C<sub>100</sub>H<sub>162</sub>N<sub>31</sub>O<sub>28</sub>S [M + 3H]<sup>3+</sup>: 759.5. found: 759.5.

**(S)-4-(Benzyloxycarbonylamino)-3-((1R,3R)-3-methoxycarbonyl-2,2-dimethylcyclobutyl) butanoic acid, **86**:**



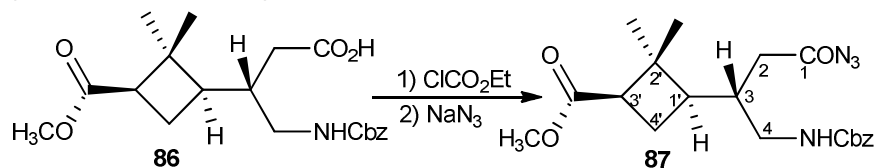
A mixture containing compound **15** (2.14 g, 4.9 mmol), trifluoroacetic acid (4.6 mL, 63.7 mmol, 13 eq) and triethyl silane (1.3 mL, 7.9 mmol, 1.6 eq) in anhydrous dichloromethane (40 mL) was stirred at room temperature for 18 h. Solvent was evaporated and the excess of trifluoroacetic acid was removed by liophilization affording acid **86** as a yellowish oil which was identified by its <sup>1</sup>H NMR spectrum and used in the next step without purification (1.73 g, 93% yield).

**Spectroscopic data for compound 86:**

$^1\text{H NMR}$  (250 MHz,  $\text{CDCl}_3$ )  $\delta$  0.98 (s, 3H, *trans*- $\text{CH}_3$ ), 1.25 (s, 3H, *cis*- $\text{CH}_3$ ), 1.71-2.44 (c.a., 6H,  $\text{H}_{4'a}$ ,  $\text{H}_{1'}$ ,  $\text{H}_{4'b}$ ,  $\text{H}_{2a}$ ,  $\text{H}_{2b}$ ,  $\text{H}_3$ ), 2.58-2.77 (m, 1H,  $\text{H}_{3'}$ ), 2.95-3.18 (m, 1H,  $\text{H}_{4a}$ ), 3.23-3.43 (m, 1H,  $\text{H}_{4b}$ ), 3.67 (s, 3H,  $\text{CO}_2\text{CH}_3$ ), 5.09-5.22 (m, 2H,  $\text{CH}_2\text{Bn}$ ), 6.33 (bs, 1H, NH), 7.30-7.45 (c.a., 5H,  $\text{H}_{\text{Ar}}$ ), 7.75 (broad singlet, 1H, COOH).

$^{13}\text{C NMR}$  (62.5 MHz,  $\text{CDCl}_3$ )  $\delta$  17.1 (*trans*- $\text{CH}_3$ ), 23.5 ( $\text{C}_{4'}$ ), 30.8 (*cis*- $\text{CH}_3$ ), 37.0 ( $\text{C}_2$ ), 42.0 ( $\text{C}_{2'}$ ), 42.8 ( $\text{C}_4$ ), 43.7 ( $\text{C}_{1'}$ ), 45.5 ( $\text{C}_{3'}$ ), 51.5 ( $\text{CO}_2\text{CH}_3$ ), 67.3 ( $\text{CH}_2\text{Bn}$ ), 128.2, 128.3, 128.4, 128.6, 136.1 (6C,  $\text{C}_{\text{Ar}}$ ), 157.4 ( $\text{CO}_{\text{carbamate}}$ ), 173.5 ( $\text{CO}_2\text{CH}_3$ ), 177.8 ( $\text{CO}_2\text{H}$ ).

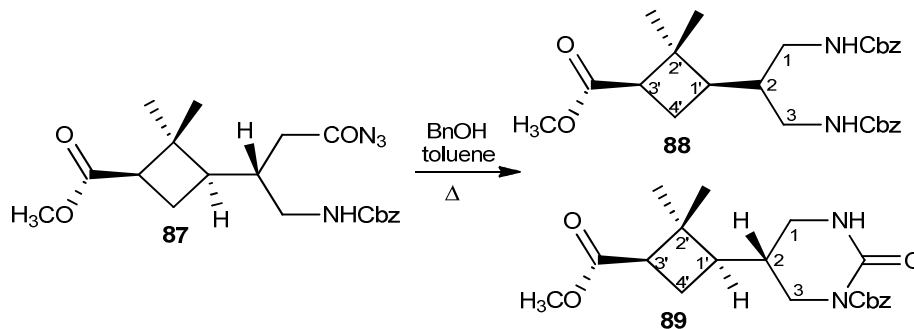
**(1*R*,3*R*)-Methyl 3-((*S*)-4-azido-1-(benzyloxycarbonylamino)-4-oxobutan-2-yl)-2,2-dimethylcyclobutane carboxylate, 87:**



To an ice-cooled solution of carboxylic acid **86** (1.86 g, 4.9 mmol) in 40 mL of anhydrous acetone, triethylamine (1.8 mL, 12.4 mmol, 2.5 eq) and ethyl chloroformate (0.75 mL, 7.4 mmol, 1.5 eq) were subsequently added. The mixture was stirred at 0 °C for 30 minutes. Then, sodium azide (0.52 g, 7.9 mmol, 1.6 eq) in 5 mL of water was added and the resultant solution was stirred at room temperature for 1.5 h. The reaction mixture was extracted with dichloromethane (4 x 15 mL), and the organic extracts were dried over magnesium sulfate. Solvents were removed under reduced pressure to give acyl azide **87** as a colourless oil (1.83 g, 92% yield), which was characterised by its spectroscopic data and used in the next step without further purification.

**Spectroscopic data of compound 87:**

IR ( $\text{cm}^{-1}$ ) 3350 ( $\text{NH}_{\text{st}}$ ), 2953 ( $\text{CH}_{\text{st}}$ ), 2134 ( $\text{N}_3$ ), 1702 (CO).

**(1*R*,3*R*)-Methyl 3-(3,9-dioxo-1,11-diphenyl-2,10-dioxo-4,8-diazaundecan-6-yl)-2,2-dimethylcyclobutane carboxylate, **88**:**

A solution of azyl azide **87** (1.83 g, 4.5 mmol) and benzyl alcohol (1.2 mL, 9.5 mmol, 2.1 eq) in toluene (30 mL) was heated to reflux for 18 hours under nitrogen atmosphere (the reaction progress was monitored by IR following the signals for the acyl azide at 2136 cm<sup>-1</sup> and the corresponding isocyanate at 2260 cm<sup>-1</sup>). Toluene was removed at reduced pressure and then excess of benzyl alcohol was eliminated by vacuum distillation. The residue was chromatographed on silica gel (ethyl acetate-hexane, 1:4 to 1:1 to ethyl acetate to methanol) to afford carbamate as a yellow oil which was crystallised (ether-pentane) to afford pure orthogonally protected amino acid **88** (0.75 g, 32% yield) and cyclic urea **89** (0.84 g, 50% yield) as a white solid.



**Spectroscopic data and physical constants for compound 88:**

$[\alpha]_D = -24.7$  ( $c$  0.60,  $\text{CH}_2\text{Cl}_2$ ).

IR (ATR): 3352 ( $\text{NH}_{\text{st}}$ ), 2953 ( $\text{CH}_{\text{st}}$ ), 1702 (bs,  $\text{CO}_{\text{ester}} + \text{CO}_{\text{carbamate}}$ ), 1522, 1457, 1373.

$^1\text{H NMR}$  (360 MHz,  $\text{CDCl}_3$ )  $\delta$  1.02 (s, 3H, *trans-CH*<sub>3</sub>), 1.24 (s, 3H, *cis-CH*<sub>3</sub>), 1.58-1.76 (c.a., 2H,  $\text{H}_{4'a}$ ,  $\text{H}_{1'}$ ), 1.88-2.02 (c.a., 2H,  $\text{H}_{4'b}$ ,  $\text{H}_2$ ), 2.55-2.81 (m, 2H,  $\text{H}_{1a}$ ,  $\text{H}_{3a}$ ), 2.82-2.95 (m, 1H,  $\text{H}_{3'}$ ), 3.23-3.44 (m, 2H,  $\text{H}_{1b}$ ,  $\text{H}_{3b}$ ), 3.65 (s, 3H,  $-\text{OCH}_3$ ), 5.01-5.20 (m, 4H,  $-\text{CH}_2\text{Bn}$ ), 5.28 (bs, 1H, NH), 5.66 (bs, 1H, NH), 7.30-7.41 (c.a., 10H,  $\text{H}_{\text{Ar}}$ ).

$^{13}\text{C NMR}$  (90 MHz,  $\text{CDCl}_3$ )  $\delta$  20.0 (*trans-CH*<sub>3</sub>), 25.7 ( $\text{C}_{4'}$ ), 33.7 (*cis-CH*<sub>3</sub>), 41.5, 42.9 (2C,  $\text{C}_1$ ,  $\text{C}_3$ ), 43.8 ( $\text{C}_2$ ), 44.2 ( $\text{C}_{1'}$ ), 45.4 ( $\text{C}_{2'}$ ), 48.3 ( $\text{C}_{3'}$ ), 54.1 ( $-\text{OCH}_3$ ), 69.5 ( $-\text{CH}_2\text{Bn}$ ), 69.7 ( $-\text{CH}_2\text{Bn}$ ), 130.8, 130.9, 131.0, 131.3 (10C,  $\text{C}_{\text{Ar}}$ ), 139.2 ( $\text{C}_{\text{Ar}}$ ), 139.4 ( $\text{C}_{\text{Ar}}$ ), 159.8 ( $\text{CO}_{\text{carbamate}}$ ), 160.1 ( $\text{CO}_{\text{carbamate}}$ ), 175.8 ( $\text{CO}_{\text{ester}}$ ).

**High resolution mass spectrum:** calculated for  $\text{C}_{27}\text{H}_{34}\text{N}_2\text{NaO}_6$  ( $\text{M}+\text{Na}$ )<sup>+</sup>: 502.2309, Found: 502.2316.

**Spectroscopic data and physical constants for compound 89:**

$[\alpha]_D = +3.0$  (c 0.46, CH<sub>2</sub>Cl<sub>2</sub>).

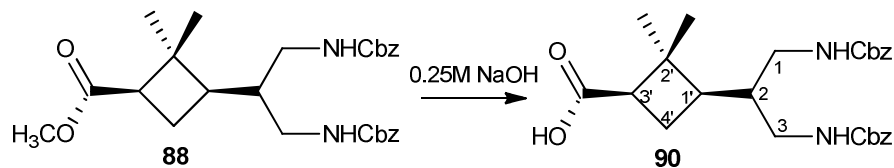
**IR** (ATR): 3243 (NH<sub>st</sub>), 2949 (CH<sub>st</sub>), 1709 (bs, CO<sub>ester</sub> + CO<sub>carbamate</sub>), 1656 (CO<sub>urea</sub>), 1462, 1381.

**<sup>1</sup>H NMR** (360 MHz, CDCl<sub>3</sub>) δ 0.97 (s, 3H, *trans*-CH<sub>3</sub>), 1.20 (s, 3H, *cis*-CH<sub>3</sub>), 1.69-1.90 (m, 1H, H<sub>4'a</sub>), 1.92-2.10 (c.a., 3H, H<sub>1'</sub>, H<sub>4'b</sub>, H<sub>2</sub>), 2.68 (t, *J* = 9.0 Hz, 1H, H<sub>3'</sub>), 2.80-2.99 (m, 1H, H<sub>1a</sub>), 3.16-3.38 (c.a., 2H, H<sub>1b</sub>, H<sub>3a</sub>), 3.67 (s, 3H, -OCH<sub>3</sub>), 3.83 (dd, *J* = 12.9 Hz, *J* = 3.4 Hz, 1H, H<sub>3b</sub>), 5.27 (s, 2H, -CH<sub>2</sub>Bn), 6.46 (bs, 1H, NH), 7.30-7.52 (c.a., 5H, H<sub>Ar</sub>).

**<sup>13</sup>C NMR** (90 MHz, CDCl<sub>3</sub>) δ 17.5 (*trans*-CH<sub>3</sub>), 22.5 (C<sub>4'</sub>), 30.7 (*cis*-CH<sub>3</sub>), 33.7 (C<sub>1</sub>), 42.3 (C<sub>3</sub>), 42.5 (C<sub>2</sub>), 44.5 (C<sub>1'</sub>), 45.4 (C<sub>2'</sub>), 46.6 (C<sub>3'</sub>), 51.3 (-OCH<sub>3</sub>), 68.2 (-CH<sub>2</sub>Bn), 128.0, 128.1, 128.4 (5C, C<sub>Ar</sub>), 135.6 (C<sub>Ar</sub>), 139.4 (C<sub>Ar</sub>), 152.9, 153.6 (2C, CO<sub>carbamate</sub>, CO<sub>urea</sub>), 172.7 (CO<sub>ester</sub>).

**High resolution mass spectrum:** calculated for C<sub>20</sub>H<sub>26</sub>N<sub>2</sub>NaO<sub>5</sub>, (M+Na)<sup>+</sup>: 397.1734, Found: 397.1736.

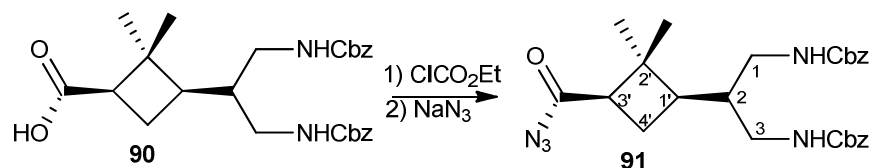
**(1*R*,3*R*)-3-(3,9-Dioxo-1,11-diphenyl-2,10-dioxa-4,8-diazaundecan-6-yl)-2,2-dimethylcyclobutane carboxylic acid, 90:**



A mixture of **88** (0.75 g, 1.6 mmol) in 10:1 H<sub>2</sub>O-THF (44 mL) and 0.25 M NaOH (37.5 mL, 9.6 mmol, 6.0 eq) was stirred at 0 °C for 6 days. Then the reaction mixture was washed with CH<sub>2</sub>Cl<sub>2</sub>, and 4 M HCl was added to the aqueous layer to reach pH 2. Then the acid aqueous phase was extracted with dichloromethane, and the solvent was removed at reduced pressure to afford acid **90** as a white solid (0.73 g, quantitative yield), which was characterised by its spectroscopic data and used in the next step without further purification.

**Spectroscopic data for compound 90:**

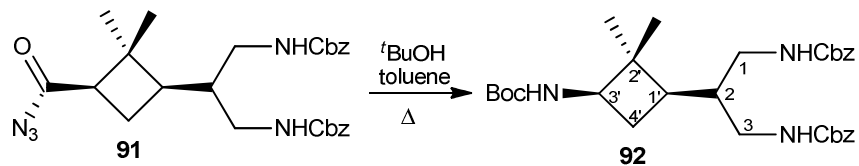
$^1\text{H NMR}$  (360 MHz,  $\text{CDCl}_3$ )  $\delta$  1.14 (s, 3H, *trans*- $\text{CH}_3$ ), 1.28 (s, 3H, *cis*- $\text{CH}_3$ ), 1.76-2.04 (c.a., 4H,  $\text{H}_{4'a}$ ,  $\text{H}_{1'}$ ,  $\text{H}_{4'b}$ ,  $\text{H}_2$ ), 2.60-2.79 (m, 1H,  $\text{H}_{3'}$ ), 2.97-3.38 (c.a., 4H,  $\text{H}_{1a}$ ,  $\text{H}_{1b}$ ,  $\text{H}_{3a}$ ,  $\text{H}_{3b}$ ), 5.04-5.23 (c.a., 4H,  $-\text{CH}_2\text{Bn}$ ), 5.30 (bs, 1H, NH), 5.69 (bs, 1H, NH), 7.31-7.43 (c.a., 10H,  $\text{H}_{Ar}$ ).

**Dibenzyl (2-((1*R*,3*R*)-3-(azidocarbonyl)-2,2-dimethylcyclobutyl)propane-1,3-diyl)dicarbamate, 91:**

To an ice-cooled solution of free acid **90** (0.73 g, 1.6 mmol) in 20 mL of anhydrous acetone, triethylamine (0.6 mL, 3.9 mmol, 2.5 eq) and ethyl chloroformate (0.2 mL, 2.3 mmol, 1.5 eq) were subsequently added. The mixture was stirred at 0 °C for 30 minutes. Then, sodium azide (0.16 g, 2.5 mmol, 1.6 eq) in 5 mL of water was added and the resultant solution was stirred at room temperature for 1.5 h. The reaction mixture was extracted with dichloromethane (4 x 15 mL), and the organic extracts were dried over magnesium sulfate. Solvents were removed under reduced pressure to give acyl azide **91** as a colourless oil (0.75 g, 97% yield), which was characterised by its spectroscopic data and used in the next step without further purification.

**Spectroscopic data of compound 91:**

**IR** ( $\text{cm}^{-1}$ ) 3350 ( $\text{NH}_{\text{st}}$ ), 2954 ( $\text{CH}_{\text{st}}$ ), 2134 ( $\text{N}_3$ ), 1706 (bs,  $\text{CO}_{\text{ester}} + \text{CO}_{\text{carbamate}}$ ).

Cyclobutane triamine, **92**:

A solution of azyl azide **91** (0.75 g, 1.5 mmol) in *tert*-butanol (80 mL, 842.8 mmol, 561.9 eq) was heated to reflux for 18 hours under nitrogen atmosphere (the reaction progress was monitored by IR following the signals for the acyl azide at  $2134\text{ cm}^{-1}$  and the corresponding isocyanate at  $2260\text{ cm}^{-1}$ ). After that, the reaction crude was cooled to room temperature, 50 mL of ethyl acetate were added and the reaction mixture was washed with aqueous  $\text{NaHCO}_3$  (3 x 30 mL). The organic layer was dried over anhydrous  $\text{MgSO}_4$  and solvents removed under reduced pressure. The reaction crude was purified by column chromatography on neutral silica gel (ethyl acetate-hexane, 1:4 to 1:2 to 1:1 to 2:1 to ethyl acetate) to afford pure triamine **92** as a white solid (0.35 g, 43% yield).

**Spectroscopic data and physical constants for compound 92:**

$[\alpha]_D = +7.9$  (c 0.65 in  $\text{CH}_2\text{Cl}_2$ )

**Melting point:** Below 25 °C (ethyl acetate/hexane).

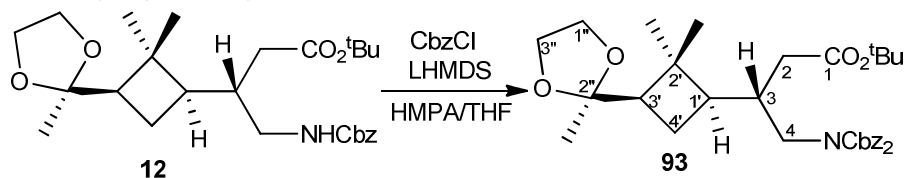
**IR (ATR):** 3335 ( $\text{NH}_{\text{st}}$ ), 2952 ( $\text{CH}_{\text{st}}$ ), 1687 (bs,  $\text{CO}_{\text{carbamate}}$ ), 1512, 1454, 1366.

**$^1\text{H}$  NMR** (360 MHz,  $\text{CDCl}_3$ )  $\delta$  0.97 (s, 3H, *trans*- $\text{CH}_3$ ), 1.16 (s, 3H, *cis*- $\text{CH}_3$ ), 1.43 (s, 9H,  $\text{O}^t\text{Bu}$ ), 1.56-1.71 (m, 1H,  $\text{H}_{4'a}$ ), 2.15-2.36 (m, 1H,  $\text{H}_{1'}$ ), 2.57-2.95 (c.a., 2H,  $\text{H}_{4'b}$ ,  $\text{H}_2$ ), 3.18-3.44 (m, 2H,  $\text{H}_{1a}$ ,  $\text{H}_{3a}$ ), 3.44-3.88 (m, 2H,  $\text{H}_{1b}$ ,  $\text{H}_{3b}$ ), 4.48-4.67 (m, 1H,  $\text{H}_{3'}$ ), 4.98-5.18 (c.a., 5H,  $-\text{CH}_2\text{Bn}$ , NH), 5.52 (bs, 1H, NH), 5.66 (bs, 1H, NH), 7.28-7.43 (c.a., 10H,  $\text{H}_{\text{Ar}}$ ).

**$^{13}\text{C}$  NMR** (90 MHz,  $\text{CDCl}_3$ )  $\delta$  15.7 (*trans*- $\text{CH}_3$ ), 28.4 ( $\text{C}(\text{CH}_3)_3$ ), 29.7 ( $\text{C}_{4'}$ ), 30.0 (*cis*- $\text{CH}_3$ ), 38.3, 39.0 (2C,  $\text{C}_1$ ,  $\text{C}_3$ ), 40.2 ( $\text{C}_2$ ), 40.9 ( $\text{C}_{1'}$ ), 43.4 ( $\text{C}_{2'}$ ), 50.8 ( $\text{C}_{3'}$ ), 66.7, 66.8 (2C,  $-\text{CH}_2\text{Bn}$ ), 79.2 ( $\text{C}(\text{CH}_3)_3$ ), 128.0, 128.1, 128.5, 136.5, 136.6 (10C,  $\text{C}_{\text{Ar}}$ ), 155.4, 157.1, 157.3 (3C,  $\text{CO}_{\text{carbamate}}$ ).

**High resolution mass spectrum:** calculated for  $\text{C}_{30}\text{H}_{41}\text{N}_3\text{NaO}_6$ ,  $(\text{M}+\text{Na})^+$ : 562.288, Found: 562.2883.

**(S)-tert-Butyl 4-((dibenzoyloxycarbonylamino)-3-((1R,3R)-2,2-dimethyl-3-(2-methyl-1,3-dioxolan-2-yl)cyclobutyl)butanoate, 93:**



To a stirred solution of monoprotected amine **12** (200 mg, 0.4 mmol) in THF (7.5 mL) and HMPA (1.5 mL, 8.6 mmol, 20 eq) was added LHMDS (0.5 mL, 1 M, 0.5 mmol, 1.3 eq) at -78 °C. The mixture was additionally stirred for 15 min at -78 °C and CbzCl (80  $\mu\text{L}$ , 0.5 mmol, 1.3 eq) was slowly added by syringe. The reaction mixture was stirred for 18 h at room temperature. Then the reaction mixture was quenched with a saturated aqueous solution of

NH<sub>4</sub>Cl and extracted with EtOAc. The combined organic phases were washed with brine, dried over MgSO<sub>4</sub>, and filtered and the solvent was evaporated. The crude was purified by silica gel column chromatography (1:5 to 1:1 ethyl acetate-hexane) to afford diprotected amine **93** (150 mg, 58% yield) as a colourless oil.

**Spectroscopic data and physical constants for compound 93:**

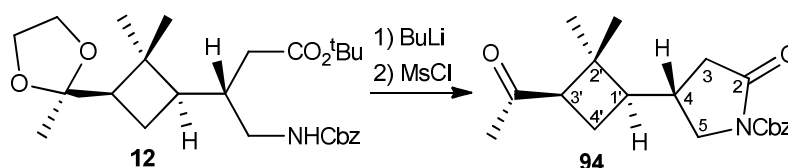
$[\alpha]_D = +8.5$  (c 0.65, CH<sub>2</sub>Cl<sub>2</sub>).

IR (ATR): 2952 (CH<sub>st</sub>), 1728 and 1695 (bs, CO<sub>ester</sub> + CO<sub>carbamate</sub>), 1452, 1366.

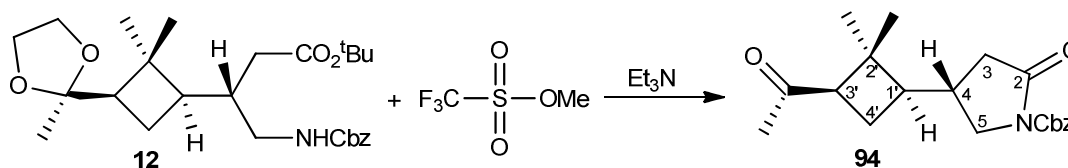
<sup>1</sup>H NMR (250 MHz, CDCl<sub>3</sub>) δ : 1.06 (s, 3H, *trans*-CH<sub>3</sub>), 1.15 (s, 3H, *cis*-CH<sub>3</sub>), 1.21 (s, 3H, CH<sub>3</sub><sub>ketal</sub>), 1.40 (s, 9H, <sup>t</sup>Bu), 1.53–1.66 (c.a., 2H, H<sub>4'a</sub>, H<sub>1'</sub>), 1.71–1.85(m, 1H, H<sub>4'b</sub>), 1.88–2.28 (c.a., 4H, H<sub>3</sub>, H<sub>3'</sub>, H<sub>2a</sub>, H<sub>2b</sub>), 2.31–2.55 (m, 1H, H<sub>4a</sub>), 3.56–3.89 (c.a., 4H, -OCH<sub>2</sub>CH<sub>2</sub>O-), 3.90–4.01 (m, 1H, H<sub>4b</sub>), 5.20–5.30 (c.a., 4H, CH<sub>2</sub>Bn), 7.32–7.45 (c.a., 10H, H<sub>Ar</sub>).

<sup>13</sup>C NMR (90 MHz, CDCl<sub>3</sub>) δ 16.5 (*trans*-CH<sub>3</sub>), 23.9 (C<sub>4'</sub>), 23.9 (CH<sub>3</sub><sub>ketal</sub>), 28.1 (C(CH<sub>3</sub>)<sub>3</sub>), 32.1 (*cis*-CH<sub>3</sub>), 35.5 (C<sub>3</sub>), 37.4 (C<sub>2</sub>), 41.5 (C<sub>2'</sub>), 44.5 (C<sub>4</sub>), 49.5 (C<sub>1'</sub>), 49.7 (C<sub>3'</sub>), 63.7 (-OCH<sub>2</sub>CH<sub>2</sub>O-), 65.5 (-OCH<sub>2</sub>CH<sub>2</sub>O-), 68.7 (2C, CH<sub>2</sub>Bn), 80.3 (C(CH<sub>3</sub>)<sub>3</sub>), 109.7 (C<sub>ketalic</sub>), 128.3, 128.4, 128.6, 135.3 (12C, C<sub>Ar</sub>), 153.6 (2C, CO<sub>carbamate</sub>) 171.7 (CO<sub>2</sub><sup>t</sup>Bu).

**High resolution mass spectrum:** calculated for C<sub>34</sub>H<sub>45</sub>NNaO<sub>8</sub>, (M+Na)<sup>+</sup>: 618.3037, Found: 618.3030.

**(S)-benzyl 4-((1R,3R)-3-acetyl-2,2-dimethylcyclobutyl)-2-oxopyrrolidine-1-carboxylate, **94**:**Method 1:

A solution of **12** (0.20 g, 0.4 mmol) in 5 mL of anhydrous THF under N<sub>2</sub> atmosphere was cooled to -80 °C with an ethyl acetate/N<sub>2</sub> bath. Afterwards 2.5 M butyl lithium in hexane (0.34 mL, 0.8 mmol, 2.0 eq) was added and the solution was stirred for 10 min. Next, the reaction was warmed up to -30 °C, mesyl chloride (0.06 mL, 0.8 mmol, 2.0 eq) was added and the reaction was stirred for 4 h at room temperature. After that, an aqueous solution of NH<sub>4</sub>Cl (20 mL) was added and the resultant solution was extracted with CH<sub>2</sub>Cl<sub>2</sub> (3 x 15 mL). The organic extracts were dried over anhydrous MgSO<sub>4</sub> and solvents removed under reduced pressure to afford lactam **94** (0.14 g, quantitative yield) as a colourless oil.

Method 2:

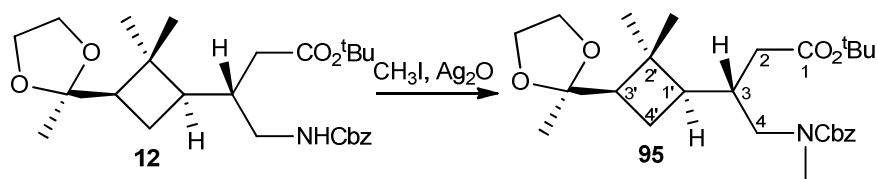
To a stirred solution of **12** (100 mg, 0.2 mmol) in anhydrous CH<sub>2</sub>Cl<sub>2</sub> (5 mL) were subsequently added Et<sub>3</sub>N (0.04 mL, 0.3 mmol, 1.5 eq) and methyl triflate (0.03 mL, 0.2 mmol, 1.1 eq) under nitrogen atmosphere. The resulting mixture was stirred overnight at room temperature. Solvents and the reactants in excess were evaporated under reduced pressure and the crude was poured into EtOAc (20 mL) and washed with aqueous NaHCO<sub>3</sub> (3 x 20 mL). The organic phase was dried over MgSO<sub>4</sub> and concentrated *in vacuo* to obtain **94** as the main product.

**Spectroscopic data for compound 94:**

$^1\text{H NMR}$  (250 MHz,  $\text{CDCl}_3$ )  $\delta$  0.94 (s, 3H, *trans*- $\text{CH}_3$ ), 1.28 (s, 3H, *cis*- $\text{CH}_3$ ), 1.73-1.89 (c.a., 3H,  $\text{H}_{4'a}$ ,  $\text{H}_{4'b}$ ,  $\text{H}_{1'}$ ), 1.99-2.12 (c.a., 4H,  $\text{CH}_3\text{CO}$ ,  $\text{H}_4$ ), 2.21-2.36 (m, 1H,  $\text{H}_3$ ), 2.39-2.54 (m, 1H,  $\text{H}_{3a}$ ), 2.66-2.84 (m, 1H,  $\text{H}_{3b}$ ), 3.19-3.30 (m, 1H,  $\text{H}_{5a}$ ), 3.36-3.50 (m, 1H,  $\text{H}_{5b}$ ), 5.09 (s, 2H,  $\text{CH}_2\text{Bn}$ ), 7.32-7.50 (c.a., 5H,  $\text{H}_{\text{Ar}}$ ).

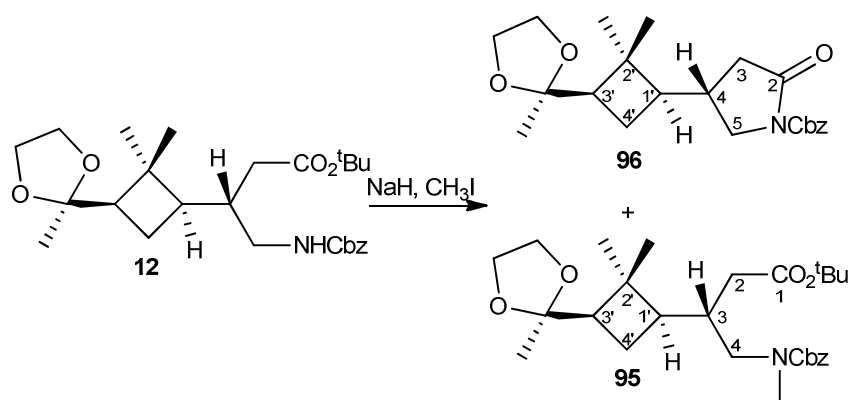
**(S)-tert-Butyl 4-(benzyloxycarbonylmethylamino)-3-((1*R*,3*R*)-2,2-dimethyl-3-(2-methyl-1,3-dioxolan-2-yl)cyclobutyl)butanoate, **95**:**

Method 1:



To a solution of **12** (100 mg, 0.2 mmol) in anhydrous DMF (5 mL) were subsequently added  $\text{Ag}_2\text{O}$  (1.20 g, 5.2 mmol, 25.0 eq) and  $\text{CH}_3\text{I}$  (0.32 mL, 5.2 mmol, 25.0 eq), the reaction was protected from light and stirred for 7 days at room temperature. Afterwards, excess of  $\text{CH}_3\text{I}$  was eliminated in the rotary evaporator, the solution was filtered through Celite<sup>®</sup> and the filtrate was washed with a saturated aqueous solution of  $\text{NaHCO}_3$ . The organic layer was dried over anhydrous  $\text{MgSO}_4$  and solvents removed under reduced pressure. The reaction crude was purified by column chromatography on neutral silica gel (ethyl acetate-hexane, 1:9 to 2:8) to afford pure methyl-amine **95** as a yellow oil (20 mg, 25 % conversion).



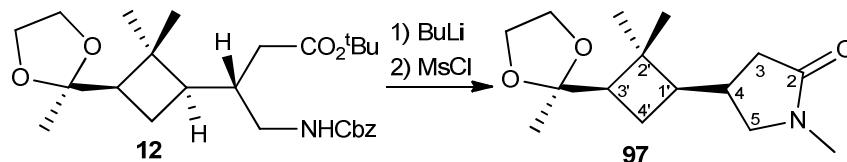
Method 2:

To a stirred solution of **12** (80 mg, 0.2 mmol) in anhydrous THF (4 mL) were subsequently added CH<sub>3</sub>I (0.05 mL, 0.9 mmol, 5.0 eq) and NaH (10 mg, 0.3 mmol, 1.5 eq) dissolved in 4 mL of anhydrous THF at 0 °C under nitrogen atmosphere. The resulting mixture was stirred overnight at room temperature. Solvents and the reactants in excess were evaporated under reduced pressure and the crude was poured into EtOAc (20 mL) and washed with aqueous NaHCO<sub>3</sub> (3 x 20 mL). The organic phase was dried over MgSO<sub>4</sub> and concentrated in vacuum. The crude was controlled by NMR and showed to be a 7:3 mixture of **95** and **96**.

**Spectroscopic data for compound 95:**

<sup>1</sup>H NMR (360 MHz, CDCl<sub>3</sub>) δ 1.12 (s, 3H, *trans*-CH<sub>3</sub>), 1.18 (s, 3H, *cis*-CH<sub>3</sub>), 1.23 (s, 3H, CH<sub>3</sub><sub>ketal</sub>), 1.45 (s, 9H, O<sup>t</sup>Bu), 1.73-1.94 (c.a., 2H, H<sub>4'a</sub>, H<sub>1'</sub>), 1.95-2.15 (c.a., 3H, H<sub>4'b</sub>, H<sub>3</sub>, H<sub>3'</sub>), 2.21-2.40 (c.a., 2H, H<sub>2a</sub>, H<sub>2b</sub>), 2.92 (s, 3H, NCH<sub>3</sub>), 3.10-3.41 (c.a., 2H, H<sub>4a</sub>, H<sub>4b</sub>), 3.76-4.08 (c.a., 4H, -OCH<sub>2</sub>CH<sub>2</sub>O-), 5.06-5.25 (m, 2H, CH<sub>2</sub>Bn), 7.33-7.50 (c.a., 5H, H<sub>Ar</sub>).

**4-((1*R*,3*R*)-2,2-Dimethyl-3-(2-methyl-1,3-dioxolan-2-yl)cyclobutyl)-1-methylpyrrolidin-2-one, **97**:**



To a stirred solution of **12** (100 mg, 0.2 mmol) in anhydrous THF (5 mL) was added 2.5 M butyl lithium in hexane (2.33 mL, 1.1 eq) at 0 °C under nitrogen atmosphere. The resulting mixture was stirred for 30 min. Methyl iodide (0.07 mL, 1.1 mmol, 5.0 eq) was then added, the resulting reaction mixture was stirred for 1 night. Solvents and the reactants in excess were evaporated under reduced pressure and the crude was poured into EtOAc (20 mL) and washed with aqueous NaHCO<sub>3</sub> (3 x 20 mL). The organic phase was dried over MgSO<sub>4</sub> and concentrated in vacuum. The obtained residue was purified by flash chromatography on silica gel (EtOAc-hexane, 1:1 to EtOAc) to give compound **97** (47 mg, 70% yield) as a mixture of the two epimers (*S* to *R* ratio 3:2).

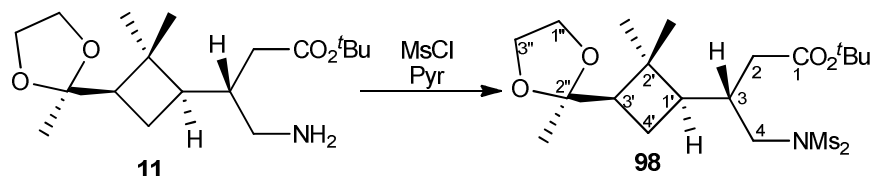
**Spectroscopic data for compound **97**:**

<sup>1</sup>H NMR (360 MHz, CDCl<sub>3</sub>) δ 1.08 (s, 3H, *trans*-CH<sub>3</sub> *S* enantiomer), 1.10 (s, 3H, *trans*-CH<sub>3</sub> *R* enantiomer), 1.17 (s, 3H, *cis*-CH<sub>3</sub> *S* enantiomer), 1.19 (s, 3H, *cis*-CH<sub>3</sub> *R* enantiomer), 1.24 (s, 3H, CH<sub>3</sub> *ketal R* enantiomer), 1.25 (s, 3H, CH<sub>3</sub> *ketal S* enantiomer), 1.41-1.59 (m, 1H, H<sub>4'a</sub>), 1.69-2.18 (c.a., 5H, H<sub>1'</sub>, H<sub>4'b</sub>, H<sub>3a</sub>, H<sub>3'</sub>, H<sub>4</sub>), 2.25-2.55 (m, 1H, H<sub>3b</sub>), 2.83 (s, 3H, N-CH<sub>3</sub>), 2.88-3.01 (m, 1H, H<sub>5a</sub>), 3.09-3.24 (m, 1H, H<sub>5b</sub> *R* enantiomer), 3.31-3.47 (m, 1H, H<sub>5b</sub> *S* enantiomer), 3.75-4.06 (c.a., 4H, -OCH<sub>2</sub>CH<sub>2</sub>O-).

Spectroscopic data are consistent with those reported in reference:

Dr. Jordi Aguilera, PhD thesis, 2010.

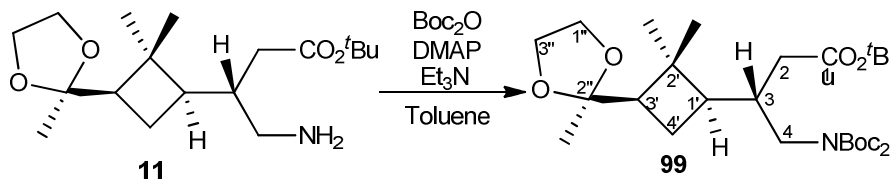
**(S)-tert-Butyl 3-((1R,3R)-2,2-dimethyl-3-(2-methyl-1,3-dioxolan-2-yl)cyclobutyl)-4-(N-(methylsulfonyl)methylsulfonamido)butanoate, 98:**



A mixture containing amine **11** (0.20 g, 0.6 mmol), pyridine (0.31 mL, 3.9 mmol, 7.0 eq) and mesyl chloride (0.15 mL, 1.7 mmol, 3.0 eq) in anhydrous  $\text{CH}_2\text{Cl}_2$  (15 mL) was refluxed under nitrogen atmosphere for 18 hours.

The solvent was evaporated under vacuum. The crude was then solved in EtOAc (30 mL) and washed with a saturated aqueous solution of  $\text{NaHCO}_3$  (3 x 15 mL), dried over  $\text{MgSO}_4$  and evaporated at reduced pressure. The NMR and TLC analysis of the crude showed that it was an unpurifiable mixture of **98** and several other side-products.

**(S)-tert-Butyl 4-(di(tert-butoxycarbonyl)amino)-3-((1R,3R)-2,2-dimethyl-3-(2-methyl-1,3-dioxolan-2-yl)cyclobutyl)butanoate, 99:**



A mixture containing amine **11** (80 mg, 0.2 mmol), DMAP (11 mg, 0.1 mmol, 0.5 eq),  $\text{Et}_3\text{N}$  (0.1 mL, 0.7 mmol, 4.0 eq) and *tert*-butyl dicarbonate (0.34 mL, 0.7 mmol, 4.0 eq) in anhydrous toluene (5 mL) was refluxed under nitrogen atmosphere for 60 hours.

The solvent was evaporated under vacuum. The crude was then solved in EtOAc (30 mL) and washed with a saturated aqueous solution of  $\text{NaHCO}_3$  (3x15 mL), dried over  $\text{MgSO}_4$  and evaporated at reduced pressure. The residue was chromatographed (ethyl acetate-hexane, 1:10 to 1:4) to afford pure **99** as a colourless oil (67 mg, 75% yield).

**Spectroscopic data and physical constants for compound 99:**

$[\alpha]_D^{25} = +4.3$  (c 0.26 in  $\text{CH}_2\text{Cl}_2$ )

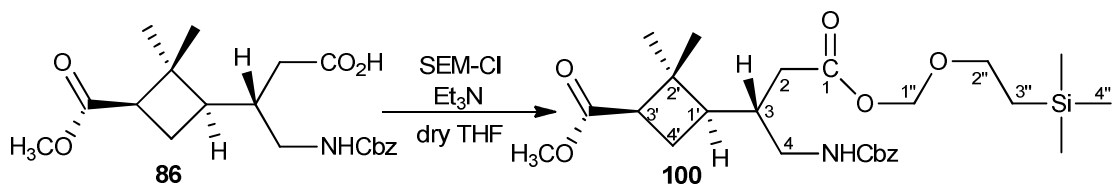
IR (ATR): 2978 ( $\text{CH}_{\text{st}}$ ), 1786 and 1730 (bs,  $\text{CO}_{\text{ester}} + \text{CO}_{\text{carbamate}}$ ), 1457, 1367.

$^1\text{H NMR}$  (250 MHz,  $\text{CDCl}_3$ )  $\delta$  1.11 (s, 3H, *trans*- $\text{CH}_3$ ), 1.17 (s, 3H, *cis*- $\text{CH}_3$ ), 1.24 (s, 3H,  $\text{CH}_3_{\text{ketal}}$ ), 1.44 (s, 9H,  $\text{O}^t\text{Bu}$ ), 1.53 (s, 18H, Boc), 1.61-1.70 (c.a., 2H,  $\text{H}_{4'a}$ ,  $\text{H}_{1'}$ ), 1.77-1.94 (m, 1H,  $\text{H}_{4'b}$ ), 1.97-2.23 (c.a., 3H,  $\text{H}_3$ ,  $\text{H}_{3'}$ ,  $\text{H}_{2a}$ ), 2.23-2.47 (m, 1H,  $\text{H}_{2b}$ ), 3.44-3.64 (m, 2H,  $\text{H}_4$ ), 3.74-4.06 (c.a., 4H,  $-\text{OCH}_2\text{CH}_2\text{O}-$ ).

$^{13}\text{C NMR}$  (62.5 MHz,  $\text{CDCl}_3$ )  $\delta$  17.1 (*trans*- $\text{CH}_3$ ), 24.1 ( $\text{C}_{4'}$ ), 24.3 ( $\text{CH}_3_{\text{ketal}}$ ), 28.5, 28.6 ( $\text{C}(\text{CH}_3)_3$ ), 32.5 (*cis*- $\text{CH}_3$ ), 35.8 ( $\text{C}_3$ ), 37.5 ( $\text{C}_2$ ), 41.9 ( $\text{C}_{2'}$ ), 45.0 ( $\text{C}_4$ ), 49.1 ( $\text{C}_{1'}$ ), 50.3 ( $\text{C}_{3'}$ ), 64.1 ( $-\text{OCH}_2\text{CH}_2\text{O}-$ ), 65.9 ( $-\text{OCH}_2\text{CH}_2\text{O}-$ ), 80.5, 82.4 ( $\text{C}(\text{CH}_3)_3$ ), 110.2 ( $\text{C}_{\text{ketalic}}$ ), 153.0 ( $\text{CO}_{\text{carbamate}}$ ) 171.9 ( $\text{CO}_2^t\text{Bu}$ ).

**High resolution mass spectrum:** calculated for  $\text{C}_{28}\text{H}_{49}\text{NO}_8$  ( $\text{M}^+$ ): 550.3350, Found: 5501.3349.

**(1*R*,3*R*)-Methyl 3-((*S*)-14,14-dimethyl-3,8-dioxo-1-phenyl-2,9,11-trioxa-4-aza-14-silapentadecan-6-yl)-2,2-dimethylcyclobutanecarboxylate, 100:**



To a cooled (0 °C) and stirred solution of the crude material **86** (147 mg, 0.4 mmol) in anhydrous THF (3 mL) under nitrogen atmosphere were added  $\text{Et}_3\text{N}$  (0.16 mL, 1.2 mmol, 3.0 eq) and SEMCl (2-(Trimethylsilyl)ethoxymethyl chloride) (80  $\mu\text{L}$ , 0.4 mmol, 1.1 eq). The mixture was stirred at room temperature for 18 h and then diluted with saturated aqueous  $\text{NH}_4\text{Cl}$  (15 mL). This was extracted with  $\text{CH}_2\text{Cl}_2$  (3 x 15 mL). The combined organic layers were dried and concentrated in vacuo. The residue was purified by column chromatography on

silica gel (ethyl acetate-hexane, 1:5 to 1:3) to provide 160 mg (81% yield) of **100** as a colourless oil.

**Spectroscopic data and physical constants for compound 100:**

$[\alpha]_D = +14.7$  (c 0.31 in  $\text{CH}_2\text{Cl}_2$ )

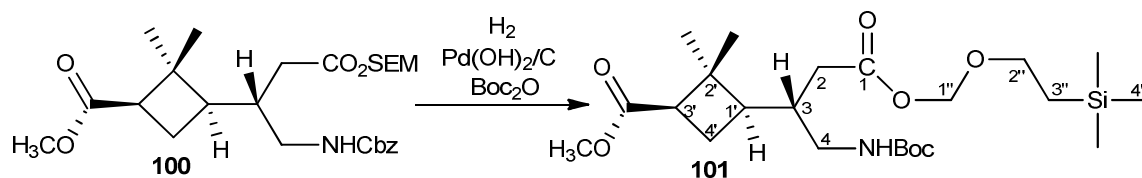
IR (ATR): 3358 ( $\text{NH}_{\text{st}}$ ), 2957 ( $\text{CH}_{\text{st}}$ ), 1727 (bs,  $\text{CO}_{\text{carbamate}} + \text{CO}_{\text{esters}}$ ), 1515, 1448.

$^1\text{H NMR}$  (400 MHz,  $\text{CDCl}_3$ )  $\delta$  0.01 (s, 9H,  $\text{H}_{4''}$ ), 0.83-1.03 (c.a., 5H, *trans*- $\text{CH}_3$ ,  $\text{H}_{3''}$ ), 1.25 (s, 3H, *cis*- $\text{CH}_3$ ), 1.68–1.86 (m, 1H,  $\text{H}_{4'a}$ ), 1.87–2.20 (c.a., 4H,  $\text{H}_{4'b}$ ,  $\text{H}_{1'}$ ,  $\text{H}_3$ ,  $\text{H}_{2a}$ ), 2.22–2.39 (m, 1H,  $\text{H}_{2b}$ ), 2.51–2.70 (m, 1H,  $\text{H}_{3'}$ ), 2.90–3.15 (m, 1H,  $\text{H}_{4a}$ ), 3.21–3.40 (m, 1H,  $\text{H}_{4b}$ ), 3.52-3.77 (c.a., 5H,  $\text{CO}_2\text{CH}_3$ ,  $\text{H}_{2''}$ ), 4.97-5.12 (c.a., 3H,  $\text{CH}_2\text{Bn}$ , NH), 5.14-5.32 (m, 2H,  $\text{H}_{1''}$ ), 7.29–7.41 (c.a., 5H,  $\text{H}_{\text{Ar}}$ ).

$^{13}\text{C NMR}$  (100 MHz,  $\text{CDCl}_3$ )  $\delta$  -1.5 ( $\text{C}_{4''}$ ), 17.1 (*trans*- $\text{CH}_3$ ), 18.0 ( $\text{C}_{3''}$ ), 23.6 ( $\text{C}_{4'}$ ), 30.8 (*cis*- $\text{CH}_3$ ), 36.9 ( $\text{C}_2$ ), 42.1 ( $\text{C}_{2'}$ ), 42.6 ( $\text{C}_4$ ), 43.9 ( $\text{C}_{1'}$ ), 45.5 ( $\text{C}_{3'}$ ), 51.1 ( $\text{CO}_2\text{CH}_3$ ), 66.6 ( $\text{CH}_2\text{Bn}$ ), 67.9 ( $\text{C}_{2''}$ ), 89.0 ( $\text{C}_{1''}$ ), 128.0, 128.4, 136.5 (6C,  $\text{C}_{\text{Ar}}$ ), 156.5 ( $\text{CO}_{\text{carbamate}}$ ), 172.1 and 172.8 ( $\text{CO}_2\text{SEM} + \text{CO}_2\text{CH}_3$ ).

**High resolution mass spectrum:** calculated for  $\text{C}_{26}\text{H}_{45}\text{NNaO}_7\text{Si}$  ( $\text{M}+\text{Na}$ ) $^+$ : 530.2550, Found: 530.2549.

**(1*R*,3*R*)-Methyl 2,2-dimethyl-3-((*S*)-2,2,15,15-tetramethyl-8,13-dioxo-5,7,14-trioxo-12-aza-2-silahexadecan-10-yl)cyclobutane carboxylate, 101:**



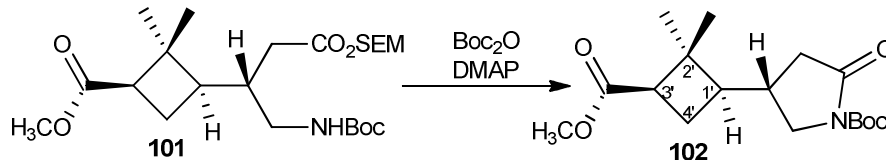
Compound **100** (150 mg, 0.3 mmol) in methanol (10 mL) was hydrogenated under 5 atmospheres of pressure in the presence of  $\text{Boc}_2\text{O}$  (0.1 mL, 0.5 mmol, 1.6 eq) and 20%  $\text{Pd}(\text{OH})_2/\text{C}$  (100 mg, 13% in weight of Pd) overnight. The reaction mixture was filtered through Celite<sup>®</sup> and solvent was removed under reduced pressure. The resulting crude was

purified by column chromatography on silica gel (1:3 ethyl acetate-hexane) to provide **101** (150 mg, quantitative yield) as a colourless oil slightly contaminated with the unreacted  $\text{Boc}_2\text{O}$ . The product was used in the next step without further purification.

**Spectroscopic data for compound 101:**

$^1\text{H NMR}$  (250 MHz,  $\text{CDCl}_3$ )  $\delta$  0.03 (s, 9H,  $\text{H}_{4''}$ ), 0.92-1.07 (c.a., 5H, *trans*- $\text{CH}_3$ ,  $\text{H}_{3''}$ ), 1.26 (s, 3H, *cis*- $\text{CH}_3$ ), 1.44 (s, 9H,  $\text{O}^t\text{Bu}$ ), 1.59-1.70 (m, 1H,  $\text{H}_{4'a}$ ), 1.77-1.90 (m, 1H,  $\text{H}_{4'b}$ ), 1.97-2.37 (c.a., 4H,  $\text{H}_{1'}$ ,  $\text{H}_3$ ,  $\text{H}_{2a}$ ,  $\text{H}_{2b}$ ), 2.56-2.72 (m, 1H,  $\text{H}_{3'}$ ), 2.85-3.07 (m, 1H,  $\text{H}_{4a}$ ), 3.16-3.33 (m, 1H,  $\text{H}_{4b}$ ), 3.64-3.78 (c.a., 5H,  $\text{CO}_2\text{CH}_3$ ,  $\text{H}_{2''}$ ), 4.71 (bs, 1H, NH), 5.23-5.36 (m, 2H,  $\text{H}_{1''}$ ).

**(S)-Tert-butyl 4-((1R,3R)-3-(methoxycarbonyl)-2,2-dimethylcyclobutyl)-2-oxopyrrolidine-1-carboxylate, 102:**



A mixture containing mono-protected amine **101** (140 mg, 0.3 mmol), DMAP (21 mg, 0.2 mmol, 0.5 eq),  $\text{Et}_3\text{N}$  (90  $\mu\text{L}$ , 0.6 mmol, 2.0 eq) and *tert*-butyl dicarbonate (0.3 mL, 0.6 mmol, 2.0 eq) in anhydrous toluene (5 mL) was refluxed under nitrogen atmosphere for 60 hours.

The solvent was evaporated under vacuum. The crude was then solved in EtOAc (30 mL) and washed with a saturated aqueous solution of  $\text{NaHCO}_3$  (3 x 15 mL), dried over  $\text{MgSO}_4$  and evaporated at reduced pressure. The residue was chromatographed (ethyl acetate-hexane, 1:6 to 1:4) to afford pure **102** as a colourless oil (67 mg, 75% yield).

**Spectroscopic data for compound 102:**

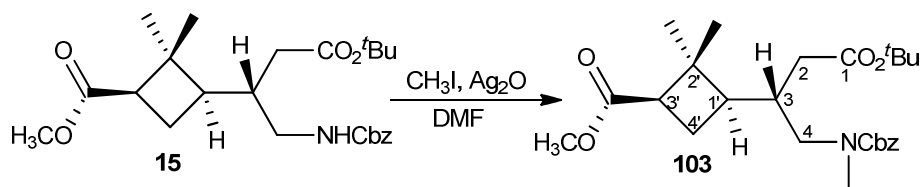
$^1\text{H NMR}$  (250 MHz,  $\text{CDCl}_3$ )  $\delta$  0.97 (s, 3H, *trans*- $\text{CH}_3$ ), 1.31 (s, 3H, *cis*- $\text{CH}_3$ ), 1.42 (s, 9H,  $\text{C}(\text{CH}_3)_3$ ), 1.73 (m, 1H,  $\text{H}_{4'a}$ ), 1.83-2.34 (c.a., 5H,  $\text{H}_3$ ,  $2\text{H}_4$ ,  $\text{H}_{4'b}$ ), 2.56 (m, 1H,  $\text{H}_{1'}$ ), 2.94 (m, 1H,  $\text{H}_{2a}$ ), 3.21 (m, 1H,  $\text{H}_{2b}$ ), 3.67 (s, 3H,  $\text{CO}_2\text{CH}_3$ ), 3.70 (s, 3H,  $\text{CO}_2\text{CH}_3$ ), 4.75 (broad singlet, 1H, NH).

$^{13}\text{C NMR}$  (62.5 MHz,  $\text{CDCl}_3$ )  $\delta$  16.9 (*trans*- $\text{CH}_3$ ), 23.5 ( $\text{C}_4$ ), 28.0 ( $\text{C}(\text{CH}_3)_3$ ), 30.8 (*cis*- $\text{CH}_3$ ), 35.4 ( $\text{C}_{4'}$ ), 36.9 ( $\text{C}_{3'}$ ), 41.7 ( $\text{C}_{2'}$ ), 42.7 ( $\text{C}_1$ ), 45.5 ( $\text{C}_{2'}$ ), 51 and 51.31 ( $\text{CO}_2\text{CH}_3$ ), 80.1 ( $\text{C}(\text{CH}_3)_3$ ), 155.9 ( $\text{CO}_{\text{carbamate}}$ ), 172.9 ( $\text{CO}_2\text{CH}_3$ ).

Spectroscopic data are consistent with those reported in reference:

Dr. Jordi Aguilera, PhD thesis, 2010.

**(1*R*,3*R*)-Methyl 3-((*S*)-1-(benzyloxycarbonyl(methyl)amino)-4-(*tert*-butoxy)-4-oxobutan-2-yl)-2,2-dimethylcyclobutanecarboxylate, 103:**



To a solution of **15** (0.56 g, 1.3 mmol) in anhydrous DMF (5 mL) were subsequently added  $\text{Ag}_2\text{O}$  (2.3 mg, 10.4 mmol, 8.0 eq) and  $\text{CH}_3\text{I}$  (1.0 mL, 16.3 mmol, 12.5 eq), the reaction was protected from light and stirred for 7 days at room temperature. Afterwards, excess of  $\text{CH}_3\text{I}$  was eliminated in the rotary evaporator, the solution was filtered through Celite<sup>®</sup> and the filtrate was washed with a saturated aqueous solution of  $\text{NaHCO}_3$ . The organic layer was dried over anhydrous  $\text{MgSO}_4$  and solvents removed under reduced pressure. The reaction crude was purified by column chromatography on neutral silica gel (ethyl acetate-hexane, 1:9 to 2:8) to afford pure methyl-amine **103** as a yellow oil (0.30 g, 52 % yield).

**Spectroscopic data and physical constants for compound 103:**

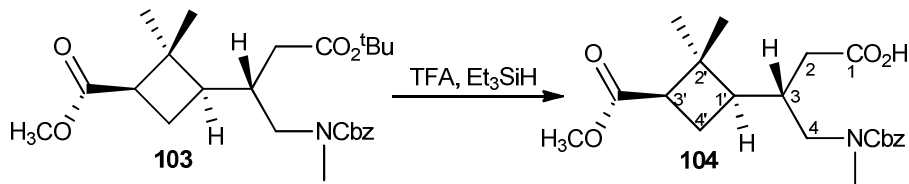
$[\alpha]_D^{25} = +2.2$  (c 0.67 in  $\text{CH}_2\text{Cl}_2$ )

**IR** (ATR): 3029 ( $=\text{CH}_{\text{st}}$ ), 2970 and 2951 ( $\text{CH}_{\text{st}}$ ), 1727 (bs,  $\text{CO}_{\text{carbamate}} + \text{CO}_{\text{esters}}$ ), 1586, 1366.

**$^1\text{H}$  NMR** (360 MHz,  $\text{CDCl}_3$ )  $\delta$  0.97 (s, 3H, *trans*- $\text{CH}_3$ ), 1.22 (s, 3H, *cis*- $\text{CH}_3$ ), 1.41 (s, 9H,  $^t\text{Bu}$ ), 1.66–2.34 (c.a., 6H,  $\text{H}_{4'a}$ ,  $\text{H}_{4'b}$ ,  $\text{H}_{1'}$ ,  $\text{H}_3$ ,  $\text{H}_{2a}$ ,  $\text{H}_{2b}$ ), 2.46–2.70 (m, 1H,  $\text{H}_{3'}$ ), 2.91 (s, 3H, N- $\text{CH}_3$ ), 3.00–3.35 (c.a., 2H,  $\text{H}_{4a}$ ,  $\text{H}_{4b}$ ), 3.65 (s, 3H,  $\text{CO}_2\text{CH}_3$ ), 5.01–5.21 (m, 2H,  $\text{CH}_2\text{Bn}$ ), 7.29–7.44 (c.a., 5H,  $\text{H}_{\text{Ar}}$ ).

**$^{13}\text{C}$  NMR** (90 MHz,  $\text{CDCl}_3$ )  $\delta$  17.1 (*trans*- $\text{CH}_3$ ), 24.0 ( $\text{C}_{4'}$ ), 28.1 ( $\text{C}(\text{CH}_3)_3$ ), 30.9 (*cis*- $\text{CH}_3$ ), 37.0 ( $\text{C}_2$ ), 41.5 ( $\text{C}_{2'}$ ), 43.1 ( $\text{C}_4$ ), 43.9 ( $\text{C}_{1'}$ ), 45.9 ( $\text{C}_{3'}$ ), 46.9 (N- $\text{CH}_3$ ), 51.2 ( $\text{CO}_2\text{CH}_3$ ), 67.0 ( $\text{CH}_2\text{Bn}$ ), 80.5 ( $\text{C}(\text{CH}_3)_3$ ), 127.8, 127.9, 128.1, 128.5, 136.8 (6C,  $\text{C}_{\text{Ar}}$ ), 156.2 ( $\text{CO}_{\text{carbamate}}$ ), 171.4 and 172.9 ( $\text{CO}_2^t\text{Bu} + \text{CO}_2\text{CH}_3$ ).

**High resolution mass spectrum:** calculated for  $\text{C}_{25}\text{H}_{37}\text{NNaO}_6$ ,  $(\text{M}+\text{Na})^+$ : 470.2513, Found: 470.2526.

**(S)-4-(Benzyloxycarbonyl(methyl)amino)-3-((1R,3R)-3-(methoxycarbonyl)-2,2-dimethylcyclobutyl)butanoic acid, 104:**

A mixture containing compound **103** (0.27 g, 0.6 mmol), trifluoroacetic acid (0.6 mL, 8.3 mmol, 13.8 eq) and triethyl silane (0.22 mL, 1.3 mmol, 2.2 eq) in anhydrous dichloromethane (15 mL) was stirred at room temperature for 18 h. Solvent was evaporated and the excess of trifluoroacetic acid was removed by liophilization affording acid **104** as a yellowish oil which was identified by its  $^1\text{H}$  NMR spectrum and used in the next step without purification (0.24 g, quantitative yield).

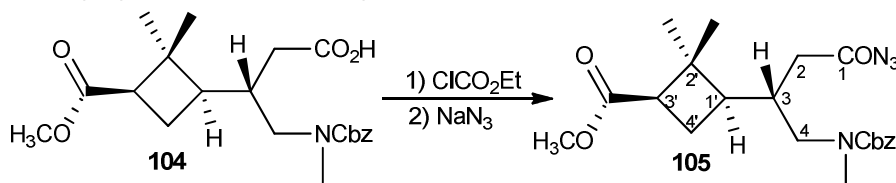


**Spectroscopic data for compound 104:**

$^1\text{H NMR}$  (400 MHz,  $\text{CDCl}_3$ )  $\delta$  0.98 (s, 3H, *trans*- $\text{CH}_3$ ), 1.24 (s, 3H, *cis*- $\text{CH}_3$ ), 1.69-2.36 (c.a. , 6H,  $\text{H}_{4'a}$ ,  $\text{H}_{1'}$ ,  $\text{H}_{4'b}$ ,  $\text{H}_{2a}$ ,  $\text{H}_{2b}$ ,  $\text{H}_3$ ), 2.53-2.71 (m, 1H,  $\text{H}_{3'}$ ), 2.89 (s, 3H, N- $\text{CH}_3$ ), 3.05-3.19 (m, 1H,  $\text{H}_{4a}$ ), 3.20-3.43 (m, 1H,  $\text{H}_{4b}$ ), 3.67 (s, 3H,  $\text{CO}_2\text{CH}_3$ ), 4.98-5.22 (m, 2H,  $\text{CH}_2\text{Bn}$ ), 7.29-7.42 (c.a., 5H,  $\text{H}_{\text{Ar}}$ ), 9.40 (broad singlet, 1H,  $\text{COOH}$ ).

$^{13}\text{C NMR}$  (100 MHz,  $\text{CDCl}_3$ )  $\delta$  16.9 (*trans*- $\text{CH}_3$ ), 23.7 ( $\text{C}_{4'}$ ), 30.7 (*cis*- $\text{CH}_3$ ), 35.6 ( $\text{C}_2$ ), 41.4 ( $\text{C}_{2'}$ ), 43.0 ( $\text{C}_4$ ), 44.1 ( $\text{C}_{1'}$ ), 45.7 ( $\text{C}_{3'}$ ), 46.8 (N- $\text{CH}_3$ ), 51.2 ( $\text{CO}_2\text{CH}_3$ ), 67.6 ( $\text{CH}_2\text{Bn}$ ), 127.7, 128.1, 128.2, 128.4, 136.1 (6C,  $\text{C}_{\text{Ar}}$ ), 157.1 ( $\text{CO}_{\text{carbamate}}$ ), 173.2 ( $\text{CO}_2\text{CH}_3$ ), 177.0 ( $\text{CO}_2\text{H}$ ).

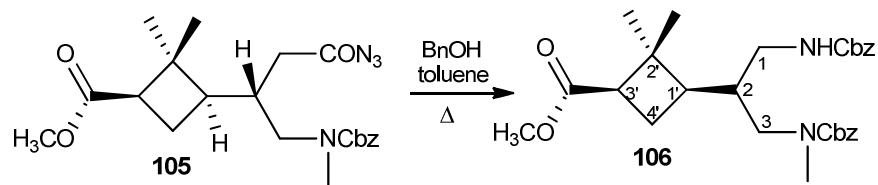
**(1*R*,3*R*)-methyl 3-((*S*)-4-azido-1-(benzyloxycarbonyl(methyl)amino)-4-oxobutan-2-yl)-2,2-dimethylcyclobutanecarboxylate, 105:**



To an ice-cooled solution of carboxylic acid **104** (0.26 g, 0.7 mmol) in 15 mL of anhydrous acetone, triethylamine (0.15 mL, 1.0 mmol, 1.5 eq) and ethyl chloroformate (0.1 mL, 1.0 mmol, 1.5 eq) were subsequently added. The mixture was stirred at 0 °C for 30 minutes. Then, sodium azide (73 mg, 1.1 mmol, 1.7 eq) in 5 mL of water was added and the resultant solution was stirred at room temperature for 1.5 h. The reaction mixture was extracted with dichloromethane (4 x 15 mL), and the organic extracts were dried over magnesium sulfate. Solvents were removed under reduced pressure to give acyl azide **105** as a colourless oil (0.26 g, 94% yield), which was characterised by its spectroscopic data and used in the next step without further purification.

**Spectroscopic data for compound 105:**

IR ( $\text{cm}^{-1}$ ) 3347 ( $\text{NH}_{\text{st}}$ ), 2952 ( $\text{CH}_{\text{st}}$ ), 2134 ( $\text{N}_3$ ), 1705 (CO).

**(1*R*,3*R*)-Methyl 2,2-dimethyl-3-((*R*)-4-methyl-3,9-dioxo-1,11-diphenyl-2,10-dioxo-4,8-diazaundecan-6-yl)cyclobutanecarboxylate, **106**:**

A solution of azyl azide **105** (0.26 g, 0.7 mmol) and benzyl alcohol (0.15 mL, 1.3 mmol, 1.9 eq) in toluene (30 mL) was heated to reflux for 18 hours under nitrogen atmosphere (the reaction progress was monitored by IR following the signals for the acyl azide at 2136  $\text{cm}^{-1}$  and the corresponding isocyanate at 2260  $\text{cm}^{-1}$ ). Toluene was removed at reduced pressure and then excess of benzyl alcohol was eliminated by vacuum distillation. The residue was chromatographed on silica gel (ethyl acetate-hexane, 1:9 to 1:1 to ethyl acetate) to afford carbamate **106** (0.22 g, 74% yield) as a yellow oil.

**Spectroscopic data and physical constants for compound **106**:**

$[\alpha]_{\text{D}} = +2.8$  (c 0.48 in  $\text{CH}_2\text{Cl}_2$ )

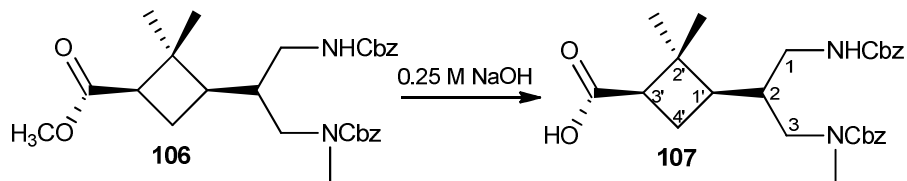
IR (ATR): 3343 ( $\text{NH}_{\text{st}}$ ), 3040 ( $=\text{CH}_{\text{st}}$ ), 2950 ( $\text{CH}_{\text{st}}$ ), 1686 (bs,  $\text{CO}_{\text{carbamates}} + \text{CO}_{\text{ester}}$ ), 1516, 1361

$^1\text{H NMR}$  (360 MHz,  $\text{CDCl}_3$ )  $\delta$  1.05 (s, 3H, *trans*- $\text{CH}_3$ ), 1.30 (s, 3H, *cis*- $\text{CH}_3$ ), 1.56-1.71 (m, 1H,  $\text{H}_{4'a}$ ), 1.76-2.01 (c.a., 3H,  $\text{H}_{1'}$ ,  $\text{H}_{4'b}$ ,  $\text{H}_2$ ), 2.56-2.72 (m, 1H,  $\text{H}_{3'}$ ), 2.90 (s, 3H, N- $\text{CH}_3$ ), 2.96-3.04 (m, 1H,  $\text{H}_{1a}$ ), 3.04-3.23 (m, 2H,  $\text{H}_{1b}$ ,  $\text{H}_{3a}$ ), 3.25-3.38 (m, 1H,  $\text{H}_{3b}$ ), 3.67 (s, 3H, - $\text{OCH}_3$ ), 5.00-5.26 (m, 4H, - $\text{CH}_2\text{Bn}$ ), 6.13 (bs, 1H, NH), 7.28-7.48 (c.a., 10H,  $\text{H}_{\text{Ar}}$ ).

$^{13}\text{C NMR}$  (90 MHz,  $\text{CDCl}_3$ )  $\delta$  17.2 (*trans*- $\text{CH}_3$ ), 23.3 ( $\text{C}_{4'}$ ), 30.95 (*cis*- $\text{CH}_3$ ), 35.1 (N- $\text{CH}_3$ ), 39.0 ( $\text{C}_1$ ), 40.0 ( $\text{C}_2$ ), 41.4 ( $\text{C}_{1'}$ ), 43.0 ( $\text{C}_{2'}$ ), 45.7 ( $\text{C}_{3'}$ ), 48.3 ( $\text{C}_3$ ), 51.2 (- $\text{OCH}_3$ ), 66.3, 67.4 (2C, - $\text{CH}_2\text{Bn}$ ), 127.8, 127.9, 128.0, 128.1, 128.5, 136.6, 137.0 (12C,  $\text{C}_{\text{Ar}}$ ), 156.7 ( $\text{CO}_{\text{carbamate}}$ ), 157.4 ( $\text{CO}_{\text{carbamate}}$ ), 173.2 ( $\text{CO}_{\text{ester}}$ ).

**High resolution mass spectrum:** calculated for  $\text{C}_{28}\text{H}_{36}\text{N}_2\text{NaO}_6$ ,  $(\text{M}+\text{Na})^+$ : 519.2466, Found: 519.2480.

**(1*R*,3*R*)-2,2-Dimethyl-3-((*R*)-4-methyl-3,9-dioxo-1,11-diphenyl-2,10-dioxo-4,8-diazaundecan-6-yl)cyclobutanecarboxylic acid, **107**:**

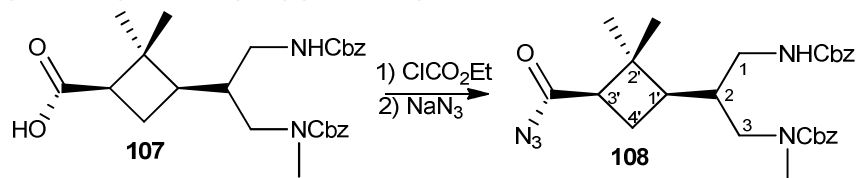


A mixture of **106** (0.18 g, 0.36 mmol) in 10:1 H<sub>2</sub>O-THF (11 mL) and 1.0 M LiOH (3.0 mL, 3.0 mmol, 8.3 eq) was stirred at 0 °C for 6 days. Then the reaction mixture was washed with CH<sub>2</sub>Cl<sub>2</sub>, and 4 M HCl was added to the aqueous layer to reach pH 2. Then the acid aqueous phase was extracted with dichloromethane, and the solvent was removed at reduced pressure to afford acid **107** as a white solid (0.17 g, quantitative yield), which was characterised by its spectroscopic data and used in the next step without further purification.

**Spectroscopic data and physical constants for compound **107**:**

<sup>1</sup>H NMR (250 MHz, CDCl<sub>3</sub>) δ 1.15 (s, 3H, *trans*-CH<sub>3</sub>), 1.27 (s, 3H, *cis*-CH<sub>3</sub>), 1.77-2.04 (c.a., 4H, H<sub>4'a</sub>, H<sub>1'</sub>, H<sub>4'b</sub>, H<sub>2</sub>), 2.59-2.80 (m, 1H, H<sub>3'</sub>), 2.92 (s, 3H, N-CH<sub>3</sub>), 2.97-3.40 (c.a., 4H, H<sub>1a</sub>, H<sub>1b</sub>, H<sub>3a</sub>, H<sub>3b</sub>), 5.03-5.24 (c.a., 4H, -CH<sub>2</sub>Bn), 6.13 (bs, 1H, NH), 7.29-7.47 (c.a., 10H, H<sub>Ar</sub>).

**Benzyl ((*R*)-2-((1*R*,3*R*)-3-(azidocarbonyl)-2,2-dimethylcyclobutyl)-3-((benzyloxycarbonylamino)propyl)(methyl)carbamate, **108**:**



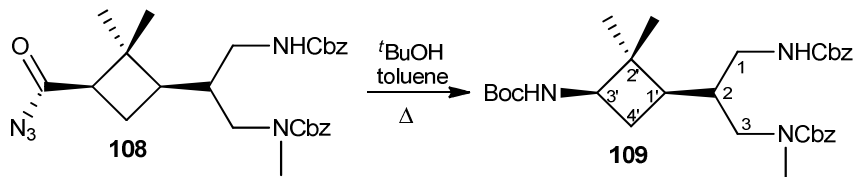
To an ice-cooled solution of half-ester **107** (0.14 g, 0.3 mmol) in 12 mL of anhydrous acetone, triethylamine (0.12 mL, 0.9 mmol, 3.0 eq) and ethyl chloroformate (0.05 mL, 0.4

mmol, 1.5 eq) were subsequently added. The mixture was stirred at 0 °C for 30 minutes. Then, sodium azide (31 mg, 0.5 mmol, 1.7 eq) in 2 mL of water was added and the resultant solution was stirred at room temperature for 1.5 h. The reaction mixture was extracted with dichloromethane (4 x 15 mL), and the organic extracts were dried over magnesium sulfate. Solvents were removed under reduced pressure to give acyl azide **108** as a colourless oil (0.14 g, 97% yield), which was characterised by its spectroscopic data and used in the next step without further purification.

#### Spectroscopic data of compound **108**:

IR (cm<sup>-1</sup>) 3347 (NH<sub>st</sub>), 2955 (CH<sub>st</sub>), 2134 (N<sub>3</sub>), 1708 (bs, CO<sub>ester</sub> + CO<sub>carbamate</sub>).

#### *N*-methyl cyclobutane triamine, **109**:



A solution of acyl azide **108** (0.14 g, 0.3 mmol) in *tert*-butanol (20 mL, 210.7 mmol, 702.3 eq) was heated to reflux for 18 hours under nitrogen atmosphere (the reaction progress was monitored by IR following the signals for the acyl azide at 2134 cm<sup>-1</sup> and the corresponding isocyanate at 2260 cm<sup>-1</sup>). After that the reaction crude was cooled to room temperature. Then, 20 mL of ethyl acetate were added and the reaction mixture was washed with aqueous NaHCO<sub>3</sub> (3 x 30 mL). The organic layer was dried over anhydrous MgSO<sub>4</sub> and solvents removed under reduced pressure. The reaction crude was purified by column chromatography on neutral silica gel (ethyl acetate-hexane, 1:4 to 1:3 to 1:2 to 2:1 to methanol) to afford pure triamine **109** as a colourless oil (90 mg, 43 % yield).

**Spectroscopic data and physical constants for compound 109:**

$[\alpha]_D^{25} = +0.5$  (c 1.59 in  $\text{CH}_2\text{Cl}_2$ )

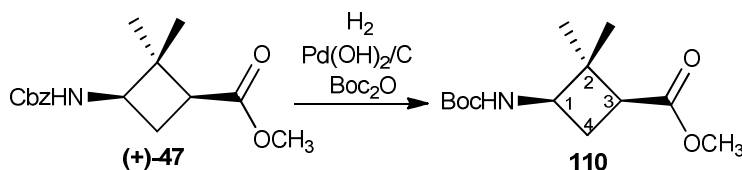
IR (ATR): 3341 ( $\text{NH}_{\text{st}}$ ), 3037 ( $=\text{CH}_{\text{st}}$ ), 2954 ( $\text{CH}_{\text{st}}$ ), 1688 (bs,  $\text{CO}_{\text{carbamates}}$ ), 1518, 1366.

$^1\text{H NMR}$  (250 MHz,  $\text{CDCl}_3$ )  $\delta$  1.09 (s, 3H, *trans*- $\text{CH}_3$ ), 1.26 (s, 3H, *cis*- $\text{CH}_3$ ), 1.45 (s, 9H,  $\text{O}^t\text{Bu}$ ), 1.72-1.97 (c.a., 4H,  $\text{H}_{4'a}$ ,  $\text{H}_{1'}$ ,  $\text{H}_{4'b}$ ,  $\text{H}_2$ ), 2.48-2.62 (m, 1H,  $\text{H}_{3'}$ ), 2.92 (s, 3H,  $\text{N-CH}_3$ ), 3.04-3.45 (c.a., 4H,  $\text{H}_{1a}$ ,  $\text{H}_{1b}$ ,  $\text{H}_{3a}$ ,  $\text{H}_{3b}$ ), 4.99-5.28 (c.a., 5H,  $-\text{CH}_2\text{Bn}$ ,  $\text{NH}$ ), 6.13 (broad singlet, 1H,  $\text{NH}$ ), 7.31-7.45 (c.a., 10H,  $\text{H}_{\text{Ar}}$ ).

$^{13}\text{C NMR}$  (90 MHz,  $\text{CDCl}_3$ )  $\delta$  15.6 (*trans*- $\text{CH}_3$ ), 28.4 ( $\text{C}(\text{CH}_3)_3$ ), 29.6 ( $\text{C}_{4'}$ ), 30.1 (*cis*- $\text{CH}_3$ ), 35.6 ( $\text{N-CH}_3$ ), 38.8 ( $\text{C}_1$ ), 39.9 ( $\text{C}_2$ ), 40.2 ( $\text{C}_{1'}$ ), 43.6 ( $\text{C}_{2'}$ ), 48.8 ( $\text{C}_{3'}$ ), 50.9 ( $\text{C}_3$ ), 66.4, 67.5 ( $2\text{C}$ ,  $-\text{CH}_2\text{Bn}$ ), 79.2 ( $\text{C}(\text{CH}_3)_3$ ), 127.8, 127.9, 128.0, 128.1, 128.4, 128.5, 136.5, 137.0 ( $12\text{C}$ ,  $\text{C}_{\text{Ar}}$ ), 155.4, 156.7, 157.5 ( $3\text{C}$ ,  $\text{CO}_{\text{carbamate}}$ ).

**High resolution mass spectrum:** calculated for  $\text{C}_{31}\text{H}_{43}\text{N}_3\text{NaO}_6$ ,  $(\text{M}+\text{Na})^+$ : 576.3044, Found: 576.3059.

**(1*S*,3*R*)-Methyl 3-(*tert*-butoxycarbonylamino)-2,2-dimethylcyclobutane carboxylate, 110:**



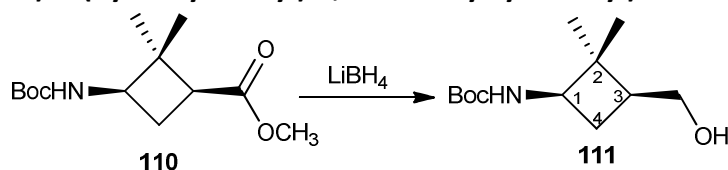
Compound **(+)-47** (0.47 g, 1.8 mmol) in methanol (15 mL) was hydrogenated under 5 atmospheres of pressure in the presence of  $\text{Boc}_2\text{O}$  (0.45 mL, 2.3 mmol, 1.3 eq) and 20%  $\text{Pd}(\text{OH})_2/\text{C}$  (180 mg, 8% in weight of Pd) overnight. The reaction mixture was filtered through Celite<sup>®</sup> and solvent was removed under reduced pressure. The resulting crude was purified by column chromatography on silica gel (ethyl acetate-hexane, 1:10 to 1:4) to provide **110** (0.46 mg, quantitative yield) as a colourless oil.

**Spectroscopic data and physical constants for compound 110:**

$^1\text{H NMR}$  (250 MHz,  $\text{CDCl}_3$ )  $\delta$  0.92 (s, 3H, *trans*- $\text{CH}_3$ ), 1.32 (s, 3H, *cis*- $\text{CH}_3$ ), 1.57 (s, 9H,  $\text{O}^t\text{Bu}$ ), 1.97-2.13 (m, 1H,  $\text{H}_{4a}$ ), 2.28-2.44 (m, 1H,  $\text{H}_{4b}$ ), 2.51-2.68 (m, 1H,  $\text{H}_3$ ), 3.82-4.00 (m, 1H,  $\text{H}_1$ ), 4.85 (bs, 1H, NH), 5.04-5.20 (c.a., 2H,  $\text{CH}_2\text{Bn}$ ), 7.31-7.45 (c.a., 5H,  $\text{H}_{\text{Ar}}$ ).

Spectroscopic data are consistent with those reported in reference:

Dr. Jordi Aguilera, PhD thesis, 2010.

***tert*-Butyl ((1*R*,3*S*)-3-(hydroxymethyl)-2,2-dimethylcyclobutyl)carbamate, 111:**

To a solution of ester **110** (0.38 g, 1.5 mmol) in anhydrous THF (20 mL) was added a 2 M solution of  $\text{LiBH}_4$  in THF (2.3 mL, 4.6 mmol, 3.1 eq). The mixture was stirred under nitrogen atmosphere for 18 h. Excess hydride was eliminated by slow addition of methanol (5 mL), and water (30 mL). The resultant solution was extracted with dichloromethane, and the combined extracts were dried over  $\text{MgSO}_4$ . Solvents were removed at reduced pressure, and the residue was chromatographed (EtOAc-hexane, 4:1) to provide alcohol **111** as a colourless oil (0.33 g, quantitative yield).

**Spectroscopic data and physical constants for compound 111:**

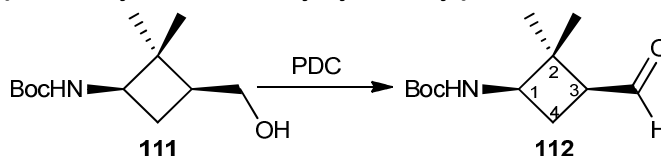
$[\alpha]_D^{25} = +5.9$  (c 0.3 in  $\text{CH}_2\text{Cl}_2$ )

IR (ATR): 3337 (bs,  $\text{OH}_{\text{st}}$ ,  $\text{NH}_{\text{st}}$ ), 2961 ( $\text{CH}_{\text{st}}$ ), 1685 ( $\text{CO}_{\text{carbamate}}$ ), 1527, 1365.

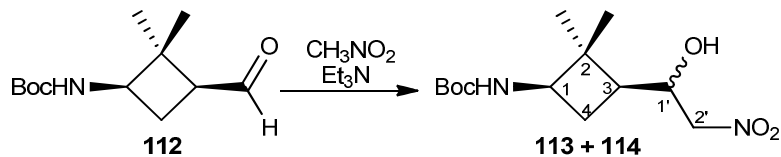
$^1\text{H NMR}$  (360 MHz,  $\text{CDCl}_3$ )  $\delta$  0.92 (s, 3H, *trans*- $\text{CH}_3$ ), 1.14 (s, 3H, *cis*- $\text{CH}_3$ ), 1.40 (s, 9H,  $\text{O}^t\text{Bu}$ ), 1.79-1.94 (m, 1H,  $\text{H}_{4a}$ ), 1.98-2.17 (m, 1H,  $\text{H}_{4b}$ ), 2.19-2.33 (m, 1H,  $\text{H}_3$ ), 3.47-3.61 (m, 2H,  $\text{CH}_2\text{OH}$ ), 3.61-3.74 (m, 1H,  $\text{H}_1$ ), 4.64 (bs, 1H, NH).

$^{13}\text{C NMR}$  (90 MHz,  $\text{CDCl}_3$ )  $\delta$  15.8 (*trans*- $\text{CH}_3$ ), 28.3 ( $\text{C}(\text{CH}_3)_3$ ), 28.5 ( $\text{C}_4$ ), 29.4 (*cis*- $\text{CH}_3$ ), 40.6 ( $\text{C}_2$ ), 42.9 ( $\text{C}_3$ ), 50.9 ( $\text{C}_1$ ), 63.0 ( $\text{CH}_2\text{OH}$ ), 79.1 ( $\text{C}(\text{CH}_3)_3$ ), 155.4 ( $\text{CO}_{\text{carbamate}}$ ).

**High resolution mass spectrum:** calculated for  $\text{C}_{12}\text{H}_{23}\text{NNaO}_3$  ( $\text{M}+\text{Na}$ ) $^+$ : 252.1570, Found: 252.1564.

***tert*-Butyl ((1*R*,3*S*)-3-formyl-2,2-dimethylcyclobutyl)carbamate, 112:**

A mixture of alcohol **111** (140 mg, 0.6 mmol) and PDC (0.40 g, 1.2 mmol, 2.0 eq) in anhydrous dichloromethane was stirred at room temperature overnight under nitrogen atmosphere (the reaction progress was monitored by TLC. If needed, more PDC was added). Then a small portion of Florisil was added and stirring was continued for 30 minutes. The reaction mixture was filtered on Celite® and solvent was removed at reduced pressure to afford crude aldehyde **112** (132 mg, quantitative yield) as a rather unstable oil that was immediately used in the condensation step without purification.

**((1*R*,3*S*)-3-(1-hydroxy-2-nitroethyl)-2,2-dimethylcyclobutyl)carbamate, **113+114**:**

To a mixture of aldehyde **112** (132 mg, 0.6 mmol) and nitromethane (2 mL, 36.9 mmol, 61.5 eq) under nitrogen atmosphere was added triethylamine (40  $\mu$ L, 0.3 mmol, 0.5 eq). The reaction was stirred at room temperature for 2 h. Afterwards the excess of nitromethane was evaporated under vacuum and the resulting crude was purified by column chromatography on silica gel (1:4 to 1:1 ethyl acetate-hexane) to provide a mixture of aminoalcohols **113** and **114** (156 mg, 90% yield) as a colourless oil.

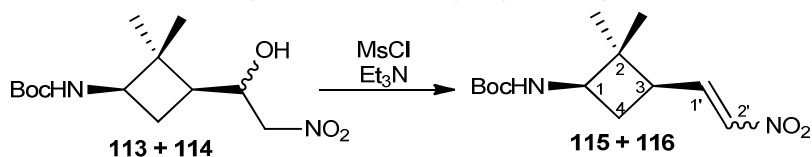
**Spectroscopic data and physical constants for compounds **113** and **114**:**

**IR** (ATR): 3340 (bs, OH<sub>st</sub>, NH<sub>st</sub>), 2961 (CH<sub>st</sub>), 1683 (CO<sub>carbamate</sub>), 1551, 1366.

**<sup>1</sup>H NMR** (360 MHz, CDCl<sub>3</sub>)  $\delta$  1.04 (s, 3H, *trans*-CH<sub>3</sub>), 1.24 (s, 3H, *cis*-CH<sub>3</sub>), 1.44 (s, 9H, O<sup>t</sup>Bu), 1.62-1.81 (m, 1H, H<sub>4a</sub>), 2.30-2.51 (m, 1H, H<sub>4b</sub>), 2.72-2.94 (m, 1H, H<sub>3</sub>), 3.66-3.86 (m, 1H, H<sub>1</sub>), 4.36-4.64 (c.a., 3H, H<sub>1'</sub>, H<sub>2'</sub>).

**<sup>13</sup>C NMR** (90 MHz, CDCl<sub>3</sub>)  $\delta$  16.0 (*trans*-CH<sub>3</sub>), 28.1 (C<sub>4</sub>), 28.3 (C(CH<sub>3</sub>)<sub>3</sub>), 29.7 (*cis*-CH<sub>3</sub>), 41.1 (C<sub>2</sub>), 43.9 (C<sub>3</sub>), 50.7 (C<sub>1</sub>), 70.2 (C<sub>2'</sub>), 79.1 (C(CH<sub>3</sub>)<sub>3</sub>), 79.8 (C<sub>2'</sub>), 155.2 (CO<sub>carbamate</sub>)

**High resolution mass spectrum:** calculated for C<sub>13</sub>H<sub>24</sub>N<sub>2</sub>NaO<sub>5</sub> (M+Na)<sup>+</sup>: 311.1577, found: 311.1569.

***tert*-Butyl ((1*R*,3*R*)-2,2-dimethyl-3-(2-nitrovinyl)cyclobutyl)carbamate, **115+116**:**



Nitroalcohols **113** and **114** (0.24 g, 0.8 mmol) was dissolved in anhydrous  $\text{CH}_2\text{Cl}_2$  (5 mL) and the resulting solution was cooled down with an ice bath. After that triethylamine (0.23 mL, 1.6 mmol, 2.0 eq) and mesyl chloride (80  $\mu\text{L}$ , 1.0 mmol, 1.3 eq) were subsequently added and the reaction was stirred overnight at room temperature. Then the solvent and excess of reactants were removed under vacuum and the resulting crude was purified by column chromatography on silica gel (ethyl acetate-hexane, 1:4 to 2:1) to afford a mixture of olefins **115** and **116** (173 mg, 80% yield) as a colourless oil.

#### Spectroscopic data and physical constants for compound **115** and **116**:

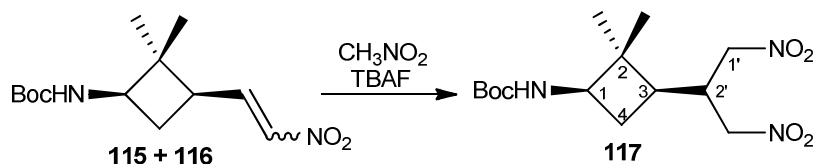
IR (ATR): 3340 ( $\text{NH}_{\text{st}}$ ), 3040 ( $=\text{CH}_{\text{st}}$ ), 2961 ( $\text{CH}_{\text{st}}$ ), 1693 ( $\text{CO}_{\text{carbamate}}$ )

$^1\text{H NMR}$  (360 MHz,  $\text{CDCl}_3$ )  $\delta$  0.92 (s, 3H, *trans*- $\text{CH}_3$ ), 1.17 (s, 3H, *cis*- $\text{CH}_3$ ), 1.38 (s, 9H,  $\text{O}^t\text{Bu}$ ), 1.72 (q, 1H,  $J_{\text{H-H}} = 10.2$  Hz,  $\text{H}_{4\text{a}}$ ), 2.33-2.56 (m, 1H,  $\text{H}_{4\text{b}}$ ), 3.76-3.95 (m, 1H,  $\text{H}_1$ ), 4.74 (broad singlet, 1H, NH), 6.88 (d, 1H,  $J_{\text{H-H}} = 13.4$  Hz,  $\text{H}_{2'}$ ), 7.16 (dd, 1H,  $J_{\text{H-H}} = 13.3$  Hz,  $J_{\text{H-H}} = 8.0$  Hz,  $\text{H}_2$ ).

$^{13}\text{C NMR}$  (90 MHz,  $\text{CDCl}_3$ )  $\delta$  17.0 (*trans*- $\text{CH}_3$ ), 28.0 ( $\text{C}_4$ ), 30.0 ( $\text{C}(\text{CH}_3)_3$ ), 30.9 (*cis*- $\text{CH}_3$ ), 38.4 ( $\text{C}_2$ ), 47.2 ( $\text{C}_3$ ), 51.3 ( $\text{C}_1$ ), 79.5 ( $\text{C}(\text{CH}_3)_3$ ), 139.7 ( $\text{C}_{2'}$ ), 142.1 ( $\text{C}_{1'}$ ), 155.3 ( $\text{CO}_{\text{carbamate}}$ )

High resolution mass spectrum: calculated for  $\text{C}_{13}\text{H}_{22}\text{N}_2\text{NaO}_4$  ( $\text{M}+\text{Na}$ ) $^+$ : 293.1465, found: 293.1472.

#### *tert*-Butyl ((1*R*,3*R*)-3-(1,3-dinitropropan-2-yl)-2,2-dimethylcyclobutyl)carbamate, **117**:



To a solution of alkenes **115** and **116** (110 mg, 0.4 mmol) in 5 mL of anhydrous THF under nitrogen atmosphere were subsequently added nitromethane (30  $\mu\text{L}$ , 0.5 mmol, 1.3 eq) and 1.0 M TBAF in THF (0.47 mL, 0.5 mmol, 1.3 eq). The resulting mixture was let to stir for 18 h at room temperature. Next, the solvent was evaporated at reduced pressure, and

the resulting crude was chromatographed on silica gel (ethyl acetate-hexane, 1:10 to 1:1) to afford compound **117** as a colourless oil (110 mg, 83 % yield).

**Spectroscopic data and physical constants for compound 117:**

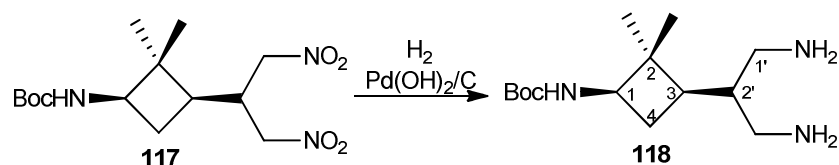
IR (ATR): 3355 (bs, OH<sub>st</sub>, NH<sub>st</sub>), 2970 (CH<sub>st</sub>), 1723 (CO<sub>carbamate</sub>), 1555, 1366.

<sup>1</sup>H NMR (360 MHz, CDCl<sub>3</sub>) δ 1.02 (s, 3H, *trans*-CH<sub>3</sub>), 1.22 (s, 3H, *cis*-CH<sub>3</sub>), 1.45 (s, 9H, O<sup>t</sup>Bu), 1.53-1.80 (c.a., 2H, H<sub>4a</sub>, H<sub>2'</sub>), 2.33-2.48 (m, 1H, H<sub>4b</sub>), 2.75-2.91 (m, 1H, H<sub>3</sub>), 3.67-3.83 (m, 1H, H<sub>1</sub>), 4.37-4.62 (c.a., 4H, H<sub>1'</sub>).

<sup>13</sup>C NMR (90 MHz, CDCl<sub>3</sub>) δ 15.7 (*trans*-CH<sub>3</sub>), 28.3 (C(CH<sub>3</sub>)<sub>3</sub>), 29.3 (*cis*-CH<sub>3</sub>), 29.7 (C<sub>4</sub>), 37.5 (C<sub>2'</sub>), 37.8 (C<sub>3</sub>), 43.9 (C<sub>2</sub>), 50.4 (C<sub>1</sub>), 74.4 (2C, C<sub>1'</sub>, C<sub>2'</sub>), 79.6 (C(CH<sub>3</sub>)<sub>3</sub>), 155.1 (CO<sub>carbamate</sub>).

**High resolution mass spectrum:** calculated for C<sub>14</sub>H<sub>25</sub>N<sub>3</sub>NaO<sub>6</sub> (M+Na)<sup>+</sup>: 354.1641, found: 354.1647.

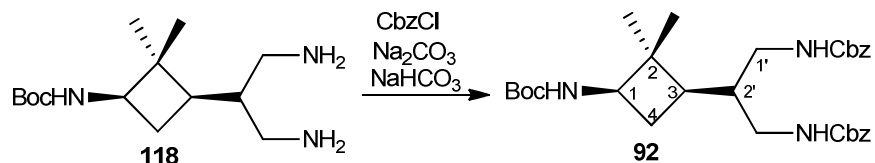
***tert*-Butyl ((1*R*,3*R*)-3-(1,3-diaminopropan-2-yl)-2,2-dimethylcyclobutyl)carbamate, **118**:**



Compound **117** (80 mg, 0.4 mmol) in methanol (5 mL) was hydrogenated under 5 atmospheres of pressure in the presence 20% Pd(OH)<sub>2</sub>/C (100 mg, 25% in weight of Pd) overnight. The reaction mixture was filtered through Celite<sup>®</sup> and solvent was removed under reduced pressure. The resulting crude diamine **118** (100 mg, quantitative yield) was used without further purification in the next step.

**Spectroscopic data and physical constants for compound 118:**

$^1\text{H NMR}$  (360 MHz,  $\text{CDCl}_3$ )  $\delta$  1.05 (s, 3H, *trans*- $\text{CH}_3$ ), 1.20 (s, 3H, *cis*- $\text{CH}_3$ ), 1.43 (s, 9H,  $\text{O}^t\text{Bu}$ ), 1.78-2.10 (m, 1H,  $\text{H}_{4a}$ ), 2.17-2.46 (c.a., 2H,  $\text{H}_{2'}$ ,  $\text{H}_{4b}$ ), 2.67-2.96 (c.a., 3H,  $\text{H}_3$ ,  $\text{H}_{1'a}$ ,  $\text{H}_{2'a}$ ), 3.04-3.35 (m, 2H,  $\text{H}_{1'b}$ ,  $\text{H}_{2'b}$ ), 3.58-3.81 (m, 1H,  $\text{H}_1$ ), 4.65 (broad singlet, 1H,  $\text{NH}_{\text{carbamate}}$ ).

**(1*R*,2*S*)-Methyl 2-(((benzyloxycarbonylamino)cyclobutanecarboxylate, 92:**

To a solution of **118** (100 mg, 0.4 mmol) in water-acetone(10:1, 6.8 mL) were subsequently added Na<sub>2</sub>CO<sub>3</sub> (90 mg, 0.8 mmol, 2.0 eq), NaHCO<sub>3</sub> (20 mg, 0.4 mmol, 1.0 eq) and CbzCl (0.16 mL, 1.1 mmol, 3.0 eq). The resulting mixture was stirred overnight at room temperature. Afterwards, the reaction mixture was extracted with dichloromethane, and the combined extracts were dried over MgSO<sub>4</sub>. Solvents were removed at reduced pressure, and the residue was chromatographed (EtOAc-hexane, 1:4) to provide carbamate **92** as a white solid (140 mg, 65 % yield).

**Spectroscopic data and physical constants for compound 92:**

$[\alpha]_D = +7.9$  (c 0.65 in  $\text{CH}_2\text{Cl}_2$ )

**Melting point:** Below 25 °C (ethyl acetate/hexane).

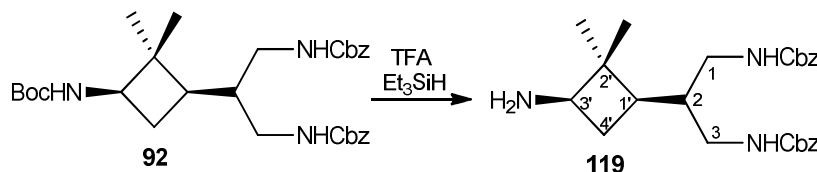
**IR (ATR):** 3335 ( $\text{NH}_{\text{st}}$ ), 2952 ( $\text{CH}_{\text{st}}$ ), 1687 (bs,  $\text{CO}_{\text{carbamate}}$ ), 1512, 1454, 1366.

**$^1\text{H}$  NMR** (360 MHz,  $\text{CDCl}_3$ )  $\delta$  0.97 (s, 3H, *trans*- $\text{CH}_3$ ), 1.16 (s, 3H, *cis*- $\text{CH}_3$ ), 1.43 (s, 9H,  $\text{O}^t\text{Bu}$ ), 1.56-1.71 (m, 1H,  $\text{H}_{4'a}$ ), 2.15-2.36 (m, 1H,  $\text{H}_{1'}$ ), 2.57-2.95 (c.a., 2H,  $\text{H}_{4'b}$ ,  $\text{H}_2$ ), 3.18-3.44 (m, 2H,  $\text{H}_{1a}$ ,  $\text{H}_{3a}$ ), 3.44-3.88 (m, 2H,  $\text{H}_{1b}$ ,  $\text{H}_{3b}$ ), 4.48-4.67 (m, 1H,  $\text{H}_{3'}$ ), 4.98-5.18 (c.a., 5H,  $-\text{CH}_2\text{Bn}$ , NH), 5.52 (bs, 1H, NH), 5.66 (bs, 1H, NH), 7.28-7.43 (c.a., 10H,  $\text{H}_{\text{Ar}}$ ).

**$^{13}\text{C}$  NMR** (90 MHz,  $\text{CDCl}_3$ )  $\delta$  15.7 (*trans*- $\text{CH}_3$ ), 28.4 ( $\text{C}(\text{CH}_3)_3$ ), 29.7 ( $\text{C}_{4'}$ ), 30.0 (*cis*- $\text{CH}_3$ ), 38.3, 39.0 ( $\text{C}_2$ ,  $\text{C}_1$ ,  $\text{C}_3$ ), 40.2 ( $\text{C}_2$ ), 40.9 ( $\text{C}_{1'}$ ), 43.4 ( $\text{C}_{2'}$ ), 50.8 ( $\text{C}_{3'}$ ), 66.7, 66.8 ( $\text{C}_2$ ,  $-\text{CH}_2\text{Bn}$ ), 79.2 ( $\text{C}(\text{CH}_3)_3$ ), 128.0, 128.1, 128.5, 136.5, 136.6 ( $10\text{C}$ ,  $\text{C}_{\text{Ar}}$ ), 155.4, 157.1, 157.3 ( $3\text{C}$ ,  $\text{CO}_{\text{carbamate}}$ ).

**High resolution mass spectrum:** calculated for  $\text{C}_{30}\text{H}_{41}\text{N}_3\text{NaO}_6$ ,  $(\text{M}+\text{Na})^+$ : 562.288, Found: 562.2883.

**Dibenzyl (2-((1*R*,3*R*)-3-amino-2,2-dimethylcyclobutyl)propane-1,3-diyl)dicarbamate, **119**:**

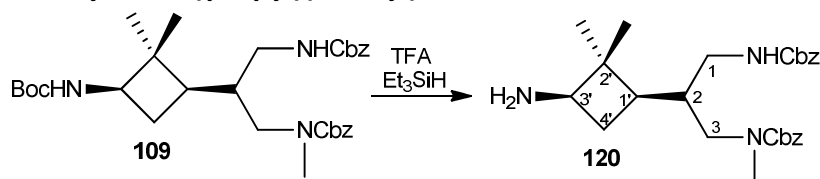


A mixture containing compound **92** (0.12 g, 0.2 mmol), trifluoroacetic acid (0.22 mL, 2.9 mmol, 13 eq) and triethyl silane (80  $\mu\text{L}$ , 0.6 mmol, 2.5 eq) in anhydrous dichloromethane (5 mL) was stirred at room temperature for 2 h. Solvent was evaporated and the excess of trifluoroacetic acid was removed by liophilization affording amine **119** as a colourless oil which was identified by its  $^1\text{H}$  NMR spectrum and used in the next step without purification (95 mg, 98% yield).

**Spectroscopic data for compound 119:**

$^1\text{H NMR}$  (250 MHz,  $\text{CDCl}_3$ )  $\delta$  0.95 (s, 3H, *trans*- $\text{CH}_3$ ), 1.128 (s, 3H, *cis*- $\text{CH}_3$ ), 1.68-1.82 (m, 1H,  $\text{H}_{4'a}$ ), 2.120-2.46 (m, 1H,  $\text{H}_{1'}$ ), 2.68-2.93 (c.a., 3H,  $\text{H}_{4'b}$ ,  $\text{H}_2$ ,  $\text{H}_{1a}$ ), 3.15-3.42 (m, 3H,  $\text{H}_{3a}$ ,  $\text{H}_{1b}$ ,  $\text{H}_{3b}$ ), 3.63-3.81 (m, 1H,  $\text{H}_{3'}$ ), 4.97-5.22 (m, 4H,  $-\text{CH}_2\text{Bn}$ ), 5.67 (bs, 1H, NH), 7.30-7.46 (c.a., 10H,  $\text{H}_{\text{Ar}}$ ).

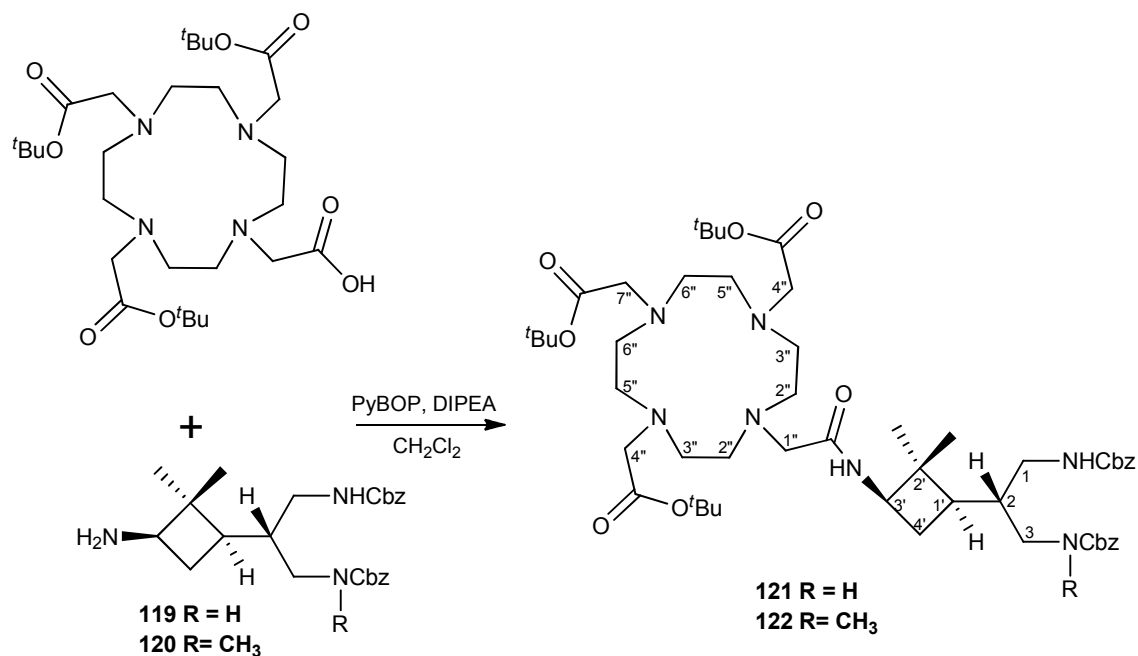
**Benzyl ((*R*)-2-((1*R*,3*R*)-3-amino-2,2-dimethylcyclobutyl)-3-(benzyloxycarbonylamino)propyl)(methyl)carbamate, 120:**



A mixture containing compound **109** (60 mg, 0.1 mmol), trifluoroacetic acid (0.12 mL, 1.6 mmol, 13.0 eq) and triethyl silane (30  $\mu\text{L}$ , 0.2 mmol, 2.0 eq) in anhydrous dichloromethane (5 mL) was stirred at room temperature for 2 h. Solvent was evaporated and the excess of trifluoroacetic acid was removed by liophilization affording amine **120** as a colourless oil which was identified by its  $^1\text{H NMR}$  spectrum and used in the next step without purification (53 mg, 97% yield).

**Spectroscopic data for compound 120:**

$^1\text{H NMR}$  (250 MHz,  $\text{CDCl}_3$ )  $\delta$  0.88 (s, 3H, *trans*- $\text{CH}_3$ ), 1.21 (s, 3H, *cis*- $\text{CH}_3$ ), 1.63-1.92 (c.a., 4H,  $\text{H}_{4'a}$ ,  $\text{H}_{1'}$ ,  $\text{H}_{4'b}$ ,  $\text{H}_2$ ), 2.13-2.41 (m, 1H,  $\text{H}_{3'}$ ), 2.90 (s, 3H, N- $\text{CH}_3$ ), 3.01-3.42 (c.a., 4H,  $\text{H}_{1a}$ ,  $\text{H}_{1b}$ ,  $\text{H}_{3a}$ ,  $\text{H}_{3b}$ ), 4.98-5.25 (c.a., 5H,  $-\text{CH}_2\text{Bn}$ , NH), 6.19 (broad singlet, 1H, NH), 7.30-7.44 (c.a., 10H,  $\text{H}_{\text{Ar}}$ ).

General procedure for the <sup>t</sup>Bu-DOTA-cyclobutane peptide coupling:

To a solution of <sup>t</sup>Bu-DOTA (0.12 g, 0.2 mmol) in 5 mL of DMF were subsequently added PyBOP (0.13 g, 0.2 mmol, 1.1 eq), DIPEA (0.15 mL, 0.9 mmol, 4.0 eq) and amine **119** (95 mg, 0.2 mmol, 1.0 eq). The reaction was stirred for 18 hours, poured into 20 mL of a saturated NaHCO<sub>3</sub> solution and extracted with dichloromethane (3 x 20 mL). The organic extracts were dried over magnesium sulfate. Solvents were removed under reduced pressure to give crude product **121** (0.25 g), which was used in the next step without further purification.

**Tri-*tert*-butyl 2,2',2''-(10-(2-(((1*R*,3*R*)-3-(3,9-dioxo-1,11-diphenyl-2,10-dioxo-4,8-diazaundecan-6-yl)-2,2-dimethylcyclobutyl)amino)-2-oxoethyl)-1,4,7,10-tetraazacyclododecane-1,4,7-triyl)triacetate, 121:**

**Spectroscopic data and physical constants for compound 121:**

<sup>1</sup>H NMR (360 MHz, CDCl<sub>3</sub>) δ 0.99 (s, 3H, *trans*-CH<sub>3</sub>), 1.11 (s, 3H, *cis*-CH<sub>3</sub>), 1.45 (s, 27H, O<sup>t</sup>Bu), 1.78-1.89 (m, 1H, H<sub>4'a</sub>), 2.01-3.45 (c.a., 30H, H<sub>1'</sub>, H<sub>2''</sub>, H<sub>3''</sub>, H<sub>5''</sub>, H<sub>6''</sub>, H<sub>4'b</sub>, H<sub>2</sub>, H<sub>1a</sub>, H<sub>3a</sub>, H<sub>1''</sub>, H<sub>4''</sub>, H<sub>7''</sub>), 3.57-3.78 (m, 2H, H<sub>1b</sub>, H<sub>3b</sub>), 3.81-3.93 (m, 1H, H<sub>3'</sub>), 5.02-5.15 (m, 4H, -CH<sub>2</sub>Bn), 5.20 (bs, 1H, NH), 5.73 (bs, 1H, NH), 6.11 (bs, 1H, NH), 7.29-7.41 (c.a., 10H, H<sub>Ar</sub>).

<sup>13</sup>C NMR (90 MHz, CDCl<sub>3</sub>) δ 16.0 (*trans*-CH<sub>3</sub>), 28.0 (9C, C(CH<sub>3</sub>)<sub>3</sub>), 29.7 (C<sub>4'</sub>), 31.7 (*cis*-CH<sub>3</sub>), 38.6, 39.1 (2C, C<sub>1</sub>, C<sub>3</sub>), 40.2 (C<sub>2</sub>), 40.9 (C<sub>1'</sub>), 43.8 (C<sub>2'</sub>), 48.3, 49.7 (8C, C<sub>2''</sub>, C<sub>3''</sub>, C<sub>5''</sub>, C<sub>6''</sub>), 51.7, 52.5 (4C, C<sub>1''</sub>, C<sub>4''</sub>, C<sub>7''</sub>), 55.7 (C<sub>3'</sub>), 66.6, 66.8 (2C, -CH<sub>2</sub>Bn), 81.9 (3C, C(CH<sub>3</sub>)<sub>3</sub>), 128.0, 128.1, 128.5, 132.1, 132.2, 136.5, 136.7 (12C, C<sub>Ar</sub>), 157.0, 157.5 (2C, CO<sub>carbamate</sub>), 171.5, 172.5 (4C, CO<sub>ester</sub>, CO<sub>amide</sub>).

**High resolution mass spectrum:** calculated for C<sub>53</sub>H<sub>83</sub>N<sub>7</sub>NaO<sub>11</sub>, (M+Na)<sup>+</sup>: 1016.6048, Found: 1016.6052.

Tri-*tert*-butyl 2,2',2''-(10-(2-(((1*R*,3*R*)-2,2-dimethyl-3-((*R*)-4-methyl-3,9-dioxo-1,11-diphenyl-2,10-dioxo-4,8-diazaundecan-6-yl)cyclobutyl)amino)-2-oxoethyl)-1,4,7,10-tetraazacyclododecane-1,4,7-triyl)triacetate, **122**:

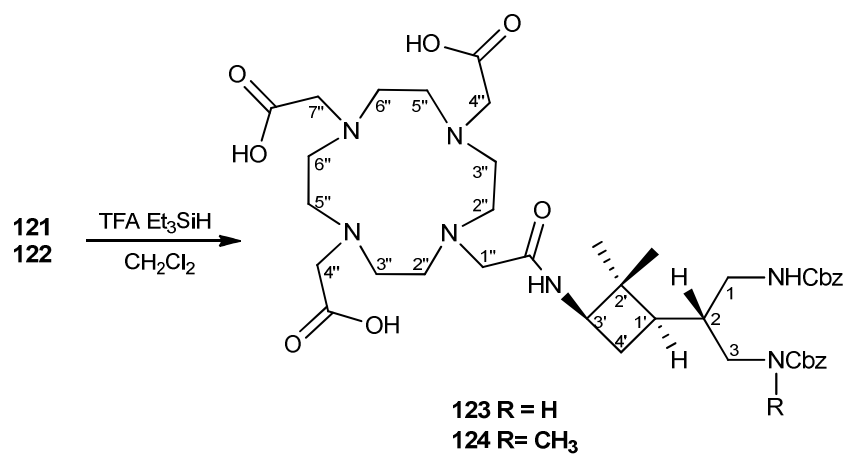
**Spectroscopic data and physical constants for compound 122:**

$^1\text{H NMR}$  (250 MHz,  $\text{CDCl}_3$ )  $\delta$  1.00 (s, 3H, *trans*- $\text{CH}_3$ ), 1.16 (s, 3H, *cis*- $\text{CH}_3$ ), 1.44 (s, 27H,  $\text{O}^t\text{Bu}$ ), 1.67-1.77 (m, 1H,  $\text{H}_{4'a}$ ), 2.66-3.09 (c.a., 33H,  $\text{H}_{1'}$ ,  $\text{H}_{2''}$ ,  $\text{H}_{3''}$ ,  $\text{H}_{5''}$ ,  $\text{H}_{6''}$ ,  $\text{H}_{4'b}$ ,  $\text{H}_2$ , N- $\text{CH}_3$ ,  $\text{H}_{1a}$ ,  $\text{H}_{3a}$ ,  $\text{H}_{1''}$ ,  $\text{H}_{4''}$ ,  $\text{H}_{7''}$ ), 3.24-3.36 (c.a., 5H,  $\text{H}_{3'}$ ,  $\text{H}_{1a}$ ,  $\text{H}_{1b}$ ,  $\text{H}_{3a}$ ,  $\text{H}_{3b}$ ), 5.02-5.18 (m, 4H,  $-\text{CH}_2\text{Bn}$ ), 6.14 (bs, 1H, NH), 6.32 (bs, 1H, NH), 7.30-7.42 (c.a., 10H,  $\text{H}_{Ar}$ ).

$^{13}\text{C NMR}$  (62.5 MHz,  $\text{CDCl}_3$ )  $\delta$  18.8 (*trans*- $\text{CH}_3$ ), 26.7, 26.9 (9C,  $\text{C}(\text{CH}_3)_3$ ), 29.8 ( $\text{C}_{4'}$ ), 30.1 (*cis*- $\text{CH}_3$ ), 35.3 (N- $\text{CH}_3$ ), 37.5, 38.4 (2C,  $\text{C}_1$ ,  $\text{C}_3$ ), 40.7 ( $\text{C}_2$ ), 41.0 ( $\text{C}_{1'}$ ), 41.8 ( $\text{C}_{2'}$ ), 46.7 (8C,  $\text{C}_{2''}$ ,  $\text{C}_{3''}$ ,  $\text{C}_{5''}$ ,  $\text{C}_{6''}$ ), 53.0, 53.9 (4C,  $\text{C}_{1''}$ ,  $\text{C}_{4''}$ ,  $\text{C}_{7''}$ ), 56.0 ( $\text{C}_{3'}$ ), 68.0, 68.3 (2C,  $-\text{CH}_2\text{Bn}$ ), 82.2 (3C,  $\text{C}(\text{CH}_3)_3$ ), 127.8, 128.4, 128.7, 129.0, 129.1, 136.3, 137.1 (12C,  $\text{C}_{Ar}$ ), 155.6, 156.3 (2C,  $\text{CO}_{\text{carbamate}}$ ), 170.4, 171.8 (4C,  $\text{CO}_{\text{ester}}$ ,  $\text{CO}_{\text{amide}}$ ).

**High resolution mass spectrum:** calculated for  $\text{C}_{54}\text{H}_{85}\text{N}_7\text{NaO}_{11}$ ,  $(\text{M}+\text{Na})^+$ : 1030.6199, Found: 1030.6214.

**General procedure for the  $^t\text{Bu}$ -DOTA-cyclobutane deprotection:**





A mixture containing compound **121** (0.25 g, 0.2 mmol), trifluoroacetic acid (3.0 mL, 40.0 mmol, 200.0 eq) and triethyl silane (40  $\mu$ L, 0.3 mmol, 1.5 eq) was stirred at room temperature for 18 h. The reaction mixture was evaporated and dissolved in methanol (5 mL) and **123** was isolated as a white solid through the addition of diethyl ether drops (82 mg, 49% overall yield for the 2 steps).

The same procedure was applied for **122** to obtain **124** (48 mg, 45% overall yield for the 2 steps).

**2,2',2''-(10-(2-(((1*R*,3*R*)-3-(3,9-dioxo-1,11-diphenyl-2,10-dioxa-4,8-diazaundecan-6-yl)-2,2-dimethylcyclobutyl)amino)-2-oxoethyl)-1,4,7,10-tetraazacyclododecane-1,4,7-triyl)triacetic acid, **123**:**

**Spectroscopic data for compound 123:**

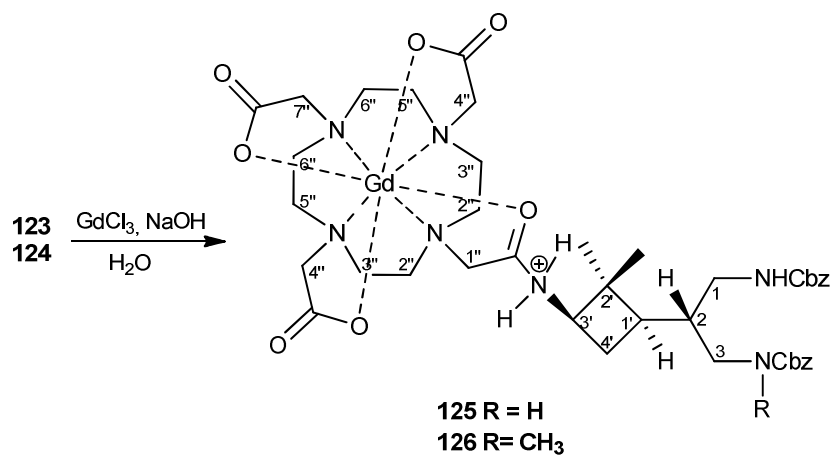
**MALDI-TOF spectrum:** calculated for  $C_{41}H_{60}N_7O_{11}$ ,  $(M+H)^+$ : 826.435, Found: 826.418.

**2,2',2''-(10-(2-(((1*R*,3*R*)-2,2-Dimethyl-3-((*R*)-4-methyl-3,9-dioxo-1,11-diphenyl-2,10-dioxa-4,8-diazaundecan-6-yl)cyclobutyl)amino)-2-oxoethyl)-1,4,7,10-tetraazacyclododecane-1,4,7-triyl)triacetic acid, **124**:**

**Spectroscopic data for compound 124:**

**MALDI-TOF spectrum:** calculated for  $C_{42}H_{62}N_7O_{11}$ ,  $(M+H)^+$ : 840.450, Found: 840.479.

## General procedure for the Gd complexation:



Tri-carboxylic acid **123** (14.9 mg, 0.02 mmol) was dissolved in 0.7 mL of water to which  $\text{GdCl}_3 \cdot 6\text{H}_2\text{O}$  (6.2 mg, 0.02 mmol, 1.0 eq) was added, the pH was adjusted to 6.5 with 0.1 mM NaOH and the reaction was stirred at room temperature until completed. The reaction progress was monitored using the xylenol orange test (detects free  $\text{Gd}^{3+}$ ). After that the solvent was eliminated in the anhydrous freezer to obtain **125** as a white solid.

The same procedure was applied for **124** to obtain **126** as a white solid.

**Annex I**

Coupling Agents



## 8. ANNEX I: COUPLING REAGENTS

We have used three different kind of coupling reagents in the peptide synthesis, **EDAC** (1-[3-(dimethylamino)propyl]-3-ethylcarbodiimide hydrochloride, *carbodiimide type*) and **PyBOP** (benzotriazol-1-yl-oxytripyrrolidinophosphonium hexafluorophosphate, *phosphonium type*) and **HATU** (O-(7-Azabenzotriazol-1-yl)-N,N,N',N'-tetramethyluronium hexafluorophosphate, *aminium type*):

**Carbodiimide reagents** have been widely used in peptide synthesis because they show a moderate activity and they are reasonably cheap (**Figure 71**). DCC was first reported by Sheehan in 1955.<sup>162</sup> The urea by-product was insoluble in most organic solvents and hence was easily separable from the product.

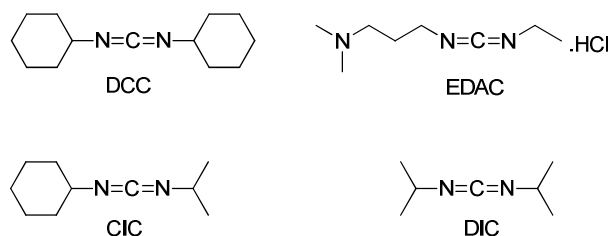
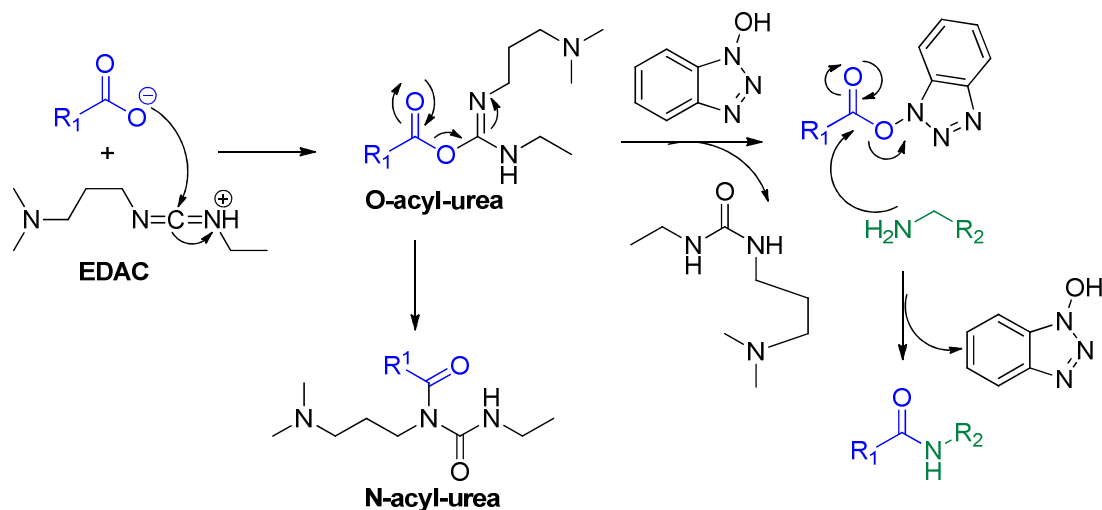


**Figure 71:** Common carbodiimide reagents.

As has been shown before, when coupling *via* carbodiimide, as in with the rest of the coupling agents, the carboxyl group is usually activated to speed up the reaction yielding a highly reactive *O*-acyl-urea (**Scheme 59**). To enhance the electrophilicity of the carboxylate group, the negatively charged oxygen must first be "activated" into a better leaving group. Nevertheless, the by-product *N*-acyl-urea is sometimes formed in important amounts when carbodiimides are used in the formation of amide bonds and they can therefore cause racemisation if there is a stereogenic centre in the  $\alpha$ -position of the carboxyl group. This problem was solved when HOBt (hydroxybenzotriazole) was added to the reaction mixture, which circumvents the use of excess reagent that was typical in similar processes before its use. This additive reacts with activated acyl groups (for example, carboxylic acid + EDAC as in

**Scheme 20)** to form activated molecules that are referred to as *activated esters*. Under these conditions, chiral integrity is usually retained and there is no need for protecting sensitive functional groups such as the free hydroxyl moiety. Since the successful launch of DCC/HOBt in peptide synthesis,<sup>163</sup> carbodiimides have dramatically expanded their scope with the aid of various additives (such as HOPO, HOAt, etc.). These additives have complemented the weakness of coupling reagents by enhancing the reaction rate and reducing the racemisation.



**Scheme 59:** Reaction mechanism for the carbodiimide-mediated peptide coupling.

**Phosphonium reagents:** Since the discovery of HOBt-attached coupling reagents was successful, many racemisation suppressants have been exploited as a part of compositions of new peptide coupling reagents (**Figure 72**).<sup>164, 165, 166, 167, 168</sup>

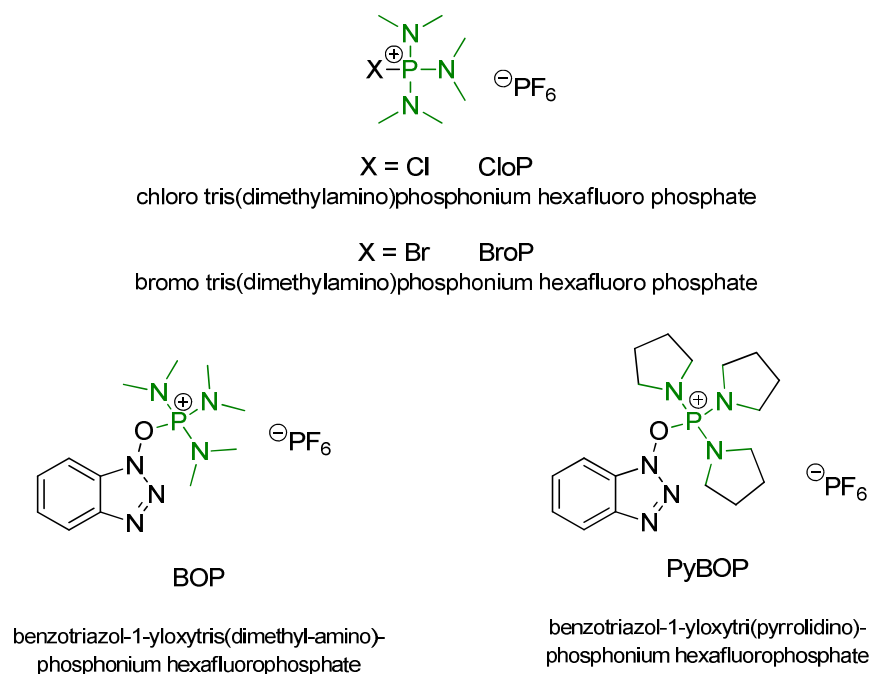
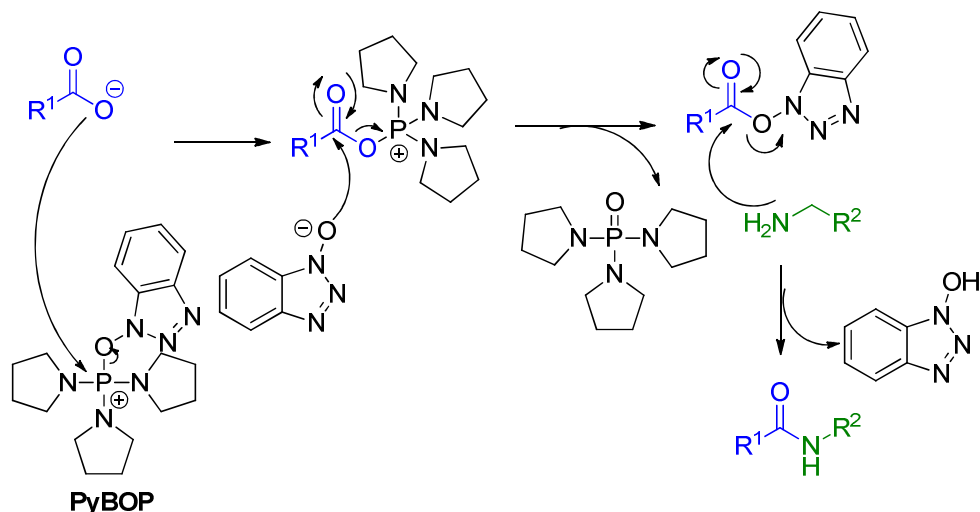


**Figure 72:** Common phosphonium reagents used in peptide synthesis.

The use of the effective couple EDAC/HOBt led to satisfactory results in the peptide coupling. Nevertheless, the reaction time required for completing the condensation between to cyclobutane amino acids was long, from 2 to 4 days, in comparison with the reaction times described for peptide coupling using *phosphonium reagents*.

These results are in agreement with those in the literature, where the coupling reagents are differently effective depending on the electronic and steric characteristics of the acid and the amine coupled in a new amide bond formation. On the other hand, the obtained results are also in agreement with the fact that *BOP reagents* provide usually higher yields of products than carbodiimide ones due to the fact that undesired *N*-acyl-urea cannot be formed (**Scheme 60**) and, in most of cases, keeping stable the optical integrity.



**Scheme 60:** Reaction mechanism for the phosphonium-mediated peptide coupling.

**Aminium reagents:** Gross introduced HBTU as the progenitor of uronium reagents in 1978.<sup>164</sup> Since then, various analogues of HBTU have been prepared and investigated by Knorr (**Figure 73**).<sup>166</sup> The tetrafluoroborate or hexafluorophosphate anion is generally used as the non-nucleophilic counterion in uronium reagents.

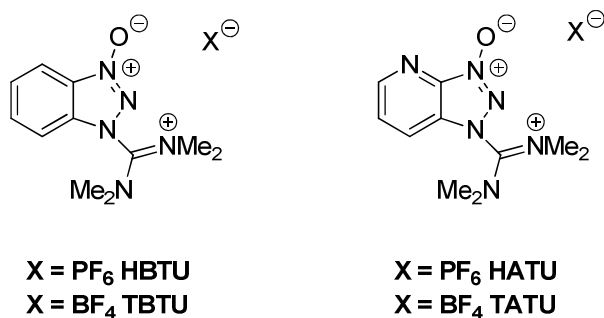


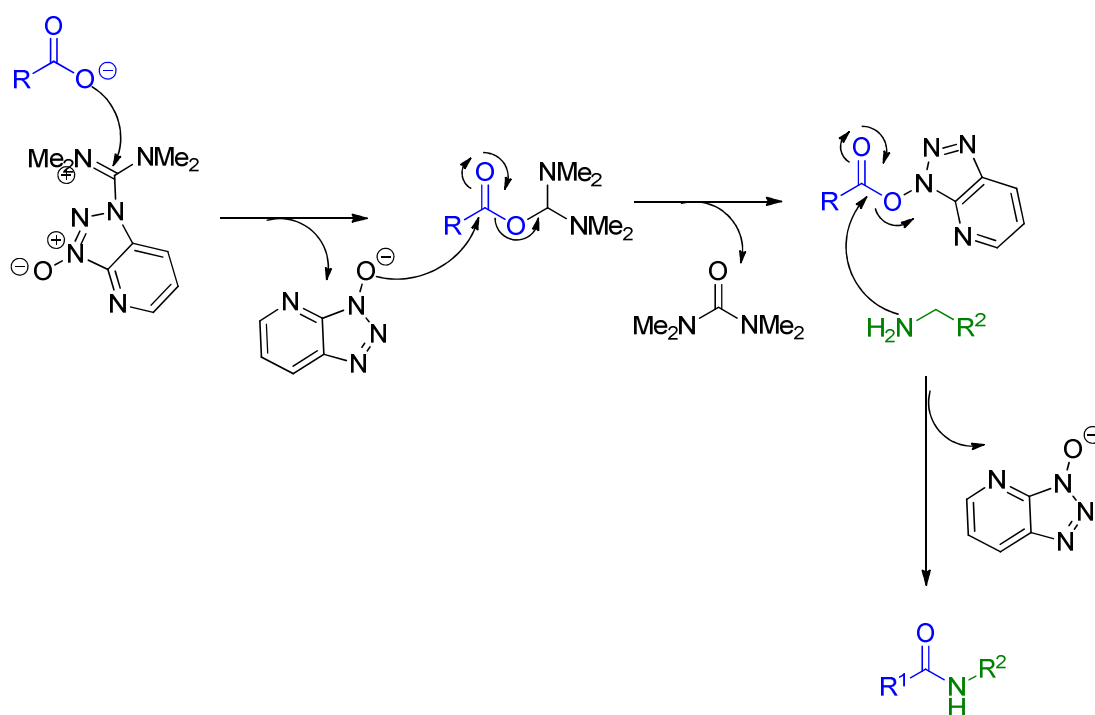
**Figure 73:** Common aminium reagents used in peptide synthesis.

For a long time, the active HBTU and its family were believed to possess an uronium structure, but intensive studies provided evidence for the formulation of guanidinium *N*-oxides.<sup>168</sup> Nevertheless, by custom, they are still called uronium type reagents. Unlike carbodiimides or phosphonium reagents, uronium salts could form tetramethylguanidinium derivatives with free amines. To circumvent this side reaction, excess reagent should be



avoided and pre-activation of the carboxylic acid component is recommended before adding the amine.

Besides HBTU and TBTU, several other members of the uronium family are worthy of attention. The 7-aza-analogue of HBTU called HATU (1-[Bis-(dimethylamino)methyliumyl]-1H-1,2,3-triazolo[4,5-b]pyridine-3-oxide hexafluorophosphate) can be considered today's gold standard of peptide coupling reagents. It has been used for difficult amide bond formation in solution and solid-phase (e.g., PNAs) synthesis.<sup>169</sup> It is especially superior for macrocyclization, fragment condensation, and the coupling of *N*-substituted amino acids. Reaction mechanism is depicted in **Scheme 61**.



**Scheme 61:** Reaction mechanism for the aminium-mediated peptide coupling.



## **Annex II**

NMR studies of cyblobutane-cored dendrimers



## 9. ANNEX II: NMR STUDIES OF CYCLOBUTANE-CORED DENDRIMERS

In order to test the capability of cyclobutane ring to induce defined secondary structures in solution, a structural study using different NMR techniques was carried out for the series of orthogonally protected hybrid cyclobutane-GABA peptides. The followed procedure can be summarised in the following steps:

1. NMR spectra of the peptide series assignment ( $^1\text{H}$  and  $^{13}\text{C}$ )
2. Recording of SELTOCSY spectra (bond coupling) for each NH
3. Recording of SELTOCSY spectra (space coupling) for each NH
4. Superposition and comparison of SELTOCSY and SELNOESY spectra

Here are shown the superpositions of SELTOCSY and SELNOESY spectras for each of the NHs of each of the peptides.

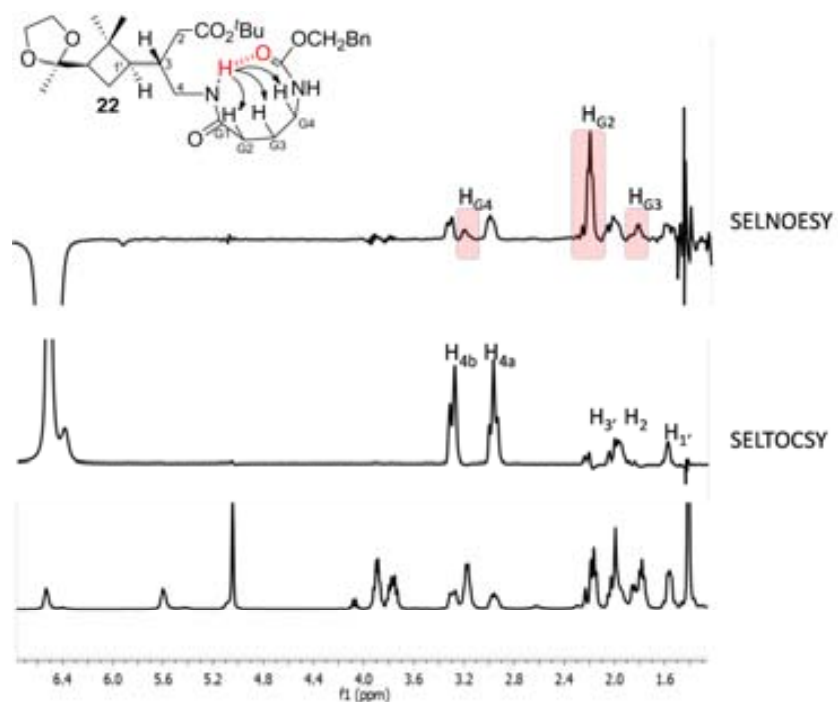
**Dipeptide 22**

Figure 74: Overlay of the  $^1\text{H}$ , SELTOCSY (6.53 ppm) and SELNOESY (6.53 ppm) spectra of dipeptide **22**.

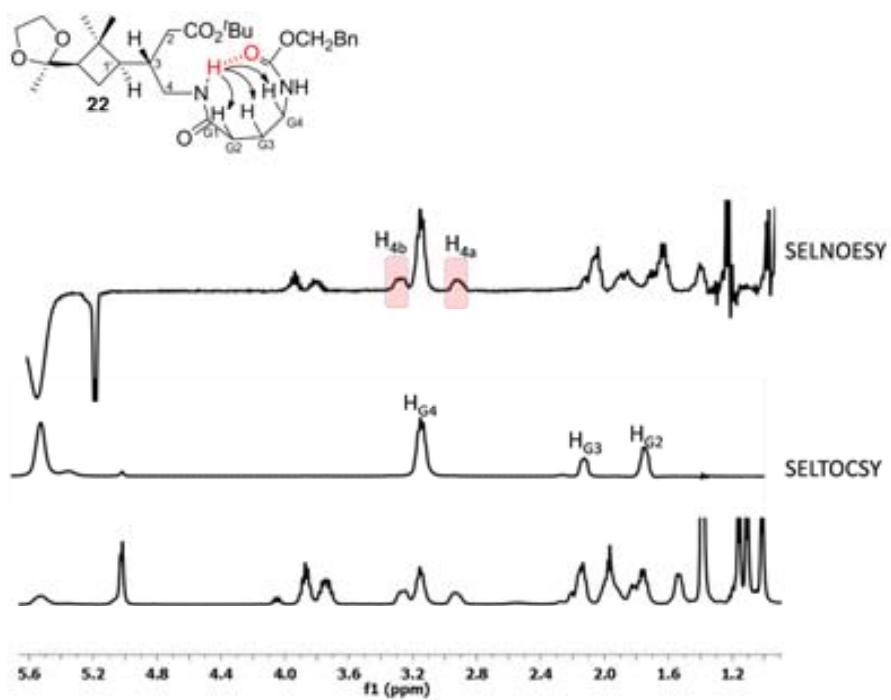


Figure 75: Overlay of the  $^1\text{H}$ , SELTOCSY (5.60 ppm) and SELNOESY (5.60 ppm) spectra of dipeptide **22**.

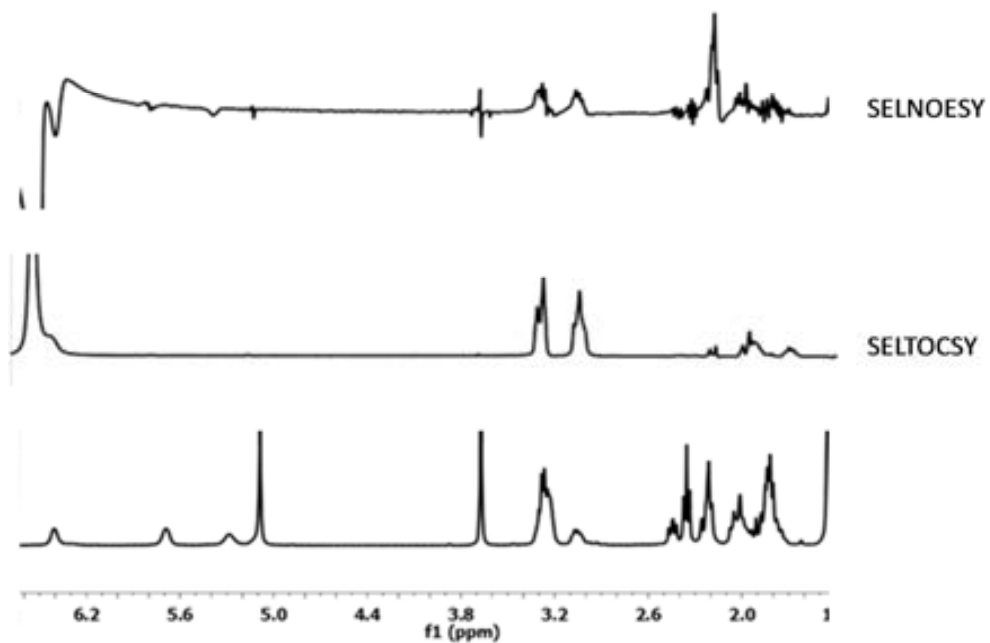
**Tripeptide 25**

Figure 76: Overlay of the  $^1\text{H}$ , SELTOCSY (6.39 ppm) and SELNOESY (6.39 ppm) spectra of tripeptide 25.

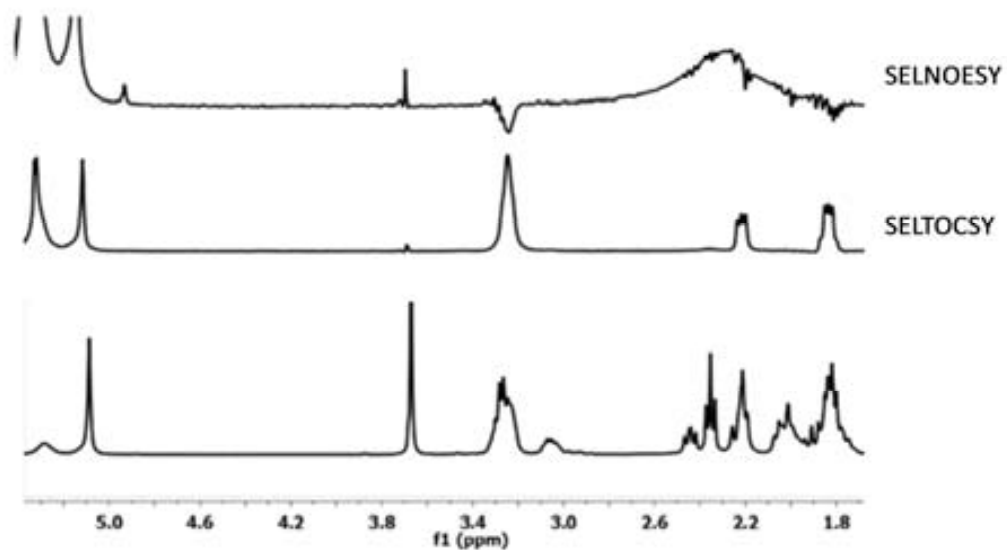
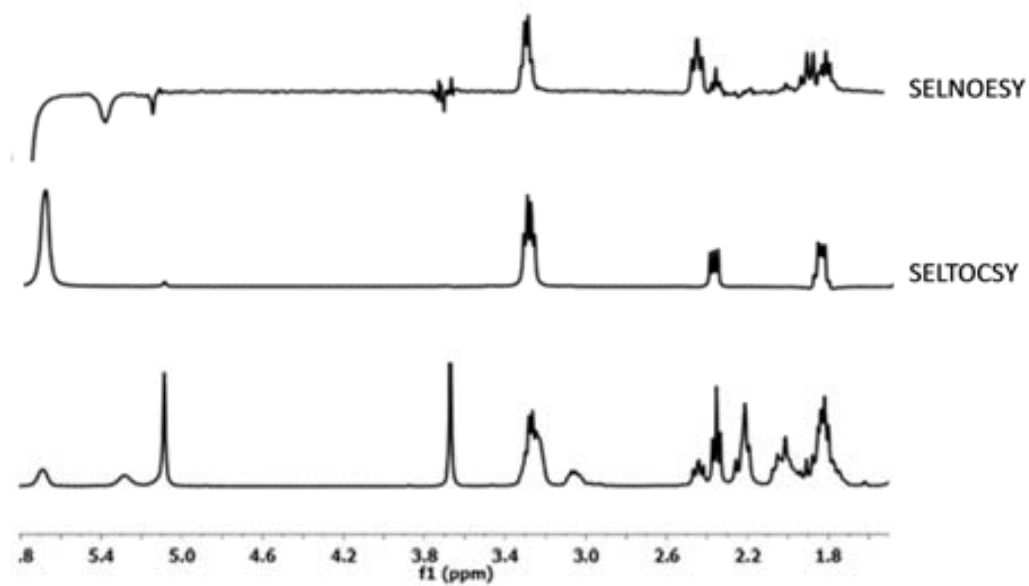


Figure 77: Overlay of the  $^1\text{H}$ , SELTOCSY (5.28 ppm) and SELNOESY (5.28 ppm) spectra of tripeptide 25.



**Figure 78:** Overlay of the  $^1\text{H}$ , SELTOCSY (5.69 ppm) and SELNOESY (5.69 ppm) spectra of tripeptide **25**.



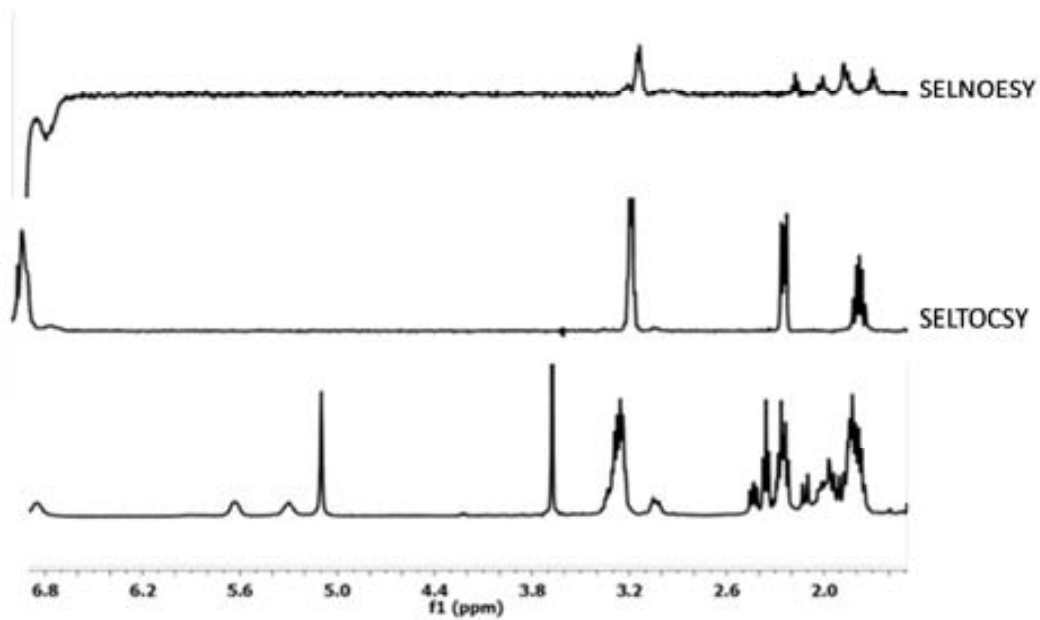
**Tetrapeptide 27**

Figure 79: Overlay of the  $^1\text{H}$ , SELTOCSY (6.99 ppm) and SELNOESY (6.99 ppm) spectra of tetrapeptide 27.

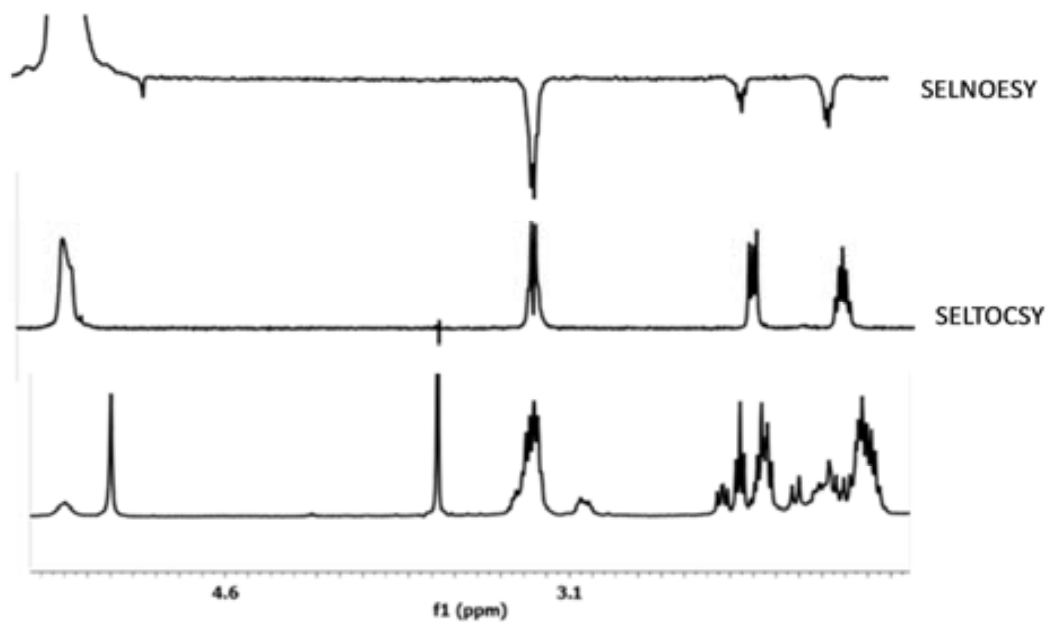


Figure 80: Overlay of the  $^1\text{H}$ , SELTOCSY (5.38 ppm) and SELNOESY (5.38 ppm) spectra of tetrapeptide 27.

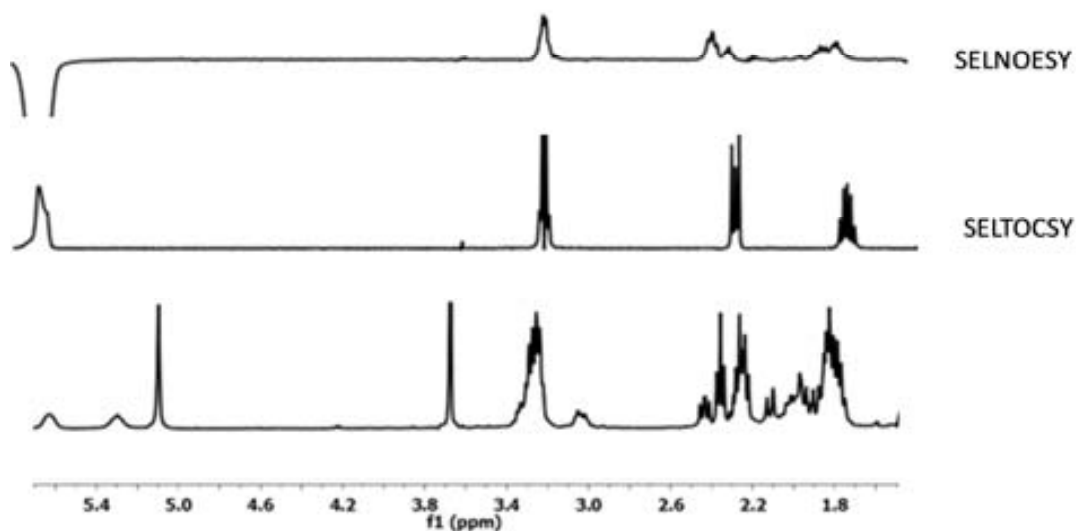


Figure 81: Overlay of the  $^1\text{H}$ , SELTOCSY (5.70 ppm) and SELNOESY (5.70 ppm) spectra of tetrapeptide 27.

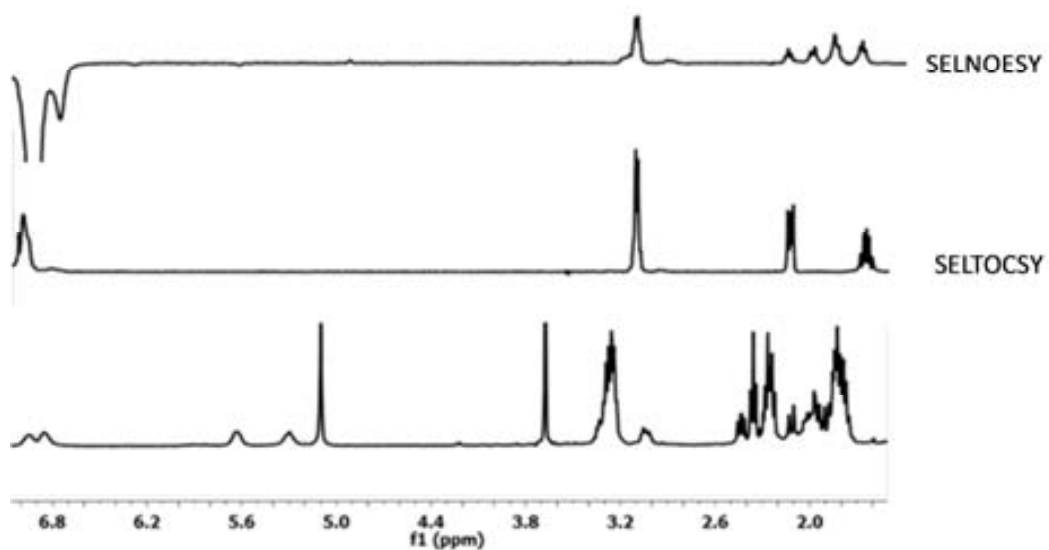


Figure 82: Overlay of the  $^1\text{H}$ , SELTOCSY (7.14 ppm) and SELNOESY (7.14 ppm) spectra of tetrapeptide 27.

### **Annex III**

Detailed NMR studies on hybrid cyclobutane-proline  $\gamma$ ,  $\gamma$ -peptides



## 10. ANNEX III: DETAILED NMR STUDIES ON HYBRID CYCLOBUTANE- PROLINE $\gamma$ , $\gamma$ -PEPTIDES

### Compound 55

$^1\text{H}$  spectrum of triprotected 4-aminoproline **55** acquired at 273K clearly shows split resonances in most of the protons. It is widely known that dynamic rotation of the conjugated NC bond Boc is very slow within the NMR time scale giving rise to *trans/cis* conformers. The key point for the unambiguous assignment of both conformers is the NOE contacts observed in *tert*-Bu group. While *trans* isomer correlates *tert*-Bu with  $\text{H}^5$  protons, *cis* isomers does it with  $\text{Me}^1$  and  $\text{H}^3$  proton. Both conformers are almost equally populated (**Figure 83**).

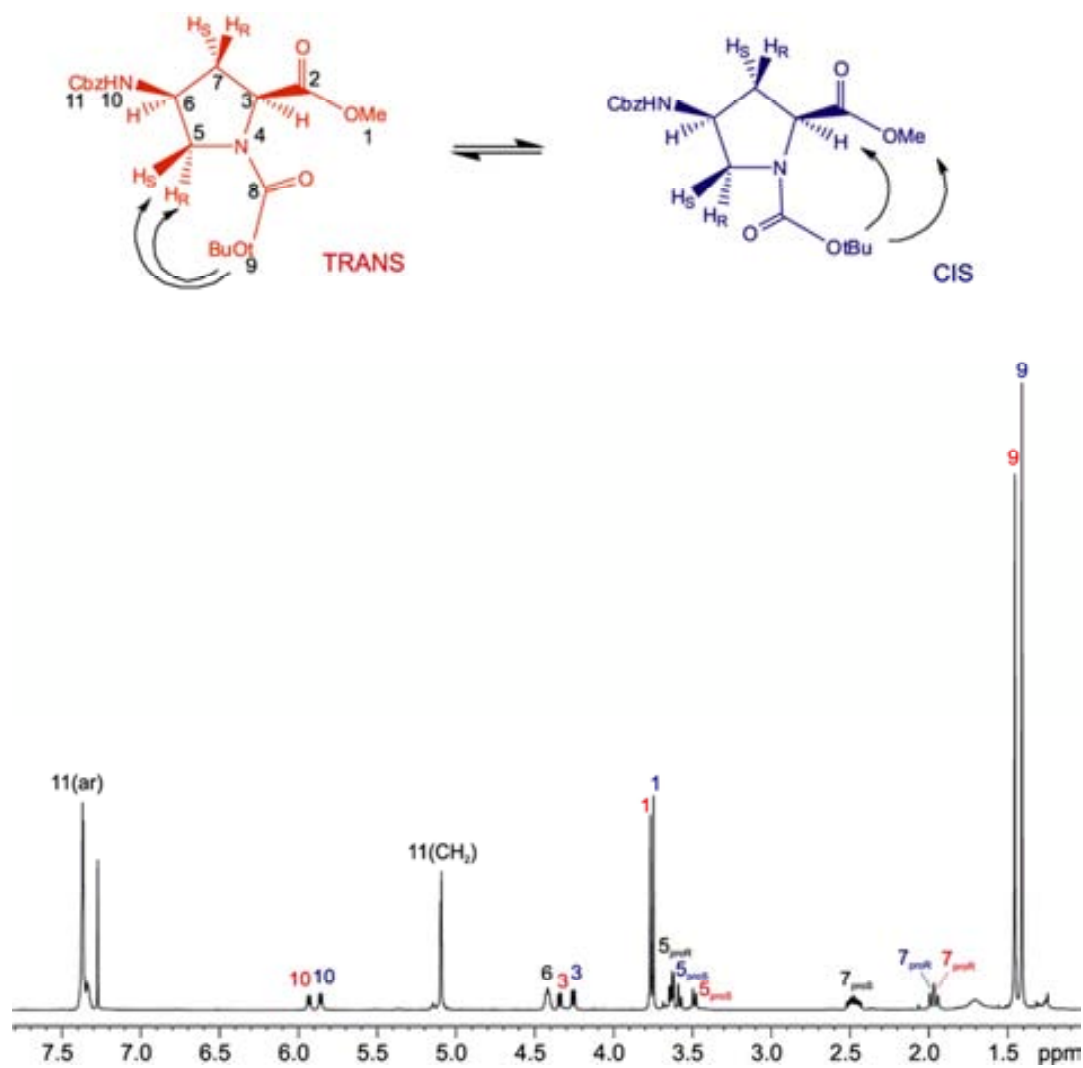


**Figure 83:**  $^1\text{H}$  spectrum of **55** acquired in a Bruker 600 MHz spectrometer at 273K. *Trans* isomer is marked red and *cis* isomer is marked blue. Overlapped *trans/cis* signals are not colored.

1D selective TOCSY experiment irradiating at  $H^{10}$  protons led to obtain *cis/trans* proline protons in separate subspectra (**Figure 84**), thus facilitating the *cis/trans* chemical shift assignment.

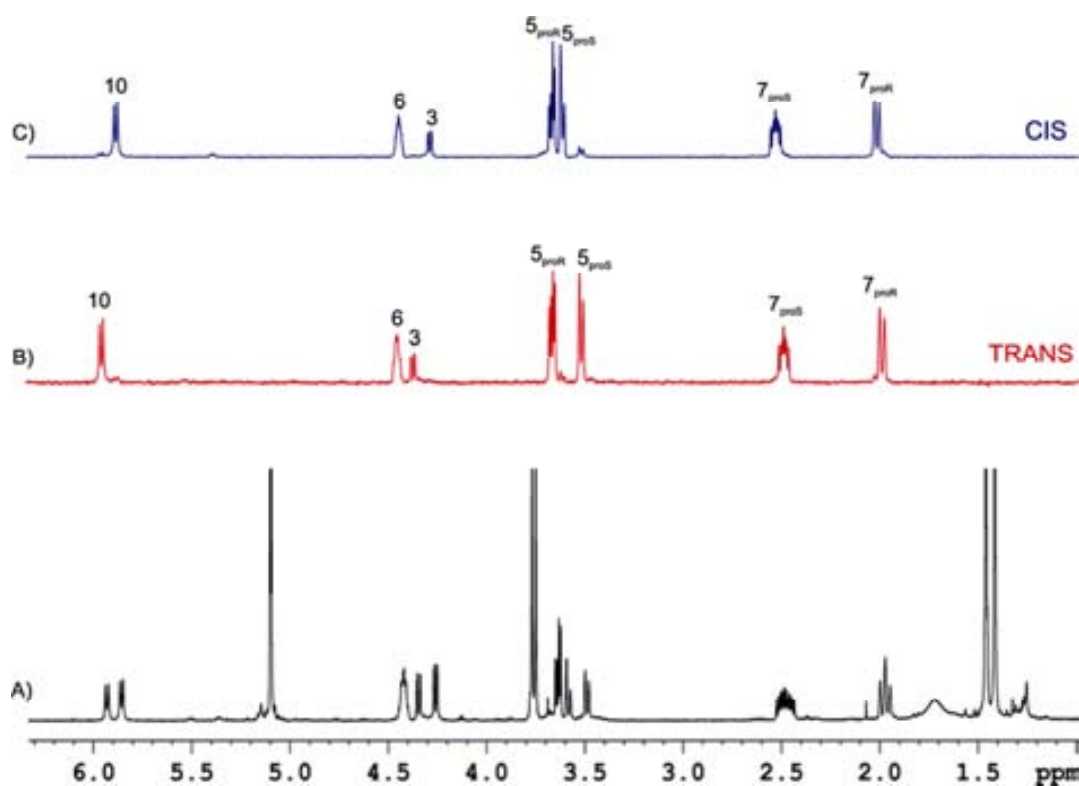


**Figure 84:** A)  $^1H$  NMR spectrum (black) obtained at 600 MHz,  $CDCl_3$ . B) 1D selective TOCSY experiment irradiating  $H^{10}$  *trans* proton (140 ms mixing time). C) 1D selective TOCSY experiment irradiating  $H^{10}$  *cis*-proton (140 ms mixing time).

<sup>13</sup>C NMR spectrum acquired at 273K also exhibits split resonances for most of the signals due to *cis/trans* isomers (**Figure 85**). It is noticeable that  $CO^8$  signal difference between *trans* and *cis* isomer is about 113 Hz, while the differences encountered between *cis/trans* isomers in carbonyls  $CO^2$  and  $CO^{11}$  are much lower (16 Hz and 9 Hz, respectively), therefore confirming that conformational rotational barrier is due to NC bond in Boc group.

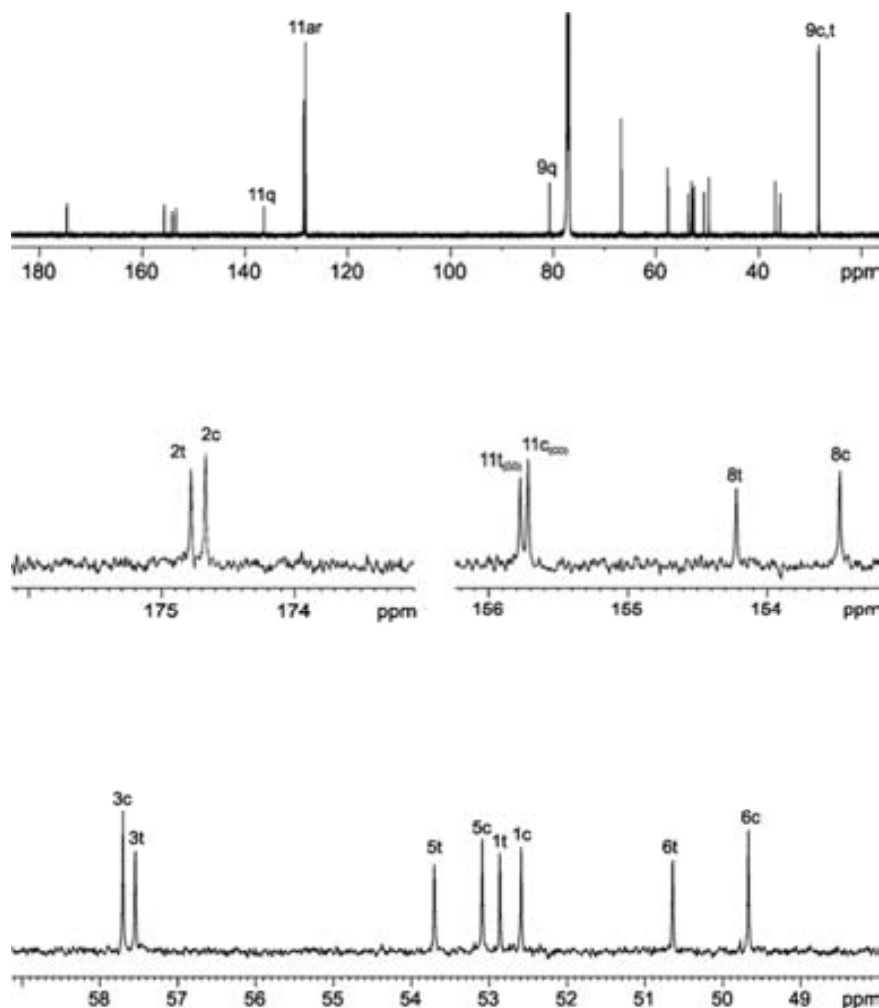


**Figure 85:**  $^{13}\text{C}$  NMR spectrum of **55** recorded in a Bruker 600 MHz spectrometer in  $\text{CDCl}_3$  at 273K. Several expanded regions clearly show *trans* and *cis* isomer signals which are fully assigned and marked with the subscript t or c respectively.

The experiment that is the key point to assign unequivocally *trans* and *cis* isomers is 2D-NOESY spectrum acquired at 273K (**Figure 86**). The expanded region presenting *tert*-butyl cross peaks shows that the slightly major component has cross peaks with  $\text{H}^3$  and  $\text{Me}^1$  protons, therefore can be attributed to *cis* conformer. On the other hand, minor component correlates with  $\text{H}^5$  protons, therefore assigned to *trans* conformer.



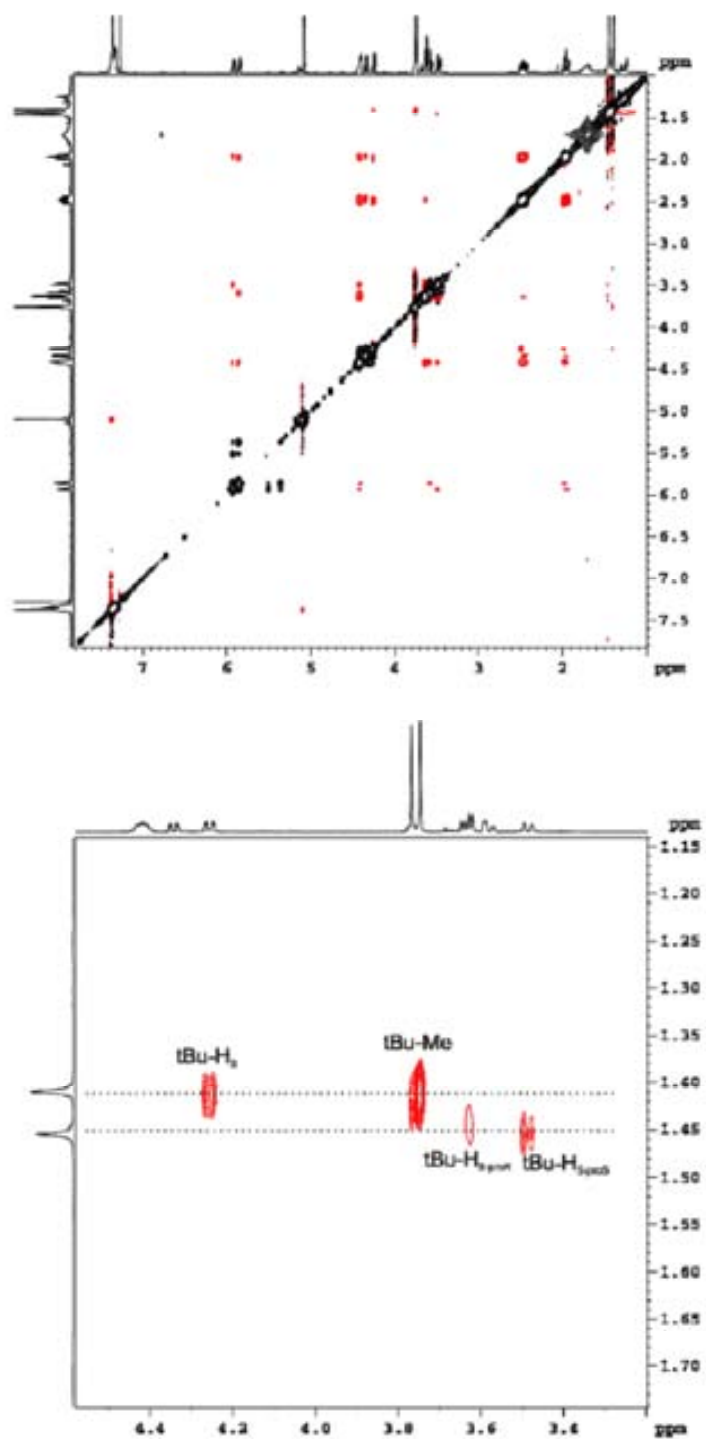


**Figure 86:** 2D-NOESY spectrum recorded in a Bruker 600 MHz spectrometer in CDCl<sub>3</sub> at 273 K (mixing time was set to 500 ms). Expanded region showing cross <sup>t</sup>Bu cross peaks is shown.

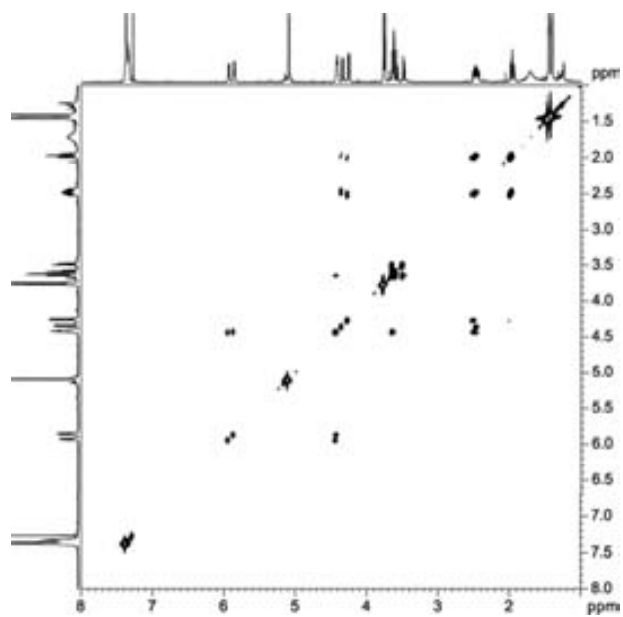


**Figure 87:** COSY spectrum recorded in a Bruker 600 MHz spectrometer in CDCl<sub>3</sub> at 273 K.

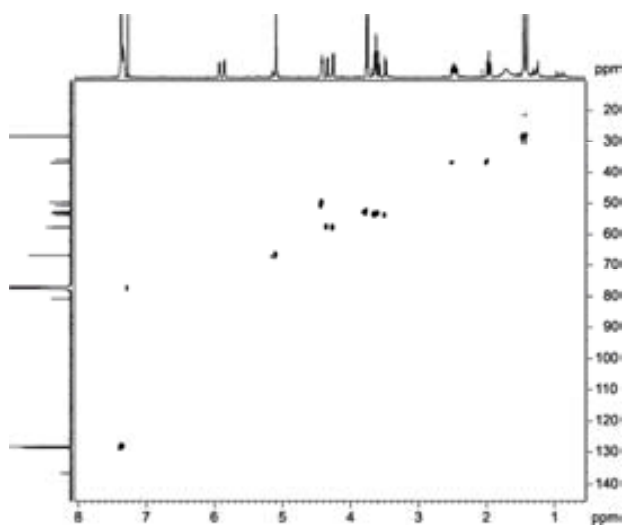


**Figure 88:** H<sup>1</sup>QC spectrum recorded in a Bruker 600 MHz spectrometer in CDCl<sub>3</sub> at 273 K.

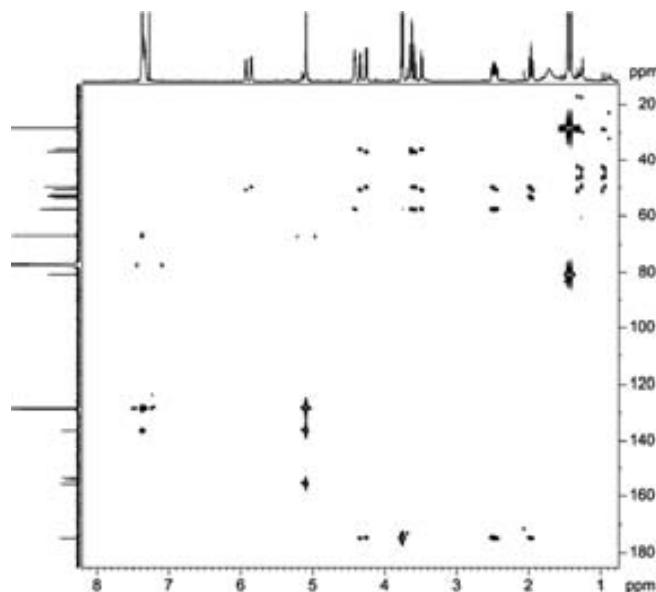


**Figure 89:** HMBC spectrum recorded in a Bruker 600 MHz spectrometer in  $\text{CDCl}_3$  at 273 K.

Interestingly, while inverting  $\text{H}^{10}$  proton in 1D selective NOE experiment, independently of *cis* or *trans* isomer (**Figure 90**), NOE effects are observed at *pro-S*  $\text{H}^5$  and *pro-R*  $\text{H}^7$ , suggesting that  $\text{NH}^{10}$  in both conformers is pointing to the carbonyl of the methyl ester group ( $\text{CO}^2$ ) probably due to the presence of a hydrogen bond. Also, conformational exchange signals are detected in that experiment between *cis* and *trans* isomers (see detailed expanded spectra in **Figure 91**). Furthermore, two small signals resonating  $\sim 0.5$  ppm downfield with respect to the major signals were observed. Those are assigned to minor conformations without such hydrogen bonding.

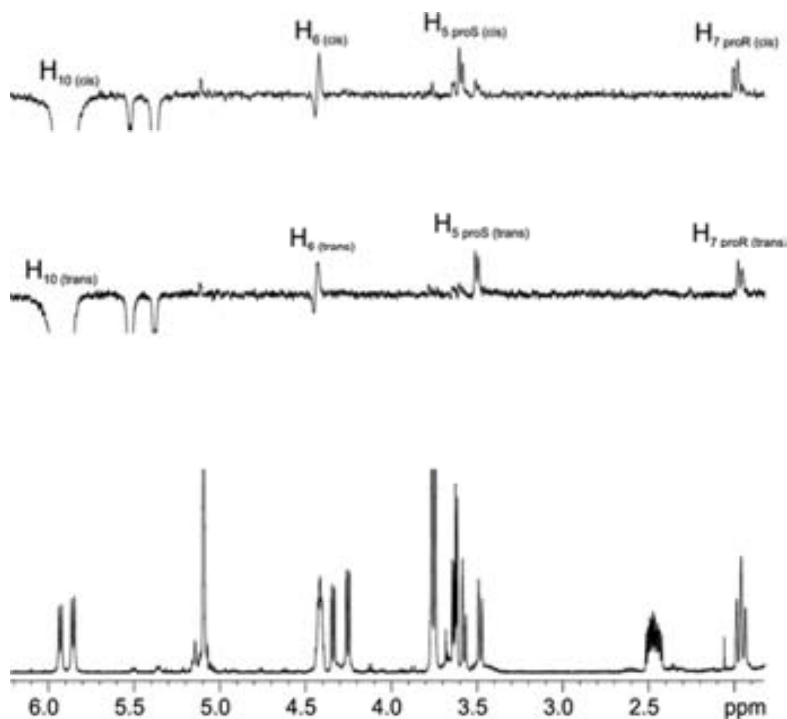


**Figure 90:** 1D selective NOE experiments at  $H_{10(cis)}$  and  $H_{10(trans)}$  protons recorded in a Bruker 600 MHz spectrometer in  $CDCl_3$  at 273 K. Mixing time was set to 500 ms, ns 1k.

Also, conformational exchange signals are detected in that experiment between *cis* and *trans* isomers (see detailed expanded spectra of **Figure 90** in **Figure 91**). Furthermore, two small signals resonating  $\sim 0.5$  ppm upfield with respect to  $H^{10}$  (*trans/cis*) major signals are observed. Those are attributed to  $H^{10}$  (*trans/cis*) minor conformations without such hydrogen bonding.

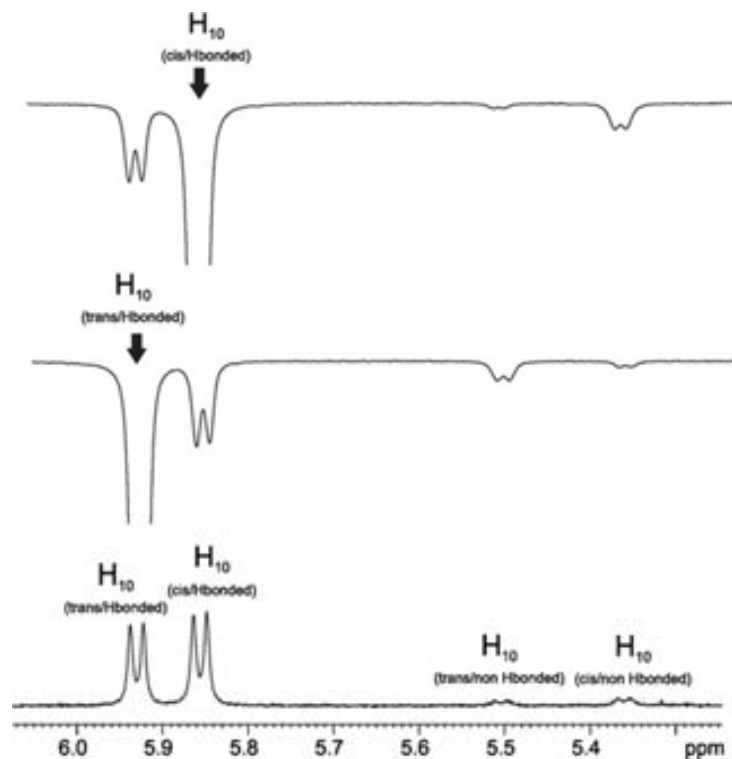


**Figure 91:** Expanded region of spectra shown in **Figure 90**. Chemical exchange peaks (EXSY peaks) are clearly seen in 1D-selective experiments corresponding to non-hydrogen bonded conformers for both *cis* and *trans* isomers.

According to all NMR experiments performed, the conformational equilibrium of triprotected 4-aminoproline **55** can be depicted as shown in **Figure 92**.

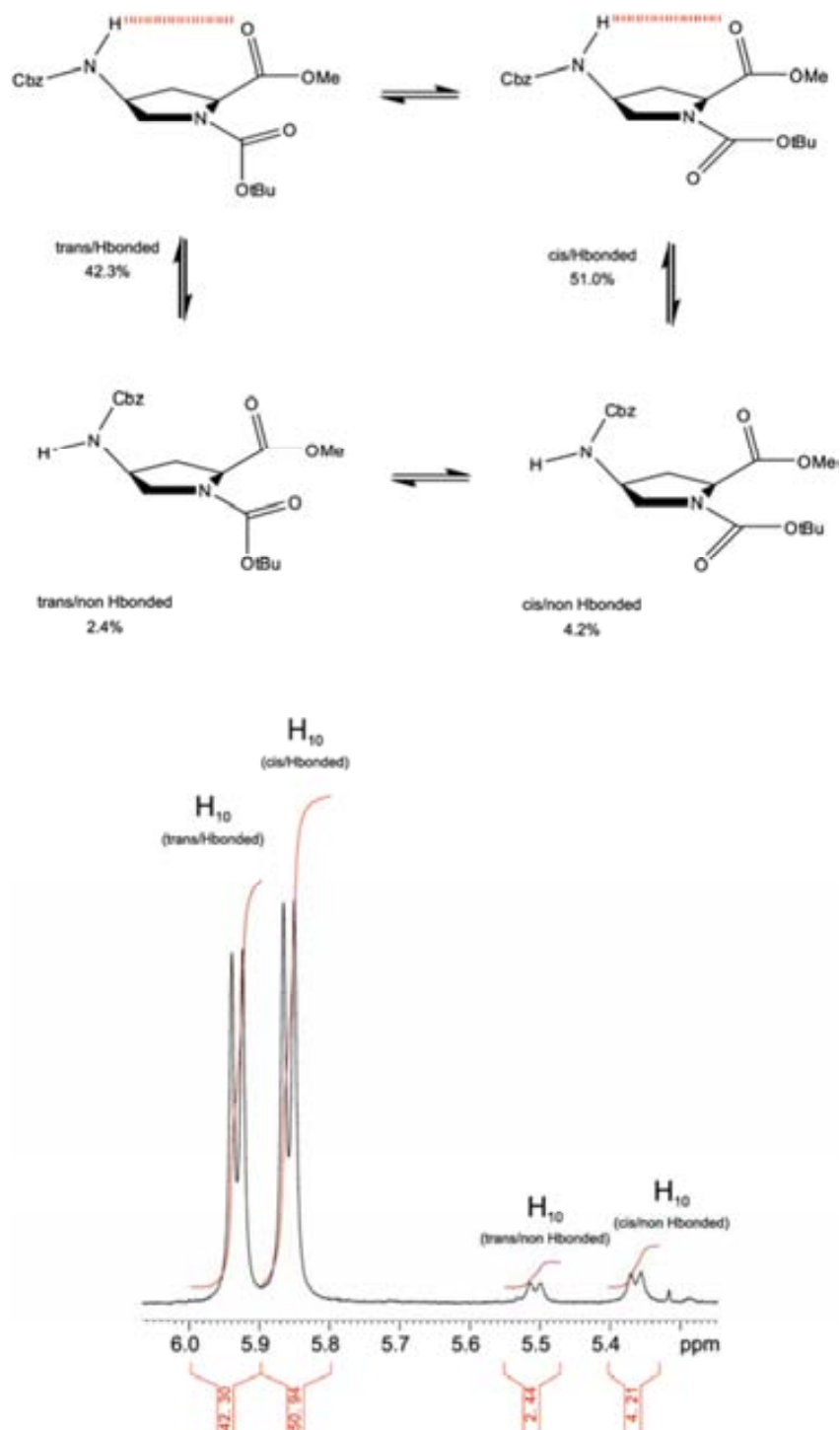


**Figure 92:** Expanded region of  $^1\text{H}$  NMR spectrum at 273K with the detailed integration values for each conformer.

Variable  $^1\text{H}$ -NMR temperature experiments led to visualize the coalescence temperature between major *cis/trans* Boc isomers (**Figure 93**). As conformers populations are almost equal, Eyring's equation is used to approximately determine a rotational barrier of 18,1 kcal/mol for the *cis/trans* equilibrium.

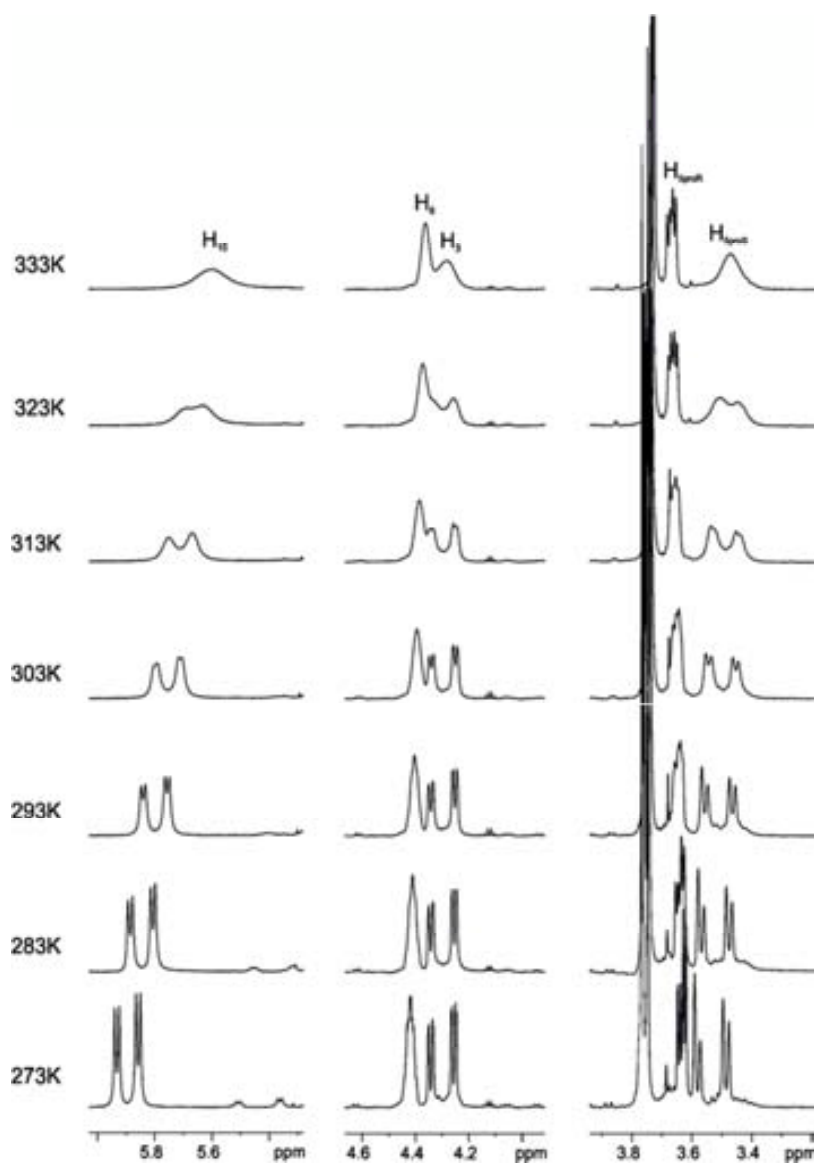


**Figure 93:** Variable temperature experiments, acquired at 600 MHz Bruker spectrometer. Temperature equilibration period was set to 10 minutes.

**Dipeptide 63**

Differently to 4-aminoproline **55**,  $^1\text{H}$  NMR spectrum of the dipeptide **63** clearly shows a single major conformation (**Figure 94**). Strongly deshielded position of  $\text{H}^9$  suggests a hydrogen bond between  $\text{NH}^9$  and  $\text{CO}^{16}$  building a 7-membered ring stacked to 5-membered proline ring, therefore fixing Boc rotamer to *trans* position. NOE experiments confirm such hypothesis as will be explained later on.

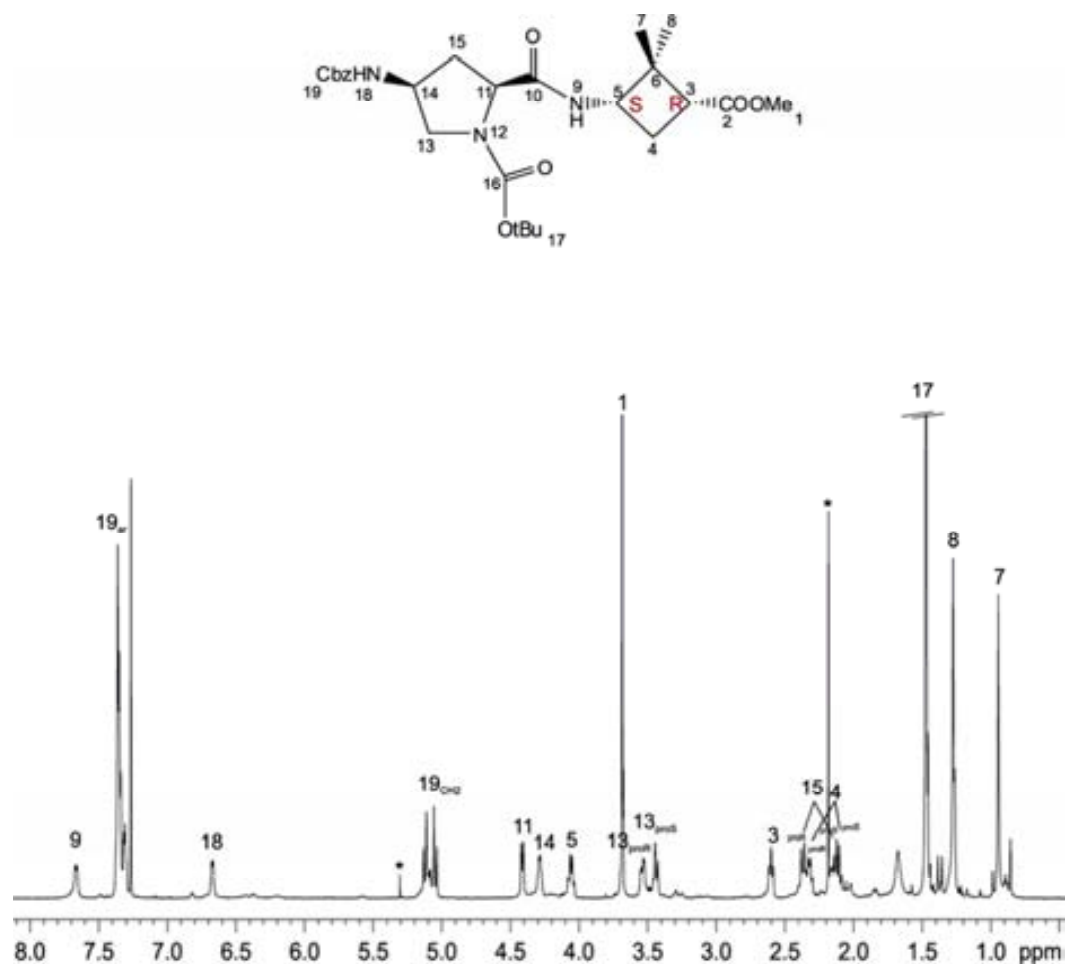


**Figure 94:**  $^1\text{H}$  NMR spectrum of dipeptide **63** acquired in a Bruker 600 MHz spectrometer at 298K.



1D selective TOCSY experiments irradiating at  $NH$  protons allows the separation of proline and cyclobutane subspectra, which affords a clear visualization of the correct proton assignment of the molecule (**Figure 95**).

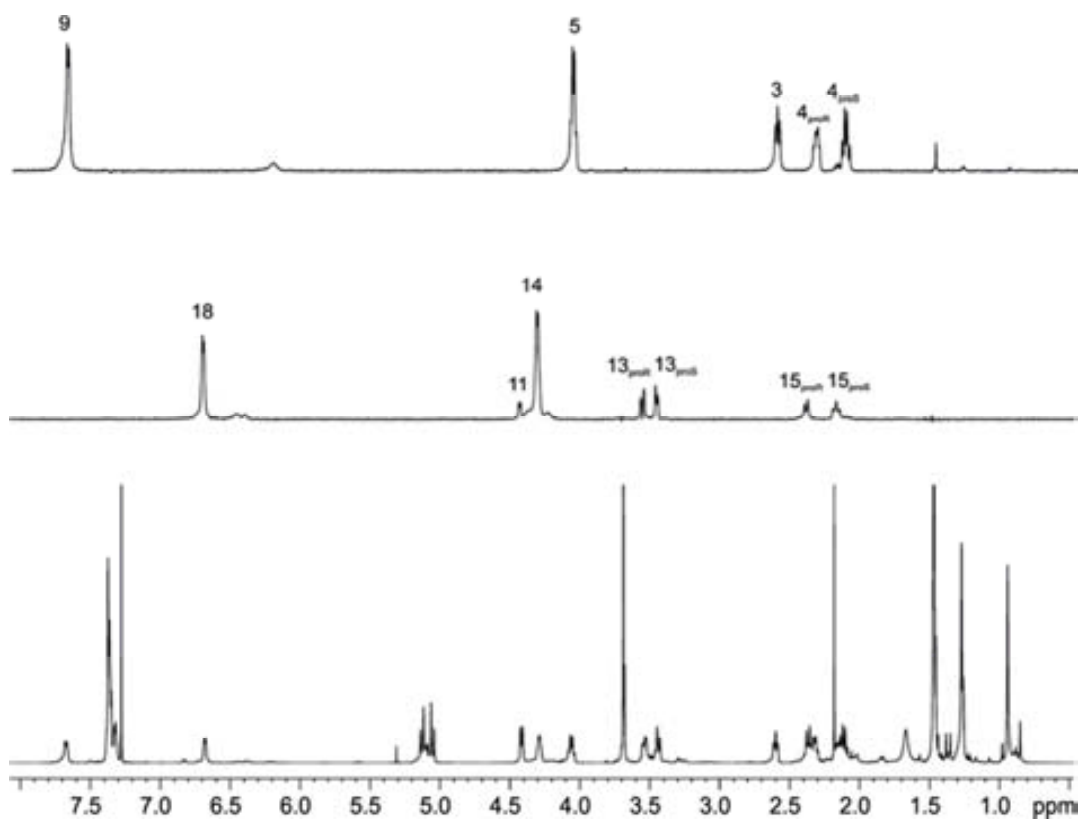


**Figure 95:** A)  $^1H$  NMR spectrum recorded at 600 MHz,  $CDCl_3$ . B) 1D selective TOCSY experiment irradiating  $H^{18}$  proton. Mixing time was set to 60 ms in both experiments. C) 1D selective TOCSY experiment irradiating  $H^9$  proton.

### Conformational details

$J$  coupling values together with 1D selective NOE experiments (**Figure 96**) over NH protons give an excellent visualization of the conformational structure of the molecule.

Selective inversion of H<sup>9</sup> gives a strong NOE effect with H<sup>11</sup>. That, together with the highly deshielded position encountered for that proton, clearly indicates a strong hydrogen bond formation with Boc carbonyl. Furthermore, coupling constant  $J_{H^9H^5}^3 = 7.8$  Hz (dihedral angle  $\sim 150^\circ$ ) and NOE effects observed with H<sup>5</sup>, H<sup>4S</sup> and Me<sup>8</sup> indicate how cyclobutane ring is spatially situated.

Equally to what was observed for triprotected 4-aminoproline **55**, NH<sup>18</sup> proton has an uncommon deshielded position suggesting the formation of a hydrogen bond with CO<sup>10</sup>. That is corroborated by NOE effects observed with H<sup>15R</sup> and H<sup>13S</sup>. However, there are slight differences in NOE intensities compared to **55**. In the dimer **63**, comparatively, more NOE signal is observed for H<sup>15R</sup> with respect to H<sup>13S</sup> proton indicating a shift toward this proton. That can be explained due to the conformational restrain given to CO<sup>10</sup> belonging to the new 7-membered ring and consequently shifting a bit the hydrogen bond CO<sup>10</sup>-NH<sup>18</sup>. The slight change is also noticeable in  $J_{H^{14}H^{18}}^3$  coupling value, which changed from 8.8 Hz (dihedral angle  $\sim 160^\circ$ ) in triprotected proline **55** to 6.5 Hz in the dimer **63** (dihedral angle  $\sim 140^\circ$ ).

Furthermore, exchange peaks are observed in selective NOE experiment indicating the presence of minor conformations during the NMR experiment time scale (500 ms). Those conformers can be seen in the <sup>1</sup>H NMR spectrum background but close to noise level, making their study difficult. However, the broadness and the chemical shift position of the exchange peaks observed in NOE experiments give an idea of the nature of the different conformers. For instance, NH<sup>9</sup> exchanges with a broad peak ( $\sim 40$  Hz at half height) that resonates at 6.2 ppm, 1.5 ppm far away from its initial 7.7 ppm position. The large displacement and the broadness of the line suggest that finding H<sup>9</sup> in this position is due to the loss of the hydrogen bond. On the other hand, NH<sup>18</sup> behavior is more difficult to explain because several exchange lines are observed. Two signals (6.4 and 6.5 ppm) which are very close to the initial peak position (6.7 ppm) are observed. Those signals

are equally broad at half height of the inverted peak ( $\sim 20$  Hz). Slight chemical shift displacement and almost the same signal broadness suggest that peaks come from a conformational exchange without hydrogen bond breaking, thus from another part of the molecule, probably Cbz rotation to a *cis* position and the above mentioned  $H^9$  hydrogen bond loss. Also, although small, a broad peak appears at 5.9 ppm ( $\sim 40$  Hz at half height) which is attributed to hydrogen bond breaking. Low intensity is explained because once the bond is broken water can have access to that proton and exchange with it, which is in fact seen in the spectrum.

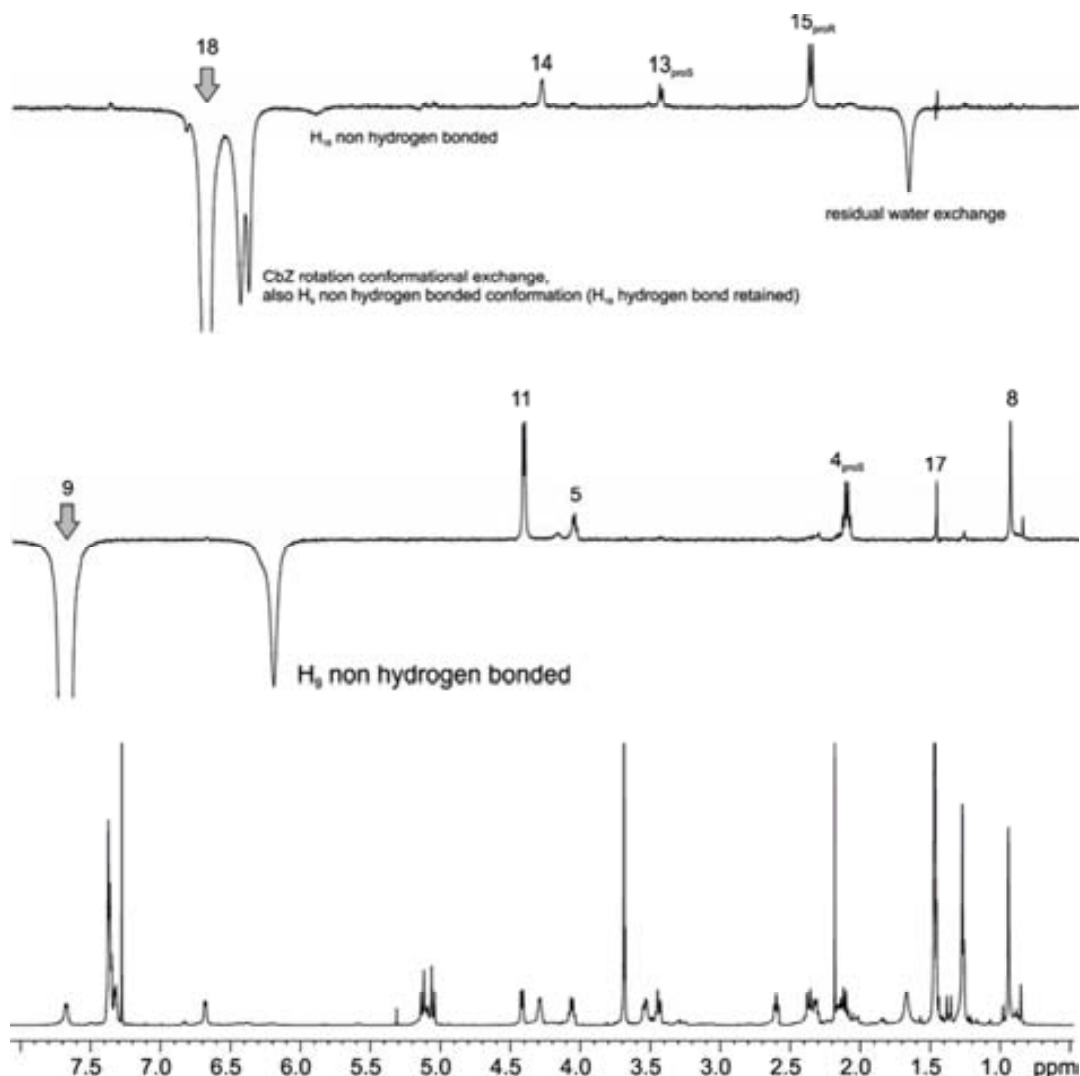


**Figure 96:** 1D selective NOESY experiments irradiating NH protons. Mixing time was set to 500 ms.  $^1H$  spectrum is added for comparison. A part from NOE peaks, exchange peaks are also observed.

A pictorial conformational structure of the major conformer of **63** is depicted in **Figure 97**.

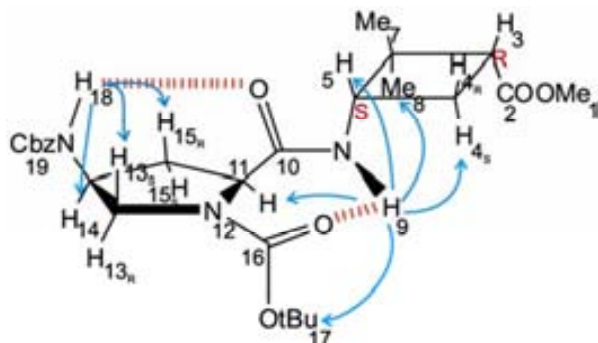


**Figure 97:** Conformation for **63** deduced from NOEs and  $J$  coupling values. NOE effects are indicated with a blue arrow and hydrogen bond indicated with red lines.

In order to qualitatively compare hydrogen bonding strength of  $\text{NH}^9$  and  $\text{NH}^{18}$ , 50  $\mu\text{L}$  of deuterated methanol were added into the NMR tube. The tube was then hand-shaken and left to equilibrate for 10 minutes. The spectrum (**Figure 98**) clearly shows that while approximately half of the signal of  $\text{NH}^9$  prevails,  $\text{NH}^{18}$  has completely disappeared indicating a total deuterium exchange, therefore being experimentally demonstrated that  $\text{NH}^9$  hydrogen bond is less accessible than  $\text{NH}^{18}$  one, suggesting a stronger hydrogen bond.

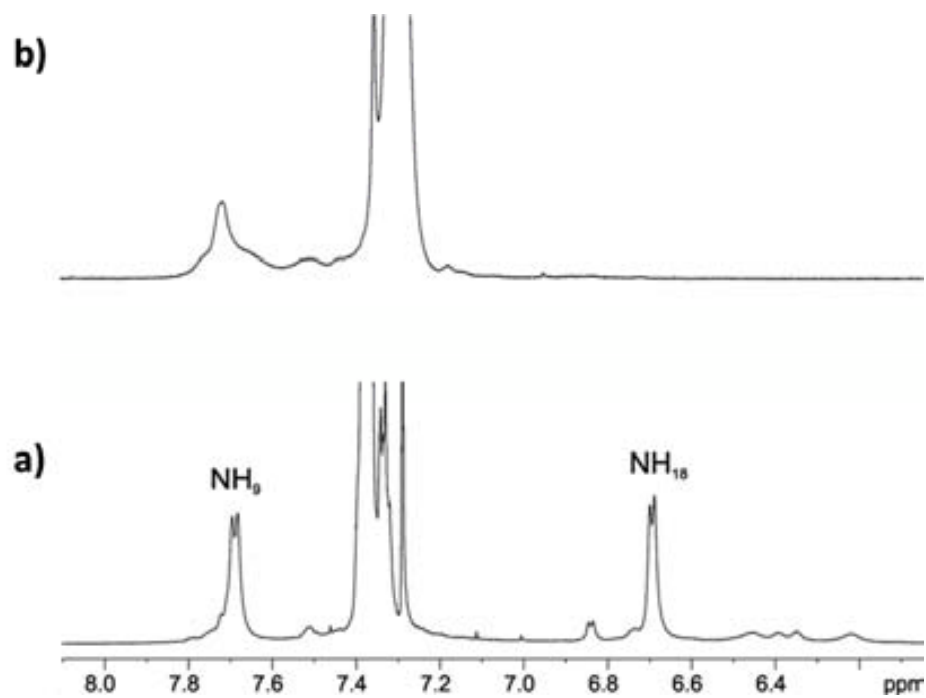
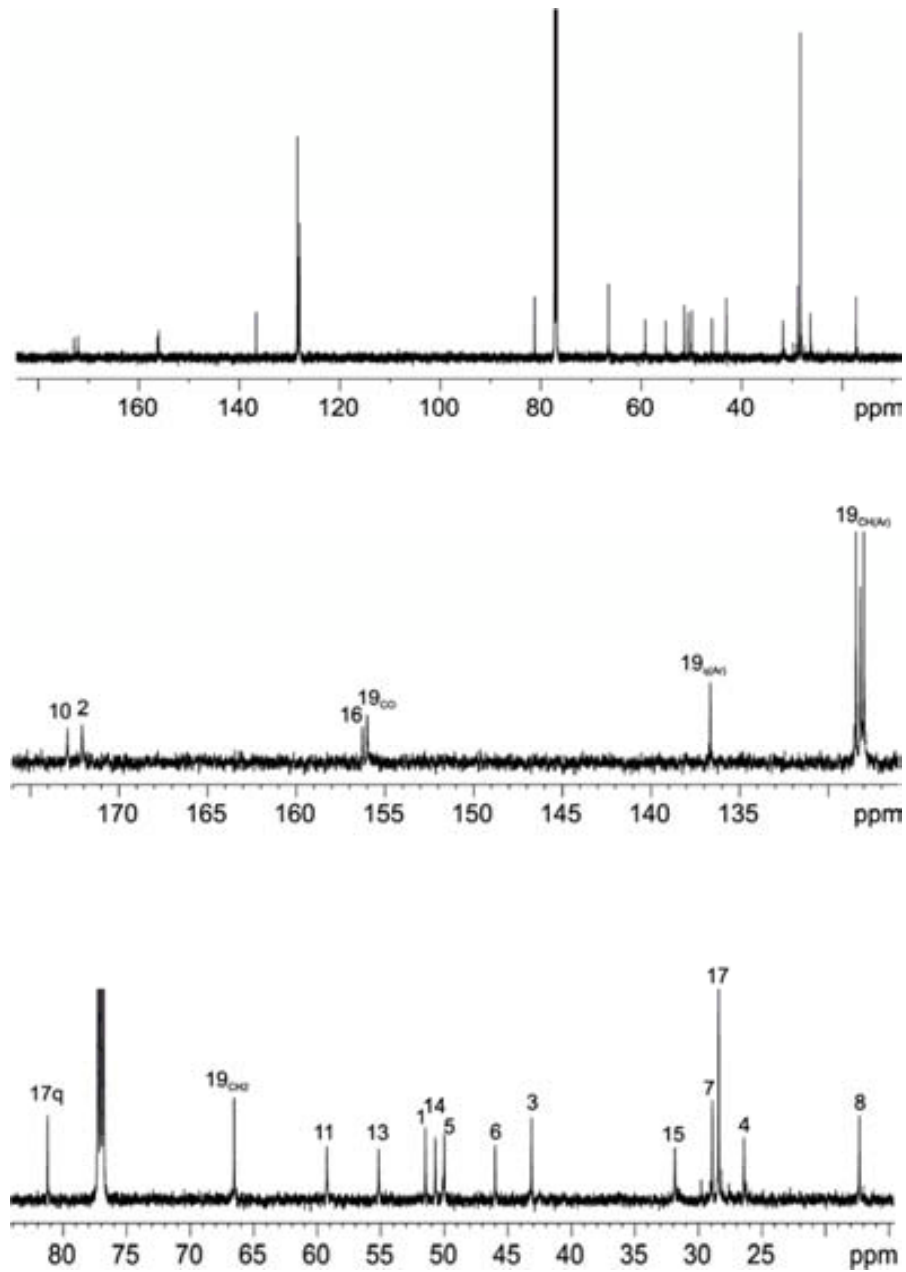
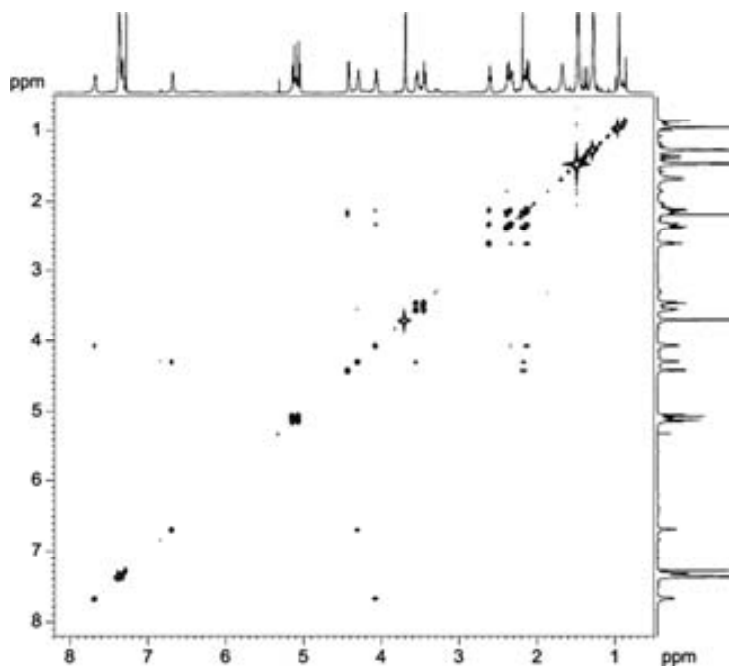


Figure 98: MeOD exchange experiment. a) before MeOD addition; b) after MeOD addition

## SUPPORTING FIGURES FOR PRODUCT 63



**Figure 99:**  $^{13}\text{C}$  NMR spectrum of **63** recorded in a Bruker 600 MHz spectrometer in  $\text{CDCl}_3$  at 298 K. Several expanded regions are shown.



**Figure 100:** COSY spectrum recorded in a Bruker 600 MHz spectrometer in CDCl<sub>3</sub> at 298 K.

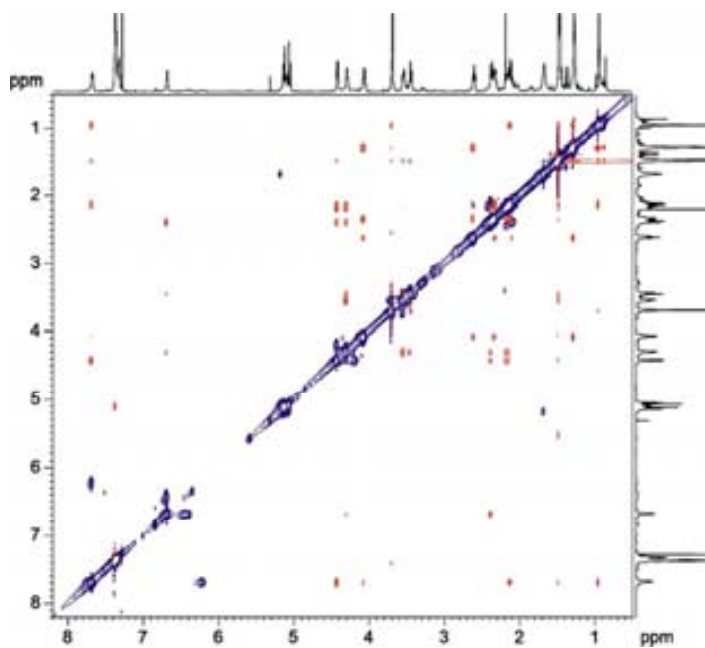


**Figure 101:** 2D-NOESY spectrum recorded in a Bruker 600 MHz spectrometer in CDCl<sub>3</sub> at 298K (mixing time was set to 500 ms).

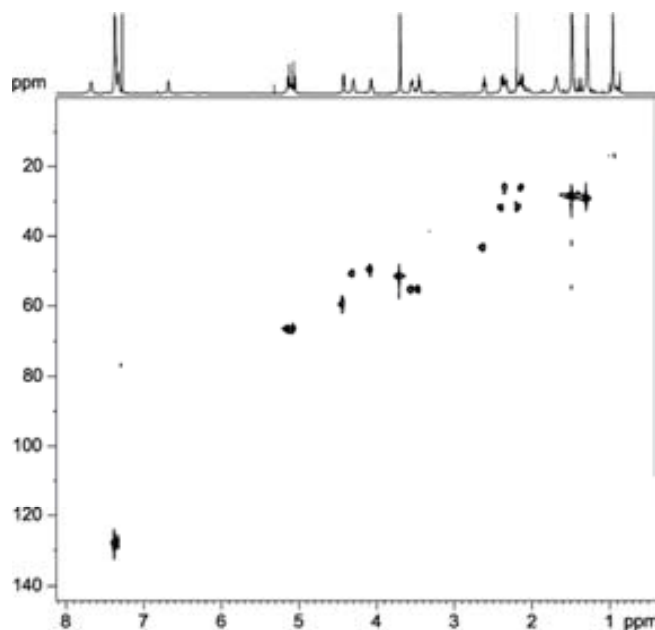


**Figure 102:** HMQC spectrum recorded in a Bruker 600 MHz spectrometer in  $\text{CDCl}_3$  at 298 K.

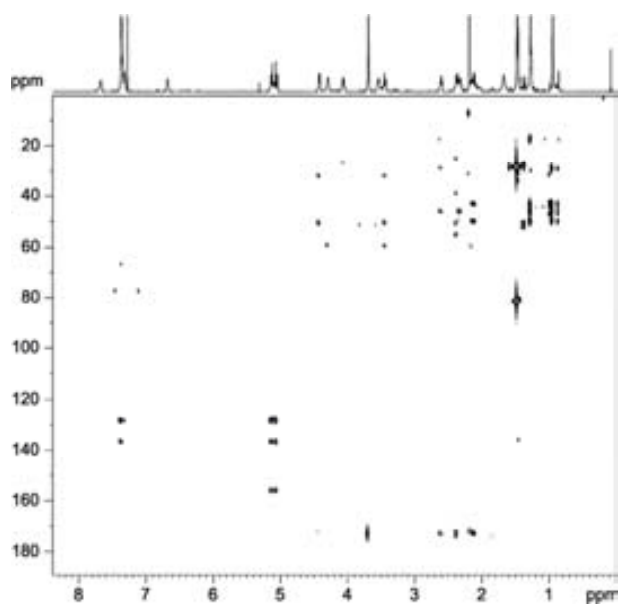
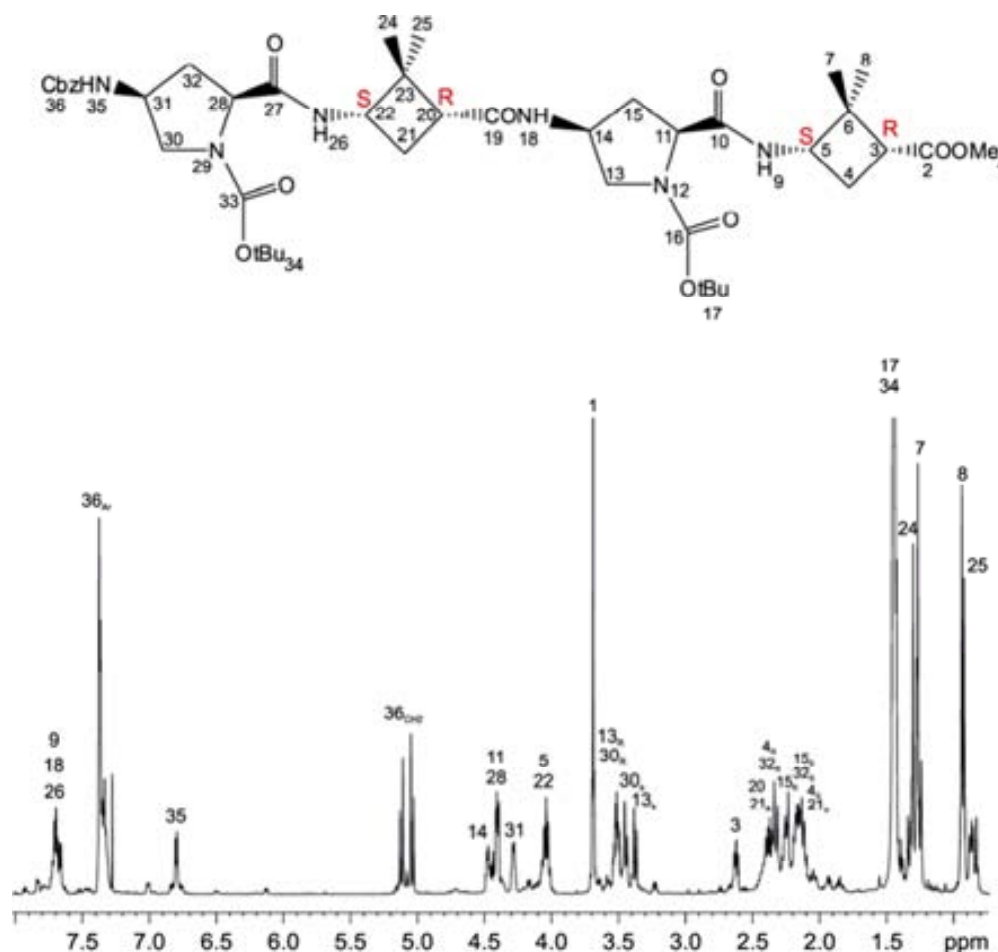


**Figure 103:** HMBC spectrum recorded in a Bruker 600 MHz spectrometer in  $\text{CDCl}_3$  at 298 K.



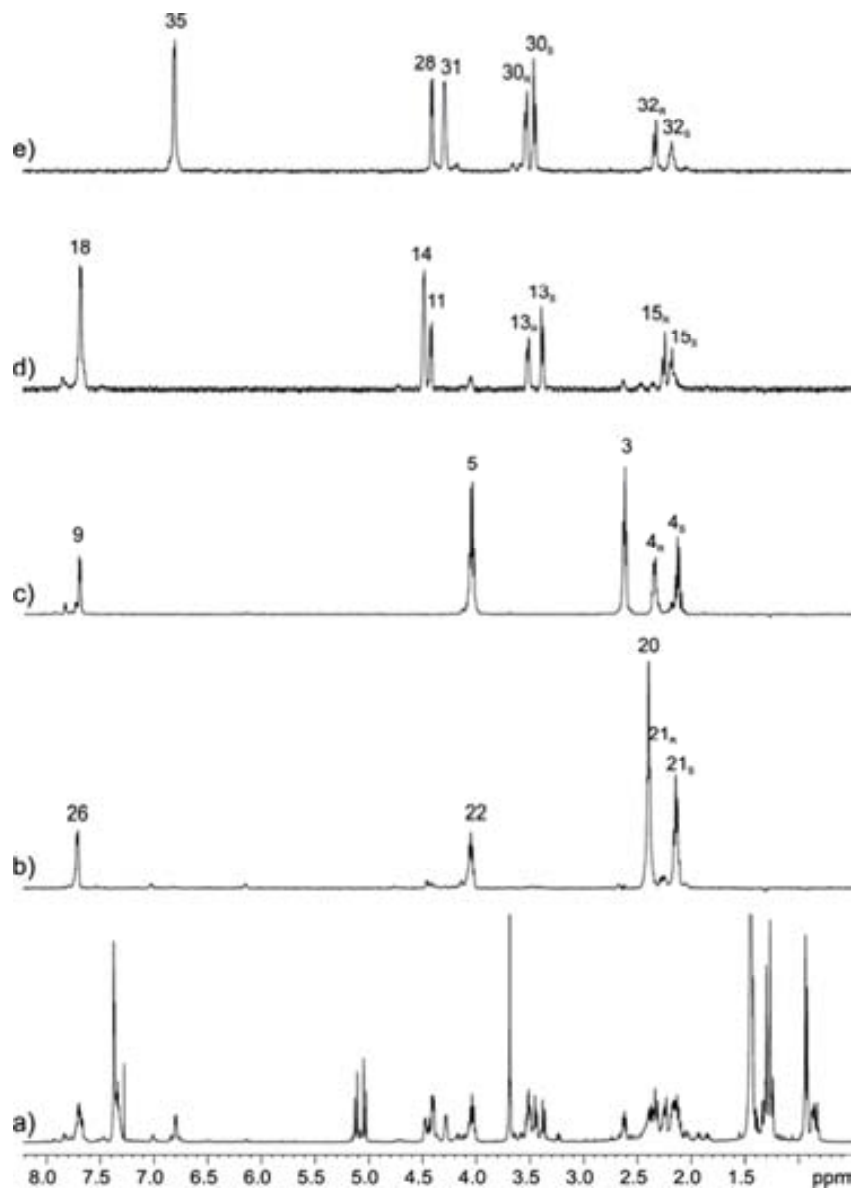
**Tetrapeptide 66**

$^1\text{H}$  NMR spectrum of the  $\gamma$ -tetrapeptide **66** clearly shows a single major conformation although several minor conformers are visible in the spectrum (**Figure 104**).



**Figure 104:**  $^1\text{H}$  NMR spectrum of tetrapeptide **66** acquired in a Bruker 600 MHz spectrometer at 273K.

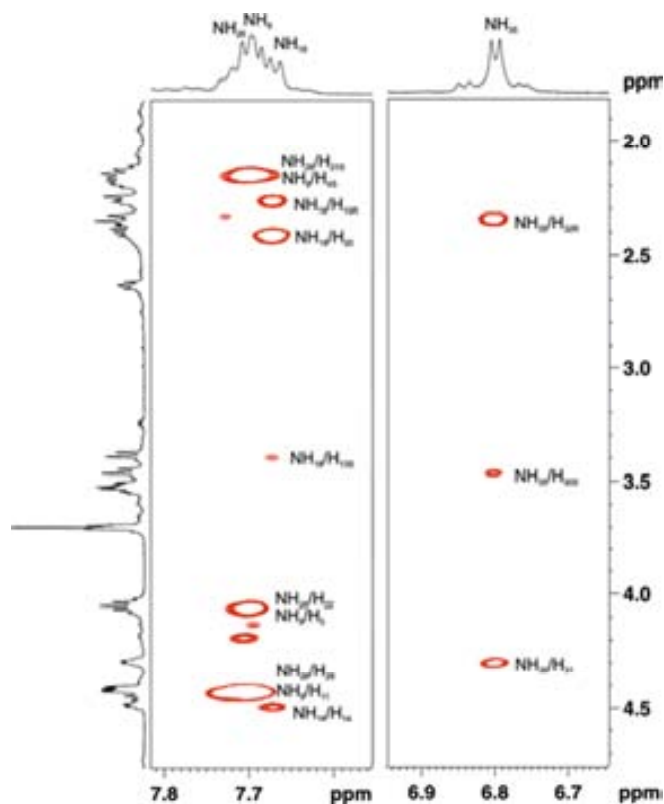
All  $^1\text{H}$  and  $^{13}\text{C}$  resonances have been assigned with the help of standard 2D NMR experiments which are presented in the supporting figures (COSY, ROESY, HSQC and HMBC). Furthermore, a series of the 1D selective TOCSY experiments have been an important tool to afford a separated visualization of spin systems belonging to proline and cyclobutane skeletons (**Figure 105**).



**Figure 105:** A)  $^1\text{H}$  NMR spectrum recorded at 600 MHz,  $\text{CDCl}_3$ , 273 K. B) 1D selective TOCSY experiment from  $\text{H}^{20}$  proton. C) 1D selective TOCSY experiment from  $\text{H}_3$  proton position. D) 1D selective TOCSY experiment from  $\text{H}^{18}$ . E) 1D selective TOCSY experiment irradiating from  $\text{H}^{35}$  proton. TOCSY mixing time was set to 60 ms in all experiments.

**Conformational details:**

Strongly deshielded positions are encountered for all NH protons. That suggests that four hydrogen bonds are responsible of fixing a major conformer. 2D-ROESY experiment (**Figure 106**) shows that the major conformer follows the same proton pattern encountered for dipeptide **69**, therefore confirming that four hydrogen bonds are responsible for the conformer stabilization. Those hydrogen bonds are NH<sup>9</sup>-CO<sup>16</sup>, NH<sup>18</sup>-CO<sup>10</sup>, NH<sup>26</sup>-CO<sup>33</sup> and NH<sup>35</sup>-CO<sup>27</sup>. It is noticeable that NH<sup>35</sup> resonates at a lower frequency (6.7 ppm) compared to those NH belonging to an amide group (around 7.7 ppm), that is due to the nature of the carbamate group. Nevertheless, ROE contacts avoid any doubt of hydrogen bond formation.

**Figure 106:** 2DROESY.

Furthermore,  $J$  coupling values for tetramer involving NH protons are very close to the values found for the dimer **63**, corroborating that an analogous hydrogen bond pattern is maintained from dimer to tetramer (**Table 9**).

**Table 9:**  $J$  coupling values

| Dimer <b>63</b>              | Tetramer <b>66</b>                           |
|------------------------------|--|
| $^3J_{\text{NH9H5}} = 7.8$   | $^3J_{\text{NH9H5}} = 7.7 (\pm 150^\circ)$   |
|                              | $^3J_{\text{NH26H22}} = 7.6 (\pm 150^\circ)$ |
| $^3J_{\text{NH18H14}} = 6.5$ | $^3J_{\text{NH18H14}} = 6.4 (\pm 140^\circ)$ |
|                              | $^3J_{\text{NH35H31}} = 7.0 (\pm 145^\circ)$ |

$J$  coupling values (**Table 9**) together with 1D selective NOE experiments (**Figure 106**) over NH protons give an excellent visualization of the conformational structure of the molecule.

Taking into account chemical shift positions, ROE contacts encountered and  $J$  values a pictorial conformational structure of the major conformer is depicted in **Figure 107**.

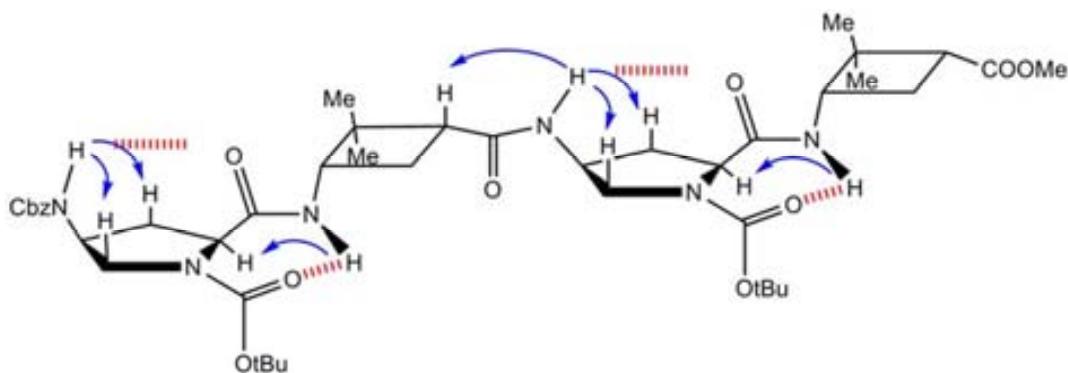


**Figure 107:** Main conformation for tetrapeptide **66** deduced from ROE connections and  $^3J_{\text{NHCH}}$  coupling values. Hydrogen bonds are indicated with red lines. ROE contacts are indicated with blue arrows.

## SUPPORTING FIGURES FOR 66

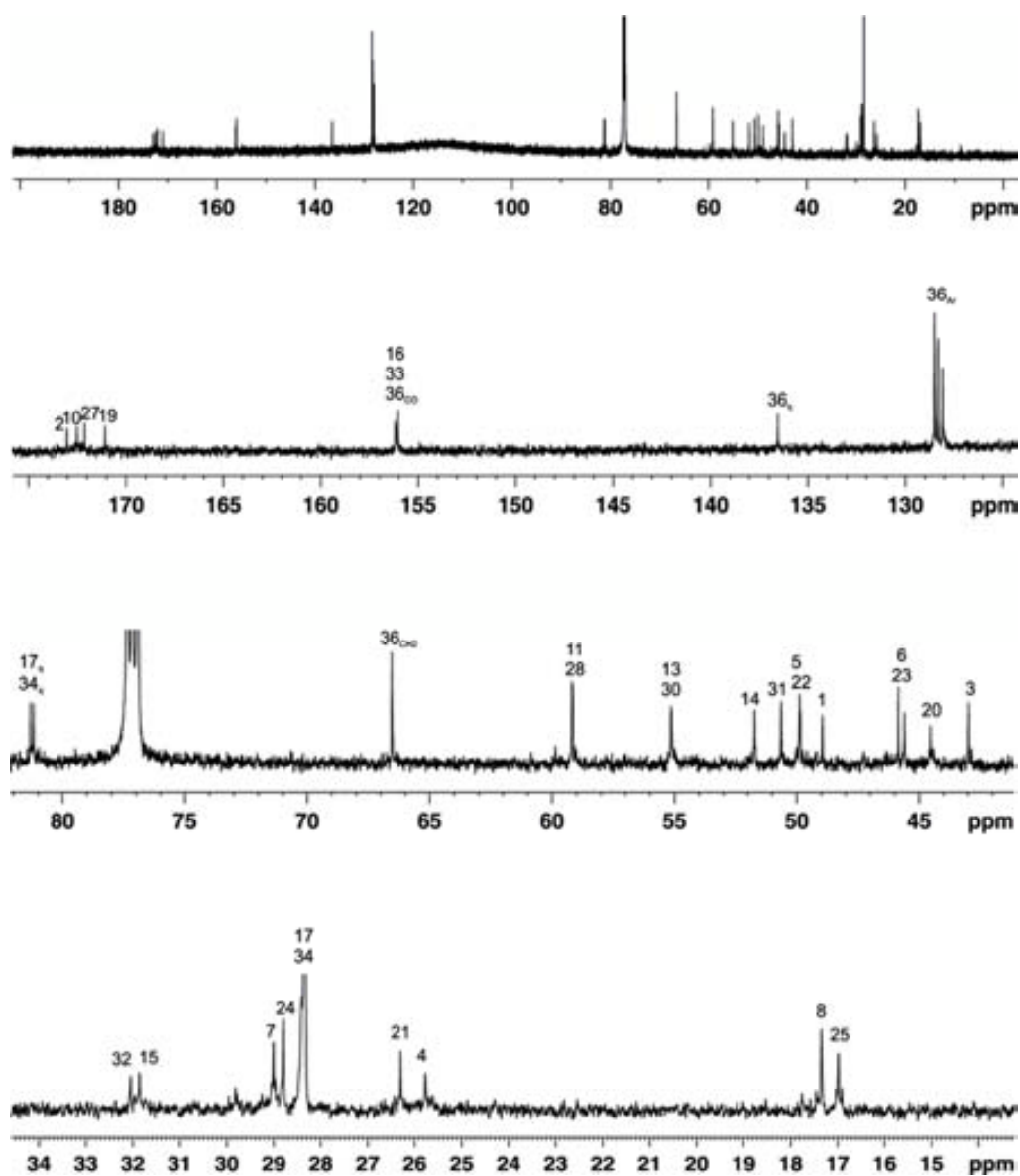
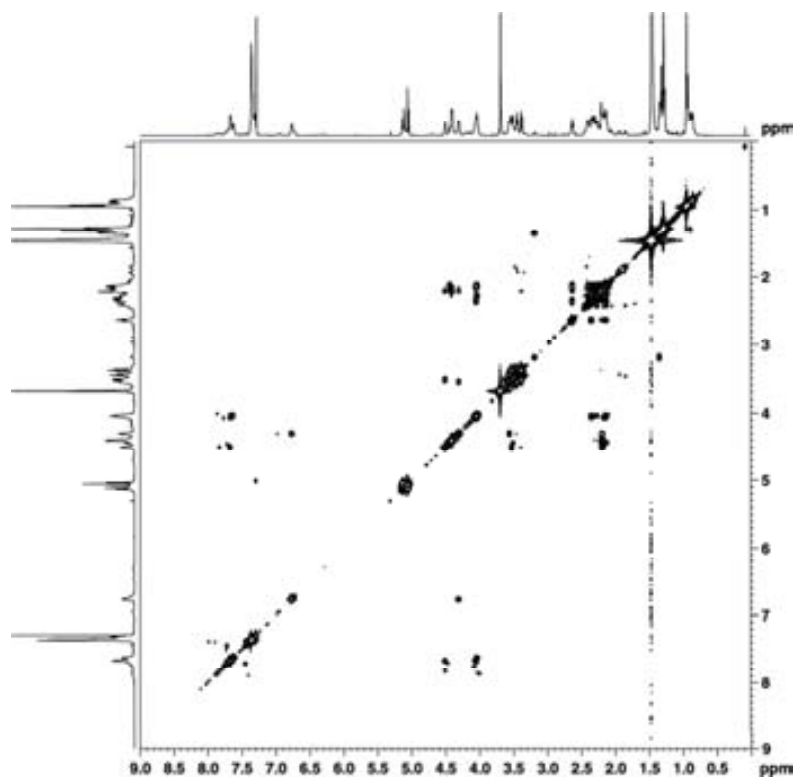
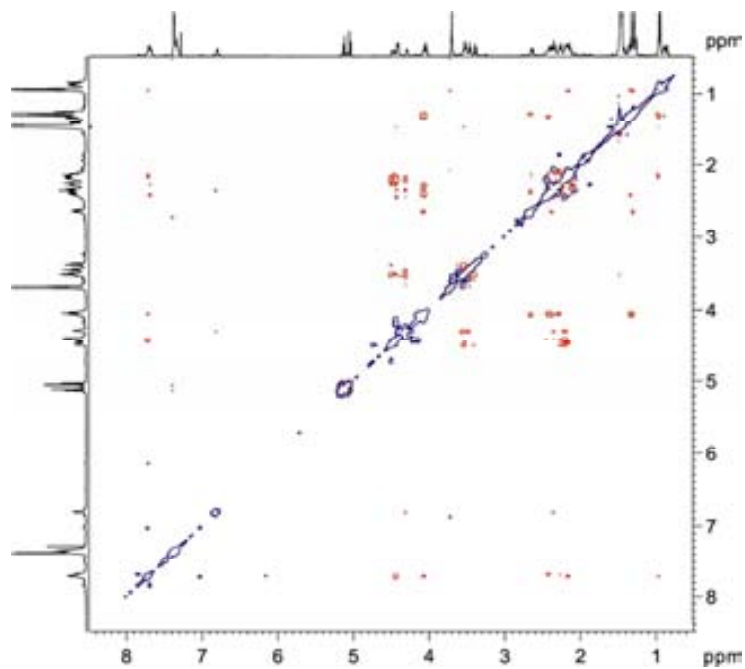


Figure 108:  $^{13}\text{C}$  NMR spectrum of 66 recorded in a Bruker 600 MHz spectrometer in  $\text{CDCl}_3$  at 298 K.



**Figure 109:** COSY spectrum recorded in a Bruker 600 MHz spectrometer in CDCl<sub>3</sub> at 298 K.



**Figure 110:** 2D-ROESY spectrum recorded in a Bruker 600 MHz spectrometer in CDCl<sub>3</sub> at 298 K (mixing time was set to 500 ms).

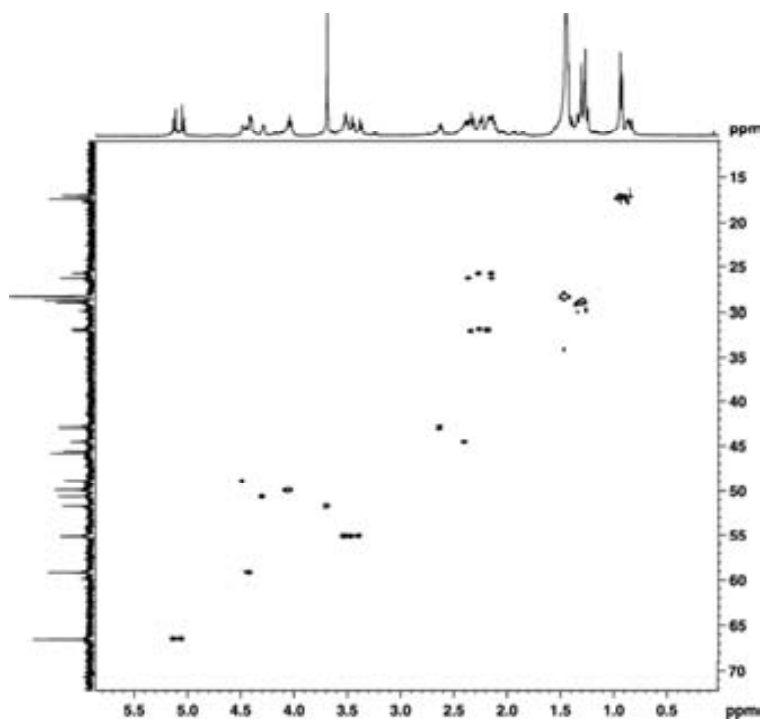


Figure 111: HOSQC spectrum recorded in a Bruker 600 MHz spectrometer in CDCl<sub>3</sub>

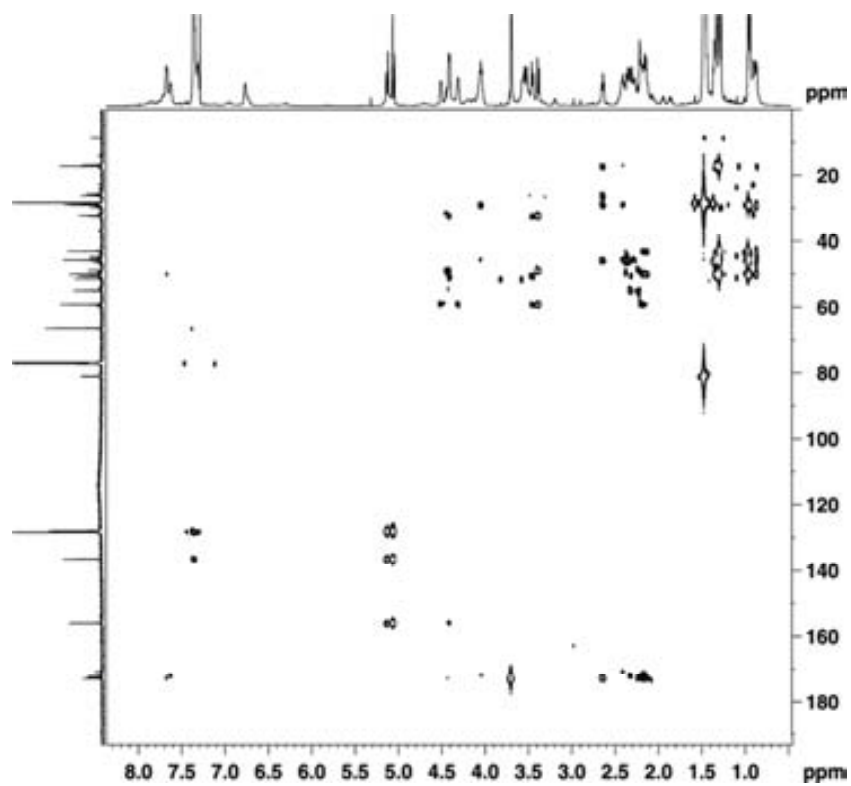
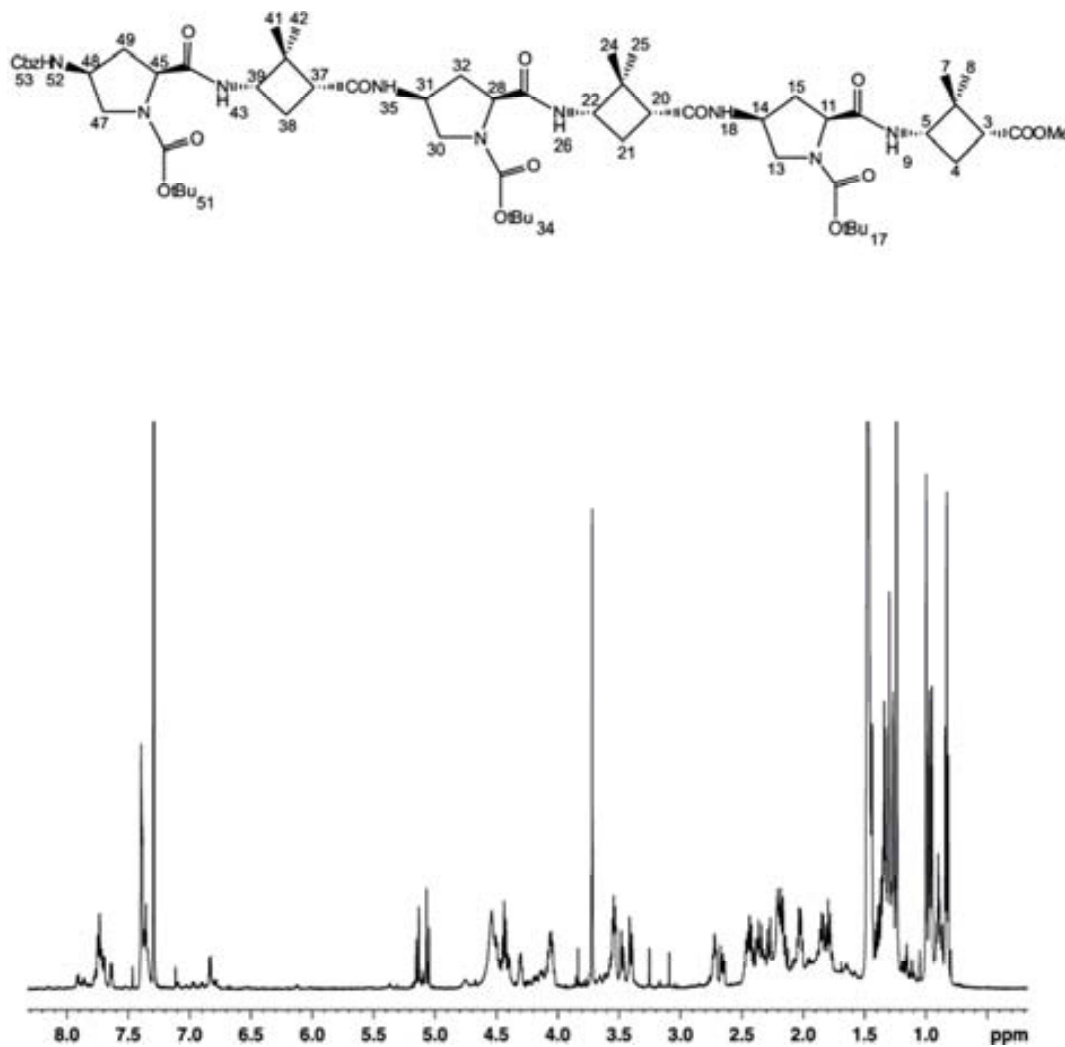


Figure 112: HMBC spectrum recorded in a Bruker 600 MHz spectrometer in CDCl<sub>3</sub> at 298 K.

**Hexapeptide 68**

$^1\text{H}$  NMR spectrum of the  $\gamma$ -hexapeptide **68** clearly shows a single major conformation although several minor conformers are visible in the spectrum (**Figure 113**).



**Figure 113:**  $^1\text{H}$  NMR spectrum of hexapeptide **68** acquired in a Bruker 600 MHz spectrometer at 298K.



SUPPORTING FIGURES FOR 68

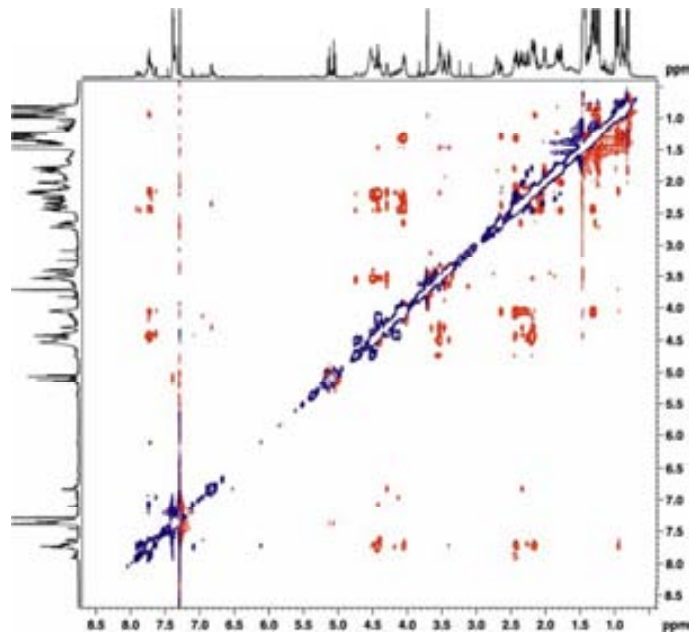


Figure 114: 2D ROESY experiment.

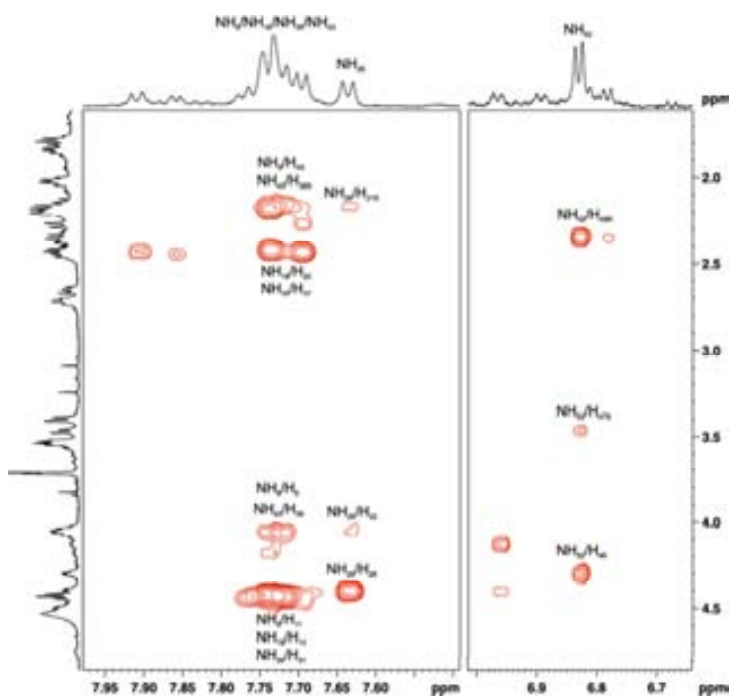
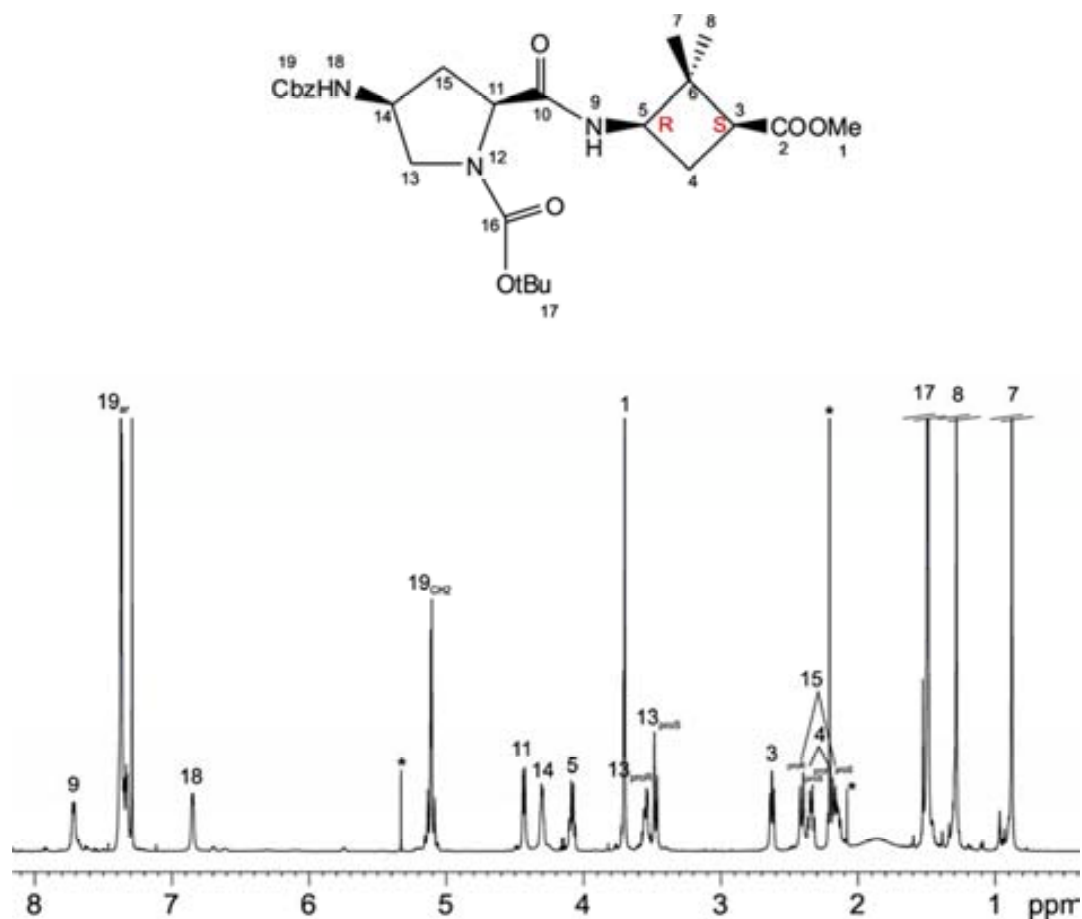


Figure 115: 2D ROESY experiment.

### Dipeptide 57

Similarly to what was found for dipeptide **63**, and differently to triprotected 4-aminoproline **55**,  $^1\text{H}$  NMR spectrum of dipeptide **57** clearly shows a single major conformation (**Figure 116**). Strongly deshielded position of  $\text{H}^9$  suggests a hydrogen bond between  $\text{NH}^9$  and  $\text{CO}^{16}$  building a 7-membered ring stacked to 5-membered proline ring, therefore fixing Boc rotamer to *trans* position. NOE experiments confirm such hypothesis, which is analogous to that explained for dipeptide **63**.



**Figure 116:**  $^1\text{H}$  NMR spectrum of dipeptide **57** acquired in a Bruker 600 MHz spectrometer at 298K.

1D selective TOCSY experiments irradiating *NH* protons allows the separation of proline and cyclobutane subspectra, which affords a clear visualization for the correct proton assignment of the molecule (**Figure 117**).

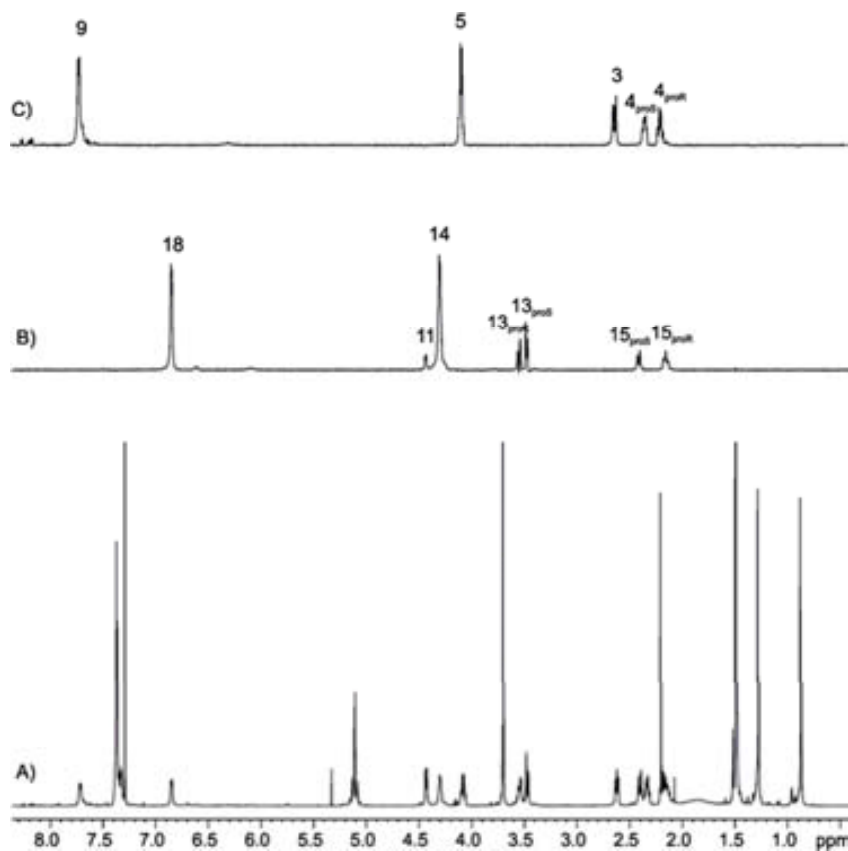


**Figure 117:** A)  $^1\text{H}$  NMR spectrum for **57** recorded in a 600 MHz,  $\text{CDCl}_3$ . B) 1D selective TOCSY experiment irradiating  $\text{H}^{18}$  proton. Mixing time was set to 60 ms in both experiments. C) 1D selective TOCSY experiment irradiating  $\text{H}^9$  proton.

**Conformational details:**

An analogous explanation given for dipeptide **63** is valid for this diastereomer.  $J$  coupling values together with 1D selective NOE experiments (**Figure 118**) over  $NH$  protons give an excellent visualization of the conformational structure of the molecule. A pictorial conformational structure of the major conformer is depicted in **Figure 119**.

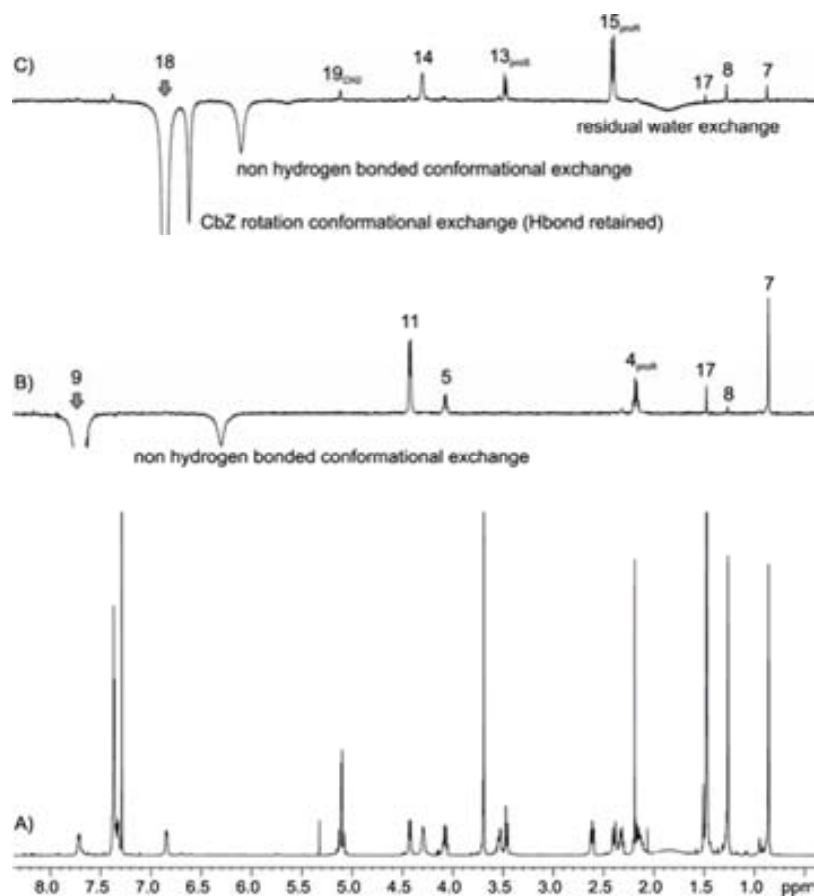


**Figure 118:** 1D selective NOESY experiments irradiating  $NH$  protons. Mixing time was set to 500 ms.  $^1H$  NMR spectrum is added for comparison. Apart from NOE peaks, exchange peaks are also observed.

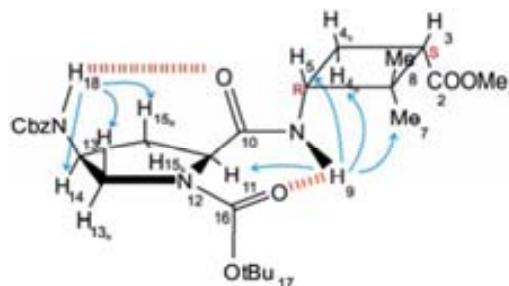


**Figure 119:** Conformation for **57** deduced from NOEs and  $J$  coupling values. NOE effects are indicated with a blue arrow and hydrogen bond indicated with red lines.

Analogously to what was found for dipeptide **63**, 50  $\mu$ L of deuterated methanol addition in an exchange test demonstrates that NH<sup>9</sup> hydrogen bond is slightly less accessible than NH<sup>18</sup> one, suggesting a stronger hydrogen bond for NH<sup>9</sup> position (**Figure 120**).

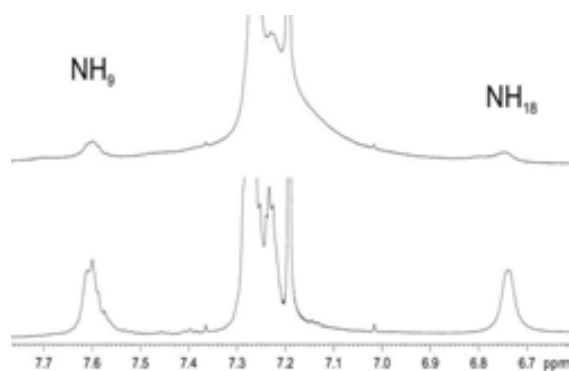


**Figure 120:** MeOD exchange.

## SUPPORTING FIGURES FOR 57

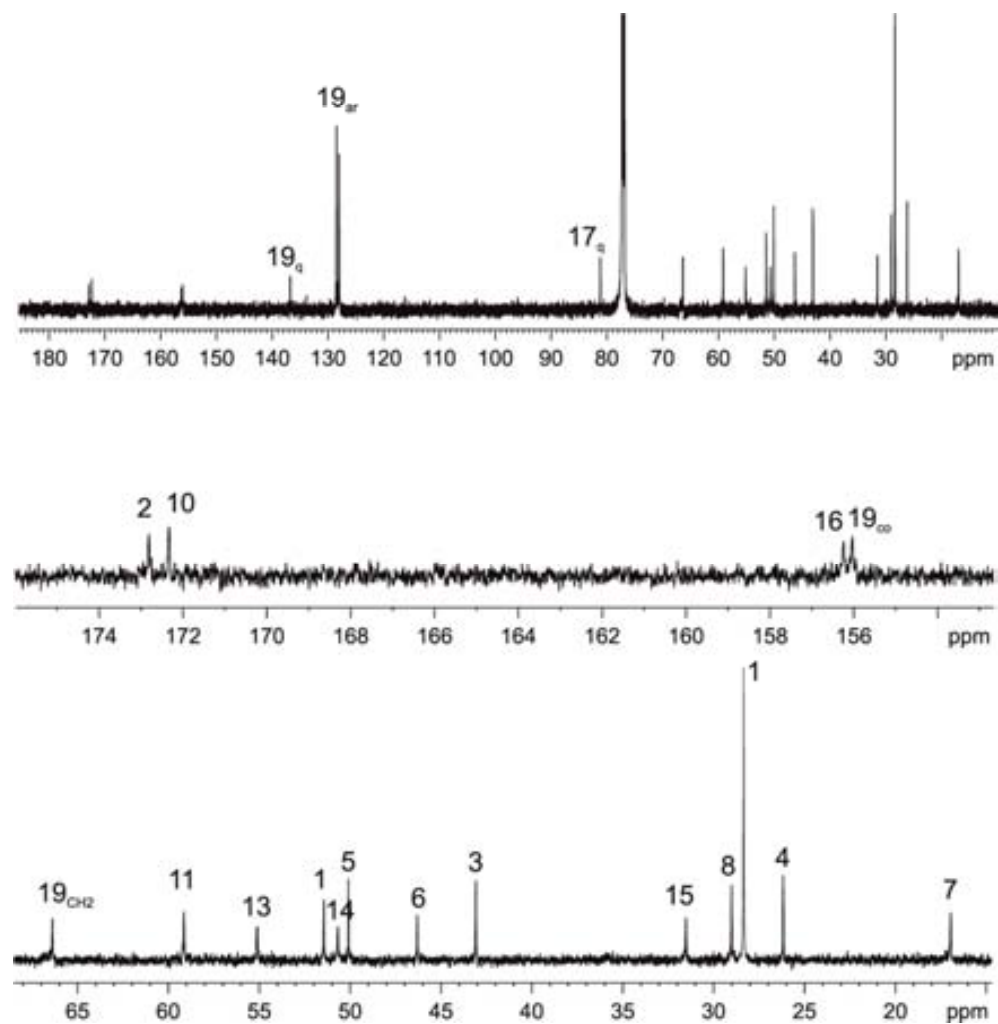


Figure 121:  $^{13}\text{C}$  NMR spectrum of **57** recorded in a Bruker 600 MHz spectrometer in  $\text{CDCl}_3$  at 298 K.

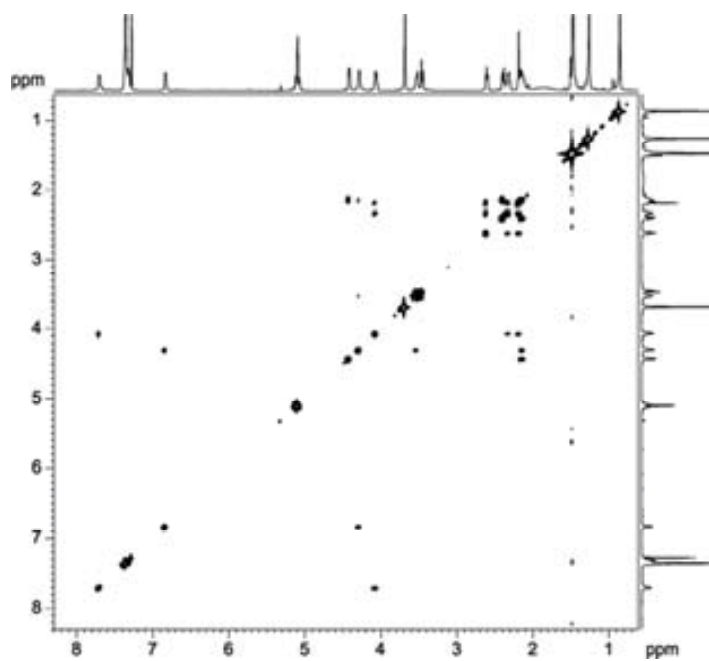


Figure 122: COSY spectrum recorded in a Bruker 600 MHz spectrometer in CDCl<sub>3</sub> at 298 K.

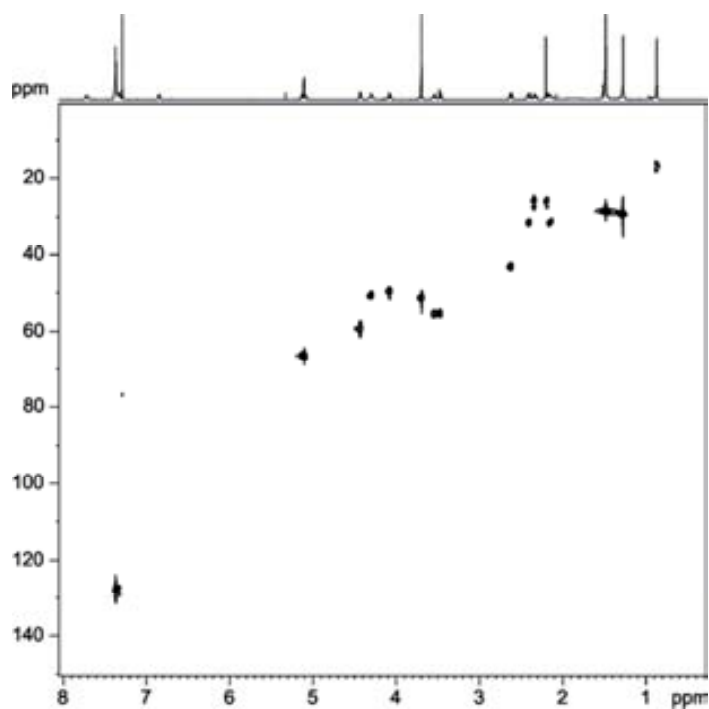
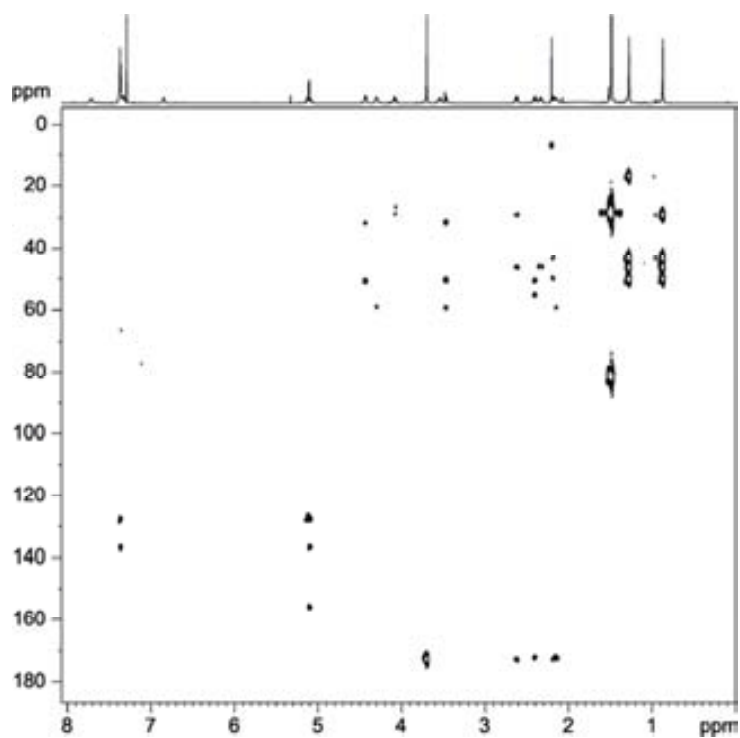


Figure 123: H<sup>1</sup>QC spectrum recorded in a Bruker 600 MHz spectrometer in CDCl<sub>3</sub> at 298 K.



**Figure 124:** HMBC spectrum recorded in a Bruker 600 MHz spectrometer in CDCl<sub>3</sub> at 298 K.



**Tetrapeptide 60**

$^1\text{H}$  NMR spectrum (**Figure 125**) of the tetrapeptide **60** clearly shows a single major conformation although several minor conformers are visible in the spectrum and as exchange peaks in 2D ROESY spectrum. All  $^1\text{H}$  and  $^{13}\text{C}$  resonances have been assigned with the help of standard 2D NMR experiments which are reported below (TOCSY, ROESY, HSQC and HMBC).

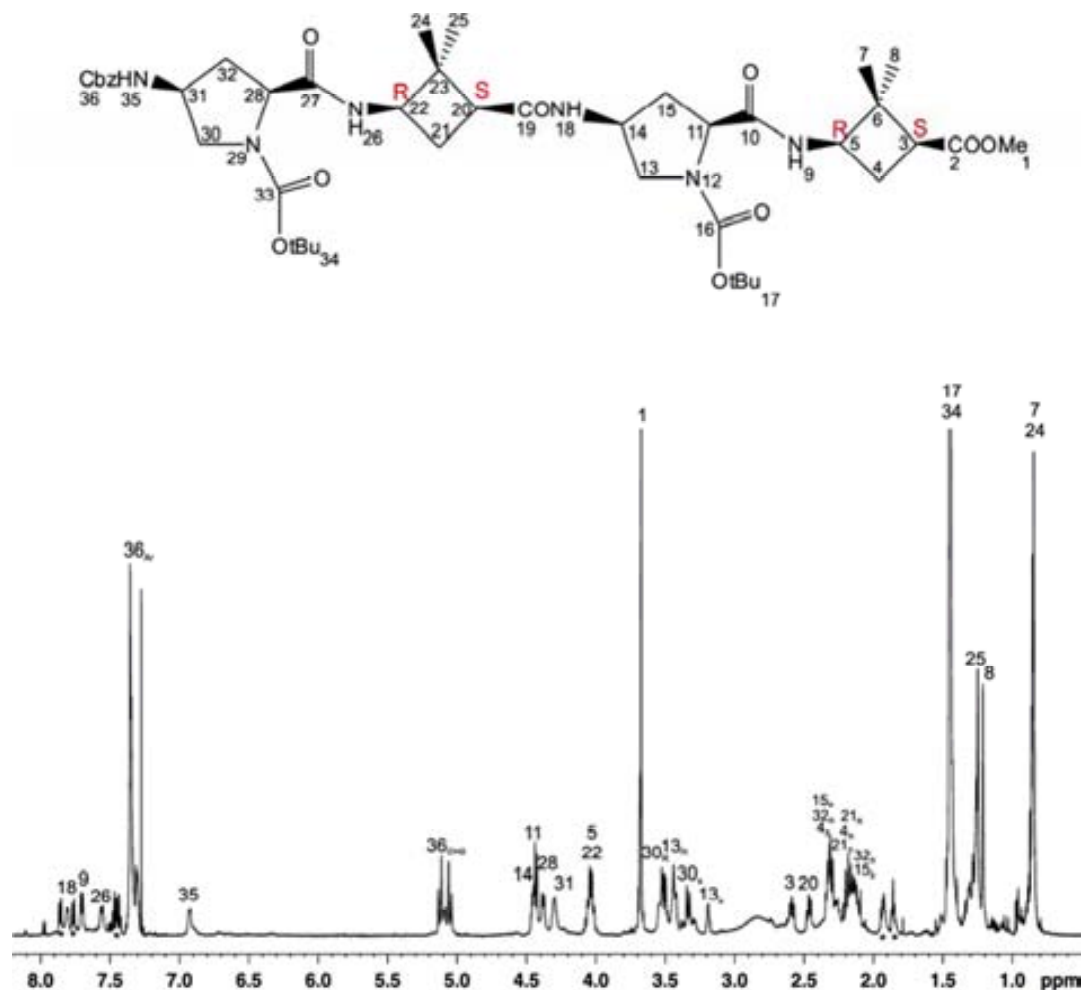


**Figure 125:**  $^1\text{H}$  NMR spectrum of tetrapeptide **60** acquired in a Bruker 600 MHz spectrometer at 273K. Impurities are marked \*

### Conformational details

Analogously to its diastereomeric tetrapeptide **66**, strongly deshielded positions are encountered for all NH protons. Therefore, suggesting that the four hydrogen bonds responsible for fixing a major conformer are maintained in this molecule. Correlation signals seen in the 2D-ROESY experiment show that the major conformer follows the same proton pattern found for dipeptide **57**, therefore confirming that four hydrogen bonds are responsible for the conformer stabilization (**Figure 126**). Those hydrogen bonds are NH<sup>9</sup>-CO<sup>16</sup>, NH<sup>18</sup>-CO<sup>10</sup>, NH<sup>26</sup>-CO<sup>33</sup> and NH<sup>35</sup>-CO<sup>27</sup>.

It is noticeable that the main difference with the ROE pattern encountered for its diastereomeric tetrapeptide **66** is the ROE contact observed between NH<sup>18</sup> and H<sup>21R</sup> proton in **60**.

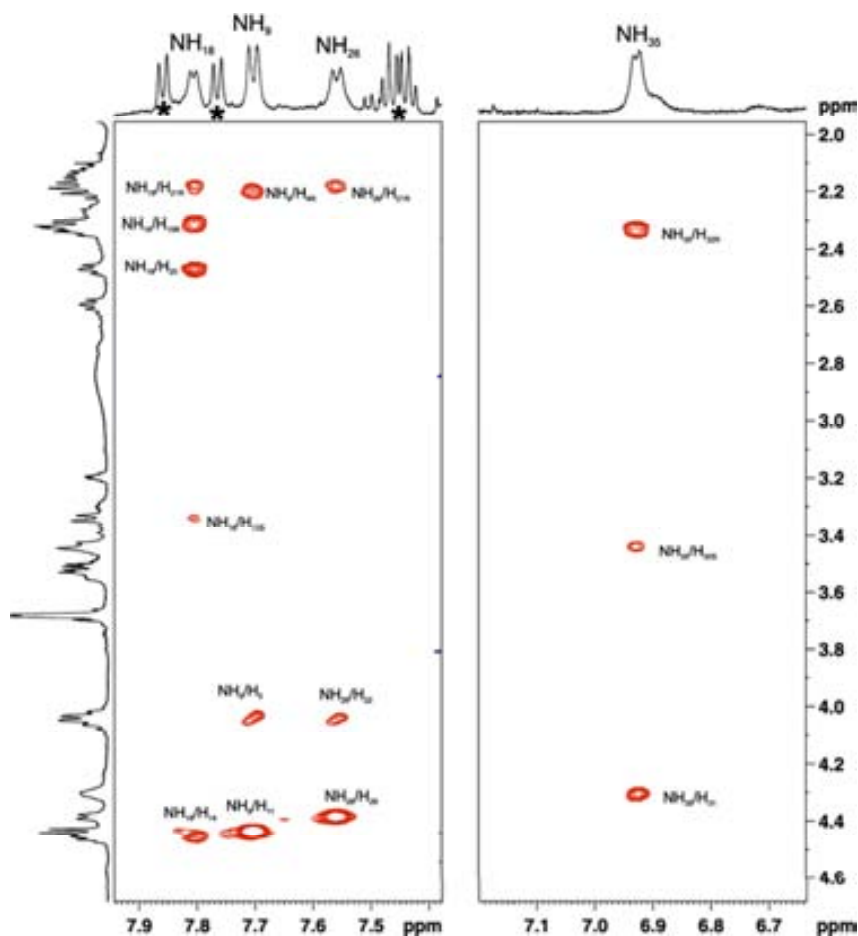


Figure 126: 2D ROESY experiment.

Furthermore,  $J$  coupling values for tetramer involving NH protons are very close to the values found for the dimer, corroborating that an analogous hydrogen bond pattern is maintained from dimer to tetramer (**Table 10**).

**Table 10:**  $J$  coupling values.

| Dimer <b>57</b> (298K)       | Tetramer <b>60</b> (298K)    |
|------------------------------|------------------------------|
| $^3J_{\text{NH9H5}} = 8.2$   | $^3J_{\text{NH9H5}} = 8.5$   |
|                              | $^3J_{\text{NH26H22}} = 8.2$ |
| $^3J_{\text{NH18H14}} = 6.2$ | $^3J_{\text{NH18H14}} = 6.2$ |
|                              | $^3J_{\text{NH35H31}} = 6.1$ |

$J$  coupling values together with 1D selective NOE experiments over NH protons give an excellent visualization of the conformational structure of the molecule.

Taking into account chemical shifts positions, ROE contacts encountered and  $J$  values a pictorial conformational structure of the major conformer is depicted in **Figure 127**.

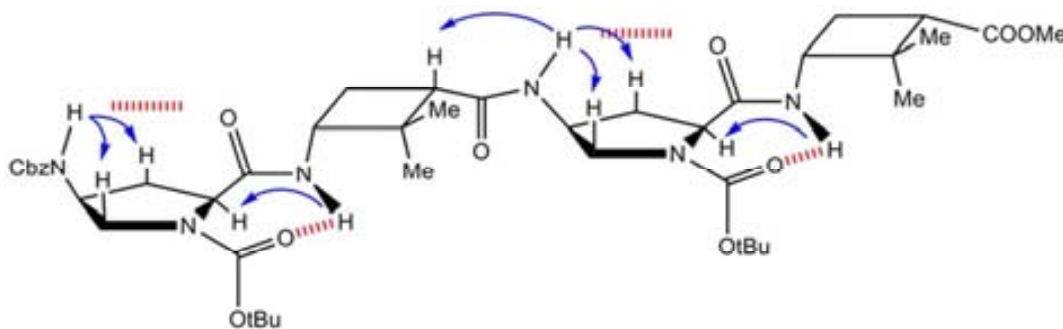


**Figure 127:** Conformation for **60** deduced from ROE connections and  $^3J_{\text{NHCH}}$  values. Important ROE effects corroborating hydrogen bonding are indicated with a blue arrow. Hydrogen bonds are indicated with red lines.

## SUPPORTING FIGURES FOR 60

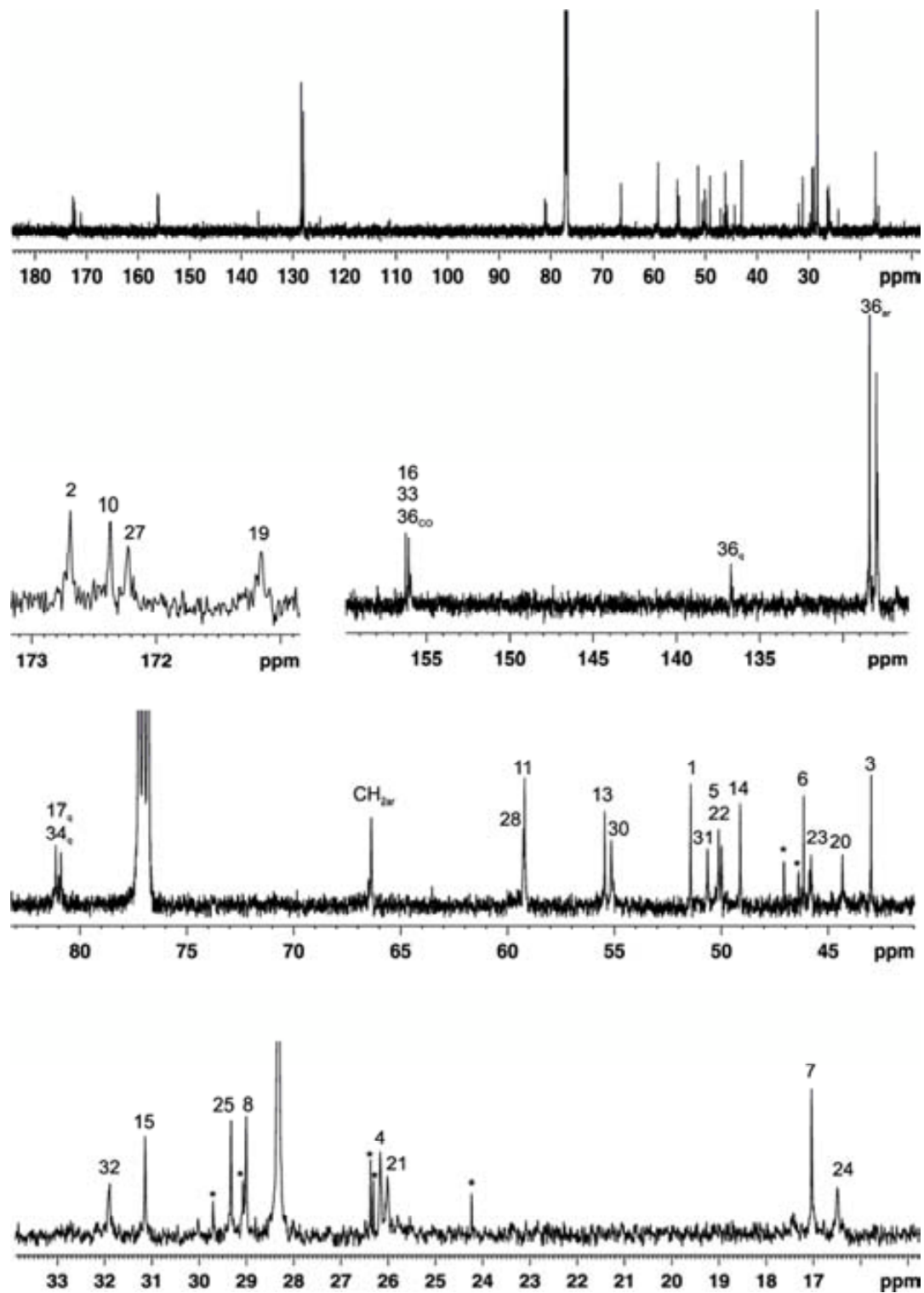
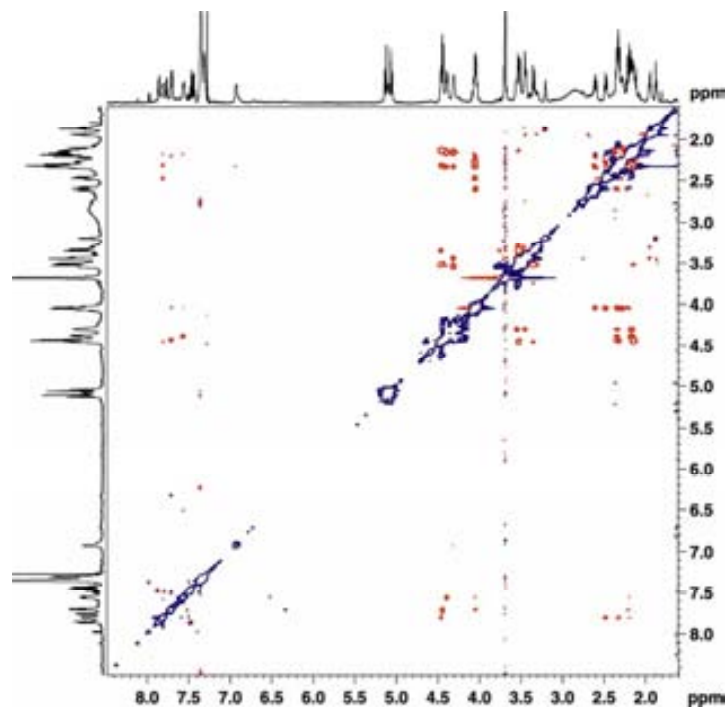
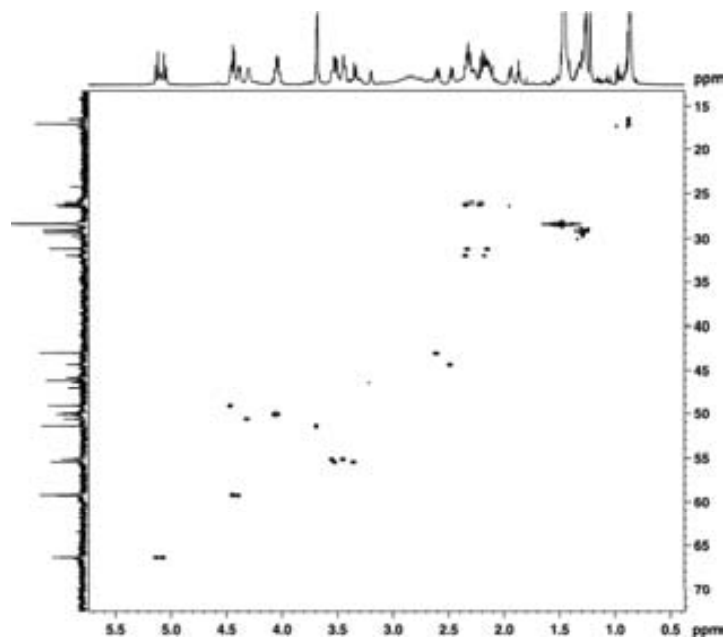


Figure 128:  $^{13}\text{C}$  NMR spectrum for **60** obtained in a Bruker 600 MHz spectrometer in  $\text{CDCl}_3$  at 298 K.



**Figure 129:** 2D-ROESY spectrum recorded in a Bruker 600 MHz spectrometer in  $\text{CDCl}_3$  at 298 K (mixing time was set to 500 ms).



**Figure 130:** HQC spectrum recorded in a Bruker 600 MHz spectrometer in  $\text{CDCl}_3$  at 298 K.

**Hexapeptide 62**

$^1\text{H}$  NMR spectrum of the  $\gamma$ -hexapeptide **62** clearly shows a single major conformation although several minor conformers are visible in the spectrum (**Figure 131**).

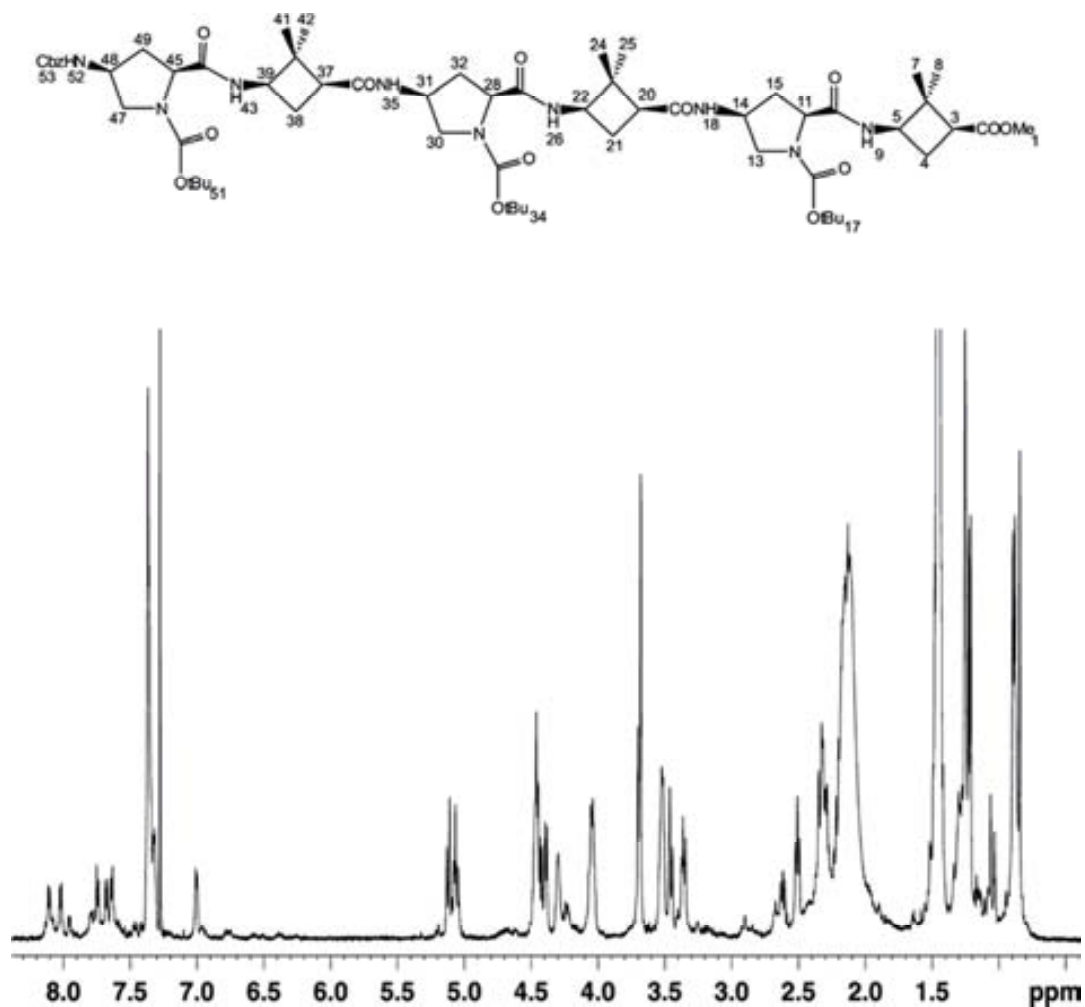


**Figure 131:**  $^1\text{H}$  NMR spectrum of hexapeptide **62** acquired in a Bruker 600 MHz spectrometer at 298 K.

SUPPORTING FIGURES FOR 62

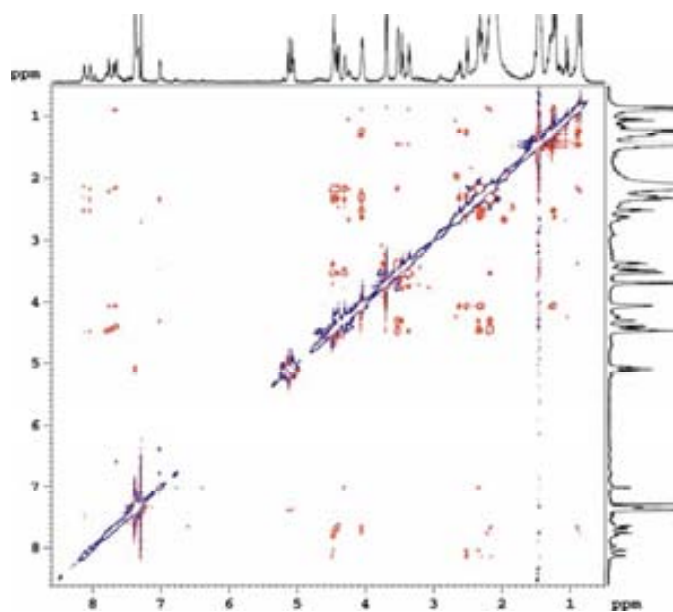


Figure 132: 2D ROESY experiment.

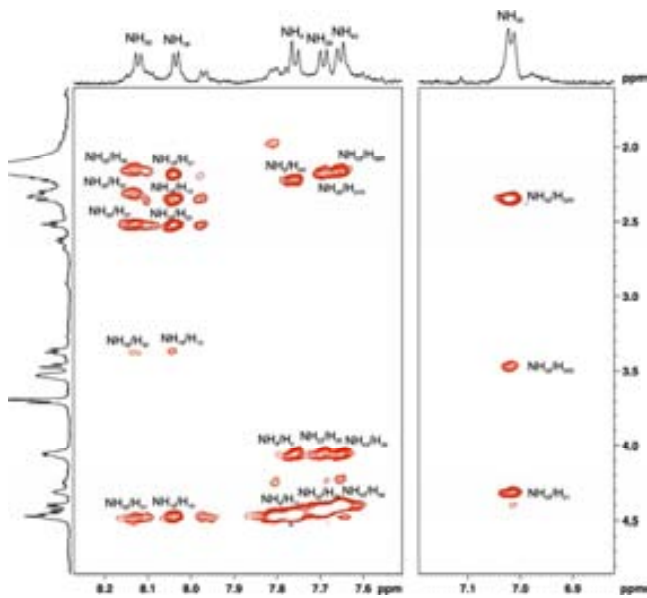


Figure 133: 2D ROESY experiment.





## **Annex IV**

Computational Methods for cyclobutane-proline  $\gamma,\gamma$ -peptides modelling



## **11.ANNEX IV: COMPUTATIONAL METHODS FOR CYCLOBUTANE-PROLINE $\gamma,\gamma$ -PEPTIDES MODELLING**

A mixed Monte-Carlo<sup>170</sup>/Low-Mode<sup>171, 172</sup> Conformational Search was done using the MMFF<sup>173</sup> (Merck Molecular Force Field) force field implemented in the Macromodel 9.8 program.<sup>174</sup> Restrictions have been introduced to reproduce the NOE-derived distances and dihedral angles from coupling constants and NOEs experiments. The solvent effect has been included using the GB/SA<sup>175</sup> method implemented in Macromodel with chloroform as solvent. We have also done Molecular Dynamics calculations with Macromodel 9.8 program using the MMFF force field at 300K.

Moreover, for representative structures, geometry optimisations have been carried out at B3LYP<sup>176</sup>/6-31G(d) level of theory in gas phase with Gaussian09 package.<sup>177</sup> Frequency calculations in gas phase have been done to verify that the final geometries are minima. Geometry optimisations in chloroform using the continuum model implemented<sup>178, 179</sup> in Jaguar 7.7 program<sup>180</sup> have also been done for tetramer compounds. On the other hand, for hexamer compounds, the geometries of representative structures have been optimised at B3LYP/6-31G(d) level of theory in gas phase with Gaussian09 package.

### **Tetrapeptides 60 and 66 results**

For an energy window of 2 kcal·mol<sup>-1</sup>, 855 structures were generated for compound **60** and 240 for **66**. A structure with 5 hydrogen bonds is the preferred one for tetrapeptide **60** while two representative structures, a folded one and another extended have been found for **66**, both with 4 hydrogen bonds.

The geometries of the two conformers of **66** have been optimised in chloroform solution. These results show that the extended conformation is 2.6 kcal·mol<sup>-1</sup> more stable than the folded one, so, the extended conformation will be considered as the more probable for **66**.

The optimised structures in chloroform are shown in **Figure 134**.

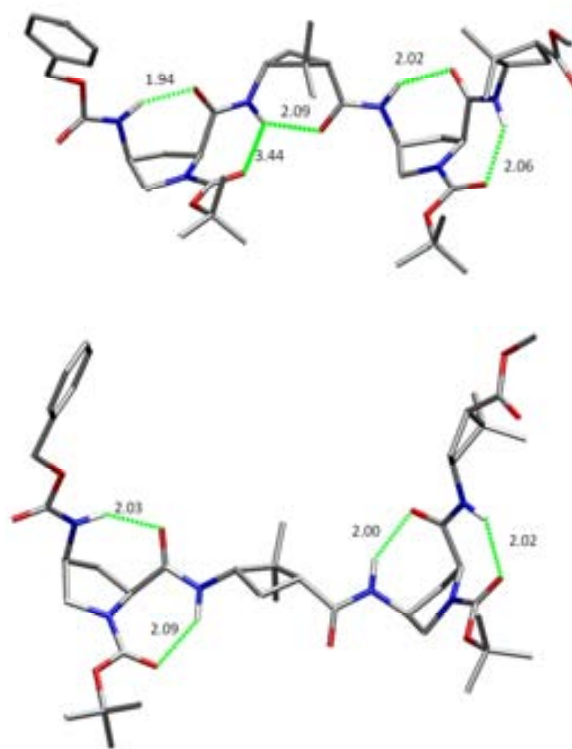
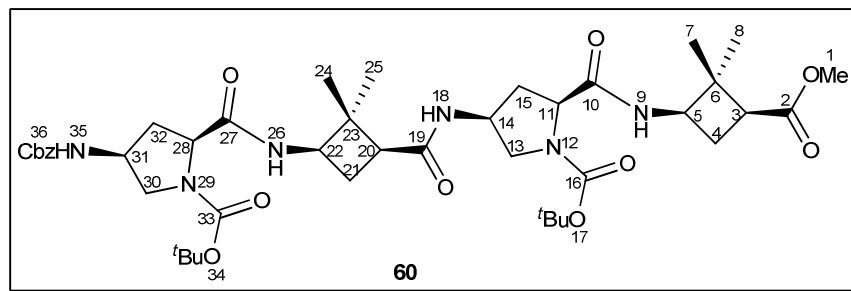


**Figure 134.** Geometries obtained at B3LYP/6-31G(d) level of theory in chloroform solvent for a) **60** and b) **66** conformers. Distances in Å. All hydrogen atoms with the exception of N-H have been deleted for clarity.

For **60** and **66** representative conformers obtained from the conformational search, Molecular Dynamics calculations were also done to monitor H-O distance using the MMFF force field in chloroform at 300K (equilibration time 250 ps, molecular dynamic 750 ps). Molecular Dynamics results also show that the folded structure is not favourable for **66**, so it varies to the extended one during the dynamics (**Table 11**).

It has to be mentioned that the Molecular Dynamics have been performed without any restriction and, moreover, monitoring the relevant NOEs distance to confirm that the NOEs interactions are always present during the dynamics. For the three representative structures considered, tetrapeptide **60** and tetrapeptide **66** extended and folded conformers, the distances between the significant atoms are always in agreement with a NOE interaction from the beginning to the end of the dynamics.

**Table 11:** Starting and average relevant distances of tetrapeptides **60** and **66** from 750 ps Molecular Dynamics. The starting structures are selected from the conformational search.



|                                   | Tetrapeptide <b>60</b> |         | Tetrapeptide <b>66</b> |         |          |         |
|-----------------------------------|------------------------|---------|------------------------|---------|----------|---------|
|                                   | Starting               | Average | Extended               |         | Folded   |         |
|                                   |                        |         | Starting               | Average | Starting | Average |
| O <sup>27</sup> -NH <sup>35</sup> | 2.001                  | 4.347   | 2.006                  | 4.821   | 2.006    | 5.026   |
| O <sup>33</sup> -NH <sup>26</sup> | 2.054                  | 2.105   | 1.840                  | 2.088   | 1.793    | 1.998   |
| O <sup>19</sup> -NH <sup>26</sup> | 2.303                  | 4.984   | 5.338                  | *       | 5.395    | *       |
| O <sup>10</sup> -NH <sup>18</sup> | 2.039                  | 4.637   | 2.017                  | 3.789   | 1.992    | 4.954   |
| O <sup>16</sup> -NH <sup>9</sup>  | 1.864                  | 2.391   | 1.828                  | 1.936   | 1.808    | 1.832   |
| O <sup>2</sup> -NH <sup>35</sup>  | 16.607                 | *       | 14.880                 | 19.184  | 3.639    | 22.961  |

\*Not monitored distance

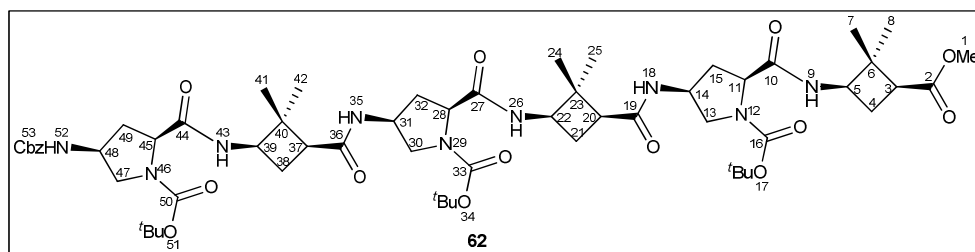
Analysing these results for tetrapeptide **60**, we observe that H<sup>26</sup>-O<sup>33</sup>, H<sup>9</sup>-O<sup>16</sup> hydrogen bonds are always present during the dynamics while H<sup>35</sup>-O<sup>27</sup>, H<sup>26</sup>-O<sup>19</sup>, H<sup>18</sup>-O<sup>10</sup> not. This fact can be related to the strength of the hydrogen bonds suggested by the NMR titration experiments with MeOD carried out for both dipeptides **57** and **64**, being stronger those ones in which the NH group belongs to the cyclobutane amino acid. On the other hand, for peptide **66** it was found that the folded structure varies to the extended one during the dynamics (see distance O<sup>2</sup>-NH<sup>35</sup> in **Table 11**). Analogously to what was found for compound **60** we observed that H<sup>26</sup>-O<sup>33</sup>, H<sup>9</sup>-O<sup>16</sup> hydrogen bonds are always present during the dynamics while H<sup>35</sup>-O<sup>27</sup>, H<sup>18</sup>-O<sup>10</sup> are not. Those results are again in agreement with the NMR experiments and can be related to the higher strength of those hydrogen bonds in which the NH group belongs to the cyclobutane amino acid.

**Hexapeptides 62 and 68 results**

For an energy window of 2 kcal mol<sup>-1</sup>, 402 structures were generated for compound **62** and 362 for **68**. For peptide **62**, two representative structures were found, one with 7 hydrogen bonds (called **62a**) and another one with 8 hydrogen bonds (**62b**). For peptide **68**, in the same way to what happened for tetrapeptide **66**, two representative conformers, a folded one and another extended, were selected, both with 6 hydrogen bonds.

For **62** and **68** representative conformers obtained from the conformational search, Molecular Dynamics calculations were also done to monitor H-O distance using the MMFF force field in CHCl<sub>3</sub> at 300K (equilibration time 250 ps, molecular dynamic 750 ps). Molecular Dynamics results also show that the folded structure is not favourable for **68** and it varies to the extended one during the dynamics.

**Table 12:** Starting and average relevant distances of hexapeptides **62** and **68** from 750 ps Molecular Dynamics. The starting structures are selected from the Conformational Search.



|                                   | Hexapeptide <b>62</b> |         |                  |         | Hexapeptide <b>68</b> |         |          |         |
|-----------------------------------|-----------------------|---------|------------------|---------|-----------------------|---------|----------|---------|
|                                   | 7 hydrogen bonds      |         | 8 hydrogen bonds |         | Extended              |         | Folded   |         |
|                                   | Starting              | Average | Starting         | Average | Starting              | Average | Starting | Average |
| O <sup>44</sup> -NH <sup>52</sup> | 1,999                 | 3,198   | 1,992            | 4,312   | 1,963                 | 3,694   | 2,020    | 3,193   |
| O <sup>50</sup> -NH <sup>43</sup> | 4,237                 | 2,566   | 2,068            | 2,127   | 1,818                 | 2,664   | 1,884    | 2,681   |
| O <sup>36</sup> -NH <sup>43</sup> | 1,958                 | 5,024   | 2,193            | 5,189   | 5,319                 | *       | 6,114    | *       |
| O <sup>27</sup> -NH <sup>35</sup> | 2,040                 | 3,367   | 1,985            | 4,208   | 2,045                 | 3,293   | 1,947    | 3,063   |
| O <sup>33</sup> -NH <sup>26</sup> | 1,898                 | 2,373   | 1,899            | 2,186   | 1,821                 | 2,627   | 1,761    | 2,543   |
| O <sup>19</sup> -NH <sup>26</sup> | 2,961                 | 4,830   | 2,890            | 5,217   | 5,383                 | *       | 5,394    | *       |
| O <sup>10</sup> -NH <sup>18</sup> | 1,850                 | 2,589   | 1,891            | 3,751   | 1,966                 | 2,631   | 2,055    | 2,871   |
| O <sup>16</sup> -NH <sup>9</sup>  | 1,931                 | 2,374   | 1,950            | 2,145   | 1,831                 | 2,330   | 1,865    | 2,582   |
| O <sup>10</sup> -NH <sup>43</sup> | 14,218                | *       | 14,635           | *       | 11,799                | 14,104  | 4,469    | 13,990  |

\*Not monitored distance

Analysing results in **Table 12**, for peptide **62**, we observe that similar average distances are obtained for **62a** and **62b** conformers. Moreover, we have optimised the structures of **62a** and **62b** conformers at B3LYP/6-31G(d) level of theory in gas phase and they both evolve to the same structure shown in **Figure 135a**.

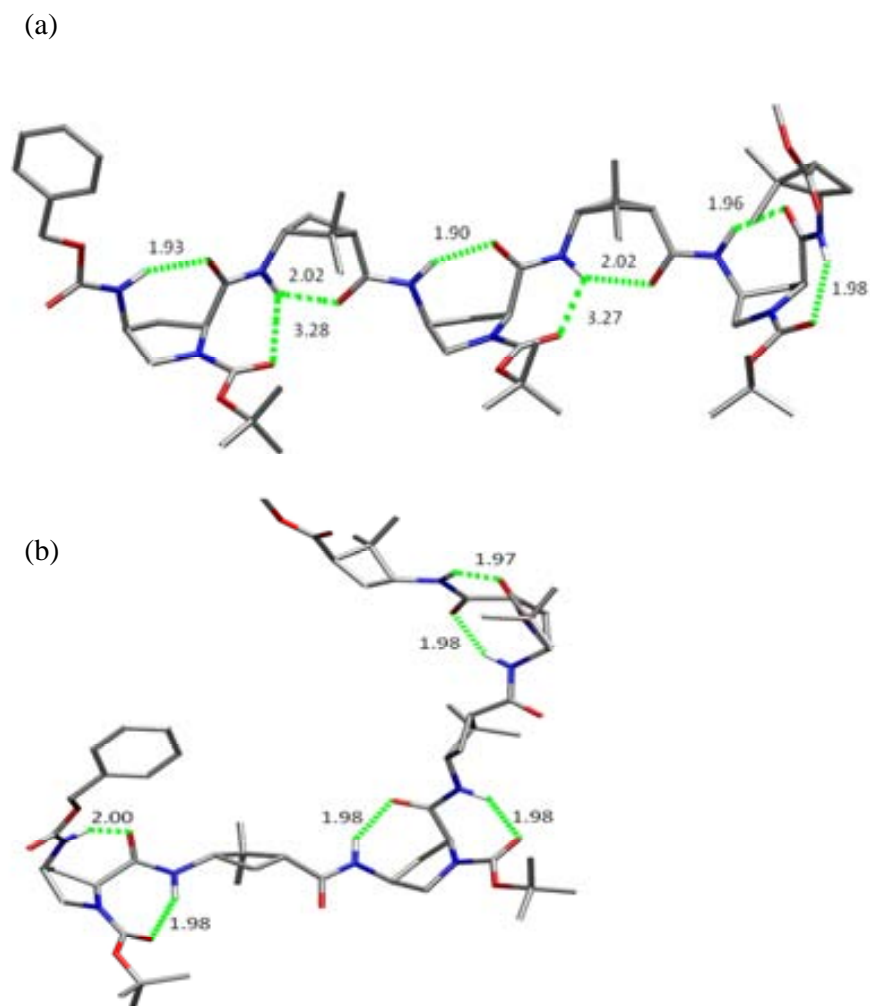


**Figure 135:** Preferred conformations for hexapeptides **62** (a) and **68** (b) as obtained at B3LYP/6-31G(d) level of theory in gas phase. Distances are in Å. All hydrogen atoms except *NH* have been omitted for clarity.

In the same way that it was observed for tetrapeptide **60**,  $H^{43}-O^{50}$ ,  $H^{26}-O^{33}$ ,  $H^9-O^{16}$ ,  $H^{18}-O^{10}$  hydrogen bonds are always present during the dynamics while  $H^{52}-O^{44}$ ,  $H^{35}-O^{27}$  are not. Those results are again in agreement with the NMR experiments and can be related to the higher strength of those hydrogen bonds in which the *NH* group belongs to the cyclobutane amino acid. Moreover, we can conclude that as we move from the *N*-terminus

to the C-terminus, hydrogen bonds become stronger due to some kind of “zip-effect”. On the other hand, for hexapeptide **68** it was found that the folded structure varies to the extended one during the dynamics (see distance  $O^{36}-H^3$  in **Table 12**). Analogously to what was found for compound **66** we observed that  $H^{43}-O^{50}$ ,  $H^{26}-O^{33}$ ,  $H^9-O^{16}$ ,  $H^{18}-O^{10}$  hydrogen bonds are always present during the dynamics while  $H^{52}-O^{44}$ ,  $H^{35}-O^{27}$  are not. Those results are again in agreement with the NOE experiments and can be related to the higher strength of those hydrogen bonds in which the NH group belongs to the cyclobutane amino acid.

Comparing the calculated structures for **62** and **8** some features are remarkable. The first one is that, in **62**, each cyclobutane NH proton is involved, in average, in a bifurcated hydrogen bond, that means an inter residual  $NH^{(i)}\dots OC^{(i-1)}$  hydrogen bond with the carbamate of the sequentially preceding proline moiety and a second one with the amide carbonyl of the same residue,  $NH^{(i)}\dots OC^{(i)}$ . This last interaction is not observed in the terminal cyclobutane residue. In contrast, for hexapeptide **68**, only inter residual hydrogen bonding is predicted due to steric effects resulting from *gem*-dimethyl and the molecule is more twisted than **62** (**Figure 135**). The presence of the intra and inter residue hydrogen bonds in **62** originates a differentiated chemical environment for each NH proton, which in turn explains the split pattern in the NH region of the  $^1H$  NMR spectra. In contrast, the preferred conformation for **68** presents a similar environment for all NH protons, thus resulting in an overlapping of the corresponding NH signals. Therefore, there is a tight relationship between cyclobutane stereochemistry and secondary structure of hybrid peptide.



**Annex V**

Biological Assays of CPPs



## **12. ANNEX V: BIOLOGICAL ASSAYS OF CPPs**

### **MTT cytotoxicity assay**

The viability of HeLa cells in the presence of the peptides was tested using the 3-(4,5-dimethyl-thiazol-2-yl)-2,5-diphenyltetrazolium bromide (MTT) assay. To avoid saturation in cell growth after 24 h of peptide incubation,  $7 \times 10^3$  cells/well were seeded on a 96-well plate (Nange Nunc) for each assay. After 24 h, the culture medium was discarded and replaced by a new medium containing different CF-peptide concentrations. Cells were incubated for 2 h and 24 h at 37 °C under 5% CO<sub>2</sub> atmosphere, and MTT (0.5 mg/mL) was added 2 h before the end of incubation. After 2 h of incubation with MTT, the medium was discarded by aspiration and 2-propanol was added to dissolve formazan, a dark blue coloured crystal observed in the wells. Absorbance was measured at 570 nm in a spectrophotometric Elx800 Universal microplate reader (Bio-Tek), 30 min after the addition of 2-propanol. Cell viability is expressed as a percent ratio of cells treated with peptide to untreated cells, which were used as a control.

### **Flow cytometry**

Flow cytometry was used to study the penetrating properties of the peptides. HeLa cells were seeded onto 35-mm plates at a concentration of  $21.4 \times 10^3$  cells/cm<sup>2</sup>. After 24 h, cells were then incubated for 2 h at 37 °C. After incubation time, cells were washed 3 times with PBS, detached with 0.25% trypsin-EDTA, centrifuged at 1000 × g, and washed again. To remove fluorescence of CF or CFpeptides bound to the plasma membrane, the pH of the PBS solution was brought down to 6 by the addition of 1 N HCl just before measuring fluorescence. At pH = 6, extracellular fluorescence of CF is quenched without altering cell mechanisms. Fluorescence analysis was performed with an Epics XL flow cytometer (Coulter). Triplicates of each sample were performed for each condition, and results from independent experiments were normalised by subtraction of the auto fluorescence control value from each value and considering the value of TAT reference under the same experimental conditions as 100.



**Annex VI**

Biological Assays of NPY Analogues



## **13. ANNEX VI: BIOLOGICAL ASSAYS OF NPY ANALOGUES**

### **13.1 Assay Protocols**

#### **13.1.1 Binding studies: Flow cytometric binding studies**

##### **Peptides and reagents**

Porcine NPY (pNPY), human pancreatic polypeptide (HPP), [K<sup>4</sup>]-HPP and GW1229<sup>181</sup> (also designated GR231118 or 1229U91) were a gift of Prof. Cabrele (Ruhr-Universität Bochum, Germany). The cyanine dye labeled fluorescent peptides cy5-pNPY and cy5-[K<sup>4</sup>]HPP were prepared in Prof. Buschauer laboratory as described previously.<sup>143, 144</sup>

Unless otherwise indicated, chemicals, buffers and reagents were purchased from Merck (Darmstadt, Germany). Millipore water was used throughout. HEPES and bovine serum albumin (BSA) were purchased from Serva (Heidelberg, Germany). FCS was obtained from Biochrom (Berlin, Germany), cy5-succinimidyl ester from Amersham Biosciences (Little Chalfont, UK).<sup>144</sup> Stock solutions of compounds **76-85** (10 mM or 1 mM) for binding studies and functional assays were prepared in Millipore water and stored at -20 °C.

##### **Cell culture**

Except for HEL cells, all cells were genetically engineered to stably express the receptor of interest.

HEL (human erythroleukemia) cells, expressing the NPY Y<sub>1</sub> receptor (Y<sub>1</sub>R)<sup>182</sup>, HEC-1-B-Y<sub>5</sub><sup>183</sup> cells, CHO-hY<sub>2</sub> and CHO -hY<sub>4</sub> cells<sup>142, 143</sup> were maintained as described. HEL cells (suspension) were passaged in RPMI with FCS (5 %). HEC-1-B-Y<sub>5</sub> cells (Y<sub>5</sub>R) were cultured in EMEM with FCS (10 %) and G418 (400 µg/mL) as described previously.<sup>184</sup> CHO cells, expressing Y<sub>2</sub>R or Y<sub>4</sub>R were grown in Ham's F12 medium supplemented with FCS (10 %) and G418 (400 mg/mL), hygromycin (400 mg/mL) and zeocin (200 mg/mL).<sup>142, 143</sup>

## **Assay Procedure**

Compounds **76-85** were investigated with respect to binding affinity of the Y<sub>4</sub>R and to receptor subtype selectivity (Y<sub>1</sub>R, Y<sub>2</sub>R and Y<sub>5</sub>R) by flow cytometry, using cy5-[K<sup>4</sup>]-HPP (final concentration 3 nM) or cy5-pNPY or (5 nM), respectively, as fluorescent receptor ligands. For all experiments, HEPES (25 mM) buffer (pH 7.4), containing CaCl<sub>2</sub>·2 H<sub>2</sub>O (2.5 mM) and MgCl<sub>2</sub> (1.5 mM), was supplemented with bovine serum albumin (BSA, 1 %) and bacitracin (0.1 g/L). All binding assays were performed in a final volume of 500 μL. Saturation binding assays were performed in the presence of increasing concentrations of compounds **76-85**. Unspecific binding was determined by addition of an excess (final concentration 1 μM) of either GW1229 (Y<sub>4</sub>R) or pNPY (Y<sub>1</sub>R, Y<sub>2</sub>R, Y<sub>5</sub>R). The samples were incubated in “siliconised” (Sigmacote, Sigma-Aldrich, Taufkirchen, Germany) Eppendorf reaction vessels at rt for 90–120 min and analysed by a FacsCalibur™ flow cytometer (Becton Dickinson, Heidelberg, Germany). The procedure and the instrument settings have been described in detail previously.<sup>142-144</sup>

### **13.1.2 Functional Studies: GTPase assay**

The steady state GTPase activity assay was performed as described previously.<sup>145-147</sup>

#### **Membrane preparation**

Sf9 cells were infected with a dilution of high-titer hY<sub>4</sub>R and Gα<sub>i2</sub>/Gα<sub>o</sub> baculovirus stocks.<sup>145</sup> After culturing for 24 – 48 h, the cells were lysed using 1 mM ethylenediamine tetraacetic acid (EDTA) (Merck, Darmstadt, Germany), 0.2 mM phenylmethylsulfonyl fluoride (Sigma, Munich, Germany), 10 μg/mL benzamide (Sigma, Munich, Germany), and 10 μg/mL leupeptin (Calbiochem, Darmstadt, Germany) as protease inhibitors in 10 mM Tris/HCl (pH 7.4), followed by multiple homogenization and centrifugation steps. For storage at -80 °C, the membranes were suspended in binding buffer (12.5 mM MgCl<sub>2</sub>, 1 mM EDTA, and 75 mM Tris/HCl, pH 7.4) at 0.5 – 1.0 mg protein/mL. For detailed information see.<sup>147</sup>



**Assay protocol**

Membranes were thawed, sedimented, and resuspended in 10 mM Tris-HCl (pH 7.4). Assay tubes contained Sf9 membranes expressing Y<sub>4</sub>R-Gα<sub>i2</sub>/Gα<sub>o</sub> fusion proteins (10 µg of protein/tube in 20 µL), 1.0 mM MgCl<sub>2</sub>, 0.1 mM EDTA, 0.1 mM ATP, 100 nM GTP, 0.1 mM adenylyl imidodiphosphate, 5 mM creatine phosphate, 40 µg of creatine kinase, and 0.2 % (w/v) BSA in 50 mM Tris-HCl, (pH 7.4, 50 µL), and Y<sub>4</sub>R agonists at various concentrations (10 uL). After incubation of the reaction mixtures (80 µL) at 25 °C for 2 min, 20 µl of [γ-<sup>33</sup>P]-GTP (0.1 µCi/tube) were added. All stock and work solutions of [γ-<sup>33</sup>P]-GTP were prepared in 20 mM Tris-HCl (pH 7.4). Reactions were terminated by addition of 900 µL of a slurry consisting of 5 % (w/v) activated charcoal and 50 mM NaH<sub>2</sub>PO<sub>4</sub> (pH 2.0). Charcoal-quenched reaction mixtures were centrifuged for 7 min at room temperature at 15,000 *g*. Six hundred microliters of the supernatant of the reaction mixtures were removed, and <sup>33</sup>P<sub>i</sub> was determined by liquid scintillation counting using Optiphase Supermix<sup>®</sup> (Perkin Elmer, Rodgau, Germany). Enzyme activities were corrected for spontaneous hydrolysis of [γ-<sup>33</sup>P]GTP, which was determined in tubes containing all of the above-described components plus a very high concentration of unlabeled GTP (1 mM). In the presence of Sf9 membranes this high excess of unlabeled GTP prevents enzymatic hydrolysis of [γ-<sup>33</sup>P]GTP. Spontaneous hydrolysis of [γ-<sup>33</sup>P]GTP amounted to < 1 % of the total amount of radioactivity added.<sup>145, 146</sup>

**Assay Results****Determination of NPY Y<sub>4</sub>R affinity and subtype selectivity by flow cytometric binding studies****Table 13:** Summary of results of the binding studies at all NPY receptor subtypes (Y<sub>1</sub>, Y<sub>2</sub>, Y<sub>4</sub>, Y<sub>5</sub>)

|          | Y <sub>4</sub>      | Y <sub>1</sub>      | Y <sub>2</sub>      | Y <sub>5</sub>        |       |     |        |     |
|----------|---------------------|---------------------|---------------------|-----------------------|-------|-----|--------|-----|
|          | CHO-hY <sub>4</sub> | HEL                 | CHO-hY <sub>2</sub> | HEC-1B-Y <sub>5</sub> |       |     |        |     |
|          | K <sub>i</sub> [nM] | K <sub>i</sub> [nM] | K <sub>i</sub> [nM] | K <sub>i</sub> [nM]   |       |     |        |     |
|          | mean                | sem                 | mean                | sem                   | mean  | sem | mean   | sem |
| 76       | 71.6                | 7.2                 | > 1000              | /                     | >1000 | /   | > 1000 | /   |
| 77       | > 1000              | /                   | > 1000              | /                     | >1000 | /   | > 1000 | /   |
| 77a      | > 1000              | /                   | > 1000              | /                     | >1000 | /   | > 1000 | /   |
| 77b      | > 1000              | /                   | > 1000              | /                     | >1000 | /   | > 1000 | /   |
| 78       | 35.3                | 1.9                 | > 1000              | /                     | >1000 | /   | > 1000 | /   |
| 78a      | 41.2                | 8.2                 | > 1000              | /                     | >1000 | /   | > 1000 | /   |
| 79       | > 1000              | /                   | > 1000              | /                     | >1000 | /   | > 1000 | /   |
| 79a      | > 1000              | /                   | > 1000              | /                     | >1000 | /   | > 1000 | /   |
| 80 + 80a | > 1000              | /                   | > 1000              | /                     | >1000 | /   | > 1000 | /   |
| 81       | > 1000              | /                   | > 1000              | /                     | >1000 | /   | > 1000 | /   |
| 82       | 92.8                | 4.3                 | > 1000              | /                     | 708.5 | 107 | > 1000 | /   |
| 82a      | 563.4               | 59.8                | > 1000              | /                     | >1000 | /   | > 1000 | /   |
| 83a      | > 1000              | /                   | > 1000              | /                     | >1000 | /   | > 1000 | /   |
| 83b      | > 1000              | /                   | > 1000              | /                     | >1000 | /   | > 1000 | /   |
| 84       | 70.0                | 9.0                 | > 1000              | /                     | >1000 | /   | > 1000 | /   |
| 85       | 119.9               | 29.5                | > 1000              | /                     | *1    | /   | > 1000 | /   |
| 85a      | > 1000              | /                   | > 1000              | /                     | >1000 | /   | > 1000 | /   |

|                          |      |      |   |   |     |     |   |   |
|--------------------------|------|------|---|---|-----|-----|---|---|
| HPP <sup>143</sup>       | 6.55 | 0.06 | / | / | /   | /   | / | / |
| pNPY <sup>142, 143</sup> | 9.62 | 0.07 | / | / | 0.8 | 0.2 | / | / |

Flow cytometric binding studies at  $Y_1$ ,  $Y_2$  and  $Y_5$  receptors were performed by displacement of cy5-pNPY (5 nM); competition binding experiments at the  $Y_4$ R were performed with cy5-[K<sup>4</sup>]-HPP (3 nM); cell lines used in the different experiments:  $Y_1$ : HEL cells expressing the  $Y_1$ R,  $Y_2$  and  $Y_4$ : CHO- $Y_2$ / $Y_4$  cells expressing the  $Y_2$  or  $Y_4$  receptor,  $Y_5$ : HEC-1B- $Y_5$ ;  $K_i$  was calculated according to the Cheng-Prusoff equation<sup>185</sup> ( $K_D$ (cy5-pNPY) = 5.2 nM; c(cy5-pNPY) = 5.0 nM,  $K_D$ (cy5-[K<sup>4</sup>]-HPP) = 5.62 nM; c(cy5-[K<sup>4</sup>]-HPP) = 3.0 nM ( $K_D$ (cy5-pNPY) = 5.2 nM; conc. (cy5-pNPY) = 5.0 nM); mean and sem were calculated from three independent experiments performed in duplicate; \*<sup>1</sup>  $K_i$  in the same range as that of RGA 13, but due to limited amount of material estimated from only one experiment; \*<sup>2</sup> Only 45 to 50 % displacement of cy5-pNPY by NPY B2/B3 at 1  $\mu$ M concentration  $\rightarrow$   $IC_{50} > 1000$  nM ( $K_D$ (cy5-pNPY) = 5.2 nM; conc. (cy5-pNPY) = 5.0 nM)

#### Summary and explanation of the results:

- All NPY analogues containing  $\gamma$ -amino acids didn't show any affinity towards the NPY  $Y_4$ R or the other NPY receptor subtypes
- Peptides containing a sulfonate residue (**77a**, **77b**, **78a**, **79a**, **80a**, **82a**, **83a**, **83b**, **85a**) showed no (**77a**, **77b**, **79a**, **80a**, **83a**, **83b**, **85a**) or, in case of **93a** compared to **93**, reduced  $Y_4$ R affinity; exception: the  $Y_4$ R affinity of **78a** was comparable to that of the non-sulfonated analogue **78**
- The NPY analogue **81**, which is extended by five amino acids, didn't show any affinity for the  $Y_4$ R, whereas the corresponding elongated HPP analogue **85** ( $K_i$  = 120 nM) showed only a minimal decrease in affinity compared to the truncated analogue **82** ( $K_i$  = 92.8)

**Functional activity at the NPY Y<sub>4</sub> receptor determined in the steady state GTPase assay**

**Table 14:** Results of the GTPase assay (agonist mode) of all Y<sub>4</sub>R affinic ligands. Means ± sem were obtained in at least three independent experiments performed in duplicate. The assay procedure is described in the appendix.

|                           | Y <sub>4</sub> R      |       |          |
|---------------------------|-----------------------|-------|----------|
|                           | EC <sub>50</sub> [nM] |       | Efficacy |
|                           | mean                  | sem   |          |
| <b>76</b>                 | 122.01                | 28.29 | 0.67     |
| <b>78</b>                 | 66.16                 | 25.48 | 0.76     |
| <b>78a</b>                | 69.95                 | 19.10 | 0.65     |
| <b>82</b>                 | 284.17                | 46.36 | 0.74     |
| <b>82a</b>                | 214.19                | 67.46 | 0.58     |
| <b>84</b>                 | 75.82                 | 21.06 | 0.70     |
| <b>85</b>                 | 223.70                | 34.08 | 0.51     |
| <b>HPP<sup>145</sup></b>  | 11.0                  | 3.6   | /        |
| <b>pNPY<sup>145</sup></b> | 416.9                 | 42    | /        |

All analogues show partial agonism at the NPY Y<sub>4</sub>R in the steady state GTPase assay.

## **Bibliography**



**14. BIBLIOGRAPHY**

- Otvos, L., *Peptide-Based Drug Design*. Humana Press: New York, 2008; Vol. 494.
- Abell, A., *Advances in Amino Acid Mimetics and Peptidomimetics*. JAI Press Inc.: Greenwich, 1997; Vol. 1.
- Smith, A. B.; Guzman, M. C.; Sprengeler, P. A.; Keenan, T. P.; Holcomb, R. C.; Wood, J. L.; Carroll, P. J.; Hirschmann, R., *J. Am. Chem. Soc.* **1994**, *116*, (22), 9947-9962.
- Gellman, S. H., *Acc. Chem. Res.* **1998**, *31*, (4), 173-180.
- Seebach, D.; L. Matthews, J., *Chem. Commun.* **1997**, (21), 2015-2022.
- Baldauf, C.; Günther, R.; Hofmann, H.-J., *Helv. Chim. Acta* **2003**, *86*, (7), 2573-2588.
- Dembitsky, V., *Journal of Natural Medicines* **2008**, *62*, (1), 1-33.
- Hansen, T. V. S., Yngve Naturally Occurring Cyclobutanes. In *Org. Synth.: Theory Appl.*, Hudlicky, T., Ed. Elsevier Science: Oxford, 2001; Vol. 5, pp 1-38.
- Bell, E. A.; Qureshi, M. Y.; Pryce, R. J.; Janzen, D. H.; Lemke, P.; Clardy, J., *J. Am. Chem. Soc.* **1980**, *102*, (4), 1409-1412.
- Austin, G. N.; Baird, P. D.; Chow, H.-F.; Fellows, L. E.; Fleet, G. W. J.; Nash, R. J.; Peach, J. M.; Pryce, R. J.; Stirton, C. H., *Tetrahedron* **1987**, *43*, (8), 1857-1861.
- Avotins, F. M., *Russ. Chem. Rev.* **1993**, *62*, (9), 897.
- Miles, D. H.; Tunsuwan, K.; Chittawong, V.; Kokpol, U.; Choudhary, M. I.; Clardy, J., *Phytochemistry* **1993**, *34*, (5), 1277-1279.
- Stevens, C. V.; Smaghe, G.; Rammeloo, T.; De Kimpe, N., *J. Agric. Food Chem.* **2005**, *53*, (6), 1945-1948.
- Mehta, L. K.; Parrick, J.; Gordon, W. G. a. T. L. G., Chapter 4.2 Four-membered ring systems. In *Progress in Heterocyclic Chemistry*, Elsevier: 2000; Vol. Volume 12, pp 77-91.
- Rappoport, Z. L., J. F., *The Chemistry of Cyclobutanes*. John Wiley & Sons: Hoboken, 2006.
- Burgess, K.; Li, S.; Rebenspies, J., *Tetrahedron Lett.* **1997**, *38*, (10), 1681-1684.
- Baxendale, I. R.; Ernst, M.; Krahnert, W.-R. d.; Ley, S. V., *Synlett* **2002**, (10), 1641-1644.
- Bolm, C.; Schiffers, I.; Atodiresei, I.; Hackenberger, C. P. R., *Tetrahedron: Asymmetry* **2003**, *14*, (22), 3455-3467.
- Aitken, D. J.; Gauzy, C.; Pereira, E., *Tetrahedron Lett.* **2004**, *45*, (11), 2359-2361.
- Gauzy, C.; Pereira, E.; Faure, S.; Aitken, D. J., *Tetrahedron Lett.* **2004**, *45*, (38), 7095-7097.
- Ortuño, R. M. I., S.; Holenz, J.; Corbera, J.; Cuberes, M. R. WO 2008015266, 2008.
- Fernández, D.; Torres, E.; Avilés, F. X.; Ortuño, R. M.; Vendrell, J., *Bioorg. Med. Chem.* **2009**, *17*, (11), 3824-3828.
- Torres, E.; Puigmarti-Luis, J.; Perez del Pino, A.; Ortuño, R. M.; Amabilino, D. B., *Org. Biomol. Chem.* **2010**, *8*, (7), 1661-1665.
- Torres, E.; Gorrea, E.; Burusco, K. K.; Da Silva, E.; Nolis, P.; Rua, F.; Bousert, S.; Diez-Perez, I.; Dannenberg, S.; Izquierdo, S.; Giral, E.; Jaime, C.; Branchadell, V.; Ortuño, R. M., *Org. Biomol. Chem.* **2010**, *8*, (3), 564-575.
- Torres, E.; Gorrea, E.; Silva, E. D.; Nolis, P.; Branchadell, V.; Ortuño, R. M., *Org. Lett.* **2009**, *11*, (11), 2301-2304.
- Gorrea, E.; Nolis, P.; Torres, E.; Da Silva, E.; Amabilino, D. B.; Branchadell, V.; Ortuño, R. M., *Chem. Eur. J.* **2011**, *17*, (16), 4588-4597.
- Martín-Vilà, M.; Muray, E.; Aguado, G. P.; Alvarez-Larena, A.; Branchadell, V.; Minguillón, C.; Giral, E.; Ortuño, R. M., *Tetrahedron: Asymmetry* **2000**, *11*, (17), 3569-3584.
- Izquierdo, S.; Rúa, F.; Sbai, A.; Parella, T.; Álvarez-Larena, Á.; Branchadell, V.; Ortuño, R. M., *J. Org. Chem.* **2005**, *70*, (20), 7963-7971.
- Rúa, F.; Bousert, S.; Parella, T.; Díez-Pérez, I.; Branchadell, V.; Giral, E.; Ortuño, R. M., *Org. Lett.* **2007**, *9*, (18), 3643-3645.

30. Gorrea, E. Cyclobutane peptides and ureas: synthesis, folding, self-assembling and some biological properties. PhD Thesis. Universitat Autònoma de Barcelona, 2012.
31. Celis, S.; Gorrea, E.; Nolis, P.; Illa, O.; Ortuño, R. M., *Org. Biomol. Chem.* **2012**, 10, (4), 861-868.
32. Izquierdo, S.; Kogan, M. J.; Parella, T.; Moglioni, A. G.; Branchadell, V.; Giralt, E.; Ortuño, R. M., *J. Org. Chem.* **2004**, 69, (15), 5093-5099.
33. Aguado, G. P.; Moglioni, A. G.; García-Expósito, E.; Branchadell, V.; Ortuño, R. M., *J. Org. Chem.* **2004**, 69, (23), 7971-7978.
34. Aguado, G. P.; Alvarez-Larena, A.; Illa, O.; Moglioni, A. G.; Ortuño, R. M., *Tetrahedron: Asymmetry* **2001**, 12, (1), 25-28.
35. Moglioni, A. G.; García-Expósito, E.; Alvarez-Larena, A.; Branchadell, V.; Moltrasio, G. Y.; Ortuño, R. M., *Tetrahedron: Asymmetry* **2000**, 11, (24), 4903-4914.
36. Moglioni, A. G.; García-Expósito, E.; Aguado, G. P.; Parella, T.; Branchadell, V.; Moltrasio, G. Y.; Ortuño, R. M., *J. Org. Chem.* **2000**, 65, (13), 3934-3940.
37. Aguado, G. P.; Moglioni, A. G.; Ortuño, R. M., *Tetrahedron: Asymmetry* **2003**, 14, (2), 217-223.
38. Aguado, G. P.; Moglioni, A. G.; Brousse, B. N.; Ortuño, R. M., *Tetrahedron: Asymmetry* **2003**, 14, (16), 2445-2451.
39. Moglioni, A. G.; Muray, E.; Castillo, J. A.; Álvarez-Larena, Á.; Moltrasio, G. Y.; Branchadell, V.; Ortuño, R. M., *J. Org. Chem.* **2002**, 67, (8), 2402-2410.
40. Moglioni, A. G.; Brousse, B. N.; Álvarez-Larena, Á.; Moltrasio, G. Y.; Ortuño, R. M., *Tetrahedron: Asymmetry* **2002**, 13, (5), 451-454.
41. Rouge, P. D.; Moglioni, A. G.; Moltrasio, G. Y.; Ortuño, R. M., *Tetrahedron: Asymmetry* **2003**, 14, (2), 193-195.
42. Aguilera, J.; Gutiérrez-Abad, R.; Mor, À.; Moglioni, A. G.; Moltrasio, G. Y.; Ortuño, R. M., *Tetrahedron: Asymmetry* **2008**, 19, (24), 2864-2869.
43. Aguilera, J.; Moglioni, A. G.; Moltrasio, G. Y.; Ortuño, R. M., *Tetrahedron: Asymmetry* **2008**, 19, (3), 302-308.
44. Dado, G. P.; Gellman, S. H., *J. Am. Chem. Soc.* **1994**, 116, (3), 1054-1062.
45. Roberts, E.; Frankel, S., *J. Biol. Chem.* **1950**, 187, (1), 55-63.
46. Krogsgaard-Larsen, P.; Frolund, B.; Frydenvang, K., *GABA uptake inhibitors. Design, molecular pharmacology and therapeutic aspects*. 2000; Vol. 6, p 1193-209.
47. Bormann, J., *Trends Pharmacol. Sci.* **2000**, 21, (1), 16-19.
48. Smart, T. G., In *Amino acid neurotransmission*, Stephenson, F. A., Ed. Portland Press: London, 1998; pp 37-63.
49. Seebach, D.; Hook, D. F.; Glättli, A., *Peptide Science* **2006**, 84, (1), 23-37.
50. Brea, R. J.; Amorín, M.; Castedo, L.; Granja, J. R., *Angew. Chem. Int. Ed.* **2005**, 44, (35), 5710-5713.
51. Woll, M. G.; Lai, J. R.; Guzei, I. A.; Taylor, S. J. C.; Smith, M. E. B.; Gellman, S. H., *J. Am. Chem. Soc.* **2001**, 123, (44), 11077-11078.
52. Hintermann, T.; Gademann, K.; Jaun, B.; Seebach, D., *Helv. Chim. Acta* **1998**, 81, (5-8), 983-1002.
53. Seebach, D.; Brenner, M.; Rueping, M.; Schweizer, B.; Jaun, B., *Chem. Commun.* **2001**, (2), 207-208.
54. Hanessian, S.; Luo, X.; Schaum, R.; Michnick, S., *J. Am. Chem. Soc.* **1998**, 120, (33), 8569-8570.
55. Hanessian, S.; Luo, X.; Schaum, R., *Tetrahedron Lett.* **1999**, 40, (27), 4925-4929.
56. Seebach, D.; Brenner, M.; Rueping, M.; Jaun, B., *Chem. Eur. J.* **2002**, 8, (3), 573-584.
57. Seebach, D., *Angew. Chem. Int. Ed.* **1990**, 29, (11), 1320-1367.
58. Kennewell, P. D.; Matharu, S. S.; Taylor, J. B.; Westwood, R.; Sammes, P. G., *J. Chem. Soc., Perkin Trans. 1* **1982**, 2553-2562.
59. Kennewell, P. D.; Matharu, S. S.; Taylor, J. B.; Westwood, R.; Sammes, P. G., *J. Chem. Soc., Perkin Trans. 1* **1982**, 2563-2570.
60. Vögtle, F.; Richard, G.; Werner, N., *Dendrimer Chemistry*. Wiley-VCH: 2009.



61. Buhleier, E.; Wehner, W.; VÃ–gtle, F., *Synthesis* **1978**, 1978, (02), 155,158.
62. Newkome, G. R.; Yao, Z.; Baker, G. R.; Gupta, V. K., *J. Org. Chem.* **1985**, 50, (11), 2003-2004.
63. Tomalia, D. A.; Baker, H.; Dewald, J.; Hall, M.; Kallos, G.; Martin, S.; Roeck, J.; Ryder, J.; Smith, P., *Polymer Journal* **1985**, 17, (1), 117-132.
64. Sadler, K.; Tam, J. P., *Reviews in Molecular Biotechnology* **2002**, 90, (3â€“4), 195-229.
65. Lee, C. C.; MacKay, J. A.; Frechet, J. M. J.; Szoka, F. C., *Nat Biotech* **2005**, 23, (12), 1517-1526.
66. Hodge, P., *Nature* **1993**, 362, (6415), 18-19.
67. Hawker, C. J.; Frechet, J. M. J., *J. Am. Chem. Soc.* **1990**, 112, (21), 7638-7647.
68. Kristiansen, M.; Smith, P.; Chanzy, H.; Baerlocher, C.; Gramlich, V.; McCusker, L.; Weber, T.; Pattison, P.; Blomenhofer, M.; Schmidt, H.-W., *Cryst. Growth Des.* **2009**, 9, (6), 2556-2558.
69. Mohmeyer, N.; Behrendt, N.; Zhang, X.; Smith, P.; AltstÃ¤dt, V.; Sessler, G. M.; Schmidt, H.-W., *Polymer* **2007**, 48, (6), 1612-1619.
70. Blomenhofer, M.; Ganzleben, S.; Hanft, D.; Schmidt, H.-W.; Kristiansen, M.; Smith, P.; Stoll, K.; MÃ¤rder, D.; Hoffmann, K., *Macromolecules* **2005**, 38, (9), 3688-3695.
71. Kreger, K.; Wolfer, P.; Audorff, H.; Kador, L.; Stingelin-Stutzmann, N.; Smith, P.; Schmidt, H.-W., *J. Am. Chem. Soc.* **2009**, 132, (2), 509-516.
72. Smulders, M. M. J.; Pilot, I. A. W.; Leenders, J. M. A.; van der Schoot, P.; Palmans, A. R. A.; Schenning, A. P. H. J.; Meijer, E. W., *J. Am. Chem. Soc.* **2009**, 132, (2), 611-619.
73. Smulders, M. M. J.; Stals, P. J. M.; Mes, T.; Paffen, T. F. E.; Schenning, A. P. H. J.; Palmans, A. R. A.; Meijer, E. W., *J. Am. Chem. Soc.* **2009**, 132, (2), 620-626.
74. Matsuura, K.; Matsuyama, H.; Fukuda, T.; Teramoto, T.; Watanabe, K.; Murasato, K.; Kimizuka, N., *Soft Matter* **2009**, 5, (12), 2463-2470.
75. Huang, Y.; Cong, Y.; Li, J.; Wang, D.; Zhang, J.; Xu, L.; Li, W.; Li, L.; Pan, G.; Yang, C., *Chem. Commun.* **2009**, (48), 7560-7562.
76. Van Gorp, J. J.; Vekemans, J. A. J. M.; Meijer, E. W., *Mol. Cryst. Liq. Cryst.* **2003**, 397, (1), 191-205.
77. P. Lightfoot, M.; S. Mair, F.; G. Pritchard, R.; E. Warren, J., *Chem. Commun.* **1999**, (19), 1945-1946.
78. Zhou, Y.; Xu, M.; Li, T.; Guo, Y.; Yi, T.; Xiao, S.; Li, F.; Huang, C., *J. Colloid Interface Sci.* **2008**, 321, (1), 205-211.
79. Pichon, B. P.; Wong Chi Man, M.; Dieudonné, P.; Bantignies, J. L.; Bied, C.; Sauvajol, J. L.; Moreau, J. J. E., *Adv. Funct. Mater.* **2007**, 17, (14), 2349-2355.
80. de Loos, M.; van Esch, J. H.; Kellogg, R. M.; Feringa, B. L., *Tetrahedron* **2007**, 63, (31), 7285-7301.
81. van Gorp, J. J.; Vekemans, J. A. J. M.; Meijer, E. W., *J. Am. Chem. Soc.* **2002**, 124, (49), 14759-14769.
82. Yasuda, Y.; Iishi, E.; Inada, H.; Shirota, Y., *Chem. Lett.* **1996**, 25, (7), 575-576.
83. Danila, I.; Riobe, F.; Puigmarti-Luis, J.; Perez del Pino, A.; Wallis, J. D.; Amabilino, D. B.; Avarvari, N., *J. Mater. Chem.* **2009**, 19, (26), 4495-4504.
84. Zhou, Y.; Xu, M.; Yi, T.; Xiao, S.; Zhou, Z.; Li, F.; Huang, C., *Langmuir* **2006**, 23, (1), 202-208.
85. Jia, T.; Zhao, Y.; Xing, F.; Shao, M.; Zhu, S.; Li, M., *J. Mol. Struct.* **2009**, 920, (1-3), 18-22.
86. Birkmann, B.; Fröhlich, R.; Hahn, F. E., *Chem. Eur. J.* **2009**, 15, (37), 9325-9329.
87. Caulder, D. L.; Brückner, C.; Powers, R. E.; König, S.; Parac, T. N.; Leary, J. A.; Raymond, K. N., *J. Am. Chem. Soc.* **2001**, 123, (37), 8923-8938.
88. Müller, M. K.; Brunsveld, L., *Angew. Chem. Int. Ed.* **2009**, 48, (16), 2921-2924.
89. Trouche, N.; Wieckowski, S. b.; Sun, W.; Chaloin, O.; Hoebeke, J.; Fournel, S.; Guichard, G., *J. Am. Chem. Soc.* **2007**, 129, (44), 13480-13492.
90. Kotha, S.; Shah, V. R., *Amino Acids* **2008**, 35, (1), 83-88.
91. van den Hout, K. P.; Martín-Rapún, R.; Vekemans, J. A. J. M.; Meijer, E. W., *Chem. Eur. J.* **2007**, 13, (29), 8111-8123.
92. Matsuura, K.; Murasato, K.; Kimizuka, N., *J. Am. Chem. Soc.* **2005**, 127, (29), 10148-10149.

93. Tor, Y.; Libman, J.; Shanzer, A.; Felder, C. E.; Lifson, S., *J. Am. Chem. Soc.* **1992**, 114, (17), 6653-6661.
94. Jeong, M. J.; Park, J. H.; Lee, C.; Chang, J. Y., *Org. Lett.* **2006**, 8, (11), 2221-2224.
95. Pehere, A. D.; Abell, A. D., *Tetrahedron Lett.* 52, (13), 1493-1494.
96. Inanaga, J. H., K.; Saeki, H.; Katsuki, T.; Yamaguchi, M., *Bull. Chem. Soc. Jpn.* **1979**, 52, 1989-1993.
97. Lee, K. K., D.-K., *J. Korean Chem. Soc.* **2004**, 48, 161-170.
98. Hirst, A. R.; Escuder, B.; Miravet, J. F.; Smith, D. K., *Angew. Chem. Int. Ed.* **2008**, 47, (42), 8002-8018.
99. Cheng, R. P.; Gellman, S. H.; DeGrado, W. F., *Chem. Rev.* **2001**, 101, (10), 3219-3232.
100. De Pol, S.; Zorn, C.; Klein, C. D.; Zerbe, O.; Reiser, O., *Angew. Chem. Int. Ed.* **2004**, 43, (4), 511-514.
101. Horne, W. S.; Gellman, S. H., *Acc. Chem. Res.* **2008**, 41, (10), 1399-1408.
102. Hayen, A.; Schmitt, M. A.; Ngassa, F. N.; Thomasson, K. A.; Gellman, S. H., *Angew. Chem. Int. Ed.* **2004**, 43, (4), 505-510.
103. Berlicki, Ł.; Pilsl, L.; Wéber, E.; Mándity, I. M.; Cabrele, C.; Martinek, T. A.; Fülöp, F.; Reiser, O., *Angew. Chem. Int. Ed.* **2012**, 51, (9), 2208-2212.
104. Brenner, M.; Seebach, D., *Helv. Chim. Acta* **2001**, 84, (8), 2155-2166.
105. Koglin, N.; Zorn, C.; Beumer, R.; Cabrele, C.; Bubert, C.; Sewald, N.; Reiser, O.; Beck-Sickinger, A. G., *Angew. Chem. Int. Ed.* **2003**, 42, (2), 202-205.
106. Lang, M.; Bufe, B.; De Pol, S.; Reiser, O.; Meyerhof, W.; Beck-Sickinger, A. G., *J. Pept. Sci.* **2006**, 12, (4), 258-266.
107. Farrera-Sinfreu, J.; Zaccaro, L.; Vidal, D.; Salvatella, X.; Giralt, E.; Pons, M.; Albericio, F.; Royo, M., *J. Am. Chem. Soc.* **2004**, 126, (19), 6048-6057.
108. Woods, C. R.; Ishii, T.; Boger, D. L., *J. Am. Chem. Soc.* **2002**, 124, (36), 10676-10682.
109. Zhang, A.; Rodríguez-Ropero, F.; Zanuy, D.; Alemán, C.; Meijer, E. W.; Schlüter, A. D., *Chem. Eur. J.* **2008**, 14, (23), 6924-6934.
110. Rodríguez-Ropero, F.; Canales, M.; Zanuy, D.; Zhang, A.; Schlüter, D.; Alemán, C., *J. Phys. Chem. B* **2009**, 113, (45), 14868-14876.
111. Farrera-Sinfreu, J.; Giralt, E.; Castel, S.; Albericio, F.; Royo, M., *J. Am. Chem. Soc.* **2005**, 127, (26), 9459-9468.
112. Davidson, B. L.; Breakefield, X. O., *Nat. Rev. Neurosci.* **2003**, 4, (5), 353-364.
113. Zhang, S.; Xu, Y.; Wang, B.; Qiao, W.; Liu, D.; Li, Z., *J. Controlled Release* **2004**, 100, (2), 165-180.
114. Vivès, E.; Brodin, P.; Lebleu, B., *J. Biol. Chem.* **1997**, 272, (25), 16010-16017.
115. Nakase, I.; Akita, H.; Kogure, K.; Gräslund, A.; Langel, Ü.; Harashima, H.; Futaki, S., *Acc. Chem. Res.* **2012**, doi: 10.1021/ar200256e.
116. Goun, E. A.; Pillow, T. H.; Jones, L. R.; Rothbard, J. B.; Wender, P. A., *ChemBioChem* **2006**, 7, (10), 1497-1515.
117. Gupta, B.; Levchenko, T. S.; Torchilin, V. P., *Adv. Drug Deliv. Rev.* **2005**, 57, (4), 637-651.
118. Deshayes, S.; Morris, M. C.; Divita, G.; Heitz, F., *Cell. Mol. Life Sci.* **2005**, 62, (16), 1839-1849.
119. Schwarze, S. R.; Ho, A.; Vocero-Akbani, A.; Dowdy, S. F., *Science* **1999**, 285, (5433), 1569-1572.
120. Tréhin, R.; Merkle, H. P., *Eur. J. Pharmaceut. Biopharmaceut.* **2004**, 58, (2), 209-223.
121. Singh, D.; Kiarash, R.; Kawamura, K.; LaCasse, E. C.; Gariépy, J., *Biochemistry* **1998**, 37, (17), 5798-5809.
122. Brokx, R. D.; Bisland, S. K.; Gariépy, J., *J. Controlled Release* **2002**, 78, (1-3), 115-123.
123. Umezawa, N.; Gelman, M. A.; Haigis, M. C.; Raines, R. T.; Gellman, S. H., *J. Am. Chem. Soc.* **2001**, 124, (3), 368-369.
124. Rueping, M.; Mahajan, Y.; Sauer, M.; Seebach, D., *ChemBioChem* **2002**, 3, (2-3), 257-259.
125. García-Echeverría, C.; Ruetz, S., *Bioorg. Med. Chem. Lett.* **2003**, 13, (2), 247-251.
126. Jacek, H., *Curr. Opin. Immunol.* **1997**, 9, (2), 189-194.

127. Sadler, K.; Eom, K. D.; Yang, J.-L.; Dimitrova, Y.; Tam, J. P., *Biochemistry* **2002**, 41, (48), 14150-14157.
128. Fernández-Carneado, J.; Kogan, M. J.; Castel, S.; Giralt, E., *Angew. Chem. Int. Ed.* **2004**, 43, (14), 1811-1814.
129. Kern, D.; Schutkowski, M.; Drakenberg, T. r., *J. Am. Chem. Soc.* **1997**, 119, (36), 8403-8408.
130. Wang, K.; Yan, X.; Cui, Y.; He, Q.; Li, J., *Bioconjugate Chemistry* **2007**, 18, (6), 1735-1738.
131. Yan, X.; He, Q.; Wang, K.; Duan, L.; Cui, Y.; Li, J., *Angew. Chem. Int. Ed.* **2007**, 46, (14), 2431-2434.
132. Yan, X.; Cui, Y.; He, Q.; Wang, K.; Li, J.; Mu, W.; Wang, B.; Ou-yang, Z.-C., *Chem. Eur. J.* **2008**, 14, (19), 5974-5980.
133. Ghosh, S.; Reches, M.; Gazit, E.; Verma, S., *Angew. Chem. Int. Ed.* **2007**, 46, (12), 2002-2004.
134. Ghosh, S.; Singh, S. K.; Verma, S., *Chem. Commun.* **2007**, (22), 2296-2298.
135. Ghosh, S.; Verma, S., *Chem. Eur. J.* **2008**, 14, (5), 1415-1419.
136. Nelson-Rees, W. A.; Flandermeyer, R. R., *Science* **1976**, 191, (4222), 96-98.
137. Abes, R.; Moulton, H. M.; Clair, P.; Yang, S.-T.; Abes, S.; Melikov, K.; Prevot, P.; Youngblood, D. S.; Iversen, P. L.; Chernomordik, L. V.; Lebleu, B., *Nucleic Acids Res.* **2008**, 36, (20), 6343-6354.
138. Gray, T. S.; Morley, J. E., *Life Sci.* **1986**, 38, (5), 389-401.
139. Michel, M. C.; Beck-Sickinger, A.; Cox, H.; Doods, H. N.; Herzog, H.; Larhammar, D.; Quirion, R.; Schwartz, T.; Westfall, T., *Pharmacological Reviews* **1998**, 50, (1), 143-150.
140. Allen, J.; Novotný, J.; Martin, J.; Heinrich, G., *Proc. Natl. Acad. Sci. U. S. A.* **1987**, 84, (8), 2532-2536.
141. Beck-Sickinger, A. G.; Weland, H. A.; Wittneben, H.; Willim, K.-D.; Rudolf, K.; Jung, G., *Eur. J. Biochem.* **1994**, 225, (3), 947-958.
142. Ziemek, R.; Brennauer, A.; Schneider, E.; Cabrele, C.; Beck-Sickinger, A. G.; Bernhardt, G. n.; Buschauer, A., *Eur. J. Pharmacol.* **2006**, 551, (1-3), 10-18.
143. Ziemek, R.; Schneider, E.; Kraus, A.; Cabrele, C.; Beck-Sickinger, A. G.; Bernhardt, G.; Buschauer, A., *J. Recep. Signal Transduction* **2007**, 27, (4), 217-233.
144. Schneider, E.; Keller, M.; Brennauer, A.; Hoefelschweiger, B. K.; Gross, D.; Wolfbeis, O. S.; Bernhardt, G.; Buschauer, A., *ChemBioChem* **2007**, 8, (16), 1981-1988.
145. Pop, N.; Igel, P.; Brennauer, A.; Cabrele, C.; Bernhardt, G. n.; Seifert, R.; Buschauer, A., *J. Recep. Signal Transduction* **2011**, 31, (4), 271-285.
146. Preuss, H.; Ghorai, P.; Kraus, A.; Dove, S.; Buschauer, A.; Seifert, R., *J. Pharmacol. Exp. Ther.* **2007**, 321, (3), 983-995.
147. Seifert, R.; Lee, T. W.; Lam, V. T.; Kobilka, B. K., *Eur. J. Biochem.* **1998**, 255, (2), 369-382.
148. García, A. I.; Insuasty, B.; Herranz, M. Á.; Martínez-Álvarez, R.; Martín, N., *Org. Lett.* **2009**, 11, (23), 5398-5401.
149. Danila, I.; Riobé, F.; Piron, F.; Puigmartí-Luis, J.; Wallis, J. D.; Linares, M.; Agren, H.; Beljonne, D.; Amabilino, D. B.; Avarvari, N., *J. Am. Chem. Soc.* **2011**, 133, (21), 8344-8353.
150. Yelamaggad, C. V.; Achalkumar, A. S.; Rao, D. S. S.; Prasad, S. K., *J. Org. Chem.* **2007**, 72, (22), 8308-8318.
151. Nicole, L.; Rozes, L.; Sanchez, C., *Adv. Mat.* **2006**, 22, (29), 3208-3214.
152. Sanchez, C.; Ribot, F., *New J. Chem.* **1994**, 18, (10), 1007-1047.
153. Weisskoff, R. M. E., R. R., Basic principles of MRI. In *Clinical Magnetic Resonance imaging*, Edelman, R. R. H., J. R.; Zlatkin, M. B., Ed. Saunders: Philadelphia, 1996; Vol. 1, pp 3-51.
154. Bonnet, C. S.; Tóth, É., *Am. J. Neuroradiol.* **2010**, 31, (3), 401-409.
155. Port, M.; Idée, J.-M.; Medina, C.; Robic, C.; Sabatou, M.; Corot, C., *BioMetals* **2008**, 21, (4), 469-490.
156. Caravan, P., *Chem. Soc. Rev.* **2006**, 35, (6), 512-523.
157. Ceccherelli, P.; Curini, M.; Marcotullio, M. C.; Epifano, F.; Rosati, O., *Synth. Commun.* **1998**, 28, (16), 3057-3064.
158. Iwasawa, Y.; Shibata, J.; Nonoshita, K.; Arai, S.; Masaki, H.; Tomimoto, K., *Tetrahedron* **1996**, 52, (44), 13881-13894.

159. Barge, A.; Cravotto, G.; Gianolio, E.; Fedeli, F., *Contrast Media Mol. Imaging* **2006**, 1, (5), 184-188.
160. Caravan, P.; Ellison, J. J.; McMurry, T. J.; Lauffer, R. B., *Chem. Rev.* **1999**, 99, (9), 2293-2352.
161. Chan, K. W.-Y.; Wong, W.-T., *Coord. Chem. Rev.* **2007**, 251, (17-20), 2428-2451.
162. Sheehan, J. C.; Hess, G. P., *J. Am. Chem. Soc.* **1955**, 77, (4), 1067-1068.
163. König, W.; Geiger, R., *Chem. Ber.* **1970**, 103, (3), 788-798.
164. Dourtoglou, V.; Ziegler, J.-C.; Gross, B., *Tetrahedron Lett.* **1978**, 19, (15), 1269-1272.
165. Dourtoglou, V.; Gross, B.; Lambropoulou, V.; Zioudrou, C., *Synthesis* **1984**, 1984, (07), 572,574.
166. Knorr, R.; Trzeciak, A.; Bannwarth, W.; Gillessen, D., *Tetrahedron Lett.* **1989**, 30, (15), 1927-1930.
167. Carpino, L. A.; Henklein, P.; Foxman, B. M.; Abdelmoty, I.; Costisella, B.; Wray, V.; Domke, T.; El-Faham, A.; Mügge, C., *J. Org. Chem.* **2001**, 66, (15), 5245-5247.
168. Carpino, L. A.; Imazumi, H.; El-Faham, A.; Ferrer, F. J.; Zhang, C.; Lee, Y.; Foxman, B. M.; Henklein, P.; Hanay, C.; Mügge, C.; Wenschuh, H.; Klose, J.; Beyermann, M.; Bienert, M., *Angew. Chem. Int. Ed.* **2002**, 41, (3), 441-445.
169. Uhlmann, E.; Peyman, A.; Breipohl, G.; Will, D. W., *Angew. Chem. Int. Ed.* **1998**, 37, (20), 2796-2823.
170. Chang, G.; Guida, W. C.; Still, W. C., *J. Am. Chem. Soc.* **1989**, 111, (12), 4379-4386.
171. Kolossváry, I. n.; Guida, W. C., *J. Am. Chem. Soc.* **1996**, 118, (21), 5011-5019.
172. Kolossváry, I.; Guida, W. C., *J. Comput. Chem.* **1999**, 20, (15), 1671-1684.
173. Halgren, T. A., *J. Comput. Chem.* **1996**, 17, (5-6), 490-519.
174. Mohamadi, F.; Richards, N. G. J.; Guida, W. C.; Liskamp, R.; Lipton, M.; Caufield, C.; Chang, G.; Hendrickson, T.; Still, W. C., *J. Comput. Chem.* **1990**, 11, (4), 440-467.
175. Qiu, D.; Shenkin, P. S.; Hollinger, F. P.; Still, W. C., *J. Phys. Chem. A* **1997**, 101, (16), 3005-3014.
176. Becke, A. D., *J. Chem. Phys.* **1993**, 98, (7), 5648-5652.
177. M. J. Frisch, G. W. T., H. B. Schlegel, G. E. Scuseria, M. A. Robb, J. R. Cheeseman, G. Scalmani, V. Barone, B. Mennucci, G. A. Petersson, H. Nakatsuji, M. Caricato, X. Li, H. P. Hratchian, A. F. Izmaylov, J. Bloino, G. Zheng, J. L. Sonnenberg, M. Hada, M. Ehara, K. Toyota, R. Fukuda, J. Hasegawa, M. Ishida, T. Nakajima, Y. Honda, O. Kitao, H. Nakai, T. Vreven, J. A. Montgomery, Jr., J. E. Peralta, F. Ogliaro, M. Bearpark, J. J. Heyd, E. Brothers, K. N. Kudin, V. N. Staroverov, R. Kobayashi, J. Normand, K. Raghavachari, A. Rendell, J. C. Burant, S. S. Iyengar, J. Tomasi, M. Cossi, N. Rega, J. M. Millam, M. Klene, J. E. Knox, J. B. Cross, V. Bakken, C. Adamo, J. Jaramillo, R. Gomperts, R. E. Stratmann, O. Yazyev, A. J. Austin, R. Cammi, C. Pomelli, J. W. Ochterski, R. L. Martin, K. Morokuma, V. G. Zakrzewski, G. A. Voth, P. Salvador, J. J. Dannenberg, S. Dapprich, A. D. Daniels, Ö. Farkas, J. B. Foresman, J. V. Ortiz, J. Cioslowski, and D. J. Fox *Gaussian 09, Revision B.01*, Gaussian, Inc.: Wallingford CT, 2009.
178. Marten, B.; Kim, K.; Cortis, C.; Friesner, R. A.; Murphy, R. B.; Ringnalda, M. N.; Sitkoff, D.; Honig, B., *J. Phys. Chem.* **1996**, 100, (28), 11775-11788.
179. Tannor, D. J.; Marten, B.; Murphy, R.; Friesner, R. A.; Sitkoff, D.; Nicholls, A.; Honig, B.; Ringnalda, M.; Goddard, W. A., *J. Am. Chem. Soc.* **1994**, 116, (26), 11875-11882.
180. *Jaguar, version 7.7*, Schrodinger, LLC: New York, 2010.
181. Balasubramaniam, A.; Mullins, D. E.; Lin, S.; Zhai, W.; Tao, Z.; Dhawan, V. C.; Guzzi, M.; Knittel, J. J.; Slack, K.; Herzog, H.; Parker, E. M., *J Med Chem* **2006**, 49, (8), 2661-5.
182. Martin, P.; Papayannopoulou, T., *Science* **1982**, 216, (4551), 1233-5.
183. Moser, C.; Bernhardt, G.; Michel, J.; Schwarz, H.; Buschauer, A., *Can J Physiol Pharmacol* **2000**, 78, (2), 134-42.
184. Moser, C.; Bernhardt, G.; Michel, J.; Schwarz, H.; Buschauer, A., *Can. J. Physiol. Pharmacol.* **2000**, 78, (2), 134-142.
185. Cheng, Y.; Prusoff, W. H., *Biochem Pharmacol* **1973**, 22, (23), 3099-108.